5th INTERNATIONAL SYMPOSIUM on DAM SAFETY

27 October - 01 November 2018
DSI-Orhantepe Convention Center
Cevahir Asia Hotel - ISTANBUL / TURKEY

5 UBGS 2018 Istanbul Turkey

www.damsafety2018.com

PROCEEDINGS: VOLUME II

General Directorate of State Hydraulic Works
was established
for use of earth and water resources in Turkey
by Law No. 6200.
We think that
all intellectuals throughout the country
have to support its institutional studies.

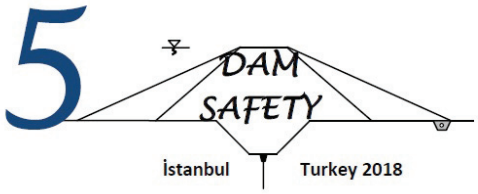

5th INTERNATIONAL SYMPOSIUM
on
DAM SAFETY

27 October – 1 November 2018

İstanbul / TURKEY

VOLUME II

Edited by:

Prof. Dr. Hasan TOSUN

Prof. Dr. M. Emin EMİROĞLU

Assoc. Dr. Şerife Yurdagül KUMCU

C. Eng. Turgut Vatan TOSUN

Proceedings for dam safety 2018

ISBN: 978-9444-0782-7-6
BASKI: Uzman Matbaacılık Kağıt Yayın Ticaret Ltd. Şti
İvedik Org. San. Bölgesi Matbaacılar Sitesi 1514 Sk.
No:44 İvedik /Ankara

Organizing Committee

Chairman
Hasan TOSUN
Co-Chairman
Murat DAĞDEVİREN
Co-Chairman
Feyza ÇİNİCİOĞLU
Co-Chairman
Sedat ÖZPINAR
Secretary
Kasım YENİGÜN
Co-Secretary
Şerife Yurdagül KUMCU, NEÜ
Members
Mustafa Hakkı AYDOĞU, HÜ
Tevfik Baran ÖNDER, BGD
Mehmer BERİLGEN, YTÜ
Veysel GÜMÜŞ, HÜ
Murat HATİPOĞLU, DSİ
Müge İNANIR, ZMGM
İlker PEKER, DSİ
Saim ŞEN, BGD
Turgut Vatan TOSUN, BGD
Mustafa TUNÇ, FÜ
Hasan USUL, BGD
Kemal YÜKSEL, DSİ

Members of The Honor Board

Binali YILDIRIM, Chairman of the Grand National Assembly of Turkey
Bekir PAKDEMİRLİ, Minister of the Agriculture and Forestry
Fatih DÖNMEZ, Minister of Energy and Natural Resources
Akif ÖZKALDI, Deputy Minister of the Agriculture and Forestry
Mücahit DEMİRTAŞ, Deputy Minister of Environment and Urban Planning
Mevlüt UYSAL, Mayor of İstanbul Metropolitan Municipality
Prof. Dr. Erhan GÜZEL, Rector of Kultur University
Prof.Dr. Kemal ŞENOCAK, Eskişehir Osmnagazi University
Hasan MANDAL, President of Scientific and Technological Research Council
Mehmet GÜLLÜOĞLU, Head of Disaster and Emergency Management Presidency Mevlüt AYDIN, General Director of State Hydraulic Works
Fatih TURAN, General Director of Istanbul Water and Sewerage Administration.
Zekai ŞEN, Director of Water Foundation
Hasan TOSUN, President of National Dam Safety Association
İlyas DEMİRCİ, General Secretary of TDMMB

Local Advisory Committee

Dincer AYDOĞAN, DSİ
M.Emin EMİROĞLU, FÜ
Kamil EREN, İKÜ
Nazmi KAĞNICIOĞLU, DSI
Zafer KARAYILANLIOĞLU, YEGM
Celal KOLOĞLU, İNTES
Selami OĞUZ, BGD
Mehmet Uğur YILDIRIM, DSİ
Turgut UZEL İKÜ
Kasım YENİGÜN HÜ
Kemal KARAKUŞ, DSİ
Seyfullah YILMAZ, Eti Maden
Mithat YÜKSEL, EUAŞ
Munis ÖZER, TMMMB
Cemal GÖKÇE, İMO

International Advisory Committee

Altan Abdulamit, Romania
Mevlüt Aydın, Turkey
Marla Barnes, USA
Erich Bauer, Austria
Tony Bennett, Canada
George Dounias, Greece
Tuncer Edil, USA
Jean Jacques Fry, France
Mazza Guido, Italy
Michel Lino, France
Dimitur Kisliakov, Bulgaria
E. Miljkovic, Bosnia Herz.
Laurent Mouvet, Switzerland
Rakesh Nath, India
Ali Noorzad, İran
Vladimir Pelehtin, Russia
Ljupcho Petkovski, Macedonia
Mahdi Rashid Mahdi, Iraq
Illahi B. Shaikh, Pakistan
Anton J.Scheiss, Switzerland
Vache Tokmajyan, Armenia
G.Vashetti, Italy
Martin Wieland, Switzerland
Tracey Williamson, UK
Gerald Zenz, Austria
P. Zielinski, Canada

International Scientific Committee

Mohammad Alembagheri, Iran
M. Amin Hariri-Ardebili, USA
Eduardo E. Alonso, Spain
Arash Barjasteh, Iran
Erich Bauer, Austria
David S.Bowles, USA
Laura Calderia, Portugal
Georges R. Darbre, Switzerland
Behrouz Gordan, Iran
Dean B. Durkee, USA
Babak Ebrahiman, Iran
Tuncer Edil, USA
Mohsen Ghaemian, Iran
Yusof Gnaaat, USA
Feng Jin, China
Seyedmehdi Mohammadizadeh, Iran
Laurent Mouvet, Switzerland
Ljupcho Petkovski, Macedonia
Adrian Popovic, Romania
Anton J.Scheiss, Switzerland
Carlos Ventura, Canada
Jin-Ting Wang, China
Martin Wieland, Switzerland
Gerald Zenz, Austria
Andy P. Zielinski, Canada
Fu Zhongzhi, China

Local Scientific Comittee

Süleyman Adanur, Karadeniz Technical University
Necati Ağıralioğlu, Antalya Bilim University
Ahmet Can Altınışık, Karadeniz Technical University
S.Oğuzhan Akbaş, Gazi University
Mustafa Tamer Ayvaz, Pamukkale University
Mehmet Berilgen, Yıldız Technical University
Ayla Bilgin, Çoruh University
Barış Binici, Middle East Technical University
Zekai Celep, İstanbul Teknik Üniversitesi
Barış Sevim, Yıldız Technical University
Zafer Bozkuş, Middle East Technical University
U.Şafak Çavuş, Süleyman Demirel University
Yusuf Calayır, Fırat University
S.Feyza Çinicioğlu, Özyeğin University
Ayşe Edinçliler, Boğaziçi University
Kemal Önder Çetin, Middle East Technical University
Erdal Çokça, Middle East Technical University
Ender Demirel, Eskişehir Osmangazi University

Ahmet Doğan, Yıldız Technical University Şebnem
Şeker Elçi, İzmir İnstitute of Technology M.Emin
Emiroğlu, Fırat University
Mustafa Erdik, Boğaziçi University
Kamil Eren, İstanbul Kültür University
Erol Güler, Boğaziçi University
Necati Gülbahar, İstanbul Gelişim University Murat
Günaydın, Gümüşhane University
Ayhan Gürbüz, Gazi University
Tefaruk Haktanır, Erciyes University
Yılmaz İçağa, Afyon Kocatepe University
Mete İncecik, İstabul Teknik University
Yunus Kalkan, İstanbul Technical University
Halil Karadeniz, İstanbul University
Muhammet Karaton, Fırat University
Murat Emre Kartal, İzmir Demokrasi University
C. Melek Kazezyılmaz ALHAN, Istanbul University
Ayhan Koçbay, DSİ
Selami Oğuz, Dam Safety Association
Ali Rıza Öç, Temelsu Int.
Kutay Özaydın, Yıldız Technical University
A.Tolga Özer, Okan University
Evren Seyrek, Dumlıpınar University
Zekai Şen, Water Foundation
Gökmen Tayfur, İzmir İnstitute of Technology
Kasım Yenigün, Harran University
Yalçın Yüksel, Yıldız Technical University
Turgut Uzel, İstanbul Kültür University

Study Groups

Technical Committee on Dictionary for Dams and Auxiliary Structures
Technical Committee on Design of Tailing Dams
Technical Committee on Upstream Flood Control for Reservoir and Siltation
Technical Committee on Slope Stability in Reservoir

Awards

Competition on M.S Thesis
Competition on Ph.D Thesis

Dear Ladies and Gentlemen,

Working under the Ministry of the Agriculture and Forestry, there are main governmental agencies responsible for development of water resources all over Turkey. In terms of water resources, we consider two main problems in Turkey: Flood and Drought. These natural disasters can result in social and economic damages. Scientific studies point out that as a result of the global warming and climate change, water related natural disasters experienced in many countries have been occurring more destructive with larger scales than those happened in the past. Impacts of global warming and climate change have been intensified with each passing day in the world and in our region. These conditions add to the weight of water administration in the semiarid zones in which Turkey is located as well.

Our Ministry and other related organizations have accomplished a great deal towards completing facilities mitigating the adverse effects of flood and drought disasters. I would like our national organizations to continue on achievements and efforts for this challenge. We also try to discuss water resources problems in conferences, congresses and symposiums. This international symposium and exhibition is one of the important events to discuss our water problems with neighboring countries. We think that special technical sessions will be presented on large dam projects, which have been completed or under construction now in Turkey and other countries.

The purpose of this symposium is to provide opportunity for the dam safety community to share important information, lessons learned and new technology.

We are very glad to see you and your family members in Istanbul and wish you many stimulating professional and personal experiences.

Have a great symposium!

Dr. Bekir PAKDEMİRLİ
Minister of the Agriculture and Forestry

Dear Participants,

Turkey is in the semi-arid zone and so the precipitation shows differences according to regions and seasons. In recent years, upwards trends in temperature and changing precipitation patterns have been recorded all around the world due to the climate change impacts. Moreover, climate change in most regions will likely increase the probability and severity of floods. Although a large amount of rain falls down usually during the winter season however the water consumption increases a large amount in the summer times. Parallel to the population growth, there is a large increase in water demand in drinking, use and industry sectors, especially in agriculture in our country as well as in the world. As a consequence of climate change, receding in the amount of water brings need for effective and sustainable water resources utilization and enforces the countries to implement water saving technologies in all water sectors, particularly in irrigation.

Water demand of the future generation should be guaranteed without compromising the ability of them to meet their own needs by water storage structures for achieving water sustainability. Water resources should also be increased in order to avoid water scarcity problems, in particular, in arid periods. Preservation and extension of life-time of storage facilities has vital importance in Turkey. On the other hand, as Turkey is one of the most quake-prone countries in the world, the safety of the water storage facilities in all stages like from planning and design to construction and operation must also be planned by taking into account of the deformation risk of the construction materials. For this purpose, technical and academic studies are extensively carried out in Turkey. The fifth International Symposium on Dam Safety and Exhibition activity is a part of the our studies. We will be very pleased to see you among us at this symposium.

I would like to say “welcome” for all guests and participants in order to have enjoyable time and see the beauties of Istanbul and also Turkey and I wish the event has a great success.

Akif ÖZKALDI
Deputy Minister of the Agriculture and Forestry

Ladies and Gentlemen,

Turkey is rich by means of land resources and sufficient in terms of water resources. Almost one third of Turkey's total area (78 million ha) is arable land (28 million ha). Comprehensive studies pointed indicate that 8,5 million ha of the arable land is economically irrigable in Turkey. 5,9 million ha of this irrigable area have been equipped with irrigation facilities being 3,61 million ha developed by DSİ with modern irrigation network systems.

The average annual precipitation of Turkey is 501 cubic km (501 billion cubic m) per year. 274 billion cubic m of this amount is assumed to evaporate from surface and transpire through plants. 69 billion cubic m of precipitation directly recharges the aquifers, whereas 158 billion cubic m forms the precipitation runoff. There is a continuous interaction between surface runoff and groundwater, but it is estimated that a net 28 billion cubic m of groundwater feeds the rivers.

In summary, surface water and ground water potential has an average of 112 billion cubic m per year and of which 44 billion cubic m is consumed.

The General Directorate of State Hydraulic Works (DSI) is the primary executive state agency of Turkey and the main objective of DSI is to develop planning and designing projects for efficiently use of all water and land resources in Turkey. Additionally, it follows closely the improvements related with its subject and efforts for cooperating with organizations such as ICOLD in order to find out technical solutions rationally. 5th International Symposium on Dam Safety and Exhibition is one of these collaborations. Many scientists, researchers and field engineers of various countries are expected to participate this symposium and many presentation will be held on by invited speakers who are professional in their area.

Turkey has an important amount of knowhow about the assessment of water and land resources. I wish this conference will give an opportunity to share these knowledges and to exchange informations between the participants. I hope that this conference in which many issues discussed will be very useful for all of you and I as the President of TRCOLD would like to invite all of you to Istanbul.

Mevlüt AYDIN
General Director of State Hydraulic Works

Dear Colleagues, Ladies and Gentlemen,

Fifth International Symposium on Dam Safety was organized by National Association on Dam Safety, TRCOLD, Water Foundation, National Association on Soil Mechanics and Geotechnical Engineering and Eskisehir Osmangazi University between October 27 and November 1, 2018 in Istanbul, Turkey. On behalf of the Organizing Committee, I am very glad to join with you in the 5th International Symposium on the Safety of Dams. The Conference Center is located in a pleasant, calm and intimate atmosphere of the historic city of Istanbul, which lies on and around the Bosphorus between Asia and Europe.

The aim of the symposium is to provide participants with a forum to exchange experiences and information about new technologies. The Organizing Committee works extremely hard to present an interesting and innovative program that will also include excursions to dams in Istanbul. In addition to workshops and lectures, there are also be a special technical meeting on the major dam projects already completed or under construction in Turkey and neighboring countries. In the symposium, we organized information days for some countries with presentations on local water resources and hydraulic structures and panel discussions on safety of dams and other related structures.

The organizing committee is proud to offer the opportunity to the delegate taking part a high technical program including 240 abstracts and 132 full papers with different subject. The papers focused on the topics such as geotechnical problems of foundation and embankments, innovative technology on hydrology, use of geographical information system for dam issues, static and dynamic stability analyses, dam surveillance, maintenance, instrumentation and monitoring, foundation treatments and cut-off structures, environmental issues and also hydro politics.

I hope that the symposium has been an opportunity for engineers, consultants and scientists working in the field of dam safety and other dam issues to meet and to present new ideas, achievements and experiences and to incorporate of the latest knowledge into practice. Also it has provided an enjoyable experience for cultural and social activities with the background of ancient city of the World for the delegates and accompanying people.

Discover the historical, cultural and culinary side of Turkey.

We look forward to welcoming you to Istanbul.

Have a great symposium.

Prof. Dr. Hasan TOSUN, Chairman
Organizing Committee

İÇİNDEKİLER/CONTENTS

PROCEEDINGS

5th International Symposium on Dam Safety

October 27-31, 2018

EARTHQUAKE SAFETY OF LARGE DAMS LOCATED IN KUCUK MENDERES BASIN, WEST TURKEY

Hasan TOSUN[1], Turgut Vatan TOSUN[2]

ABSTRACT

There are so many factors acting on total risk for a dam structure. Design engineers consider the risk rating of the completed structure and the seismic hazard rating of dam site as the main factors. The Kucuk Menderes basin, which is located in the western country, includes eight large dams having heights of 15.3 m to 84.5m from river bed. These are mainly used for providing domestic water for Izmir province. These are namely Alacatlı Kutlu Aktas, Balcova, Beydağ, Burgaz, Kavaklıdere, Seferihisar, Tahtalı and Urkmez dams. The study area is structurally cut by numerous faults, which are resulted by horst-graben system in west Anatolia. The deterministic seismic hazard analyses have indicated that values of peak ground acceleration range from 0.116g to 0.310g at the 50th percentile and from 0.189g to 0.482g at the 84th percentile for eight dam sites of this area. The total risk analyses have concluded that seven large dams have high-risk class in the basin.

Keywords: Dam, seismic hazard, total risk, basin.

INTRODUCTION

Design engineers generally consider two main factors acting on dam safety. These are the seismic hazard rating of dam site and the risk rating of the dam and appurtenant structures. The seismic hazard of a dam site can be based on the peak ground acceleration. This value derived from the defined design earthquake produces the main seismic loads. The risk rating of the dam should be based on the capacity of the reservoir, the height of the dam, the evacuation requirements, and the potential downstream damages. In general, the seismic and risk ratings are evaluated separately (ICOLD,1989). However, Bureau (2003) combined these two factors to define the total risk factor for dam structure.

The type of dam is an important parameter impacting the total risk rating. Safety concerns for embankment dams subjected to earthquakes involve either the loss of stability due to a loss of strength were combined in the embankment or foundation materials or excessive deformations such as slumping, settlement, cracking and planar or rotational slope failures (ICOLD,2016). The simplified procedures can be used for designing the embankment dams to obtain preliminary information about seismic parameters of the dam materials (Tosun, 2002).

[1] Professor, Department of Civil Engineering, Eskişehir Osmangazi University, Eskisehir, Turkey, e-posta: hasantosun26@gmail.com

[2] Civil engineer, TVT Hydrotech Bureau, Ahmet Mithat Efendi sok. 40/12 Cankaya, Ankara, Turkey, e-posta: barajproje@gmail.com

In the study eight large dams in Kucuk Menderes basin were considered. These basins cover totally an area of 7.2 sq.km at the west Anatolia and have a water yield resources of 2.40 L/s/km^2. This paper deals with an evaluation of seismic hazard and local site effects and evaluates their total risk of all dams, which have a structural height greater than 25 m, in the Kucuk Menderes basin (Table 1).

Table 1. Physical properties of dams considered for this study (DSI, 2016).

No	Dam	River	Aim *	Type (**)	Height from river bed (m)	Completed Year	Volume of embankment (hm^3)	Volume of reservoir (hm^3)
1	A.Kutlu Aktaş	Hırsız	D	EF	15.3	1997	0.28	16.61
2	Balcova	Ilıca	D	RF	63.4	1980	1.11	8.10
3	Beydağ	K.Menderes	I	HF	51.0	2009	2.37	248.27
4	Burgaz	Falaka	I	EF	84.5	2013	4.70	33.00
5	Kavaklıdere	Kavaklıdere	I+F	EF	36.5	2006	2.10	13.88
6	Seferihisar	Yassı	I	EF	54.0	1984	1.49	29.10
5	Tahtali	Tahtalı	D	RF	54.4	1999	3.37	306.65
6	Urkmez	Urkmez	I+D	EF	32.0	1981	0.99	7.92

(*) D = Domestic water, E = Energy, F = Flood Control, I = Irrigation, IU= Industry Use
(**) EF =Earthfill, HF = Hard fill, RF = Rockfill

METHODS OF ANALYSES

The probabilistic and deterministic are generally used for seismic hazard analyses of dams and appurtenant structures. The probabilistic seismic hazard analysis is widely used and considers uncertainties in size, location and recurrence rate of earthquakes. Kramer (1996) states that the probabilistic seismic hazard analysis provides a framework in which uncertainties can be identified and combined in a rational manner to provide a more complete picture of the seismic hazard. The deterministic seismic hazard analysis considers a seismic scenario that includes a four-step process. It is a very simple procedure and gives rational solutions for large dams because it provides a straightforward framework for the evaluation of the worst ground motions. Due to the unavailability of strong motion records, various attenuation relationships were adopted to calculate the peak ground acceleration (PGA) acting on dam sites. Krinitzsky (2005) states that deterministic seismic hazard analysis considers geology and seismic history to identify earthquake sources and to interpret the strongest earthquake with regardless of time.

For this study, earthquake definitions given by FEMA (2005) were considered for seismic hazard analyses. The Operating Basis Earthquake (OBE), which was defined by means of the probabilistic methods mentioned above, is the earthquake that produces the ground motions at the site that can reasonably be expected to occur within the service life of the project. MDE is normally characterized by a level of motion equal to that expected at the dam site from the occurrence of deterministically evaluated MCE. Safety Evaluation Earthquake (SEE) is the level of shaking for which damage can be accepted but for which there should be no uncontrolled release of water from the reservoir. Author states that most of large dams in Turkey were analyzed by using these definitions in past. ICOLD (2016) also some earthquake definitions for dynamic analysis of dams. Author mentions these definitions more detail on their research (Tosun and Tosun, 2017; Tosun, 2018).

Some methods are used to quantify the total risk factor of a dam. One of them considers the seismic hazard of the dam site and the risk rating of the structure separately (ICOLD, 1989 and DSI, 2012). According to this method, the seismic hazard of the dam site regardless of type of dam, can be classified into four groups from low to extreme. This is a quick way for rating the seismic hazard. The hazard class of a dam site obtained from this method provides a preliminary indication of seismic evaluation requirements. Other one is Bureau method, which considers various risk factors and weighting points to quantify the total risk factor (TRF) of any dam (Bureau, 2003). In this methods the TRF depends on the dam type, age, size, downstream risk and vulnerability, which depends on the seismic hazard of the site.

The peak ground acceleration was determined by two methods discussed above. For this study eight separate predictive relationships for horizontal peak ground acceleration were considered. However, some data have been excluded for the study because of giving extreme values. Only three predictive relationships were taken into account for this study (Campbell, 1981; Boore et al, 1993; Boore et al, 1997). All procedures mentioned above can be executed by the DAMHA program that is working on the basis of geographic information system (GIS). For total risk of dams, two different methods mentioned above are used for all dams considered for this study.

ICOLD (2016) states that the Maximum Credible Earthquake (MCE) is the largest reasonably conceivable earthquake magnitude that is considered possible along a recognized fault or within a geographically defined tectonic province. According to this specification, the Safety Evaluation Earthquake (SEE) is defined as the maximum level of ground motion for which the dam should be designed or analyzed. For the dams with high total risk, it is recommended that the SEE should be characterized by a level of motion equal to that expected at the dam site from the occurrence of a deterministically-evaluated maximum credible earthquake or of the probabilistically-evaluated earthquake ground motion with a very long return period.

SEISMIC HAZARD ANALYSES AND RESULTS

For the seismic hazard analyses of the dam site in the Kucuk Menderes basin, a detailed study was performed to identify all possible seismic sources, as based on the seismic zonation map of Turkey, given in Figure 1. The National Disaster Organization and other Institutes prepared the map for general use. But it was modified by the author and co-workers to use for dam projects at the Earthquake Research Center in Eskişehir Osmangazi University. Local geological features and seismic history were used to quantify the rate of seismic activity in the basin. As a result of detailed evaluation, total area covering all basins was separated into five seismic zones. Figure 2 introduces the model used for seismic hazard analyses of this study.

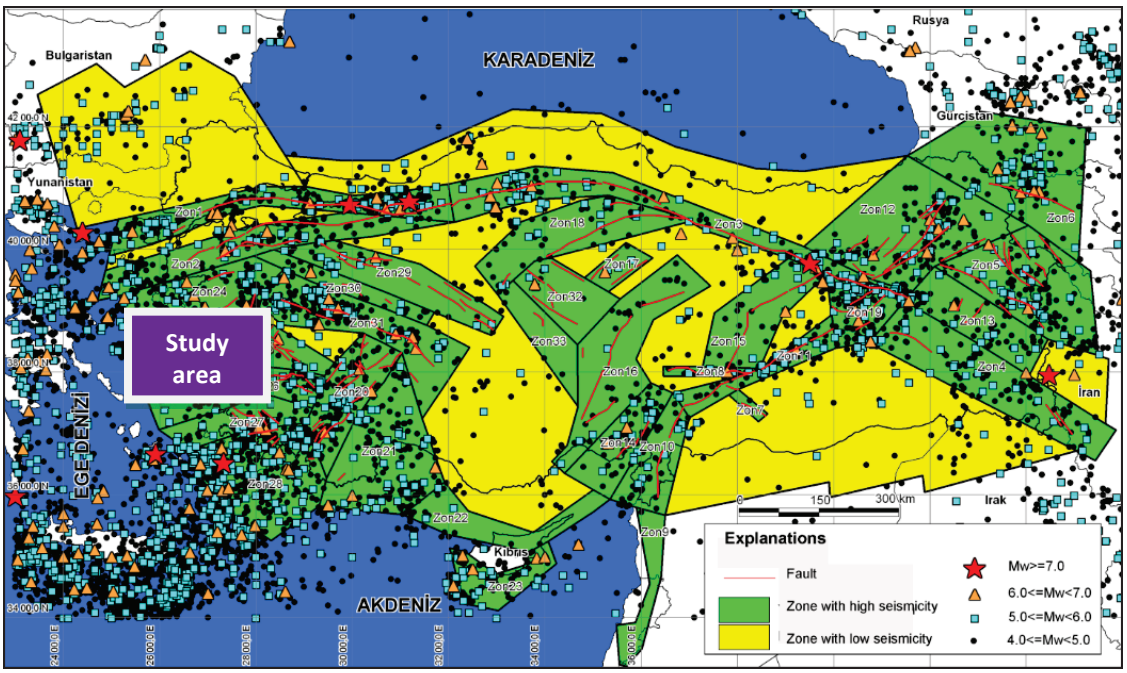

Figure 1. Seismo-tectonic map of Turkey and location of study area.

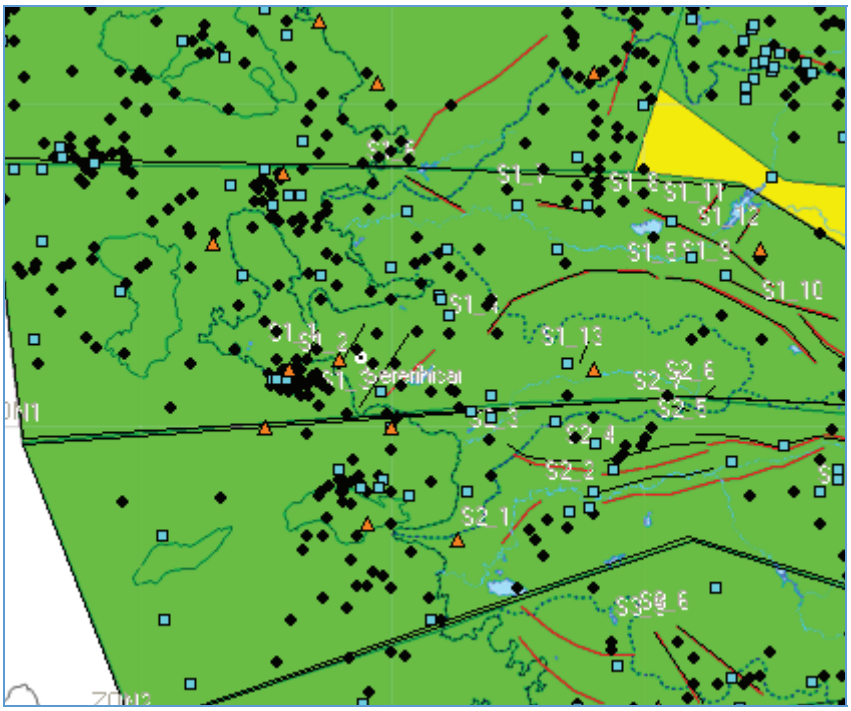

Figure 2. Seismological sources and earthquakes for the dams in Kucuk Menderes basin.

In Turkey, a new seismo-tectonic map was released to public by National Geological Survey (MTA, 2013). According to this map, seven large dams considered for this study are under near source effect. ICOLD (2016) defined the near-field motion, which is ground motion recorded in the vicinity of a fault. In this specification, a correlation between radius of near field area and earthquake magnitude is suggested as based on the cases on West United States. Author established limits of near-field motion for the investigation area. According to this model, there are seven dams, which are under the near-field motion. These dams can be subjected to earthquake having a magnitude of 5.3 and 6.2 are the minimal distance to fault segment is between 1.9 and 10.1 km (Table 2).

Table 2. Results of deterministic analyses

No	Dam	Deterministic Method *			
		M_{max}	R_{min} (km)	Mean PGA + 50 %	Mean PGA + 84 %
1	A.Kutlu Aktaş	6.1	10.1	0.116	0.189
2	Balcova	6.1	2.4	0.288	0.450
3	Beydağ	5.3	2.4	0.239	0.371
4	Burgaz	5.4	1.7	0.276	0.427
5	Kavaklıdere	6.2	4.7	0.293	0.459
6	Seferihisar	5.9	5.3	0.245	0.374
7	Tahtali	5.7	1.9	0.277	0.431
8	Urkmez	5.7	1.7	0.310	0.482

(*) M_{maks} = Maximum earthquake magnitude in M_w
R_{min} = Minimum distance to fault segment
Mean PGA + 50% = Mean Peak Ground Acceleration at the 50th percentile
Mean PGA + 84% = Mean Peak Ground Acceleration at the 84th percentile

The deterministic analyses indicate that peak ground acceleration (PGA) changes within a wide range. The PGA values ranges from 0.116g to 0.310g for the mean Peak Ground Acceleration at the 50th percentile and from 0.189g to 0.482g for the mean Peak Ground Acceleration at the 84th percentile

given in table 2. According to the updated DSI guidelines, the PGA values at the 84th percentile should be taken into account for four dams analyzed throughout the study, when considered deterministic approach (DSI, 2012). For Alacati Kutlu Aktas, Beydag and Seferihisar dams, the PGA values at the 50th percentile should be considered for dynamic analyses according to DSI seismic guidelines.

Throughout this study, two methods have been considered to quantify the total risk for dam structures. In DSI guidelines, total risk factor depends to reservoir capacity, height, evacuation requirement and potential hazard (DSİ, 2012). According to DSI Guidelines all dams are categorized in III and IV risk classes with high and very high risk rating. Following Bureau's method, seven large dams are classified in risk class III, a high-risk rating. One of them, namely Beydag dam, is categorized in risk class of II with moderate risk ratio. In Bureau method, the values of the TRF range from 99.3 to 188.5. This means that there is only one dam having a risk class II when considered all dams for this study. Author thinks that the solution obtained from Bureau method is more rational than that of the DSI guidelines.

Table 3. Total risk of large dams ın Kucuk Menderes Basin.

No	Dam	Hazard Analysis		Total Risk (ICOLD,1989)			Total Risk (Bureau, 2003)		
		Class	Hazard Ratio	Risk factor	Risk class	Risk ratio	Risk factor	Risk class	Risk ratio
1	A.K. Aktaş	II	Moderate	30	III	High	163.4	III	High
2	Balcova	IV	Very high	34	IV	Very high	187.6	III	High
3	Beydağ	II	Moderate	36	IV	Very high	99.3	II	Moderate
4	Burgaz	IV	Very high	34	IV	Very high	162.8	III	High
5	Kavaklıdere	IV	Very high	32	IV	Very high	184.8	III	High
6	Seferihisar	II	Moderate	34	IV	Very high	180.2	III	High
7	Tahtali	IV	Very high	36	IV	Very high	186.6	III	High
8	Urkmez	IV	Very high	32	IV	Very high	188.5	III	High

DISCUSSIONS

There are six large dams located in Izmir Metropolitan Area for providing domestic water. Four of them are located on the turbidities of Kucuk Menderes river while other two were constructed in Gediz basin. The earthquake safety and total risk of these dams are evaluated more detail as given below (Tosun, 2018).

Alacatı Kutlu Aktas Dam is a 15.3 m high-earthfill dam with a total embankment volume of 280 000 m^3. It is located on Hirsiz river in Kucuk Menderes basin. Its construction was finished in 1997. When the reservoir is at operation stage with maximum water level, the facility approximately will impound 16.60 hm^3 of water with a reservoir surface area of 2.55 km^2. It is mainly designed to provide domestic water with annual capacity of 3.0 hm^3. The side slopes of main embankment is 3.0H:1V for upstream and 2.5H:1V for downstream (H=horizontal and V=vertical) (Fig. 2). On the section there is a central impervious zone, which is composed of impervious clay and a transition section of sand, gravel and small-sized crushed rock was designed over rockfill materials (Figure 2). The shell fill in downstream and upstream parts is composed of semi-pervious clayey material. The alluvium on river bed was removed before beginning the construction of the main embankment. The seismic hazard analyses performed throughout this study indicates that this dam is less critical dam within the Izmir Metropolitan Area. It will be subjected to a peak ground acceleration of 0.116 g by an earthquake of 6.1 magnitude and it is only 10.1 km far away from an active fault given in new seismo-tectonic map of Turkey in 2013. Its TRF value is 163.4 and it is identified as risk class of III. The 21-years old embankment is in excellent condition.

Balcova dam is a rockfill dam on Ilica River in the Izmir Metropolitan Area. It has a 63.4 m height from river bed. When the reservoir is at maximum capacity, the facility impounds 7.76 hm^3 of water with a reservoir surface area of 0.69 km^2. Its construction was finished in 1980. It was designed to provide domestic water with annual capacity of 12 hm^3. The crest length is 231 m and the side slopes of main embankment is 3.5H:1V for upstream and 3.0H:1V for downstream (H=horizontal and V=vertical) (Fig. 3). On the section there is a central impervious core, which is composed of compacted impervious clay and a transition section of sandy and gravelly aggregates was designed between the core and semi-pervious soils. The alluvium on river bed, which is composed of different size of river bed material, was removed before beginning the construction of the main embankment According to the seismic hazard analyses of this study, it will be subjected to a peak ground acceleration of 0.288g by an earthquake of 6.1 magnitude and its embankment is only 2.4 km far away from an active fault given in new seismo-tectonic map of Turkey in 2014. Its TRF value is 187.6, and it is identified as risk class of III. This 37-year old earthfill embankment is in excellent condition, but it cannot meet current seismic design standards. Additionally, it is under near-field motion. Therefore, its seismic upgrade should be provided soon.

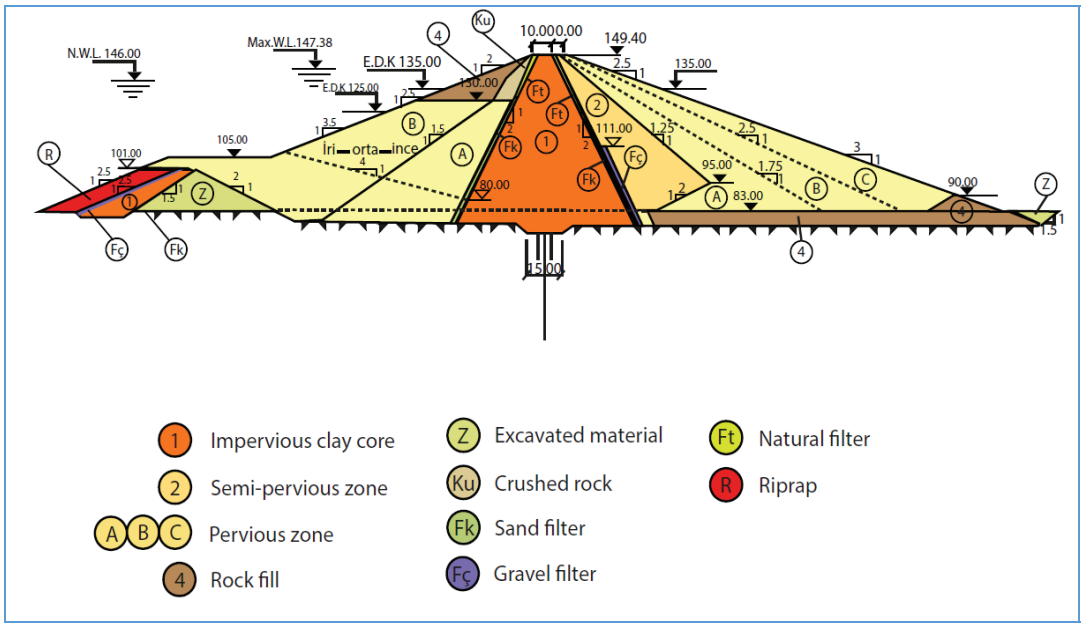

Figure 3. The maximum cross-section of embankment of Balcova dam.

The Beydag dam is a hardfill dam with a 51.0-m height from river bed. It was located on the main river of Kucuk Menderes basin. When the reservoir is at maximum capacity, the facility impounds 248.27 hm^3 of water with a reservoir surface area of 13.0 km^2. Its construction was finished in 2009. It was designed to irrigate 19 650 ha of land. The main embankment consists of hardfill materials (figure 4). The upstream and downstream slopes were covered by concrete for erosion protection and water tightness. The crest length is 797 m and the side slopes of main embankment is 0.25H:1V for upstream and 0.8H:1V for downstream (H=horizontal and V=vertical). According to the seismic hazard analyses of this study, it will be subjected to a peak ground acceleration of 0.239g by an earthquake of 5.3 magnitude. This 9-year old earthfill embankment is in excellent condition. It is categorized in risk class of II with moderate risk ratio. Figure 5 introduces a general view from the Beydag dam.

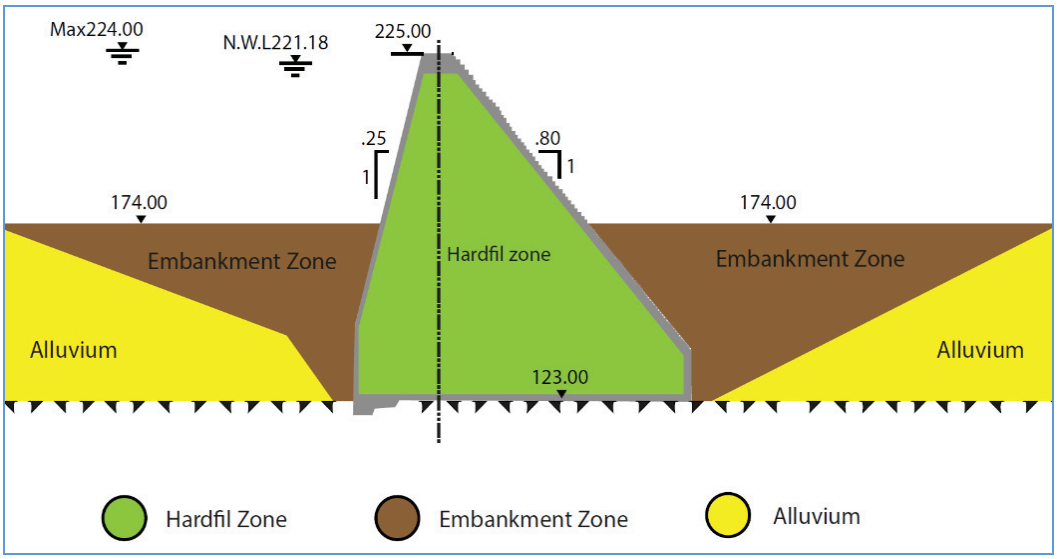

Figure 4. The maximum cross-section of the embankment of Beydag dam.

Figure 5. A general view from Beydag dam.

The Burgaz dam is a 84.5-m high earthfill dam with a total embankment volume of 4 700 000 m^3. It is located on the Falaka River in the basin. Its construction was finished in 2013. When the reservoir is at operation stage with maximum water level, the facility approximately will impound 33.00 hm^3 of water with a reservoir surface area of 1.52 km^2. It was mainly designed to irrigate 3009 ha of land. The crest width is 10 m and the side slopes of main embankment is 2.75H:1V for upstream and 2.4H:1V for downstream (H=horizontal and V=vertical). On the section there is a central impervious core, which is composed of compacted low-plasticity sandy clay and a transition section of sand and gravel was designed between the core and earth materials for upstream and downstream parts. The alluvium on river bed, which is composed of mixtures of fine to large size grains, was removed before beginning the construction of the main embankment. It has a positive cutoff. In other words, there is grouting curtain in foundation soil. The seismic hazard analyses performed throughout this study indicates that dam is one of the most critical dams within the basin.

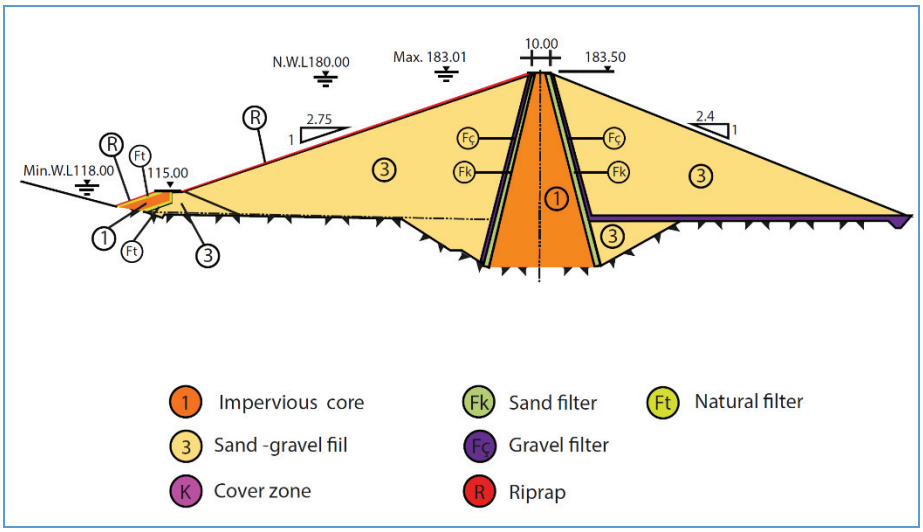

Figure 6. The maximum cross-section of the embankment of Burgaz dam.

Figure 7. A general view from Burgaz dam.

The Kavaklidere dam is a 36.5 m high-earthfill dam with a total embankment volume of 2 100 000 m^3. It is located on Kavaklidere river in Kucuk Menderes basin. Its construction was finished in 2006. When the reservoir is at operation stage with maximum water level, the facility approximately will impound 13.8 hm^3 of water with a reservoir surface area of 0.96 km^2. It is mainly designed to irrigate 560 ha of land. The side slopes of main embankment is 3.0H:1V for upstream and 2.5H:1V for downstream (H=horizontal and V=vertical) (Fig. 8). On the section there is a central impervious zone, which is composed of impervious clay and a transition section of sand was designed over earthfill materials (Figure 2). The shell fill in downstream and upstream parts is composed of semi-pervious sandy-gravelly material. The alluvium on river bed was removed before beginning the construction of the main embankment. The seismic hazard analyses performed throughout this study indicates that this dam is critical dam within the basin. It will be subjected to a peak ground acceleration of 0.459 g by an earthquake of 6.2 magnitude and it is only 4.7 km far away from an active fault given in new seismo-tectonic map of Turkey in 2013. Its TRF value is 184.8 and it is identified as risk class of III. The -years old embankment is in excellent condition.

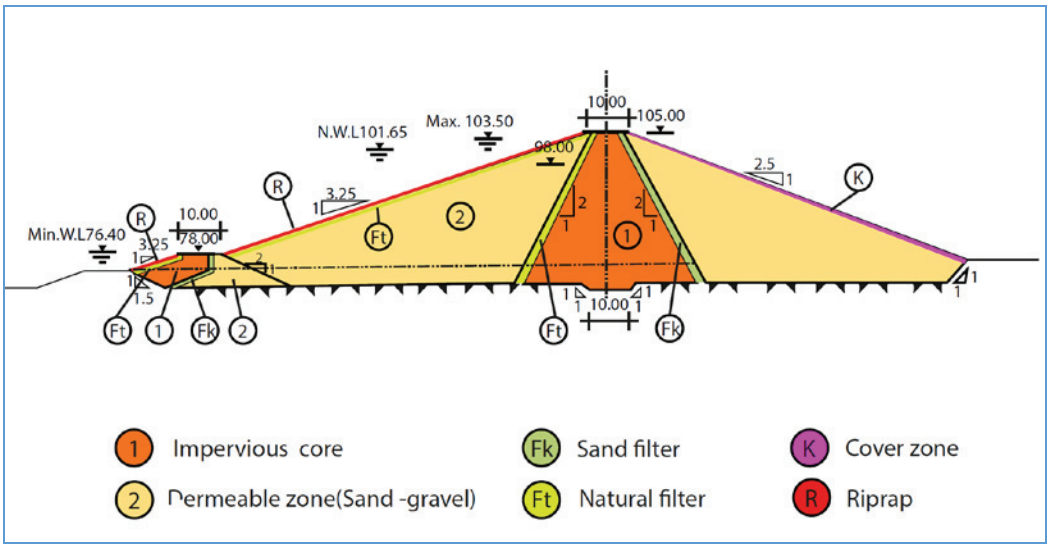

Figure 8. The maximum cross-section of the embankment of Kavaklıdere dam.

The Seferihisar dam is a earthfill dam on Yassı River in the basin. It has a 54.0 m height from river bed. When the reservoir is at maximum capacity, the facility impounds 29.1 hm^3 of water with a reservoir surface area of 1.79 km^2. Its construction was finished in 1984. The crest length is 231 m and the side slopes of main embankment is 3.0H:1V for upstream and 2.5H:1V for downstream (H=horizontal and V=vertical) (Fig. 9). On the section there is a central impervious core, which is composed of compacted impervious clay and a transition section of sandy and gravelly aggregates was designed between the core and semi-pervious soils. The alluvium on river bed, which is composed of different size of river bed material, was removed before beginning the construction of the main embankment. According to the seismic hazard analyses of this study, it will be subjected to a peak ground acceleration of 0.374g by an earthquake of 5.9 magnitude and its embankment is only 5.3 km far away from an active fault given in new seismo-tectonic map of Turkey in 2014. Its TRF value is 180.2 and it is identified as risk class of III. This 34-year old earthfill embankment is in excellent condition, but it cannot meet current seismic design standards. Therefore, its seismic upgrade should be provided soon.

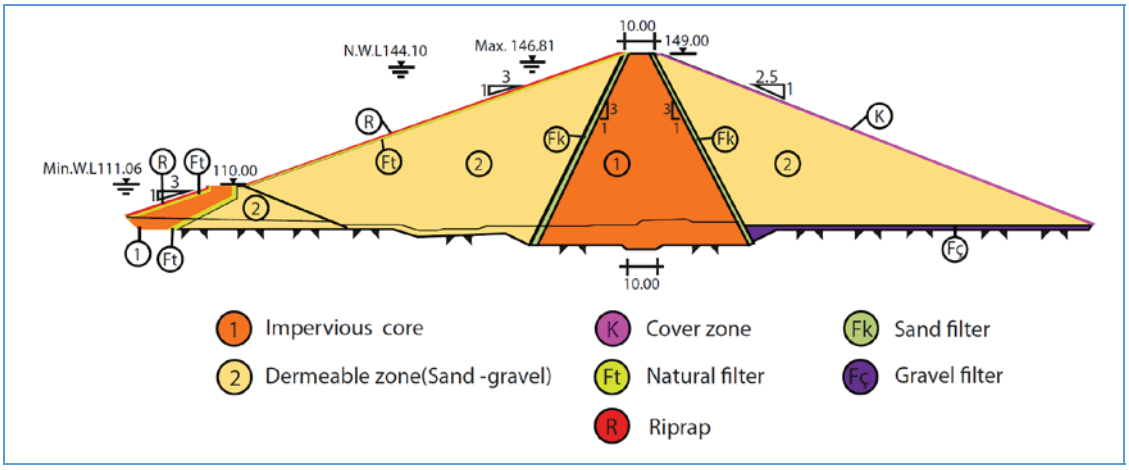

Figure 9. The maximum cross-section of the embankment of Seferihisar dam.

Tahtalı dam is a rockfill dam on Tahtalı River near Gumuldur County in the Izmir Metropolitan Area. It has a 54.4 m height from river bed. When the reservoir is at maximum capacity, the facility impounds 306.6 hm^3 of water in its reservoir. Its construction was finished in 1999. It was designed to provide domestic water with an active volume of 287 hm^3. Fig.10 shows a general view from

Tahtali dam. On the section there is a central impervious core, which is composed of compacted impervious clay and a transition section of sandy and gravelly aggregates was designed between the core and semi-pervious soils. The alluvium on clay core was removed before beginning the construction of the main embankment. A low-strength concrete wall was constructed for providing impermeability in dense alluvial soil. According to the seismic hazard analyses of this study, it will be subjected to a peak ground acceleration of 0.277g by an earthquake of 5.7 magnitude and its embankment is only 1.9 km far away from an active fault given in the updated seismo-tectonic map of Turkey. Its TRF value is 188.6 and it is identified as risk class of III. It is at second place after Gordes dam when regarding the total capacity of reservoir and one of the most critical dams in Izmır Metropolitan Area. This 19-year old earthfill embankment is in excellent condition, but it cannot meet current seismic design standards. Additionally, it is under near-field motion. Therefore, its seismic upgrade should be provided soon.

Figure 10. A general view from Tahtali dam

Urkmez dam is a earthfill dam on Urkmez River near Seferihisar County. It has a 32.0 m height from river bed. When the reservoir is at maximum capacity, the facility impounds 7.92 hm^3 of water with a reservoir surface area of 0.61 km^2. Its construction was finished in 1991. It was designed to provide water for irrigation of 370 ha and drinking water with annual capacity of 0.78 hm^3. The crest length is 428 m and the side slopes of main embankment is 3.0H:1V for upstream and 2.5H:1V for downstream (H=horizontal and V=vertical) (Figure 11). On the section there is a central impervious core, which is composed of compacted impervious clay and a transition section of sandy and gravelly aggregates was designed between the core and pervious coarse grained soils. The alluvium under clayey impervious core, which is composed of different size of river bed material, was removed before beginning the construction of the main embankment According to the seismic hazard analyses of this study, it will be subjected to a peak ground acceleration of 0.310 g by an earthquake of 5.7 magnitude and its embankment is 1.7 km far away from an active fault given in the updated seismo-tectonic map of Turkey. Its TRF value is 188.5, and it is identified as risk class of III. This 37-year old earthfill embankment is in excellent condition, but it cannot meet current seismic design standards. It will be under near-field motion during earthquake. Therefore, its seismic upgrade should be provided soon.

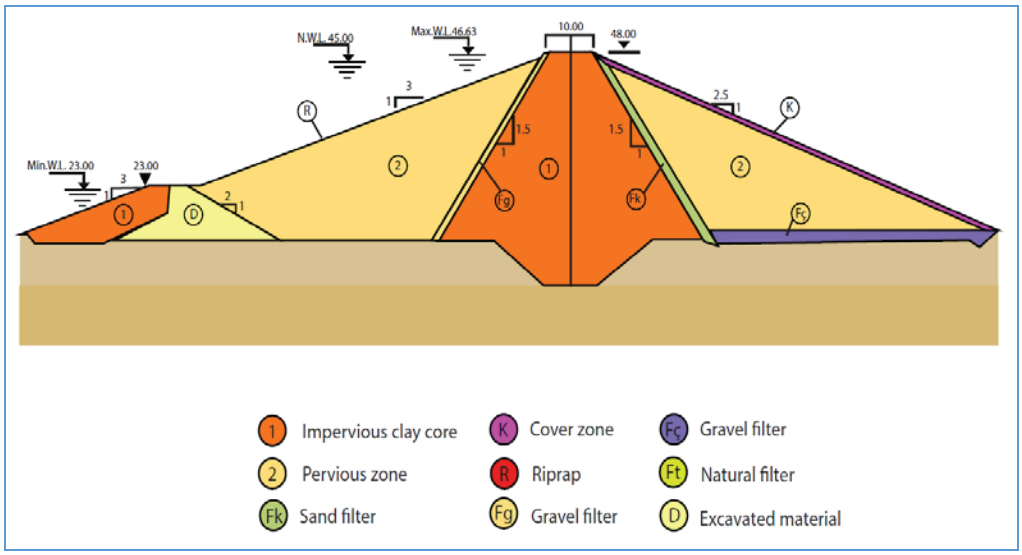

Figure 11. The maximum cross-section of the embankment of Urkmez dam.

CONCLUSIONS

Design engineers in Turkey believe that embankment dams, which are well compacted according to the specification, are suitable type for regions having high seismic activity. Whereas it is a well-known fact that strong ground shaking can result to instability on embankment and loss of strength at the foundations. Additionally, active faults, which are very close to the foundation of dams, have the potential to cause damaging displacement of the structure. This paper summarizes the seismic hazard and total risk analyses of six large dams, which are located in Kucuk Menderes basin, Turkey, as based on a preliminary study. Some of them are used for domestic water for Izmir Metropolitan Area. Therefore, they are critical structures for water safety for a metropolitan area as well as public safety. The study identified that seven of them are under near source effect. As a result of this study, 87.5 percent of dams has extremely high of risk class while others are classified in high risk class according to ICOLD classification. Therefore, detail seismic hazard analyses should be performed for these structures as based on the updated seismic data and design code under circumstances of the study of a national safety program for dam. In other words, these dams must be re-analyzed by selecting appropriate seismic parameters. Then they should be rehabilitated as considering design and construction measures, if necessary.

AKNOWLEDGEMENTS

Authors would like to thank to DSI General Director, who is the owner of state dams in Turkey and his co-workers.

REFERENCES

Boore, DM, Joyner, WB. and Fumal, TE (1993). *Estimation of response spectra and peak accelerations from Western North American earthquakes*. An interim report. Open file report 93-509.U.S.G.S.

Boore, DM., Joyner, WB. and Fumal, TE (1997*). Equation for Estimating Horizontal Response Spectra and Peak Acceleration from Western North American Earthquakes.* A Summary of recent Work. Sesimological Reseach Letters, V.68, N.1, January /February, 128-153.

Bureau, GJ (2003). *Dams and Appurtenant Facilities in Earthquake Engineering Handbook edited by Chenh, W.F and Scawthorn,C.* CRS press, Bora Raton 26.1-26.47.

Campbell, KW (1981). N*ear-Source Attenuation of Peak Horizontal Acceleration*: Bulletin Seism. Soc. Am., V.71, N.6, 2039-2070.

DSİ (2012). *Selection of Seismic Parameters for Dam Design*. State Hydraulic Works, Ankara, 29 p (in Turkish).

DSİ (2016). *Dams of Turkey*. TR-COLD, Ankara, 602 p.

FEMA (2005). *Federal Guidelines for Dam Safety—Earthquake Analyses and Design of Dams*.

ICOLD (2016). *Selecting Seismic Parameters for Large Dams-Guidelines*. ICOLD, Bulletin 148.

ICOLD (1989). *Selecting Parameters for Large Dams-Guidelines and Recommendations*. ICOLD Committee on Seismic Aspects of Large Dams, Bulletin 72.

Kramer, SL (1996). *Geotechnical Earthquake Engineering:* Prentice-Hall, Upper Saddle River, NJ 653 p.

Krinitzsky, E. (2005). Discussion on Problems in the Application of the SSHAC Probability Method for Assessing Earthquake Hazards at Swiss nuclear power plants. Eng. Geol. 78 285-307; Eng.Geo. 82, 62-68.

MTA (2013) Scale 1/1.125.000 Turkey Live Fault Map. General Directorate of Mineral Research and Exploration. Special publications series, Ankara, Turkey

Tosun, H (2002). *Earthquake-Resistant Design for Embankment Dams*: Publication of General Directorate of State Hydraulic Works, Ankara. 208 pp. (in Turkish).

Tosun, H and Tosun,V (2017) Total risk and seismic hazard analyses of large dams in northwest Anatolia, Turkey. 85th Annual Meeting of International Commission on Large Dams, July 3-7, Prague.

Tosun, H. (2018) Safety assessment for large reservoir constructed for domestic water near urban areas and a case study. 86th Annual Meeting of International Commission on Large Dams, July 1-7, Vienna.

5th International Symposium on Dam Safety

October 27-31, 2018

SAFETY ASSESSMENT FOR EXISTING LARGE RESERVOIRS CONSTRUCTED IN ISTANBUL METROPOLITAN AREA

Hasan TOSUN [1], Tefik Baran ÖNDER[2]

ABSTRACT

Earthquake safety is one of important task of total safety assessment for the structures, at where are constructed on the seismically active regions in the world. There are some metropolitan provinces, which are under threatening of earthquakes. One of them is Istanbul Metropolitan Area with fifteen million people. Major earthquakes with the potential of threatening life and property occur frequently here. There are seven large dams for providing domestic water for Istanbul province. These are namely Alibey, Büyükçekmece, Darlık, Elmalı I, Elmalı II, Ömerli and Sazlıdere dams. The seismic hazard analyses have indicated that peak ground acceleration changes within a wide range (0.176 g and 0.374 g) for the six dam sites of this area. For each dam pseudo-static and numerical analyses were performed to relieve excessive deformations such as slumping, settlement, cracking and planar or rotational slope failures for embankment dams and overall stability of the structure for concrete dams.

Key words: dam, domestic water, earthquake safety, seismic hazard, total risk

INTRODUCTION

Reservoir behind a dam poses potential energy which creates a hazard to life and property located downstream. Therefore, dams must be properly planned, designed, constructed and operated to safely fulfill their intended function. To attain this goal, the organizations (state or private) have to use a system of checks and reviews within their constitution supplemented by independent outside consultation. The contemporary engineers believe the fact that safety assessment of existing dams is a most significant concept for large reservoir, especially constructed in or near urban area.

Increasing demand for water results to construct large reservoirs in or near urban areas. Same situation can be resulted by extending settlement area around reservoirs, which were constructed many years ago. Therefore, dams with large reservoirs, which are located in or near urban areas, have a high-risk potential for downstream life and property. In other words, a problem on public safety can raise up for people and live life on downstream for urban areas.

The seismic hazard rating of dam site and the risk rating of the dam and appurtenant structures are two important factors acting on total risk for dam structures. The seismic hazard of a dam site can be based on the peak ground acceleration. This value derived from the defined design earthquake produces the main seismic loads. For a preliminary study, the existing map of seismic zones can be used to estimate the seismic hazard of a dam site. The risk rating of the dam should be based on the capacity of the reservoir, the height of the dam, the evacuation requirements, and the potential

[1] Professor, Department of Civil Engineering, Osmangazi University University, Eskisehir, Turkey, e-posta: hasantosun26@gmail.com
[2] Civil Engineeer, Dam Safety Association, Ankara, Turke,

downstream damages. In general, the seismic and risk ratings are evaluated separately for ICOLD method. However, BUREAU method combined these two factors to define the total risk factor for dam structure.

In the study six existing dams, which located within Istanbul Metropolitan Area, were considered to assess their toral risk for life and property in downstream. These, namely Alibey, Buyukcekmece, Darlık Elmali II, Omerli and Sazlidere dams in Marmara basin, have completed between 1955 and 1996. These dams are totally utilized for providing domestic water of Istanbul Metropolitan Area. In 2017, the water demand was totally 964 million cubic meter per year for this area. The 97 percent of this demand was provided by surface water, which are impounded in the reservoirs of dams mentioned above while others provided by groundwater resources. Total storage capacity is about 868 million cubic meter for Istanbul Metropolitan Area. The sixty percent of this capacity is provided by the reservoir of the dams considered this study. This paper deals with an evaluation of seismic hazard and local site effects for six large dams, which have a height from river bed between 10.1 m and 52.0 m in the Istanbul Metropolitan Area (Table 1).

Table 1. Physical properties of dams considered for this study.

Dam		River	Aim (*)	Height from river bed (m)	Completed Year	Type (**)	Volume of embankment (hm^3)	Volume of reservoir (hm^3)
No	Name							
1	Alibey	Alibey	D+F	28.0	1983	EF	1.927	65.00
2	B.cekmece	Karasu-Sarısu	D	10.1	1987	EF	1.718	172.45
3	Darlık	Yeşildere	D		1988	RF	1.600	107.00
4	Elmalı II	Göksu	D	42.5	1955	CG	0.103	10.31
5	Omerli	Riva	D	52.0	1972	EF	1.650	436.53
6	Sazlidere	Sazlıdere	D	23.0	1996	RF	1.780	131.50

(*) D = Domestic water, F = Flood Control,
(**) EF =Earthfill, RF = Rockfill CG= Concrete Gravity

METHODS OF ANALYSIS

For this study seismic analyses have been carried out by deterministic and probabilistic methods. The deterministic seismic hazard analysis (DSHA) defines a seismic scenario that includes a four-step process. It is a very simple procedure and gives rational solutions for large dams because it provides a straightforward framework for the evaluation of the worst ground motions. The probabilistic seismic hazard analysis (PSHA), which is widely used for dam sites, considers uncertainties in size, location and recurrence rate of earthquakes. For the seismic hazard analysis of each dam site, all possible seismic sources were identified and their potential was evaluated in detail, as based on the guidelines given by Fraser and Howard (2002) and the unified seismic hazard modeling for Mediterranean region introduced by Jiminez (2001). Four separate predictive relationships for horizontal peak ground acceleration were used for this study (Campbell, 1981; Boore et al, 1993; Boore et al, 1997; Gülkan and Kalkan, 2002).

Some institutions have defined some earthquake levels for dynamic analysis of dam structures. In this study, earthquake definitions given by FEMA were considered for seismic hazard analyses (FEMA, 2005). The Operating Basis Earthquake (OBE), which was defined by means of the probabilistic methods mentioned above, is the earthquake that produces the ground motions at the site that can reasonably be expected to occur within the service life of the project. MDE is normally characterized by a level of motion equal to that expected at the dam site from the occurrence of deterministically evaluated MCE. Safety Evaluation Earthquake (SEE) is the level of shaking for which damage can be accepted but for which there should be no uncontrolled release of water from the reservoir. Author states that most of large dams in Turkey were analyzed by using these definitions in past. ICOLD

(2016) also some earthquake definitions for dynamic analysis of dams. Author mentions these definitions more detail on their research (Bureau, 2003).

Some methods are used to quantify the total risk factor of a dam. One of them considers the seismic hazard of the dam site and the risk rating of the structure separately (Tosun and Tosun, 2017). According to this method, the seismic hazard of the dam site regardless of type of dam, can be classified into four groups from low to extreme. This is a quick way for rating the seismic hazard. The hazard class of a dam site obtained from this method provides a preliminary indication of seismic evaluation requirements. Other one is Bureau method, which considers various risk factors and weighting points to quantify the total risk factor (TRF) of any dam /ICOLD, 1989). In this methods the TRF depends on the dam type, age, size, downstream risk and vulnerability, which depends on the seismic hazard of the site.

For all analyses throughout this study, the peak ground acceleration was determined by two methods discussed above. Both results obtained by DSHA and PSHA were submitted in this study. All procedures of seismic study mentioned above can be executed by the DAMHA program that is working on the basis of geographic information system (GIS). For total risk of dams, two different methods mentioned above are used for all dams considered for this study.

ANALYSES AND RESULTS

A detailed study was performed to identify all possible seismic sources for the seismic hazard analyses of the dam sites, as based on the macro seismo-tectonic model of Turkey. The National Disaster Organization and other Institutes prepared the map for general use. But it was modified by the author and his co-workers to use for dam projects at the Earthquake Research Center in Osmangazi University. Local geological features and seismic history were also taken into account to quantify the rate of seismic activity in dam sites. As a result of detailed evaluation, total area covering all basins was separated into four seismic zones. These seismic zones and historical earthquakes are given in Figure 1. These zones including faults and earthquakes occurred in the basin along last 100 years. The number of earthquakes having a magnitude on the basis of surface wave (Ms), which is greater than 4.0, is 1455. The numbers of earthquakes with Ms that are greater than 6.0 are 34 for dam sites .There are two earthquakes having a magnitude greater than 7.0 in the relating area.

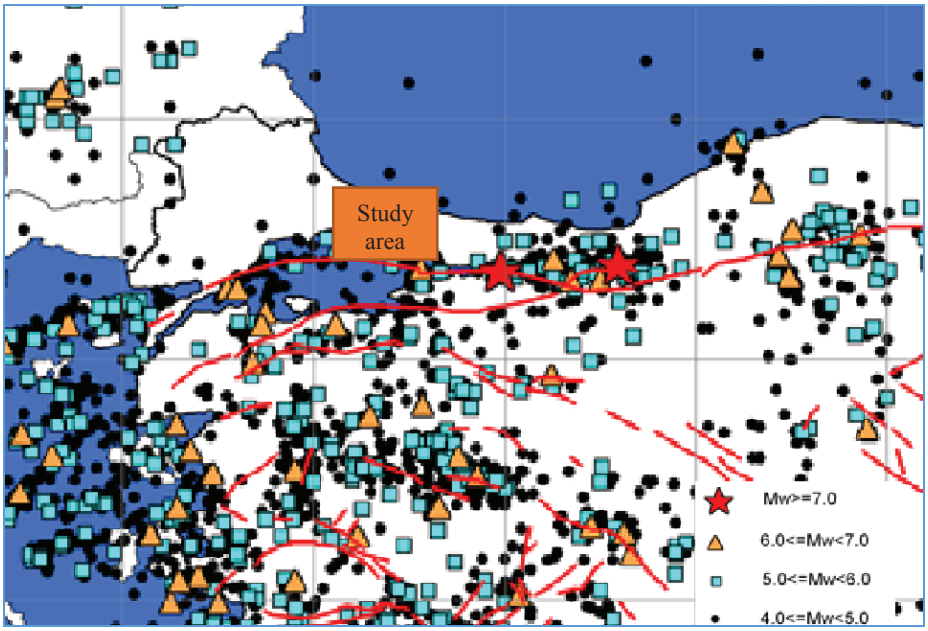

Figure 1. Energy sources and earthquakes around the study area.

ICOLD defined the near-field motion, which is ground motion recorded in the vicinity of a fault [8]. All existing dams considered for this study are not under near source effect (MTA, 2013). Author established limits of near-field motion for the investigation area. According to this model, the maximum moment magnitude of the earthquakes ranges from 7.5 to 7.7 and the minimal distance to fault segment is between 14.8 and 41.2 km for six dams (Table 2). The Büyükçekmece dam, is closest dam with minimal distance to fault segment is 14.8 km. The Darlık dam is most far away from fault segment (41.2 km).

Table 2. The results of deterministic seismic hazard analyses

Dam No	Dam	Deterministic Method *				Probabilistic Method **		
		M_{max}	R_{min} (km)	Mean PGA + 50 %	Mean PGA + 84 %	OBE	MDE	SEE
1	Alibey	7.5	25.1	0.191	0.313	0.229	0.298	0.413
2	B.çekmece	7.5	14.8	0.281	0.468	0.286	0.393	0.558
3	Darlık	7.7	41.2	0.141	0.230	0.146	0.195	0.268
4	Elmalı II	7.5	27.3	0.178	0.292	0.210	0.285	0.394
5	Ömerli	7.7	34.6	0.164	0.267	0.178	0.238	0.329
6	Sazlıdere	7.5	23.0	0.205	0.335	0.225	0.306	0.428

(*) M_{maks} = Maximum earthquake magnitude in M_w
R_{min} = Minimum distance to fault segment
Mean PGA + 50% = Mean Peak Ground Acceleration at the 50th percentile
Mean PGA + 84% = Mean Peak Ground Acceleration at the 84th percentile
(**) OBE = Operational Based Earthquake
MDE = Maximum Design Earthquake
SEE = Safety Evaluation Earthquake

The results of the DSHA and PSHA are given in table 2. In this table, M_{max} is the maximum earthquake magnitude in M_w and R_{min} is the minimum distance to fault segment. Mean PGA + 50% and Mean PGA + 84% are mean values for peak ground acceleration at the 50th and 84th percentile, respectively. This table also includes the levels of peak ground acceleration for defined earthquakes (OBE, MDE and SEE) as a result of PSHA.

Table 3. Total risk of dams considered for this study.

No	Dam	Hazard Analysis		Total Risk (ICOLD,1989)			Total Risk (Bureau, 2003)		
		Class	Hazard Ratio	Risk factor	Risk class	Risk ratio	Risk factor	Risk class	Risk ratio
1	Alibey	III	High	30	III	High	223.3	III	High
2	B.çekmece	III	High	22	III	High	150.8	III	High
3	Darlık	II	Moderate	32	IV	Very high	160.3	III	High
4	Elmalı II	III	High	32	IV	Very high	180.2	III	High
5	Ömerli	II	Moderate	36	IV	Very high	217.0	III	High
6	Sazlıdere	III	High	32	IV	Very high	158.4	III	High

The deterministic analyses indicate that peak ground acceleration (PGA) changes within a wide range. The PGA values ranges from 0.141g to 0.281g for the mean Peak Ground Acceleration at the 50th percentile and from 0.230g to 0.468g for the mean Peak Ground Acceleration at the 84th percentile given in table 2. The results of PSHA also change within a wide range. The values of PGA for OBE and MDE range from 0.146g to 0.286g and from 0.195g to 0.393g, respectively.

The total risk analyses were performed for six dams throughout this study. The results with total risk of each dam are given table 3. All dams with exception of Darlık and Omerli dams are identified in class of III with high hazard rating. Two dam sites have moderate hazard rating and are identified as hazard class of II. For these dams, the distance from dam site to active faults, which are given on updated seismic maps, ranges from 14.8 km to 41.2 km. The hazard classes were defined from moderate to high hazard ratios because of being all large dams not under the influence of the near-field motion.

Throughout this study, two methods have been considered to quantify the total risk for dam structures. In DSI guidelines, total risk factor depends to reservoir capacity, height, evacuation requirement and potential hazard (DSİ, 2012). According to DSI Guidelines all dams are categorized in II and III risk classes with moderate and high risk rating. Following Bureau's method, all large dams are classified in risk class III, a high-risk rating. In Bureau method, the values of the TRF range from 150.8 to 223.8. This means that there is no dam having a risk classes of I and II for all dams considered for this study. Author thinks that the solution obtained from Bureau method is more rational than that of the DSI guidelines.

Table 4 shows the summary of DSI seismic guidelines for dynamic analyses. According to these updated DSI guidelines, The PGA values should be taken at the 50th percentile for two dams while others at the 84th percentile for DSHA. The values of PGA should be selected as MDE for two dams and SEE with Tr of 975 years for others when considered the PSHA.

Table 4. Selection of Design Earthquake as based on risk classification [13]

Hazard Analysis		Deterministic Method	Probabilistic Method
Class	Hazard Ratio		
I	Low	50 %	T_R = 224 years $^{(*)}$
II	Moderate	50 %	T_R = 475 years
III	High	84 %	T_R = 975 years
IV	Very high	84 %	T_R = 2475 years

$^{(*)}$ Tr = Return time

DISCUSSIONS

There are fifteen existing large dams and four regulators located in Istanbul vicinity for providing domestic water. Six of them are located on the Istanbul Metropolitan Area. The earthquake safety and total risk of these dams are evaluated more detail as given below.

Alibey Dam is a earthfill dam 28.0-m high with a total embankment volume of 1 927 000 m^3. It is located on Alibey river in Marmara basin. Its construction was finished in 1983. When the reservoir is at operation stage with maximum water level, the facility approximately will impound 65.0 hm^3 of water with a reservoir surface area of 4.75 km^2. It is mainly designed to provide domestic water with annual capacity of 33.0 hm^3. The side slopes of main embankment is 2.0H:1V for both upstream and downstream (H=horizontal and V=vertical) (Fig. 2). On the section there is a central impervious zone, which is composed of impervious clay and a transition section of sand, gravel and small-sized crushed rock was designed to protect impervious zone. The shell fill in downstream and upstream parts is composed of semi-pervious clayey material. Vertical sand drains were used in the soft alluvium on

river bed. The seismic hazard analyses performed throughout this study indicates that this dam is one of more critical dam within the Istanbul Metropolitan Area. It will be subjected to a peak ground acceleration of 0.191g by an earthquake of 7.5 magnitude according to DSHA. As based on PSH the values of peak ground acceleration for OBE and MDE are 0.229g and 0.298g, respectively. It is 25.1 km far away from an active fault given in new seismo-tectonic map of Turkey adopted in 2013. Its TRF value is 223.3 and it is identified as risk class of III. The 35-years old embankment is in excellent condition. However, its seismic upgrade should be provided soon. Figure 3 shows a general view from Alibey dam.

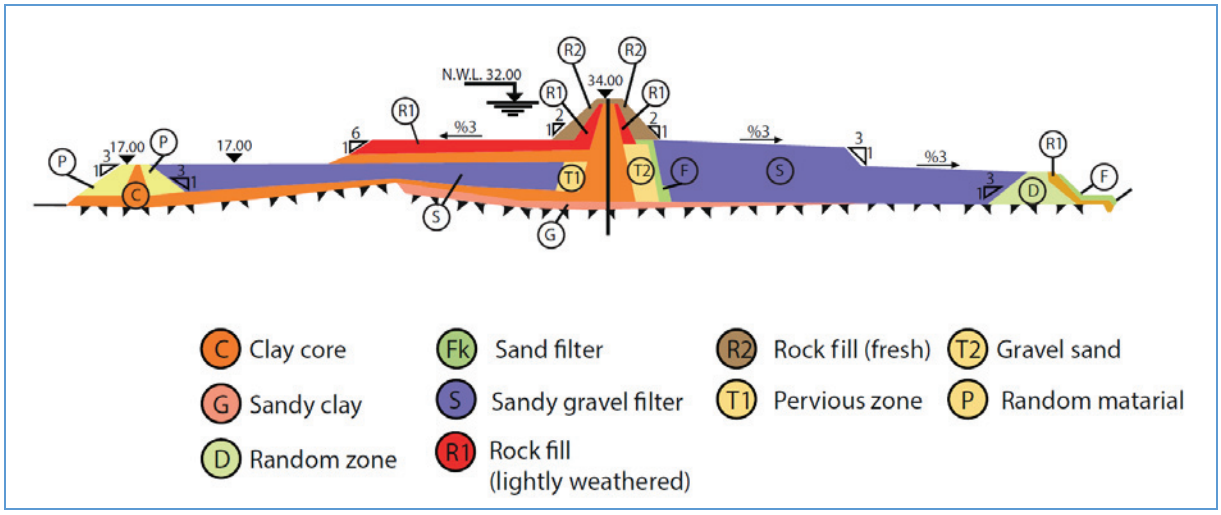

Figure 2. The maximum cross-section of embankment of Alibey dam (DSI, 2016).

Figure 3. A general view from Alibey dam.

Buyuk Cekmece dam is a earthfill dam on Karasu and Sarısu Rivers in the Istanbul Metropolitan Area. It has only a 10.1 m height from river bed, however its total storage capacity is relatively high. When the reservoir is at maximum capacity, the facility impounds 172.5 hm^3 of water with a reservoir surface area of 28.58 km^2. Its construction was finished in 1987. It was designed to provide domestic water with annual capacity of 82 hm^3. The crest length is 2 476 m and the side slopes of main embankment is 3.0H:1V for both upstream and downstream side (H=horizontal and V=vertical)

(Figure 4). On the section there is a central impervious core, which is composed of compacted impervious clay and a transition section of sandy and gravelly aggregates was designed between the core and semi-pervious soils. The alluvium on river bed, which is composed of different size of river bed material, was removed before beginning the construction of the main embankment. According to the deterministic seismic hazard analyses, it will be subjected to a peak ground acceleration of 0.281g by an earthquake of 7.5 magnitude. As based on PSHA the values of peak ground acceleration for OBE and MDE are 0286g and 0.393g, respectively. Its embankment is only 14.8 km far away from an active fault given in new seismo-tectonic map of Turkey adopted for 2013. Its TRF value is 150.8, and it is identified as risk class of III. This 31-year old earthfill embankment is in excellent condition, but it cannot meet current seismic design standards. Additionally, it is relatively close to the active energy source. Therefore, its seismic upgrade should be provided soon. Figure 5 indicates the location of Büyük Cekmece dam within settlement area.

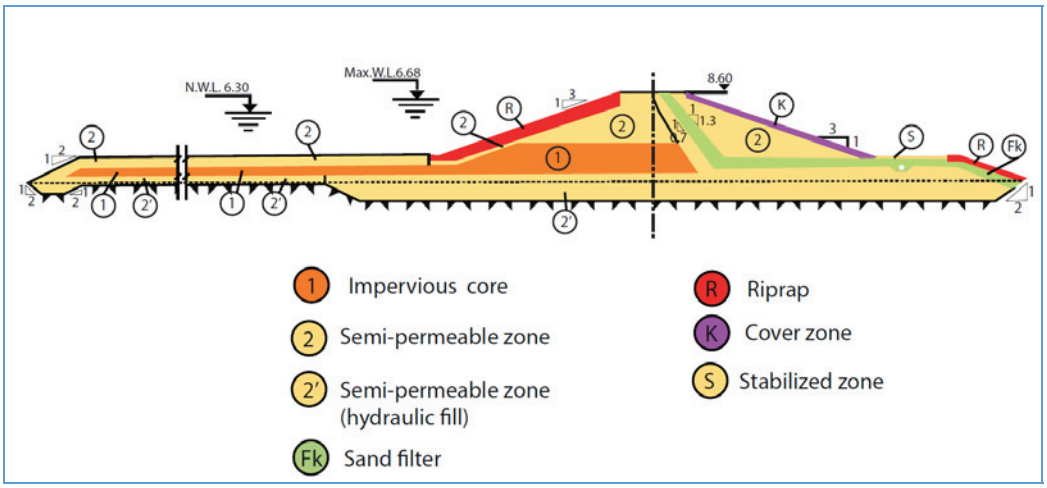

Figure 4. The maximum cross-section of embankment of Buyuk Cekmece dam (DSI, 2016).

Figure 5. General view from Buyuk Cekmece dam.

Darlik dam is a rockfill dam on Yesildere river near Sile County in the Istanbul Metropolitan Area. It has a 70 m height from foundation. Its construction was finished in 1988. It was designed to provide domestic water with an active volume of 107 hm^3. On the section there is a central impervious core,

which is composed of compacted impervious clay and a transition section of sandy-gravelly aggregates and rock crush zone was designed between the core and rock materials. The alluvium on clay core was removed before beginning the construction of the main embankment. According to the seismic hazard analyses of this study, it will be subjected to a peak ground acceleration of 0.141g by an earthquake of 7.7 magnitude and its embankment is 41.2 km far away from an active fault given in the updated seismo-tectonic map of Turkey. PSHA indicates that the values of peak ground acceleration for OBE and MDE are 0.146g and 0.195g, respectively. Its TRF value is 160.3 and it is identified as risk class of III. This 30-year old earthfill embankment is in excellent condition.

Elmalı-II dam is unique rigid type structure of the basin with volume of 0.10 hm^3 of concrete gravity type (Figure 4). It is located on the Goksu river in the Istanbul Metropolitan Area. . Its construction was finished in 1955. Its height from river bed is 42.5 m. When the reservoir is at operation stage with maximum water level, the facility approximately will impound 10.31 hm^3 of water with a reservoir surface area of 42 km^2. It is mainly designed to provide domestic water for Istanbul city. The alluvium on river bed was removed before beginning the construction of the main embankment. The seismic hazard analyses performed throughout this study indicates that this dam is one of safe dams within the Marmara basin. It will be subjected to a peak ground acceleration of 0.178g by an earthquake of 7.5 magnitude and it is 27.3 km far away from an active fault. PSHA indicates that the values of peak ground acceleration for OBE and MDE are 0.210g and 0.285g, respectively. Its TRF value is 158.4 and it is identified as risk class of III. Elmalı-II dam, which is oldest one of the dams considered for this study (63-years old concrete gravity dam) is in excellent condition. However, its seismic upgrade should be provided soon. Figure 6 shows a general view from Elmalı-II dam.

Figure 6. A general view from Elmalı-II dam.

Omerli dam is one of the main structures when considered the storage capacity. It is located on the Riva river in Marmara basin. Its construction was finished in 1972. Its height from river bed is 52.0 m and its type is earthfill. When the reservoir is at maximum capacity, the facility impounds 436.53 hm^3 of water with a reservoir surface area of 23.92 km^2. It was designed to provide domestic water for Istanbul city. The main embankment consists of crushed rock and transition zone to concrete face. The upstream and downstream fills are large-sized crushed rocks at which the most durable and high strengthened ones are located on the outer part of the shell. The crest width is 10 m and the side slopes of main embankment is 2.5H:1V for upstream and 3.0H:1V for downstream (H=horizontal and

V=vertical) (Figure 7). According to the seismic hazard analyses of this study, it will be subjected to a peak ground acceleration of 0.164g by an earthquake of 7.7 magnitude. PSHA indicates that the values of peak ground acceleration for OBE and MDE are 0.178g and 0.238g, respectively. Its TRF value is 217.0 and it is identified as risk class of III. Omerli dam, which is largest capacity of the dams considered for this study. It is a key structure for water safety of Istanbul Metropolitan Area. This 45-year old earthfill embankment is in excellent condition, but it cannot meet current seismic design standards. its seismic upgrade should be provided soon. Figure 8 introduces a general view from Omerli dam.

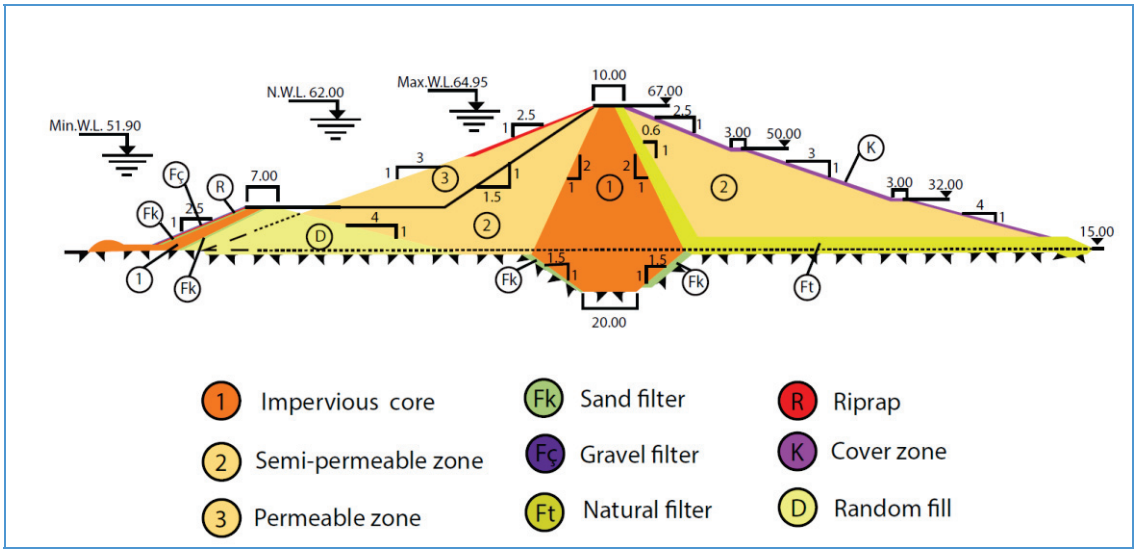

Figure 7.The maximum cross-section of embankment of Omerli dam (DSI, 2016).

Figure 8. General view from Buyuk Cekmece dam.

Sazlıdere dam is a rockfill dam on Sazlıdere River near Arnavutköy County. It has a 23.0 m height from river bed. When the reservoir is at maximum capacity, the facility impounds 131.50 hm^3 of

water with a reservoir surface area of 11.77 km^2. Its construction was finished in 1996. It was designed to provide domestic water with annual capacity of 55.0 hm^3. The crest length is 435 m and the side slopes of main embankment is 2.25H:1V for upstream and 2.0H:1V for downstream (H=horizontal and V=vertical) (Figure 9). On the section there is a central impervious core, which is composed of compacted impervious clay and a transition section of sandy and gravelly aggregates was designed between the core and pervious coarse grained soils. The alluvium under all embankment, which is composed of different size of river bed material, was removed before beginning the construction. According to the seismic hazard analyses of this study, it will be subjected to a peak ground acceleration of 0.335 g by an earthquake of 7.5 magnitude and its embankment is 23.0 km far away from an active fault given in the updated seismo-tectonic map of Turkey. PSHA indicates that the values of peak ground acceleration for OBE and MDE are 0.225g and 0.306g, respectively. Its TRF value is 158.4, and it is identified as risk class of III. This 22-year old rockfill embankment is in excellent condition.

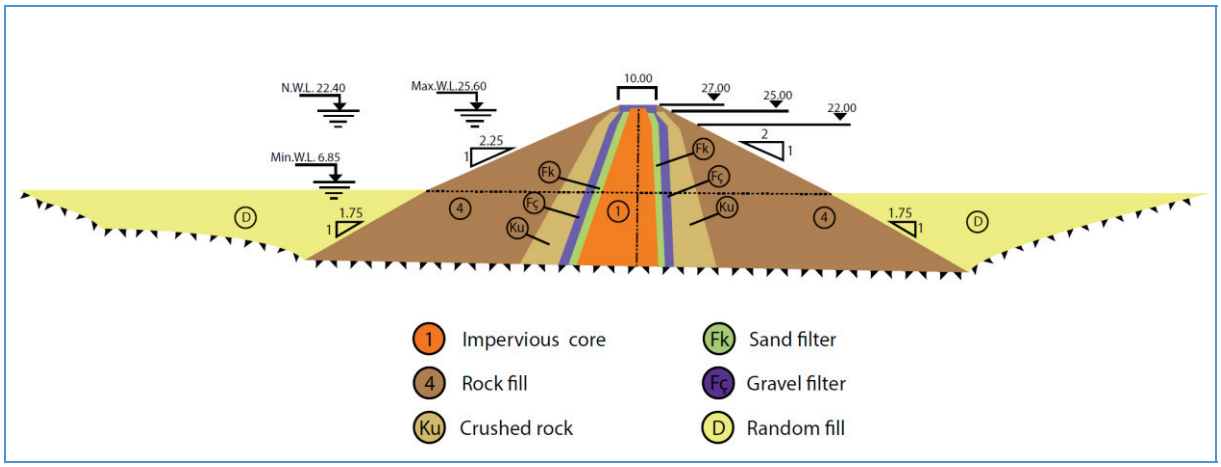

Figure 9.The maximum cross-section of embankment of Sazlıdere dam (DSI, 2016).

CONCLUSIONS

In this study, the seismic hazard rating of the dam site and the risk rating of the complete structures were determined and possible modes of failure were estimated for the existing large dams within the Istanbul Metropolitan Area. The study identified that all dams located in Istanbul Metropolitan area are not under near source effect. As a result of this study, 66.7 percent of dams has extremely high of risk class while others are classified in high risk class. Therefore, detail seismic hazard analyses are needed for these structures as based on the updated seismic data and design code under circumstances of the study of a national safety program for dam. In other words, these dams must be re-analyzed by selecting appropriate seismic parameters. All dams are critical structures for public safety because of being within settlement area. However, Omerli and Buyuk Cekmece dam are also more critical water storage structures when compared with others considered in this study.

REFERENCES

Boore, DM, Joyner, WB. and Fumal, TE (1993). *Estimation of response spectra and peak accelerations from Western North American earthquakes*. An interim report. Open file report 93-509.U.S.G.S.

Boore, DM., Joyner, WB. and Fumal, TE (1997*). Equation for Estimating Horizontal Response Spectra and Peak Acceleration from Western North American Earthquakes.* A Summary of recent Work. Sesimological Reseach Letters, V.68, N.1, January /February, 128-153.

Bureau, GJ (2003). *Dams and Appurtenant Facilities in Earthquake Engineering Handbook edited by Chenh, W.F and Scawthorn,C.* CRS press, Bora Raton 26.1-26.47.

Campbell, KW (1981). N*ear-Source Attenuation of Peak Horizontal Acceleration*: Bulletin Seism. Soc. Am., V.71, N.6, 2039-2070.

DSİ (2012). *Selection of Seismic Parameters for Dam Design.* State Hydraulic Works, Ankara, 29 p (in Turkish).

DSİ (2016). *Dams of Turkey*. TR-COLD, Ankara, 602 p.

FEMA (2005). *Federal Guidelines for Dam Safety—Earthquake Analyses and Design of Dams*.

Fraser, WA and Howard, JK (2002). *Guidelines for Use of the Consequence-Hazard matrix and Selection of Ground Motion Parameters:* Technical Publication, Department of Water Resources, Division of Safety of Dams.

Gülkan, P and Kalkan,E (2002). *Attenuation modeling of recent earthquakes in Turkey.* Journal of Seismology, 6(3), 397-409.

ICOLD (1989). *Selecting Parameters for Large Dams-Guidelines and Recommendations*. ICOLD Committee on Seismic Aspects of Large Dams, Bulletin 72.

ICOLD (2016). *Selecting Seismic Parameters for Large Dams-Guidelines*. ICOLD, Bulletin 148.

Jiminez, MJ, Giardini, D and Grünthal, G (2001). *Unified Seismic Hazard Modelling throughout the Mediterranean Region.* Bolettino di Geofisica Teorica ed Applicata, Vol.42, N.1-2, Mar-Jun., 3-18.

MTA (2013) Scale 1/1.125.000 Turkey Live Fault Map. General Directorate of Mineral Research and Exploration. Special publications series, Ankara, Turkey

Tosun, H and Tosun,V (2017) Total risk and seismic hazard analyses of large dams in northwest Anatolia, Turkey. 85th Annual Meeting of International Commission on Large Dams, July 3-7, Prague.

5th International Symposium on Dam Safety

October 27-31, 2018

DEVELOPMENT OF SOFTWARE TO PREDICT THE MODAL PARAMETERS AND STRUCTURAL BEHAVIOR OF SINGLE CURVED ARCH DAMS

Ebru KALKAN [1], Ahmet Can ALTUNIŞIK [2], Hasan Basri BAŞAĞA [3], Barış SEVİM [4]

ABSTRACT

The dams are among the most important building elements and fields of study of Civil Engineering when considering the reasons such as the duties they undertake, the difficulties in construction stages and high cost. Analyzes carried out by expert engineers are also taking considerable time due to the difficult and challenging of parts of modeling, analysis and interpretation. In the scope of this paper, general engineering software has been developed in order to facilitate the analysis of the dam which takes considerable time due to the reasons explained above and to have a quick knowledge about the structural behavior. Modal analysis, static analysis and dynamic analysis results can be obtained by considering the soil-structure interaction for single curved arch dams within the scope of the developed software. As the initial model, a single curved Type-1 arch dam selected that is one of five types of arch dam, presented in the "Arch Dams Symposium" in 1968. Detailed studies have been carried out on the reference type 1-arch dam, built on a certain scale in the laboratory environment and verified by environmental vibration tests, taking into account the different scales (1, 10, 20, 30, ..., 500) through the finite element model created by the ANSYS program. In the analyses, dam height, material property, mass, soil class, seismic load reduction factor, effective ground acceleration coefficient, soil-structure interaction etc. are used as variable parameters. In the end of analyses, static and modal analysis results (frequency, period, displacement, strain and deformation) with the most appropriate equations obtained by the regression analysis, dynamic analysis results (displacement, stress and deformation) are expressed by the equations of field. Software interface has been developed using the EXCEL program in order to combine the large number of formulas, equations and results obtained.

Keywords: Arch dam, modal parameters, software, structural behavior, Type-1 arch dam.

INTRODUCTION

With the development of the technology age and the concept of time being so important, there is an increasing trend towards software operations to ensure ease of process. Peng and Law (2002) introduced a software framework, which will serve as the core for collaborative structural analysis

[1] Dr., Department of Civil Engineering, Karadeniz Technical University, Trabzon, Turkey, e-posta: ebrukalkan@ktu.edu.tr
[2] Professor, Department of Civil Engineering, Karadeniz Technical University, Trabzon, Turkey, e-posta: ahmetcan8284@hotmail.com
[3] Asst. Prof. Dr., Department of Civil Engineering, Karadeniz Technical University, Trabzon, Turkey, e-posta: hasanbb69@hotmail.com
[4] Assoc. Prof. Dr, Department of Civil Engineering, Yildiz Technical University, Istanbul, Turkey, e-posta: basevim@yildiz.edu.tr

program development. Özdemir (2004) analyzed the effects of main and interdependence of data on linear regression and knowledge transfer by aiming to mathematically and structurally define reciprocal dependency structure between two periodic-stochastic hydrological processes. Mittrup and Hartmann (2005) studied on software development for structural control of dams. For this purpose, it is selected Ennepe Dam that gravity dam. The correctness of the software is proved by the tests conducted at the Ennepe Dam and the usage of the application has been recommended. Beşiktaş (2010) used the data of some flow observation stations in the Eastern Black Sea Region to estimate flow rates of previously unmeasured points by using the regression analysis method the flow continuity curves. Şahin (2009) presented a new algorithm developed to minimize the torsional effects in asymmetric tall buildings. Qiujing et al. (2012) aimed to estimated horizontal displacements, stress and safety of high arch dams during construct and first water storage. Parameters are selected as water level, change of temperature, time, elasticity modulus of rock and concrete. It is aimed to develop formula for obtained dynamic characteristic of historical arch bridges by Bayraktar et al. (2014). Within the scope of the Sümerkan (2014) thesis, he developed a formula based on environmental vibration data and finite element analysis to predict the natural frequencies of post-tensioned balanced console bridges. Serhatoğlu (2015) examined the dynamic characteristics and performances of historical minarets. For this purpose, in the scope of the thesis, experimental works and finite element analyses are carried out on 15 historical minarets in Bursa. Within the thesis of Atmaca (2016), software named structGIS is developed in order to complete the earthquake inventory of the existing building stock, which is one of the important stages of earthquake damage estimation and loss reduction studies. Many studies conducted on the subject show that the software and scaling studies are getting more and more important (Chan et al. 2010, Gu and Özçelik 2011, Xiang et al. 2011, Cheng 2012, Yılmaz and Şahin 2013, Altunışık et al. 2018a, 2018b, 2018c, 2018d).

Software is being developed and continuously updated to facilitate the works done in many areas of engineering and to provide save time. It is seen that the need for software is increasing day by day when the researches done are examined. Within the scope of study, it is aimed to obtain the results of the structural behavior of arch dams under dynamic analysis depending on the desired parameters

SCOPE AND USAGE AREA OF SCALING

Scaling is a work that can be done in every area, by shrinking large elements or systems and by enlarge small elements or systems in a certain way to make it easier to work on. The main purpose of the scaling concept used in many areas is basically the same, and the main purpose is to simplify the work by making the hard and time-consuming systems smaller and simpler to test. The study areas of Civil Engineering are multi-story buildings, dams, airports etc. examining and testing such prototypes is a very expensive, time-consuming and difficult-to-control process. For this reason, it is very easy and convenient to do the desired work on the small models created by scaling the prototype. Due to the similarity between the prototype and the model, the results obtained in the small model will be interpreted so that the behavior of the prototype can be predicted.

In its broadest terms, there are two main ways to relate the model to the prototype. Similarity conditions are derived from the relevant field equations if the system has a mathematical model or by dimensional analysis if the mathematical model of the system is not valid. In dimensional analysis, all parameters and variables that affect the behavior of the system have to be known. The obtained equation is the dimensionless product of system parameters and variables. Thus, similarity conditions can be created on the basis of the generated equation.

Since there is a corresponding mathematical model for the frequency value, similarity relations are obtained with depending on the geometric, mass and material scales and the results are compared with each other. Mathematical formulas of different systems are changing. For example, the frequency formula of the simple column element whose results are known is chosen. The obtained similarity formula can be generalized and used in different systems.

By establishing a relationship between the prototype and the scaled model of the column;

$$\frac{f_{n(\text{Model})}}{f_{n(\text{prototype})}} = \frac{\sqrt{E_m}\,S}{\sqrt{E_p}} \quad \Rightarrow \quad f_{n(m)} = S\sqrt{\frac{E_m}{E_p}}\,f_{n(p)} \tag{1}$$

Eq. 1 is a similarity formula obtained for the frequency value. The general formulas expressing the scale model and prototype between the similarity relation established by using mathematical models of displacement, principal stress and principal strain, are presented in Table 1.

Table 1. Similarity formulas for displacement, principal stress and principal strain

Structural Behavior	Formül
Frequency	$f_m = S\frac{\sqrt{E_m}}{\sqrt{E_p}} f_p$
Displacement	$\delta_m = \frac{E_p}{E_m}\frac{1}{S^2}\delta_p$
Principal Stress	$\sigma_m = \frac{1}{S}\frac{\gamma_m}{\gamma_p}\sigma_p$
Principal Strain	$\varepsilon_m = \frac{1}{S}\frac{\gamma_p}{\gamma_m}\frac{E_p}{E_m}\varepsilon_p$

These formulas are formed by using a column sample. In the example, the prototype is used for the real column size and the model is called for the scaled columns. For the application of the formulas to the dam, a small scaled dam with a laboratory model are named as a prototype and the enlarged scale dams are named as model and the similarity formulas are rearranged (Table 2).

Table 2. Rearranged similarity formulas for displacement, principal stress and principal strain

Structural Behavior	Formül
Frequency	$f_m = \frac{1}{S}\frac{\sqrt{E_m}}{\sqrt{E_p}} f_p$
Displacement	$\delta_m = \frac{E_p}{E_m}\frac{\gamma_m}{\gamma_p}S^2\,\delta_p$
Principal Stress	$\sigma_m = S\frac{\gamma_m}{\gamma_p}\sigma_p$
Principal Strain	$\varepsilon_m = S\frac{\gamma_p}{\gamma_m}\frac{E_p}{E_m}\varepsilon_p$

TYPE-1 ARCH DAM

There are five types of arch dams with different geometries proposed in the symposium "Arch Dams (1968)" held in England in 1968. From this dam types, in order to study in the laboratory were selected model small-scaled Type-1 arch dam. The Type-1 arch dam has geometry that a constant radius, angle and a single curvature. The geometrical characteristics of the Type-1 arch dam are shown in Figures 1 and 2.

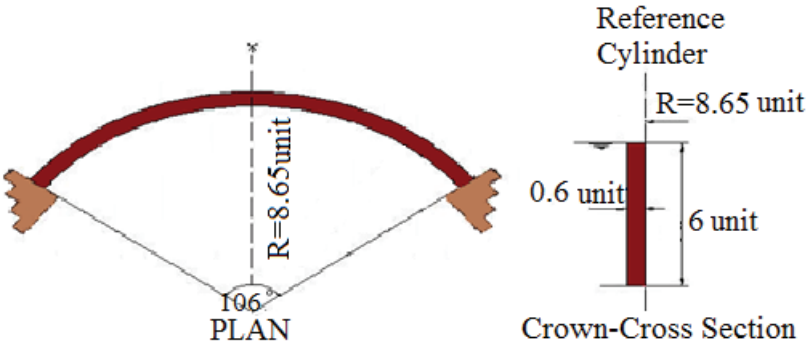

Figure 1. Geometry properties of Type-1 Arch Dam (Arch Dams, 1968)

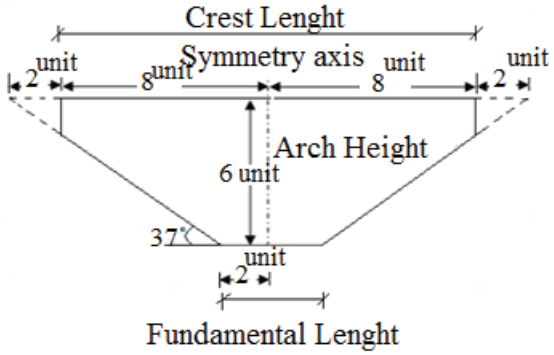

Figure 2. The cross-section of the valley where the Type-1 arch dam is located

Constitution of Laboratory Model

In the Type-1 arch dam whose dimensions are given in units, 1 unit=10cm is selected and the laboratory model is created. According to the obtained data, the dam height (H) is 60cm, the crest and the base width are 6cm and the crest length of the dam is calculated as 171.13cm in the upstream face and 160.03cm in the downstream face. In the studies conducted within the scope of the thesis, the dam model has been developed to include base and reservoir in order to realistically determine the dynamic behavior of the Type-1 arch dam (Sevim 2010). The three-dimensional soil-structure interaction model and laboratory model of the Type-1 arch dam prepared according to these properties and the dimensions of this model are given in Figure 3.

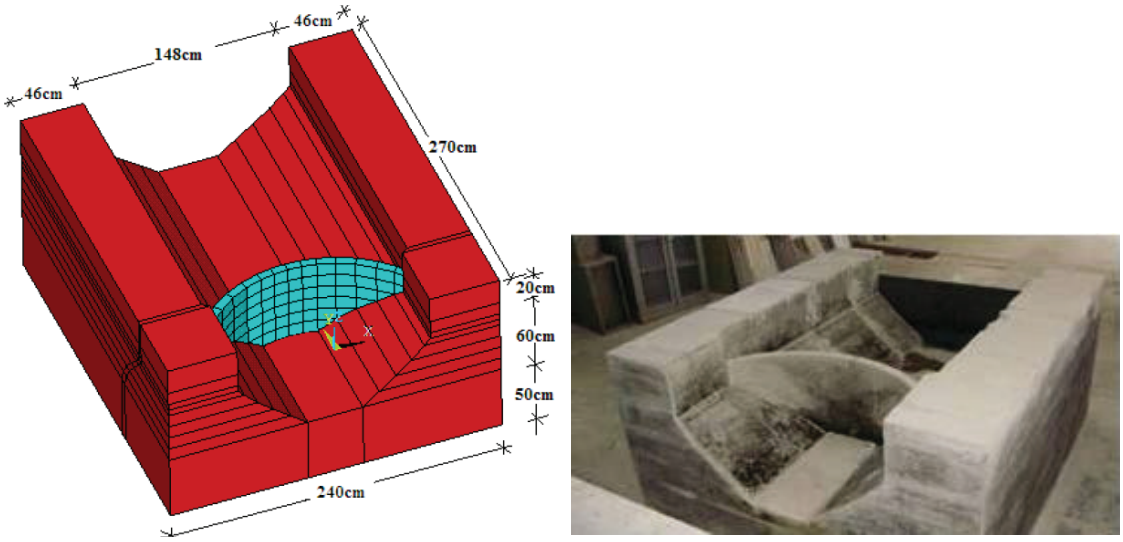

Figure 3. 3D and laboratory model of Type-1 arch dam

Modal Parameters of Laboratory Model of Type-1 Arch Dam

By using the finite element model of the Type-1 arch dam formed in the thesis study done by Sevim (2010), is purposed developing the software to predict the static, dynamic characteristics and structural characteristics of the dams. Non-destructive experimental measurements such as ambient vibration and forced vibration tests are conducted on the dam body to extract the natural frequencies. Table 3 summarizes the first nine numerically and experimentally identified natural frequencies.

Table 3. Numerical and experimental first nine natural frequencies

Mod Number	Frequency Values (Hz)		
	Finite Element Analysis	Ambient Vibration Test	Forced Vibration test
1	348.87	339.2	340
2	364.81	372.6	372
3	510.22	552.3	552
4	658.45	619.8	616
5	680.42	----	----
6	701.66	----	----
7	740.70	741.1	740
8	793.32	----	----
9	836.73	839.0	828

Results of Finite Element Model of Type-1 Arch Dam

In order to verify the results given in Table 3 and obtain the displacements with principal stresses and strain, finite element model of the Type-1 arch dam is constituted in ANSYS software (2016). It is aimed to use these results as initial and references parameters for scaling.

The analyses are carried out Soil-structure interaction conditions. Empty reservoir condition is taken into consideration. For the next studies, it is aim to investigate the reservoir and dynamic load effects on structural response. Modal analyses are done and first ten natural frequencies, period values and mode shapes are obtained. Table 4 presents the related results. In the finite element analysis, the material properties are selected as E=150000MPa for dam body and foundation according to the updated finite element results by experimental measurement.

Table 4. Dynamic characteristics of Type-1 arch dam for soil-structure interaction

Mod Number	Finite Element Analysis Results		
	Frequency (Hz)	Period (s)	Mod Shape
1	344.58706	0.002020	Anti-Symmetrical Mode
2	361.20676	0.002768	Symmetrical Mode
3	505.56430	0.001978	Symmetrical Mode
4	652.08387	0.001534	Anti-Symmetrical Mode
5	674.36188	0.001483	Vertical Mode
6	860.11709	0.001163	Vertical Mode
7	890.79624	0.001125	Symmetrical Mode
8	917.23440	0.001090	Vertical Mode
9	954.16860	0.001048	Symmetrical mode
10	958.79734	0.001043	Symmetrical mode

Static analyses of the Type-1 arch dam are carried out under its own weight considering empty reservoir water and soil-structure interaction. Displacements, principal stresses and principal strains are calculated at the all nodal points of upstream and downstream faces (Figure 4) of dam body. A

total of 346 nodal points are located on the upstream and downstream faces of dam body. 10 critical nodal points are selected to display the changes of displacements and internal forces.

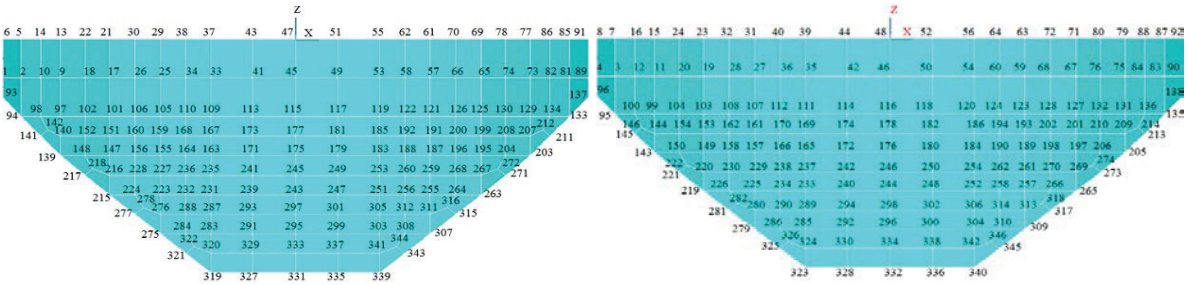

a) Upstream Surface b) Downstream Surface

Figure 4. Nodal points numbers of upstream and downstream surface of Type-1 arch dam

Determination of Real Arch Dam Model Results

To investigate the real arch dam response using scaling laws and similarity requirements with related formulas, four different arch dams (Model-1, Model-2, Model-3 and Model-4) are selected as an example. Table 5 present the detail information such as scaling factors, arch heights, arch interior radius and thickness with modulus of elasticity considered in the analyses to reflect the real arch dam models (Model-1, Model-2, Model-3 and Model-4).

Table 5. Dynamic characteristics of Type-1 arch dam for soil-structure interaction

Type-1 Arch Dam	Scale	Arch Height (m)	Arch Interior Radius (m)	Crest and Fundamental Thickness (m)	Modulus of Elasticity (MPa)
Prototype	1	0.60	0.8650	0.06	15000
Model-1	335	201	289.78	20.1	34000
Model-2	400	240	346.00	24.0	34000
Model-3	416.67	250	360.42	25.0	34000
Model-4	450	270	389.25	27.0	34000

Considering frequency formula in Table 2 and the frequency values of prototype Type-1 arch dam given in Table 4 including soil-structure interaction, the first natural frequencies of Model-1 and Model-2 are calculated;

$$\left.\begin{aligned} f_{m_1} &= \frac{1}{S}\frac{\sqrt{E_{m_1}}}{\sqrt{E_p}} f_p \\ f_{m_1} &= \frac{1}{335}\frac{\sqrt{34000}}{\sqrt{15000}} 344.58706 = 1.548611\,\text{Hz} \end{aligned}\right\} \quad (2)$$

$$\left.\begin{aligned} f_{m_2} &= \frac{1}{S}\frac{\sqrt{E_{m_2}}}{\sqrt{E_p}} f_p \\ f_{m_2} &= \frac{1}{400}\frac{\sqrt{34000}}{\sqrt{15000}} 344.58706 = 1.2969786\,\text{Hz} \end{aligned}\right\} \quad (3)$$

Table 6 presents the first ten natural frequencies of scaled arch dam models (Model-1, Model-2, Model-3 and Model-4) using finite element analysis and related formula soil-structure interaction. It can be seen from these table that there is a good agreement between finite element results and related formula (for frequencies, displacements, principal stresses and principal strains) of all models.

Table 6. The first ten natural frequencies of scaled arch dam models using FE analyses and formula for soil-structure interaction

Mod Numbers	Frequency (Hz)							
	Model-1		Model-2		Model-3		Model-4	
	ANSYS	Formula	ANSYS	Formula	ANSYS	Formula	ANSYS	Formula
1	1.5486	1.5486311	1.297	1.2969786	1.2451	1.2450895	1.1529	1.1528698
2	1.6233	1.6233228	1.3595	1.3595329	1.3051	1.3051411	1.2085	1.2084736
3	2.2721	2.2720894	1.9029	1.9028749	1.8267	1.8267453	1.6914	1.6914444
4	2.9306	2.9305726	2.4544	2.4543545	2.3562	2.3561615	2.1816	2.1816485
5	3.0307	3.0306936	2.5382	2.5382059	2.4367	2.4366582	2.2562	2.256183
6	3.8655	3.8655082	3.2374	3.2373631	3.1078	3.1078437	2.8777	2.8776561
7	4.0034	4.0033854	3.3528	3.3528352	3.2187	3.2186961	2.9803	2.980298
8	4.1222	4.1222028	3.4523	3.4523449	3.3142	3.3142246	3.0688	3.068751
9	4.2882	4.2881912	3.5914	3.5913601	3.4477	3.4476782	3.1923	3.1923201
10	4.309	4.3089935	3.6088	3.6087821	3.4644	3.4644031	3.2078	3.2078063

Dynamic Analysis Results of Laboratory Model of Type-1 Arch Dam

Under the time-dependent changing loads, it seems that there are disproportional between displacements, principal stresses and principal strains values obtained from the prototype and different scale of dam. In other words, the ratio of values obtained at any nodal points on between the dams that enlarged at a certain scale and prototype are not the same as the ratios of values at the between different nodal points on dams. This shows that the values obtained at result of dynamic analysis (displacement, principal stress and strain) can not be generalized with a single formula. For this reason, a regression analysis is used, which is a statistical method for obtaining of the results of large scale real systems according to the prototype results, achieving the desired data by fitting a curve between the results. In regression analysis, which is a parametric study, a curve is obtained by performing a regression analysis with the results of analyzes obtained with different combinations of the desired data in Type-1 arch dam, it is reached the result together with the formula of curve. It has been seen that the expression of the desired values using a single curve at all the nodal points on the dam is not a correct approach. Thus, developed different formulas are reflected the results of each nodal point in the dam.

Selection of Analysis Parameters

Taking into consideration soil-structure interaction of the Type-1 arch dam, it is obtained a total of 102 unit finite element models as 1, 10, 20, ..., 500 times scale. When the scales are expressed as arch height, they take values ranging between 0.60-300m and these values are also the first parameter for regression analysis. In the Modulus of Elasticity selected as the second parameter, for each model is taken into consideration nine different concrete strength class as C14/16, C16/20, C18/22.5, C20/25, C25/30, C30/37, C35/45, C40/50 and C45/55. Based on these two parameters, 918 different models are created and 3672 response spectrum analysis is applied by considering four different soil classes that is Z1, Z2, Z3 and Z4. All analyses are performed with ANSYS (2010) finite element program.

The results obtained in each of the nodal points for 102 different models with respect to nine different concrete strength classes are arranged, making them suitable for regression analysis. The data for each nodal point is obtained for all ground classes, fixed conditions and soil-structure interaction model, and a total of 2768 txt files have been created.

The first step is to evaluate whether there is any relationship between the obtained data or a linear or non-linear relationship if there is a relationship. Within the scope of this study, the desired graphics are created with EXCEL software and the relationship between the data is examined in detail. As a result of the review, a linear relationship is generally determined in the scatterplot of the data

pertaining to displacement. Nonetheless, nonlinear relationships exist at some nodal points. For this reason, it is evaluated which kind of range is suitable in each nodal points for the displacement results. Scatterplots of some nodal points related to displacement are given in Figure 5. Once the trendline of the obtained scatterplot is constructed, the R^2 value indicating how the gradient represents the data is readable. It is seen that these values are about 97-98% for some nodal points shown in Figure 5.

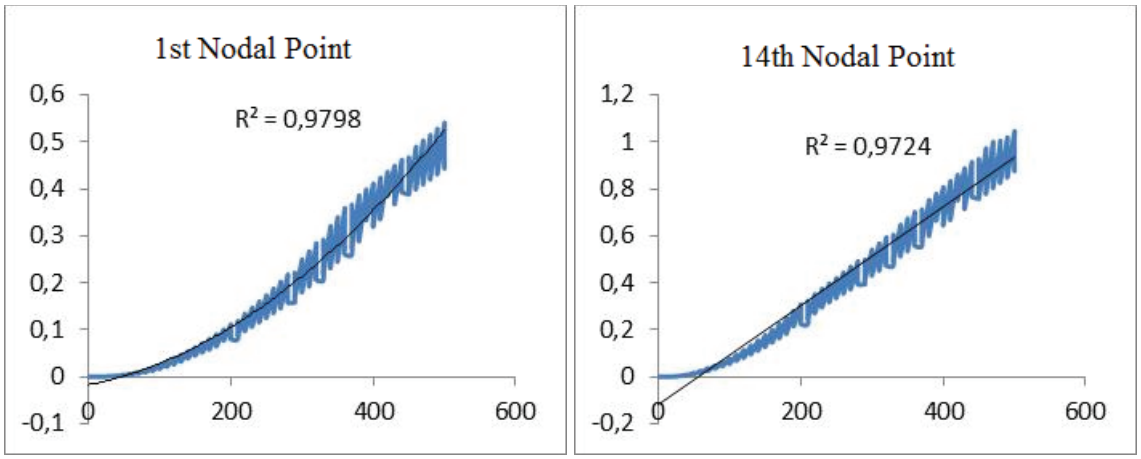

Figure 5. Scatterplots of the displacement results for some nodal points

Application of Appropriate Regression Analyzes for Results

Two-parameter regression analyses are performed by considering the scale and the modulus of elasticity as parameters. Linear regression analysis is performed at nodal points where the linear relationship is valid for the displacement results. However, for the non-linear relationship, the program code of the 2nd degree regression analysis based on the Least Squares Method given in the thesis study by Başağa (2009) is rearranged according to the two-parameter method.

Comparison of ANSYS and Regression Analysis Results

The results of the regression analysis are compared with the results obtained from the ANSYS program and the error rates are examined. When the results are analyzed, it is seen that 10% of the error rates are not exceeded. When comparing for the 50-times scaled of Type-1 arch dam, error rates reach 20-40%. This height is considered as the lower limit because the error rate at the scale value corresponding to a dam height of 30m is high. The upper limit used in the regression analysis is 300 meters arch height which corresponds to 500-times scale. It is decided that the formulas obtained for this reason are suitable for dam heights between 30m and 300m. It appears that errors of the predicted results of the formulas of any arch height value in outside these limits will more than 10%. Figure 6 shows the comparison the error rates of the results obtained according to different selected parameter values in some nodal points.

Development of Software

In the scope of the work done in Type-1 dam, it is not easy to present the desired results due to the reasons such as the excess of the variable parameters and the combination of these parameters, long and specific of the formulas obtained for each nodal point. It is a very difficult process to find and store a desired data from within the plenty data. For this reason, it is aimed to develop a software that will only allow the results of the desired data to be obtained at a selected nodal point and display various graphs and contour diagrams of these results. With the help of the software designed in the EXCEL program, the parameters are asserted the user selection and the static and dynamic analytical results are displayed with the formulas obtained from the regression analysis of the desired nodal

point at the arch dam. At the same time, depending on the selected parameters, the change on sectional and the contour diagrams of the results of the arch can be obtained at any nodal point.

Displacement			
500 Scale, Ao=4, R=1, C30/37, Z1			
Nodal Points	ANSYS	Formula	%Error
1.	1,912806	1,872897	2,086368
10.	3,043458	3,221922	-5,86386
19.	7,591565	7,561946	0,390151
31.	12,77068	12,48698	2,22151
37.	16,31958	16,74372	-2,59896
47.	28,29404	27,3858	3,21
48.	28,33737	27,3858	3,358014
50.	14,99984	14,2395	5,068934
72.	12,42	12,21506	1,65014
81.	2,167173	2,332794	-7,64224
90.	1,977952	1,872897	5,311278
105.	6,075831	6,33973	-4,34342

Maximum Principal Strain			
350 Scale, Ao=4, R=1, C20/25, Z1			
Nodal Points	ANSYS	Formula	%Error
1.	0,000115	0,000116	-0,91788
10.	0,000179	0,000183	-2,2075
19.	0,000349	0,000356	-2,0922
31.	0,000561	0,000552	1,591474
37.	0,000556	0,000551	0,91254
47.	0,000682	0,000676	0,910996
48.	0,000489	0,000491	-0,37904
50.	0,000453	0,000444	1,864185
72.	0,000494	0,000496	-0,23052
81.	0,000197	0,000203	-3,1155
93.	0,000106	0,000103	2,319356
105.	0,000328	0,000327	0,396926

Figure 6. Comparison of the results obtained for some nodal points

The Figurations for the appearance and use of the developed software are shown in detail in Figures 7-10.

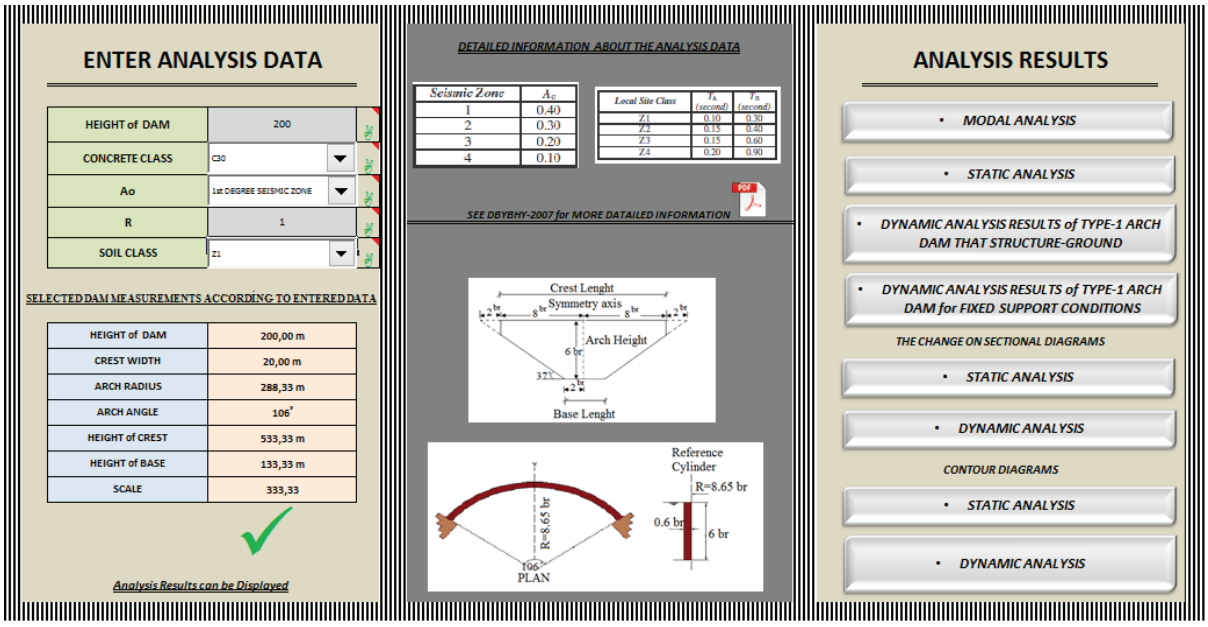

Figure 7. Input of data into home page of the software

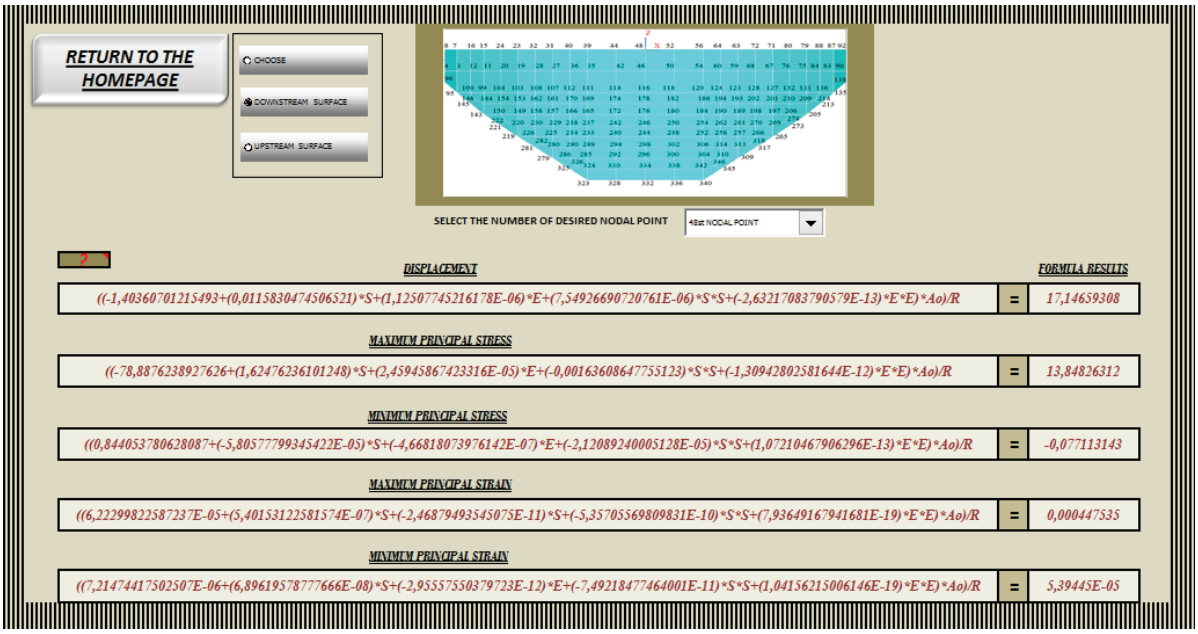

Figure 8. Displaying the related formulas and results of 48 nodal point at dynamic analysis results page of Type-1 arch dam that building ground interaction

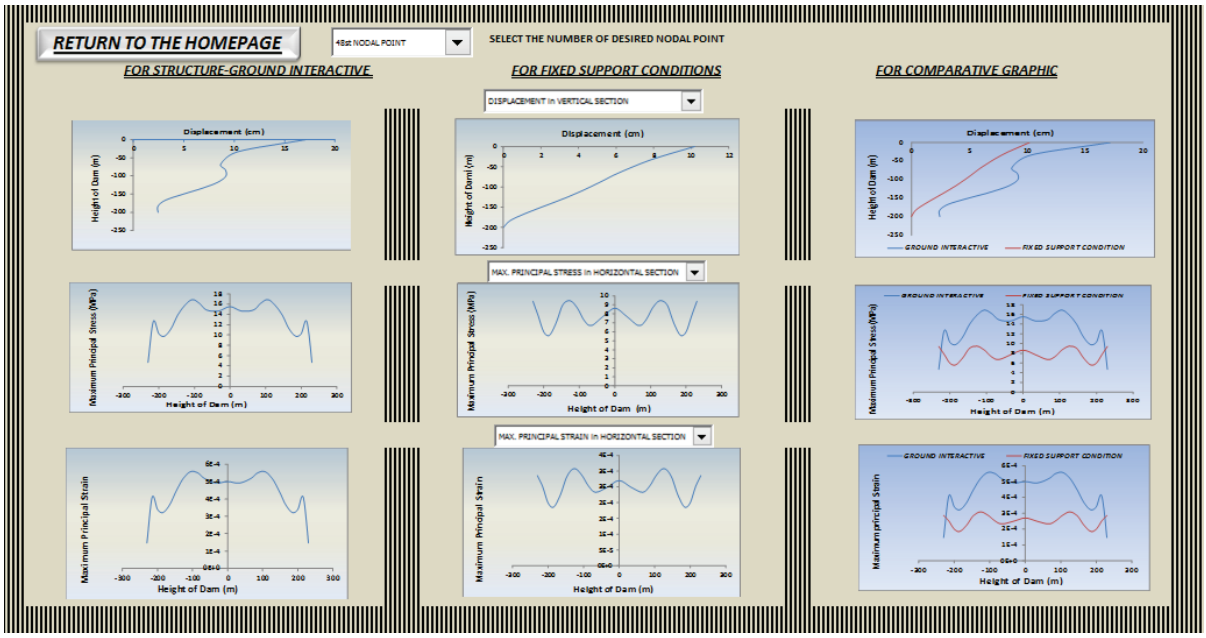

Figure 9. Displaying the change on sectional diagrams of 48th nodal point at section diagrams page obtained with dynamic analysis

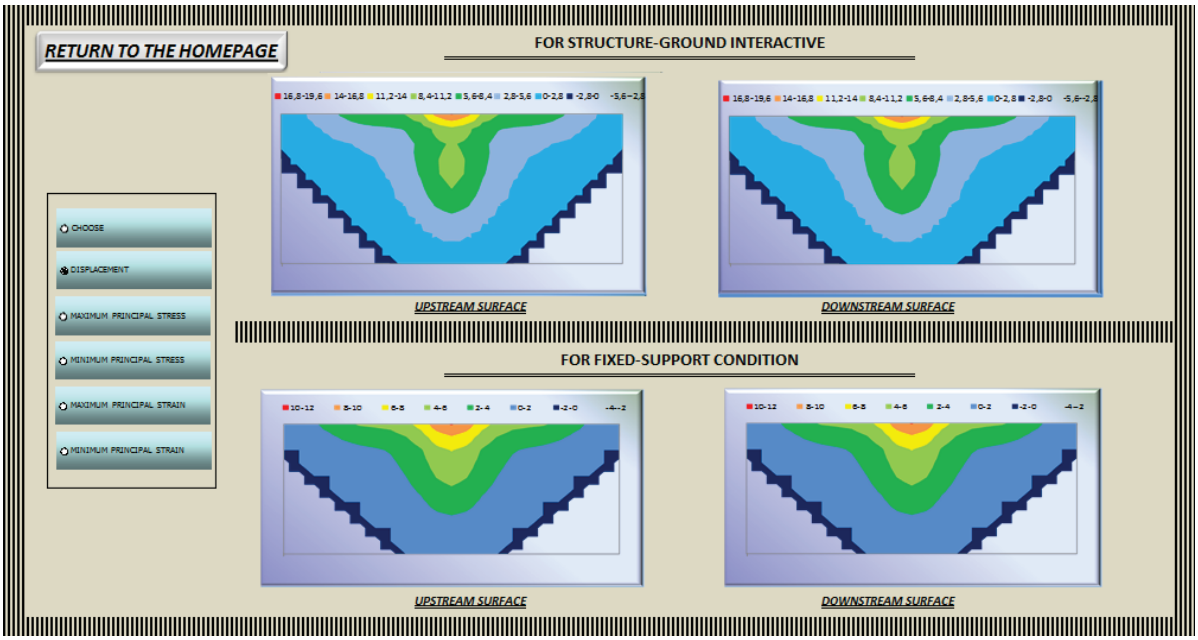

Figure 10. Displaying the change on sectional diagrams of 48th nodal point at section diagrams page obtained with dynamic analysis

CONCLUSION

In this study, engineering software is developed to predict the structural behavior of arch dams. By using the finite element model of the Type-1 arch dam modeled in the laboratory, dams are scaled to different heights and dynamic analyses are made. Taking into consideration the fixed support conditions and structure-foundation interaction of the Type-1 arch dam, it is obtained a total of 102 unit finite element models as 1, 10, 20, ..., 500 times scale. When the scales are expressed as arch height, they take values ranging between 0.60-300m and these values are also the first parameter for regression analysis. Modulus of elasticity are selected as second parameter and nine different concrete strength class (C14/16, C16/20, C18/22.5, C20/25, C25/30, C30/37, C35/45, C40/50 and C45/55) are considered for each structural model. Based on these two parameters, 918 different models are created and 3672 response spectrum analyses are applied by considering four different soil classes that is Z1, Z2, Z3 and Z4. All analyses are performed with ANSYS (2010) finite element program. The data for each nodal point on Type-1 arch dam is obtained for all ground classes, fixed support conditions and soil-structure interaction model, and a total of 2768 txt files are created. For regression analysis, the first step is to evaluate whether there is any relationship between the obtained data or a linear or non-linear relationship if there is a relationship. As a result of the review, a linear relationship was generally determined in the scatterplot of the data pertaining to displacement. Nonetheless, nonlinear relationships exist at some nodal points. However, it is seen nonlinear relationship in the scatterplot of data of the principal stress and principal strain. In each of the 346 nodal points on the arch body, a total of 13840 formulas are created represented of five different structural behavior, including displacement, maximum and minimum principal stresses, and maximum and minimum principal strains. The results of the regression analysis are compared with the results obtained from the ANSYS program and the error rates are examined. When the results are analyzed, it is seen that 10% of the error rates are not exceeded. In the scope of the work done in Type-1 dam, it is not easy to present the desired results due to the reasons such as the excess of the variable parameters and the combination of these parameters, long and specific of the formulas obtained for each nodal point. For this reason, it is aimed to develop a software that will only allow the results of the desired data to be obtained at a selected nodal point and display various graphs and contour diagrams of these results.

REFERENCES

Altunışık A.C., Kalkan E., Başağa, H.B., 2018a. "Development of Engineering Software to Predict the Structural Behavior of Arch Dams". Advances in Computational Design, vol. 3, N.1, pp. 87-112.

Altunışık A.C., Kalkan E., Başağa, H.B., 2018b. "Creation of Similarity Requirement with Field Equations in Steel Bearing Systems". The Open Civil Engineering Journal, vol. 12, N.1, pp. 134-149.

Altunışık A.C., Kalkan E., Başağa, H.B., 2018c. "Structural behavior of arch dams considering experimentally validated prototype model using similitude and scaling laws". Computers and Concrete, vol. 22, N.1, pp. 101-116.

Altunışık A.C., Kalkan E., Başağa, H.B., 2018d. "Structural Response Relationship Between Scaled and Prototype Concrete Load Bearing Systems Using Similarity Requirements". Computers and Concrete, vol. 21, N.4, pp. 385-397.

Arch Dams., 1968. "A review of British research and development". Proceedings of the Symposium held at the Institution of Civil Engineers, March, London, England.

Atmaca, H., 2016. "System Development for Full Scale Modeling and Analysis of Building Inventory". Master Thesis, Yıldız Technical University, İstanbul, Turkey.

Başağa, H.B., 2009. "An Approach for Reliability Analysis of Structures: Improved Response Surface Method". PhD Thesis, Karadeniz Technical University, Trabzon, Turkey.

Bayraktar, A., Türker, T., Altunışık, A.C., 2014. "Experimental frequencies and damping ratios for historical masonry arch bridges". Construction and Building Materials, vol. 75, pp. 234-241.

Beşiktaş, M., 2010. "Determination of Flow Duration Curves by Regression Analysis in the Eastern Black Sea and Current Estimation". Master Thesis, İstanbul Technical University, İstanbul, Turkey.

Chan, Y.K., Lu, Y.K., Albermani, F.G., 2010. "Performance-based structural fire design of steel frames using conventional computer software", Steel and Composite Structures, vol. 10, N.3, pp. 207-222.

Cheng, J., 2012. "Development of computational software for flutter reliability analysis of long span bridges", Wind and Structures, vol. 15, N. 3, pp. 209-221.

Gu, Q., Özçelik, Ö., 2011. "Integrating OpenSees with other software-with application to coupling problems in civil engineering". Structural Engineering and Mechanics, vol. 40, pp. 85-103.

Mittrup, I., Hartmann, D., 2005. "Structural monitoring of dams using software agents". Computing in Civil Engineering, ASCE, pp. 1-7.

Özdemir, Y., 2004. "Information Transfer via Regression among Periodic-Stochastic Hydrologic Processes". PhD Thesis, Dokuz Eylül University, İzmir, Turkey

Peng, J., Law, K.H., 2002. "A prototype software framework for internet-enabled collaborative development of a structural analysis program". Engineering with Computers, vol. 18, pp. 38-49.

Qiujing, Z., Guoxin, Z., Haifeng, L., Yi, L., Bo, Y., 2012. "Study on regression analysis and simulation feedback-prediction methods of super high arch dam during construction and first impounding process", Earth and Space, ASCE, pp. 1024-1033.

Serhatoğlu, C., 2015. "Numerical and Empirical Investigation of Dynamic Performance of Historical Masonry Minarets in Bursa". Master Thesis, Uludağ University, Bursa, Turkey.

Sevim, B., 2010. "Determination of Dynamic Behavior of Arch Dams using Finite Element and Experimental Modal Analysis Methods", PhD Thesis, Karadeniz Technical University, Trabzon, Turkey.

Sümerkan, S. 2014. "Natural frequency formula for post tensioned balanced cantilever bridges", Master Thesis, Karadeniz Technical University, Trabzon, Turkey.

Şahin, A., 2009. "Digital Signal Processing, Dynamic Characteristic Identification and Finite Element Model Updating Software for Experimental and Operational Modal Testing of Structures: SignalCAD-ModalCAD-FemUP", PhD Thesis, Karadeniz Technical University, Trabzon, Turkey.

Xiang, J., Jiang, Z., Wang, Y., Chen, X., 2011. "Study on Damage Detection Software of Beam-like Structures". Structural Engineering and Mechanics, vol. 39, N. 1, pp. 77-91.

Yılmaz, O., Şahin, A., 2013. "Educational Software Development for Design of Steel Structures Lesson". Sigma Journal of Engineering and Natural Sciences, vol. 31, N. 4, pp. 571-581.

5th International Symposium on Dam Safety

October 27-31, 2018

DAM EXPERT PANEL IN THE FRAMEWORK OF DAM SAFETY MANAGEMENT OF BENER DAM, INDONESIA

Cristina D. YULININGTYAS[1], Amos SANGKA[2]

ABSTRACT

Bener Dam is the highest concrete face rock fill dam in Indonesia with 159 m height (from plinth) and 169 m from the deepest foundation with 712.13 m length and has 90.4 million m^3 total storage on flood water level.

In order to manage Bener Dam safety, dam safety evaluation is still needed to be done by dam expert panel activity which is planned to be done at the beginning of construction. This activity refers to the Minister Regulation of Public Works and Housing No. 27/2015 on Dam that for dams with height of 75 m or more from river base need expert technical advice beyond the advice from Dam Safety Commission.

The important notes to be followed up on the activities of the Dam Experts Panel have been agreed between the stakeholders and the Dam Safety Commission as recommender that the design of the Bener Dam can be constructed.

Keywords: Bener Dam, CFRD, Dam Expert Panel

[1] Young Dam Engineer, Serayu Opak River Basin Unit, Ministry of Public Works and Housing, Indonesia. e-posta: cristinadwi87@gmail.com

[2] General Manager of Dam Construction, Serayu Opak River Basin Unit, Ministry of Public Works and Housing, Indonesia. e-posta: bajul.mati@yahoo.com

INTRODUCTION

Bener Dam is a Concrete Face Rock Fill Dam with 159 m height from plinth and 169 m from the deepest foundation with 712.13 m length and has a total storage of 90.4 million m^3 at flood water level.

Spillway is designed as side spillway, located on the left bank with a 90 m long and USBR Type II stilling basin. The diversion channel is designed as circular tunnel with Φ7 m, 763.85 m long and at the Q_{25} design flood elevation. The intake structure is designed as tower (shaft) with 114 m height and very high / extreme hazard level classification.

Figure 1. Location of The Bener Dam

The purposes of Bener Dam are:
- Irrigation of 1,940 Ha (new) and 15,519 Ha existing.
- water supply of 1,500 l/s
- Hydro Power Plant of 6 MW

DETAIL DESIGN CRITERIA

General

Dam type was chosen based on topographic, geological and availability of embankment material around the dam location. Based on these considerations, the Bener Dam is designed concrete face rockfill dam (CFRD).

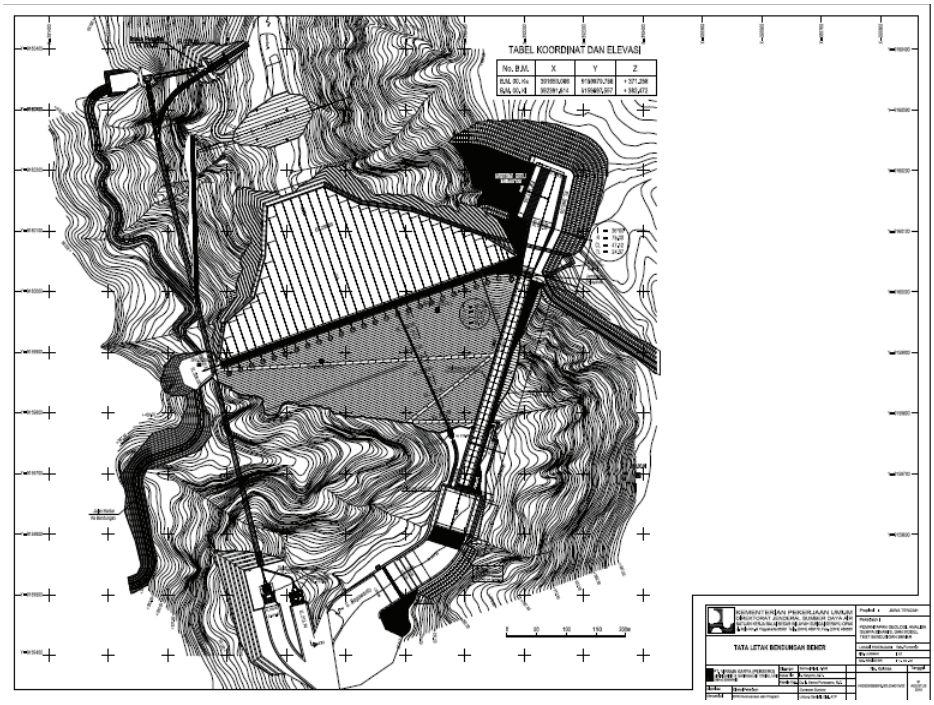

Figure 2. Bener Dam Layout

Dam Zoning

The principle of this dam is material availability from quarry. Zoning is divided based on material sources and requirements, including shear strength, permeability, compressibility by considering efficiency and economic aspects.

Bener Dam zoning design as follows:

1. Zone 1 Upstream Counterweight
   - 1A : silt or fine – coarse non cohessive material < 150 mm,
   - 1B : random fine – coarse material
2. Zone 2 Filter
   - 2A fine filter
   - 2 B coarse filter (3 m width)
3. 3A as transition
4. Rockfill embankment zone
   - 3B
   - 3C
5. 3D : rip rap

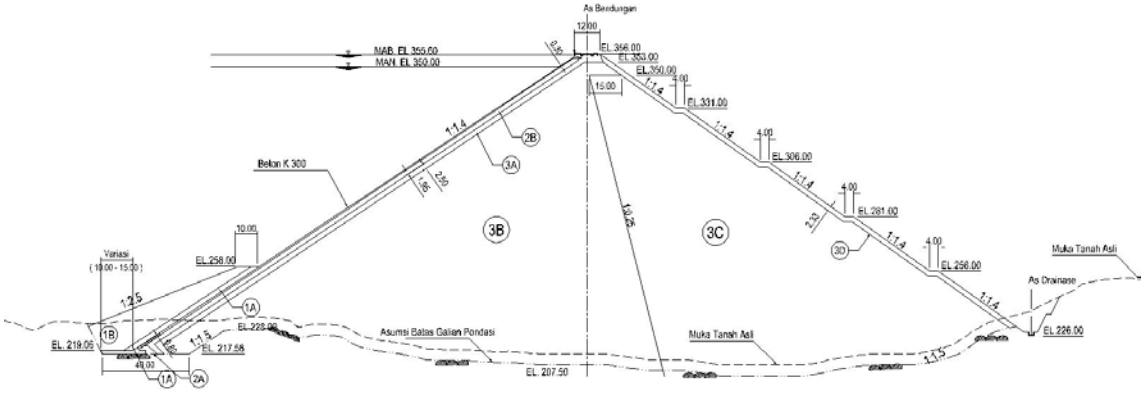

Figure 3. Cross Section of Bener Dam

Plinth

The plinth structure connects the foundation with the slab which are functioned as impermeable layer between the slab and the foundation, grout cap, and initial position of slab slipform equipment.

Determination of the width and thickness of the plinth was based on the hydraulic gradient in the table of Guidelines for Design and Construction of Concrete Face Rockfill Dam where the value taken for the Bener Dam is 20 so that the plinth length is 8.0 m and 1.0 m thickness with K-300 concrete quality.

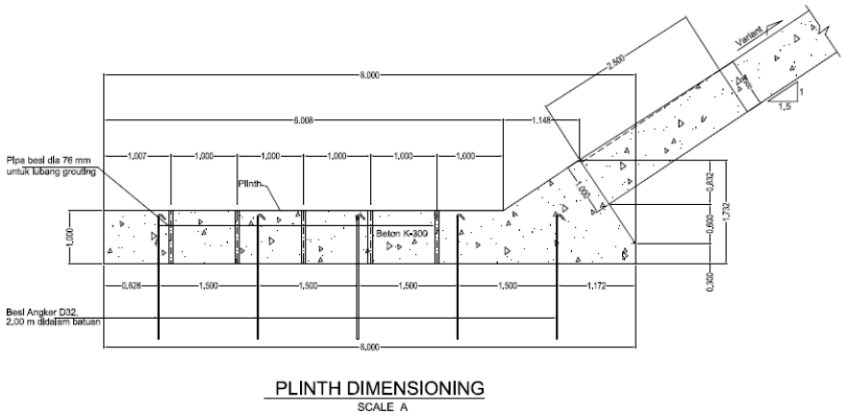

Figure 4. Plinth

Slab

The slab is a impermeable layer on upstream. The determination of the slab segment is based on the body deformation estimation of the dam and construction conditions. The Bener Dam is designed with 15 m segment width where the distance between vertical joint is usually between 12 ~ 18 m. Thickness of slab designed conservatively with thickness from bottom to top is 1.0 m - 0.5 m with K-250 concrete quality.

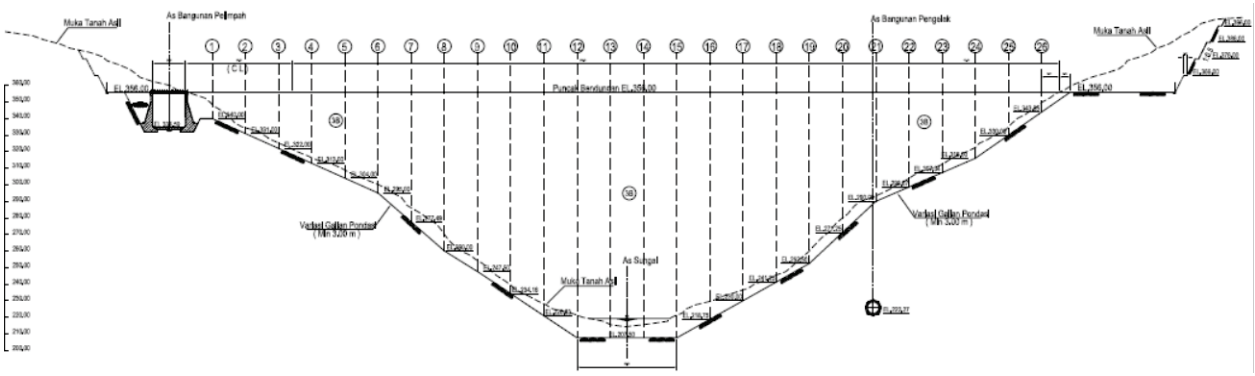

Figure 5. Slab Segment

Spillway

The spillway is designed as side spillway type without gate (overflow) located on the left bank with 90 m long and 113 m long of USBR type II stilling basin where dimensions and types are made followed the results of hydraulic model test.

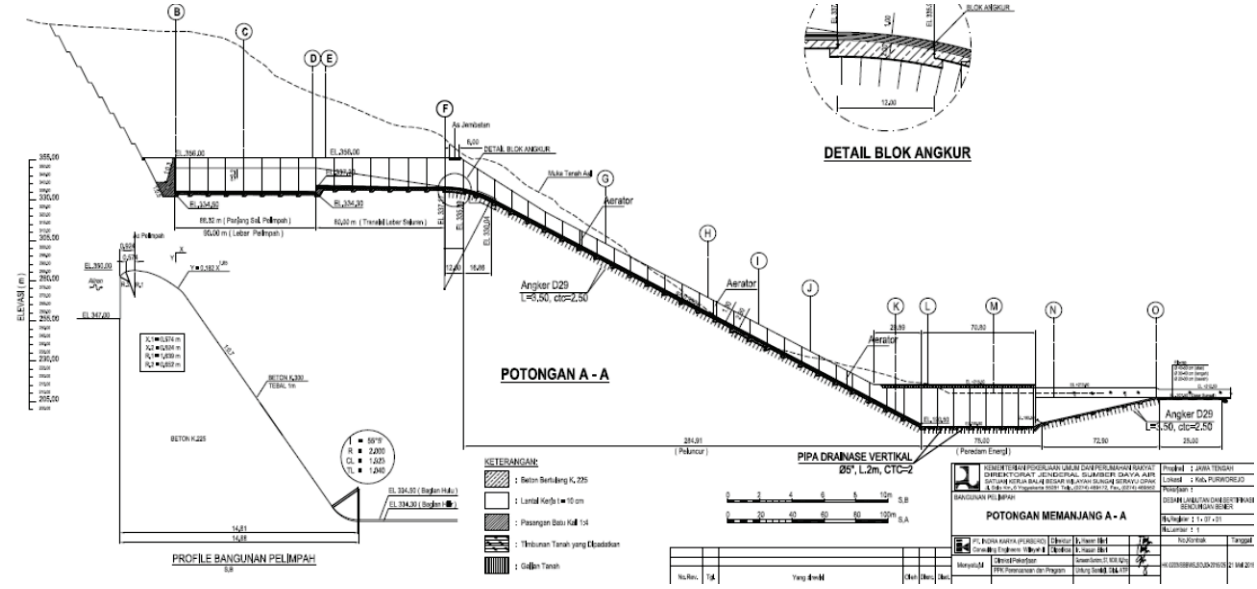

Figure 6. Spillway

Intake

Intake is designed to secure the work site especially the dam body against the Bogowonto river flow when constructed. This intake system consists of cofferdam in the upstream and downstream side of the main dam and diversion channel. Due to dam site topography as narrow river valley, the diversion channel is designed with tunnel of Q_{25} design capacity.

The waterway was planned to diameter 1.4 m from 7.0 m in the downstream section for the purposes of water supplay, irrigation, and hydropower whose output will be adjusted to the emergency release opening.

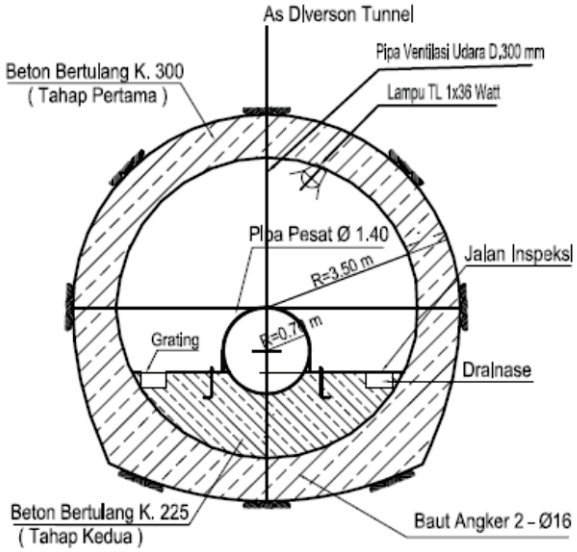

Figure 7. Diameter 7.0 m of Tunnel to 1.4 m of Waterway

DESIGN OPTIMIZATION

Design optimization is carried out in order to manage the dam security more efficiently and effectively. Based on Ministry of Public Works and Housing Regulation no. 27/2015 of Dams article no.150 concerning of Dam Panel Expert stated that:

(1) Dalam pelaksanaan pembangunan dan pengelolaan bendungan dengan kriteria tertentu, Pembangun dan Pengelola bendungan berkewajiban menunjuk panel ahli bebas.

(2) Bendungan dengan kriteria tertentu sebagaimana dimaksud pada ayat (1), meliputi:

a. bendungan dengan tinggi 75 (tujuh puluh lima) meter atau lebih diukur dari lembah terdalam dengan daya tampung waduk sekurang-kurangnya 100.000.000 (seratus juta) meter kubik;

b. bendungan yang mempunyai permasalahan teknik yang kompleks; atau

c. bendungan yang menerapkan teknologi baru sesuai dengan rekomendasi Komisi Keamanan Bendungan.

(3) Panel ahli bebas sebagaimana dimaksud pada ayat (1), mempunyai tugas memberikan pertimbangan teknis yang lebih mendalam mengenai keamanan bendungan.

For Bener Dam, the criteria above must be fulfilled by appointing Dam Panel Expert team, where according to the results of the previous discussion either in the technical meeting or the plenary session of the Dam Safety Commission it is necessary to study in depth, namely:

1) Bottom Outlet
   The proposed structure is intended to empty the reservoir where from the inlet to the deepest reservoir is still about 40 m below.

2) Gallery on half sides (under plinth on the riverbed until the left side).
   This gallery structure was recommended to monitor the possibility of seepage flowing through the slab / plinth.

3) Zone of 1A and 1B
   Based on the guidelines for design and construction of CFRD, it is known that this zone serves to fill cracks that maybe occur at concrete membranes when initial filling. But in the discussion that has been carried out there is a plan to replace this zone with geotextile if the function is as a impermeable zone which the use is in the outer zone of the dam so that if necessary to replace it won't make much failure potential to increase damage to the concrete membrane.

CONCLUSION

Based on the results of the detailed design discussion was carried out that the design of the Dam was recommended for the construction implementation. The important note to be carried out is the activity of the Dam Panel Expert in the early stages of the construction, especially when the excavation of the dam foundation is carried out with the main topics being:

1) Bottom Outlet
   The proposed structure is intended to empty the reservoir where from the inlet to the deepest reservoir is still about 40 m below.

2) Gallery on half sides (under plinth on the riverbed until the left side).
   This gallery structure was recommended to monitor the possibility of seepage flowing through the slab / plinth.

3) Zone of 1A and 1B
   Based on the guidelines for design and construction of CFRD, it is known that this zone serves to fill cracks that maybe occur at concrete membranes when initial filling. But in the discussion that has been carried out there is a plan to replace this zone with geotextile if the function is as a impermeable zone which the use is in the outer zone of the dam so that if necessary to replace it won't make much failure potential to increase damage to the concrete membrane.

AKNOWLEDGEMENTS

The authors would like to thank to Dam Safety Unit and Serayu Opak River Basin Unit, Directorate General of Water Resources, Ministry of Public Works and Housing for the authorization to publish the main result of the present study.

REFERENCES

Ministry of Public Works and Housing Regulation no. 27/2015 of Dams.
Ministry of Public Works, 2011. "Guidelines for Design and Construction of CFRD".
Yulinintyas, Cristina Dwi, 2018. "Dam Safety Management of Bener Dam Design". Paper on Inacold Symposium.
Virama Karya. Ltd and Indra Karya, Ltd, 2015. "Final Report of Bener Dam Design and Certification".
Virama Karya. Ltd and Indra Karya, Ltd, 2015. "Design Drawing of Bener Dam Design and Certification".

DAMAGE OF THE DERBENDIKHAN DAM DURING THE LAST Mw 7.3 HALABJA EARTHQUAKE

İdris BEDİRHANOĞLU[1], Çağrı MOLLAMAHMUTOĞLU[2*], M. Şefik İMAMOĞLU[3]

ABSTRACT

In this study we have investigated the effects of the recent earthquake (M 7.3) on the Derbendikhan Dam which occurred at Iraq/Iran border and devastated the Halabja/Suleymaniyah regions of Northern Iraq. For this purpose a technical visit to the dam was conducted and failures occurred in the structure of dam were examined on-site. Moreover structures around dam region were also investigated. Conclusions were made for the probable epicenter of the earthquake through evaluation of the damages of dam structure. Finally it is concluded that the first announced epicenter of the earthquake is more likely to be the true epicenter.

KeyWords: Derbendikhan dam, earthquake, epicenter, damage.

INTRODUCTION

The earthquake occurred with a magnitude of 7.3 Mw on 12.11.2017 at 18:18:17 local time around the part of Bitlis-Zagğros mountain range near Iraq-Iran border which is 30 Km south of Halabja province. A scientific team was formed from the members of Dicle University College of Engineering in order to investigate the effects of the earthquake on-site. Assist. Prof. Dr. M. Şefik İmamoğlu from the Department of Geology of Mining Engineering, Assoc. Prof. Dr. İdris Bedirhanoğlu from the Department of Structures of Civil Engineering and CE Nihat Noyan from the Chamber of Civil Engineers/Diyarbakır branch arrived at the earthquake effected region on 14.11.2017 and started investigations just after three days passed the occurrence. First of all local administrators were contacted and asked if any major damage had occurred in city centers of Zaho, Duhok and Suleymaniyah. Then earthquake records were examined in Suleymaniyah Earthquake Center and regions with major damages were identified. Eventually it was seen that the most effected city is Derbendikhan city and especially the dam near the city, Derbendikhan Dam, sustained serious damage to its structure. Thus investigation efforts were first directed to the dam and later to the heavily damaged structures in Derbendikhan city. Reference to detailed reports on the subject is given at the end of the literature section; (İmamoğlu, M.Ş. ve Bedirhanoğlu, İ. (2017) and Bedirhanoğlu, İ. ve İmamoğlu, M.Ş. (2017).

SEISMIC ACTIVITY of MIDDLE EAST and SURROUNDING REGIONS

Middle East region is rich in terms of active fault zones which are capable to produce severely devastating earthquakes. Main mechanism of this seismic activeness is due to the movement of African, Arabian and Indian plates along north/north-east direction towards Eurasian Plate. The Tetis oceanic plate, located between mentioned plates, is squeezed and a compressional region with tectonically active properties is formed along Bitlis-Zagğros suture belt. The thrust between these plates when combined with the westbound movement of the Anatolian plate play the major role in the seismic activeness of Middle East and surrounding region. The northbound movement of the African plate and a rupture zone along Red Sea together cause a slip of Middle East region towards north, northwest direction with rates of 20-24 mm and 28 mm per year respectively (Figure 1). When this slip mechanism is arrested at some locations tremendous levels of stress develops and finally energy is discharged with ruptures and breaks which manifest themselves as earthquakes. The severity of the earthquake is depending on the size of the rupture occurring at these concentration points.

Bitlis-Zagros suture belt is under the effect of a tectonically active compression zone with a length of over 300 Km.

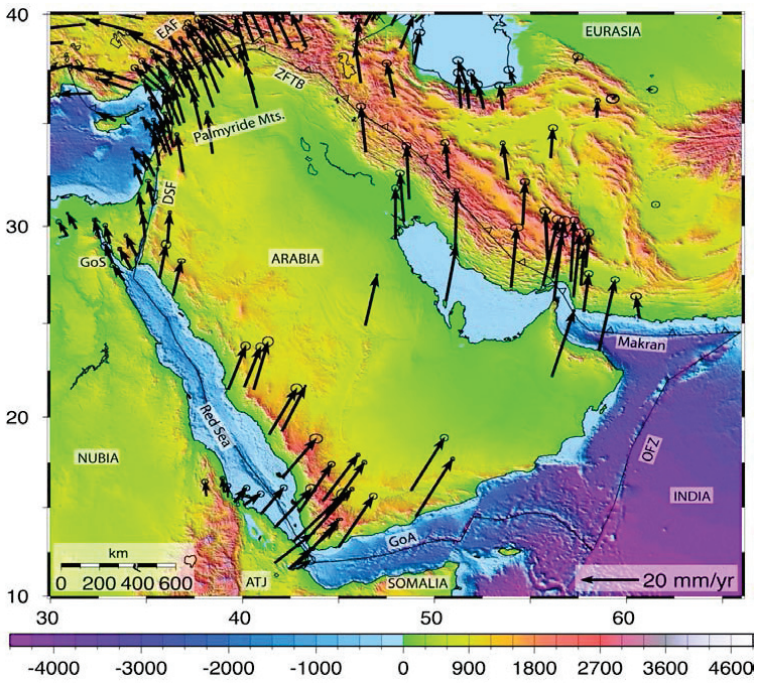

Figure 1. 1988-2005 Global Position System GPS results show slip rates and directions of the plates **(**it is estimated that the slip rate is 20-30mm/year) (Reilinger *et al.*, 2009, in Hafidh et al. 2012).

The largest recorded earthquake which has occurred in the last 100 years is the earthquake which occurred in the Makran region, North of Gulf of Oman in 1945 with a moment magnitude of M8.1 (Figure 2). This severe earthquake caused a tsunami in the Gulf of Oman and Arabian Sea which resulted to the deaths of over 4000 people. In 1505 the Chaman Fault zone near Afghanistan Kabul fractured and devastated the nearby villages. In the same region

on 30 May 1935 Suleymaniyah region, Quetta, Pakistan an earthquake (M7.6) caused deaths of 30000 to 60000 people (USGS).

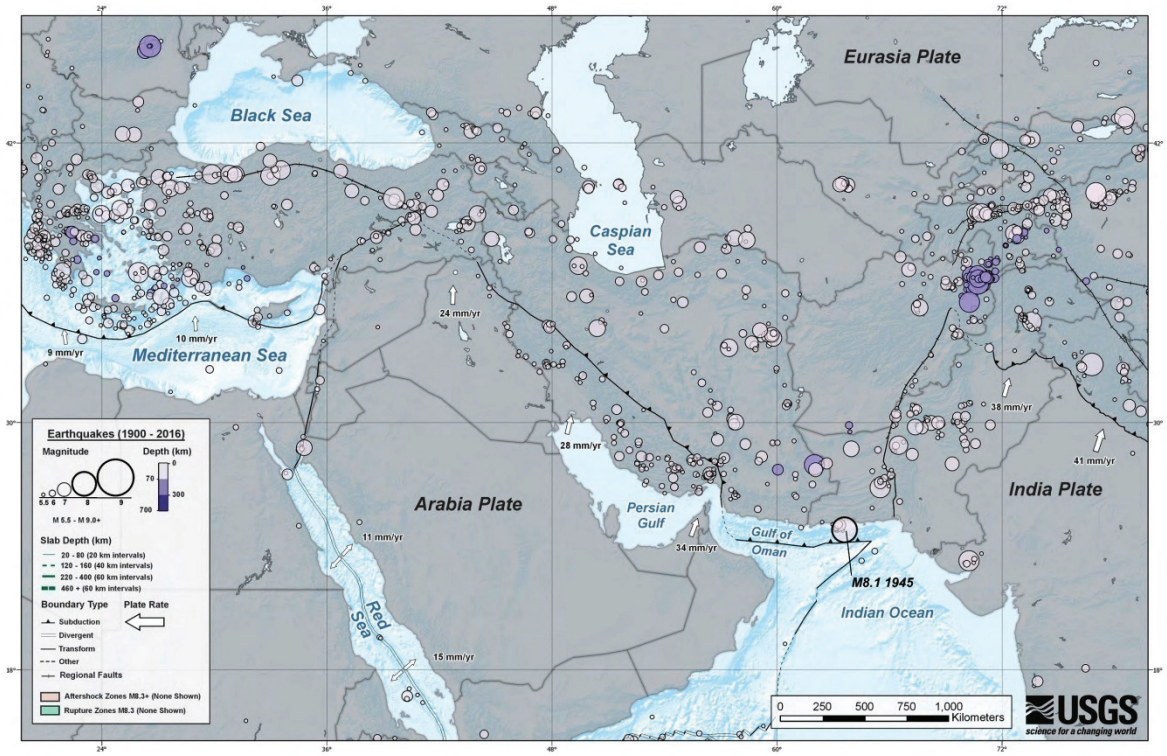

Figure2. Earthquakes of Middle East between 1900-2016 with a magnitude over M 5.5 and slip of surrounding plates (USGS)

1930 Hakkari Earthquake, 1975 Lice Earthquake and 2011 Van Earthquake are the major earthquakes of this seismic activeness which occurred as direct result of Bitlis-Zagğros suture belt in Turkey. 1930 Hakkari Earthquake occurred at Turkey-Iran border at 00:34 local time (UTC 21:34) on 7 May 1930 and devastated the city center of Hakkari. With a moment magnitude of 7.2M this earthquake resulted in the deaths of 2514 people and damaged around 3000 structures. 1975 Lice Earthquake occurred in the Lice district and surrounding villages of Diyarbakır province at 12.20 local time (UTC 09:20) with a magnitude of M 6.6. During the 23 seconds lasting severe earthquake 2385 people lost their lives and 8149 structures were damaged.

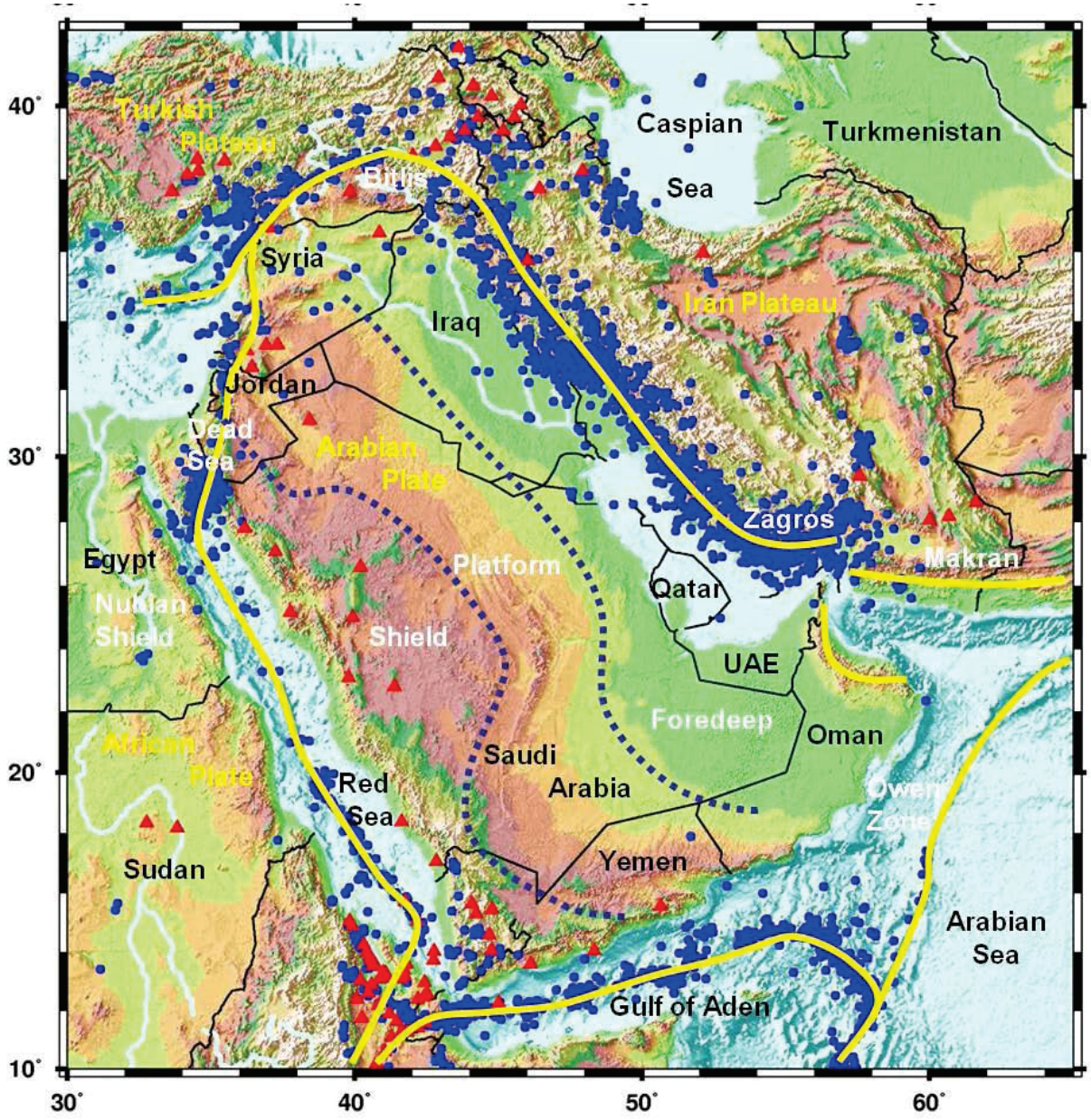

Figure3. Arabian plate and seismotechtonics of the surrounding region.(blue dots denote earthquakes, red dots denote volcanoes.) (Reilinger, R. F., (2009; in Hafidh et al. 2012)

Last major earthquake of this mechanism in Turkey is the Van Earthquake in 2011 which has an epicenter located in the Tabanlı village of Van province. The severe (M 7.2) earthquake was felt in almost the complete southeast region of Turkey including provinces Ağrı, Bitlis, Erzurum, Iğdır, Kars, Siirt, Bingöl, Muş, Diyarbakır, Tunceli, Batman, Erzincan which caused mass panic. In this earthquake thousands of structures were completely destroyed or heavily damaged beyond repair. Especially the RC structures in the downtown of Erciş district performed relatively poor and hundreds of them were annihilated. Due to the poor structural

performance and severe damages earthquake took a heavy toll: 604 people mainly from Erçiş died and well over 2000 people injured.

As a conclusion from the Figures 2-3 no major earthquakes have happened in the Northern Iraq and in fact in Iraq as general in the last 100 years. This fact has an important outcome which effects the characteristics of the existing structures in this region as people forgot have not mind the devastating effects of a major earthquake when constructing.

THE Mw 7.3 EARTHQUAKE at IRAQ-IRAN BORDER - 30 Km SOUTH of HALABJA

The earthquake focused in this study was occurred on 12.11.2007 at UTC 18:18:17 (21:18:17 local time) at 30 Km south of city of Halabja, Suleymaniyah/Iraq on the Bitlis-Zagğros rupture zone near Iraq-Iran border. The faults of the rupture zone produced an earthquake with a magnitude of 7.3 Mw.

USGS firstly announced that the epicenter is located at **34.957°N 45.792°E** with a depth of **25 km**. Later revised the location value as farther to east **34.905°N 45.956°E** and the depth is revised as **19 km**. Thus the territorial address of the epicenter was changed from Suleymaniyah/Iraq to Kermanshah/Iran (Figure 4).

Figure 4. First and final epicenters announced and their distances with respect to Derbendikhan dam structure

The earthquake was felt in a vast region including Iraq's Baghdad, Basra, Mosul; Turkey's Diyarbakır, Van; Iran's Tabriz, Tehran and Ahvaz. Table 1 documents the major residential areas which are nearest to the epicenter and their populations.

Table 1. Nearest major residential areas to the epicenter of the earthquake and their populations (USGS)

ResidentialArea	Distance w/ respect to the firstly announced epicenter	Distance w/ respect to the revised epicenter	Population
Derbendikhan, Irak	19.7 km (12.3 mi)	31.8 km (19.8 mi)	>20,000
Halabja, Iraq	30.2 km (18.8 mi)	30.4 km (18.9 mi)	57,333
Pāveh Iran	52.4 km (32.6 mi)	39.6 km (24.6 mi)	17,779
Sarpol-e Ẕahāb, Iran	55.4 km (34.4 mi)	50.0 km (31.1 mi)	51,611
Suleymaniyah	75.0 km (46.6 mi)	87.3 km (54.3 mi)	723,170

Earthquake caused severe damage at the epicenter and immediate nearby with the classification of VIII level of Mercalli scale. As moving away from the epicenter the devastating effect of earthquake has diminished. For Batman which is 543 km far away level V, for Diyarbakir which is 612 km away approximately level IV is registered in terms of Mercalli scale.

.

DARBANDIKHAN DAM and SURROUNDING AREA

Darbandikhan (Derbendixan) dam is located inside a narrow valley near Darbandikhan district along north-northeast direction.(Figure5). Darbandikhan district in turn is located at the near south of Suleymaniyah province (Figure6).

The 535 m long dam is constructed on a thick limestone layer which is split off narrowly by the streams feeding the reservoir and which sits on an alternate formation of mudstone and silt stone (Figure 7). It was constructed between the years 1956-1961 as a rock fill dam, has a height of 128 m and has a reservoir capacity of 3 billion m^3 (Figure 7). Geometrical data were measured from Google Earth as views were given in Figures 8-9.

Figure 5. Close up of Darbandikhan district

Figure 6. Location of Darbandikhan District

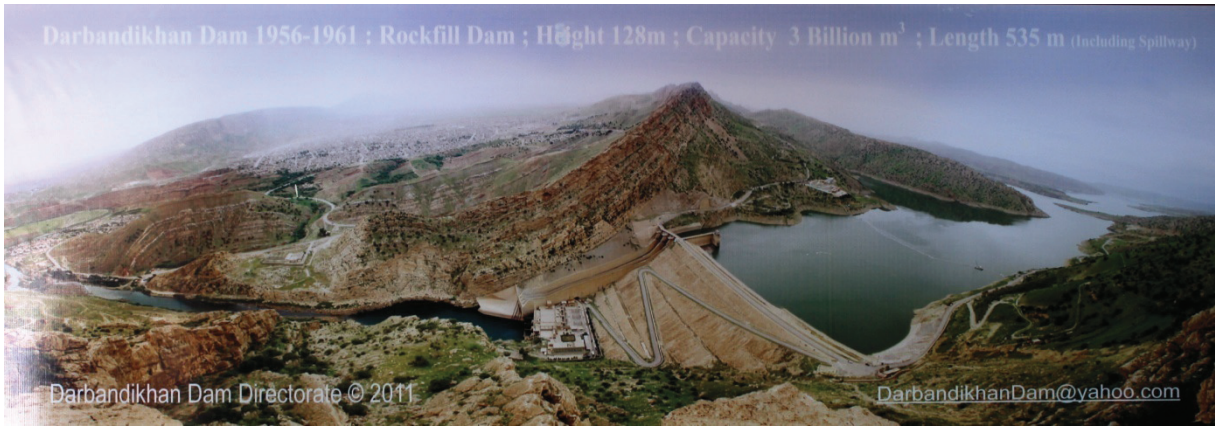

Figure7 . Darbandikhan (Derbendixan) Dam view of right bank

Figure 8. Darbandikhan Dam geometrical dimensions

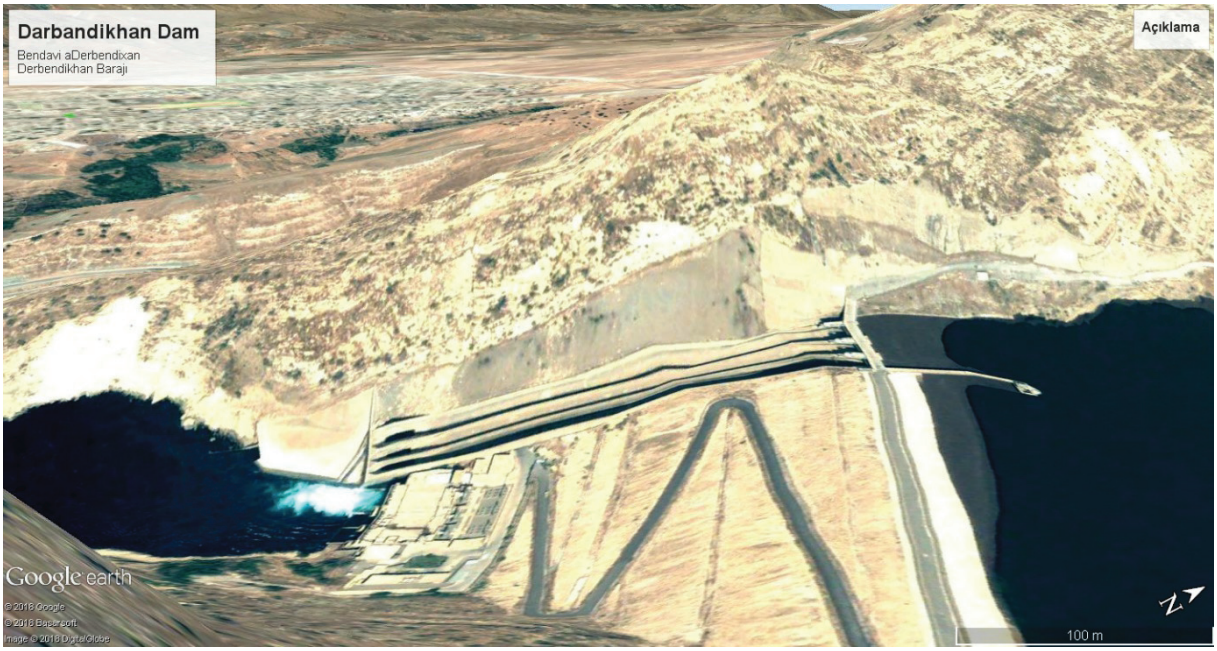

Figure 9. Darbandikhan Dam from profile via Google Earth

DAMAGE OCCURRED IN THE DAM STRUCTURE

Derbendikhan dam is the largest structure with concerning damages because of the wide, long and penetrating cracks occurred on structure during the earthquake. There are two main crack directions in the structure which are shown with green and red lines in Figure 10. The first type of cracks which occurred longitudinally and especially more pronounced at the center section resulted in up to 21 cm wide penetrating gaps at the downstream side of the clay core (Figure 10-11). Also a 20-30 cm depression was observed at the downstream side of the downstream crack. These longitudinal cracks reveal that serious dynamic effects had occurred along lateral direction to the dam structure. The compressed clay core has more flexibility with respect to the surrounding rock fill section of the structure. The lateral dynamic effects caused to split off the core clay and the rock fill as their responses are quite different. The clay flexed like a lateral spring and separated from the more rigid rock fill section which manifested as longitudinally continuous deep cracks both on the downstream sides of the dam structure. The upstream rock fill section is under continuous water pressure which prevented the separation from the clay core whereas the downstream rock fill section separated from the clay core because of dynamic effects.

The second type of cracks occurred laterally on both ends of the dam structure parallel to the stream direction and thus perpendicular to the first type of cracks (red lines in Figure 10). The distance which is over 500 m between these end cracks reveals that earthquake had a cyclic effect which rocked the whole dam structure both along the upstream and downstream directions. Another manifestation of these cyclic whole motion is that crack openings on both ends have approximately equal sizes.

In figure 13 investigative excavations were conducted on these end cracks and it was seen that they were penetrating deep inside the structure.

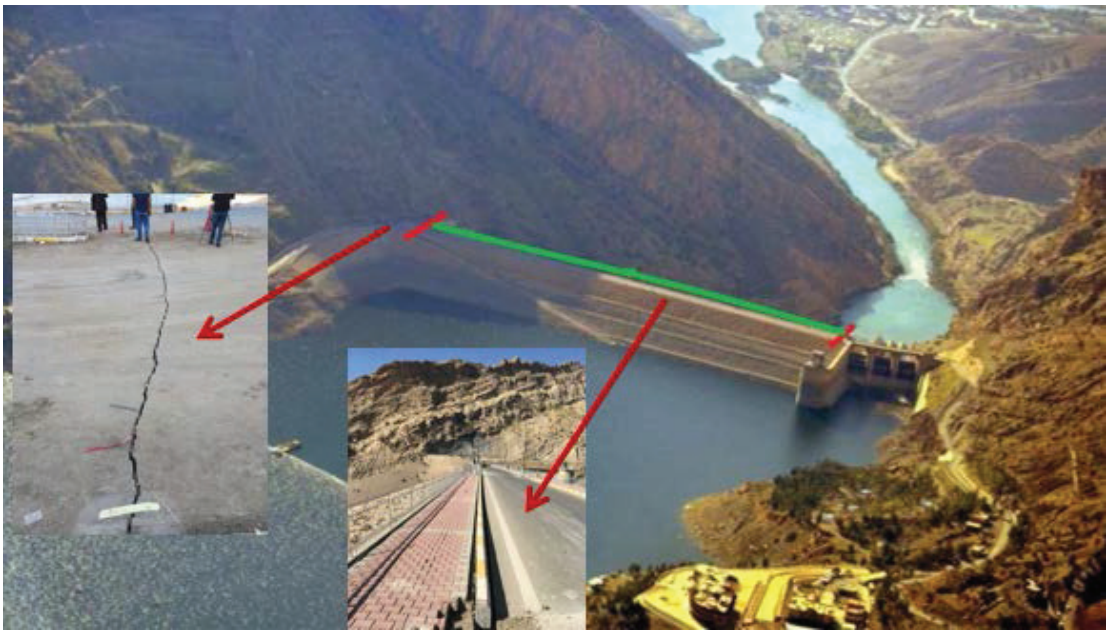

Figure 10. Major Cracks occurred on Darbandikhan (Derbendixan) Dam structure

Figure11. Major downstream crack occurred on the Darbandikhan (Derbendixan) Dam

Figure 12. Depression near the downstream longitudinal crack

Figure 13. Investigation of the penetrating end crack with excavation

THE RELATION BETWEEN THE DAMAGE MECHANISM IN THE DAM STRUCTURE and THE POSSIBLE EPICENTER of THE EARTHQUAKE

Two different epicenters were announced for the earthquake by different agencies around the world. The first one was given as a location which is 30 km south of Halabja, northern Iraq Suleymaniyah region, on the Iraq-Iran border within the Bitlis-Zagğros suture belt. The second revised location for the epicenter was given inside the Kermanshah/Iran. In this study the evaluation of the most probable location for the epicenter is based on the major effective direction of the ground motion and the damages sustained by the dam structure rather than the data collected by the earthquake recording centers.

Figure 14 shows the locations of these two epicenters with respect to the Darbandikhan dam. The first epicenter is just 19 km away from the dam structure whereas the second one is over 30 km away. When a straight line is drawn between the dam location and the second epicenter it becomes parallel to the dam structure. It is not realistic that the major effective ground motion direction is parallel along the 500 m dam structure since the observed crack formations seem unlikely with longitudinal effects. When a line is drawn from the first epicenter to the dam we see that it crosses the dam structures with an inclination of approximately 30°-40° and in this case the structure is under forced vibration in both longitudinal and lateral directions. Thus the first epicenter location seems to be more likely the reasonable one. Also since the longitudinal crack becomes wider as one moves from the ends towards to the center of the dam we can conclude that a strong dynamic force effected the dam structure in perpendicular direction.

Figure 14. Satellite view of the general location of the Darbandikhan (Derbendixan) Dam with respect to the epicenters

CONCLUSION

Üniversitesi Mühendislik Fakültesi Maden Mühendisliği Bölümü Genel Jeoloji Anabilim Dalı Başkanlığı, 29 Kasım 2017, DİYARBAKIR

Bedirhanoğlu, İ. ve İmamoğlu, M.Ş. (2017). 12 Kasım 2017 Halepçe Depremi Ön Değerlendirme Raporu, Dicle Üniversitesi Mühendislik Fakültesi Maden Mühendisliği Bölümü Genel Jeoloji Anabilim Dalı Başkanlığı, 29 Kasım 2017, DİYARBAKIR

In this studyan on-site investigation of the damages sustained by the Darbandikhan dam due to latest 7.3 Mw earthquake which was occurred at Iraq-Iran border.As two different epicenters were announced by the agencies, the most probable epicenter of the earthquake is evaluated with respect to the damages sustained by the dam structure. Longitudinal cracks which become wider at the center and separate the clay core from the rock fill were observed on the structure. Also lateral cracks have been observed at the both ends of dam structure which was found to be deeply penetrating when examined via excavation. It is concluded that these type damage mechanism with observed cracks reveals that the structure were under the effects of strong cyclic ground motion perpendicular to the dam's structural body. Thus it is highly unlikely that the epicenter was located somewhere which could produce cyclic effects almost only parallel to the dam's body. Therefore the first announced epicenter which is located inside Northern Iraq about 30 kM south of Halabja provinve of Suleymaniyah. seems to be more probable as it fits more properly within the explanation of the sustained damage which was evaluated on-site.

ACKNOWLEDGEMENTS

We deeply appreciate the supports of Diyarbakir Branch of Chamber of Civil Engineer and its member Civil Engineer Nihat Noyan who took a part in our investigation group. Dicle University Physics Department's graduate student Mr. Kadri Yusufwho accompanied us with his vehicle and also acted as our translator and guide. We also thank to the Dr. Ramazan Hamza Muhammed from Duhok University, Department of Geogly, and members of Duhok Seismology and Meteorology Institute; Head Dara Hasan Faraj, seismologs Bakir M Saeed Ali, Aras Muhammed Tofig, Omid Muhammed Mahsun, Borhan İbrahim Salih for their companionship during the on-site investigations. We need to also mention the helps of Union of Engineers Duhok Chamber members Abdul Emir and Diler Abo. We also wants to thanks Dicle University Engineering department and Dean of Engineering Faculty Prof. Dr. Abdullah Toprak, who made this site visit possible.

REFERENCES

KOERI, 2010. www.koeri.boun.edu.tr.

USGS, 2010. www.usgs.govs

Saad Z. Jassim and Jeremy C. Goff, 2006. Geology of Iraq, Edited by Saad Z. Jassim and Jeremy C. Goff

Hafidh A. A. Ghalib, Ghassan I. Aleqabi, Eid Al-Tarazi, TawfiqGh. Al-Yazjeen,Omar Q. Ahmed, Bakir S. Ali, KhozgaQadr, Ali A. Ali, 2012. A Proposal to Establish a Middle East Seismographic Network .Sulaimaniyah Kurdistan Directorate General of Meteorology and Seismology Ç

Reilinger, R. F., (2009). Seismotectonics of the Arabian Plate and its boundaries III, EOS Trans AGU, 90 (52), Fall Meeting Suppl. Abstract T54C-2011.

İmamoğlu, M.Ş. ve Bedirhanoğlu, İ. (2017). 12 Kasım 2017 M 7.3 -Halepçe'nin 30 km Güneyi Irak-İran Sınır Bölgesi Depremi'nin Sismotektonik Ön Değerlendirme Raporu, Dicle

5th International Symposium on Dam Safety

October 27-31, 2018

DAM SAFETY IN BULGARIA – SOME RECENT DEVELOPMENTS, POLICIES AND PRACTICE

Dimitar S. KISLIAKOV[1]

ABSTRACT

This work is a summary report about the current frame conditions for the dam safety regulation and management in Bulgaria. The contemporary situation in the field of dam safety is analysed based on the recent economic, political and social developments in the country after 1989. This background is traced in its relation to the whole process of preliminary studies, design, construction and operation of dams. The presentation is based on both literature survey and specific national experience, and it results in the performed qualitative analysis from the point of view of the following aspects of dam safety:

- Legislative base, codes and guidelines and their development, administrative procedures, financial mechanisms, international recommendations and good practices.
- Physical aspects of the operation of large and small dams aiming at technical and operational reliability in connection with the most commonly used structural solutions for these facilities;
- Regulatory environment and formulation of some design load cases and operational conditions, respectively.

Finally, based on the presented findings and considerations, conclusions are drawn with respect to particular contemporary research, administrative and implementation needs.

Keywords: dam safety, Bulgaria, recent developments, regulatory base, needs and solutions

INTRODUCTION

Dams are complex multi-purpose engineering facilities which are always built in connection with a characteristic particular set of local conditions (hydrological, geological, topographical, economic etc.). Their construction is a result of complicated investment process consisting of several simultaneously running lines of activities such as administrative, financial, technical, economical, social, environmental. One activity of special importance in this spectrum is the technical design in all its particular fields and phases. In the design namely, all parameters, scenarios and modes of the operational life of the dam and its appurtenant facilities incl. the reservoir are formulated with respect to the particular water resources management tasks to be solved and to the requirements of the currently active codes and other regulations. It is well known in this connection that the operational life of the dam as a set of hydraulic structures essentially depends on the maintenance of the facilities. The latter's performance in fulfillment of the formulated operational tasks is not possible without such proper surveillance and maintenance. The operation of the dam and its structures ends with conservation or removal of the dam, and such activity also is subject to the development of special and very particular design solutions and their subsequent constructional implementation.

[1] Professor, Dr., MSc (CEng), Department of Hydraulic, Irrigation and Drainage Engineering, University of Architecture, Civil Engineering and Geodesy (UACEG), 1, Hr.Smirnenski Blvd., 1046 Sofia, Bulgaria,
e-mail: kiss_fhe@uacg.bg

It is well known as well that the safety of the dams – both structural and operational, is an aspect of special importance related to these facility complexes due to their high secondary risk since possible failure scenarios may have in many cases devastating consequences. Such scenarios can have different roots because dam-reservoir-foundation systems are complex ones subjected to a wide spectrum of possible loads and impacts with different probability of occurrence during their long operational life. The real-world phenomena and the more than century-long experience in the field of Dam Engineering have made the Dam Safety a separate scientific branch with especially intensive development in the last decades and a large number of papers, reports and regulative documents as a product. Only in the International Commission on Large Dams (ICOLD), this development resulted in the issue of two important documents quite recently – the Bulletins 154 (ICOLD, 2017) and 167 preprint (ICOLD, 2018).

The present work constitutes an attempt for a short analysis of the current status in the field of Dam Safety in Bulgaria considering its more recent historical development as well as the wide variety of related problems and the activities undertaken for their solution. This is not the first study of these problems, moreover since they became more topical with the time. Here in this connection, the works (Toshev et al., 2012), (Stankulova, 2017) on general and particular issues of the small dams should be mentioned where some operation and maintenance problems became more obvious lately. Of course, a complete study would require large amount of reliable input data, its statistical processing over decades and a comprehensive multi-disciplinary analysis with the boundary conditions of the overall national development in the considered time period. Since such task would go far beyond the frame of this short report, further below we'll aim mainly at the qualitative presentation of the main dam safety related groups of problems, the sources of these problems and some ideas for solutions. The emphasis below is on the operation of dams although in the analysis of dam safety issues, the whole process of preliminary studies, design, construction, operation and maintenance up to the possible decommissioning should be always kept in mind.

DAM SAFETY IN BULGARIA – RECENT DEVELOPMENTS

Historical background

The construction of larger dam reservoirs began in Bulgaria shortly before the Second World War but the actual intensive Hydraulic Engineering construction including building of almost all dams now in operation was carried out after 1945, during the so-called socialist development. There are more than 6500 water objects in Bulgaria currently subject to water right permits. More than 4000 of them are small dams as covered by Bulletin 157 (ICOLD, 2016). They were built predominantly in the 1960s and 1970s serving most of all agricultural purposes – local irrigation and stock farming. With very few exceptions as parts of some industrial facilities, these are embankment dams. In the decades of socialism after 1944, large profiled state design and construction enterprises with their local branches were engaged in the design and construction of such dams on the whole territory of Bulgaria for enabling the development of local agriculture besides the large national irrigation systems.

The large dams in Bulgaria according to the definition of ICOLD are 212. With very few exceptions, they all were built after 1944, and about 10 of them were completed after 1989. The state-owned National Electricity Company (in Bulgarian: Национална електрическа компания ЕАД) owns and operates 29 large dams (12 concrete, 11 embankment and 6 masonry ones) and 12 small dams (11 embankment and 1 concrete one). The state-owned enterprise "Irrigation Systems" (in Bulgarian: Напоителни системи ЕАД) owns and operates 138 large and 50 small dams. With some very few exceptions, they all are earth-fill dams. In general, the remaining large dams are owned and/or operated by the water supply companies.

With very few exceptions, all dams in Bulgaria were designed, built and are still operated only by Bulgarian engineers and technical personnel. At the same time, the related national codes and

regulations for preliminary surveys, design and maintenance of dams were developed from the very beginning after 1944 with respect to the obtained experience and the current best practices not only of the Soviet Union and the other socialist countries (Petranov et al., 1955) but also of the world leading countries in the field of Dam Engineering. As a result, simultaneously with the use of leading foreign regulative documents, the national codes and guidelines were developed covering particular technical fields and types of facilities.

At the time of in-depth political change in Bulgaria in November 1989, all large dams were state-owned and operated either for electricity production, or for irrigation, or for water supply by the corresponding state enterprises. Since Bulgaria is a country with relatively quite poor water resources per inhabitant, many of these large dams were designed and built as multi-purpose reservoirs. The coordination of the water resources management by these reservoirs also was centralized and carried out by state structures. Due to the importance of the large dams and their reservoirs for the overall development of the country, the state enterprises responsible for the operation of dams had clear structures, resources and personnel for fulfillment of their tasks. After 1989, despite of the deep administrative and political changes, almost all large dams remained owned either by the National Electricity Company, or by "Irrigation Systems", or by the water supply enterprises. In general, the local structures for dam operation remained kept in these fields of water management with their particular experience and knowledge, and only the continuously growing lack of resources remained the most severe problem. Thus, the structural and operational safety with respect to the large dams remained in general well preserved.

In the field of small dams, the development was more turbulent (Nikolov and Kisliakov, 2018). After the fundamental political change in Bulgaria in 1989, all cooperative farms and so-called agricultural-industrial complexes were liquidated. The related administrative procedures were forced in time in connection with the restitution of the land property nationalized after 1944. In the frame of this process, many small dams owned previously by cooperative farms were sold, however, with deal conditions according to the state of the legislative environment in the field at that time. Later on, some conditions related to this legislation changed, and this caused on its part severe problems for some of the new dam owners. Furthermore, all responsibilities for the further operation of all remaining small dams were administratively transferred to the local municipalities. On the one hand, they had neither the qualified personnel nor the financial resources to perform proper maintenance of the dams and their facilities. On the other hand, due to the collapse of the national agriculture and the steady evacuation of the land population, there is currently in fact almost no need more for the water from all these small reservoirs. As a result, the technical maintenance of the small dams as an inherent operation component was disregarded for years with all related consequences.

The further development in the field of small dams up to now is also characterized by two other features. The municipalities owning small dams always tried to find mechanisms for financing the technical maintenance of the facilities. Some solutions were found, however, they caused some other problems which will be addressed further below. At the same time, there were continuous and intensive attempts for corresponding development of the complicated legislative environment in the field which had to enable general solutions of the most important problems related to the dam safety above all.

All above considerations are related to the technical maintenance of the dams and their facilities as well as to the dam safety, respectively. The other side of the problem is presented by the water resources management of the small dam reservoirs in particular, that is, by their operational safety. As already mentioned, after both the collapse of the Bulgarian agriculture and the population migration following the political change in 1989, many of these reservoirs were simply not needed anymore. Hence, the interest for their ownership, operation and maintenance was not directly present. This was a severe problem since on the one hand, these small dams are extremely valuable facilities of the water infrastructure in the conditions of relatively scarce water resources in Bulgaria. Furthermore, although small but numerous, they contribute to the damping of the peaks of flood events in whole

catchment areas as this was the case of the flood in August 2014 in Northwestern Bulgaria (Kisliakov, 2015). On the other hand however, the long-term absence of proper technical maintenance substantially reduces their safety with all negative consequences.

In the last several years, intensive work was done by all involved parties for qualitative improvement of the conditions for technical maintenance of the dams in Bulgaria. In fact, there are no substantial issues with the large ones owned either by the National Electricity Company and serving with priority production of electricity from hydropower, or by the state enterprise "Irrigation Systems", or by the water supply companies. They all have special operational units with experienced staff and resources for proper maintenance of the facilities. The main problems with the status – both technical and operational, are connected most of all with the small dams owned by local municipalities. However, a key person in the latter relation is the local district governor who is directly responsible for the safety of every dam in the district and its appurtenant structures. Once a year, he/she must organize an expert commission for analysis of the status of these facilities. Twice yearly, every dam owner must arrange thorough technical review of the facilities. In general, this has become a working mechanism recently, however, the governors hardly have the resources needed for implementation of the results from these analyses.

Legislative environment

Currently, there are more than 40 acts and subordinated legislative documents covering the whole spectrum of hierarchical range which regulate all aspects of the technical operation of the dams in Bulgaria, their safety and the technical maintenance of the facilities (www.lex.bg). Presenting and discussing them here would go far beyond the frame of the present short report. A special feature in this connection is the fact that the property and the operation of the water body in the reservoir is still separated from the operation of the dam and its facilities. Moreover, different ministries are responsible for these management fields. In some cases, this causes some issues in the operation as a whole set of interrelated activities, and attempts at highest administrative level are made currently for overcoming this formal separation.

It should be noted that this regulatory system is a dynamic structure being continuously in development and improvement in terms of more adequate reflection of the reality for decrease of the identified problems – technical, administrative, legislative, operational, environmental etc., and increase of the structural and operational safety, respectively. It also has to be emphasized that the safety of a dam is an issue which has to be addressed during the whole development process of a dam project – from the first reconnaissance works and preliminary studies to the end of the operational life of the dam and its possible decommissioning. As already mentioned above, the national system of particular technical codes and guidelines exists and is being upgraded, although relatively slow. For all appurtenant structures, the Eurocode (EN) is valid as well with all corresponding national annexes. In the field of Dam Engineering, the Bulgarian codes about hydraulic structures in general and about embankment dams clearly introduce importance classes of the dams and their facilities, according to which all activities in the mentioned project development process are specified. Furthermore, levels of impact (for example – annual probability of exceedance of design flood) are specified as well according to the particular class of importance. The Bulgarian code for seismic resistant design of buildings and facilities of 2012 comprises dams (unlike Eurocode) and specifies the necessary design requirements for seismic impact.

In all cases when a particular problem is not clearly covered by the current national regulations, the most advanced solutions to this problem available worldwide are applied with corresponding justification. In such cases, the owner as client usually organizes special expert meetings with external reviewers for ensuring the safest and technically most appropriate solution. For example, recommendations like ICOLD documents – Bulletin 168 (ICOLD, 2017) should be mentioned here in addition to the above cited bulletins, serve this purpose. Furthermore, EU Directives and related documents, internationally recognized recommendations and guidelines as well as modern best practices are implemented in such cases. Other established related sources are considered, too –for

example (Degoutte, 2002) in the field of small dams, or (Tanchev, 2014) in general. Special attention is paid to the recent research activities in this field as well, especially to the ones covering similar problems, such as (Meghella et al., 2008). The vast amount of publications in profiled journals as well as the proceedings of the numerous special scientific forums in the field of Dam Safety serve as intensive and reliable research information stream in this connection.

A key issue related to the dam safety management is the ownership of the dam and its appurtenant structures. A central role in the contemporary national legislation after 1989 in this field has the Water Act (first release in 1999). The water in the surface water bodies (including the dam reservoirs) is public state property while the dam itself and its facilities may be owned by a different type of company. The largest dams in Bulgaria and their reservoirs are called complex (in the sense of multi-purpose ones) and important dams and are listed in the special Annex 1 to the Water Act. In the latest issue of the Water Act of 3^{d} July 2018, there are 53 such large dams listed in Annex 1. They (i.e. these dams and their appurtenant facilities, and not only the reservoirs) also constitute public state property although operated by different companies, mostly state-owned ones.

It also should be mentioned in this connection that the most recent and important changes of the Water Act will result in corresponding changes in several subordinated documents as well. The most important one is the Ordinance about the technical operation of the dams and their appurtenant facilities. The first version of this Ordinance was issued in January 2004 (the so-called Ordinance 13). A more recent version of the document was of October 2016 and now, a next release of this decisive regulative document is being prepared with respect to the last state of the legislative environment in the field.

The environmental aspects of dams are subject to special concern, too. Recently, the legislative component of these aspects is rapidly growing, especially with the implementation of the strategies, policies and directives of the European Union. One important issue related to the operation of dams is the water quality in the reservoir. This requires better care not only for the water quality in the dam reservoir itself but also for the run-off and pollution prevention in the whole catchment area, respectively. Furthermore, the necessity of regular preparation of plans for assessment and management of flood risks (which are important regulatory documents together with the River Basin Management Plans) is both formally obligatory and directly related to the dam safety.

Dam operation and administrative developments

Since July 2015, the State Agency for Metrological and Technical Surveillance – SAMTS (Bulgarian: ДАМТН) is officially responsible for all issues of the technical operation of the dams in Bulgaria and their safety. This transition was accompanied by a still running substantial transformation of both administrative structures and regulatory documents.

The Main Directorate “Supervision of dams and their appurtenant structures” at SAMTS has only control functions, i.e. it is not engaged itself in performing technical operation and / or maintenance of dams and their facilities. In general, the experts there examine the technical state of the dams periodically, formulate improvement requirements if necessary and control latter’s fulfillment. Currently, a global national information system is being developed with online platform for data management and status monitoring of all dams in Bulgaria.

Although the SAMTS works together with all related parties if necessary, some administrative tension sometimes arises, especially when contradictory interests are present – for example, when an act of violation is drawn up of a dam owner while it is objectively evident that he/she has not had the possibility to ensure the required activities for the maintenance needed.

With the mentioned above last changes and amendments of the national Water Act of July 2018, a new State Enterprise Management and Operation of Dams – SEMOD (Bulgarian: ДПУСЯ) was created. This company will perform complex management of dams which constitute public and

private state property. For this purpose, the state by decision of the Council of Ministers grants the company such type of property, including dams, the property on which municipalities have gratuitously placed at the disposal of the state or in cases when the property is not cleared yet. The dams owned or operated by the National Electricity Company, "Irrigation Systems", "Zeminvest" EAD (company of the Ministry of Agriculture and Foods, owner of numerous small dams in the whole country) as well as by water supply companies with state or municipal participation or water supply companies under concession with the duty of the licensee to carry out rehabilitation of the facilities, remain outside of the scope of activities of the new company. The financing mechanism and the structure of the executive board of SEMOD were formulated as well. The interested municipalities were given 3 months to apply for such transfer of owned by them dams which they are unable to maintain properly according to the formulated procedure. The government authorized the State Consolidation Company to carry out the necessary maintenance, repair and rehabilitation works on the dams where necessary, upgrading its budget, respectively.

This was a very important regulation step. As mentioned above, the municipalities obtained administratively the property on large number of dams, however, without the resources for their maintenance and repair when necessary. According to recent reports, over 800 dams need repair works, for about 400 of them this need is urgent, however, still without direct thread to the population downstream. The new regulation will enable the direct involvement of the state in the solution of these problems.

PROBLEMS, ACTIVITIES, RECOMMENDATIONS

Legal and administrative issues

In this section, the following main issues can be formulated as currently identified in the operation and maintenance of dams:

- After having become owners of numerous small dams without having the needed resources for their proper maintenance, many municipalities gave the reservoirs for rent. As a result, the renter usually not only restricted the access of any other parties to the reservoir but also to all dam facilities for maintenance. At the same time, the renter had no responsibility for the technical status of the dam and its appurtenant structures. In most cases, the renter used the dam reservoir as a fish farm and installed meshes at the spillway for preventing the fish to escape. Although such installations are indeed extremely dangerous for the dam structural integrity, deficiencies in the actual regulations and in the particular contract formulations made them happen in many cases for years.
- As mentioned above, the land property was restituted in general in the 1990s. However, during the liquidation of the cooperative farms, many small dams were sold by tenders. Later on, it became obvious in many cases that the legal owner of the dam didn't have in fact anything more since the land below the reservoir was returned to its previous owners, and the water in the dam reservoir is public state property. Thus, the dam owner had often even no more access possibility to the facilities for whose technical state and safety he/she was directly responsible. This is indeed a severe issue in many cases still open and directly related to the maintenance and safety of the dam and its structures.
- The previous issue is directly related to the next one as already mentioned above – the separation between dam with its appurtenant structures and the water in the reservoir. These two items are inherently connected by the purpose of the dam as well as by the hydraulic and structural engineering facilities serving the reservoir water management. Attempts are currently made for overcoming this problem by sharing responsibilities or by better consideration of the reservoir management with respect to the maintenance and operation of the dam and its facilities. This issue holds in general for all dams – both small and large ones.
- The lack of resources for technical maintenance of the small dams and their structures brought some small dam owners to the necessity either to keep the corresponding reservoir

permanently empty or to cut the dam body and thus to prevent any further impounding. So, they also prevented any flood risks for the downstream residents. Such destruction was usually performed without any technical design and compliance with the related regulative requirements. Of course, the result is devastating for the materials of the dam body, too.

- The lack of resources (i.e. finances, qualified personnel, equipment etc.) for technical maintenance of the small dams and their facilities including for carrying out reparatory works sets many municipalities as dam owners between the hammer of the legal requirements and the anvil of resources. The constitution of the new state enterprise SEMOD with the last release of the Water Act of July 2018 as mentioned above gives many such municipalities the chance to hand over the duty for proper further maintenance of particular dams to the state.
- The emphasis on environmental friendliness has led recently to some curious legal requirements. For example, every new dam (no matter how large) must have a fish pass according to the Act for Fishery and Aquacultures. In the process of legislation development, such examples of nonsense should be cleared.

Problems of the technical maintenance

The following issues due to the lack or even absence of technical maintenance can be formulated with respect to the performance exclusively of small dams, mainly according to (Nikolov and Kisliakov, 2018):

- In many cases, there has been no technical maintenance of the dams and their facilities. There is no monitoring system, no measurements and analyses of the technical conditions are carried out. Usually, there is no technical documentation including design and/or as-built drawings left.
- Settlement of the embankment, mostly at the central part of the dam. Thus, the dam crest level has sunk below the maximum water level in the reservoir, and the risk of crest overflow during flood conditions strongly increases with all negative consequences of such event.
- The legal requirement for cleaning the river bed 500 m downstream of the dam is in general not held by the dam owner.
- Many small dams have suffered some damages over the years of operation without proper maintenance. The need for a serious and urgent repair for restoring their full operational functionality only increases with the time. Otherwise, subsequent load impacts and floods could lead to heavy damages of the dam body with possibly uncontrolled release of the impounded water. Independantly how small this volume might be, the resulting flood wave could certainly have severe consequences.
- Erosion of the streambed downstream of the spillway. In some cases, the structure of the spillway itself is in a good condition. However, the following spillway race and the stilling basin (if available) have been for years subjected to erosion without maintenance and repair. Under some particular geological conditions, this erosion may have become quite intensive.
- Damaged or clogged bottom outlet which leads to the necessity of draining the reservoir only by means of an external temporary siphon.
- With the time and without any maintenance, the spillway inlets of numerous small embankment dams have clogged by floating debris during relatively small flood events. Every time when there was flow in such spillways, additional amounts of debris were added. Thus, without cleaning the spillway inlet, the risk of dam crest overflow increases.
- Non-maintained downstream dam slopes with developed dense plant and tree cover. These surface conditions on the slopes often hinder the access to the dam crest and all appurtenant structures.

Problems due to impacts exceeding the extreme design load cases

It is well known that each dam with its appurtenant facilities belonging to some class of importance is designed for certain combinations of loads and impacts of some intensity. Some of these impacts have stochastic nature (floods, wind waves, earthquakes). According to the active national codes and guidelines, an intensity with different annual probability of exceedance (APE) of these impacts is assigned to the dams and facilities of different importance class. The lower the class of importance is, the lower the design intensity of impacts with

stochastic nature and the higher the probability of exceeding of these intensities during the operational life of the dam, respectively. A question of crucial importance for the safety of the dam and its facilities arises, what will happen if this design intensity is exceeded. Such scenario corresponds to the so-called "overload conditions" although the importance class is to be increased by one level if population would be endangered in the case of dam failure according to the active national regulations. Moreover, the structural integrity of the dam is to be proved and ensured for load and impact intensities corresponding to the next higher importance class, too. For large dams, this gives impact levels corresponding to the most recent recommendations of ICOLD. For dams of the highest class of importance, PMF and SEE / MCE have to be additionally accounted for, respectively.

The situations of "overload conditions" are especially realistic for the small dams. The problem is that the design of such dams is performed with relatively high probability of exceedance of the design loads and impacts according to the code requirements. Thus, it is quite possible that such damages occur during their operational life. This only emphasizes the importance of proper regular maintenance and carrying out of all necessary repair works on time. For example, at several small dams during past flood events, the dam crest was overtopped as well (Kisliakov, 2015). Fortunately, in the most cases these dams retained their overall structural integrity, and no uncontrolled release of the reservoir content occurred. However, the dam body in such cases was damaged, and all necessary repair works had to be carried out as soon as possible.

Most recently, special and growing attention is paid to the performance of the dam and its facilities in the case of "overload conditions" as crucial for its safety (Pohl, 2018). There also are regulative documents already developed especially considering such conditions and supplying both valuable theoretical background and recommendations for the practical implementation (Gemeinsamer Themenband, T1/2017).

Solution approaches and some recommendations

Based on the above summarizing presentation of the main safety conditions, issues and considerations of the dams currently in Bulgaria, the following recommendations may be formulated:

- The necessary administrative work has to be done for overcoming the separation in the technical and operational management of the dams between the dam with its structures and the water reservoir. Careful and justified distribution of the activities and responsibilities, respectively, has to be carried out together with a better coordinated complex management of both the reservoir and the dam with its facilities.
- The performance of the facilities under so-called "overload conditions" for the particular class of importance has to be regulated more precisely and upgraded with respect to the state-of-the-art in this field.
- The property issues related to the dams, their appurtenant facilities and the land beneath the reservoirs need solution of the open issues in every particular case based of course on the common national legislative base.
- Highest priority has to be assigned to the repair of dams with structural damages of the dam body and to works for restoring the operational ability of the safety-related appurtenant structures.

CONCLUSIONS

From the performed short analysis of the dam safety status in Bulgaria, the following conclusions can be drawn. Most of all, these facilities are the key components of the national water resources management infrastructure at every (i.e. from the lowest up to the highest) structural level. Hence, their safety – both structural and operational (including all related activities for operation and

technical maintenance) should be a matter of highest priority in the strategic national policy in this field.

There are some open issues in several fields related to the dam safety and to the operation and maintenance mostly of small dams in Bulgaria, as shortly discussed above. The nature of the required solutions is very complex and requires on the one hand, interdisciplinary approach by broader teams of experts. On the other hand, a long-term strategic national policy is needed in the field of water resources management and infrastructure in general and of the dams and their safety in all aspects in particular for further development of all necessary political, administrative and financial mechanisms for improvement of the existing well built national network of dams and their facilities.

It is quite clear, however, that the process of developing and implementing such solutions is complicated and requires besides expert knowledge high-level skills in the management of sometimes contradictive interests. Moreover, these solutions need considerable resources but they have no alternative with respect to the dam safety. However, although possible removal of some small dams which currently seem to be not needed anymore (which also would require corresponding design, administrative and construction activities and financing of the implementation) looks like to be a solution, their subsequent building if needed again will be much more difficult and expensive. Hence, similar decisions with long-term effect have to be made very carefully.

We are glad to find out that currently, there is not only the expert but also the political and administrative will for solving the open issues with the status and operation of the dams in Bulgaria for improving their overall safety and operational reliability.

AKNOWLEDGEMENTS

Special thanks for the kindly supplied information go to the Technical Director Dr. V.Slavov, MSc, for the dams owned / operated by “Napoitelni sistemi” EAD as well as to Mrs. T.Opalchenska, MSc, for the dams owned / operated by “Natsionalna elektricheska kompania” EAD.

REFERENCES

Bulgarian legislation gateway – www.lex.bg

Degoutte, G. (ENGREF, Coordination), 2002. Small Dams. Guidelines for design, construction and monitoring, French Committee on Large Dams.

ICOLD Bulletin 157, 2016. Small Dams: Design, Surveillance and Rehabilitation, International Commission on Large Dams (ICOLD).

ICOLD Bulletin 154, 2017. Dam Safety Management: Operational phase of the dam life cycle, International Commission on Large Dams (ICOLD).

ICOLD Bulletin 167 preprint, 2018. Regulation of Dam Safety: An overview of current practice world wide, International Commission on Large Dams (ICOLD).

ICOLD Bulletin 168, 2017. Recommendations for operation, maintenance and rehabilitation, International Commission on Large Dams (ICOLD).

Kisliakov, D., 2015. “Performance and role of the small dams during the flood in North-Western Bulgaria in August 2014”, Proceedings of Conference on topic: The State of the Water Economy Infrastructure, 18th-19th September 2015, Macedonian Committee on Large Dams, Skopje, Republic of Macedonia, 85-92.

Meghella, M., Bueno, I.E., Ortuño, M.M., Lombillo, A.S., 2008. DAMSE – A European Methodology for the Security Assessment of Dams, Deliverable 3 - v.02, EC funded project, JLS/2006/EPCIP/001.

Nikolov, B., Kisliakov, D., 2018. Operation of small agricultural dams in Bulgaria – state-of-the-art ICOLD 2018 Symposium Hydro Engineering, Vienna 2018.

Petranov, Hr., Valchanov, L., Antonov, L., Mitev, D., Popov, B., 1955. Small dams – reconnaissance, design, construction, Zemizdat, Sofia, (in Bulgarian).

Pohl, R., 2018. Dams Beyond Design Assumptions. Daniel Bung, Blake Tullis, 7th IAHR International Symposium on Hydraulic Structures, Aachen, Germany, 15-18 May. doi: 10.15142/T3KM0T (978-0-692-13277-7)

Research project „Assessment of the combined impacts from hydropower plants on the ecosystems and on the ecological conditions of the rivers – ANCHOR", 2015 – 2016. Financial mechanism of the EEA 2009-2014, EEA Grants, Program BG02 „Integrated management of the sea and land waters",Regional Environmental Center (REC) for Central and Eastern Europe, Branch Bulgaria.

Stankulova, D., 2017. "State and operation control of the small dams", Report presented at Water day, April 2017, Sofia, (in Bulgarian), not published

Stauanlagensicherheit und Folgen bei Überschreitung der Bemessungsannahmen nach DIN 19700, 2017. Gemeinsamer Themenband der DGGT, DTK und DWA, T1/2017, 126p.

Tanchev, L., 2014. Dams and Appurtenant Hydraulic Structures. Taylor & Francis Group, London, UK, 1073p.

Toshev, D., Cholakov, T., Todorov, O., Lissev, N., 2012. "State of small dams in Republic of Bulgaria", Vodno delo, Nr.5/6, 2-8, (in Bulgarian)

https://www.juridipedia.com/BG/Targovishte/1521044598125356/%D0%90%D0%B4%D0%B2%D0%BE%D0%BA%D0%B0%D1%82-%D0%92%D0%B0%D0%BD%D1%8F-%D0%9D%D0%B5%D0%B4%D0%B5%D0%B2%D0%B0 (accessed 14.08.2018)

http://iconomist.bg/%D1%8E%D1%80%D1%83%D1%88-%D0%BD%D0%B0-%D1%8F%D0%B7%D0%BE%D0%B2%D0%B8%D1%80%D0%B8%D1%82%D0%B5/ (accessed 14.08.2018)

http://iconomist.bg/%d0%b4%d1%8a%d1%80%d0%b6%d0%b0%d0%b2%d0%bd%d0%be-%d0%bf%d1%80%d0%b5%d0%b4%d0%bf%d1%80%d0%b8%d1%8f%d1%82%d0%b8%d0%b5-%d1%89%d0%b5-%d1%81%d1%82%d0%be%d0%bf%d0%b0%d0%bd%d0%b8%d1%81%d0%b2%d0%b0-%d1%8f/ (accessed 14.08.2018)

5th International Symposium on Dam Safety

October 27-31, 2018

KEY ELEMENTS OF NATIONAL DAM SAFETY REGULATION – THE EXAMPLE OF GREEK DAM SAFETY REGULATION

George DOUNIAS [1]

ABSTRACT

The paper presents the critical elements of National Dam Safety Regulations (NDSR). The ICOLD and World Bank studies are mentioned and the main reasons for the establishment of a general application Dam Safety Regulation are presented. The key elements for a successful NDSR are described. Some dam failures and incidents of Greek dams are briefly mentioned. Then, the steps that where followed for drafting the DSR in Greece are presented, followed by a summary of the DSR, where the main points are elaborated. Finally the first reaction to the DSR and the challenges that are met are described.

Keywords: dam safety regulation, supervising authority, dam surveillance, dam safety review

INTRODUCTION

Dam failures, often catastrophic have occurred since the beginning of dam construction. But "every cloud has a silver lining". For centuries, the failures of dams have provided an opportunity for the advancement of engineering through the investigations that followed. Empirical rules for the design of dams were initially formed, followed later by scientific theories. Hydrology, hydraulic engineering, soil mechanics, engineering geology and other disciplines have advanced following analysis of failures. But the cost for this knowledge has been great.

At present, after the evolution of the disciplines related to dam construction and operation, the existing state of the art is so advanced that if properly applied the risk to the dam works and public safety is minimized. Yet dam failures still occur at a high frequency. Looking into the causes of the recent dam failures it is alarming to note that the great majority of them are caused by well-known mechanisms that were ignored in the design, construction or operation of the works.

Application of "good practice" or "state of the art" was for many years left to individual experts or institutions. Regulations for dam construction still are far behind the regulations for other engineering works. In many countries, permits to erect and operate a dam are concerned more about financial and environmental issues and less about public safety.

The need for general application National Regulations regarding dam safety became apparent and many countries instigated regulations, usually following dam failures. In the United Kingdom, the first Reservoirs Act was passed in 1930, following two dam failures in Scotland and Wales in 1925. It was later updated in 1975 and again with Flood and Water Management Act 2010. The first French regulations were established in the early 1960's following the failure of Malpasset Dam in 1959.

[1] Visiting Professor, Department of Civil Engineering, Imperial College, London, UK – EDAFOS SA, Greece
e-mail: gdounias@edafos.gr

Many more countries have established national general application legislations in the past 40 years.

The international status on Dam Safety Regulations is included in the preprint of ICOLD Bulletin B167 (2017), prepared by the ICOLD Technical Committee on Dam Safety, providing information on 44 countries. The World Bank report by Bradlow et al. (2002) includes information on 22 countries. The report of the working group of the ICOLD European Club (2007 - constantly updated) includes information on European countries. Relevant information is also included in the ICOLD Bulletin B154 "Dam safety management: Operational phase of the dam life cycle".

According to ICOLD B169, the legal and administrative regulations are considered the top priority component for dam safety (Fig, 1).

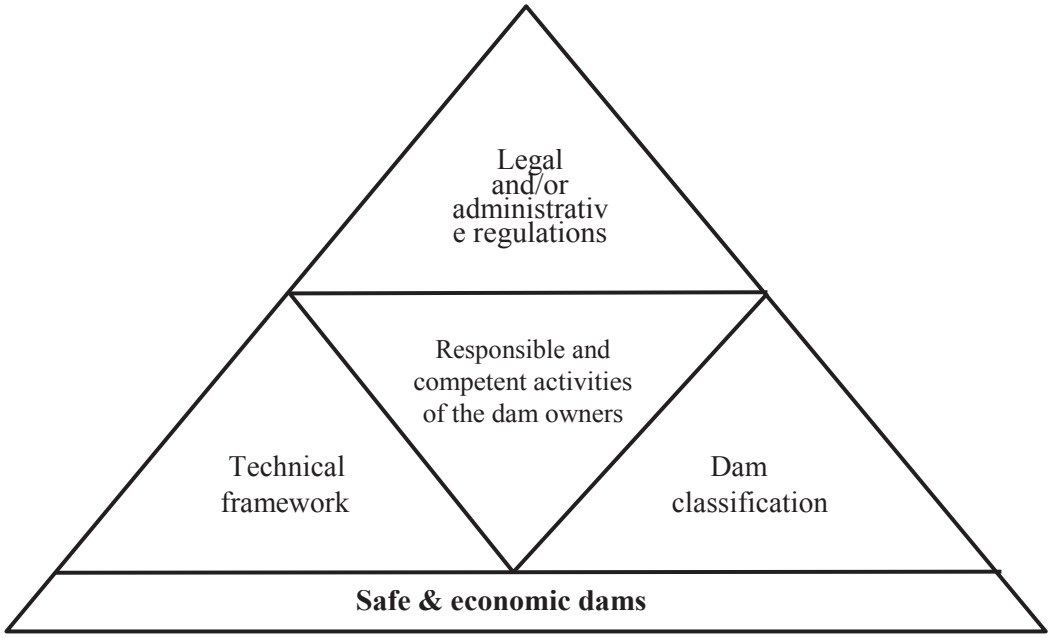

Figure 1. Components of dam safety (ICOLD Bulletin B169 – Preprint)

WHY A NATIONAL DAM SAFETY REGULATION IS NEEDED

Bradlow et al. (2002) argue for the need of dam safety regulations. The reasons they give are:

1. It is essential that each dam owner be able to ensure that its dams are safe and do not pose an unacceptable risk to life, human health, property, or the environment.
2. Dam safety directly influences the sustainability of dam projects and the extent of their potential environmental and social impacts and therefore it is an important consideration at all stages of the dam's life cycle.
3. Dam safety is relevant to a state's ability to comply with its international obligations including transboundary watercourses and the environment, the ability to perform its international financial obligations etc..
4. Dam safety is a matter of great importance in many countries, where a substantial stock of dams exists, because their failure could have significantly adverse social, economic, and environmental consequences.

One could argue that the above targets can be met by individual dam owners following generally accepted guidelines and recommendations. Indeed that is the case in many countries where technical guidance and framework exist. There are though some very strong arguments for a unified national

legislation of general application that will ensure that the technical framework is obeyed. These arguments are supported by numerous examples of ill practice and failures. Some of the reasons for establishment of central dam safety regulation are:

- IMPORTANCE. The dam safety is too important for any country and therefore the central government should have a strong control.
- SAFETY LEVEL. It is fair that the required safety level, i.e. a balance between the risks and the benefits and between social equity and economic efficiency should be defined by legislation for all types of reservoirs.
- UNIFORMITY. It is difficult to have uniformity in the approach to dam safety in all dam owners i.e. state, individuals, municipalities etc., without a national legislation.
- COMPLIANCE. Without a national legislation, compliance to "state of the art" dam safety is left to the dam owner's good will. Often, financial implications impede or delay considerably dam safety measures.
- ORPHAN DAMS. There are dams that were built a long time ago and their present ownership is complicated to such a degree that there is no one clearly responsible for their maintenance.

It has been observed that even very large and competent organizations operating a large number of dams show signs of overconfidence and complaisance regarding safety issues.

In some countries a large number of old dams exist and very few, if any at all, new dams are being built. For such countries, the safety of existing dams is the most important issue related to dams.

Throughout the article the term national is used. In federal countries like the USA or Canada, they use the term federal legislation to distinguish from individual state regulations. In the USA it became apparent that although many individual state regulations exist, there was a need for a federal (national) regulation, established gradually since 1986.

KEY ELEMENTS OF A NATIONAL DAM SAFETY REGULATION

Throughout the ICOLD and World Bank studies mentioned above, there are some key elements that are considered necessary for the formation of a National Dam Safety Regulation, briefly presented in the following paragraphs.

Classification of dams and field of application

Classification of dams, with respect to size of dam and reservoir and with respect to risks posed, is the basis for the regulation. The structures that fall within the regulation should be then defined together with the required actions per dam category.

National dam inventory and Ownership

An inventory of all existing dams and their reservoirs that fall within the National Regulation should be compiled. It is important that the ownership is defined at this stage as the Owner is legally responsible for applying the DSR

Owner responsibilities

Owner responsibilities should be clearly defined for all stages of the dam life cycle including design, construction, first filling, operation and decommissioning. The Owner's responsibilities should be detailed in the Operation and Maintenance manuals and in the Emergency Preparedness Plan (EPP), where his role in emergencies and extreme events and his cooperation with Disaster Protection public agencies should be defined

Paramount for dam safety is that the dam Owner allocates a highly experienced engineer to act as Dam Safety Engineer responsible for the application of the regulation requirements and react

promptly to any incident that poses a threat to safety. This engineer must either belong to an accredited body or be approved by a National Dam Safety Authority and be assisted by personnel depending on the size of the dam works.

The Owner should comply with the DSR regarding keeping data on the dam, surveillance and periodic dam safety reports etc. He should regularly report to the National Authority according to the DSR.

State responsibilities – Technical Framework
An important element is the formation of an Authority, State or independent, which will supervise the application of the DSR and will impose penalties on Dam Operators that do not conform to it.

The Authority should prepare new or adopt existing Technical Framework in order to provide clear guidance and rules for all the issues concerning dam safety.

It is common in all countries to have a multitude of legislations, including Technical Framework, issued by different federal, state or municipal authorities, often with conflicting contents. The task of the central Authority should be to clarify and unify the existing legislation and propose the adoption of new legislation if needed.

The Authority should regularly examine the application of the DSR and update or amend the DSR and the Technical Framework.

Transition period
A transition period should be defined in order to allow adequate time for dam Owners to comply with the NDSR, depending on the stage of the dam, i.e. construction, first filling operation or decommissioning.

Means of enforcing the regulation
The Authority should be given the legal means to ensure the application of the NDSR. Such means can include financial and legal penalties, withdrawal of licenses etc.

DAM INCIDENTS AND FAILURES IN GREECE

Large dams constructed and operated by the Public Power Corporation, the Ministry for Infrastructure, the Athens Water and Sewage Company etc. are managed well and are behaving very well (Dounias et al, 2012). In many of the smaller dams though, poor standards of design and construction were followed and problems appeared since their first impoundment. Some examples of failures are given here. All these failures would have been avoided if the procedures included in the recent DSR were followed.

Monolithi dam was a homogeneous embankment 8m high that was breached due to internal erosion in 1993, soon after its first filling in the same year (Photograph 1, Nikos Naskos, personal communication). Many such small dams built without proper design and construction had a similar fate in the early 1990's.

Triadi Dam, Thermi, Prefecture of Thessaloniki (Photograph 1, Kazilis, 2008), is a 36.5m high homogeneous embankment dam that was built in 1997. Soon after its first filling, seepage was observed on the downstream face that evolved slowly over the years. In July 2007, with the reservoir almost full, a large pipe (approximately 1m diameter at its exit) was formed close to the right abutment, 25m below crest level. The reservoir was emptied above this level, and the dam suffered cracks and slumps on the upstream face but it did not collapse. It was later repaired and now it is a touristic attraction.

Photograph 1. Monolithi Kilkis Dam failure (N. Naskos, personal communication 1993)

Photograph 2. Triadi Dam, 2007, Thermi (Kazilis, 2008)

Kamares dam on Sifnos Island, a 21m high masonry structure, developed a large gap on the right abutment following overtopping when the dam was 6m from completion. It was mainly due to inadequate diversion provisions and poor foundation contact (Photograph 3, Moutafis, 2008). It was later repaired and now is operating properly.

Gennas Dam on the Island of Crete, an approximately 11m high concrete dam, developed a large hole near the right abutment mainly due to inadequate foundation contact (Photograph 4, Nikos Moutafis, personal communication).

Photograph 3. Kamares Dam, Sifnos Island 2003 (Moutafis, 2008)

Photograph 4. Gennas Dam failure, 2014 (N. Moutafis, personal communication)

Sparmos dam in the Municipality of Elassona, a 16m high homogeneous embankment was breached in March 2016 due to internal erosion (Photograph 5, Dounias et al, 2017). The dam was built in 1990 and developed seepage on the downstream slope soon after its first filling. It is surprising that internal erosion was evolving gradually for almost 25 years before uncontrolled piping developed, leading to the dam breach.

There are many more incidents that have occurred on relatively small dams with a height of up to 45m. It has been extremely fortunate that all dam incidents and failures caused no human fatalities and the loss of property was small. Some recent failures of similar size dams have caused many deaths in other parts of the world. Incidents creating a high risk of failure have been in some cases repaired with proper design and construction.

Photograph 5. Sparmos Dam failure, 2016 (Dounias et al, 2017) Photo by Eurokinissi

THE GREEK DAM SAFETY REGULATION

Status before the establishment of the DSR

There are approximately 250 dams in Greece of which approximately 150 are large dams according to the ICOLD criteria. Many more dams are currently under construction. The main purposes of large dams are power production, irrigation and domestic water supply. The very large dams were built mainly by the Public Power Corporation, a state owned company, by the Ministry for Public Works (Infrastructure), by the Ministry for Agriculture and by regional governments or municipalities. Very few privately owned dams were recently built mainly for energy production.

A large number of dams were built after 1990, normally following high standards of design and good construction practice. There were though many instances of dams 10 to 25m high that were constructed by municipalities with only rudimentary designs and by non-experienced contractors. That has resulted in a large number of unsatisfactory dams with poor safety performance. To make bad things worse, the ownership of many of these dams is disputed and they are practically unattended.

Dam Safety Regulations or Guidelines did not exist in Greece before 2017. However, a recent law concerning environmental licensing imposed the dam owner to provide a safety surveillance program for all dams (both existing and new dams). Also, legislation for dam design imposed a dam break study to be conducted in order to proceed with licensing for construction of a dam. In addition, an Emergency Plan had to be drawn up for all dams. This task was carried out by the regional administrations, where the dam is located, with the assistance of the dam owner.

Steps taken towards a National Dam Safety Regulation

Initially, a working group by the GCOLD drafted a proposal for a DSR after studying relevant regulations from many countries. A workshop was organized with invited speakers from relevant Dam Safety Authorities from Europe and the USA. Then a broad working group was formed by the Ministry for Infrastructure with the participation of all interested stakeholders. Many agencies dealing with design, construction and operation of dams participated and a final DSR was produced together with a proposal for the formation of a Dam Administration Authority. The Dam Administration

Authority is operating within the Ministry for Infrastructure, headed by the General Director of Hydraulic Works.

Main elements of the Greek Dam Safety Regulation (DSR)
The main provisions of the DSR are briefly described in the following paragraphs, article by article.

Article 1: Purpose of DSR
The purpose of the Dam Safety Regulation is the establishment of rules and procedures for the reviews – inspections of dams, private or public during the period of their construction and operation, aiming at their safety, so that conditions that could endanger human life, properties, structures and the environment, are prevented. The Dam Owner (DO) is responsible for the application of and compliance with the DSR.

The DSR does not lift or suspend any obligations and responsibilities of the Owner that are defined by the existing laws and regulations. The same holds true for any institutions or persons that are delegated by the Owner and participate in any of the dam life stages from the design till the abandonment or/and the decommissioning.

The Dam Administration Authority (DAA), constituted as Committee with the new legislation, is responsible for ensuring conformity and compliance with the DSR. The DAA will take the initiative for the preparation of a complete Technical Framework (guidelines) incorporating any current regulations according to the existing legislation.

Article 2: Area of Application
The DSR applies to all dams that form reservoirs or control water flow when:

- The visible dam height is larger than or equal to 10m, or
- The visible dam height is from 5m to 10m and the reservoir has a capacity equal to or greater than 50.000 m^3.

The visible dam height signifies the height of the structure above the river bed and is considered critical for dam safety issues. It is different than the dam height as defined by the International Commission of Large Dams (ICOLD), where it is measured from the deepest point of the foundation to the crest. Based on the dam height and the reservoir volume, the dams are classified in three (3) categories:

Table 1. Dam Classification

DAM CATEGORY	DESCRIPTION
I	Visible dam height, H ≥ 40 m. or Reservoir volume > 10.000.000 m^3, irrespective of dam height
II	Visible dam height 40 m. > H ≥ 20 m. or Reservoir volume ≥ 1.000.000 m^3, , irrespective of dam height
III	Dams that are not classified in categories I and II

Dams that are initially classified according to the above criteria in Categories II or III, can be moved to the immediately higher category after a substantiated decision of the Dam Safety Authority. Also dams that are initially classified according to the above criteria in Classes I or II, can be moved to the immediately lower category, only if their possible failure does not entail risk of human losses, or considerable economic losses or serious environmental consequences.

Article 3: Definitions
A complete set of definitions is included for the most important elements of the DSR.

Article 4: General obligations of the Dam Owner
a. The Dam Owner (DO) must comply with the present DSR in all stages of life of the structure and to notify and receive the necessary approvals from the Dam Administration Authority (DAA).
In any case the DO is solely responsible for the application of the DSR and to ensure the dam safety thought-out its life cycle.

b. The DO is obliged to define, or form, the Dam Construction Body (DCB) before the beginning of construction and to submit the information to the DAA.

c. The DO should define or form the Dam Operation Body (DOB) before the commencement of the first filling and submit the information to DAA for review and approval. First filling cannot be undertaken without an approved DOB.

d. The DO is obliged to submit for notification and approval by the DAA the following folders:
- A Dam Construction Folder (DCF) before the start of construction
- An Approval of First Filling Forder (AFFF) before the plugging of the diversion and the start of impoundment.
- An Approval for Abandonment Folder (AAF) or an Approval for Removal Folder (ARF)

e. The DO is also obliged to inform on time the DAA before the application of any substantial changes and repairs on the dam, following an incident or after review of the design criteria.

f. The DO is obliged to perform surveillance and review, as they defined by Article 16, and submit the relevant reports to the DAA.

Article 5: Dam Construction Body (DCB)
This article describes the DO responsibilities and interaction with the DAA during the design stage up to the beginning of construction. Before the beginning of construction, the DO should define the Dam Construction Body (DCB), the body that will undertake the management and supervision of construction and will be responsible for the application of the DSR up to the time that the dam will be handed over completely to the Dam Operation Body (DOB). The requirements for the staffing of the DCB are outlined including a Dam Safety Engineer (DSE).

Article 6: Dam Operation Body (DOB)
The DOB is proposed by the DO and is approved by DAA before the approval of the first impoundment. The DOB can be a public or a private organization that is staffed with the appropriate personnel and has the ability for the satisfactory and safe operation of the dam. This article describes the obligations of the DOB and its interaction with the DAA, including the appointment of the Dam Safety Engineer (DSE).

Article 7: Design Stage - Obligations during Design
The procedures for the design of dams are outlined in this article. The design of the dam and its auxiliary structures is prepared according to appropriate design criteria that guarantee its safety, with respect to hydraulic, geotechnical and structural design, and regarding the operation of the dam and the environmental impacts. Integral part of the design is the preparation of the following manuals that when necessary are updated before the first impoundment:
- Operation and Maintenance manual
- The Dam Surveillance Manual
- Emergency Preparedness Plan including flood propagation studies
- First impoundment manual

Article 8: Design Stage - Surveillance Manual
It outlines the contents of the Surveillance Manual to be initially prepared by the designer and updated as necessary during construction.

Article 9: Design Stage - First Filling Manual
It outlines the contents of the First Filling Manual to be initially prepared by the designer and updated as necessary during construction.

Article 10: Design Stage - Emergency Preparedness Plan (EPP)
It outlines the contents of the Emergency Preparedness Plan to be initially prepared by the designer and updated as necessary during construction. The obligations of the Dam Owner are covered by this EPP. The EPP after approval is submitted to the national and local Disaster Prevention Organizations in order to be incorporated in the general disaster prevention plans.

Article 11: Construction Stage - Dam Construction Folder (DCF)
The DO submits to the DAA for approval the Dam Construction Folder (DCF) that includes, not limited, the following:

- Approved Final Design that includes treatment of all required disciplines (geological, hydraulic, geotechnical, environmental, structural, electro-mechanical etc.)
- Basic design criteria
- Tender documents, if existing
- Program for financing of the construction
- Organization chart with personnel and duties allocated as defined in Article 5.

The DCF is submitted at least 2 months before the tender for the project. The DAA is obliged to respond within one (1) month. The one month reply period holds also for any re-submissions.

Article 12: Construction Stage - Construction
The article defines the obligations of the DCB during construction. The DAA can visit and check – inspect during construction, or/and after a request by the DCB. After every check – inspection the DAA prepares a report to the DCB. If the report includes observations or suggestions that involve the safety of the dam, the DCB must observe them. The DAA report will be filed in the Dam Register.

Article 13: Construction Stage - Approval of First Filling Folder (AFFF)
The DCB applies for approval of the first filling of the reservoir by submitting the Approval of First Filling Folder (AFFF) containing as a minimum the following:

- The setting of the Dam Operation Body (DOB)
- The updated Dam Register
- The Plan for First Filling including Organization chart with responsibilities of the personnel of the DCB and the DOB (if the presence of the DOB is foreseen during first filling)
- The Surveillance Manual
- The Operation and Maintenance Manual
- The Emergency Preparedness Plan (EPP)

The DAA is obliged to respond within one (1) month from the submission of the AFFF approving or rejecting justifiably the application, or asking for clarifications – amendments – corrections. The one month reply period holds also for any re-submissions or additions.

Article 14: First Filling Stage
This article outlines the procedures that should be followed and the obligations of the DO during the stage of first filling, as well as the communication and inspections by the DAA.

Article 15: Dam Register
The Dam Register is prepared by the DCB during construction and includes all information relevant to the design, construction, behavior, inspections etc. Later, the Register will be kept and updated, on every stage of the life of the dam, by the DOB and will be available for inspection by the DAA.

Article 16: Obligations during operation - Operation Stage
The dam is considered in the Operation Stage when it is capable of controlling or storing water. The DOB must satisfy all safety rules, check the behavior, repair any damages and maintain the dam according to the Design and the O&M Manual, even if the dam is not used as intended.

The DOB should continuously perform inspections and checks, as detailed in the O&M Manual. The various types of checks and inspections that the DOB should undertake are [a] Basic inspections, [b] Regular inspections, [c] Safety inspections, [d] Non-routine and Emergency inspections and [e] Review of design parameters and methods of analysis. The inspections and checks are carried out according to the Surveillance Manual and the present article.

Basic inspections are general quick inspections aiming at the early identification of problems. The common inspections include visual reconnaissance and instrumentation measurements.

Regular inspections are carried out at regular intervals and they include detailed visual reconnaissance, recording and interpretation of instrument readings and preparation of an inspection report that is filed in the Dam Register. The DOB should notify the DAA for the results of the regular inspections within 15 days after the report preparation.

The Safety Inspections are detailed checks of the dam performance. Special experienced experts should be employed having at least a 20 year experience. It includes all that is included in a Regular Inspection plus verification of the dam's behavior according to the design, special technical checks of the installed equipment, review of the organization and adequacy of the personnel employed on the dam safety etc. A detailed report is prepared and submitted to the DAA within one month. The DAA reviews the report, inspects the dam together with DOB personnel and approves the report. This approval acts as an approval for the continuation of the dam operation. If the DAA has observations or proposals, the DOB has to apply them within the allocated time. The approval by the DAA, or a justifiable rejection should come within 3 months.

Non-routine and Emergency Inspections are carried out after an extraordinary occurrence such as complete or very substantial lowering of the reservoir, alarming instrumentation readings, big earthquakes or floods, malfunctioning of electro-mechanical equipment that cannot be readily repaired and influence the operation of the dam etc. The DAA can participate in extraordinary inspections if asked by the DOB. The frequency of inspections per dam category is shown on Table 2.

Table 2. Frequency of inspections

INSPECTION FREQUENCY	DAM CATEGORY		
	I	II	III
Basic inspections	Daily	Weekly	Monthly
Regular inspections	Yearly	Every 2 years	Every 5 years
Safety inspections	3 years after first filling report and then every 5 years or less.	6 years after first filling report and then every 10 years or less.	10 years after first filling report and then every 20 years or less.
Non-routine and emergency inspections	When required		
Review of design parameters and method of analysis	$\leq$ 30 years	$\leq$ 60 years	If required

The inspections and checks will be carried out by experienced personnel and dam experts. The DOB is responsible for the planning and management of the inspections and for facilitating external inspections when required by the DAA. The bodies and experts participating in the inspections are as defined on Table 3.

Table 3. Bodies participating in inspections

INSPECTION TYPE	INSPECTION BODY
Basic inspections	DOB
Regular inspections	DOB
Safety inspections	DOB & DAA
Non-routine and emergency inspections	DOB (and DAA, if asked)
Review of design parameters and methods of analysis	DOB with the participation of expert engineers in dam design and operation

Article 17: Dams presently under construction, first filling or operation
Dams under construction, first filling or operation at the time of the establishment of the present DSR are given a transition period for registering with the DAA and comply with the DSR.

A three (3) year period is given for dams in operation in order to submit to the DAA all the data included in Article 13 with the exception of the First Filling Plan. Shorter periods are defined for dams under construction or first filling.

Dams that are abandoned or are not used as designed will be initially considered in operation and application to the DAA should be made for a change of status. In case that the ownership of the dam is not evident, the Regional Government should undertake the compliance with the DSR.

Irrespective of the dam category, the DO has to undertake a Safety Inspection as defined in Article 16 with four (4) years after the establishment of the DSR.

Article 18: Abandonment or Removal of a dam
The Abandonment or the Removal of a dam are the only cases where a completed dam is not considered in operation.

The Abandonment or Removal requires approval by the DAA. The DO has to prepare and submit an Approval for Abandonment Folder (AAF) or an Approval for Removal Folder (ARF). The present article outlines the contents of these folders and the procedures followed.

Article 19: Actions when there is a threat of war or sabotage
When there is a threat of war or sabotage, the DO with its relevant bodies (DCB or DOB), and in cooperation with DAA, are communicating with the relevant Ministries for the undertaking of sufficient protection measures for the safety of the dams.

Articles 20 to 29: Setting of the Dam Administration Authority
Articles 20 to 29 are dealing with the setting of the Dam Administration Authority (DAA). The DAA has presently the form of a committee attached to the Ministry for Infrastructure. The committee has a total of ten (10) regular members, and their substitutes, representing all organizations, public or private, that are involved with the design, construction and operation of dams. The committee is renewed every four (4) years.

The DAA is assisted by a Group of Dam Experts (GDE) called to form review and inspection panels for each dam that is supervised by the DAA. The GDE is formed following a selection procedure

where Universities, Organizations of Dam Owners, Consultant, and Contractors participate. Its members cover a wide spectrum of disciplines and must have extensive experience on their field.

The DAA is financed mainly by the commission that the dam owners pay for its services, plus a state subsidy in the form of personnel provision.

Disobeying the DRS will result in penalties imposed on the DO and its bodies. The type and magnitude of the penalties is proposed by the DAA to the Ministry of Infrastructure.

Initial reactions to the DSR

The new DSR was generally met with enthusiasm from the dam's community in Greece. There was some skepticism regarding its application and the financial support that it requires.

The DAA is now operating for under a year and has received a few requests for approval of first filling. Work groups have been formed within the DAA in order to issue detailed guidelines regarding its operation. The Group of Dam Experts (GDE) has been formed.

The dam owners are preparing their applications for the existing dams and it is expected that as the three (3) year deadline is approaching more and more applications will arrive.

ACKNOWLEDGEMENTS

The first draft of the DSR was prepared by a GCOLD Working Group composed of K. Anastassopoulos, G. Dounias, N. Moutafis and D. Nikolaou. The preparation group constituted by the Ministry for Infrastructure was headed by A. Kotsonis. The first formed DAA is chaired by A. Kotsonis, General Director for Hydraulic Works.

REFERENCES

Bradlow D.D., Palmieri, A.; Salman, S.M.A. (2002), "Regulatory frameworks for dam safety: a comparative study", 2002, The World Bank

Dounias G., Anastasopoulos K., and Kountouris A. (2012), "Long-term behaviour of embankment dams: seven Greek dams", Proceedings of the ICE - Geotechnical Engineering, Volume 165, Issue 3, 01 June 2012 , pages 157 –177

Dounias, G.T., Moutafis, N. and Mamasis, N. (2017) "The failure of Sparmos embankment dam of Elassona Municipality due to internal erosion – Description of the case", 3rd Greek Dams and Reservoirs Conference, Athens 2017 (in Greek)

ICOLD European Club (2014), "Dam Legislation Report", ICOLD European Club Working Group Dec 2014

ICOLD Bulletin B167 – PREPRINT (2017), "Regulation of Dam Safety: An overview of current practice world wide", ICOLD Technical Committee on Dam Safety, Preprint of B167

ICOLD Bulletin B154, (2011), "Dam safety management: Operational phase of the dam life cycle", ICOLD, 2011

Kazilis, N. (2008), "The failure conditions of Triadi dam of Thermi Municipality, Thessaloniki Prefecture, Greece, June 2007", 1st Greek Dam Conference, Larissa 2008 (in Greek)

Moutafis, N. I. (2008), "Failures and incidents of Greek Dams", 1st Greek Dam Conference, Larissa 2008 (in Greek)

5th International Symposium on Dam Safety

October 27-31, 2018

UP-TO-DATE REVIEW OF DAM-BREAK STUDIES

Gökçen BOMBAR [1], Şebnem ELÇİ [2]

ABSTRACT

Dam break disasters may cause massive losses of human lives and massive damages to infrastructure all over the world. Dam failure may mainly occur as a result of insufficient spillway, slope failure, structural deficiency, seepage and piping, earthquake, etc. According to International Commission on Large Dams ICOLD, 1973, 38% of the failures are due to insufficient spillway design, whereas 33% of the failures are due to seepage and piping that are very important problems in earth fill dams. Although it is rare, there have been concrete dam failures as St. Francis Dam in USA, Vajont Dam in Italy and Teton Dam in USA. In fact, 18 dams failed between 1900 and 1970, 17 between 1970 and 2000 and 25 after 2000. In the literature, one can find many researches on dam-break and flood wave propagation studied both by experimental and numerical methods. Of these studies, some focused on flow characteristics at the time of failure and the failure mechanism and the others focused on flood wave propagation downstream of the dam. This paper discusses experiments conducted in the laboratory for dam-break problems and summarizes numerical modelling of these experiments in 2D and 3D flow conditions. Several key points are addressed in the paper as: 1) different visualization methods for flow characteristics 2) the effects of the topography and vegetation on the flood propagation at the downstream which is mostly ignored in both numerical and experimental studies 3) scaling and distortion effects on experimental set-ups, 4) sediment transport attached with flood wave propagation, 5) downstream morphodynamic changes.

Keywords: Dam-break, Flood wave propagation, Visualization methods, Vegetation, Scaling Effect.

INTRODUCTION

Dams are recognized for their appreciated contribution to the prosperity of civilizations, while they are also usually accused for their risk of failure. Despite the failure of large dams are seldom, few of them occur in the world every year. To reduce the loss of life and damage, Emergency Action Planning (EAP) should be implemented in the downstream valley which consists of risk analysis process and a detailed prediction of the propagation of the flood wave induced by the dam failure. Then vital information and valuable data will be obtained to make the risk assessment and management of all type of structures.

Water depth and flow velocity are the main flood impact parameters accepted to characterize the flood hazard risks. For a long time, inundation depth has been accepted as the main determinant for flood damage most likely due to limited information about other parameter i.e. flow velocity characterising the flood. Nevertheless, Kelman and Spence (2004) publicised a number of damage mechanisms including hydrodynamic actions related to waves and velocity as a result of turbulence. A systematic review of flood impacts on buildings and structures revealed that the higher the flow

[1] Assoc. Professor, Department of Civil Engineering, İzmir Katip Çelebi University, İzmir, Turkey, e-posta: gokcen.bombar@ikc.edu.tr

[2] Professor, Department of Civil Engineering, İzmir Institute of Technology, İzmir, Turkey, e-posta: sebnemelci@iyte.edu.tr

velocity of the floodwater, the greater the probability of structural damage (Soetanto and Proverbs, 2004) furthermore USACE (1996) indicated that velocity is a major factor at all (Adegoke et al, 2014).

Quantitatively, Smith (1994) specified that a velocity of 3 m/s acting over a 1m depth will produce a force sufficient to breakdown of a typical domestic wall. The study shows further critical arrangements of water depth and flow velocities for building failure for three different residential building types. These range from above 0.5m water depth and 4m/s flow velocities to above 3m water depth with no flow velocity for single storey weatherboard buildings (Smith, 1994). Examining the existing literature Finnish Environment Institute (2001) proposed a failure criteria as maximum depth of 7m, and maximum velocity of 2m/s and maximum specific discharge as $7m^2/s$. Later, Erpicum et al. (2009) investigated the historical data of the dramatic real dambreak case of the Malpasset 66-m high arch-dam in France occurred on 2nd December 1959 to determine the effect of the flood wave propagation on the buildings in the Frejus plain. Three groups of houses could be identified namely detached houses, farms and industrial halls. Historic survey stated that 24 houses out of 674, 12 industrial halls out of 24 and 103 farms out of 253 have been totally destroyed during the failure of the dam. After comparing this information with their numerical model results they suggest the critical specific discharge and flow velocity should have been lower than that given by (Finnish Environment Institute, 2001). Still, the uncertainties shall be cleared by more studies, explicitly, experimentally and numerically.

LABORATORY AND NUMERICAL STUDIES

The dambreak problem has been widely studied experimentally and numerically. Laboratory experiments play crucial role in understanding the real dam-break phenomenon and validation of numerical models due to difficulties in obtaining field data. Most predictions on dam-break waves are often based upon numerical predictions, validated by limited data sets. While various numerical studies are available, a few laboratory data exist concerning dambreak flow (Bellos et al., 1992; Fraccarollo and Toro, 1995; Lauber and Hager, 1998; Stansby et al., 1998; Bukreev and Gusev, 2005; Chen et al., 2013; Ozmen-Cagatay et al., 2014; Kocaman and Ozmen-Cagatay, 2015). Moreover, physical modelling of dam-break waves is relatively limited.

With increasing capacity and performance of the computers, computational fluid dynamics (CFD) based software involving finite volume solution have been used in dam break simulations (Biscarini et al., 2010; Ozmen-Cagatay and Kocaman, 2010; Oertel and Bung, 2011; Fu and Jin, 2014). (Kocaman and Ozmen-Cagatay, 2015). In computational fluid dynamics, various turbulence models (k-e, RNG, LES etc.) can be used (Wilcox, 2000). For instance, In her Doctoral dissertation, Larocque (2012) studied dam-break and levee-breach flows experimentally and numerically by using volume of fluid (VOF) was used and Reynolds-averaged Navier-Stokes (RANS) approach and large eddy simulation (LES) modeling for turbulence. Furthermore, Kocaman and Ozmen-Cagatay (2015) presented a comparative analysis with VOF-based CFD simulations using the Reynolds Averaged Navier Stokes equations (RANS) with the k-e turbulence model and the Shallow Water Equations (SWEs). It is observed a better agreement with laboratory measurements and RANS solution was than that of SWE.

Occasionally, one-dimensional models e.g. the US Army Corps of Engineers' River Analysis System (HEC-RAS) or the US National Weather Service Flood Wave Dynamic Model (NWS-FLDWAV) are used, nevertheless for flows over flat floodplains in which the topography is two-dimensional, and the use of a one-dimensional approach may not be appropriate. Considering the limitations of one-dimensional models and the increase of computational power, two-dimensional models that solve the shallow water equations have become popular. The softwares such as MIKE, FLO-2D, DSS-WISE, TELEMAC, Iber and HEC-RAS (Version 5.0) are few examples (Álvarez et al, 2017).

OUTFLOW HYRDROGRAPH

Hooshyaripor et al (2017) claimed that the principal source of this ambiguity in many dam failure analyses refers to prediction of the reservoir's outflow hydrograph which are certainly much more devastating than the hydrologic floods from intense rainfalls. The magnitude of the peak discharge of a dambreak flood wave is greater and has a shorter time to peak and base time. The time to peak may have values ranging from only a few minutes to usually no more than a few hours. These parameters mainly depend on the type of failure which consequently is determined by the failure cause and dam type (Singh, 1996). For instance, erodible embankment dams gradually fail mostly as a consequence of piping and overtopping, whereas concrete gravity and arch dams usually fail very fast due to overturning and sliding. In the impulsive failure, dam structure is removed abruptly and the stored water is released quickly to the downstream river valley. The worst condition and the most plausible damages are likely to occur from such a failure mode (Singh, 1996). Escolano-Sánchez and Fernández-Serrano Roberto (3000) summarized the hazards caused by uncontrolled vegetation in Earth Dams. Main reasons for failure are the internal erosion (piping) induced by the decaying roots of dying woody vegetation that creates a seepage path, penetration of roots through cracks and joints in the foundation, holes caused by overturning and uprooted trees which could breach the dam or shorten the seepage path and initiate piping, reduced spillways capacity and clogging of the drainage systems. Therefore, the mechanism and reson of failure stands as a crucial point to determine the outflow hydrograph. Other parameters influencing the dam break flow features are hydrologic, hydraulic, morphologic and geotechnical factors (Hooshyaripor et al, 2017).

The first recognised experimental and analytical dam break studies were published in the 18th century Bazin (1865) and Ritter (1892). Ritter (1892) provided a one-dimensional analytical solution to the instantaneous dam break problem, where there is an infinitely long reservoir connected to a dry frictionless horizontal channel with rectangular cross sections. Accordingly, the front velocity of the floodwater increases with increased reservoir depth linearly. Dressler (1952) established a solution considering the flow resistance (Hooshyaripor et al, 2017). Su and Barnes (1970) studied the effect of cross-sectional shape of the channel for various cross sections as rectangular to triangular. Feizi Khankandi et al (2012) used a physical model to examine the effect of the reservoir's shape on the outflow hydrograph following a sudden dam failure.

Hooshyaripor et al, (2017) experimentally studied the instantaneous dam failure flood under different reservoir's capacities and lengths in which the side slopes change within a range of 30°–90°, concisely reporting the effect of the reservoir's geometry including length, volume and cross section on dam failure outflow hydrograph experimentally. They reveal that the role of the side slopes on dambreak wave, as lower side slope creates more disastrous outflow. The reservoir capacity and length are also documented to be important factors and they do has an influence on peak discharge and time to peak of the outflow hydrograph. Further detailed studies such as the experimental and theoretical study on the erosional incision and breaking of moraine damming by a large displacement wave in a glacial lake (Balmforth et al, 2008) exists.

KEY POINTS IN DAMBREAK STUDIES

The laboratory and numerical studies investigating the dambreak flood wave propagation and its consequences focused on the key points given below.

Visualization Methods for Flow Characteristics

The surge front released from the dam is a sudden discontinuity characterized by extremely rapid variations of flow depth and velocity, therefore, experimentally had not been easy to measure the characteristics of the wave until recent development of high sensitive instruments. In order to obtain the time series of flow depth and velocity mounting them at several locations of the reservoir and downstream channel, the level sensors and various ultrasonic sensors and image processing techniques etc. has been used (Hooshyaripor et al, 2017;). Even stereoscopy was used by Eaket et al.

(2005) for dam break flow measurement. High time resolution demand of the phenomenon has to be provided by the measuring techniques for extremely unsteady and speedy flow (Adegoke et al, 2014). Of late, a range of novel experimental methods based on signal and image analysis system have been developed for measuring flow depths and velocities. Among them utilization of digital image processing techniques becoming more popular due to its various advantages over other pointwise measuring techniques (Lauber and Hager, 1998; Stansby et al., 1998) and has been applied in laboratory works (Soares-Frazao and Zech, 2007; Aureli et al., 2008a; Kocaman and Ozmen-Cagatay, 2012). (Kocaman and Ozmen-Cagatay, 2015) by using a single camera or two cameras in a stereoscopic arrangement. This measuring technique does not require test repetition for obtaining panoramic view (Kocaman and Ozmen-Cagatay 2015). But still, there exists some drawbacks in this method such as the entrapped air-bubble during wave breaking processes cause unavoidable uncertainties (Chan and Melville 1988; Kobayashi and Raichle 1994).

The techniques involve the flow field being lightened with a thin light sheet from a light source and recorded by a high speed camera. By the help of using seeding particles appear in the 2D illuminated sheet, the velocity vectors can be obtained via a tracking algorithm technique based on auto-correlation, cross-correlation or Young's fringe method (Adegoke et al, 2014) after necessary corrections for considering the parallax error and interface separating materials of different refractive indexes (Bouguet 2004).

Using imaging systems to obtain quantitative velocity flow field information from particle movements comprises different methods depending on the capturing method of the image and the analysis technique employed. The particle velocities are obtained as inter-frame displacements from the particle positions using various methods. Such methods include Particle Tracking Velocimetry (PTV), Particle Image Velocimetry (PIV) and Particle Streak Velocimetry (PSV). In all the techniques, the displacement of the particles within a field of view over a known period yields information about the velocity vector field simultaneously over the whole plane. PTV requires individual particles to be located in an image and successive images to be recorded on successive frames and analyses pairs of single exposed digital images to produce whole field maps of velocity vectors. The distance travelled by an individual particle is then calculated and the velocity found knowing the time interval between images. Various correlation algorithms to allow the tracking of particles from frame to frame exists. Also, the application of particle streak in fluid mechanics are often used for qualitative flow visualisation known as PSV. This method is often used when the medium fluid has a seeding particle concentration less than that for PTV and does not require individual streak images to be overlapped and distinguished from each other. As the individual streak lengths are determined and the exposure time is known, the velocity associated with the particle streak can be obtained. In the PIV systems particles in the fluid are illuminated in a plane by a light source and recorded by a camera on a sequence of frames. In PIV, the average velocity vectors are obtained for a cloud of particles based on image cross-correlation techniques whereas for PTV the individual particle motions are resolved and full sets of particle trajectories can be reconstructed by following the same particle over many successive frames (Adegoke et al, 2014). Liem and Köngeter, (3000) claimed that in PIV, the time delay between two frames must be short enough that the motion of the particles is "frozen" during one exposure. Thus it is essential to adapt recording frequencies according to the expected velocities and the pixel resolution of the frame. In their experiments on dam break the recording frequency was selected as 750 Hz choosing a frame size of 20 cm.

Experiments conducted with a wet-bed downstream revealed that the velocity decreases as the downstream initial water depth increases (Adegoke et al, 2014).

Aleixo et al (2011) focused on the measurement of velocity profiles over the whole flow depth within the dambreak wave. They obtained the velocity field by means of a Particle Tracking Velocimetry (PTV) algorithm based on Voronoı¨ patterns' matching and compared with the application of a PIV algorithm to the raw data.

Hsu et al. (2012) determined that the behaviour of the wave front depends on the water depth ratio i.e, downstream-to-upstream water depth ratio. The forward breaking jet velocity will decrease for higher water depth ratio. There is a linear relationship between the difference of the water level in the upstream and downstream and the depth ratio. The numerical results show that an increase in the displacement of the breaking jet from the gate with increasing depth ratio.

Oertel and Bung (2011) analysed drag forces on placed obstacles in detail by using high-speed images and resulting particle image velocimetry calculations.

Ozmen-Cagatay et al (2014) simulated dam-break flow was numerically by the VOF-based CFD commercial software package FLOW-3D, which utilizes two distinct approaches, namely the Reynolds-averaged Navier–Stokes equations (RANS) with a k-ε turbulence model and the simple Shallow Water Equations (SWEs). Later Kocaman and Ozmen-Cagatay (2015) investigated the impact of dam-break induced shock waves on a vertical wall at downstream end of a channel both experimentall and numerically.

Adegoke et al. (2014) developed an indirect way of measuring the flow velocity was applied. The present study developed simple methods for estimating instantaneous dam-break floodwater front velocity over the whole flow depth in a dry channel using image acquisition techniques. The main feature of this development is its simplicity that is well-suited to initial investigations.

Effects of the Topography and Vegetation on the Flood Propagation

Downstream topography, the residential areas, orientation of the obstacles such as houses and bridges, density and type of vegetation (grasses, shrubs, and mangroves, growing in watercourses and floodplains), the dry and wet surface etc. are the affecting factors on the downstream flood wave propagation.

Obstacles

The presence of the obstacles mimic the complex behaviour of the residential areas that may be subject to flood inundation and under probable risk (Finnish Environment Institute, 2001; Erpicum et al, 2009). Additionally, the dynamics of flooding are primarily influenced by the shape and height of the underlying topography. Since the triangular shaped obstacle test case is an idealised representation of complex topography with steep dry slopes, Hiver (2000) carried out a dam-break flow over a bump at a quite large scale in the Laboratoire de Recherches Hydrauliques at Châtelet (Belgium). At that time, only gauge measurements of the water level at some specific points along the channel were acquired. After the opening of the gate, the water flows on the dry channel and once reaching the bump, part of the wave is reflected and forms a bore travelling back in the upstream direction, while the other part moves up the bump, resulting in a wave propagation on an upward dry slope. Then, after passing the top of the bump, the water flows on the downward dry slope until arriving in the pool of water at rest. There, the rapid front wave is slowed down abruptly and a bore forms. This bore reflects against the downstream wall and travels back to the bump, but the water is unable to pass the crest. A second reflection against the downstream wall is needed to give sufficient power to the wave to pass over the bump and to travel back in the upstream direction. Multiple reflections of the flow occur both against the bump and against the channel ends. (Soares et al, 3000; Erpicum et al , 2010).
Aureli et al. (1999) performed dam-break experiment in a frictional channel with two humps. The channel is 7m long and involves two trapezoidal humps. The dam is built along the central line on the top of first hump. Upstream of the dam, the initially stationary water level is set to 0.45m, and the downstream area is initially dry. Kocaman and Ozmen-Cagatay (2015) investigated the dam-break flow over dry channel with an abrupt contracting part in certain downstream section experimentally and numerically of Reynolds Averaged Navier Stokes (RANS) equations with k-ε turbulence model focusing on the formation and propagation of the negative bore due to abruptly contracting channel. Chaabelasri, (2018) used a simple radial basis function (RBF) meshless method to solve the two-

dimensional shallow water equations (SWEs) for simulation of dam break flows over irregular, frictional topography involving wetting and drying.

Soares et al, (3000) performed a series of experiments to focus on the impact of the wave against a single building located near the dam with different configurations (25° and 65°angle to the channel axis, for the latter case the building almost faces the dam). The channel was 36 m long and 3.6 m wide. The upstream reservoir was filled with 0.5 m of water. The dam is represented by a 1 m wide gate separating the reservoir from the downstream part of the channel. The building was located 1.5 m downstream from the dam, and had dimensions such that it didn't submerged by the flow. The water level evolution will be measured at some specific points by means of water level gauges, cameras were used to film the flow and pressure gauges could be used to measure the flow impact on the building. A shadow zone behind the building was formed. Although the shape of the front wave is affected by the building, its propagation speed remains almost unchanged for all angles. The building has an important influence on the flow, but only locally. It was emphasized that, the experiments a repeatability analysis should be performed and should avoid using huge load cells that will decrease the sensitivity while measuring the pressures.

Zhou et al (2004) simulated dam-break flows in general geometries with complex bed topography numerically. A vertical step in the bed is treated verified by predicting dam-break flows typical of practical situations, i.e., dam-break flows over a vertical step into bent channels and a dam-break flow over a bump in a bed over both dry and wet beds. Anne M. (2015) measured pressure of a wave striking a vertical surface to determine the strength needed in the building materials of marine structures. These waves may be caused by storms, tsunamis, or dam breaks and can cause serious damage.

Depth-averaged transport equations can be solved either on fixed (Delis and Katsaounis, 2005; Di Martino et al 2011; Knock and Ryrie, 1994; Zoppou and Roberts, 2000) or moving grids (Chen and Duan, 2008). In the case of moving grids the domain boundaries move so that computational domain exactly covers the physical domain. George and Stripling (1995) claimed that when a fixed grid is used, an appropriate strategy for moving the wetting–drying fronts on computational domain will be necessary (Larmaei and Mahdi, 2012).

An other reason to determine the behaviour of the wave propagation is to make flood mitigation plans. The frequently employed structures that increase topographic elevation are levees and sandbags. In general, the placement of these structures is typically decided in an ad hoc manner, limiting their overall effectiveness. Tasseff et al, (3000) proposed a new computational approach to the problem of optimizing flood barrier configurations under physical and budgetary constraints, albeit, future work pursues to generalize these approaches by more real-world flood scenarios. It similarly look for to state the inherent ambiguity in flood parameterizations such as topographic elevation, dam breach parameterization and bed friction.

Vegetation

Vegetation play and important role in flood control and bank stability, but they also create and undesirable obstruction effect on flood propagation in watercourses. The riparian vegetation in the waterway narrows the channel and reduces the conveyance capacity of river. The resistance due to roughness of plants markedly reduces the flow velocity and alters the fluvial processes and effects the waterway morphology.

He et al (2017a,b) presents a depth-averaged two-dimensional model for dam-break flows over mobile and vegetated beds and verified by laboratory tests. It is shown that when the area of the vegetation zone, the vegetation density, and the pattern of the vegetation distribution are varied, the resulted bed morphological change differs greatly, suggesting a great influence of vegetation on the dam-break flow evolution. Specifically, the vegetation may divert the direction of the main flow, hindering the flow and thus result in increased deposition upstream of the vegetation.

Zhang et al (2016a) establish a depth-averaged 2-D hydrodynamic and sediment transport model for the dam- break flows with vegetation effect. The generalized shallow water equations are solved for capturing the dry-to-wet moving boundary coupling the sediment transport and bed variation equations. The drag force of vegetation is modeled as the sink terms in the momentum equations. They revealed that the presence of vegetation on the floodplain can reduce the flow velocity and the shield stress in the vegetated area for protecting the riverbank and rooting the soil in the bank which in turn raises the water levels with some serious flooding damages. The riparian vegetation along the main channel sides is both beneficial for the riverbank protection and harmful for the flood control. Zhang et al (2016b) further studied the dam-break flows over fixed and mobile beds under the conditions with and without aquatic plants. The plants formed a group providing a buffer against the disturbance by reducing floodplain stripping for flood and the flow was restricted because of the narrow pass. The vegetation community also altered the flow direction and then changed the deposition hump by causing variation in flooding velocity.

Additionally, there exists field studies accomplishing numerical simulation of dam-break problems with geographic information systems and innovation maps (Seker et al, 2003). Şeker et al. (2003) used ArcView GIS to produce Digital Elevation Model to visualize the propagation of a possible flood wave in İstanbul. Álvarez et al (2017) analysed the consequences of a potential failure of Chipembe dam (Mozambique) on the 36 km downstream reach by using a two-dimensional hydrodynamic model Iber to simulate dam failure and propagation of the flood wave for a sunny day scenario considering DEM as input for the hydraulic model.

Scaling and Distortion Effects on Experimental Set-ups

Laboratory work in dambreak studies are widely used to support the numerical modelling simulations. When doing that, either reduced scale of the real dam and the related supporting hydraulic system (such as spillway, reservoir and downstream) are built or idealized models of complex features of the systems are modelled. In recent studies; the first type of modelling is rather preferred by the researchers, due to the fact that the flood wave propagation in the modelled system can be monitored accurately in the experiments. Scaled models allow the researchers to reproduce the dambreak under the controlled conditions where scaling laws can be applied and the monitored results such as water levels, arrival times and dynamic forces can be projected to real world dambreak conditions. In this type of the modelling, researchers can also control the breaching type and extent, volume released from the reservoir and even the sediment movement.

The results of an idealized model of the hydraulic system usually serves as high quality data sets for the numerical models set up by the researchers. The monitored values in the experimental setup i.e. arrival time of the flood wave after sudden opening of a gate in a flume, can be later used for calibration/validation of the numerical models without considering any scaling effects. But this type of modelling is far from simulation of real life dambreak situations.

In a physical model, hydrodynamic characteristics can be scaled to the hydraulic system when the model represents a similarity to the actual case. Similarity must be satisfied in all three dimensions and should involve geometric (i.e. dimensions), kinematic (i.e. velocities) and dynamic (i.e. forces) similarities. However in some cases, satisfying all three similarities makes monitoring of all the parameters impossible. Suppose that, physical modelling of 5 km x 5 km reservoir having 20 m of depth is required. Using a 1/200 scale model would require 25 m x 25 m laboratory model area where the reservoir water depth should be scaled to 10 cm under these conditions. When flood wave propagation after the dambreak is of interest, water levels of the flood wave should be monitored. However, in such an experiment, velocities would fluctuate in the accuracy of millimeters which would be very difficult to capture by the current velocimeters such as ADV's or laser beams those are widely utilized by the researchers. An often preferred option is to use distorted models. Distortion of vertical scales is done as compared to horizontal scales. When done carefully, the effects of the distortion are insignificant and its benefits are great in other areas. Froude similarity is applied to

vertical scale only. Consequently flow depth become larger and higher turbulence is observed. Flow depth leads to more precise measurements of water depths. Longitudinal slope, discharge ratio and time for arrival of the flood wave need to be scaled with respect to distortion ratio.

Tayfur et al (2013) and Guney et al (2014) presents a recent study where a distorted physical model of Urkmez Dam in Turkey was designed with its reservoir and downstream part to investigate the flood wave propagation following dam failure. In this study, the physical model was designed according to the Froude similarity law since the gravitational force is dominant. Froude number is defined as:

$$Fr = \frac{v_r}{\sqrt{g_r \ell_r}} = 1 \tag{1}$$

The horizontal and vertical scales of the model are selected so that it can be built and operated conveniently and still allowing the researchers to measure flow depths and flow velocities accurately. The horizontal and vertical scales are selected as 1/150 and 1/30 respectively. The arrival time of the flood waves is another important parameter and Strouhal number was considered to achieve this purpose. Strouhal number is defined as:

$$St = \frac{v_r . t_r}{\ell_r} = 1 \tag{2}$$

Where υ velocity, t : time and ℓ length (Yalın, 1971) and r : ratio of the model to the prototype. Time scale then becomes

$$t_r = \frac{\ell_r}{v_r} \tag{3}$$

As for ℓ_{xr} : horizontal scale ; ℓ_{zr} : vertical scale; ck : distortion = $\frac{\ell_{xr}}{\ell_{zr}}$; v_x : horizontal velocity component and v_z : vertical velocity component. Velocity ratio becomes

$$v_r = v_{xr} = \sqrt{\ell_{zr}} \tag{4}$$

And time ratio becomes

$$t_r = \frac{\ell_{xr}}{\sqrt{\ell_{zr}}} = c_k \sqrt{\ell_{zr}} \tag{5}$$

The authors projected the time arrival of the flood wave to residential areas and the velocities in the experimental set up to the real dambreak scenario of Urkmez Dam using these ratios.

In another study, Heller (2001) discussed limiting criterias to avoid significant scale effects and typical scales of physical hydraulic models. It was stated that if the model is long, boundary friction has to be modelled correctly. He also pointed out that obtaining model – prototype similarity is more challenging for movable bed models where the roughness and sediment properties have to be similar as well as the force ratios, or for fluid – structure interactions where the material properties have to be scaled. Series of tests involving dike breaches due to overtopping were performed by Schmocker & Hager (2009) to examine model limitations of scaling effects. They studied the required minimum sediment size, dike width, dike height and unit discharge in their laboratory experiments of non-

cohesive dike breach to avoid the side wall effect, scale effects and cohesion. They found dike height and width as 40 cm, and largest grain size as 8 mm to be used in the experiments. As concluded by the researchers, scaling effects on material type and breaching still needs further research.

Modelling of Sediment Transport Attached with Flood Wave Propagation and Downstream Morphodynamic Changes

Although appropriate modelling of sediment transport in dambreak flows plays a critical role for reliable results, physical models are not widely used in prediction of sediment transport phenomena following dam break. The reason is mainly the difficulties encountered in representing the complex characteristics of the downstream zone accurately. In some extreme flood events caused by dam failure however, flood flow might have severe sediment movement in the form of debris flows, mud flows or sediment laden currents. This would result in changes of the geometry that would affect the flood wave propagation and the arrival time of the wave to residential areas. The Chandora river dam-break flow occurred in India in 1991 for instance; scoured a 2 m thick layer of bed material from the reach immediately downstream of the dam (Capart et al. 2001). Another example is the 1996 Lake Ha! Ha! breakout flood in Québec which reshaped the downstream valley.

In addition to that, usually the type of the breaching (whether it is piping, overtopping or .breaching) of dam is unknown and depending on the type of sediments to be considered in the modelling study it would alter significantly. In dambreak modelling studies, whether it is experimental or numerical, generally breaching type and location is decided in advance and the results are predicted according to that assumption. This, of course, adds a great uncertainty to the predictions that has to be evaluated carefully.

The researchers kept the experimental designs simple in the dam break studies involving sediment transport to eliminate unnecessary unknowns considering the complexity of these experiments. These experiments have been carried out in several hydraulics laboratories, e.g. at the National Taiwan University (Capart and Young, 1998), at the Università Degli Studi di Trento, Italy, at the Université Catholique de Louvain (Capart, 2000). In these experiments, various materials have been used for the sediments i.e. PVC pellets and sand, with uniform or graded grain-size distribution. For instance; Spinewine (2005) and Spinewine and Zech (2007) conducted flume experiments where sediment layer consisted of uniform PVC pellets with an equivalent diameter of 3,5 mm and a density of 1,54 mm, was kept constant at 6 cm upstream and water depth was specified as 10 cm, and dambreak was achieved by fast rising of a gate. In their other paper; Zech et al (2006) discussed the difficulties in modeling the super and transcritical flow over a mobile bed and they proposed a two layer modeling approach to model their experimental results.

Numerical modeling studies first started with clear water simulations (Brufau and Garcia-Navarro, 2000) then sediment effects were considered by quasi-analytical solutions (Capart and Young, 1998) . Currently, researchers utilize two approaches to model the morphodynamic processes: uncoupled and coupled solutions. In order to model the morphodynamic processes caused by dambreak flows, the second method may be more suitable. The rate of change in morphodynamics of the bed is often related to the water depth variation. Early numerical models for simulating dam-break flows over mobile beds adopted uncoupled solutions that did not consider the changes in morphodynamics on the propagation of the flood wave. Fraccarollo and Capart (2002), Spinewine and Zech (2007) were the pioneer researchers to simulate dambreak flows over mobile beds. However in their 1D, two layer models they assumed a constant sediment concentration which is not realistic.

In recent studies, researchers adopted the coupled solutions to model dambreak flow over mobile beds. Cao et al (2002) studied dambreak flow on mobile bed and estimated the morphological evolution. They developed a theoretical model upon the conservative laws of shallow water hydrodynamics, and solved numerically the system of equations. They found that; after the dambreak, a heavily concentrated flood wave forms and depresses gradually as it propagates downstream. They also observed the formation of a hydraulic jump due to erosion of the bed in the early age of the dam-

break, propagating upstream and disappearing eventually. They also found that the free surface profiles and hydrographs were altered significantly by bed mobility, and this effected flooded zones. Wu and Wang (2007) also simulated the flood wave propagation under dam-break flow over movable beds using a one-dimensional model. They adopted a similar model to Cao et al (2002) and utilized the shallow water equations, while considering the effects of sediment transport and bed change on the flow. Their sediment model considered the effects of sediment concentration on the hydrodynamics and predicted the non-equilibrium transport of bed load and suspended load. They modified the Van Rijn formulas of equilibrium bed-load transport rate and near-bed suspended-load concentration for the simulation of sediment transport under high-shear flow conditions. The model has been tested in two experimental cases, with fairly good agreement between simulations and measurements.

Simpson and Castelltort (2006) extended an existing 1D coupled model of Cao et al. (2002) to a 2D model for the free surface flow, sediment transport and morphological evolution. They used Godunov-type method with a first-order approximate Riemann solver, instead of first-order numerical scheme due to the reported limitations for modelling sediment concentrations with gradient discontinuities.

Dong and Zhang (2009) adopted both finite volume method and finite difference method to disperse 1-D unsteady flow and sediment equations, for establishing 1-D dam-break flow and sediment numerical model of Xinji reservoir. They compared the model results with the results of initial impoundment period, where influence of sediment on flood routing and river bed deformation was found evident. They concluded that the sediment flood carried would not only inunduate the river channel and downstream land, but would influence the flood routing as well.

A recent study by Zhao et al (2017), presented numerical simulations of dam-break flow over a movable bed. Two different mathematical models were compared: a fully coupled formulation of shallow water equations with erosion and deposition terms (a depth-averaged concentration flux model), and shallow water equations with a fully coupled Exner equation (a bed load flux model). They utilized a source term that accounts for the sediment flux added to the bed load flux model to reflect the influence of sediment movement on the momentum of the water. They compared model results with experimental data provided by Spinewine (2005). The BF and CF models both provided good results for the morphodynamics, but for the water surface, the numerical models showed greater water depth in the wave front, which might result from non-hydrostatic flow conditions in the experiment. However, in the investigated cases, the sediment movement and its influence on the water surface elevation were relatively small, so that both models lead to similar surface water levels which as they stated for real-world applications larger differences in the water surface levels can be observed.

In conclusion, in order to improve the existing models, sediment transport mechanism should be correctly defined including the vertical component. In the downstream of the dam, geomorphic changes must be simulated where erosion and deposition processes must be predicted precisely. Here sudden enlargement of the downstream plains should also be included in the models. Also the breaching mechanism adds uncertainty to the simulations that has to be evaluated carefully.

CONCLUSION

Dams are subject to failure because of a variety of causes: landslides, earthquakes, heavy rainfall or other triggering factors. The failure of a dam can threaten people's lives and property downstream. In the literature, there exists many researches on dam-break and flood wave propagation in laboratory by physical models, idealized one dimensional flumes, numerical methods and field studies utilizing GIS. Among these studies, some focused on the failure mechanism and others on flood wave propagation downstream of the dam. This paper presents the up-to-date review of dam-break studies and

summarizes several key points related to dambreak phenomenon. Apparently, it is concluded that, along with the development in the technology of instrumentation and computers, still there will be more studies performed on this subject.

REFERENCES

Adegoke P. B., Atherton W. & Al Khaddar R. M. (2014) A novel simple method for measuring the velocity of dam-break flow www.witpress.com, ISSN 1743-3541 (on-line) WIT Transactions on Ecology and The Environment, Vol 184, © 2014 WIT Press doi:10.2495/FRIAR140031

Adrian, R., (1989) Engineering Application of Particle Image Velocimeters. Proc. of ICALOE, Laser Institute of America, pp. 56–71, 1989.

Aleixo R., Soares-Fraza˜o S., Zech Y., (2011) Velocity-field measurements in a dam-break flow using a PTV Voronoı¨ imaging technique, Exp Fluids (2011) 50:1633–1649,10.1007/s00348-010-1021-y

Álvarez M., Puertas Jerónimo, Peña Enrique and Bermúdez María, (2017) Two-Dimensional Dam-Break Flood Analysis in Data-Scarce Regions: The Case Study of Chipembe Dam, Mozambique; Water 2017, 9, 432; doi:10.3390/w9060432

Aureli F, Mignosa P and Tomirotti M. (1999) Dam-break flows in presence of abrupt bottom variations. In: Procof the XXVIII IAHR congress, Graz, Austria, 22–27 August 1999, pp.163–171.

Balmforth, N. J., J. von Hardenberg, A. Provenzale, and R. Zammett (2008), Dam breaking by wave-induced erosional incision, J. Geophys. Res., 113, F01020, doi:10.1029/2007JF000756.

Bazin H (1865) Recherches Expe´rimentales relatives aux remous et a` la propagation des ondes [Experimental research on the hydraulic jump and on wave propagation]. Deuxie`me partie des Recherches hydrauliques de Darcy et Bazin, p 148

Bouguet, J-Y., (2004), Camera Calibration Toolbox for MATLAB, http://www.vision.caltech.edu/bouguetj/calib_doc/

Capart, H. and Yung D.L. (1998). Formation of a jump by the dam-break wave over a granular bed. J. Fluid Mech. 372, 165-187.

Capart H, Young D. L, Zech Y (2001) Dam-break Induced debris flow and particulate gravity currents. In: Kneller B, McCaffrey B, Peakall J, Druitt T, editors. Special publication of the international association of sedimentologists, vol. 31.p. 149–56.

Chaabelasri, E. (2018) Numerical Simulation of Dam Break Flows Using a Radial Basis, Function Meshless Method with Artificial Viscosity, Hindawi Modelling and Simulation in Engineering, Volume 2018, Article ID 4245658, 11 pages, https://doi.org/10.1155/2018/4245658

Chan, E.S., and W.K. Melville. 1988. Deep-water plunging wave pressures on a vertical plane wall, Proceedings of the Royal Society of London Series a-Mathematical Physical and Engineering Sciences; 417(1852), 95-131.

Chen D., Duan J.G., (2008), Case study: Two-dimensional model simulation of channel migration processes in West Jordan River, Utah, J. Hydraul. Eng. 134, (2008) 315–327.

Delis A.I., Katsaounis T., (2005) Numerical solution of the two-dimensional shallow water equations by the application of relaxation methods, Appl. Math. Modell. 29 (2005) 754–783.

Di Martino B., Giacomoni C., Martin Paoli J., Simonnet P., (2011) Simulation of the spread of a viscous fluid using a bidimensional shallow water model, Appl. Math. Modell. 35 (2011) 3387–3395.

Dressler R F (1952) Hydraulic resistance effect upon the dambreak functions. J. Res. Natl. Bur. Stand. 49(3): 217–225

Eaket, J.; Hicks, F. E., Peterson, A. E., (2005) Use of Stereoscopy for Dam Break Flow Measurement Journal of Hydraulic Engineering / Volume 131 Issue 1 - January 2005

Erpicum, S., Archambeau1 P., Dewals1, B.J. 2, Ernst1 J. and Pirotton, M. (2009) Dam-break flow numerical modeling considering structural impacts on buildings, 33rd IAHR Congress: Water Engineering for a Sustainable Environment Copyright °c 2009 by International Association of Hydraulic Engineering & Research (IAHR), ISBN: 978-94-90365-01-1

Erpicuma S., Dewalsa, B.J., Archambeaua P., Pirotton M. (2010) Dam break flow computation based on an efficient flux vector splitting a, Journal of Computational and Applied Mathematics 234 (2010) 2143-2151

Escolano-Sánchez Félix, Fernández-Serrano Roberto (3000) Hazards Caused by Uncontrolled Vegetation and Inadequate Maintenance Practice in Earth Dams

Feizi Khankandi A, Tahershamsi A and Soares-Fraza˜o S (2012) Experimental investigation of reservoir geometry effect on dam-break flow. J. Hydraul. Res. 50(4): 376–387

Finnish Environment Institute (2001). Rescdam – Development of rescue actions based on dam-break flood analysis – Final report. http://www.ymparisto.fi/print.asp?contentid=78947&lan=en&clan=en#a5.

Fraccarollo, L. and Capart, H. (2002). Riemann wave description of erosional dambreak flows. Journal of Fluid Mechanics, 461, 183-228.

George K.J. and Stripling S., (1995) Improving the simulation of drying and wetting in a two-dimensional tidal numerical model, Appl. Math. Modell. 19 (1995) 2.

Guney, M.S., Tayfur, G., Bombar, G., Elci, S. (2014) Distorted physical model to study sudden partial dam break flows in an urban area. J Hydraul Eng 140(11):05014006.

Hatice Ozmen-Cagatay , Selahattin Kocaman , Hasan Guzel (2014) Investigation of dam-break flood waves in a dry channel with a hump, Journal of Hydro-environment Research, Volume 8, Issue 3, August 2014, Pages 304-315, https://doi.org/10.1016/j.jher.2014.01.005

He Z., Wu T., Weng H., Hu P. and Wu G., Numerical simulation of dam-break flow and bed change considering the vegetation effects, Journal of Hydro-environment Research, 14 (2017b) 93–104.

He Zhiguo, Wu Ting, Weng Haoxuan, Hu Peng, Wu Gangfeng, (2017a) Numerical simulation of dam-break flow and bed change considering the vegetation effects, International Journal of Sediment Research, Volume 32, Issue 1, March 2017, Pages 105-120, https://doi.org/10.1016/j.ijsrc.2015.04.004

Heller, V. (2011) Scale effects in physical hydraulic engineering models, Journal of Hydraulic Research, 49:3, 293-306, DOI: 10.1080/00221686.2011.578914.

Hooshyaripor Farhad, Tahershamsi Ahmad, and Razi, Sahand (2017) Dam break flood wave under different reservoir's capacities and lengths, Sadhana Vol. 42, No. 9, September 2017, pp. 1557–1569 Indian Academy of Sciences DOI 10.1007/s12046-017-0693-x

Hsu Hung-Chu 1 Torres-Freyermuth A. 2 Hsu Tian-Jian 3 Hwung Hwung-Hweng 4, (2012) Numerical And Experimental Study Of Dam-Break Flood Propagation And Its Implication To Sediment Erosion Coastal Engineering 2012

Kelman, I. and Spence, R., (2004) An overview of flood actions on buildings. Eng. Geol., 73, pp. 297–309, 2004.

Knock C., Ryrie S.C., (1994) Parameterization of dispersion in the depth-averaged transport equation, Appl. Math. Modell. 18 (1994) 582–587.

Kobayashi, N., and A.W. Raichle. 1994. Irregular wave overtopping of revetments in surf zones, Journal of Waterway Port Coastal and Ocean Engineering-Asce, 120(1), 56-73.

Kocaman S, and Ozmen-Cagatay H., (2015a) Dam-Break Flow Over Abruptly Contracting Channel, International Journal of Mechanical And Production Engineering, ISSN: 2320-2092, Volume- 3, Issue-8, Aug.-2015 73

Kocaman Selahattin, Ozmen-Cagatay Hatice (2015b) Investigation of dam-break induced shock waves impact on a vertical wall, Journal of Hydrology, Volume 525, June 2015, Pages 1-12, https://doi.org/10.1016/j.jhydrol.2015.03.040

LaBine, Anne M. (2015) An Experimental Investigation of Pressure of a Simple Dam Break Generated Wave Impacting a Plate, May 8, 2015 Department of Mechanical Engineering, Bachelor of Science in Mechanical Engineering

Larmaei M. Moradi 1, Mahdi Tew-Fik (2012) A new method for the treatment of wetting–drying fronts ⇑ Applied Mathematical Modelling 36 (2012) 2286–2302

Larocque, Lindsey Ann, (2012) Experimental and Numerical Modeling of Dam-Break and Levee-Breach Flows, University of South Carolina (2012) (Doctoral dissertation).

Lauber, G. and Hager, W. H., (1998) Experiments to dam-break waves: Horizontal channel. Journal of Hydraulic Research, 36 (3), pp. 291–307, 1998.

Liem Rosi and Köngeter Jürgen, (3000) Application Of High-Speed Digital Image Processing To Experiments On Dam Break Waves

Liu X, Mohammadian A, Sedano J A I (2014) A Well-Balanced 2-D Model for Dam-Break Flow with Wetting and Drying Avestia Publishing Journal of Fluid Flow, Heat and Mass Transfer Volume 1, Year 2014 Journal ISSN: 2368-6111 DOI: 10.11159/jffhmt.2014.005

Mario Oertel & Daniel B. Bung (2011) Initial stage of two-dimensional dambreak waves: laboratory versus VOF, Pages 89-97 | https://doi.org/10.1080/00221686.2011.639981

Ritter, A. (1892): „Die Fortpflanzung der Wasserwellen", [The propagation of water waves]. Zeitschrift des Vereins Deutscher Ingenieure 1892, 947 – 954

Schmocker, L., & Hager, W.H. (2009). Modelling dike breaching due to overtopping. J. Hydraulic Res. 47(5), 585–597.

Seker D.Z., Kabdasli S. and Rudvan B. , (2003) Risk Assessment of A Dam-Break Using GIS Technology Water Science & Technology · February 2003, DOI: 10.2166/wst.2003.0546

Simpson G. & Castelltort S., 2006. Coupled model of surface water flow, sediment transport and morphological evolution. Computers & Geosciences, 32: 1600–1614.

Singh V (1996) Dam breach modelling technology. Dordrecht: Kluwer

Smith, D. I., (1994) Flood damage estimation – A review of urban stage damage curves and loss functions. Water SA, 20 (3), pp. 231–238, 1994.

Soares S., Le Grelle N., Zech Y. (3000) Dam-break flow experiments in idealised representation of complex topography and urban area

Soetanto, R. and Proverbs, D. G., (2004) Impact of flood characteristics on damage caused to UK domestic properties: the perceptions of building surveyors. Str. Survey, 22 (2), pp. 95–104, 2004.

Spinewine, B., 2005. Two-layer Flow Behaviour and the Effects of Granular Dilatancy in Dam-break Induced Sheet-flow. Ph. D. Dissertation. Universite catholique de Louvain, Louvain.

Spinewine, B., Zech, Y., 2007. Small-scale laboratory dam-break waves on movable beds. J. Hydraul. Res. 45(s1), 73e86. https://doi.org/10.1080/ 00221686.2007.9521834.

Stansby, P. K., Chegini, A. H. N. and Barnes, T. C. D., The initial stages of dam-break flow. Journal of Fluid Mechanics, 374, pp. 407–424, 1998

Su S T and Barnes A H (1970) Geometric and frictional effects on sudden releases. J. Hydraul. Div. 96(11): 2185–2200

Tasseff B., Bent R., and Van Hentenryck P. (3000) Optimization of Topography-based Flood Mitigation Strategies

Tayfur, G. Guney, M.S., Bombar, G. (2013). A distorted physical model to study sudden dam break flows. 2nd International Balkans Conference on Challenges of Civil Engineering, BCCCE, 23-25 May 2013, Epoka University, Tirana, Albania.

USACE, (1996) Design of Revetments, Seawalls and Bulkheads 1614, 1996.

Wang B., Chen Y., Wu C., Peng Y., Ma X., Song J., (2017) Analytical solution of dam-break flood wave propagation in a dry sloped channel with an irregular-shaped cross-section, Journal of Hydro-environment Research, 14 (2017) 93–104.

Wu, W. And Wang, S.S. (2007). One-Dimensional Modeling of Dam-Break Flow over Movable Beds. Journal of Hydraulic Engineering, ASCE.

Yalın, M.S. (1971). Theory of Hydraulic Models, The Macmillan Press Ltd, London, UK.

Zhang Ming-liang, XU Yuan-yuan, QIAO Yang, JIANG Heng-zhi, ZHANG Zhong-zhe, ZHANG Guo-sheng, (2016a) Numerical simulation of flow and bed morphology in the case of dam break floods with vegetation effect* 2016,28(1):23-32, DOI: 10.1016/S1001-6058(16)60604-2

Zhang, Mingliang; Xu, Yuanyuan ; Li, Jin ; Qiao, Huiting ; and Zhang Hongxing, (2016b) Interactions Study of Hydrodynamic-Morphology-Vegetation for Dam-Break Flows Hindawi Publishing Corporation, Mathematical Problems in Engineering, Volume 2016, Article ID 3818591, 12 pages, http://dx.doi.org/10.1155/2016/3818591

Zhou1 Jian G.;. Causon2 Derek M; Mingham3 Clive G.; and. Ingram David M (2004) Numerical Prediction of Dam-Break Flows in General Geometries with Complex Bed Topography, Journal of Hydraulic Engineering, Vol. 130, No. 4, April 1, 2004. ©ASCE, ISSN 0733-9429/2004/4-332–340/$18.00.

Zoppou C., Roberts S., (2000) Numerical solution of the two-dimensional unsteady dam break, Appl. Math. Modell. 24 (2000) 457–475.

5th International Symposium on Dam Safety

October 27-31, 2018

GENERAL EVALUATION ON IRAQIS' DAMS AND LESSONS LEARNED

Hemn T. MOHAMMED[1], Kasım YENİGÜN[2]

ABSTRACT

This study covers a general evaluation and review on water resources of Iraq and its dams. It also covers a data survey on capacity, site selection and construction type of dams and other related information on necessity of Iraq's water resources for management by utility of the reservoirs. The article aims to evaluate the safety level and todays situation of three dams of Iraq, which are Mosul dam, Darbandikhan Dam and Harmn dam (unfinished dam). The evaluation may be related with the reasons which are mistakes in geologic surveys, earthquakes and mistakes in planning or hydrologic investigations. By the evaluation of observed data, the effects of the erosion on dam foundations or cracks on dam body or effect of floods on dam parts are shown. The destroyed Harmn dam gives that lesson to planners, policy makers and engineers; an accurate plan needs a construction process with hydrologic and geologic stages together.

Keywords: Mosul Dam, Darbandikhan Dam, Harmn Dam, Iraq dams, Safe planning.

INTRODUCTION

Dams are giant infrastructure facilities constructed for the development of the national economy investments. The safety of the dams is very important aspect for safe guarding the national investment and the benefits derived by the nation from the project. Unlike a purely technical discipline, dam safety is a techno-management discipline and can be categorized as a part of asset management for the owner and public safety assurance on the part of the government. The dams need as much attention as any other engineering structures (Koimattur, 2012).

There may be many mistakes in analyzing hydrology data; even in hydraulic structure parts especially the spillways and culverts bottom outlets which are responsible for satisfy in transfer the floods. Safety studies in the United States have found that some existing dams do not satisfy the latest estimates of the probable maximum flood (PMF), the current design standard for high hazard dams. Estimation of the PMF is less than a perfect science and efforts continue to go into its refinement, the global climate changes made vital changes in the hydrology predicts (Sun et al., 2014).

[1] PhD Student, Department of Civil Engineering, Harran University, Şanlıurfa, Turkey.
e-mail: eng.hemint@harran.edu.tr
[2] Professor, Department of Civil Engineering, Harran University, Şanlıurfa, Turkey.
e-mail: kyenigun@harran.edu.tr

Dams will make hazard to downstream life and property. The floodplain at risk in the event of catastrophic breaching may be extensive, densely populated and of considerable economic importance. In such instances dam failure can result in unacceptable fatalities and economic damage (Novak et al., 2006). There is analyzing centers established for dams' issues The Data Station for Dam Failures (DSDF) established to collects data about dam failures reported since 1980.

The data collection not only contains the descriptions of failure events including the dimensions of the affected dams and the causes of their failure but also the qualitative judgment of damages as far as they are known (Alavian et al., 2009).

A failure of a dam means collapses or movement of a part of a dam or its foundation so that the dam cannot retain the stored water. Accidents during construction are also considered as failures. According to the statistics on large dams, there were 88 failures (27% of 327 events) were caused by overtopping of dams. Different combinations of factors result in large releases from a dam and potentially dam failure, leading to damages and possibly to loss-of-life (Thompson et al., 1997).

Due to the importance of dam safety, there are many committees on Dam Safety. For example, in USA like: National Dam Safety Review Board (NDSRB), the Interagency Committee on Dam Safety (ICODS) and National Dam Safety Program (NDSP) (FEMA Strategic Plan, 2016).

The ICOLD Bulletins 130, 154, and 167 are related with dam safety.

Ancient Iraqi Civilization on Water

- Iridu Civilization (south of Nassirriya) 5000 BC- first evidence of irrigation systems.
- Sumeria-Akkadia-Ur 4000-3000 B.C. - I-tu-rungal Canal (Baghdad to Nassirriya)
- Babylonia/Hammurabi 1900-1600 B.C. Nimrud Dam on the Tigris, other dams.
- Assyrian Age 1600-700 B.C. Sennacherib's Canals, dams in Nineveh.
- Chaldean Age 700-600 B.C. Nebuchadnezzar's dams and reservoirs.
- Persian, Greek, Parthian Age 600 BC – 637 AD.
- The Great Flood of 627-628 AD (created marsh system) (Rashid, 2018).

Water Resources and Situation in Iraq

Dams are important structures for Iraq because the weather of Iraq is semi-dry at north and is dry at center and south. Their importance gets more after the global climate changes to challenge with repeated and suddenly floods or droughts. Figure 1 shows study area: Iraq and Iraq's water bodies.

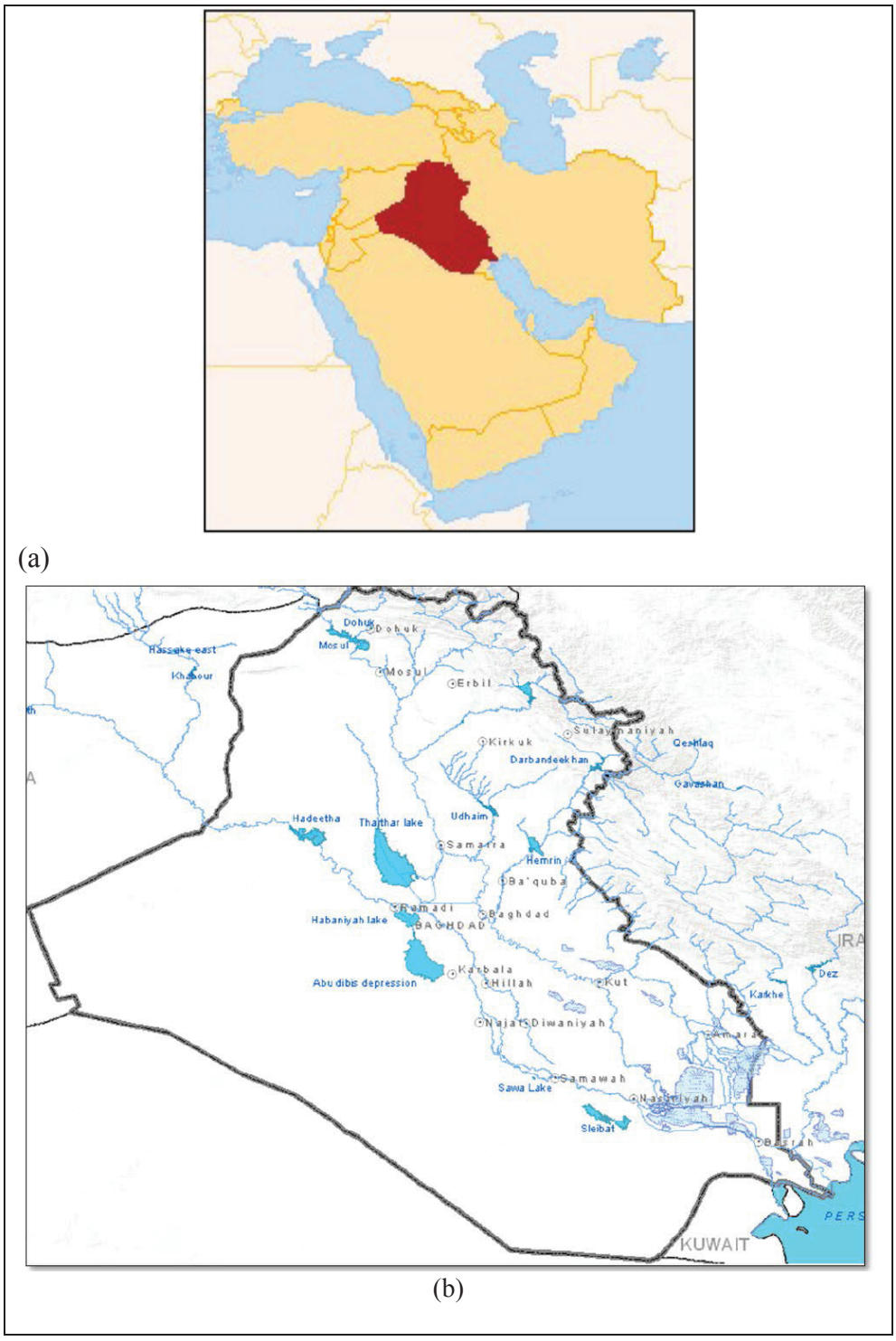

Figure 1. (a) Study area: Iraq, (b) Iraq's water bodies.

Figure 2 gives the Iraq's water balance and Table 2 show the Iraq dams and their purposes of use.

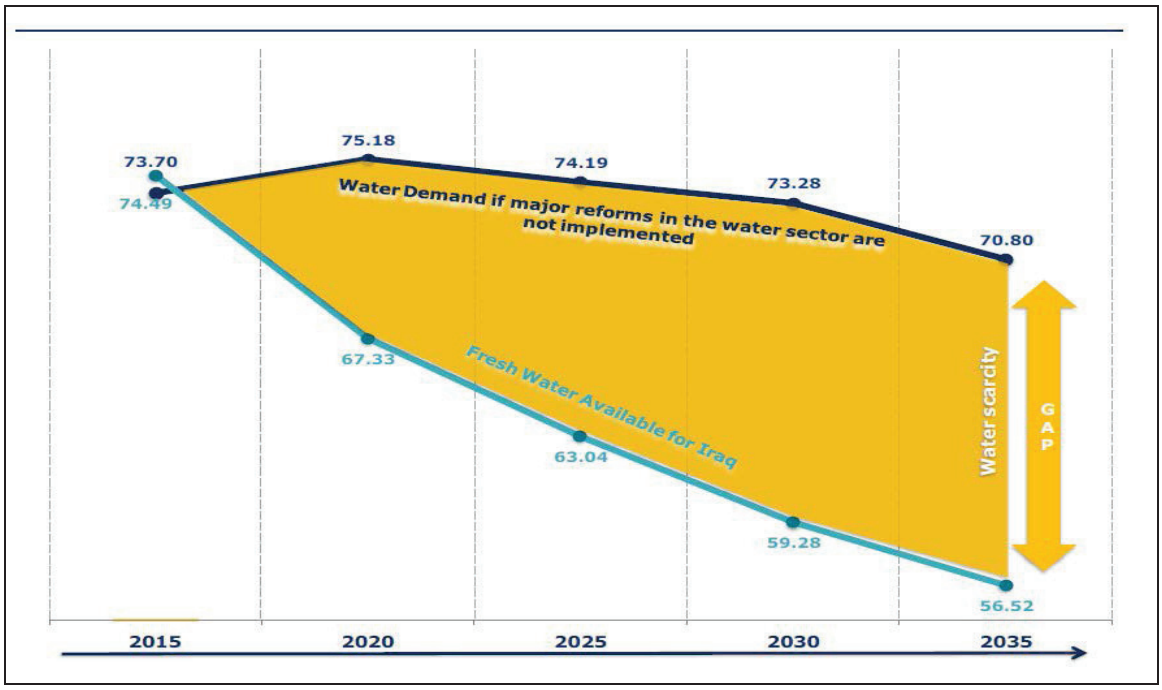

Figure 2. Iraq's water balance without the implementation of the SWLRI strategy.

Table 2 Iraq dams and their purposes of use.

	Basins and Dams	Storage Volume (Billion m^3)				Installed HPP(MW)
		Total	Flood	Irrigation & Hydropower	Dead	
Tigris	**Mosul Dam**	14.45	3.34	8.16	2.95	1010
	Dokan Dam	7.90	1.10	6.10	0.70	400
	Darbandikhan	3.80	0.80	2.54	0.46	240
	Hemrin Dam	3.95	1.45	2.20	0.30	50
	Udhaim Dam	4.00	2.5	1.00	0.5	Under Const.
	Tharthar Lake	85.00	17.00	27.70	40.3	--
	Total	119.1	26.19	47.70	45.21	1700
Euphrates	**Haditha Dam**	9.90	1.70	7.98	0.22	660
	Habbaniyah Lake	3.30	0.40	2.05	0.85	--
	Razzaza Lake	26.00	26.00	--	--	--
	Sulaibat Depression	2.50	2.50	--	--	--
	Total	41.70	30.60	10.03	1.07	660
Grand Total		160.8	56.79	57.73	46.28	2360

IRAQI DAMS REVIEW

*There are seven large dams (constructed) in Iraq; six on Tigris River and one on Euphrates River have total 29.51 B m^3 active storage.

* There are four main natural surface storages with total 47.98 B m³ active storage in 6028 km² storage area, distributed on marshes in the Southern part of Iraq (The World Bank workshop, 2017).

Figure 3 show the Tigris river tributaries and basins.

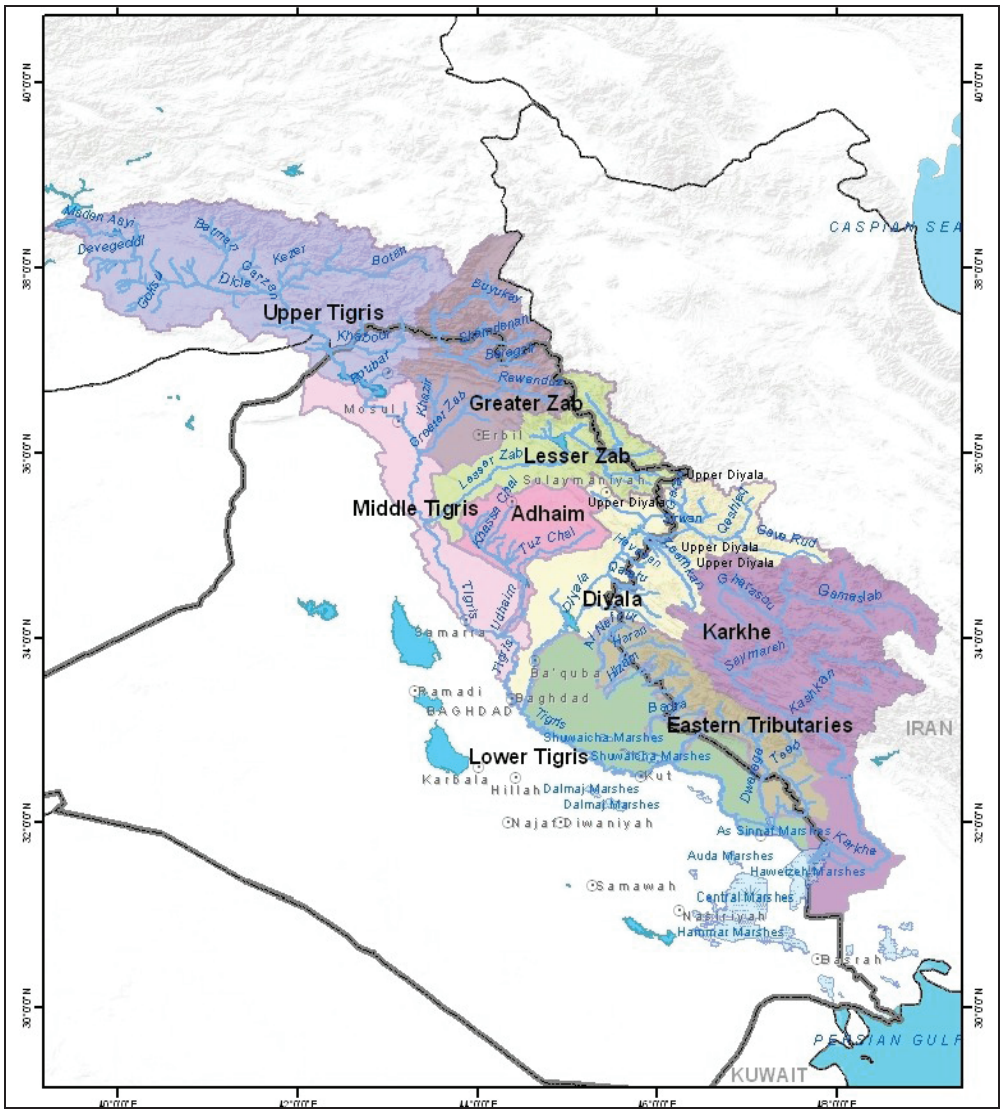

Figure 3. Tigris river tributaries and basins

River's lengths and basins of country are shown in Table 3 and 4 below.

Table 3. Tigris river tributaries and basins

Country	River Length (km)	Percentage (in country)	Basin Area (km^2)	Percentage (in country)
Turkey	400	22	44,809	12,1
Syria	44	2	864,000	00,2
Iraq	1418	76	161,250	43,4
Iran	-	-	164,815	44,3
Total	**1862**	**100**	**371,738**	**100**

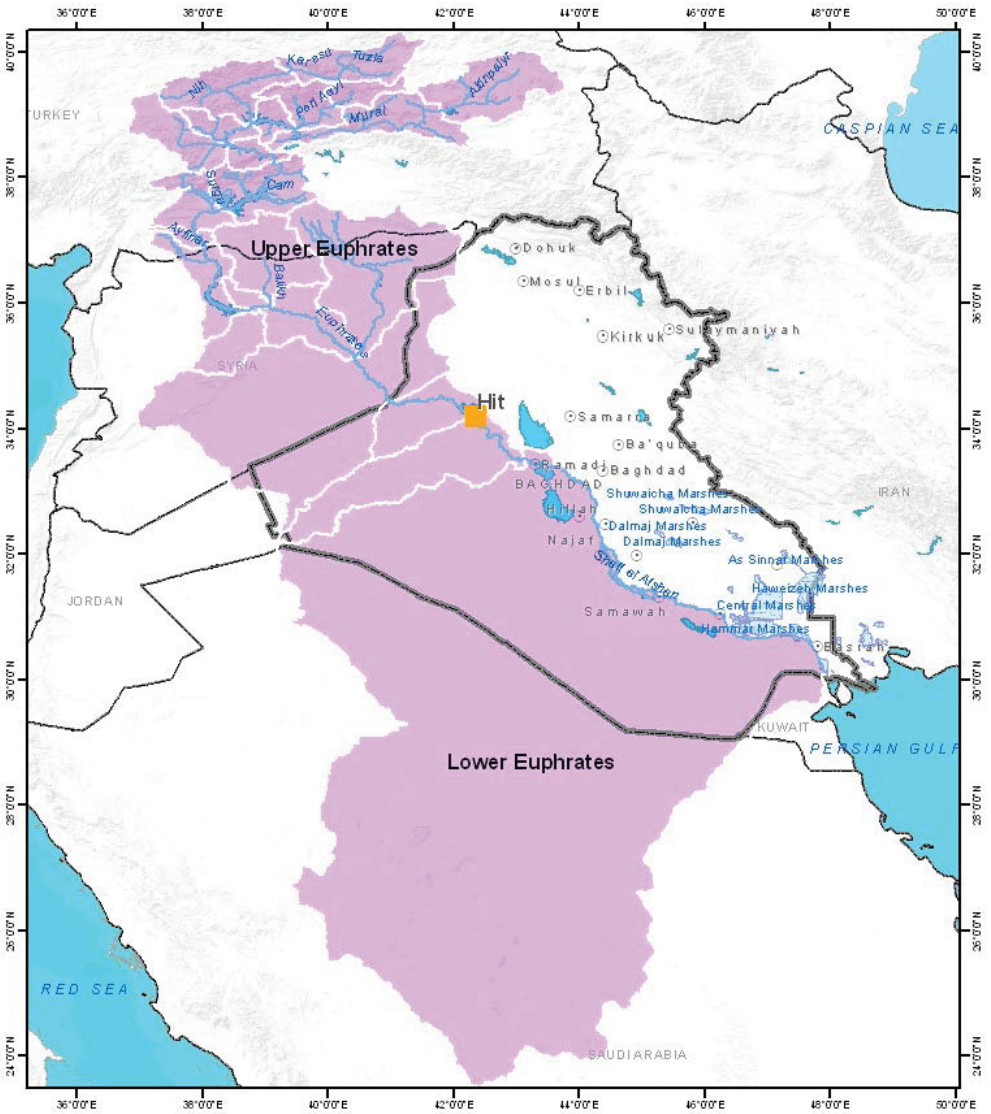

Figure 4. Euphrates river tributaries and basins

Table 4 Euphrates river tributaries and basins

Country	River Length (km)	Percentage (in country)	Basin Area (km^2)	Percentage (in country)
Turkey	1 230,0	41	121 682	13,9
Syria	710,0	24	114 505	13,0
Iraq	1 060,0	35	278 593	31,7
Saudi Arabia	-	-	363 609	41,4
Total	**3,000**	**100**	**878,39**	**100**

a) Mosul Dam safety;

- In Ninawa province, on Tigris river.
- Coordinates: N 36.63 E 42.82

- Total Storage: 14 450 M m^3
- Dead Storage: 2950 M m^3
- Dam Type: Earth-fill
- Dam Height: 113 m
- Electricity Generation: 750 MW
- Construction Date: 1986
- The construction was started in 1981 and completed in1986 (Figure 5)

After completion of the dam and commissioning in 1986, gradual deterioration of gypsum and anhydrite formations under the dam Foundation were observed, and additional grouting were necessary then led to substantial continuous re-grouting activities extended to date. Sink holes were also observed at the downstream side of the dam (Adamo and Al-Ansari, 2016)

These are all because of geologic investigation mistakes in planning. After 2003 many studies for these problems were carried out by US army and other US Consultants, generally they concluded to continue with grouting activities from the grouting gallery although it is not a permanent solution for the reduction of the dam failure.

Figure 5. Mosul dam

b) Darbandikhan Dam Safety;

- Constructed in Sulaymaniyah Province, on Diyala (Sirwan) River (Figure 6).
- Coordinates: N 45.70 E 35.11
- Total Storage: 3800 M m^3
- Dead Storage: 460 M m^3

- Dam Type: Rock-fill
- Dam Height: 127 m
- Electricity Generation: 240 MW
- Construction Date: 1962

An earthquake with magnitude 7.1 occurred in 12th of November 2017 and made losses, sliding and surface cracks on the dam body. The water level is lowered to decrease the risks on dam body another investigation done to know if the base of the dam had suffered (Figure 7).

Figure 6. Darbandikhan Dam

Figure 7. Cracks on Darbandikhan Dam crest, 2017

c) Failure on Harmn Dam

Failure of Harmn dam which is under construction at North Iraq is a sample for mistakes in planning and design as shown in Fig.8 below.

Figure 8. Location of destroyed dam (Harmn) and the paned dam upstream

The reason of the failure in the destroyed dam (Harmn dam) is amount of uncalculated floods due to hydrological mistakes in design and construction the dams. Because, the calculated catchment area was taken as 336 km², despite the actual catchment area was 526 km².

The difference of that 190 km² catchment area is leaved for a planned dam upstream of Harmn dam, but that dam didn't construct. Because of this mistake, the flood had gathered the all water of basin and affected the dam.

This mistake caused suddenly flood more than designed flood probable maximum flood (PMF), for five years (Q_5 = 239 m³/s) which the bottom outlet culvert designed to pass that water to downstream. The flood was realized as discharge of 380 m³/s. (Figure 9 and 10).

So the bottom outlet culvert failed to transfer excess water which raised water flood level with constructed cofferdam, the flood overtopped upstream cofferdam and destroyed upstream and downstream cofferdam. It had caused in losses about (520,000) USD at the dam site, roads and bridge downstream the dam.

Figure 9. Harmn dam before the flood

Figure 10 Harmn dam after the flood

CONCLUSIONS

The lesson learned from these three examples is the management of a dam in stages of construction and operation must be done in accurate plan from planning and design stages; execute stages, following up stages and maintenance. The dam has the same behavior of a baby that wants good look-out during all its life.

Mosul dam gives a sample of mistakes of geological research during the planning stage.

After the earthquake, Darbandikhan dam cracks on dam body teaches us that the seismic analyses must done more carefully and the factor of safety against earthquake must increase, also we learnt that the earth fill dams are more suitable that concrete dams for active seismic areas .

The third dam (Harmn dam) that failed by flood says us; with series of dams on one river must done in accurate plan, first must construct the dam which is more upstream river, then construct another downstream dam, also remember that the catchment area of the more upstream dam is still exist, it is big mistake to neglect this catchment area that appears during floods.

REFERENCES

Adamo,N. and Al-Ansari**,N.** , 2016. " Mosul Dam Full Story:Safety Evaluations of Mosul Dam" ,Journal of Earth Sciences and Geotechnical Engineering, vol.6, no. 3, 185-212.

Alavian V. , Qaddumi H. et al. , 2009. " Water and Climate Change: Understanding the Risks and Making Climate-Smart Investment Decisions" ,pp139.

FEMA, 2016. "Strategic Plan for the National Dam Safety Program Fiscal Years 2012 through 2016", pp. 916.

Thompson K.D., Stedinger R.J., Heath D.C., 1997, "Evaluation and presentation of dam failure and flood risks", Journal of water resources planning and management, pp224

Novak P., Moffat A.I.B., Nalluri C., and Narayanan R., 2006, Hydraulic Structures, Fourth Edition, pp289.

Rashid, L.,2018. " development of water resources in Iraq", (http://latifrashid.iq/development-of-water-resources-in-Iraq/), access 10.07.2018 .

Koimattur S.B., 2012 "Integrated approach to safety evaluation of existing dams", pp.1.

Sun W. , Wang J., Li Z., Yao X., and Yu J. ,2014 " Influences of Climate Change on Water Resources Availability in Jinjiang Basin, China", Scientific World Journal, pp2.

The World Bank, 2017 ,Workshop of " Dam Safety Appreciation through Operator Engagement",Erbil-Iraq.

5th International Symposium on Dam Safety

October 27-31, 2018

USING MACHINE LEARNING TECHNIQUES AND DEEP LEARNING IN FORECASTING THE HYDROELECTRIC POWER GENERATION IN ALMUS DAM, TURKEY

Hesham ALRAYESS [1], Salem GHARBIA [2] , Neslihan BEDEN [3], Asli ULKE KESKİN [4]

ABSTRACT

Renewable energy is considered to be a critical factor in developing wealthy and sustainable societies. However, its utilisation in the electrical power grid can be very challenging regarding the rates predictably. Renewable energy mainly depends on the local environmental conditions, such as temperature and rainfall-runoff ratios. Therefore, the expected power production heavily fluctuates, which makes calculating the feed-in into the power grid very challenging to be calculated and predicted.

Hydropower currently is the primary renewable source contributing to electricity supply, and its future contribution is anticipated to increase significantly. The accurate forecasting of energy production is a very crucial issue for the available power management process. An energy production forecast, which gives information about how much energy will be produced by a particular power station can be useful for optimising the marketing of renewable energy and hence deploy systems integration.

This paper presents the results of deploying Machine Learning Techniques in short-term forecasting of the amount of energy produced by Almus Dam and Hydroelectric Power Plant in Tokat, Turkey. This study demonstrates the use of Artificial Neural Network (ANN), Support Vector Machine (SVM) and Deep Learning (DL) in hydropower forecasting process using monthly hydroelectric power generation data from 1993 to 2013.

Keywords: Renewable energy, Hydropower, ANN, Turkey.

INTRODUCTION

The increase in world population and the developments in technology are increasing the need for energy. In sustainable development, energy is a very important point and a necessity of a modern life. Sustainable development needs a sustainable supply of energy resources (Dmitrieva, 2015). Because of the undeniable negative effects of burning fossil fuels, renewable energy sources such as hydropower and solar power have attracted an ever-increasing attention although they are still slightly more expensive (Elliot et al., 1998).

[1] PhD researcher, Department of Civil Engineering, Ondokuz Mayis University, Samsun, Turkey, e-posta: hesham.majed@hotmail.com

[2] Post-doctoral research fellow, Department of Planning and Environmental Policy, University College Dublin, Ireland, e-posta: salem.gharbia@ucd.ie

[3] Lecturer, Department of Construction, Kavak Vocational School, Samsun University, Samsun, Turkey, e-posta: neslihan.beden@omu.edu.tr

[4] Assistant Professor, Department of Civil Engineering, Ondokuz Mayis University, Samsun, Turkey, e-posta: asli.ulke@omu.edu.tr

Wind, geothermal heat, hydropower, etc. are classified as a Renewable energy sources which generally related to sustainable ones considering relatively long-term periods of time. As an example, the large-scale conventional hydroelectric stations which have water reservoirs, electricity production can be flexible since turbine systems can be adjusted to be suitable with the variation in energy demand. Energy production of hydropower plants depends on the weather situations like precipitation and temperature (Dmitrieva, 2015). A water power plant is in general a highly effective energy conversion system. There is no pollution of the environment, but objections are raised relative to the flooding of the valuable real estate and scenic areas (Kaygusuz, 2002). As a result, the energy production of such systems fluctuates and need to be forecasted. Long term electricity production forecasting is the basis for energy investment planning and plays a vital role in developing countries for governments.

Despite of parametric statistical rules and deterministic models have classified as a traditional approaches to forecasting water resources variables, many efforts have shown that when explicit information of hydrological processes are not needed. Artificial neural networks (ANN) may be more powerful and effectiveness (Maier and Dandy, 2000).

The objective is to forecast the energy production of Almus dam using different types of model. These models are Artificial Neural Networks (ANNs), Support Vector Machine (SVM) and Deep Learning (DL). This study makes a clear vision about the effective of using these models in forecasting to understand the behaviour of the system. Energy power forecasting studies on of Turkey have begun in the 1960s and starting from 1984 econometrics models have been applied for forecasting purposes (Kankal et al., 2011).

HYDROPOWER IN THE WORLD AND TURKEY

Hydroelectric energy is produced from water falling. The falling water drives an electrical generator which converts the motion into energy. Hydropower plants can quickly go from zero power to maximum output so that hydroelectric energy can be injected into the electricity system faster than that of any other energy source. Hydroelectric energy has zero emissions, low running cost (Gokgoz and Filiz, 2018).

Hydroelectric power is a clean and renewable energy source. The reasons why hydroelectric power is preferred by many countries; economic, technical and environmental benefits (Huang and Yan, 2009). Hydropower is a very essential player in many regions throughout the globe with more than 150 countries producing the hydropower and supplying approximately 19.0% of the world's total electricity supply (Altinbilek, D., 2002). Hydropower also represents more than 92.0% of electricity generated from renewable resources worldwide (Smith et al., 2012). In a hydroelectric power plant (HEPP) turbines convert water pressure into mechanical power, the power available is proportional to the product of pressure head and water discharge (Yuksek et al., 2006).

Turkey is considered as a recently developed country and an economic power house of the region. Due to fast economic growth coupled with the country's vibrant young population, Turkey's electricity demand is increasing continuously. Turkey is a net energy importer. Mainly fossil fuels and the energy import ratio is around 65.0% (Melikoglu, 2013a).

Turkey imports mostly natural gas, petroleum, and hard coal, which inevitably deranges the country's macroeconomic balances (Melikoglu, 2013b).

In Turkey, the construction of dams and subsequently hydroelectric power plants started in the second half of the 20th century and increased after that to supply water for irrigation and electricity production. Hydropower is considered the most important renewable energy source in Turkey. Moreover currently it is the second largest domestic energy source after coal (Kaygusuz, 2002).

It was estimated that Turkey has a gross annual hydroelectric potential of 432.98 GWh/year. At the end of 2016, there were more than 596 hydropower plants in operation in Turkey with a combined installed capacity of approximately 26.819 MW and an annual average generation of nearly 93.653 GWh.

STUDY AREA

The Almus Dam (Almus Barajı in Turkish) is an earthen embankment dam that is near the town of Almus (28 kilometers East of Tokat city in center north of Turkey (40°24′27″N , 36°54′11″E)) and is located on the River Yesilirmak which runs into the Black Sea as shown in Figure 1. Table 1 shows the dam and HEPP characteristics.

Irrigation, flood control and hydroelectricity are considered as the main purposes of the dams. The hydroelectricity power plant which established in 1966 at the dam has a capacity of 27 megawatts divided as three facilities at 9 megawatts each. The dam's spillway is capable of discharging a maximum 2,800 m3/s and its bottom outlet a maximum of 50 m^3/s. Figure 1 shows the location of the Almus dam and HEPP in the eastern north part of Turkey (Tokat). Table 1 shows the characteristics of the Almus dam and HEPP in meter and cubic meter units for levels and volumes, respectively.

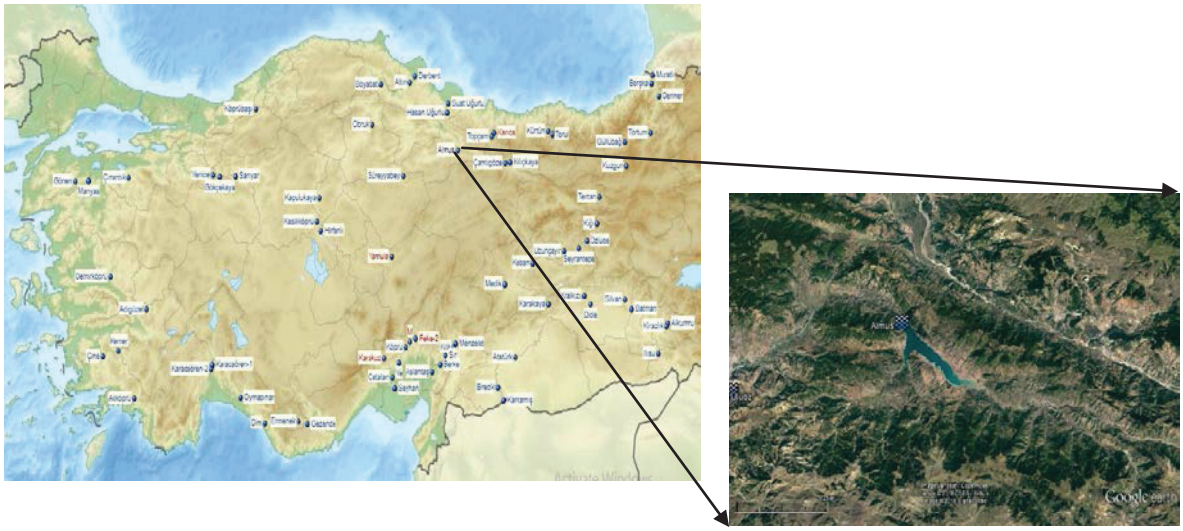

Figure 1. The location of the Almus dam and HEPP in Turkey.

Table 1. Almus Dam and HEPP Characteristics.

River	Yesilirmak
Minimum operating level (altitude)	767.37 meters
Maximum operating level (altitude)	804.5 meters
Water volume of minimum operating level	151.473 thousand m^3
Water volume of maximum operating level	1.006.730 thousand m^3
Water used for power generation	855.257 thousand m^3
Lake area	31.3 km^2
Height from the river bed	78 meters
Power	27 MW
Annual Production	99 GWh

The Data of the Almus hydropower used in the study as shown in Table 2. It is consist of the monthly data of the energy production of the dam, the total incoming water as a volume, incoming water as discharge and the lake water level as a depth.

Table 2. Part of the data input of Almus HEPP for the model.

Month	Production (KWh)	Total incoming Water (Million m^3)	Incoming flow m^3/s	Lake Water Level (m)
January-93	2,427,800	51.4	19.2	792.21
February-93	14,733,500	75.96	31.4	793.42
-	-	-	-	-
-	-	-	-	-
December-13	2,977,680	14.3	5.32	791.76

METHODS

Artificial Neural network (ANN)

In recent years there are several attempts to use intelligent computational systems such as Artificial Neural Network (ANN). ANNs inspired by biological nervous systems; algorithms that can be learned using input data, derive new information, generalize and classify algorithms (Zhang et al., 1998). ANN has been used widely in hydrology and many applications like hydropower generation forecasting. It is used to confirming the usefulness and to model different hydrological parameters. ANNs are black box models that are used for calculating, forecasting and estimating purposes in many various areas of the science and engineering. An ANN in the context of statistical analysis is an alternative to or added to multiple regressions which is an information processing model which inspired from the way biological nervous systems (Andy et al, 2004).
This growing interest among researchers is stemming from the fact that these learning machines have an excellent performance in the issues of pattern recognition and the modeling of linear and nonlinear relationships of multivariate dynamic systems. Owing to the prediction of higher accuracy, among many Artificial Intelligence (AI) built on soft computing methods, the artificial neural network (ANN) is used widely in specific operations. Therefore, the Artificial Neural Network (ANN) gives a fast and flexible passage for integration of data and the development of the model (Hammid et al., 2018). Kankal et al. (2011) has examined studies related to energy forecasting for Turkey and has found ANN, swarm optimization, genetic algorithm approach, harmony search algorithm, ARIMA methods.
Until today, ANN models have been used by many researchers to predict the production of the energy (Hamzacebi et al., 2017; Dmitrieva, 2015; Cobaner et al., 2008; Zhang et al., 1998). It was found that the ANN used in these studies gave better results than the conventional models.

Support Vector Machine (SVM)

Support vector machine (SVM) is a machine-learning algorithm, founded by Vapnik and is gaining popularity due to its good performance and attractive features. The method has been applied to several areas such as meteorology, and pavement engineering (Vapnik, 1995; Osowski and Garanty, 2007; Maalouf et al., 2008). SVM is a blend of linear modeling and instance based learning in a high-dimensional space. SVM can be applied to those problems when data cannot be separated by a line (Dmitrieva, 2015).
Application of SVM in civil engineering is an emerging area and need to be explored in other disciplines like geotechnical engineering. SVM based approaches for classification and prediction have been used in several other civil engineering disciplines and found to be working well in comparison to neural network approach (Dibike et al., 2001).
The SVM is based on statistical learning theory and implements the structural risk minimization principle rather than the empirical risk minimization principle implemented by most traditional ANN models (Vapnik, 1995). This method has been used in many searches to forecast energy production (Li et al., 2014; Lin et al., 2006).

Deep Learning

A deep learning model is used in this study at Almus dam hydropower station and show it performs well-known time-series forecasting models (Assem et al., 2017). To the best of our knowledge, this paper is the first for Deep Learning technique in hydropower sector and forecasting the energy production of this new technique. Deep learning is the developing output of ANN which make forecasting more accurately and with high percentage and gave positive results for studies of long term of periods. Deep learning can multiple layers of models to learn and support representation of data. Deep neural networks increase the performance of load forecasting by making a focus on parameter optimization (Gokgoz and Filiz, 2018).

APPLICATION AND RESULTS

In this study, ANN, SVM and DL are utilized to forecast the hydropower production of Almus dam. Two hundred and fifty monthly data samples used in this paper from Almus dam data (Production, Total incoming water, Incoming flow and Lake water level) are used for operating the three models. Figure 2 shows the relationship between the energy production and other parameters in as scatter plot figures.

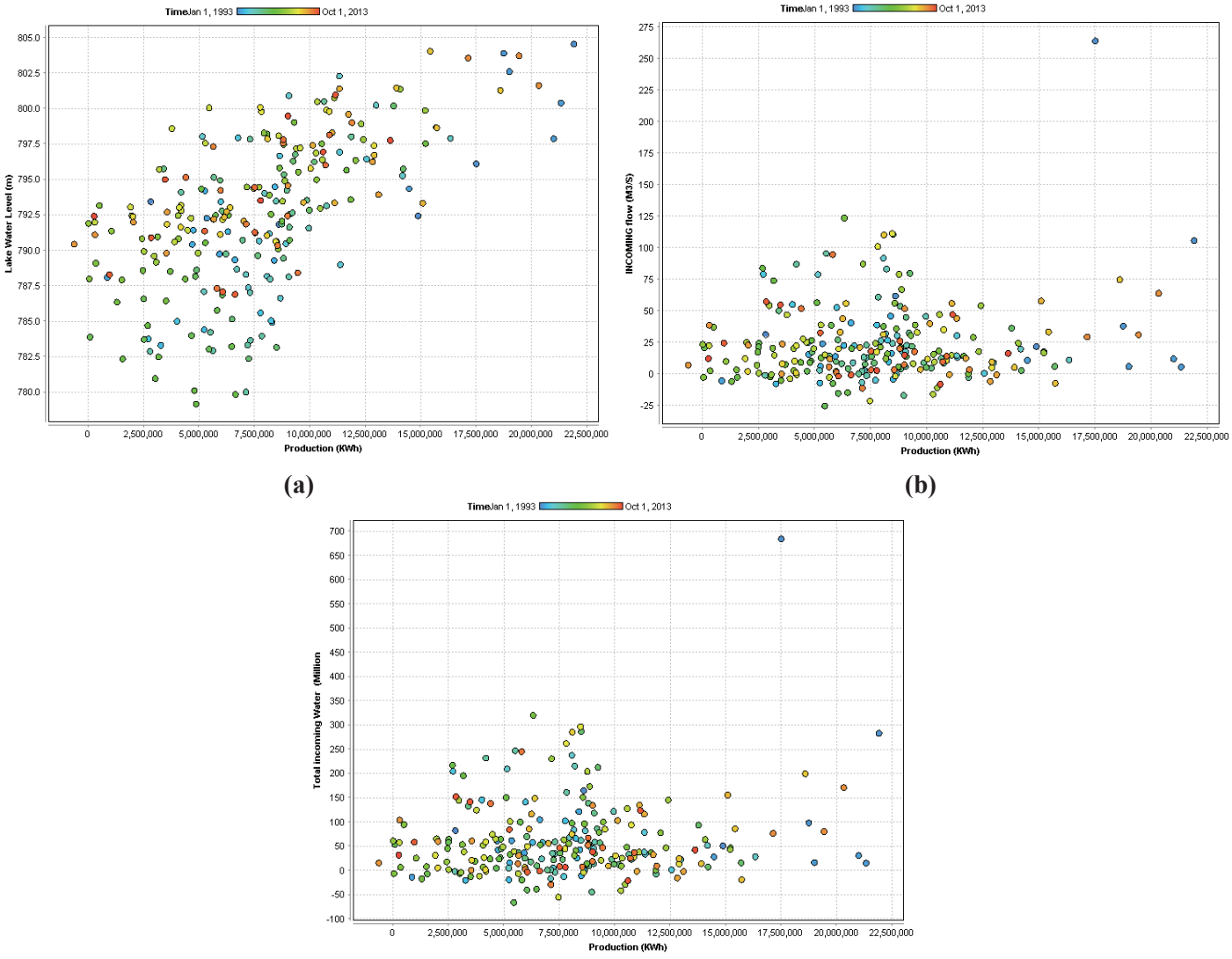

Figure 2. (a) Scatter plot between the lake water level and the energy production (b) Scatter plot between the incoming flow and the energy production (c) Scatter plot between the total incoming water and the energy production.

The scatter plots in a, b and c are described very clearly the relationship between the parameters (Production, Total incoming water, Incoming flow and Lake water level). On the other hand, Figure 3 shows the time series of the Almus dam parameters (Power production (Kwh), Incoming water, the total incoming Water (Million m^3) and the Lake Water Level (m).

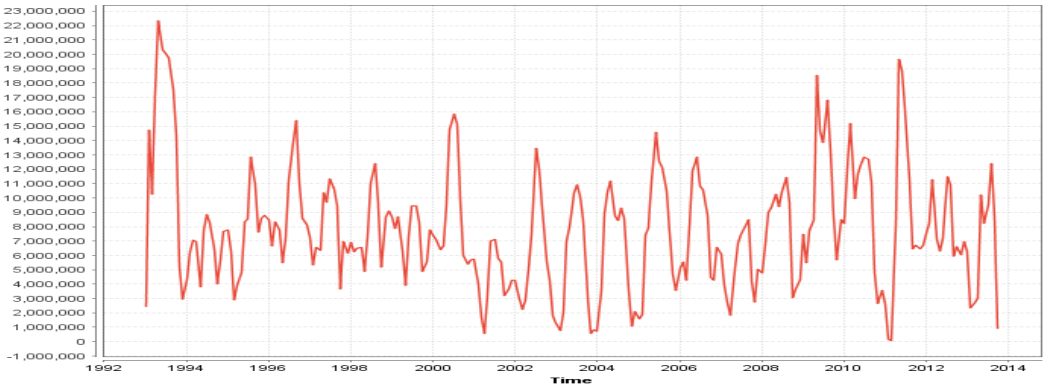

(a)

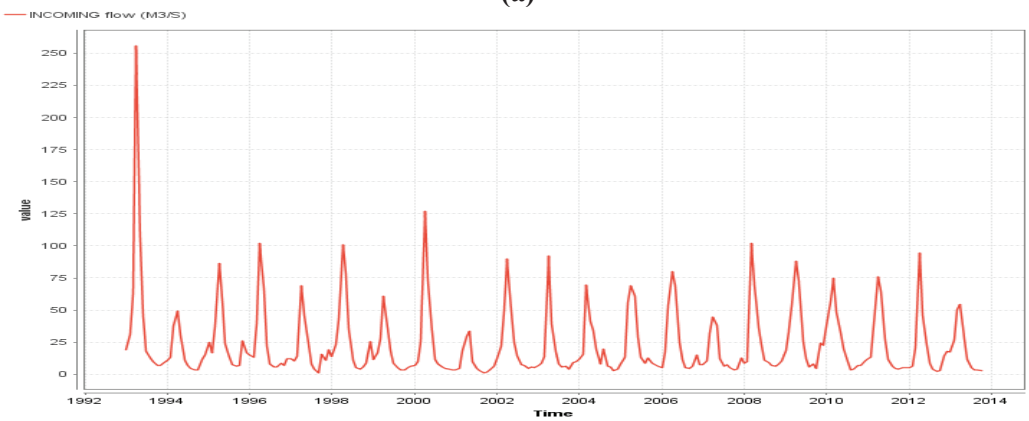

(b)

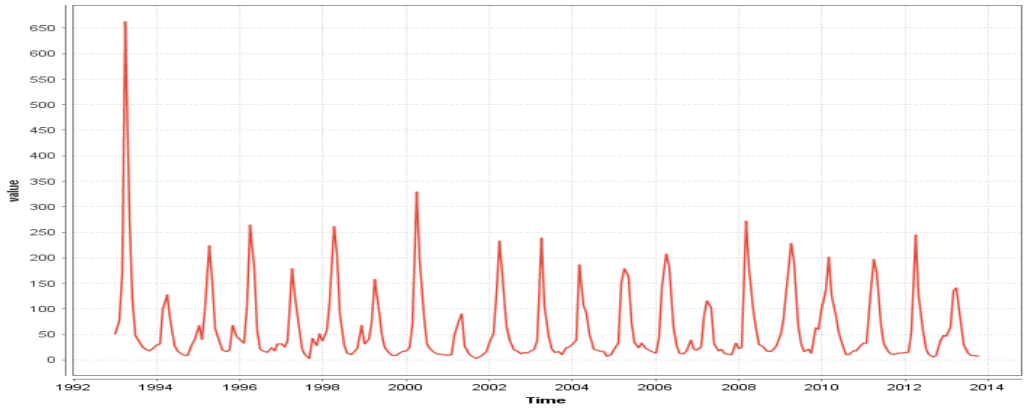

(c)

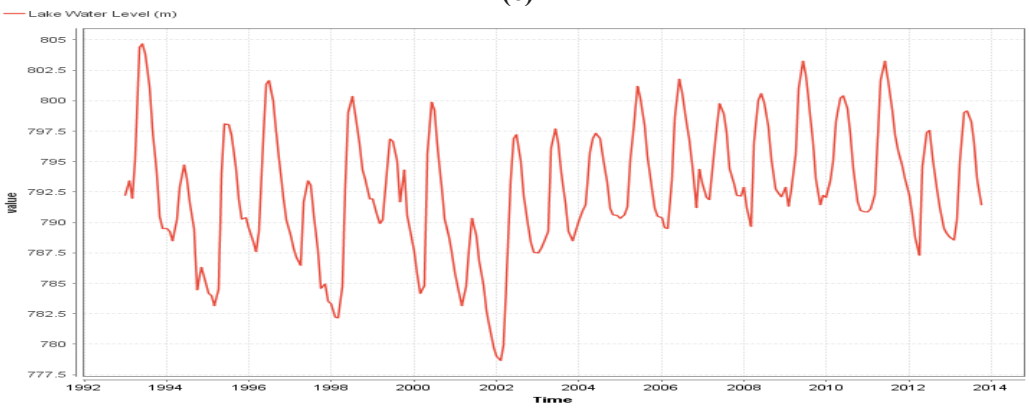

(d)

Figure 3. (a) The rate of power production (Kwh), (b) The time series of Incoming water, (c) The total incoming Water (Million m^3), (d) The Lake Water Level of Almus dam (m).

Table 3. Correlation Matrix results.

Parameter	Cell Contents	Production (KWh)	Total incoming Water	Incoming flow
Total incoming Water	Pearson correlation	0.162	-	-
	P-Value	0.010	-	-
Incoming flow	Pearson correlation	0.161	0.999	-
	P-Value	0.011	0.000	-
Lake Water Level	Pearson correlation	0.665	0.021	0.018
	P-Value	0.000	0.741	0.776

In Table 3, if the production and variable have a high correlation (equal 1) the results can give a high quality indication for the model but here only the production with the lake water level has given a good quality indication which mean that the linear model could not work as needed with the given data so a new method have to use for forecasting model. Figure 4 shows the normal distribution of energy production (Kwh), Lake water level, incoming flow and the total incoming water.

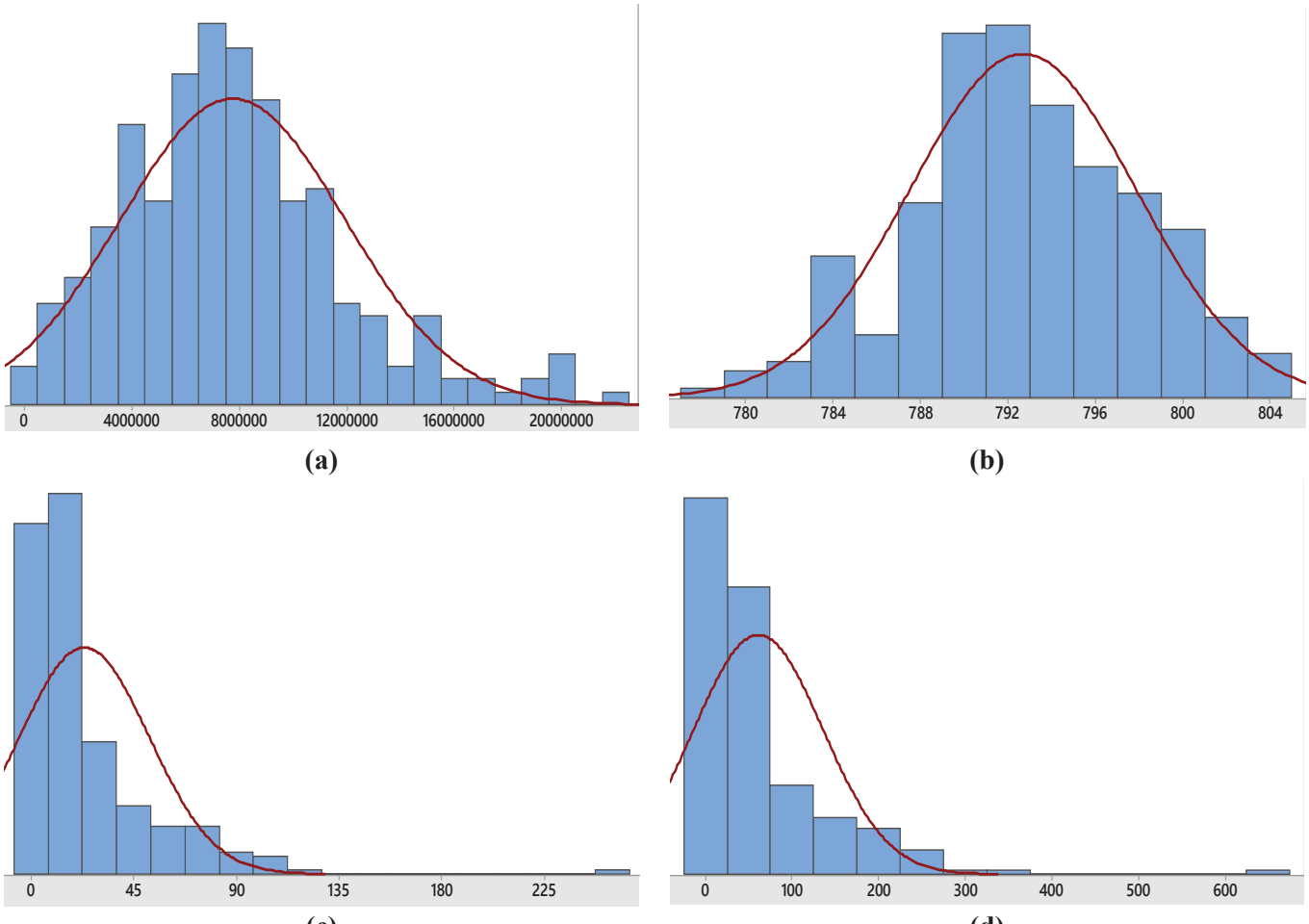

Figure 4. The distribution of (a) Energy production (Kwh), (b) Lake water level, (c) Incoming flow, (d) Total incoming water.

The distribution in a and b gave indicate that the graphs are behaved normal distributed but in c and d parts the graphs indicated that not normal distributed and non-stationary variables.

Artificial Neural network (ANN)

In this part, ANN is utilized to forecast the electricity production of Almus dam. For this purpose in ANN part, single hidden layered feed forward neural network models are used. The data used in the running of network models are obtained from the operation data of TEIAS for Almus dam.
The statistics parameters room mean square error (RMSE), the coefficient of correlation (R), the coefficient of determination (R^2) and discrepancy ratio (D) were used to get the best model out of three alternatives. Figure 5 show Three Levels of ANN is contained five hidden layers connected to five inputs and one output.

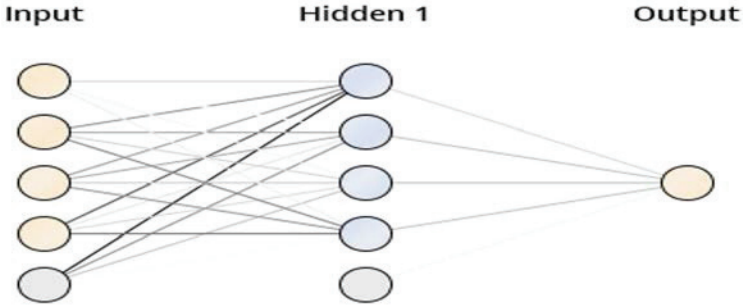

Figure 5. Structure of the ANNs.

After implementing the statistical analysis stage, the model of the neural network was simply generated by using MATLAB software that deals with applying simulation. When offered data patterns, historically measured input-output data sets relating the difficulties to be modeled, ANNs can create mapping and build up relation model for input and output data. Table 4 shows the parameters results at each nodes from Node 1 to Node 4. Beside of that, Table 5 shows the regression of the four nodes using ANN.

Table 4. The parameter of four nodes in the ANNs.

Parameters	Node 1 (Sigmoid)	Node 2 (Sigmoid)	Node 3 (Sigmoid)	Node 4 (Sigmoid)
Time	1.006	-0.008	0.259	0.411
Total incoming Water (Million m^3)	2.981	2.190	1.167	3.226
Incoming flow (m^3/s)	2.591	2.235	1.098	2.754
Lake Water Level (m)	-4.595	0.643	-1.006	3.498
Bias	6.277	-2.801	-1.475	-0.111

Table 5. Regression of four nodes in the ANNs.

Output (Regression (Linear))			
Node 1	Node 2	Node 3	Node 4
-1.018	-1.586	1.345	1.556
Threshold: 0.210			

Although the good results of ANN model Table 6 shows the comparison in the performance results between the three models. The high quality of results by using DL model are very clear from correlation and Squared correlation values which get to be near one.

Table 6. The performance results of the three models.

Parameter	ANN Performance	SVM Performance	DL Performance
Normalized absolute error	0.729	1.000	0.072
Root relative squared error	0.675	1.000	0.071
Correlation	0.766	0.682	0.998
Squared correlation	0.587	0.466	0.995
Prediction average	7795033.35 +/- 4133363.88	7795033.35 +/- 4133363.88	7795033.35 +/- 4133363.88

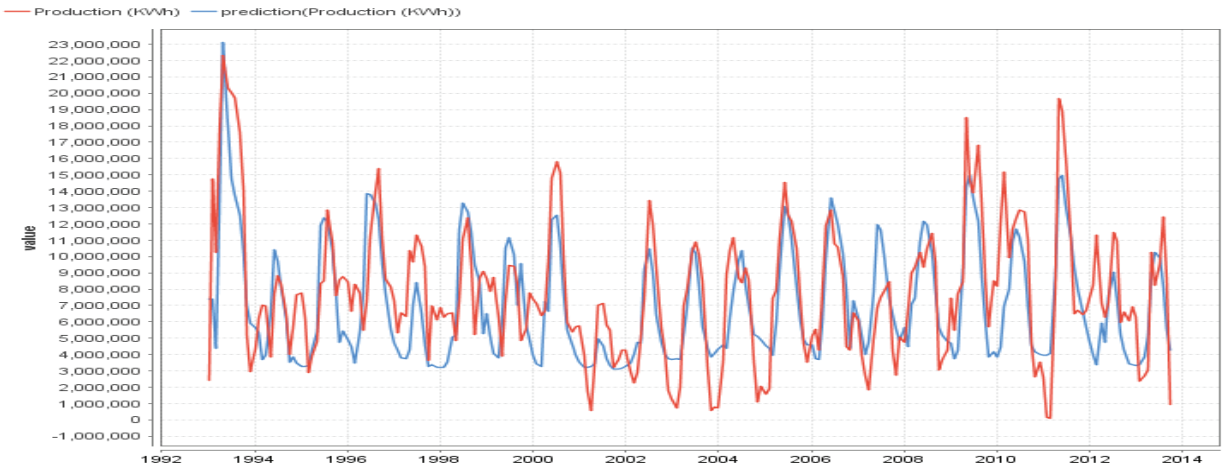

(a)ANN model

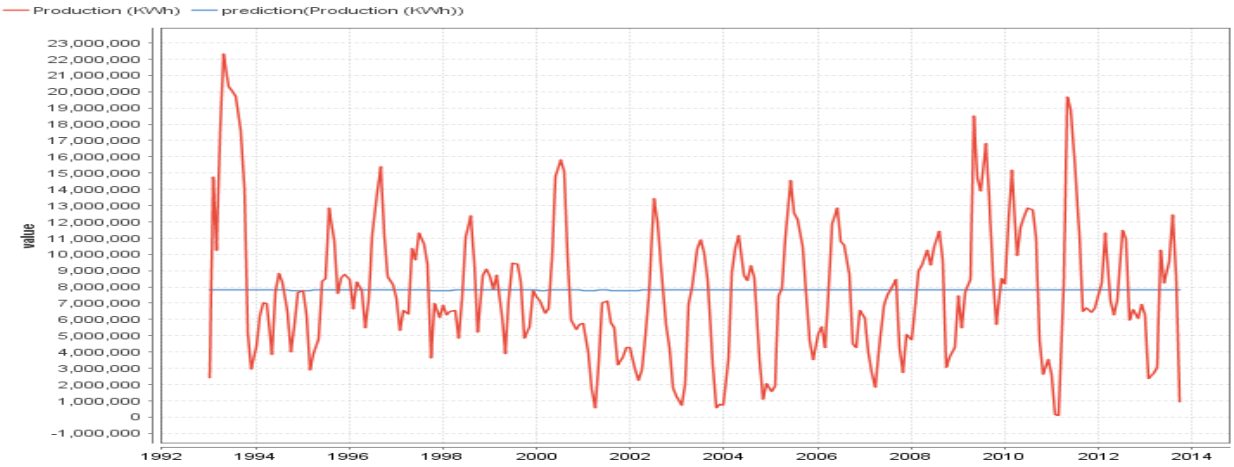

(b)SVM model

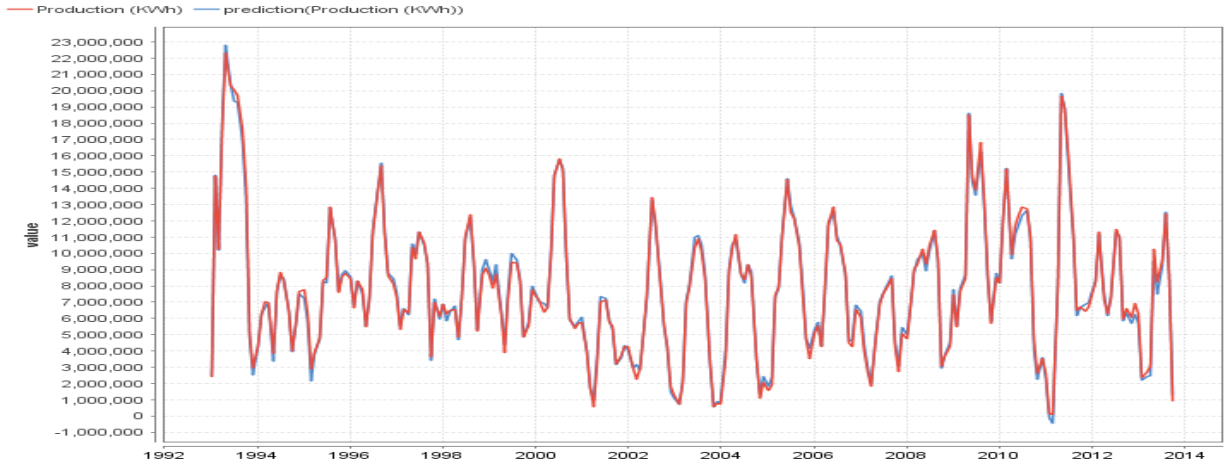

(c)DL model

Figure 6. (a), (b) and (c) the differences between production time series and predicted production curves in the three model.

In figure 6 (a) the ANN model work and acceptable just to have an idea about the forecasting stream but in (b) the SVM model did not work for forecasting the energy production. On the other hand the DL model almost the same behavior for the time series of the production. The Deep learning model is given the best result to forecast the electricity production of Almus dam.

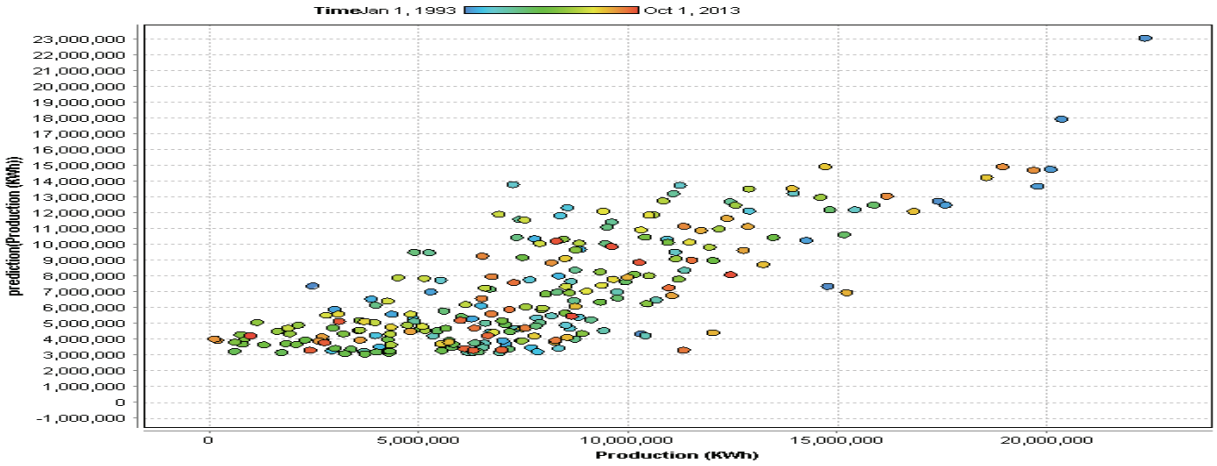

(a)ANN model

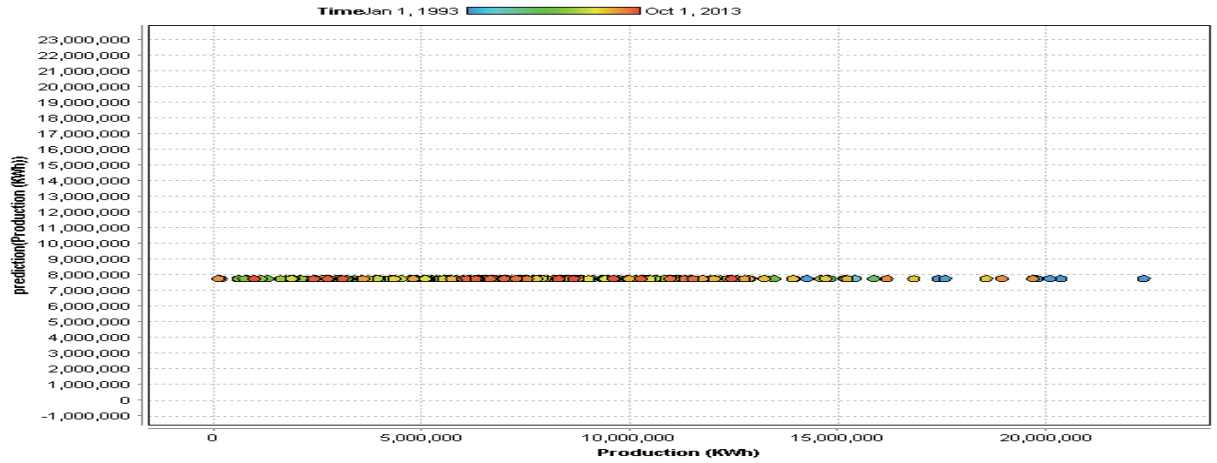

(b)SVM model

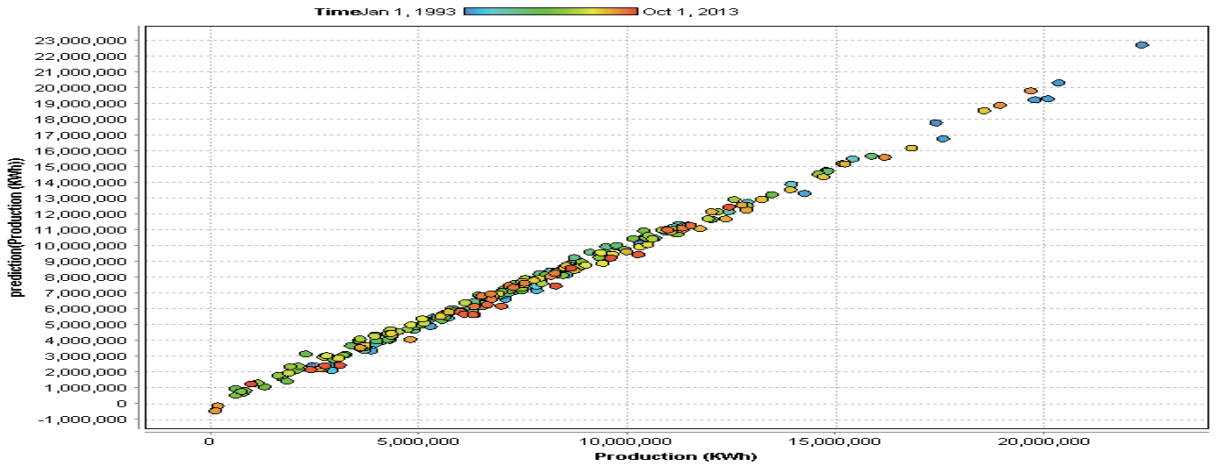

(c)DL model

Figure 7. (a), (b) and (c) the scatter plot between production and prediction of production in the three models.

The scatter plot between the production and the prediction of the energy production of the three models (ANN, SVM and DL) are shown in Figure 7. In b part, the result steady line that mean the model not work in high performance at this case study. In the opposite side, the c part result is a linear relationship which mean the model is very suitable to be using in this case study.

CONCLUSION

Renewable energy mainly depends on the local environmental conditions, such as temperature and rainfall-runoff ratios. Therefore, the expected power production heavily fluctuates, which makes calculating the feed-in into the power grid very challenging to be calculated and predicted. Hydropower is the primary renewable source contributing to electricity supply, and its future contribution is anticipated to increase significantly. This paper presented the results of deploying Machine Learning Techniques in short-term forecasting of the amount of energy produced by Almus Dam and Hydroelectric Power Plant in Tokat, Turkey.

In this study, three models (Artificial Neural Network (ANN), Support Vector Machine (SVM) and Deep Learning (DL)) are used to forecast the energy production of Almus HEPP using monthly hydroelectric power generation data from 1993 to 2013. The correlation values are 0.766, 0.682 and 0.998 for ANN, SVM and DL, respectively. Beside of that, the squared correlation values are 0.587, 0.466 and 0.995 for ANN, SVM and DL, respectively. The correlation and the squared correlation values verified that the deep learning model gives results more accurately with high performance to the case study.

The paper showed the differences between the three models and the quality of results in each model. This study makes a clear vision about the effective of using these models in forecasting to understand the behaviour of the system.

REFERENCES

Altinbilek, D., 2002. The role of dams in development. International Journal of Water Resources Development, vol. 18, issue 1, 9–24.

Andy, P.D., Peter, L.M., Goethals, W.G., Niels, D.P., 2004. Optimization of Artificial Neural Network Model Design for Prediction of Macro-invertebrates in the Zwalm River Basin, Ecological Modelling, vol.174, 161–173.

Assem, H., Ghariba, S., Makrai, G., Johnston, P., Gill, L., Pilla, F., 2017. Urban Water Flow and Water Level Prediction Based on Deep Learning. Machine Learning and Knowledge Discovery in Databases, 317-329.

Cobaner, M., Haktanir, T., Kisi, O., 2008. Prediction of Hydropower Energy Using ANN for the Feasibility of Hydropower Plant Installation to an Existing Irrigation Dam, Water Resource Manage, vol. 22, 757-774.

Dibike, Y.B., Velickov, S., Solomatine, D.P., Abbott, M.B., 2001. Model induction with support vector machines: introduction and applications. Journal of Computing in Civil Engineering, vol. 15, issue 3, 208–216.

Dmitrieva, K., 2015. Forecasting of a hydropower plant energy production. Østfold University College, Master's Thesis in Computer Science, Halden, Norway, 69p.

Elliot T.C., Chen K., Swanekamp R.C., 1998. Standard handbook of power plant engineering, second edn. McGraw-Hill, New York.

Gokgoz, F., Filiz, F., 2018. Deep Learning for Renewable Power Forecasting: An Approach Using LSTM Neural Networks. International Journal of Energy and Power Engineering, Vol.12, No.6, 412-416.

Hammid, A.T., Bin Sulaiman, M.H., Abdalla, A.N., 2018. Prediction of small hydropower plant power production in Himreen Lake dam (HLD) using artificial neural network. Alexandria Engineering Journal, vol. 57, 211-221.

Hamzacebi, C., Es, H.A., Cakmak, R., 2017. Forecasting of Turkey's monthly electricity demand by seasonal artificial neural network. Neural Computing and Applications, 1-15.

Kankal, M., Akpinar, A., Komurcu, M.I., Ozsahin T.S., 2011. Modeling and forecasting of turkey's energy consumption using socio-economic and demographic variables. Applied Energy, vol.88, No 5, 1927 – 1939.

Kaygusuz, K., 2002. Sustainable Development of Hydroelectric Power. Energy Sources, vol. 24, issue 9, 803-815.

Huang, H., Yan, Z., 2009. Present Situation and Future Prospect of Hydropower in China. Renewable and Sustainable Energy Reviews, vol. 13, issue 6, 1652-1656.

Li, G., Sun, Y., He, Y., Li, X., Tu, Q., 2014. Short-Term Power Generation Energy Forecasting Model for Small Hydropower Stations Using GA-SVM. Mathematical Problems in Engineering, 1-9.

Lin, J., Cheng, C., Chau, K., 2006. Using support vector machines for long-term discharge prediction. Hydrological Sciences Journal, vol. 51, no. 4, 599–612.

Maalouf, M., Khoury, N., Trafalis, T.B., 2008. Support vector regression to predict asphalt mix performance. International Journal for Numerical and Analytical Methods in Geomechanics, vol. 30, 1989–1996.

Maier, H.R., Dandy, G.C., 2000. Neural networks for the prediction and forecasting water resources variables: a review of modeling issues and applications. Environmental Modelling & Software, vol. 15, issue 1, 101–124.

Melikoglu, M., 2013a. Vision2023: assessing the feasibility of electricity and biogas production from municipal solid waste in Turkey. Renewable and Sustainable Energy Reviews, vol. 19, 52–63.

Melikoglu, M., 2013b. Vision2023: forecasting Turkey's natural gas demand between 2013 and 2030. Renewable and Sustainable Energy Reviews, vol. 22, 393–400.

Osowski, S., Garanty, K., 2007. Forecasting of the daily meteorological pollution using wavelets and support vector machine. Engineering Applications of Artificial Intelligence, vol. 20, issue 6, 745–755.

Smith, G., Mander, J., Callenbach, E., 2012. Nuclear roulette: the truth about the most dangerous energy source on earth. USA: Chelsea Green Publishing Company.

Vapnik, V., 1995. The Nature of Statistical Learning Theory. Springer-Verlag, New York, 1–188.
Yuksek, O., Komurcu, M.I., Yuksel, I., Kaygusuz, K., 2006. The role of hydropower in meeting Turkey's electric energy demand. Energy Policy, vol. 34, issue 17, 3093–3103.
Zhang, G.P., Patuwo, B.E., HU, M.Y., 1998. Forecasting With Artificial Neural Networks: The State Of The Art. International Journal of Forecasting, vol. 14, issue 1, 35- 62.

5th International Symposium on Dam Safety

October 27-31, 2018

EARLY WARNING SYSTEMS FOR DAM SAFETY: CASE OF LARGE ENGURI DAM, GEORGIA

Tamaz CHELIDZE[1], Alessandro TIBALDI[2], Nino TSERETELI[1], Vakhtang ABSHIDZE[1], Nodar VARAMASHVILI[1], Zurab CHELIDZE[1]

ABSTRACT

Institute of Geophysics created the Early Warning Telemetric System (EWTS), which consists of tiltmeters, laser strainmeters in the dam body and its foundation and controllers connected by the GSM/GPRS Modem to the diagnostic center. The system operates from 1998 ad operates up to now quite effectively.

Catastrophes of dam are also caused by activation of the mass-movements. At a distance of 2 km from the Enguri dam is located the most dangerous object - Khoko landslide, where field data indicate 2-5 cm/y slip rates. The monitoring system (extensiometer and GPS) was installed at the landslide in 2017. The data obtained during last 3 years show that the landslide is active and its slip-rate accelerates after heavy rainfalls.

Institute of Geophysics is developing cost-effective autonomous complex telemetric setup for signaling mass-movement initiation. Suggested EWTS implies monitoring of main factors, leading to mass-movement: soil moisture H and tilts/acceleration. The EWS after final tests will be installed on the Khoko landslide.

Keywords: Dam, Landslide, Natural catastrophe, Hazard, EWS

INTRODUCTION

The 271 m high Enguri arch dam, still one of the highest arch dam in operation in the world, was built in the canyon of the Enguri river (West Georgia) in the 1970s. It is located in a zone of high seismicity (MSK intensity IX) and close to the Ingirishi active fault. Of course, the Enguri Dam with its 1 billion cubic meters water reservoir is a potential source of large man-made catastrophe and it should be under permanent monitoring. At the same time this it is an amazing natural laboratory, where we can investigate tectonic and geotechnical strains/processes and response to the lake load-unload impact, i.e. the reaction to a controllable loading of Earth crust. This is an important scientific issue, connected with such problem as Reservoir Triggered Earthquakes.

The stability of a dam can be tested by its long-term (static) and short-term response to the water load. The dam as a whole or its individual elements may respond to certain loading conditions through time-dependent elastic and inelastic deformations. For each action a safety limit can be determined, which must not be exceeded. Due to unusual or extreme loadings or due to accumulation of damage critical conditions may occur, which are jeopardizing the safety of dam.

ENGURI HIGH DAM

The M. Nodia Institute of Geophysics and Georgian-European Centre ”Geodynamical Hazards of High Dams” operating in the frame of Open Partial Agreement on Major Disasters at the Council of Europe developed the real-time geotechnical telemetric monitoring system of large dams (DAMWATCH). This low-cost early warning system designed by Institute of Geophysics and “ALGO Ltd” (Tbilisi) consists of

[1] Institute of Geophysics, Tbilisi, Georgia: e-mail: nodar.varamashvili@tsu.ge
[2] University of Milan Bicocca, Milan, Italy

sensors (tiltmeters, APPLIED GEOMECHANICS Model 701-2 and laser strainmeters), which are connected to terminals and central controllers and by a GSM/GPRS modem transmits the data to the diagnostic center.

Fig. 1. Google view of Enguri Dam International Test Area (EDITA) territory. The arrow shows position of the major Ingirishi fault.

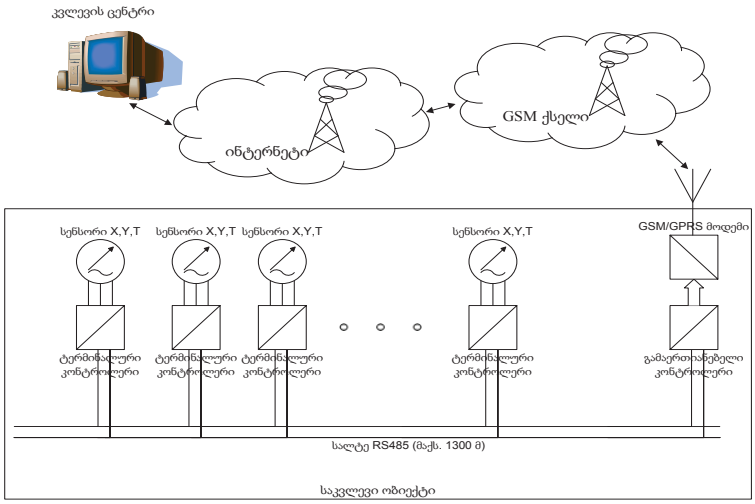

Fig. 2. The cost-effective early warning system designed by MNIG and "ALGO Ltd" (Tbilisi) consists of sensors (tiltmeters, APPLIED GEOMECHANICS Model 701-2), which are connected to terminals and central controllers and by a GSM/GPRS modem transmits the data to the diagnostic center.

The simplest approach to dam safety problem is to compare response of real strain/tilt data with design values, which as a rule use Hook's rheology (static, linear elasticity approach). If ტვე measured characteristics, e.g. strains, are close to or larger than theoretically predicted limit deformations, some

preventive measures should be realized. Of course, predictions of the model have to be compared with monitoring data (Table 1).

Table 1. Comparison of observed plumbline horizontal displacements (Bronshtein, 2008) and corresponding tiltmeters data (horizontal displacements in mm and tilts in seconds, with Root Mean Square) at maximal water level in the lake (510 m) for three sections of Enguri HPP (Abashidze et al. 2008) with theoretical (critical) admissible values of plumblines calculated by (Emukhvari, Bronshtein, 1991).

Level	Section 12			Section 18			Section 26		
	Observed plumbline data	Observed tiltmeter data	Critical Admissible values	Observed plumbline data	Observed tiltmeter data	Critical Admissible values	Observed plumbline data	Observed tiltmeter data	Critical Admissible values
360 m	20 mm	11 mm (38±5.1)''	89 (122)''	35 mm			15 mm	14 mm (46±5.6)''	88 mm
402 m	40 mm	32 mm (63±4.5)''	59 (112)''	60 mm	55 mm (70±3.9)''	55 mm	30 mm	37 mm (74±4.1)'	58 mm
475 m	60 mm	48 mm (56±8.7)''	31 (182)''	65 mm			55 mm	42 mm (55±5.5)''	26 mm

The Table 1 presents observed data: plumbline horizontal displacements (Bronshtein, 2008) and corresponding tiltmeters data (horizontal displacements in mm and tilts in seconds, with Root Mean Square) at maximal water level in the lake (510 m) for three sections of Enguri HPP (Abashidze et al. 2008) and theoretical (critical) admissible values of plumblines calculated by (Emukhvari, Bronshtein, 1991). The generally accepted approach is to compare the observed stress (strain) to calculated stresses, which correspond to some fraction of yield strength or of the ultimate strength of the material, the construction is made of.

Analysis of the Table leads to following conclusions: i. at the level 360 m all displacements are less than critical values; ii. at the level 402 m only in the central 18-th section the displacements are close to critical ones; iii. at the highest level (475 m) displacement of the side sections are larger than critical, i.e. at this level the state should be considered as diagnosis MAS or "faulty". According to Emukhvari and Bronshtein (1991) in this case it is necessary to carry out repeated diagnostics of construction on the basis of re-examination of monitoring data and correction of theoretical predictions of response of the dam to loads. The displacement observation data obtained by two different methods are in satisfactory agreement. Besides, the dam performs normally and there are no visual signs of significant damage.

This means that the theoretical model needs some development/corrections, possibly taking into account complexity of construction structure dynamic response to stress variation on different time scales from years to minutes/ seconds. Indeed, the real engineering structures manifest deviations from the simple static model and these deviations can be used for diagnostics. From above it follows that a promising technique could be analysis of deviations from static elasticity model, namely, analysis of nonlinearity of stress-strain relation such as hysteretic behavior during load-unload cycle. Figure 3 (left) shows how two

components of tilts of dam body, along (X) and normal (Y) to the dam crest at Enguri Dam respond to the seasonal recharge-discharge cycle of the reservoir; on the right the hysteresis in seismic velocities of foundation section for the same cycle is shown.

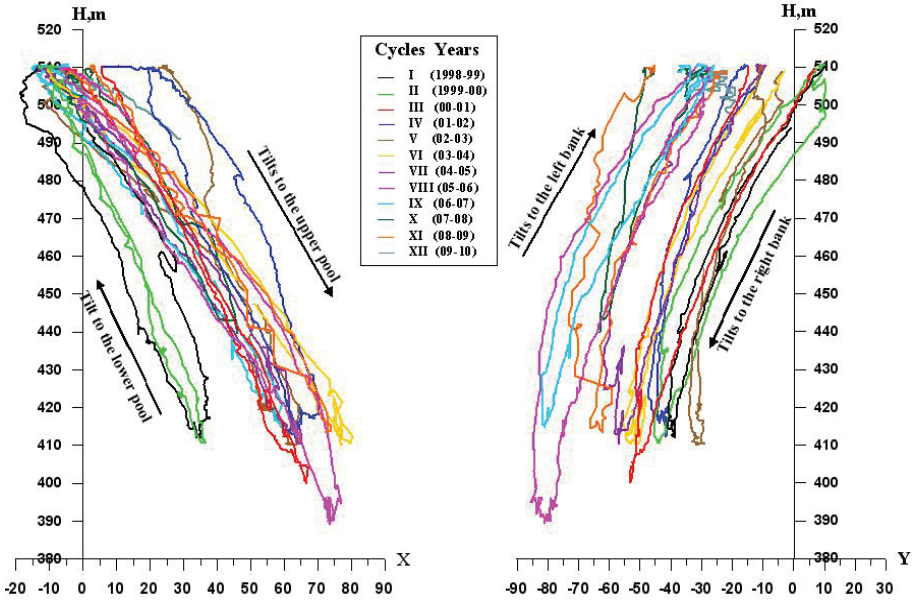

Figure 3. Left: Tilts in sec, registered in the body of Enguri High Dam, Georgia (section 12, mark 402) in two directions, along (X) and normal (Y) to the dam crest versus water level in the lake H in meters, during 12 seasonal cycles (1998-2009). Note hysteresis in load-unload response.

The interpretation of observed hysteretic stress-strain or tilt-stress diagrams (Fig.3) can be accomplished by the theory of mesoscopic elasticity (McCall&Guyer 1994, Guyer&Johnson 2009). The matter is that heterogeneous materials such as mass concrete and rocks are nonlinear and their behavior is very different from this of its homogeneous components: for example, stress-strain (or tilt) dependences manifest nonlinear hysteretic elastic behavior, namely, asymmetric response to loading and unloading of so called mesoscopic structural features (mainly compliant microcracks) to stress variation. Heterogeneous materials contain an enormous number (10^9-10^{12}) of such defects per square centimeter, which means that macroscopic elastic properties of the material depend strongly on behavior of microcracks. Thus, parameters of hysteretic cycle can be used for diagnostics of material: in the absence of cracks the brittle solid manifests linear elasticity without any hysteresis, appearance of cracks leads to hysteresis and the opening of hysteresis curve increases with the number of defects.
As a rule, nonlinear contributions to well-designed and well-constructed dam strains are small, so it can be concluded that the dam design based on linear approach works quite well, but the analysis of relatively small nonlinear effects can produce promising methods of dam safety diagnostics due to high sensitivity of nonlinear systems to small external impacts.

Short-term diagnostic tools
At present the main short-term diagnostic tool is the analysis of the eigenfrequencies of the dam based on the power spectra of dam vibrations caused by earthquakes, water discharge, turbine operation or ambient seismic noise. The record of natural dam vibrations at Enguri dam shows that the dominant frequency on the crest of the dam is about 1 Hz; this is in good agreement with results of the analysis of accelerograms recorded during the Racha earthquake (2005, M=6) and numerical analysis of a typical dam.

At the same time our data show that the Enguri Dam vibration spectrum also covers other than 1 Hz, much lower frequencies. These LF vibrations were recorded by the network of precision tiltmeters (Applied Geomechanics) and can be used for dam diagnostics.

Methods of linear and nonlinear analysis of strain and tilt time series for dam stability assessment
In order to ensure correct statistical and dynamical investigation of dam stability problem, modern methods of linear and nonlinear analysis of strain and tilt time series were used. The following time series analysis methods are used: statistical methods (moments, distribution testing), time-frequency analysis methods (power spectrum, autocorrelation function), time-frequency (wavelet transformation) and eigenvalue methods, denoising of data sets (nonlinear noise reduction), testing of memory properties of targeted process (long range correlation testing, detrended fluctuation analysis (DFA), multifractal detrended fluctuation analysis; correlation and information dimension calculation recurrence plots (RP) and recurrence quantitative analysis (RQA) (Matcharashvili et al, 2010).
Nonlinear dynamics analysis allows revealing hidden structures (regularities) in seeming random time series.

DAMTOOL- a package for operative control of engineering constructions
DAMTOOL is a program intended for visual estimate, processing and analyzing the data of large engineering constructions' (dams, bridges etc) tilt measurements. It can be used also for analysis of any monitoring time series: strains, stresses, tilts etc (Chelidze et al, 2013).
Fig. 4 demonstrates the potential of nonlinear dynamics approach to analysis of tilt time series from April 2010 to June 2010. The upper plot shows tilt time series from April to June 2010 for one of stations of our network. The lower plot shows results of processing of the tilt record by DAMTOOL package: namely, it presents percent of determinism or RQA %DET (Marwan, 2003). The deviations from the normal behavior in the mid-May and June due to fast water discharge are evident even visually, but the usage of DAMTOOL allows assessing these deviations quantitatively. Note high values of and %DET during regular regime in April and first decade of May (which points to stability of monitoring data) and strong deviations in DET% due to geotechnical impact – addition of high frequency component during intensive discharge of water through dam outlet in 12.05-22.05.2010 and 01.06-11.06.2010 time intervals.

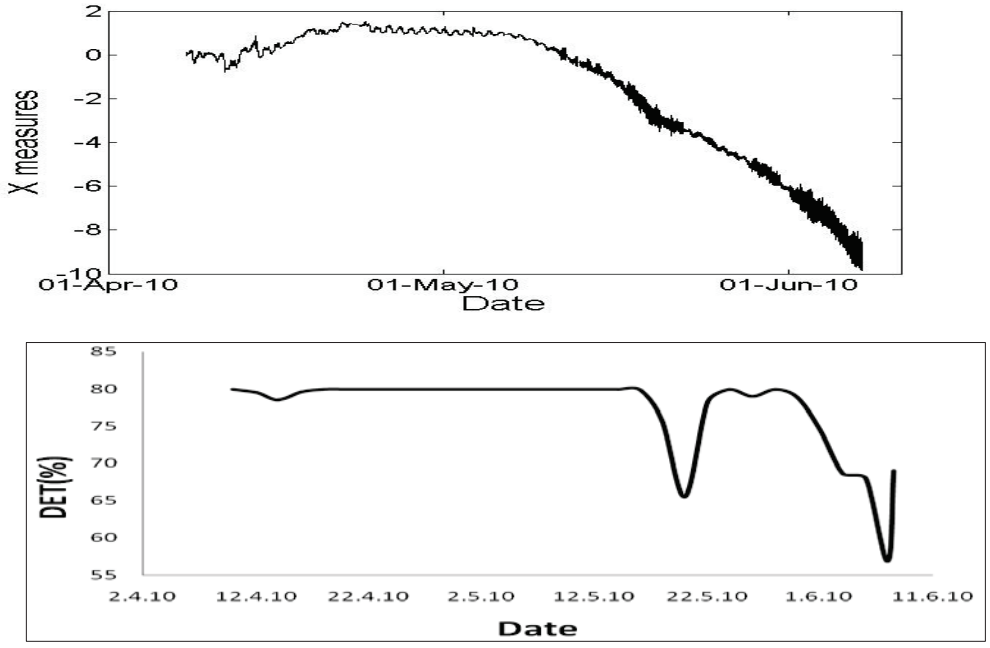

Fig. 4. The potential of nonlinear dynamics approach to analysis of tilt time series. Upper plot-original tilt time series; lower plot - RQA (% of determinism). Note high values DET during regular regime and strong deviations due to (in this case) geotechnical impact.

The data obtained already show very interesting long-term and short-term patterns of tilts' dynamics in the dam body, including tilt hysteresis during annual loading-unloading cycle, low-frequency dam oscillations etc, which can be used for dam diagnostics using packages DAMWATCH and DAMTOOL. The possible interpretation of hysteresis phenomena in by mesoelasticity (nonlinear elasticity) approach is suggested. It is shown that the main contribution to annual tilts hysteresis comes from the dam body tilts, thus these data are appropriate for dam damage diagnostics. The tiltmeter recordings with one minute resolution reveal many interesting details of dam behavior, which expand the spectrum of dam vibrations to low frequencies and give new diagnostic tools. Analysis of retrospective tilt data show that used methods are appropriate to detect and quantify dynamical changes in dam body behavior caused by different external and internal causes, though mechanism of some observed effects still need to be studied in detail.

Mass-movements can be very dangerous for dams: the example is well known 1963 Vajont dam catastrophe in Italy, where the landslide fall into the dam lake, causing enormous surge wave and killing 3000 victims. In case of Enguri dam at the distance of 2 km from it is located the most dangerous object - Khoko landslide, where field data indicate 2-5 cm/y slip rates. The monitoring system (extensiometer and GPS) was installed at the landslide in 2017 according to NATO project (Tibaldi, Tsereteli, 2017). The data obtained during last 3 years show that the landslide is active and its slip-rate accelerates after heavy rainfalls.

EARLY WARNING SYSTEM (EWS)

Taking into account importance of the problem, our institute is developing EWS project, which aims to develop a precise enough cost-effective autonomous complex telemetric setup for signaling debris flow/landslide initiation, using radio signals or Internet. The satisfaction of seemingly incompatible demands on precision and cost-effectiveness of the system became possible last years, thanks to development of new technologiēs, such as low-cost MEMS sensors and data acquisition/transfer boards (ARDUINO), having low power consumption). Exactly, the suggested EWS implies monitoring of main factors, leading to mass-movement: soil moisture H (a long-term precursor) and tilts/acceleration/low frequency (LF) acoustics/vibrations (T/A/AC/V), caused by mechanical motion (a short-term precursor). At approaching critical values of H and T/A/AC/V the EWS will issue alarm signals.

As a humidity sensor, we use high-frequency (HF) 2.7 GHz micro-radar module. The HF electro-magnetic (EM) signal, emitted by micro-radar, is partially absorbed and partially reflected by the surrounding media. The ratio of absorption/reflection depends on the value of dielectric constant (DC) of the media: as the DC of the pore water (80) is much larger, than the DC of dry porous rocks (2-5), the micro-radar's EM signal in the water-saturated rock is suppressed (it is inversely proportional to humidity of media). The laboratory test on the quartz sand of various moisture content shows synchronous drastic change of micro-radar module output and the initiation of yield of the granular mass at the volumetric water content W= 27% (Fig.5).

The cost of precise monitoring/EWS equipment is as a rule very high (of order of hundreds thousands of USD) and it is practically impossible for developing countries to purchase even one such system. If we

take into account that the number of mass-movement dangerous sources is huge – only in Georgia there are 40000 of potential debris flow/landslide sources – the financial expenses are unaffordable. Thus, the magnitude of dangerous sources, need of covering the source area by many sensors, expensiveness of supporting personnel for a long period at potential mass-movement areas, growing number of exposed vulnerable objects and limited resources of developing countries, which are most prone to mentioned hazards call for developing cost-effective and the same time accurate automatic monitoring/early warning telemetric systems. Fusion of these apparently conflicting concepts (cost-effectiveness and accuracy) became possible due to the progress of modern high-tech systems.

For monitoring short-term precursors, such as T/A/AC/V, accompanying directly mass-movement activation, we use Microelectromechanical Systems (MEMS). MEMS-micro-sensors, integrating mechanical and electrical details, could report on the physical processes, taking place in the surrounding media. Of course, the standard MEMS-sensors need modification, namely assembling special amplifiers/filters in order to have characteristics (sensitivity, frequency range), necessary for indicating adequately mass-movement initiation. Fig. 6 a shows the array of integrated MEMS-sensors, which can report changes in the humidity and temperature of soil, tilts, acceleration and vibration in the (potential) mass-movement source and Fig.6 b presents the amplifier/filter electronic scheme, assembled for the MMA7361 sensor, indicating tilts and acceleration change in the rock mass.

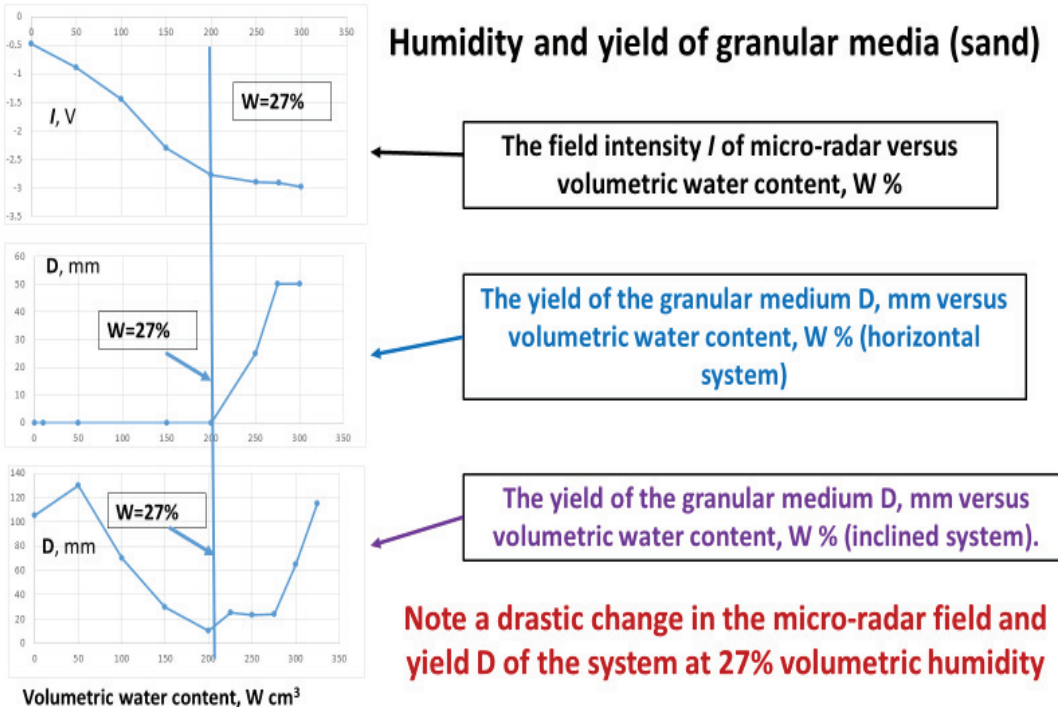

Fig.5. Humidity measurement and corresponding yield assessment in granular media (sand)

We developed differential accelerometry method, using the array of sensors (Fig.6a), where one sensor serves as a reference and others are located in the potential mass-movement source. The difference signal appears only if the latter sensors move relative to a reference one.

a.

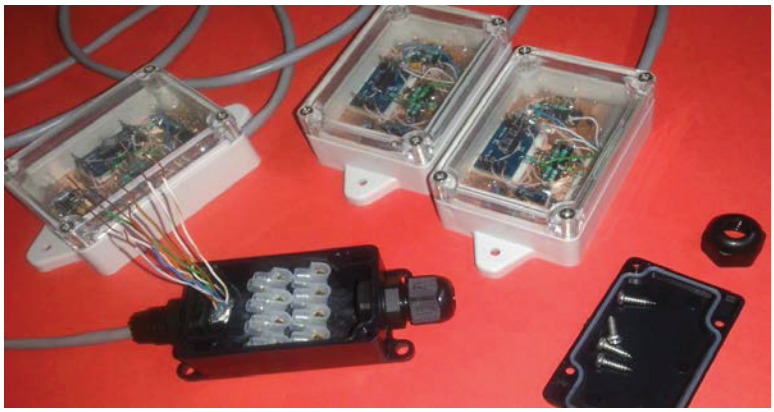

b.

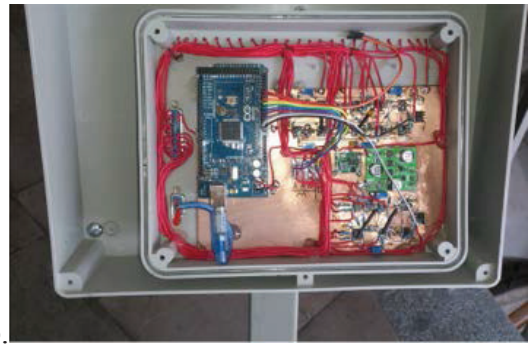

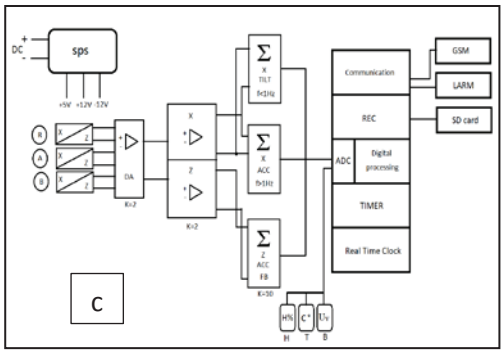

Fig. a, b. (a) Array of integrated (MMA7361)-sensors, monitoring humidity of soil, tilts, acceleration and vibration; (b) The processing platform in the double waterproof box and (c) processing platform block-scheme

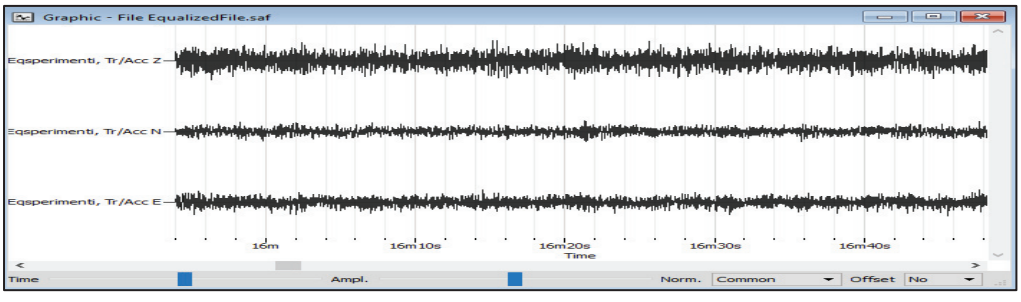

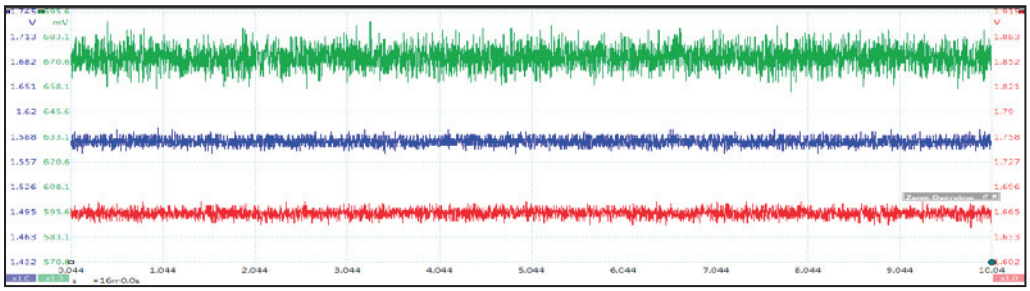

a. MEMS TROMINO

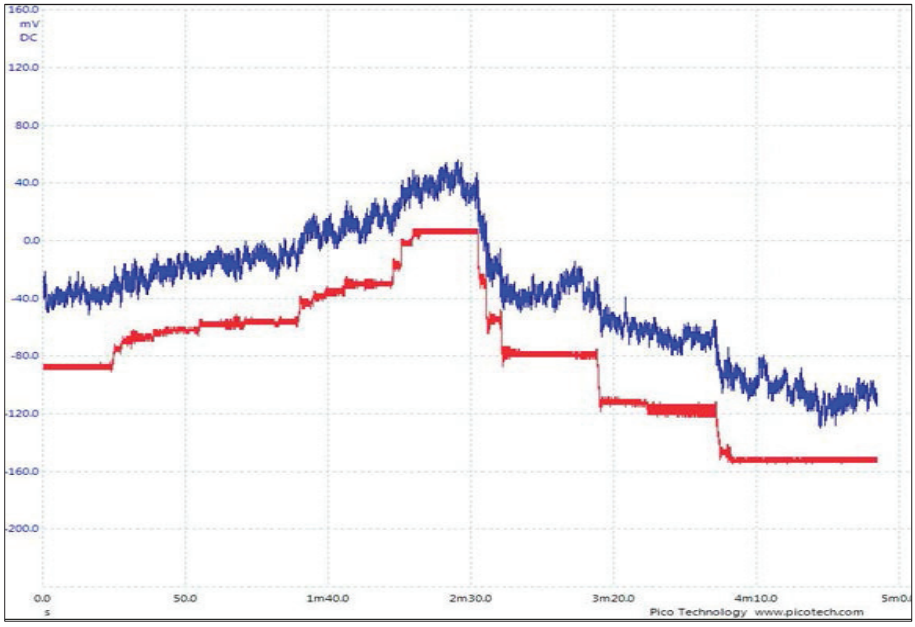

Fig. 7 a, b. (a) Acceleration records obtained by modified MEMS-sensor (Upper section) and standard accelerometer TROMINO (Lower section), in identical conditions. (b) tilt records, obtained by modified MEMS-sensor (blue) and high-class device Applied Geomechanics 701 Tiltmeter (red).

We compared recordings of tilts and acceleration provided by our (MMA7361)–based sensors with the data, obtained in the identical conditions by standard high-class devices accelerometer TROMINO (Italy) and tiltmeter Applied Geomechanics 701 (USA). The results shown in Fig. 7 a, b confirm that the recordings obtained by our system and high-class devices are almost identical. Of course, there is a difference, related to a lower signal to noise ratio in our sensors compared to the standard ones. This detail is not decisive for EWS sensors, as the main goal of such systems is fixation of significant changes in mechanical stability of media and these changes we can distinguish reliably even in our noisy records (Fig. 7). Of course, we could design amplification/filter blocks to make signal/noise ratio large, but in this case the power consumption of EWS would be significantly larger, which lead to larger power consumption.

The processing system differentiates the amplitude of the phase and the signal spectrum obtained from each sensor with respect to the information from the reference sensor. In the case of an abnormal trend, if the observed difference is greater than the site-noise of the natural trend of the data, the system generates a warning or an alarm that can be transmitted over GSM data, immediately placed on a remote server in the database and send SMS text messages to the emergency management structure or transmit coded radio signals to protect the nearest settlement that will be equipped with a radio-frequency receiver-decoder, as well as with a local sound and text alarm system.

As the EWS most likely will be installed in unpopulated areas, we developed autonomous power source, comprising solar batteries and projected all components of EWS in a low-consumption manner. We are finishing the UHF transmitter-receiver system for sending alarm signals to the nearest community under risk

CONCLUSION

The high seismic and geodynamical activities and dangerous khoko landslide near the Enguri dam together with the large number of people living downstream of the dam made the Enguri dam a potential

source of a major catastrophe in Georgia. Of course, the Enguri Dam with its 1 billion cubic meters water reservoir is a potential source of large man-made catastrophe and it should be under permanent monitoring. Catastrophes of dam are also caused by activation of the mass-movements. Each year landslides/debris-flows cause many disasters in mountainous areas all over the world. Thus, it is of great importance to create reliable and cost-effective early warning systems (EWS) for monitoring mass-movements in potentially dangerous areas (Early Warning Systems, 2012). The key elements in the solution of problem, according to the Sendai Framework for Disaster Risk Reduction are science and technology (http://www.unisdr.org/we/inform/publications/43291). The proposed early warning system, taking its parameters and price into cosideration, can play a significant role in the hazard and risk mitigation of landslides and debrisflows, which is also important for safety of high dams..

ACKNOWLEDGEMENTS

This work was supported by Shota Rustaveli National Science Foundation grant #216732, 2016.

REFERENCES

Abashidze, V., 2001. Geophysical Monitoring of Geodynamical Processes at Enguri Dam. Tbilisi

Abashidze, V., Chelidze, T., Tsaguria, T., Kobakhidze, T., 2008. "Results of research, carried out on Enguri HPP by tiltmeters". Energy, N 1, Tbilisi (in Georgian)

Analysis and assessment of the state of Enguri arch dam and its foundation,2008. recommendations for strengthening reliability and safety of exploitation. Center of geodynamical surveys in energy domain, Hydroproject and Tbilhydroproject, Moscow-Tbilisi (in Russian) Automated Dam Monitoring Systems, 2000. Bulletin of International Committee of Large Dams, N 118

Bartsh, M., Schiess Zamora, A., Steiger, K. M., 2011. "Continuous dam monitoring: An essential basis for reliable back-analysis". Hydropower and Dams, v.18, pp. 51–56

Chelidze, T., Matcharashvili, T., Abashidze, V., Kalabegashvili, M., 2011. "Real time telemetric monitoring system of large dams". In: Proceedings of the International Symposium of Dams and Reservoirs under changing challenges (edited by Shleiss, A. and Boes, R.). CD-papers, # CD_01

Chelidze, T., Kolesnikov, Yu., Matcharashvili, T., 2006. "Seismological criticality concept and percolation model of fracture". Geophysical Journal International, 164(1) pp. 125–136

Chelidze, T., Matcharashvili, T., Abashidze, V., Kalabegashvili, M., Zhukova, N., 2013. "Real time monitoring for analysis of dam stability: Potential of nonlinear elasticity and nonlinear dynamics approaches". Front. Struct. Civ. Eng. DOI 10.1007/s11709-013-0199-5

Chelidze, T., Abashidze, V., Matcharashvili, T., Tsaguria, T., Tsamalashvili, T., Amiranashvili, A., Zhukova, N., Chelidze, Z., Varamashvili, N., 2016. "Georgian-European Center "Geodynamical Hazards of High Dams" at the Council of Europe: 20 years of activity". JOURNAL OF THE GEORGIAN GEOPHYSICAL SOCIETY

Emukhvari, N., Bronshtein, V., 1991. Inguri HPP—system of allowable and limiting parameters of arch dam state for operative control of its safety during exploitation. Ministry of Energy USSR. Moscow-Tbilisi

Engineering Guidelines for the evaluation of the Hydropower projects, 1999. Chapter 11-Arch dams. Federal Energy Regulatory Commission Division of Dam Safety and Inspections. Washington, DC 20426

Guyer, R. A., Johnson, P. A., 2009. Nonlinear Mesoscopic Elasticity. Wiley-VCH

Hill, R., 1965. "A self-consistent mechanics of composite materials". Journal of the Mechanics and Physics of Solids, 13(4), pp. 213–222

Holzhausen, G., 1991. "Low cost automated detection of precursors to dam failure: Coolidge

dam, Arizona". In: Proceedings of the 8th Annual Conference ASDSO, San Diego
Kantz, H., Schreiber, T., 1997. Nonlinear Time Series Analysis. Cambridge University Press
Matcharashvili, T., Chelidze, T., Abashidze, V., Zhukova, N., Meparidze, E., 2010. "Changes in dynamics of seismic processes around Enguri High Dam Reservoir induced by periodic variation of water level". Geoplanet: Earth and Planetary Sciences, 1, pp. 273–286
Matcharashvili, T., Chelidze, T., Peinke, J., 2008. "Increase of order in seismic processes around large reservoir induced by water level periodic variation". Nonlinear Dynamics, 51, pp. 399– 407
Matcharashvili, T., Chelidze, T., Abashidze, V., Zhukova, N., Meparidze, E., 2010. "Changes in Dynamics of Seismic Processes Around Enguri High Dam Reservoir Induced by Periodic Variation of Water Level". In: Geoplanet: Earth and Planetary Sciences, Volume 1, 2010, Synchronization and Triggering: from Fracture to Earthquake Processes. Eds.V.de Rubeis, Z. Czechowski and R. Teisseyre, pp.273-286.
Matcharashvili, T., Chelidze, T., Abashidze, V., Zhukova, N., Mepharidze, N., 2011. "Evidence for changes in the dynamics of Earth crust tilts caused by the large dam construction and reservoir filling at the Enguri dam international test area (Georgia)". Nonlinear Dynamics. DOI 10.1007/s11071-010-9930-0A.
McCall, K., Guyer, R., 1994. "Equation of state and wave propagation in hysteretic nonlinear elastic materials". Journal of Geophysical Research, 99(B12), pp. 23887–23897
Mivenchi, M. R., Ahmadi, M. T., Hajmomeni, A., 2003. "Effective technique for Arch Dam Ambient Vibration Test". Journal of Seismology and Earthquake Engineering, 5, pp. 23–34
Peinke, J., Matcharashvili, T., Chelidze, T., Gogiashvili, J., Nawroth, A., Lursmanashvili, O., Javakhishvili, Z., 2006. "Influence of periodic variations in water level on regional seismic activity around a large reservoir". Physics of the Earth and Planetary Interiors, 156(1–2), pp. 130– 142
Press, W. H., Teukolsky, S. A., Vetterling, W. T., Flannery, B. P., 1996. Numerical Recipes. 3rd ed. Cambridge University Press
Savich, A., 2002. Complex Engineering-geophysical Investigations at Construction of Hydropower Objects. Moscow, (in Russian)
Savich, A., 2006. "Safety of large dams in areas of high geodynamical risk". In: Geodynamical Studies of Large Dams. Tbilisi, (in Russian)
Sprott, J. S., 2006. Chaos and Time Series Analysis. Oxford: Oxford University Press
Strogatz, S., 2003. Nonlinear Dynamics and Chaos. Westreview Press
Tibaldi, A., Tsereteli, N., 2017. "International effort tackles landslide hazards to keep the pece". EOS, 98, pp. 25-28
Varamashvili, N., Chelidze, T., Devidze, M., Chikhladze, V., Chelidze, Z., 2017. "Laboratory Research of Landslide Activation Model". Bull. Georg. Natl. Acad. Sci.
Varamashvili, N., Chelidze, T., Amilakhvari, D., Dvali, L., 2016. Laboratory modeling of landslide and seismic processes triggering JOURNAL OF THE GEORGIAN GEOPHYSICAL SOCIETY
Wieland, M., Mueller, R., 2009. ."Dam safety, emergency action plans, and water alarm systems". International Water Power and Dam Construction, January, pp. 34–38
USSD Committee on Monitoring of Dams and Their Foundations, 1989. Bulletin of International Committee of Large Dams, N 68
Zienkiewicz, O. C., Taylor, R. L., 2000. The Finite Element Method. 5th ed. Butterworth-Heinemann

5th International Symposium on Dam Safety

October 27-31, 2018

DAMS IN REPUBLIC OF MACEDONIA - THE KEY PILLAR OF THE WATER MANAGEMENT INFRASTRUCTURE

Ljupcho PETKOVSKI [1]

ABSTRACT

This year we celebrate a significant jubilee – 80 years of dam engineering in Republic of Macedonia. Planning, design, construction and maintenance of dams are among the most responsible civil engineering works. The first dam in R. Macedonia, arch dam Matka, at the canyon of Treska River, near the city of Skopje, was built in 1938. Construction of this dam and its appurtenant structures marks the beginning of dam engineering in Republic of Macedonia. At present, in 2018, we can proudly state that dam constructors in R. Macedonia are worthy heirs and prolongers of the noble work of the first dam designers, dating to 1938. Confirmation of such statement is the fact that 45 dams with regional importance and over 110 small embankment dams with local importance are the key pillar of the present water economy infrastructure. Republic of Macedonia is located in the central part of the Balkan Peninsula, and it covers an area of 25,713 km2 with a population of about 2.1 million. With over 150 built dams of basically all types (embankment and concrete dams, gravity and arch dams) categorized as "large dams" by ICOLD criteria, Republic of Macedonia, proportionally to its size, is located right at the top of dam engineering in Europe.

Keywords: embankment and concrete dams, gravity and arch dams

INTRODUCTION - MATKA, THE FIRST DAM IN R. MACEDONIA

This year we celebrate a significant jubilee – 80 Years of Dam Engineering in R. Macedonia. Back in 1938, the first dam in R. Macedonia was built – Matka arch dam. By construction of the dam and the appurtenant structures, at the exit of the canyon of river Treska close to the city of Skopje (figure 1), was created reservoir Matka (figure 2). By completion of the construction works on the hydropower plant located in the base of the dam, the power use of river Treska commenced. The Matka dam Design was prepared by academician Miladin M. Pecinar (1893-1973), figure 3, one of the pioneers in the development of contemporary "Hydraulic Engineering" in Yugoslavia. At this occasion, here below a brief overview of the rich biography of academician Pecinar is presented, which by his noble work has indebted in great deal the Civil Engineering profession in R. Macedonia.

Miladin Pecinar graduated in Belgrade at the Technical Faculty, department of Civil Engineering, in 1921. In 1925 Pecinar created its own bureau for designing of water structures, where as he designed the following hydropower plants that were later constructed: Perukachko Vrelo on river Drina (1927), Chechevo (1929), Novi Pazar (1930), St. Andreja with the arch dam Matka (1938), Temshtica (1939), Crn Timok (1940). In that period, before World War II, in several mandates, Pecinar was vice president of the Association of Yugoslavian engineers and architects. In 1946 he became president of the Yugoslav section of the International Commission on Large Dams (ICOLD). In 1948 he was elected as professor at Chair of Hydraulic structures at Civil Engineering Faculty within the Technical University in Belgrade. As the most appreciated expert in field of hydrotechnics before, during and

[1] Professor, President of MACOLD, University "Sts Cyril and Methodius", Civil Engineering Faculty, Blvd. Partizanski odredi 24, 1000, Skopje, Republic of Macedonia, e-mail: petkovski@gf.ukim.edu.mk

immediately after the World War II, Pecinar was elected as very first professor on the course "Hydraulic structures". On the XI World Conference on Energy in 1957, he was general rapporteur on the topic of the complex use of water resources. In 1959 he was elected as writing member for the Serbian Academy of Science and Arts (SASA) and later in 1963 was elected as Academy full member. He got retired in 1963 as full time professor at the Civil Engineering Faculty in Belgrade.

Figure 1. Canyon Matka on the river Treska in 1935, before construction of the arch dam

Figure 2. Downstream face of Matka dam, the first dam in R. Macedonia, built in 1938

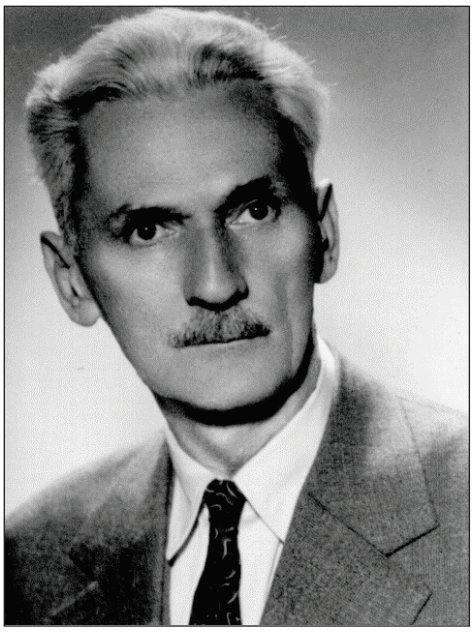

Figure 3. Academician Miladin M. Pecinar, (1893-1973)

It is worth noting that Pecinar for each hydropower plant that he designed, he also designed the appurtenant structures of the dam as well as the hydropower derivations. (Ако те сфатив добро што си сакал да кажеш би требало добро да имам поправено ама провери!) Aside from his ingenuity and enormous hydrotechnical talent, the greatness of academician Penicar was also in combining experts of different profiles thus creating both compatible and economically optimized structures, confirmed by Matka dam – a unique type of structure worldwide by many parameters. Accordingly, for the most important dam in R. Macedonia – Matka dam, the best experts at that time from various fields were in charge. Namely, the static stability analysis was made by Miodrag Marinkovic (later a professor at the Civil Engineering Faculty in Belgrade). Supervisor for concrete works was Djordje Lazarevic (later a professor at the Civil Engineering Faculty in Belgrade and full member of the Serbian Academy of Science and Art). Pavle Vukicevic was contractor of the dam (later a consultant at company Energoprojekt, Belgrade). Such approach by Pecinar resulted in building the Matka dam as "Penna Beff" type, second construction of such a dam in Europe (Denia dam in Spain was the first). In addition, Matka dam was the highest arch dam in the Kingdom of Yugoslavia (1918-1941), but also and the boldest arch dam in Yugoslavia in XX century, with slender coefficient equal to 0.054.

DYNAMICS OF LARGE DAMS CONSTRUCTION IN R. MACEDONIA

At present, in 2018, we can proudly state that dam constructors in R. Macedonia are worthy heirs and prolongers of the noble work of academician Pecinar, dating back to 1938. Confirmation of such statement is the fact that the key pillar of the our present water economy infrastructure are 45 dams with regional importance, 4 of which are tailings dams, and over 110 small fill (embankment) dams with local importance. The hydro systems with dams are mostly multipurpose, serving for irrigation, electricity production, flood control, water supply and guaranteed ecological discharge. With over 150 built dams of basically all types (embankment and concrete dams, gravity and arch dams) categorized as "large dams" by ICOLD criteria, shows that R. Macedonia, proportionally to its size, its located right at the top of dam engineering in Europe. It should be noted that the most significant water structures are designed and built by domestic companies, which is the best proof that in this period of eight decades was created well-known and respected Macedonian hydrotechnical school.

The central spot in the progress and improvement of the widely respected Macedonian school for Dam Engineering holds the Chair of Hydraulic Structures at Faculty of Civil Engineering in Skopje, created by establishment of the Technical Faculty in Skopje in 1949. The greatest merits for the development

of the Chair of Hydraulic Structures belong to the following: Chair founder, prof. Bratislav Subanovic, that lectured the first classes in courses “Utilization of Water Power” and “Hydraulic Structures” in the so far away 1950 and was the head of the Chair until 1965; his heirs, prof. Mihajlo Serafimovski (retired since 1987), leading by great number of applicative works and designs, prof. Nikola Durned (retired since 2001) and prof. Dr. Ljubomir Tanchev (retired since 2010) – a person with the greatest scientific contribution to the Chair [Tanchev, 2014] and a professor that I had the privilege to be my teacher in the "world of dams".

According to the dynamics of large dams construction in R. Macedonia, regarding the 45 hydro-systems with regional importance (figure 4), we can divide three periods with different intensity of construction of dams: (1) the period of 60-ies of XX century or “gold period” for dam construction, (2) the last decade of XX century – period of great stagnation, in which period are built very few small fill dams and (3) first two decades of XXI century – period of intensifying dam construction by various and also new dam types. By the chart on figure 4, it can be stated that R. Macedonia has a solid tradition and continuity in designing and building dams that is required for proper knowledge transfer from one generation of hydrotechnics engineers to another and maintenance of high quality of work of the engineering companies in the field of Dam Engineering.

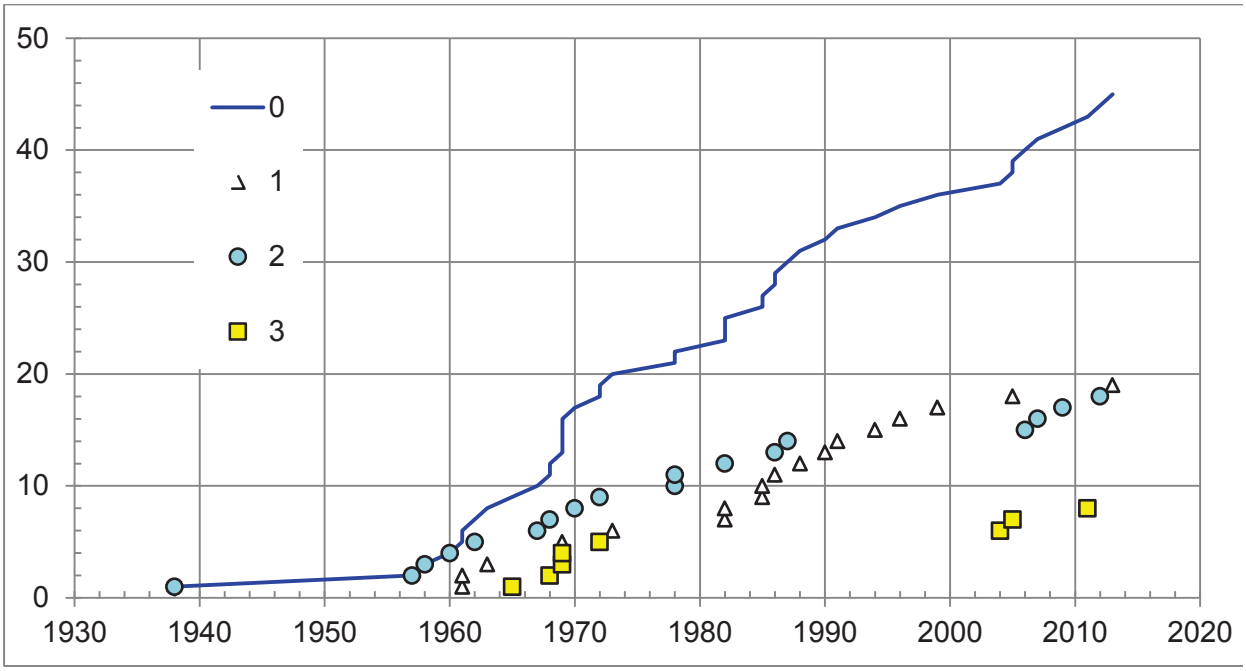

Figure 4. Dynamics of construction of large dams in R. Macedonia, for 45 hydro-systems of regional importance. (0) in total, (1) low, H < 30m, (2) medium, H < 80 m, (3) high, H < 150 m

The first embankment dam, constructed in R. Macedonia, is Mavrovo dam, near Gostivar, with structural height of Hs = 62 m, built in 1957, figure 5. The most important dams in R. Macedonia from the golden period of dams construction [YUCOLD, 1970] are: several rock-fill dams with clay, two on River Crn Drim, Globochica, near Struga, Hs = 94.5 m, built in 1965 and Shpilje, near Debar, Hs = 112 m, built in 1968, figure 6, Tikvesh, near Kavadarci, on Crna River, Hs = 114 m, built in 1968 with hydraulic compaction (the highest embankment dam in ex Yugoslavia), figure 7, Kalimanci, near M. Kamenica on river Bregalnica, Hs = 95 m, built 1969, Prilep buttress dam, Hs = 36 m, built in 1967, figure 8 and Lipkovo, near Kumanovo, arch dam Hs = 81 m, built in 1972, figure 9.

Figure 5. Mavrovo dam, constructed in 1957, first embankment dam in R. Macedonia

Figure 6. Upstream slope of Shpilje dam, constructed in 1969

Figure 7. Downstream slope of Tikvesh dam, constructed in 1968, the heighest embankment dam in ex Yugoslavia

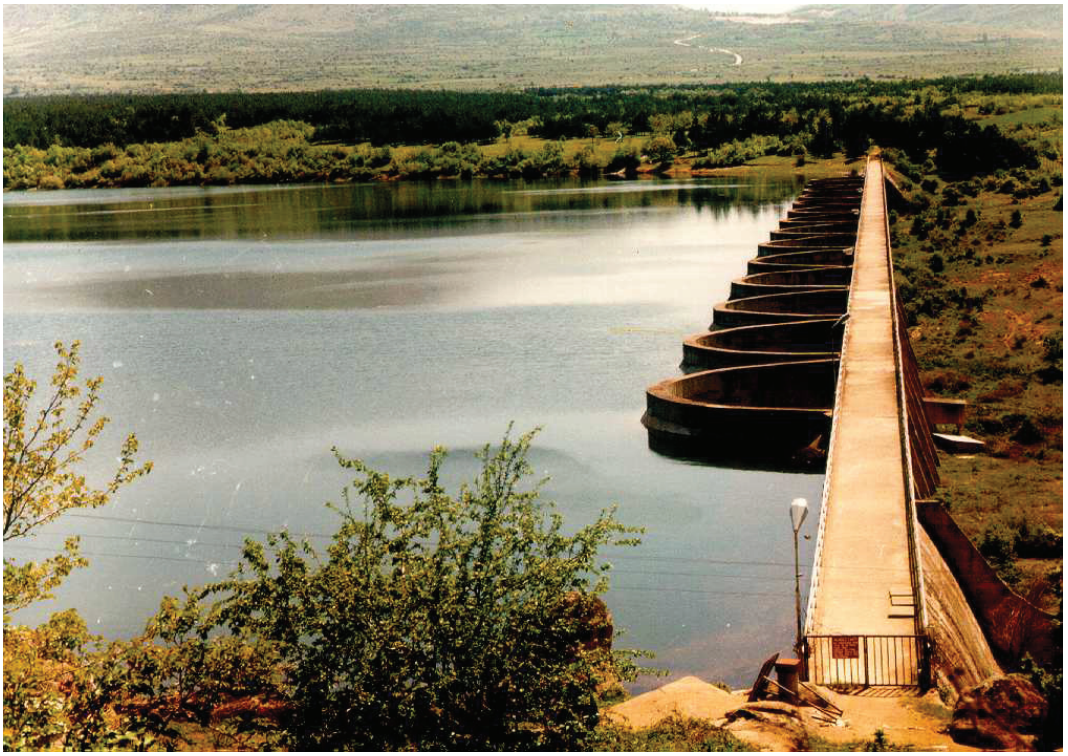

Figure 8. Priplep dam, constructed in 1967, the unique buttress dam in R. Macedonia

Figure 9. Lipkovo dam, constructed in 19672, the highest arch dam in R. Macedonia

In the past period of 80 years in R.Macedonia, practically all dam types have been built, in correlation that is common worldwide. According to the material type for dam construction (figure 10), 11 are concrete (24.4%) and 34 are embankment dams. Regarding the concrete dams, according to the structure, 8 of them are arch dams, 2 are massive dams and 1 is buttress dam. In case of fill dams, according to the local material, equally are constructed - 17 earth-fill and 17 rock-fill dams. From the rock-fill dams, mostly represented are earth-rock dams (impermeable element of natural clay material) and only 2 are rock-fill dams (with artificial impermeable element). Such dams are Loshana dam, near Delchevo, [Petkovski L., Paskalov T., 2003.], constructed in 2006 (with geomembrane facing) – first of such type in ex-Yugoslavia (figure 11), and Knezhevo dam, near Probishtip (figure 12), built in 2011 (with asphaltic core), first of such type in southeastern Europe [Petkovski L., 2007.06]. These two dam cases in most obvious manner show the boldness and inventiveness of the present generation of hydrotechnics professionals in R. Macedonia. The latest significant large dam, built in R. Macedonia is double curved arch dam St. Petka on river Treska, Hs = 64 meters, constructed in 2012, figure 13.

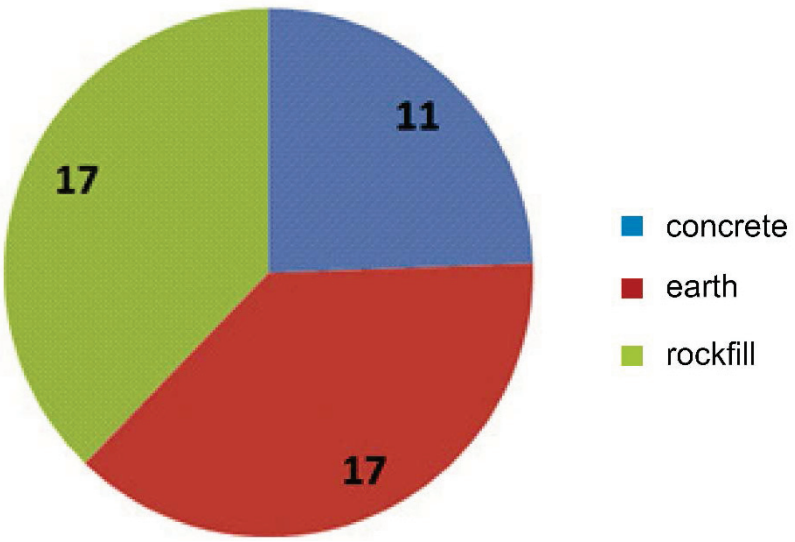

Figure 10. Division of large and important dams built in R. Macedonia, according to the

material type for construction

Figure 11. Rock-fill dam Loshana with geomembrane facing, built in 2006, Hs=45 m

Figure 12. Rock-fill dam Knezevo with asphalt core, on river Zletovska, built in 2011, Hs= 82 m

Figure 13. St. Petka arch dam on river Treska, constructed in 2012

The highest dam creating water reservoir in R. Macedonia is earth-rock dam Kozjak on river Treska [Petkovski L., Tanchev L., Mitovski S., 2007.06], built in 2006 with structural height of 126.0 m, figure 14. However, the highest fill dam in R. Macedonia is tailings dam Topolnica of mine Buchim, Radovish, [Petkovski L., Mitovski S., 2018.04] completed in 2015, with crest-to-downstream-toe height of 141.2 m, figure 15. According to the structural height of the important and large dams in R. Macedonia, figure 16, we have mostly low dams (less than 30 m) and medium high dams (30 to 80 m) – all in all, total of 19 and 18 respectively, and high dams (80 to 150 m) are total of 8 (or 17.8%), while extremely high dam (height more than 150 m) is not yet constructed in R. Macedonia.

Figure 14. Upstream view of Kozjak dam, highest earth-rock dam in R. Macedonia

Figure 15. Tailings dam Topolnica of mine Buchim, with recultivated downstream slope

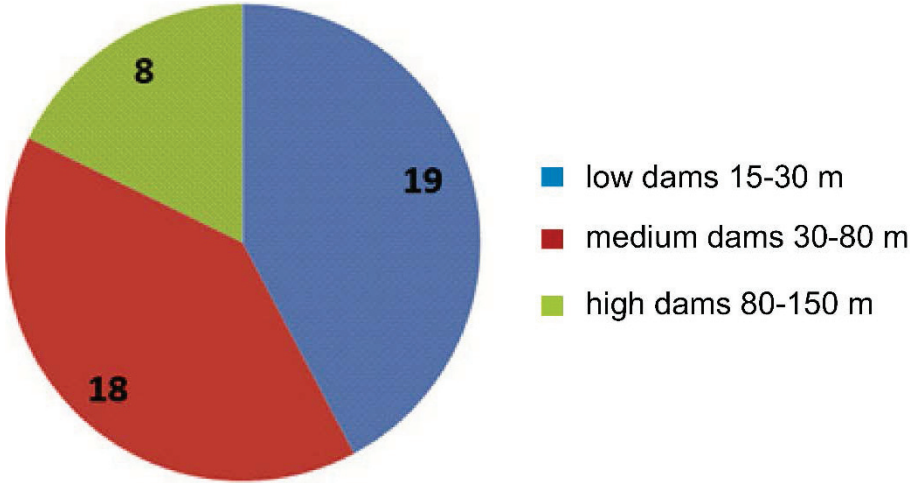

Figure 16. Division of large and important dams in R. Macedonia, according to height

CURRENT PROJECTS FOR LARGE DAMS IN R. MACEDONIA

The current projects for important dams in R. Macedonia are: (1) Shtuchka dam, figure 17, rock fill dam with geomembrane facing (GFRD) in seven stages, [Petkovski L., Mitovski S., 2015.06] near Strumica, for the tailings of mine Ilovica, Hs = 207 m, in the phase of preliminary design, (2) Slupchanska Dam, figure 18, near Kumanovo, concrete faced rock-fill dam (CFRD), Hs = 54 m, in the phase of basic design, (3) Otinja dam, figure 19, rock-fill dam with central clay core [Petkovski L., 2005.08], near Shtip, Hs = 30 m, in the phase of Review of the Basic design, which is planned for construction in 2020, (4) Orizarska dam, figure 20, rock-fill dam with geomembrane facing (GFRD), near Kochani, [Petkovski L., Mitovski S., 2013.05] Hs = 81 m, with Reviewed Basic design, which is planned for construction in 2019 and (5) Konsko dam, near Gevgelija [Petkovski L., Tančev L., Mitovski S., 2013.10], Hs = 80 m, figure 21, rock-fill dam asphalt core (ACRD), construction is started in July, 2018, figure 22.

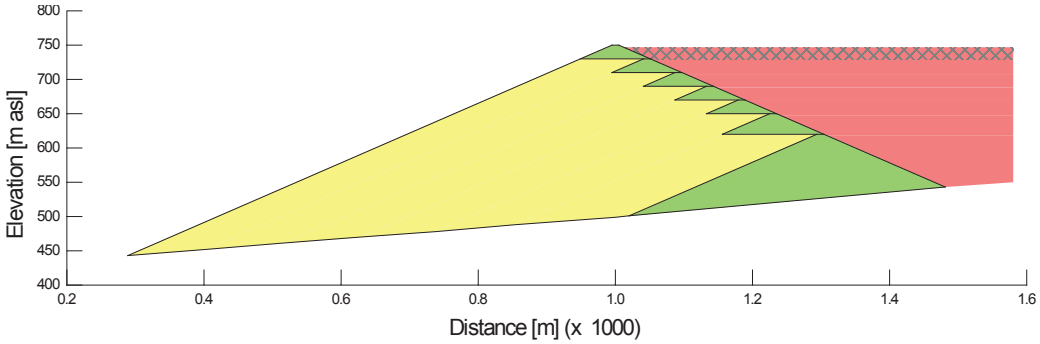

Figure 17. Shtuchka dam, Strumica, H1 = Hs = 207 m, GFRD in 7 stages

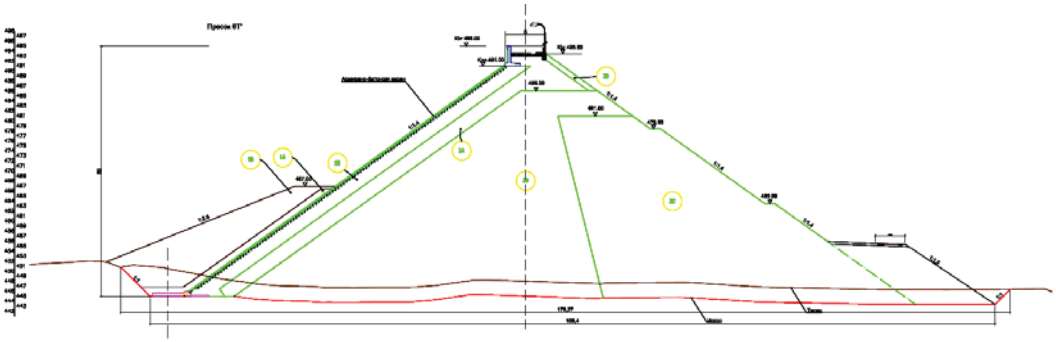

Figure 18. Slupchanska dam, Kumanovo, CFRD, Hs = 54 m

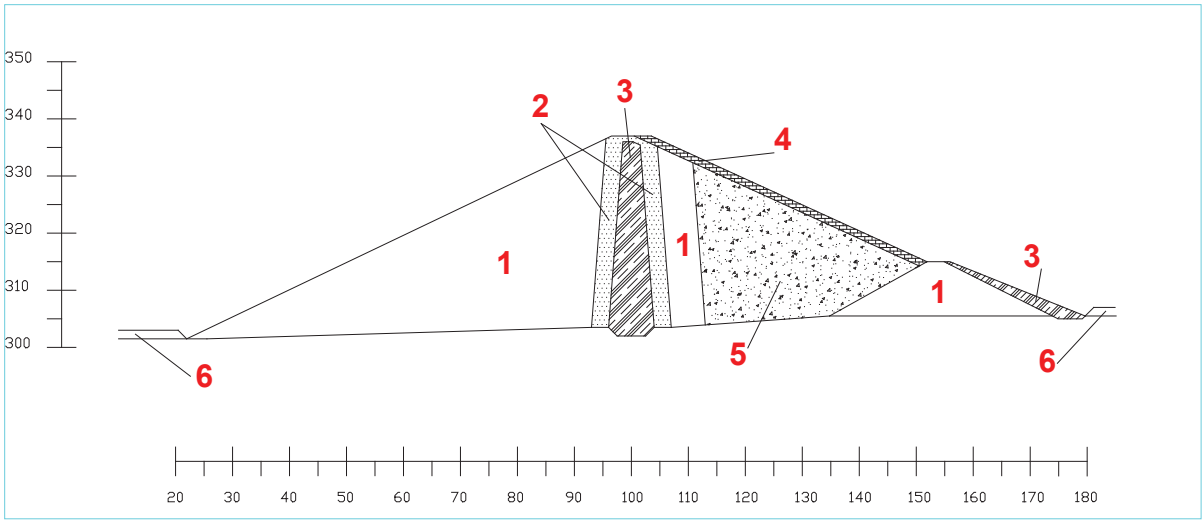

Figure 19. Otinja dam, Shtip, rock fill with clay core, Hs = 33.5 m, 1 - gravel (downstream shoulder, transition zones, upstream cofferdam), 2 - sand (filters), 3 - clay (core of dam, screen of cofferdam), 4 - masonry stone (upstream slope protection), 5 - stone-fill (upstream shoulder), 6 - alluvial deposit in riverbed

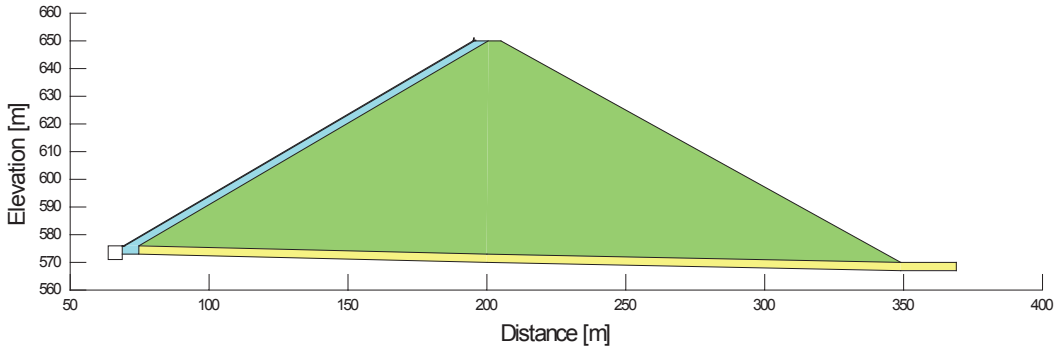

Figure 20. Rechani dam, Kochani, GFRD, Hs = 81 m, (1) foundation: deposit in the river bed, (2) filter: sub-layer of the upstream facing of geomembrane, (3) shell: rock-fill

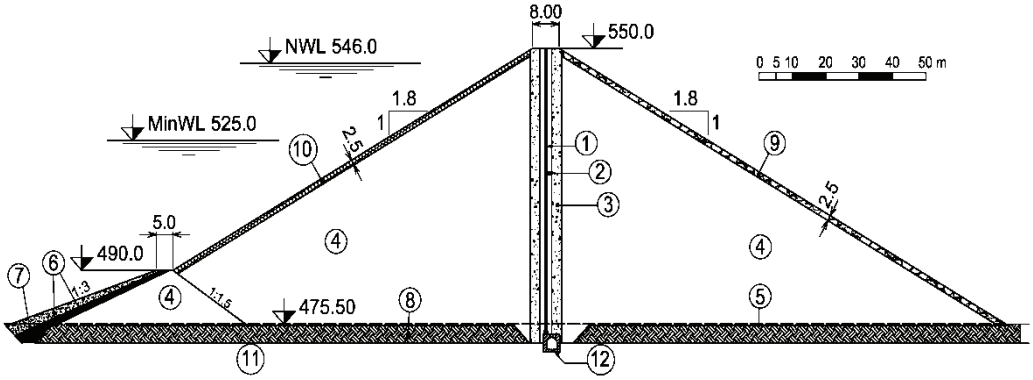

Figure 20. Konsko dam, Gevgelija, ACRD, Hs = 80 m, (1) asphalt core, (2) fine transition, (0-60) mm, (3) coarse transition, (0-250) mm, (4) rock-fill, grains to 700 mm, (5) removed humus layer, (6) cofferdam filter from river gravel, (7) cofferdam clay facing, (8) river deposit, (9) protection of the downstream slope, (10) rip-rap for protection of the upstream slope, (11) rock foundation (12) grouting gallery.

Figure 21. Ceremony at the beginning of the construction of Konsko dam, on 21st of July 2018

The Contractor of the dam Konsko, selected by the Investor – Ministry of Agriculture, Forestry and Water economy of R. Macedonia, is the company Serka-Akely Joint Venture, from Turkey. This could be an excellent example how to increase the competition, extend the transfer of knowledge and practice, and finally and to improve the Dam Engineering in South East Europe.

REFERENCES

Petkovski L., 2005.08 “Dynamic Analysis of a Rock-filled Dam with Clay Core“, paper, International Conference IZIIS 40 EE-21C, Aug 27 – Sept 01, 2005, Skopje/Ohrid, R.Macedonia, Proceedings, CD-ROM;

Petkovski L., 2007.06 “Seismic Analysis of a Rock-filled Dam with Asphalitic Concrete Diaphragm“, paper, 4th International Conference on Earthquake Geotechnical Engineering, 25-28 June 2007, Thessaloniki, Greece, paper #1261, CD-ROM;

Petkovski L., Mitovski S., 2013.05 "Comparison of linear and non-linear models on dynamic analysis of rockfill dams with facing", SE-50EEE International Conference, Skopje, R.Macedonia, CD=ID_40,

Petkovski L., Mitovski S., 2015.06 "Creating of tailings space by stage construction of rockfill dam", 25. Congress on Large Dams, ICOLD, 13–19 June 2015, Stavanger, Norway, CD Proceedings Q.98-R.4, p. 53-65

Petkovski L., Mitovski S., 2018.04 “NUMERICAL ANALYSIS OF DISPLACEMENTS IN THE POST-EXPLOITATION PERIOD OF TAILINGS DAMS WITH A COMBINED CONSTRUCTION METHOD”, Topic - Tailings Dams, USSD 38th Annual Meeting and Conference, A balancing Act: Dams, Levees and Ecosystems, April 3- May 4, 2018, Miami, Florida, USA, CD Proceedings

Petkovski L., Paskalov T., 2003. “Comparison of Dynamic Analyses of Embankment Dams by Using Lumped Mass Method and Finite Element Method“, paper, International Conference in Earthquake Engineering - Skopje Earthquake - 40 Years of Europian Earthquake Engineering, August 26-29, Skopje, Ohrid, Republic of Macedonia, Proceedings, CD-ROM;

Petkovski L., Tanchev L., Mitovski S., 2007.06 "A CONTRIBUTION TO THE STANDARDISATION OF THE MODERN APPROACH TO ASSESSMENT OF STRUCTURAL SAFETY OF EMBANKMENT DAMS", 75th ICOLD Annual Meeting, International Symposium “Dam Safety Management, Role of State, Private Companies and Public in Designing, Constructing and Operation of Large Dams”, 24-29 June 2007, St. Petersburg, Russia, Abstracts Proceedings p.66, CD-ROM;

Petkovski L., Tanchev L., Mitovski S., 2013.10 "Comparison of numerical models on research of state at first impounding of rockfill dams with an asphalt core", International symposium, Dam engineering in Southeast and Middle Europe - Recent experience and future outlooks, SLOCOLD, 16-17.10.2013 Ljubljana, Slovenia, ISBN 978-961-90207-9-1, Proceedings, 106-115

Tanchev L., 2014. “Dams and appurtenant hydraulic structures”, Second edition, A.A. Balkema Publ., CRC press, Taylor & Francis Group plc, London, UK

YUCOLD, 1970. “Dams of Macedonia, Yugoslavia”, Organization Committee for the 8th Congress of Yugoslav National Committee on Large Dams

5th International Symposium on Dam Safety

October 27-31, 2018

A REVIEW OF THE ANITA DAM INCIDENT: INTERNAL EROSION CAUSED BY A BURIED CONDUIT AND LESSONS LEARNED

Melih CALAMAK [1], Meric YILMAZ[2]

ABSTRACT

Internal erosion associated with piping is one of the main reasons for unexpected failures of embankment dams. On March 26, 1997, Anita Dam located in Montana, the United States was faced with a major threat on its safety due to internal erosion caused by the seepage around the buried steel outlet conduit used as the principal spillway. This has resulted in the drainage of the whole reservoir in one and a half day with no injury or loss of lives. The incident has changed the history of the design practice of conduits through embankment dams. The steel conduit had anti-seep collars which were known to be sufficient alone to prevent excessive seepage around buried conduits in those days. However, it was understood from this incident that they might lead to poor compaction and there is a need for filters and drains around conduits. This study reviews the mechanism of seepage around buried conduits and presents the related previous research. The Anita Dam incident is explained thoroughly by providing the reasons and the results of the failure. The lessons learned from the incident are discussed and the best practices for the design of embankment dams with buried conduits are presented.

Keywords: Embankment dam, seepage, internal erosion, conduit, failure.

INTRODUCTION

Earthen dams are made of locally available soils which may show highly variable characteristics. Design practices aim to cope with these variations for the safety of the structure. The hydraulic conductivity is one of the most prominent properties of soils that shows variation and governs the seepage through the dam. Some amount of seepage is always expected in earthen dams and it should be limited and controlled. However, excessive flow rates and preferential seepage paths may be observed due to some reasons, such as poorly graded fill material, loosely compacted soil, differential settlements, burrows and holes in the dam body, etc. Excessive seepage may trigger the initiation of movement of fine particles in the dam body which may eventually result in piping. Piping is a failure condition in an earthen dam since the formation of a breach is inevitable during piping. It can occur at any time if a discontinuity develops in the dam body at a location which is in contact with water. The statistics show that 28% to 46% of dam failures were caused by piping (Costa, 1985 and Foster et al., 2000).

The mechanism of seepage at earthen dams have been investigated by many previous studies (Calamak and Yanmaz, 2017; Calamak et al., 2017; Calamak and Yanmaz, 2018; Ahmed, 2009;

[1] Research Professor, Department of Civil and Environmental Engineering, University of South Carolina, Columbia, SC, USA,
e-posta: calamak@cec.sc.edu
[2] Adjunct Instructor, Department of Civil Engineering, Middle East Technical University, Ankara, Turkey,
e-posta: smeric@metu.edu.tr

Fenton and Griffiths, 1996; Tan et al., 2017). However, a limited number of studies presented the internal erosion process of fill material due to piping at earthen dams. Most of these studies were experimental and presented the erosion mechanism initiated by a hole or a pipe very well. The holes initiated the erosion were created at different levels and parts of the earthen bodies. The studies showed the effects of soil composition and compaction on the mechanism by presenting the changes in the depth, area, and volume of the erosion. However, in real life, piping is not caused by artificial holes and it might be observed in any level or part of the dam body which is in contact with water. The Anita Dam incident occurred in March 1997 showed that a buried conduit in the dam body may cause excessive seepage, erosion of finer particles, and eventually piping.

Conduits are one of the very common parts of embankment dams and almost any kind of hydraulic structures. Primarily, conduits convey the water from the reservoir in a controlled manner for various purposes, such as releasing water to meet the downstream requirements, evacuating the reservoir during the emergency, feeding the hydropower turbines, diverting the water during construction, etc. (FEMA, 2005). They might be located through, under or around the dam body. Many erosion and piping failure incidents caused by buried conduits through a dam were observed in the history. There are four main mechanisms for buried conduits which may lead to partial or full failure of embankment dams. These are; a hydraulic fracture caused in the earth-fill by the existence of a conduit, low compaction of the soil in the vicinity of the conduit, a void created by excessive compaction of the soil under the conduit, and the leakage of water from the conduit into the earth-fill due to aging, cavitation, corrosion etc. (FEMA, 2005). A hydraulic fraction can occur at the location where the conduit penetrates through the dam body due to poor construction or the differential settlement of the embankment [see Figure 1(a)]. A conduit may create an arching effect in the earth-fill which results in less settlement above it and more under the conduit. Another common reason for a hydraulic fraction near a conduit is the formation of a vortex. If the water level in the reservoir is less, the submergence depth at the intake of the conduit may fall below the critical limit and this may result in a vortex. A vortex nearby the embankment may erode the soil and create fractions leading to a piping failure [see Figure 1(b)].

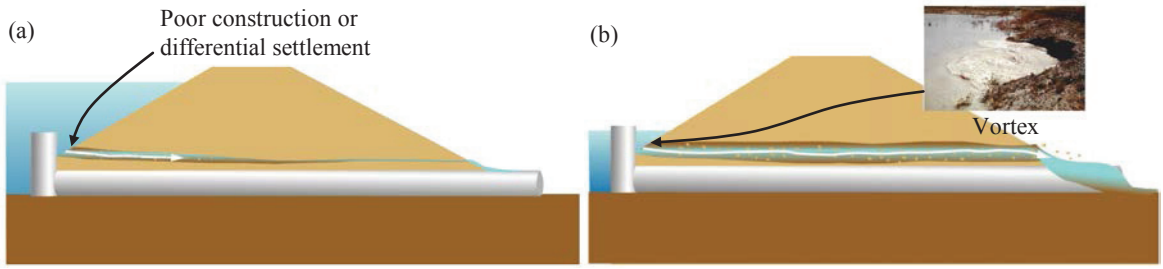

Figure 1. Piping due to a hydraulic fracture created by (a) poor construction or differential settlement; (b) a vortex (retrieved from FEMA, 2005)

The compaction process of the fill material around conduits is often difficult when compared to the regular compaction procedure. The use of a roller compactor within approximately 60 cm of a conduit is not suggested since it may damage the conduit (FEMA, 2005). Therefore, commonly, the soil around the conduit is compacted using hand compaction equipment. However, hand compaction equipment is a lightweight device. Therefore, a thinner layer of soil can be compacted at a time. This makes it slow and labor intensive. A hand compacted soil needs more often inspection, and this may tend to lag the construction. There are two possible outcomes of these: (1) either the operator of the equipment or the owner or the contractor may try to shorten the time spent for the compaction by laying thicker soil or skipping some parts; (2) or concentrate on the compaction more than required. The first outcome results in poor compaction, whereas the second one may lead to excessive compaction resulting in the lifting of the conduit. As can be seen from Figure 2(a) and (b), both cases cause the formation of voids beneath the conduit, eventually causing internal erosion and piping as shown in Figure 2(c). Along with these, if the conduit is pressurized, water may leak through a crack or a hole caused either by an improperly constructed or designed joint, corrosion, cavitation or aging.

The flow from the leak may have high velocities and this may initiate the internal erosion in the surrounding soil of the conduit and result in piping.

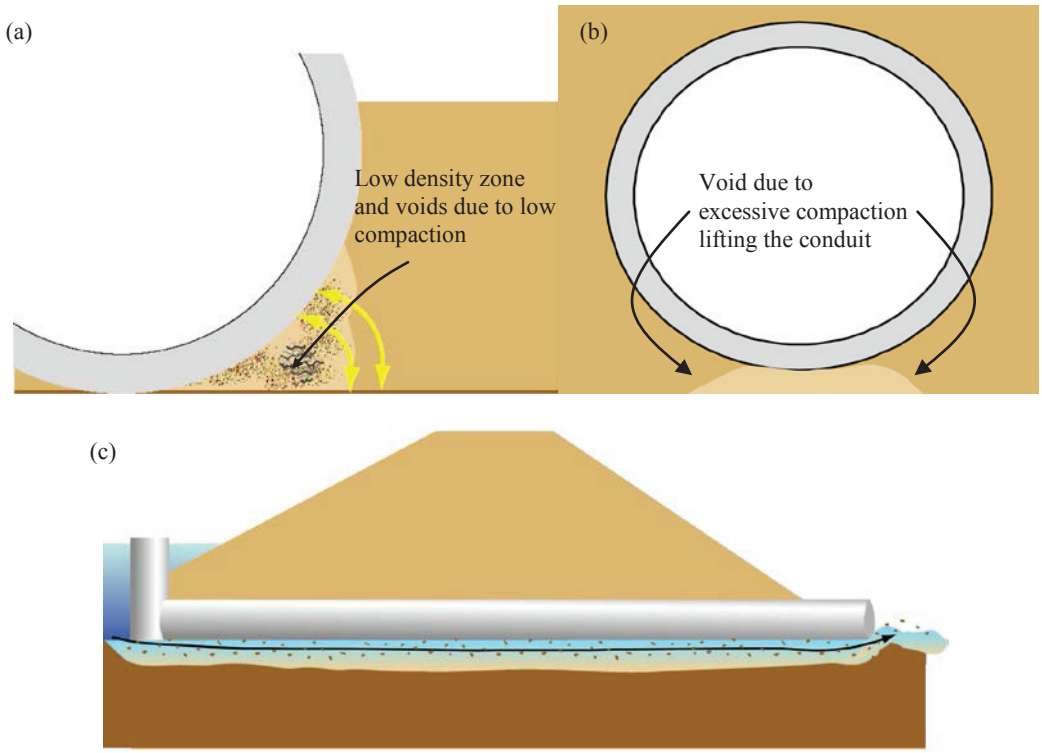

Figure 2. Voids created by (a) poor compaction; (b) excessive compaction; (c) piping due to voids beneath the conduit (retrieved from FEMA, 2005)

In history, many earthen dam failures were observed due to piping around buried conduits. Some of these failures are (1) Loveton Farms Dam failure in Maryland in 1985 due to poorly compacted fill [see Figure 3(a)]; (2) Medford Quarry Wash Water Lake Dam failure in Maryland in 1989 due to improper design and poor construction [see Figure 3(b)]; (3) Upper Red Rock Site 20 Dam failure in Oklahoma in 1986 due to a hydraulic fracture adjacent to the buried flood control conduit [see Figure 3(c)]; (4, 5, 6) the failure of Anonymous Dams 1, 2 and 3 due to a hydraulic fracture in the embankment composed of highly dispersive fine soils [see Figure 3(d), (e) and (f)] (FEMA, 2005). Apart from these, there is another dam failure which changed the history of the engineering design and practice of buried conduits through embankment dams: The Anita Dam incident. This paper is aimed at reviewing the Anita Dam failure by presenting the previous research on piping in earthen structures and providing the lessons learned from the incident. In the scope of the paper, the literature focused on dam breach due to piping, the internal erosion rate, and the time to failure in the piping is presented. Then, what caused the incident, how the causes were developed, and the consequences of the failure were provided. Finally, the lessons learned are evaluated to raise the awareness of the reader on what should be done in the design of buried conduits.

PREVIOUS RESEARCH

To the best of our knowledge, the research on the internal erosion in earthen dams has not been focused on the piping around conduits in detail yet. The study presented by Ferguson (2012) is one of the pioneering technical papers specifically focused on this topic. This study showed the potential failure modes, considerations for assessing the seepage around buried conduits, and hydraulic fracturing on two case histories. It was concluded that the identification of small defects in and around the conduit is crucial for the piping potential. The safety assessment of buried conduits was stated to be a challenging task and needed an extensive experience.

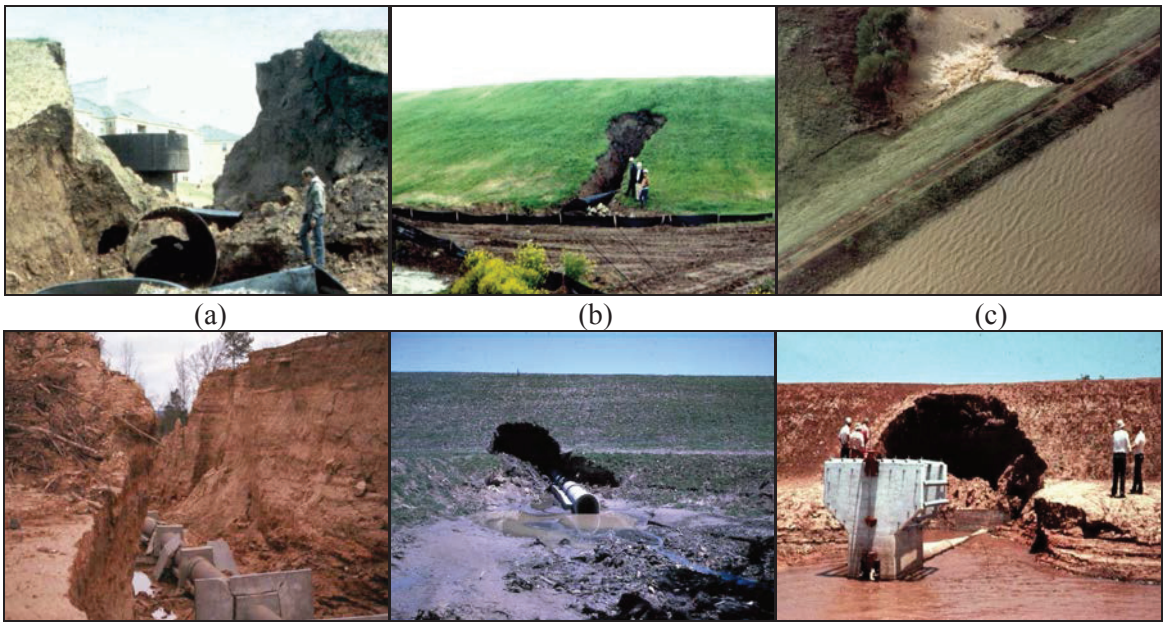

Figure 3. Some dam failures due to piping around buried conduits: (a) Loveton Farms Dam; (b) Medford Quarry Wash Water Lake Dam; (c) Upper Red Rock Site 20 Dam; (d) Anonymous Dam 1; (e) Anonymous Dam 2; (f) Anonymous Dam 3

Most of the previous research did not separate the piping process occurring around the conduits from that occurring at any level of the embankment. The researchers investigated the relationship between the piping potential and some soil parameters, the rate of erosion, the breach characteristics, and the time to failure during piping. In one of the earliest studies, Lane (1935) showed the correlation between the soil types and piping resistances of soils. Khilar et al. (1985) and Ojha et al. (2001, 2003) showed a theoretical relationship between porosity and hydraulic conductivity of soils with the critical hydraulic gradient which plays an important role for the initiation of internal erosion. In an experimental work conducted with sandy soils, Schmertmann (2000) presented that the coefficient of uniformity of the sand affects the average gradients that cause piping. Sellmeijer and Koenders (1991) and Koenders and Sellmeijer (1992) showed via a mathematical model that piping depends on the hydraulic conductivity and the D_{70} of the soil. Some of the previous studies dealt with the historical dam failure data for predicting the characteristics of dam breaches occurring after piping. MacDonald and Langridge-Monopolis (1984) introduced a breach formation factor using this kind of a data set. Tabrizi et. al. (2017) developed multivariable parametric breach models for the breach depth and width using the data of fourteen dam failures occurred during the historic 2015 flood in South Carolina, the United States.

Among recent studies, Bonelli and Benahmed (2010) conducted an experimental study on an earthen water retaining structure and proposed expressions for the time to failure in piping condition. It was found that the time of piping is a function of the initial hydraulic gradient and the coefficient of erosion. Awal et al. (2011) carried out extensive laboratory experiments on the piping of an earthen dam and found that the initial size, slope, and location of the pipe, the upstream water level and reservoir volume affect the peak discharge and the outflow hydrograph. Alamdari et al. (2012) developed a 1D numerical model utilizing mass conserving finite volume method to estimate the time of piping failure of earthen dams. Elkholy et al. (2015) studied the effects of soil composition on the internal erosion of earthen levees and it was found that the clay content of soil mixtures significantly affects the erosion rate. The study also presented an exponential equation to estimate the depth of erosion as a function of time. Sharif et al. (2015) showed the effects of soil compaction on the internal erosion rate of earthen embankments and concluded that increasing the compaction increases the time to failure of the structure; however, it has a little effect on the depth of erosion.

ANITA DAM INCIDENT

Anita Dam was designed by the Bureau of Land Management (BLM) and constructed in 1996 with a height of 11 m, a crest length of 308 m, and a crest width of 4.3 m. The dam impounds an almost 1.5 million m^3 reservoir. The embankment was a homogeneous earth-fill with riprap protection at the upstream face. The earth-fill was composed of lean clay, which was recognized to have dispersive properties after the failure. The embankment dam was constructed with a 0.91-m-diameter steel outlet conduit which was buried through the dam body and used as the principal spillway. It was surrounded by a series of concrete anti-seep collars. There were two unlined emergency spillways located on both banks to evacuate probable extreme floods (FEMA, 2015). Neither a filter diaphragm was utilized around the conduit nor it was supported by a concrete cradle. The only support for the conduit was provided by the placement of high slump soil cement backfill under the conduit between anti-seep collars (FEMA, 2005). The primary purpose of Anita Dam was flood control and it was classified as a low-hazard dam. Anita Dam is in a rural area Blaine County, Montana, the United States about 8 km south of the Canadian border. Anita Dam reservoir is on an unnamed tributary of the East Fork of the Battle Creek, flowing into the Milk River. The tributary is an ephemeral stream and it flows in response to snowmelt or heavy rain. After the completion of Anita Dam in November 1996, the reservoir was expected to be filled in 3 years (FEMA, 2015).

In the spring of 1997, the reservoir was filled only in 4 days due to an unexpectedly heavy snowpack melt. On March 26, a heavy leakage was noticed adjacent to the buried conduit and this resulted in a piping failure in the dam. In addition, multiple vortices occurred in the reservoir water surface about 45 m upstream of the dam body. The embankment did not breach; however, the outlet gate was opened as a precautionary measure and the reservoir was fully emptied. Almost 990,000 m^3 of water was drained in 36 hours, through and along the outlet conduit with a total discharge of 11.3 m^3/s [see Figure 4(a)], which was far greater than the design capacity of the conduit (FEMA, 2005 and 2015). Fortunately, the incident caused no injury or loss of lives, only four families were evacuated from the downstream. The consequences of the internal erosion became visible after the complete drainage of the reservoir on March 27. In Figure 4(b), the eroded soil around the conduit can be seen. The preferential flow path around the buried conduit completely swept away the eroded soil, resulting in the formation of caverns immediately around the anti-seep collars [see Figure 5]. The caverns were extended all along the conduit from the upstream to the downstream ends of the embankment (FEMA, 2005).

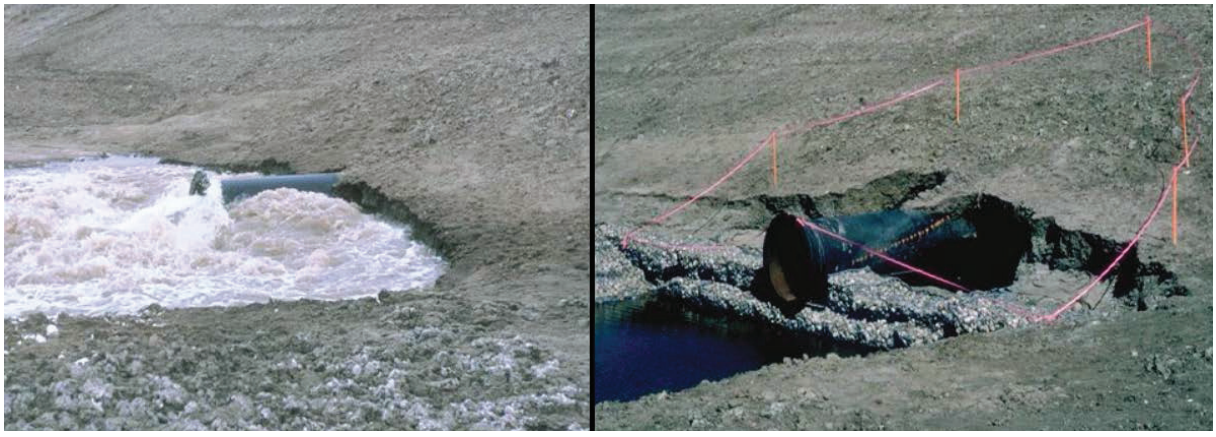

(a) (b)

Figure 4. (a) The erosion of the embankment and the flow of water through and adjacent to the conduit during the incident; (b) The embankment erosion around the conduit after the incident (retrieved from ASDSO, 2018)

Figure 5. Formation of caverns due to erosion of the backfill adjacent to the anti-seep collars at the upstream end of the conduit (retrieved from ASDSO, 2018)

A board of inquiry visited the site after the reservoir was fully drained. The board evaluated the incident and concluded that Anita Dam was failed due to internal erosion around its outlet conduit, initiated by a small flow path around the conduit (FEMA, 2015). The board reported that the combination of the following led to this rapid failure: (1) hydraulic fractures; (2) the use of anti-seep collars instead of a filter diaphragm and drain; (3) the use of cement backfill instead of a concrete cradle to support the conduit; and (4) cold airflow through the conduit creating ice lenses around the conduit. In addition, it was noted that the use of a dispersive lean clay as the fill material resulted in the accelerated enlargement of the small flow paths formed around the conduit (FEMA, 2005).

LESSONS LEARNED

Anita Dam incident was an opportunity for reconsidering the seepage control approaches in those days. Lessons learned from this failure have led to significant changes in the design considerations of embankment dams to prevent the seepage around buried conduits. These are as follows:

1) Instead of using anti-seep collars to control seepage along buried conduits through embankment dams, a filter diaphragm should be utilized with a drainage facility.

   The seepage around buried conduits in earthen dams was previously controlled using anti-seep collars that are made of concrete or metal. The collars were placed at certain intervals along the conduit [see Figure 3(d) and Figure 5]. The impermeable collars were believed to increase the length of the seepage path and decrease the hydraulic gradients around the conduit and hence, reduce the possibility of internal erosion. However, during 1980s anti-seep collars alone were recognized to be inadequate in preventing the internal erosion by US Army Corps of Engineers and US Bureau of Reclamation (FEMA, 2005). These agencies stated that the collars contributed to the differential settlement created by the buried conduit and increased the number and the length of the hydraulic fractures. The collars were also stated to obstruct the compaction of soils around the conduit. Therefore, it was noted that additional measures were needed to prevent the internal erosion. However, Anita Dam, constructed in 1996, only contained anti-seep collars as a preventive measure against the internal erosion.

A new approach is now in use for the seepage control around conduits penetrating through embankment dams. A filter zone, i.e. filter diaphragm or filter collar, is implemented in dams surrounding the buried conduits. The filter zone intercepts the water flow through the cracks in the embankment. The use of a sand filter collar is restricted to less problematic cases, where the embankment is not vulnerable to hydraulic fracturing and the soil is not a dispersive clay (FEMA, 2005). Otherwise, the use of filter diaphragms is recommended. A filter diaphragm is a zone of graded filter sand, intercepting the intergranular flow through the embankment, the flow through cracks of the earth-fill, and the flow surrounding the conduit (FEMA, 2005). A typical configuration for the filter diaphragm can be seen in Figure 6. In the case of the use of a filter diaphragm, if the fine material is eroded and carried by the flowing water through the embankment, it accumulates on the upstream face of the diaphragm and develops a layer called filter cake. The filter cake helps to prevent further erosion in the earth-fill. Further information regarding the design and construction of filter zones can be found in FEMA (2011).

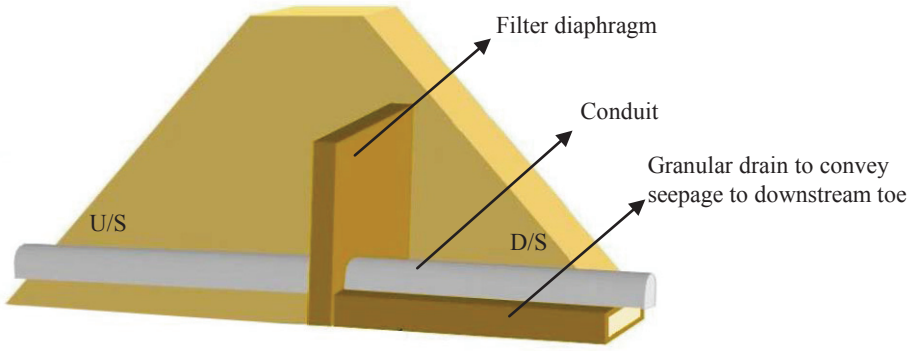

Figure 6. Typical configuration for a filter diaphragm. See the location of the filter diaphragm is as far downstream as possible, leaving adequate cover over it (retrieved from FEMA, 2005)

2) The first filling of a reservoir should be slow and monitored carefully.

The initial filling rate of the reservoir after the completion of the construction is crucial since it may create hydraulic fractures in the embankment. The initial filling may be controlled or it may occur naturally. Controlled first filling, which may take several months or years, may be performed by increasing the water level in the reservoir until it reaches the operating level (ASDSO, 2018). The initial filling rate may vary due to the location of the dam, its size and type, but typically the filling rate ranges between 0.15 to 0.6 m per day (FEMA, 2005 and ASDSO, 2018). As water penetrates the embankment, the water pressure may exceed the internal soil pressure leading to a hydraulic fracture. To avoid the risk of a failure, a proper reservoir filling rate should be selected and regulated by monitoring the response of the dam as the hydrostatic load is increased. Therefore, besides the determination of the filling rate, it is important to carefully monitor the dam during the first filling at intervals (ICOLD, 1998). In addition, construction of the outlet works should be completed, since it may be necessary to suspend filling and evacuate water to lower the reservoir level to a stage to allow the inspection of seepage and internal erosion (ASDSO, 2018).

About 48% of failure incidents due to internal erosion in the embankment have occurred during the first filling of reservoirs (Foster et al., 2000). Among those incidents, Teton Dam failure in 1976 is the well-remembered embankment dam failure due to controlled but very rapid first filling. In case of Anita Dam incident, in which the dam is constructed for only flood control purposes, the reservoir is filled for the first time naturally and unexpectedly only in 4 days due to a heavy snowpack melt.

3) A concrete encasement or cradle should be placed around the buried conduit to allow better compaction of earth-fill.

   A concrete encasement or a cradle provides a convenient shape for compaction of the earth-fill against the conduit. Among several typically used conduit shapes, precast circular conduit requires placement on a concrete cradle [see Figure 7] to provide proper compaction of the soil especially underneath the curves of the conduit (FEMA, 2005). Otherwise, differential settlement and formation of hydraulic fractures will be inevitable in the embankment. Besides its convenience in earth-fill compaction, a concrete encasement may be utilized to provide insulation of conduit against cold weather, which may prevent undesirable cracks (ASDSO, 2018).

Figure 7. Precast concrete conduit with concrete cradle support (retrieved from FEMA, 2005)

4) The flow of cold air through the conduit should be prohibited to avoid freeze and thaw of soil surrounding the conduit.

   Cold airflow through buried conduits during winter time may lead to the formation of lenses of frozen soil in the surrounding earth-fill. As happened in Anita Dam incident, the initial flow through the conduit may thaw these ice lenses resulting in a seepage path formation. Eventually, internal erosion may grow following these paths. Therefore, the conduit should be protected against cold air that may flow through it (ASDSO, 2018).

5) The dispersive soil around buried conduits may be stabilized using chemical additives.

   The cracks in dispersive soils in the embankment fill are vulnerable to erosion by flow through them. The erodibility of dispersive soils can lead to rapid enlargement of the cracks and eventually to the internal erosion as happened in Anita Dam case. To avoid the failure risk of embankment dams due to internal erosion in the dispersive soil, the soil can be modified with chemical additives to reduce its erodibility. Hydrated lime is the most commonly used additive to stabilize dispersive soils. However, although it is effective in reducing the erodibility of the soil, lime treatment is an expensive alternative and it may increase the brittleness of the soil. The use of a filter diaphragm with a proper drainage facility may be a better alternative to prevent internal erosion around buried conduits (FEMA, 2005).

SUMMARY AND CONCLUSIONS

Conduits through embankment dams are prone to seepage and internal erosion around the surrounding soil. This may be overlooked by design engineers and the embankment dams may fail due to piping. There are many piping failures occurred due to buried conduits in history. One of the well-known failures, the Anita Dam incident, has changed the design practices of conduits through the embankment dams. This specific case needed to be presented to raise an awareness of the design engineers on this incident and the lessons learned from it. To this end, this paper reviewed the Anita Dam incident regarding the literature on piping in embankment dams, the causes and the consequences of the failure, and the lessons learned from the incident. The incident occurred on March 26, 1997, was resulted due to internal erosion around the buried outlet conduit. The combination of the following led to the failure: (1) hydraulic fractures; (2) the use of anti-seep collars instead of a filter diaphragm and drain; (3) the use of cement backfill instead of a concrete cradle to support the conduit; and (4) cold airflow through the conduit creating ice lenses around it. The lessons learned from the incident and the best practices for the design of embankment dams with buried conduits are as follows: (1) filters and drains should be used to control seepage along buried conduits through embankment dams instead of anti-seep collars; (2) the first filling of a reservoir should be slow and monitored carefully; (3) a concrete encasement or cradle should be placed around the buried conduit to allow better compaction of the earth-fill; (4) the flow of cold air through the conduit should be prohibited to avoid freeze and thaw of soil surrounding the conduit; and (5) the dispersive soil around buried conduits may be stabilized using chemical additives. The authors believe that there is a need for both numerical and laboratory research on the seepage around conduits through embankment dams which is seen to be absent at present time.

REFERENCES

Ahmed, A.A., 2009. “Stochastic analysis of free surface flow through earth dams”. Computers and Geotechnics, vol. 36, N.7, pp. 1186–1190.

Alamdari, N.Z., Banihashemi, M., Mirghasemi, A., 2012. “A numerical modeling of piping phenomenon in earth dams”. World Acad. Sci. Eng. Technol., vol. 6 N.10, pp 39–41.

Association of State Dam Safety Officials (ASDSO), 2018. http://damfailures.org/case-study/anita-dam-montana-1997/ accessed on July 26, 2018

Awal, R., Nakagawa, H., Fujita, M., Kawaike, K., Baba, Y., Zhang, H., 2011. “Study on piping failure of natural dam”. Annu. Disaster Prev. Res. Inst., vol. 54, pp 539–547.

Bonelli, S., Benahmed, N., 2010. “Piping flow erosion in water retaining structures: Inferring erosion rates from hole erosion tests and quantifying the failure time”. IECS 2010, 8th ICOLD European Club Symp. Dam Safety-Sustainability in a Changing Environment, ATCOLD Austrian National Committee on Large Dams, 6.

Calamak, M., Yanmaz, A.M., 2018. “Assessment of core-filter configuration performance of rock-fill dams under uncertainties”. International Journal of Geomechanics, vol. 18, N.4, pp. 06018006.

Calamak, M., Yanmaz, A., 2017. “Uncertainty quantification of transient unsaturated seepage through embankment dams”. International Journal of Geomechanics, vol. 17, N.6, pp. 04016125.

Calamak, M., Yanmaz, A.M., Kentel, E., 2017. “Probabilistic evaluation of the effects of uncertainty in transient seepage parameters”. Journal of Geotechnical Geoenvironmental Engineering. vol. 143, N.6, pp. 06017009.

Costa, J.E., 1985. “Floods from dam failures”. U.S. Geological Survey Open-File Rep. 85-560, Denver, 54.

Elkholy, M., Sharif, Y., Hanif Chaudhry, M., Imran, J., 2015. “Effect of soil composition on piping of earthen levees”. Journal of Hydraulic Research, vol. 53 N.4, pp. 478–487.

Federal Emergency Management Agency (FEMA), 2005. Technical Manual: Conduits through Embankment Dams, Best Practices for Design, Construction, Problem Identification and Evaluation, Inspection, Maintenance, Renovation, and Repair.

Federal Emergency Management Agency (FEMA), 2011. Filters for Embankment Dams, Best Practices for Design and Construction.
Federal Emergency Management Agency (FEMA), 2015. Evaluation and Monitoring of Seepage and Internal Erosion, Interagency Committee on Dam Safety (ICODS)
Fenton, G., Griffiths, D., 1996. "Statistics of free surface flow through stochastic earth dam". Journal of Geotechnical Engineering, vol. 122, N.6, pp. 427–436.
Ferguson, K.A., 2012. "Investigation and Evaluation of Seepage Conditions and Potential Failure Modes Around Outlet Conduits". In Proceedings of the 2012 Annual Conference, United States Society on Dams (USSD), New Orleans, L.A.
Foster, M., Fell, R., Spannagle, M., 2000. "The statistics of embankment dam failures and accidents". Canadian Geotechnical Journal, vol. 37 N.5, pp. 1000–1024.
International Commission on Large Dams (ICOLD), 1988. Dam Monitoring General Considerations. Bulletin 60.
Khilar, K.C., Folger, H.S., Gray, D.H., 1985. "Model for piping plugging in earthen structures". Journal of Geotechnical Engineering, vol. 111, N.7, pp. 833–846.
Koenders, M.A., Sellmeijer, J.B., 1992. "Mathematical model for piping". Journal of Geotechnical Engineering, vol. 118, N.6, pp. 943–946.
Lane, E.W., 1935. "Security from under-seepage-masonry dams on earth foundations". Transactions of ASCE, vol. 100, N.1, pp. 1235–1272.
MacDonald, T. C., Langridge-Monopolis, J., 1984. "Breaching characteristics of dam failures". Journal of Hydraulic Engineering, vol. 110, N.5, pp. 567–586.
Ojha, C.S.P., Singh, V.P., Adrian, D.D., 2001. "Influence of porosity on piping models of levee failure". Journal Geotechnical and Geoenvironmental Engineering, vol. 127, N.12, pp. 1071–1074.
Ojha, C.S.P., Singh, V.P., Adrian, D.D., 2003. "Determination of critical head in soil piping". Journal Geotechnical and Geoenvironmental Engineering, vol. 129, N.7, pp. 511–518.
Schmertmann, J.H., 2000. "The non-filter factor of safety against piping through sand". In Judgment and innovation: the heritage and future of the geotechnical engineering profession, ASCE, Reston, VA, pp. 65–132.
Sellmeijer, J.B., Koenders, M.A. 1991. "A mathematical model for piping". Applied mathematical modeling, Oxford, U.K., vol. 115, pp. 646–661.
Sharif, Y.A., Elkholy, M., Chaudhry, M.H., Imran, J., 2015. "Experimental study on the piping erosion process in earthen embankments". Journal of Hydraulic Engineering, vol. 141, N.7, pp. 1–9.
Tabrizi, A.A., LaRocque, L.A., Chaudhry, M.H., Viparelli, E., Imran, J. 2017. "Embankment Failures during the Historic October 2015 Flood in South Carolina: Case Study". Journal of Hydraulic Engineering, vol. 143, N.8, pp. 05017001.
Tan, X., Wang, X., Khoshnevisan, S., Hou, X., & Zha, F. 2017. "Seepage analysis of earth dams considering spatial variability of hydraulic parameters". Engineering Geology, vol. 228, pp. 260-269.

5th International Symposium on Dam Safety

October 27-31, 2018

TOTAL RISK ANALYSIS OF TWENTY-FIVE LARGE DAMS IN IRAN

Mohammad DAVOODI [1], Reza AFZALSOLTANİ [2]

ABSTRACT

Iran has more than 1300 dams with different types and sizes. Iran is a vast country and great part of it is placed in a highly active seismic zone and occurred earthquakes in the past indicate that. Lots of large dams in Iran are located near the active faults and can be affected by them. As most of existing dams in Iran are designed based on old versions of codes and instructions, there is a need to evaluate the seismic safety of the existing dams based on the most recent codes; in order to do that the existing dams should be classified based on their seismic risk. Results of this classification can then be used to prioritize the safety evaluation of these dams. In this study, the total risk factor (TRF) of Iran's 25 important dams is calculated based on parameters such as each dam site's seismic activity, their physical properties and the position in the basin using the Bureau method. It is shown that many of important dams in Iran are placed in high seismic hazard category and their safety should be re-evaluated using the most recent codes and instructions.

Keywords: Dam, Dam safety, Total risk factor, Seismic risk, Earthquake, Seismic Hazard

INTRODUCTION

Although dams are designed based on codes and engineering rules, as time goes on, design instructions may be updated and dam properties may also change due to aging, so there's a need to check dams' stability and evaluate their safety factor against catastrophic loadings such as earthquake with respect to the most recent codes. There are many examples of breaking of dams in earthquakes (Azam & Li, 2010; Harder Jr, 1991; Rico, Benito, Salgueiro, Díez-Herrero, & Pereira, 2008; Seed, Lee, Idriss, & Makdisi, 1975; USCOLD., 2014; Villavicencio, Espinace, Palma, Fourie, & Valenzuela, 2013). Failure of dams can lead to loss of life and property.

Iran is a vast country with more than 1300 dams with different types and sizes and also is located in seismically active zone. Most of these dams are expected to experience few severe earthquakes during their lifetime. So, we need to evaluate the seismic safety of these dams periodically. Seismic hazard rating of dams is the first step in finding the most critical dam which has the highest risk and should be checked and rehabilitated first.

In this study, 25 of important dams in Iran are studied and the total risk factor of them are evaluated. By calculating the total factor of these dams it becomes possible to rank them to find the most critical dams, the safety of which should be re-evaluated using the most recent codes and instructions then redesigned or rehabilitated if necessary.

[1] Associate Professor, Department of Geotechnical Engineering, International Earthquake Engineering and Seismology, (IIEES), Tehran, Iran,
e-posta: m-davood@iiees.ac.ir

[2] PhD Candidate, Department of Geotechnical Engineering, International Earthquake Engineering and Seismology, (IIEES), Tehran, Iran: reza.afzalsoltani@gmail.com

METHODOLOGY

To quantify the total risk factor of a dam, one way is to consider the seismic hazard of the dam site and the risk rating of the structure separately. According to this method, the seismic hazard of the dam site regardless of type of dam can be quickly classified into the groups from low to extreme. The hazard class of a dam site obtained from this method provides a preliminary indication of seismic evaluation requirements.

ICOLD (1989) states that total risk of dams consists of structural and social-economics components. The first one is mainly based on the structural properties of the dam such as capacity of the reservoir and its height. The second factor is based on the vulnerability of downstream area due to failure of the dam. The total risk factor (TRF) is defined as a summation of these risk factors: capacity, height, evacuation requirements and potential damage. Based on the total risk factor, four risk classes are defined as low, moderate, high and extreme. Risk classification of a dam provides more detailed information for the selection of seismic evaluation parameters and methods to be used for analysis.

Bureau method considers various risk factors and weighting points to quantify approximately the total risk factor (TRF) of any dam. Bureau (2003) states that TRF depends on the dam type, age, size, downstream risk and vulnerability. The TRF in this method expressed as Eq.1 (GJ Bureau, 2003).

$$TRF = [(CRF + HRF + ARF) + DHF] \times PDF \quad (1)$$

In this equation, the dam structure influence is presented by summation of capacity risk factor (CRF), height risk factor (HRF) and age of the dam risk factor (ARF). These factors quantify the risk of a dam structure and its reservoir and indicate that higher dam with larger reservoir can cause more destructive flood. In addition, as a dam get older, it becomes more vulnerable than modern one because of possible deterioration, maintenance, siltation and etc. these risk factors can be defined from Table 1 and Table 2.

Table 1. Dams' capacity and height risk factor (CRF and HRF) (GJ Bureau, 2003)

Risk Factor	Contribution to the total risk							
	Extreme		High		Moderate		Low	
Capacity (m^3) CRF	>61,673,500	6	61,673,500-1,233,470	4	1,233,470-123,234	2	<123,347	0
Height (m) HRF	>24.38	6	24.38-12.19	4	12.19-6.1	2	<6.1	0

Table 2. Dams' age risk factor (ARF) (GJ Bureau, 2003)

Year of commissioning	< 1900	1900-1925	1925-1950	1950-1975	1975-2000	>2000
Age risk factor ARF	6	5	4	3	2	1

Downstream hazard factor (DHF) also be considered based on the population an property at risk due to failure of the dam and defined as Eq.2 and should be updated whenever new information becomes available (GJ Bureau, 2003).

$$DHF = ERF + DRI \quad (2)$$

Where ERF is evacuation requirement factor which depend on the human population at risk in the downstream of the dam and DRI is downstream damage risk index which is based on the value of private, commercial, industrial or government property in the potential flood path.

Table 3. Downstream hazard factor (GJ Bureau, 2003)

Risk Factor	Contribution to the total risk							
	Extreme		High		Moderate		Low	
Persons ERF	>1000	12	1000-100	8	100-1	4	0	1
Property value DRI	high	12	moderate	8	reduced	4	none	1

Predicted damage index (PDI) depends on the dam type and on the site seismic hazard and tectonic environment. The expected ground motion at the dam site for the scenario earthquake considered is expressed by the earthquake severity index (ESI) as expressed in Eq.3 .

$$ESI = PGA \times (M - 4.5)^3 \quad (3)$$

In this equation, PGA is peak measured ground acceleration in g and M is moment magnitude of the causative event. The PDI depends on the ESI and obtained from graphical relationship shown in figure 1.

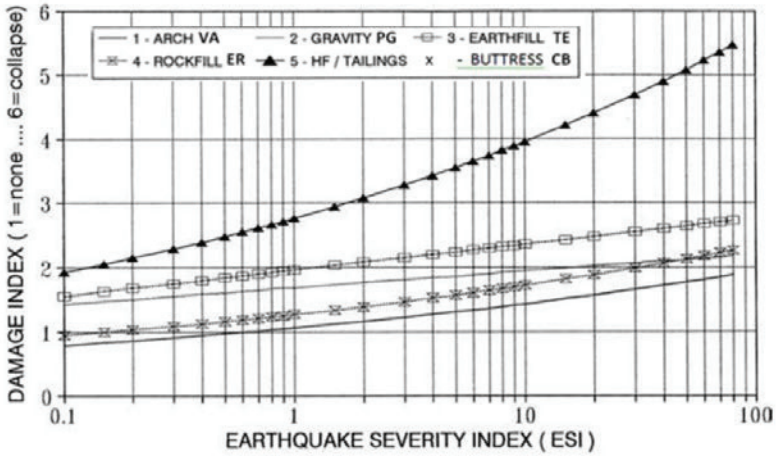

Figure 1. Dam vulnerability curves Caption (GJ Bureau, 2003)

From the computed PDI, PDF can be defined by the Eq.4 .

$$PDF = 2.5 \times PDI \quad (4)$$

The coefficient 2.5 empirically selected by Bureau and Ballentine to provide consistency between vulnerability estimates from site ground motion defined by the ESI (G Bureau & Ballentine, 2002). The PDI rates only the relative vulnerability of each dam type, and includes a significant uncertainty, especially when extrapolated to large ESI values, which can be quantified from the standard deviations associated with the mean estimates.

The final step is ranking the dams by sorting TRF and categorize them to Risk Class ranging from low risk to extreme according Table 4.

Table 4. Dams' Risk Classes (GJ Bureau, 2003)

Total Risk Factor TRF	Risk Class	Risk Explanation
2-25	I	Low
25-125	II	Moderate
125-250	III	High
>250	IV	Extreme

The method mentioned above is widely used in the literature and can be taken as a reliable approach to determine the risk of collapse in a particular dam and the importance of inspection and safety evaluations. For example, Tosun et al. (2007) evaluated the total risk of 32 large dams in Euphrates basin in turkey. Moldovan et al. (2017) used this method to rank 227 Large Romanian Dams . So, the methodology presented here was used for risk ranking of 25 important dams in Iran.

RISK RANKING OF DAMS

The source of information about studied dams are Iran Water Resources Management Company and Iranian National Committee on Large Dams (IRCOLD), that contains complete information about dams regarding commissioning year, dimensions, characteristics, etc. Table 5 shows the studied dams' informations and figure 2 shows the geographical distribution of these dams.

Table 5. Dams characteristics

Dam No.	Dam	Long.	Lat.	Type	Year of commissioning	Crest length (m)	Height (m)	Reservior Capacity (hm3)
1	Karkheh	39 S 229986	3598436	embankment	2001	3030	127	4002
2	Seymareh	38 S 704650	3685835	double arch	2014	202	180	2241
3	Karun3	39 R 414333	3518870	double arch	2004	462	205	1625
4	Dez	39 S 262001	3610371	arch	1962	212	203.5	2050
5	Shahid Abbaspour	39 S 368512	3547014	arch	1976	380	200	1446
6	Sefidrud	39 S 356114	4069357	buttress	1961	425	106	1112
7	Khoda Afarin	38 S 667160	4336283	embankment	2008	400	64	1200
8	Zayanderud	39 S 475359	3621816	double arch	1970	452	100	1450
9	Aras	38 S 534832	4326994	embankment	1971	945	40	1166.5
10	Dousti	41 S 334349	3979807	embankment	2005	655	78	950
11	Marun	39 R 438141	3398250	embankment	1999	345	165	993
12	Doroudzan	39 R 636607	3342598	embankment	1972	710	60	860
13	Lar	39 S 589840	3972002	embankment	1982	1150	107	860
14	Rayisali Delvari	39 R 508511	3277196	double arch	2007	240	115	524
15	Shahid kazemi	38 S 636974	4031914	embankment	1971	530	50	486
16	Kosar	39 R 463412	3384675	Gravity	2003	190	144	493
17	Mollasadra	39 R 603676	3390470	embankment	2007	630	75	411
18	Talegan	39 S 467121	4004834	embankment	2006	1111	109	329
19	Esteglal	40 R 511116	3004569	buttress	1984	451	59.25	270
20	Jagin	40 R 589591	2894146	RCC	2006	263	80	135
21	Masjed Soleyman	39 S 348934	3544633	embankment	2001	488	177	252
22	Gotvand	39 S 305614	3571953	embankment	2012	760	182	3470
23	Latian	39 S 508208	3979132	buttress	1967	450	107	67
24	Shahid rajaee	39 S 700241	4013847	double arch	1996	430	138	154
25	Pishin	41 R 368667	2879341	embankment	1993	400	63	167

Structural risk factors

As mentioned in pervious section, height risk factor, capacity risk factor and age risk factor are related to the structure of the dam. Using the information in Table 5, these risk factors are presented in Table 6.

Figure 2. Location of Dams in Table 5

Table 6. Dams' structural risk factors

Dam No.	Dam	HRF	CRF	ARF	Dam No.	Dam	HRF	CRF	ARF
1	Karkheh	6	6	1	14	Rayisali Delvari	6	6	1
2	Seymareh	6	6	1	15	Shahid kazemi	6	6	3
3	Karun3	6	6	1	16	Kosar	6	6	1
4	Dez	6	6	3	17	Mollasadra	6	6	1
5	Shahid Abbaspour	6	6	2	18	Talegan	6	6	1
6	Sefidrud	6	6	3	19	Esteglal	6	6	2
7	Khoda Afarin	6	6		20	Jagin	6	6	1
8	Zayanderud	6	6	3	21	Masjed Soleyman	6	6	1
9	Aras	6	6	3	22	Gotvand	6	6	
10	Dousti	6	6	1	23	Latian	6	6	3
11	Marun	6	6	2	24	Shahid rajaee	6	6	2
12	Doroudzan	6	6	3	25	Pishin	6	6	2
13	Lar	6	6	2					

Downstream hazard risk

The risk factor of the downstream water accumulations, takes into account the dam location, the villages located downstream, the distance and the height difference between them, the number of

inhabitants which should be evacuated, and the existing infrastructure (hydro-energetic plants, roads, highways, gas stations, railroads, and widely populated and visited tourist attractions) (GJ Bureau, 2003).

For studied dams, the downstream risk was calculated empirically by analyzing the maps. The localities in the downstream vicinity of the studied dams and the number of inhabitants were identified, and information regarding the value of downstream properties was obtained from related websites. The transposition of this information into risk factors was done in Table 7.

Table 7. Dams' downstream hazard factor

Dam No.	Dam	ERF	DRI	DHF	Dam No.	Dam	ERF	DRI	DHF
1	Karkheh	12	12	24	14	Rayisali Delvari	12	12	24
2	Seymareh	12	12	24	15	Shahid kazemi	12	12	24
3	Karun3	12	12	24	16	Kosar	12	12	24
4	Dez	12	12	24	17	Mollasadra	12	12	24
5	Shahid Abbaspour	12	12	24	18	Talegan	12	12	24
6	Sefidrud	12	12	24	19	Esteglal	12	12	24
7	Khoda Afarin	12	12	24	20	Jagin	12	12	24
8	Zayanderud	12	12	24	21	Masjed Soleyman	12	12	24
9	Aras	12	12	24	22	Gotvand	12	12	24
10	Dousti	12	12	24	23	Latian	12	12	24
11	Marun	12	12	24	24	Shahid rajaee	12	12	24
12	Doroudzan	12	12	24	25	Pishin	12	12	24
13	Lar	12	12	24					

Expected ground motion in dams' location

For seismic hazard analyses, in this study seismic hazard map developed by Tavakoli and Ghafory-Ashtiany (2009) is used. Tavakoli and Ghafori-Ashtiany (2009) developed a seismic hazard map of Iran based of probabilistic hazard computation and displayed the results for return period of 475 years (figure 3 and Table 8). Probabilistic seismic hazard assessment SEIS RISK III (A Computer Program for Seismic Hazard Estimation) was used to calculate peak ground accelerations. (Tavakoli & Ghafory-Ashtiany, 1999). Also, in this article we used the acceleration levels map developed by Zare (Zare, 2012) for central and southern Iran which presented in figure 4.

Estimation of seismic ground motion risk factor

The earthquake severity index (ESI) calculated from Eq. 3 according the peak ground acceleration obtained from figure 4 for a recurrence period of 475 years which corresponds to a exceeding probability of 10% in 50 years or of 0.2% in a year and the moment magnitude obtained from Figure 3 for 475 return periods. Table 9 shows the calculated ESI and PDI indices for studied dams.

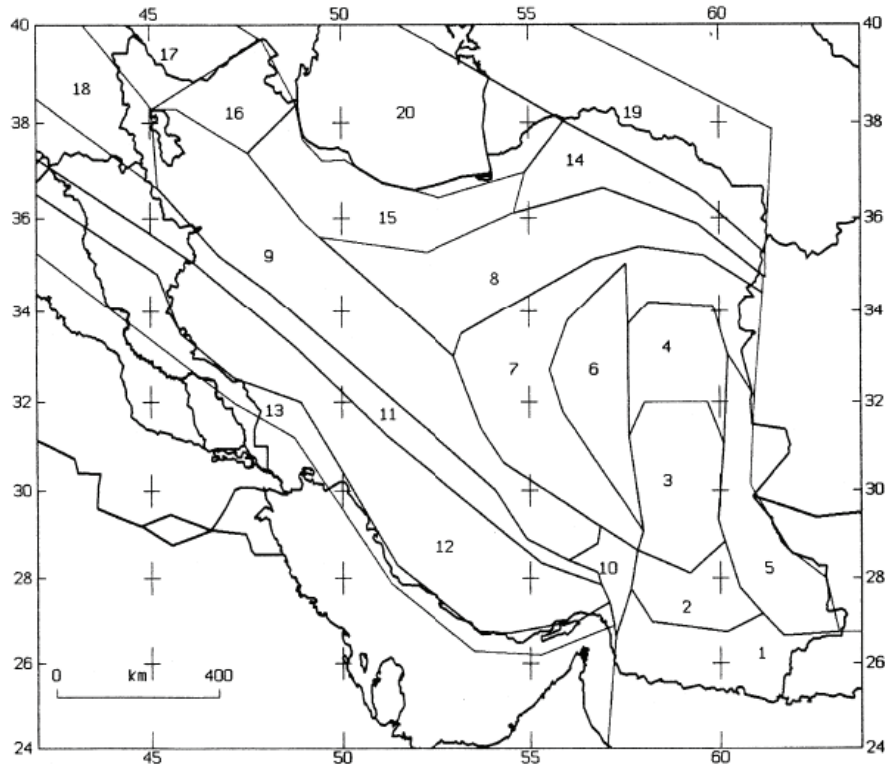

Figure 3. Seismic provinces of Iran (Tavakoli & Ghafory-Ashtiany, 1999)

Table 8. Estimated Hazard Earthquake Parameters (Tavakoli & Ghafory-Ashtiany, 1999)

Z	Span of time	Beta (KS)	b (KS)	Beta (GR)	b (GR)	CC	M_{max}	M(obs)	λ(4.5)	N
01	1926-95	1.55 ± 0.12	0.66 ± 0.05	1.54 ± 0.14	0.67 ± 0.06	0.96	8.1 ± 0.4	8.0	2.09	154
02	1963-95	1.19 ± 0.32	0.50 ± 0.13	1.17 ± 0.12	0.51 ± 0.05	0.97	7.2 ± 0.4	7.0	0.35	22
03	1960-90	1.30 ± 0.27	0.55 ± 0.11	1.13 ± 0.07	0.49 ± 0.03	0.99	7.2 ± 0.3	7.0	0.26	22
04	1941-90	1.17 ± 0.17	0.50 ± 0.07	0.93 ± 0.09	0.41 ± 0.04	0.96	7.6 ± 0.3	7.4	0.21	34
05	1927-95	1.27 ± 0.28	0.54 ± 0.12	1.27 ± 0.06	0.55 ± 0.03	0.99	7.4 ± 04	6.9	0.44	33
06	1929-95	1.39 ± 0.16	0.59 ± 0.07	1.34 ± 0.05	0.85 ± 0.02	0.99	7.6 ± 0.3	7.4	0.64	72
07	1923-95	1.95 ± 0.15	0.83 ± 0.06	1.71 ± 0.09	0.74 ± 0.04	0.99	7.5 ± 0.3	7.3	0.47	84
08	1924-95	1.99 ± 0.17	0.84 ± 0.07	1.34 ± 0.09	0.58 ± 0.04	0.98	7.4 ± 0.4	7.2	0.16	54
09	1922-95	1.94 ± 0.16	0.82 ± 0.07	1.40 ± 0.18	0.61 ± 0.08	0.97	7.3 ± 0.3	6.8	0.27	53
10	1932-95	1.47 ± 0.27	0.62 ± 0.11	2.38 ± 0.19	1.03 ± 0.08	0.98	6.6 ± 0.2	6.1	0.88	60
11	1944-95	2.24 ± 0.11	0.95 ± 0.05	1.59 ± 0.06	0.69 ± 0.03	0.99	7.6 ± 0.4	7.4	0.48	130
12	1920-95	2.12 ± 0.05	0.90 ± 0.02	1.98 ± 0.11	0.68 ± 0.05	0.99	7.2 ± 0.2	7.0	1.70	622
13	1925-95	2.49 ± 0.13	1.06 ± 0.05	1.86 ± 0.23	0.81 ± 0.10	0.98	7.0 ± 0.4	6.5	0.27	107
14	1928-95	1.98 ± 0.13	0.84 ± 0.05	1.71 ± 0.09	0.74 ± 0.04	0.99	7.6 ± 0.4	7.4	0.33	107
15	1927-95	1.41 ± 0.11	0.60 ± 0.04	1.19 ± 0.05	0.52 ± 0.02	0.99	7.9 ± 0.3	7.7	0.37	71
16	1900-92	1.68 ± 0.17	0.71 ± 0.07	1.83 ± 0.24	0.79 ± 0.10	0.96	7.6 ± 0.4	7.4	0.14	42
17	1907-92	1.72 ± 0.15	0.73 ± 0.06	1.68 ± 0.10	0.73 ± 0.04	0.98	7.5 ± 0.3	7.3	0.53	99
18	1924-92	1.61 ± 0.12	0.68 ± 0.05	1.62 ± 0.10	0.70 ± 0.04	0.99	7.9 ± 0.4	7.4	1.05	158
19	1900-95	1.68 ± 0.07	0.71 ± 0.03	1.48 ± 0.07	0.64 ± 0.03	0.99	7.9 ± 0.2	7.4	0.84	285
20	1929-95	2.32 ± 0.16	0.98 ± 0.07	1.69 ± 0.21	0.73 ± 0.09	0.95	7.5 ± 0.9	7.3	0.33	120

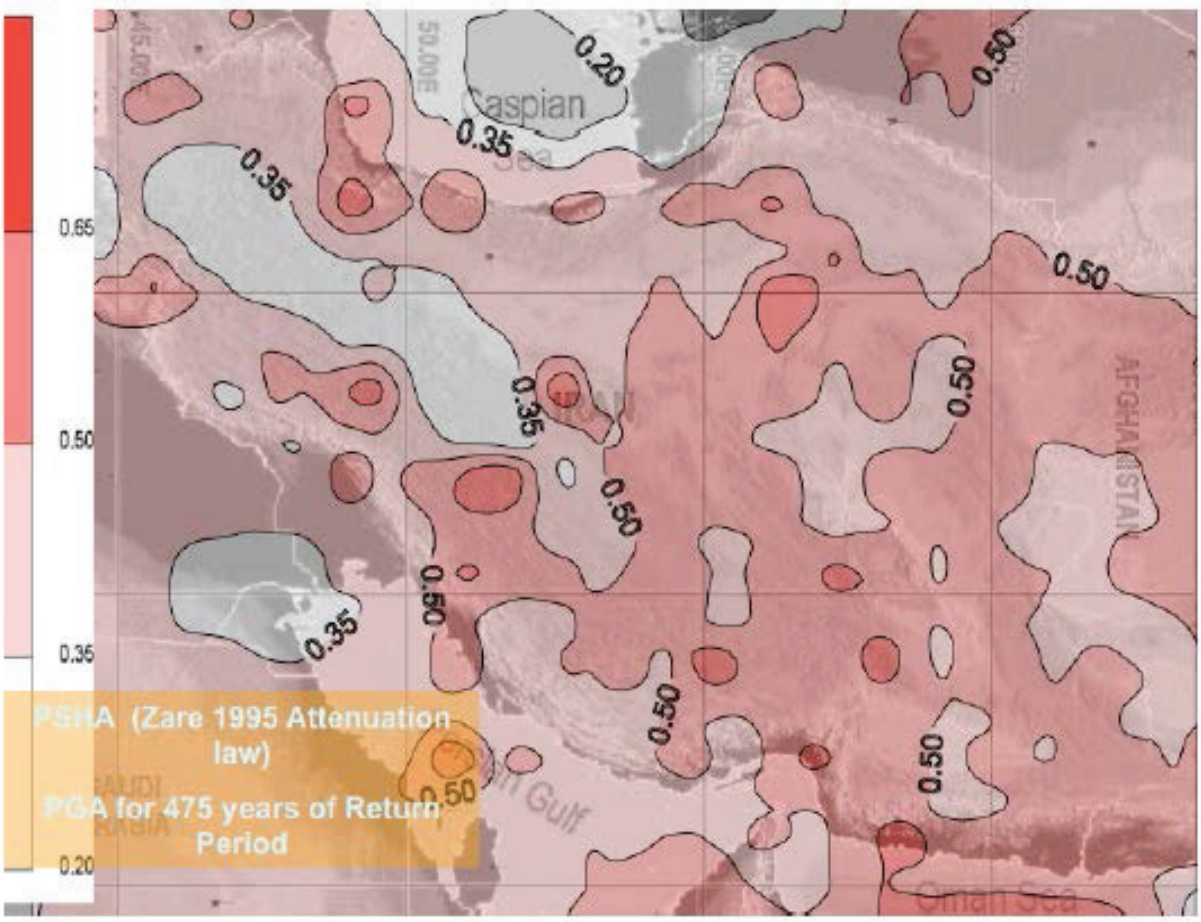

Figure 4. Seismic hazard map of Iran (Zare, 2012)

Table 9. Dams' predicted damage index

Dam No.	Dam	PGA (g)	Mw	ESI	PDI	Dam No.	Dam	PGA (g)	Mw	ESI	PDI
1	Karkheh	0.5	7	7.81	2.35	14	Rayisali Delvari	0.65	7	10.16	1.42
2	Seymareh	0.65	7	10.16	1.42	15	Shahid kazemi	0.35	6.8	4.26	2.22
3	Karun3	0.5	7	7.81	1.38	16	Kosar	0.65	7	10.16	1.73
4	Dez	0.5	7	7.81	1.38	17	Mollasadra	0.65	7.4	15.85	2.48
5	Shahid Abbaspour	0.5	7	7.81	1.39	18	Talegan	0.65	7.7	21.30	1.93
6	Sefidrud	0.5	7.7	16.38	2.00	19	Esteglal	0.8	6.1	3.28	1.81
7	Khoda Afarin	0.65	7.4	15.85	2.45	20	Jagin	0.65	8	27.87	2.07
8	Zayanderud	0.35	6.8	4.26	1.28	21	Masjed Soleyman	0. 5	7	10.16	2.39
9	Aras	0.65	7.4	15.85	2.45	22	Gotvand	0.65	7	10.16	2.39
10	Dousti	0.65	7.4	15.85	2.45	23	Latian	0.5	7.7	16.38	2.00
11	Marun	0.65	7	10.16	1.70	24	Shahid rajaee	0.5	7.7	16.38	1.54
12	Doroudzan	0.65	7	10.16	3.97	25	Pishin	0.65	8	27.87	2.50
13	Lar	0.5	7.7	16.38	2.45						

Dams rating

After finding the related risk factors (Tables 6, 7 and 9), total risk factor can be calculated according Eq. 1 .Table 10 shows the total risk factor evaluated for each dam.

Table 10. Total risk factor calculated for studied dams

Dam No.	Dam	HRF	CRF	ARF	DHF	PDF	TRF
1	Karkheh	6	6	1	24	5.9	217.4
2	Seymareh	6	6	1	24	3.6	131.4
3	Karun3	6	6	1	24	3.5	127.7
4	Dez	6	6	3	24	3.5	134.6
5	Shahid Abbaspour	6	6	2	24	3.5	132.1
6	Sefidrud	6	6	3	24	5.0	195.0
7	Khoda Afarin	6	6	1	24	6.1	226.6
8	Zayanderud	6	6	3	24	3.2	124.8
9	Aras	6	6	3	24	6.1	238.9
10	Dousti	6	6	1	24	6.1	226.6
11	Marun	6	6	2	24	4.3	161.5
12	Doroudzan	6	6	3	24	9.9	387.1
13	Lar	6	6	2	24	6.1	232.8
14	Rayisali Delvari	6	6	1	24	3.6	131.4
15	Shahid kazemi	6	6	3	24	5.6	216.5
16	Kosar	6	6	1	24	4.3	160.0
17	Mollasadra	6	6	1	24	6.2	229.4
18	Talegan	6	6	1	24	4.8	178.5
19	Esteglal	6	6	2	24	4.5	172.0
20	Jagin	6	6	1	24	5.2	191.5
21	Masjed Soleyman	6	6	1	24	6.0	221.1
22	Gotvand	6	6	1	24	6.0	221.1
23	Latian	6	6	3	24	5.0	195.0
24	Shahid rajaee	6	6	2	24	3.9	146.3
25	Pishin	6	6	2	24	6.3	237.5

CONCLUSIONS

In this paper, the total risk factor for 25 of important dams in different seismic zones in Iran are evaluated by using Bureau (2003) method based on the structural features of dams and considering the seismic risk calculations with return period of 475 years. From 25 important dams studied in this article, all have high seismic risk with total risk factor of 125 to 250. Near half of the studied dams have TRF more than 200 and should be included in a priority list for inspection, evaluation of seismic safety and increasing their seismic capacity and rehabilitation.

REFERENCES

Azam, S., & Li, Q. (2010). Tailings dam failures: a review of the last one hundred years. *Geotechnical News, 28*(4), 50-54.

Bureau, G. (2003). Dams and Appurtenant Facilities in Earthquake Engineering Handbook (edited by Chenh, WF and Scawthorn, C.): CRS press, Bora Raton.

Bureau, G., & Ballentine, G. (2002). *A comprehensive seismic vulnerability and loss assessment of the State of South Carolina using HAZUS. Part VI. Dam inventory and vulnerability assessment methodology.* Paper presented at the 7th National Conference on Earthquake Engineering, July.

Harder Jr, L. F. (1991). Performance of earth dams during the Loma Prieta earthquake.

Rico, M., Benito, G., Salgueiro, A., Díez-Herrero, A., & Pereira, H. (2008). Reported tailings dam failures: A review of the European incidents in the worldwide context. *Journal of hazardous materials, 152*(2), 846-852.

Seed, H. B., Lee, K. L., Idriss, I. M., & Makdisi, F. I. (1975). The slides in the San Fernando Dams during the earthquake of February 9, 1971. *Journal of Geotechnical and Geoenvironmental Engineering, 101*(ASCE# 11449 Proceeding).

Tavakoli, B., & Ghafory-Ashtiany, M. (1999). Seismic hazard assessment of Iran. *Annals of Geophysics, 42*(6).

USCOLD. (2014). Observed performance of dams during earthquakes. *3*.
Villavicencio, G., Espinace, R., Palma, J., Fourie, A., & Valenzuela, P. (2013). Failures of sand tailings dams in a highly seismic country. *Canadian geotechnical journal, 51*(4), 449-464.
Zare, M. (2012). *Development of seismic hazard zoning map for Iran, based on new seismic source determination.* Paper presented at the Proceedings 15th World Conference on Earthquake Engineering, Lisboa, Portugal September.

5th International Symposium on Dam Safety

October 27-31, 2018

SAFETY ASSESSMENT OF DAMS IN PAKISTAN: A CASE STUDY OF TARBELA DAM

Muhammad ZAİN[1], Muhammad USMAN[2], Khawar MUNİR[3], Zahid SHEHZAD[3], Talat IQBAL[4]

ABSTRACT

Safety assessments are essential elements that bolster the satisfactory performance of a dam. The safety does not only pertain to the structural safety against conventional loads, but its spectrum covers all aspects that can include the hydrology of a dam, performance of its instruments, conditions of the embankments, and its structural integrity against seismic excitations. The current paper presents the approach that has been employed for structural safety evaluations of dams in Pakistan for their behavior against conventional loading and the seismic excitations through a case study of Tarbela Dam, the largest earth-filled dam in the world. Thoroughly inspected structural components i.e. spillways, weirs, and powerhouse, with their contemporary issues are discussed, and recommendations are made to enhance the performance of the dam. An extensive evaluation is made to assess the performance of existing micro seismic monitoring system and the available earthquake data, and subsequently, with the prevailing information of associated seismicity, re-evaluation of seismic hazard is made. It is vehemently recommended that safety evaluations must be conducted several times during the life of dams to ensure their satisfactory performance as their unusual behavior may pose catastrophic repercussions.

Keywords: Earth-Filled Dams, Dam Safety Evaluations, Micro Seismic Monitoring System, Earthquake, Seismic Hazard Analysis.

INTRODUCTION

Safety is the fundamental element for any sort of infrastructure. For the safety of dams, an integral safety concept has been developed which is discretized into four elements i.e. structural safety, operational safety and maintenance, dam safety monitoring, and the emergency planning (Martin Wieland, 2016). The International Commission on Large Dams (ICOLD) has rendered dams higher than 15 m and/or those with storage capacity of more than 3 hm^3 as the large dams (ICOLD, 2003). ICOLD is the governing authority to establish design features of dams to effectively resist the loads. In this regard, ICOLD has established bulletins and guidelines in which Bulletin 112, 120, 123, 137, and 148 are primarily related to seismic aspects of dam design. Apart from the seismic actions, the dams have to deal with the accidents related to floods that are usually analyzed according to the storage capacity, a dam's height, spillway data, and the data pertaining to material of construction. Most of the flood related accidents that occurred have been reported for embankments capable of storing more than 10 hm^3 (F. Lemperieere, 2017).

[1] PhD Student, Department of Civil Engineering, National University of Sciences & Technology (NUST), Pakistan. e-posta: zainaltaf@hotmail.com
[2] Assistant Professor, Department of Civil Engineering, NUST, Pakistan
[3] Director, Water and Power Development Authority (WAPDA) of Pakistan
[4] Director, Centre for Earthquake Studies, National Centre for Physics, Pakistan

The ambit of research and field practice related to dam engineering covers several topics i.e. flood simulations, dam break analysis, seismic fragility assessments, etc. In this context, several researchers have published to demonstrate numerous techniques for assuring the safety of dams. For instance, Masoud and Aspasia (2018) evaluated nonlinear seismic response of a concrete dam by assuming a massless foundation; Jin-Ting and Chu (2018) performed seismic fragility of arch dams by considering aleatory and epistemic uncertainties; Luo et al. (2012) provided a review of dam-break research on earth-rock dams, and amalgamated it with dam safety management. Nevertheless, especially in developing countries, the dam safety management is abundantly lacking.

The current paper describes a case study of Tarbela Dam, which is the largest earth-filled dam in the world, and presents the findings, observations and recommendations pertaining to the Concrete Hydraulic Structures, along with the updated information about the prevailing seismicity in the Tarbela region and the north of Pakistan. Probabilistic Seismic Hazard Assessment (PSHA) has been conducted to evaluate the total hazard and to develop the updated seismic hazard curves with latest available information using the Micro Seismic Monitoring System (MSMS) at Tarbela.

OVERVIEW OF TARBELA DAM

Tarbela Dam is one of the world's largest earth and rock filled Dam that was planned and constructed under the Indus Basin Project as the greatest water resources development scheme. It had been accepted by The World Bank as an integral portion of Settlement (Replacement) plan under Indus water treaty in 1965. On behalf of Government of Pakistan, the Water And Power Development Authority (WAPDA) was entrusted with its execution. The construction of the dam was terminated in 1976. The Dam is located on the river Indus in District Sawabi of Khyber Pakhtunkhwa Province of Pakistan. Figure 1 shows an isometric view of the Tarbela Dam from satellite imagery, in which major components of the dam are identified.

The Main Dam, built of earth and rock-fill, stretches 2,743 meters (9000 ft.) from the island to the river towards right-side, and it is 143 meters (470 ft.) high with an inclined impervious earth core. A pair of auxiliary dams spans the river from the island to river left. Tarbela Dam Project is located 96.5 KMs (60 miles) North-West of Islamabad. The two spillways are located on the left bank on the auxiliary dams. The Service Spillway has a discharge capacity of 18,406 cumecs and the Auxiliary Spillway has a discharge capacity of 24,069 cumecs. Five tunnels were constructed as part of Tarbela Dam's outlet works. Presently, the Tarbela Dam Project has a maximum power generation capacity of 3,478 MW from turbines installed on tunnels 1 through 3, which were originally designed as power tunnels. For Power generation, the Units 1 to 4, each having generation capacity of 175 MW, are installed on Tunnel 1; Units 5 to 10, each having generation capacity of 175 MW, are installed at Tunnel 2, while Units 11 to 14, each with generation capacity of 432 MW, are installed at Tunnel 3. Tunnels 4 and 5 were designed for irrigation use. Both tunnels 4 and 5 are to be converted to hydropower tunnels to increase Tarbela's electricity-generating capacity.

Tunnels 1 and 2 were originally used to divert the Indus River while the dam was being constructed. Construction of a powerhouse (Tarbela 4th Extension) was in progress at the time of the inspection and is likely to be commissioned in late 2018. Under this extension, 3 units of 470 MW each (1,410 MW total) are being installed over Tunnel No. 4. After completion of the 4th Power Extension the generation capacity will increase to 4,888 MW.

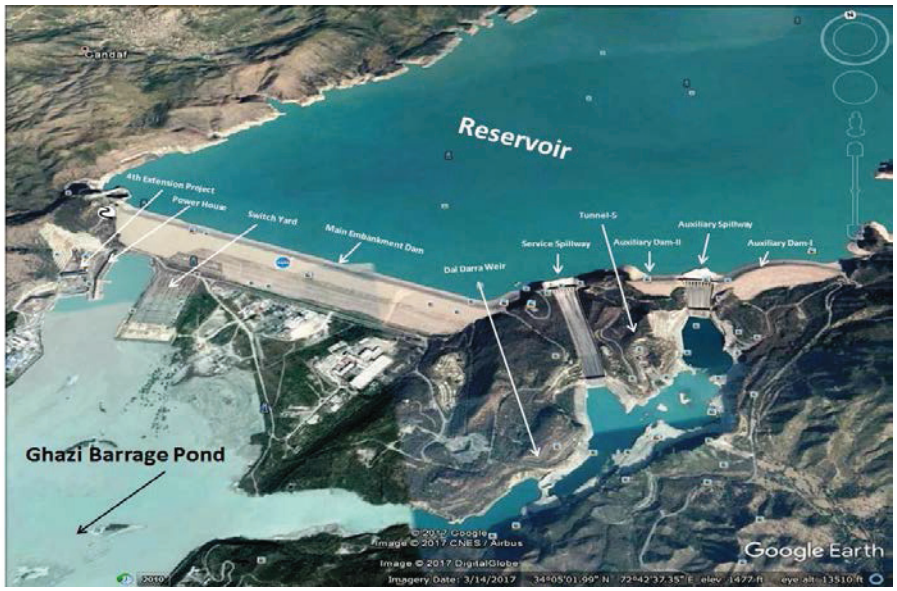

Figure 1. Satellite Image of Tarbela Dam Project from the Downstream Side showing the Salient Project Components

PHYSICAL INSPECTION OF TARBELA DAM COMPONENTS

From a dam's safety perspective, physical inspections must be carried out for embankments, instrumentation, concrete hydraulic structures i.e. spillways, weirs and powerhouse, and other appurtenant structures, and necessary actions must be taken in order to ensure the proper intended functioning of the dam. Furthermore, safety evaluations and inspections must be made numerous times during the life span of a large dam. This paper also presents the findings of physical inspection conducted at main and auxiliary spillways, Dal Darra Weir and the powerhouse, and provides essential recommendations to cope with their ongoing problems as well.

Physical Inspection of Service (Main) Spillway

The Service Spillway of Tarbela Dam is actually the main spillway and has total capacity of 18,406 cumecs (650,000 cusecs). During the time of inspection, the approach slab of the service (main) spillway was visible due to low-flow season. Figure 1 shows its precise location on the dam. At the time of inspection, the approach slab was visible and it was found in adequate condition. The spillway service bridge was also inspected from the underside. Figure 2 manifests the view of spillway service bridge from the underside. The cracking observed in the capitals of the piers and in the piers at mid-height is most likely due to Alkali-Aggregate Reaction.

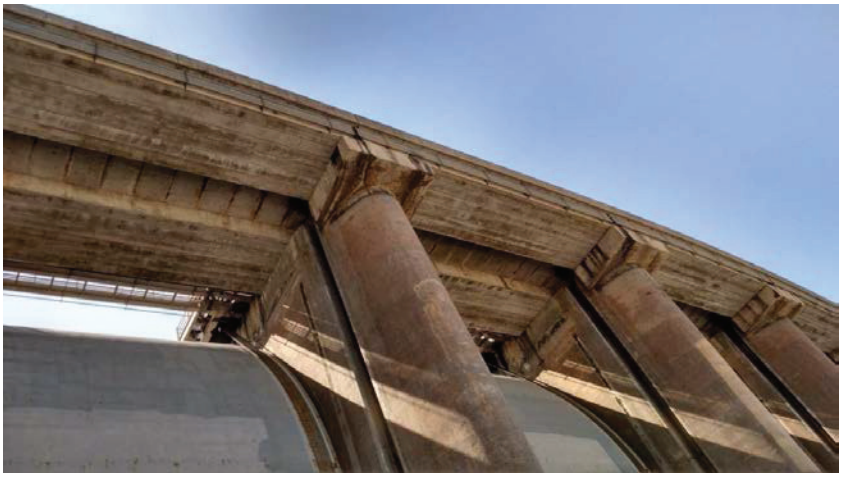

Figure 2. Service Spillway – View of the Spillway Service Bridge from underside

Settlement survey was conducted using the survey markers, installed in the bridge deck of Service Spillway. The plot of settlement of survey markers is shown in figure 3.

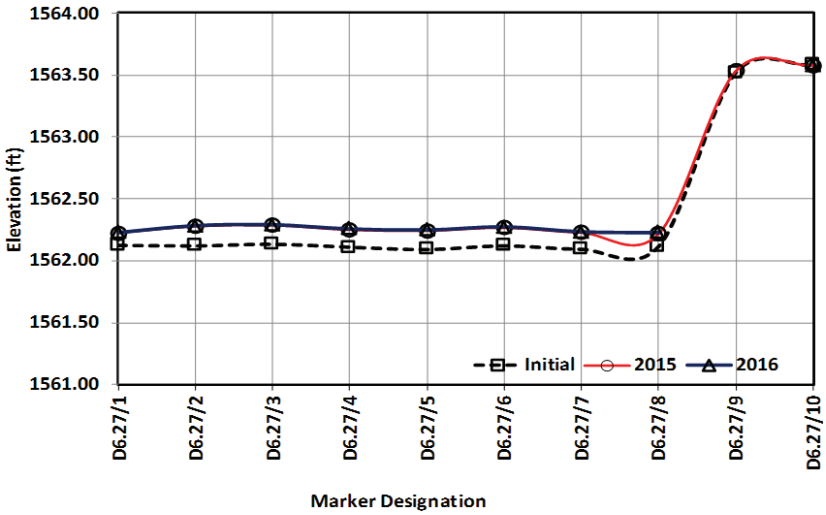

Figure 3. Service Spillway –Settlement of Survey Markers installed in the Spillway Bridge Deck

Examination of the data reveals that the Service Spillway had grown in height by about 0.15 ft. (1.8 inches or 45mm). This gain in height of the Service Spillway Piers was significant and was not because of any rock rebound as both the spillways were constructed on top of natural rock formation. The amount of rock removed for construction of the spillways was not much and therefore rock rebound was unlikely; rather, this increase in height of the Service Spillway was in all likelihood because of Alkali-Aggregate Reaction associated growth of concrete in the spillway. The most common type of Alkali-Aggregate Reaction (AAR) is Alkali-Silica Reaction, in which the alkaline cement paste and the silica bearing reactive aggregates react under favourable moisture and temperature conditions to form sodium silicate gel at cement-aggregate interfaces, causing swelling/growth of concrete. As the reaction continues over years, the hydropower structures such as dams and powerhouses exhibit increase in height and other associated deformations.

Physical Inspection of Auxiliary Spillway

The Auxiliary Spillway has total capacity of 24,069 cumecs (850,000 cusecs), and it is frequently used to spill the water in high-flow seasons in place of the Service Spillway. It was inspected from the upstream and downstream sides. There were signs of excessive leakage of grease from the wheels on some spillway gates and the staining of the piers by grease could be seen. Figure 4 presents the pier of gate No. 5, which is heavily stained by leakage of grease.

Figure 4. Significant leakage of grease from the gate wheels

At the downstream side of service spillway, the erosion of the both banks of the channel downstream of the plunge pool could be clearly observed. The remnants of the downstream weir, initially utilized during the construction process, were acting as a spur deflecting the water towards the left-bank and causing erosion. The left bank at this location consists of conglomerate of small to medium sized stones in clay matrix, which is susceptible to erosion, and further erosion is expected as a result. Figure 5 (a) provides a bigger view, while figure 5 (b) is a closer look to erosion of slope on left-bank downstream of the plunge pool.

(a) **(b)**

Figure 5. Erosion of slope on the Left-bank downstream of the Plunge Pool

A settlement survey was also conducted for auxiliary spillway with the help of survey markers installed in the spillway bridge deck. Figure 7 illustrates the plot of settlement survey conducted for auxiliary spillway.

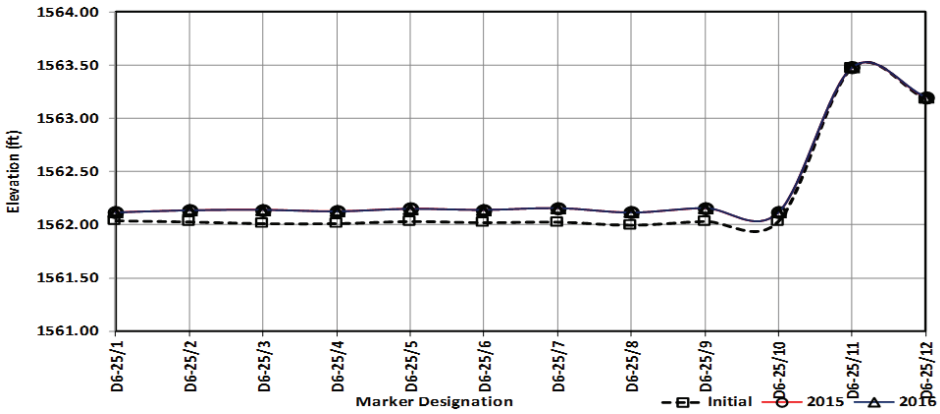

Figure 7. Settlement of Survey Markers Installed in the Spillway Bridge Deck

Examination of the data shows that the Auxiliary Spillway has grown in height by about 0.12 ft. (1.5 inches or 37 mm) since the initial survey. Similar to Main Spillway, the gain in height of the Auxiliary Spillway Piers was amply significant, and analogously, Alkali-Aggregate Reaction was seemed to be responsible for this.

Physical Inspection of Powerhouse

The powerhouse was thoroughly inspected for the cracks developed. The problems pertaining to tunnel no. 3 and the respective installed power generating units upon it i.e. Units 11 to 14, have also been discussed in this study. During the inspection, the draft tube of Unit no. 11 was inspected. The steel liner of the draft tube seemed to be progressively attaining damaged and was subsequently found dislodged from the concrete substrata. The vibration levels in the Units 11 to 14 of the Tarbela powerhouse are high. This could be due to sub-optimal performance of the turbine runners. The

possibility of cavitation in the draft tubes of Units 11-14 cannot be ruled out, rather it is quite likely the cause of damage to the steel liner.

During the inspection of the powerhouse building, the cracks were present in the downstream gallery floor. Some cracks were also present around the column perimeter in the floor but the cause of these cracks could not be ascertained, however, those cracks did not seem to be posing a safety concern contemporarily.

Figure 8 depicts cracks observed in the turbine pit of Unit 14 of the powerhouse. Glass strip tell-tales had been installed over these cracks and some were found broken. The ambient vibration levels in powerhouse-3 (Units 11 to 14) are abnormally high. The cracks in these units at the turbine floor level were most likely due to fatigue associated cracking because of high vibration levels.

Figure 8. Cracks in the Turbine Pit of Unit-14

Horizontal cracks in the downstream walls of Units 11-14 gallery at a certain elevation were observed (figure 9). The cracks were regularly spaced, pervasive, and were extended to the entire width of the unit bays. Such cracks were clearly flexural, induced by tilting of the downstream wall in the downstream direction. The cause of such tilting could not be understood. Possibility exists that the tilting of the downstream wall was due to Alkali-Aggregate Reaction associated deformations.

Figure 9. Horizontal cracks in Downstream Wall

Physical Inspection of Dal Darra Weir

The Dal Darra Weir is a massive ungated weir structure located in the channel downstream of the two spillways and Tunnel 5. The weir serves to provide impoundment of water for controlling the tail

water levels in the plunge pools of the Service and the Auxiliary Spillways and Tunnel 5. Figure 10 is a panoramic view of the Dal Darra Weir from the upstream side.

Figure 10. Panoramic view of Dal Darra Weir from Upstream Side

The weir structure appeared to be in generally fair condition. Abrasion of the Weir Crest and downstream of the crest was visible because of debris laden flows. Deficient hydraulic design of the vertical weir was resulting in inadequate energy dissipation and concrete erosion under the falling jet. Some joints among concrete panels were widely opened in the weir crest as presented in figure 11.

Figure 11. Erosion and Opeing of Concrete Panels at Dal Darra Weir

PROBABILISTIC SEISMIC HAZARD ANALYSIS OF TARBELA DAM

The seismically active nature of Pakistan and its adjacent region is well known because of the occurrence of some of the biggest earthquakes of the world. These include the 1819 Kutch earthquake, the 1931 Mach and the 1935 Quetta earthquakes, and the 1945 Makran earthquake. But none was as destructive as the October 8, 2005 Muzaffarabad-Kashmir earthquake of 7.6 Mw. At Tarbela Dam, a Micro Seismic Monitoring System (MSMS) was established near the completion of construction in 1973 and operated by Lamont-Doherty Geological Observatory (LDGO) of Columbia University, USA. The purpose of the network is to monitor any seismicity induced due to reservoir filling and to determine the active seismic sources which could affect Tarbela dam project.

As such the objective of the MSMS is to record the occurrence of earthquakes in time and space. The recorded waveform data is analyzed to access source and spectral parameters. The distribution of the earthquake epicenters is used to identify active geological structures, and together with the magnitude of each event, they can contribute to assess the seismic hazard.

The seismic design of Tarbela dam and its various structures was carried out in mid-sixties in accordance with the engineering practices prevailing at that time. Based on the identification of Darband fault crossing the dam during construction of dam and subsequent monitoring of seismicity by Tarbela seismic network, a re-evaluation of seismic design parameters in seventies and early eighties by leading experts of TAMS Consultants was made on the basis of available data. However, in the absence of any specific neo-tectonic study, several assumptions were made regarding seismic potential of the faults affecting the project.

The Tarbela microseismic network is continuously monitoring seismicity of Tarbela region since 1973. During this period, it passed through different phases of deterioration and upgradation at different times. Since 2010, an upgraded network is available with real time satellite communication and is expanded to cover the seismically active northern areas of Pakistan where a number of dam projects are being planned by WAPDA.

Existing Micro Seismic Monitoring System (MSMS)

The existing WAPDA Micro Seismic Monitoring System (MSMS) with its Central Recording Station (CRS) at Tarbela dam project is in operation since 2010. It consists of 29 seismic stations installed around Tarbela dam and various critical locations in northern Pakistan. These stations are transmitting real time data to Central Recording Station (CRS) Tarbela, through satellite link. At the CRS, online/offline processing, analysis and cataloguing of seismic data, covering an area of 450 km radius around Tarbela, is done through latest state of the art software ANTELOPE. The analysis of observed seismicity is done in two parts i.e. one for events located in 80 km radius of Tarbela dam, and other beyond the 80 km radius of Tarbela dam. Moreover, analysis of seismicity around Dasu, Bunji and Diamer-Basha, proposed Projects of WAPDA, is also conducted at Tarbela CRS.

Statistics of Recorded Earthquakes

The data recorded by Tarbela seismic network was collected from seismicity reports issued yearly by Tarbela Dam, WAPDA. The number of earthquakes recorded during each year along with data of energy release and number of earthquakes related to tectonic sources of the region are given in Table 1 for years 2006 to 2016.

Table 1. Seismicity of Tarbela Region (80 Km Radius of Tarbela) - Last Eleven Years

Year	NO. of Earthquakes	Total Energy Release (In Ergs)	No. of Earthquakes					
			Darband Fault	Panjal Fault	Hazara Thrust	MMT	IKSZ	Other Faults
2006	927	$0.134X10^{21}$	20	16	12	59	455	365
2007	324	$0.320X10^{20}$	13	9	9	43	80	170
2008	296	$0.203X10^{20}$	13	9	14	24	76	160
2009	184	$0.621X10^{20}$	14	8	3	27	15	117
2010	225	$0.349X10^{18}$	33	23	12	5	42	110
2011	140	$0.148X10^{18}$	23	17	14	1	29	56
2012	105	$0.155X10^{18}$	9	8	6	0	74	8
2013	41	$0.129X10^{18}$	6	1	3	0	28	3
2014	93	$0.320X10^{18}$	5	1	10	0	67	10
2015	226	$0.638X10^{19}$	42	9	20	0	110	45
2016	153	$0.476X10^{18}$	35	13	11	0	70	24
TOTAL	**2714**	$0.2566X10^{21}$	**213**	**114**	**114**	**159**	**1046**	**1068**
			17.60%	4.23%	4.23%	5.90%	38.82%	39.64%

In the above table, the number of recorded earthquakes does not necessarily reflect decrease or increase in seismicity of the region as the number of recorded earthquakes also depends upon the health and performance of the network during that period.

Analysis of Earthquake Data

The seismicity of the northern part of Pakistan after the 2005 devastating earthquake, which was the worst damaging earthquake in this region, as recorded by Tarbela microseismic network, was analysed. Figure 12 shows the plot of seismicity of all magnitudes recorded by Tarbela network between the periods from 2006 to 2016. Separate symbols are shown for earthquakes with magnitude less than 3 and greater than 3. Earthquakes with magnitude greater than 6 are shown by a star.

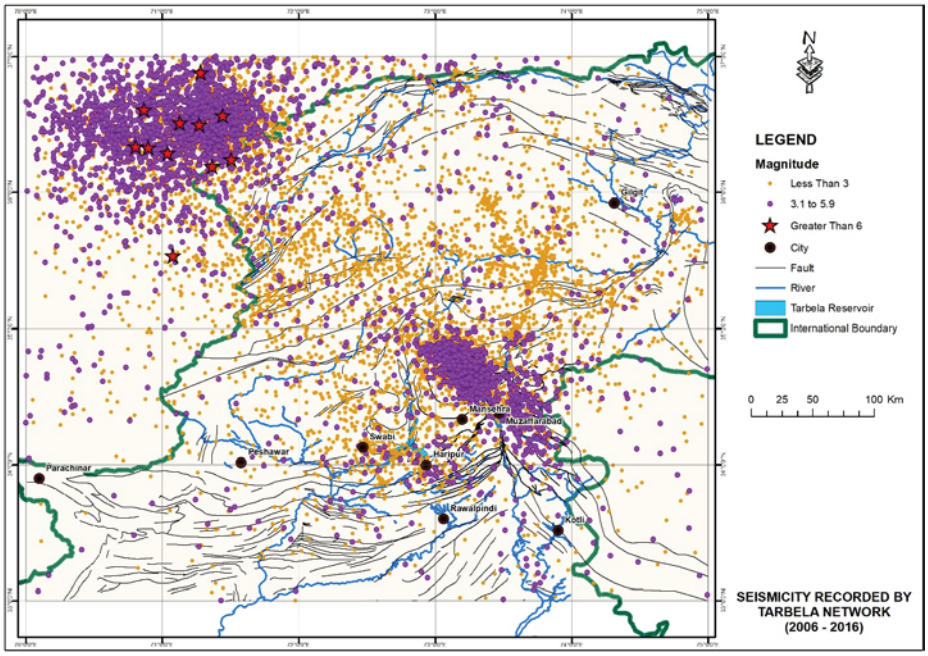

Figure 12. Seismicity Recorded by Tarbela Seismic Network - Period 2006 to 2016

During the period 2006 to 2016, a large number of earthquakes of magnitude less than 3 and of magnitude 3.1 to 5.9 have been recorded in northern Pakistan and Hindukush region. Earthquakes with magnitude greater than 6 have however been recorded in Hindukush region in Afghanistan only. Epicentral distribution of the earthquakes shown in figure 12 indicates that all of them are not associated with surface tectonic features, but appear to be randomly distributed (MonaLisa et al., 2007). This leads to the inference that besides the active surface faults, active blind faults also exist in the region. In some cases, the epicentres occur in clusters along the local tectonic features.

Apart from concentration of earthquakes in highly active Hindukush seismic zone, another concentration of earthquake, northeast of Tarbela, has also been observed which is related to Indus Kohistan Seismic Zone (IKSZ). The recorded seismicity during the last eleven years clearly demonstrates that Tarbela region and northern regions of Pakistan fall in seismically active regions.

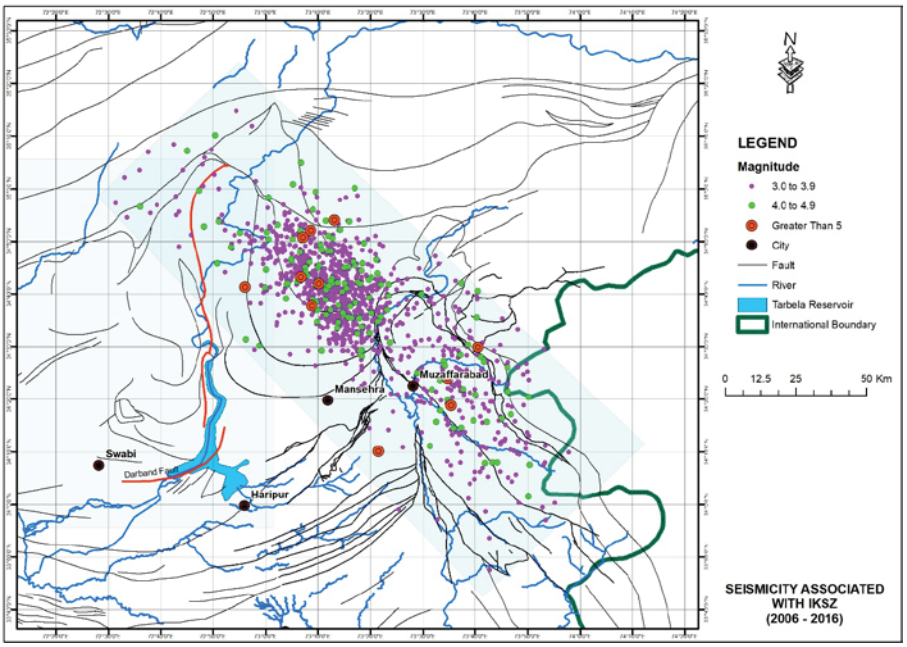

Figure 13. Seismicity Associated with Indus Kohistan Seismic Zone (IKSZ) - 2006 to 2016

Figure 13 shows a plot of seismicity of IKSZ recorded between the periods from 2006 to 2016. Recent studies by various authors indicate that the Mw 7.6 Muzaffarabad-Kashmir earthquake of October 08, 2005 was associated with the IKSZ and it occurred in a high-seismicity region. The main shock originated 90 km NE off Tarbela Dam, whereas, aftershocks primarily concentrated between the Main Mantle Thrust (MMT) and the Hindu Kush (HKS) region. Apart from being the most devastating earthquake, the Muzaffarabad-Kashmir earthquake also produced largest number of landslides locally. Locations and distribution of aftershocks in the zone indicate that the earthquake re-activated the Balakot-Bagh reverse fault and, locally, offset the Main Boundary thrust (MBT).

Revaluation of Seismic Hazard

The design of Tarbela dam project was carried out in middle sixties in accordance with the engineering practice prevailing at that time. After the knowledge of presence of active Darband fault passing below the dam, the seismic parameters were re-evaluated by leading experts in seventies on the basis of available seismotectonic information. The design of Tarbela dam project was reviewed for MCE associated with Darband and Panjal faults of 0.65-0.50g and 100-year earthquake of 0.40g. During nineties, seismotectonic studies of the project was carried out by National Engineering Services Pakistan (NESPAK) which recommended MCE ground motion of 0.52g (50 percentile) and OBE ground motion of 0.21g.

Presently, a re-evaluation of seismic hazard was carried out using probabilistic seismic hazard analysis. For a composite list of seismicity data of northern part of Pakistan recorded by the regional and local networks from 1961 up to December 2016 was compiled. The region was divided into seismic area source zones having similar tectonic and seismic characteristics. All the seismic area source zones show seismicity related to shallow crustal earthquakes except Hindukush seismic area source zone which shows deep subduction zone earthquakes. Magnitude-frequency relations and other parameters required for PSHA for each seismic area source zone were derived from the seismicity data. The results of PSHA in form of total hazard curve is shown in figure 14 (Tarbela 6th Periodic Inspection, 2018).

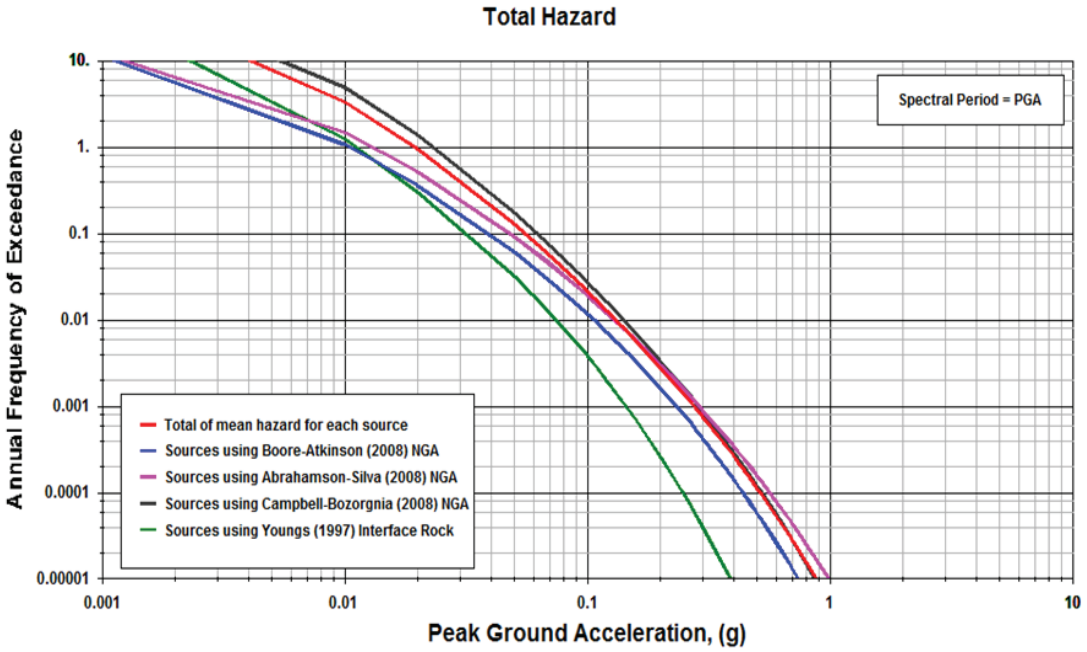

Figure 14. Total Hazard Curve for Tarbela Dam Based on Results of PSHA

For the shallow crustal seismic sources, three NGA attenuation equations (2008) developed by PEER for shallow crustal earthquakes were used. For the Hindukush deep seismic zone, Young et al. (1997) equation was used. PSHA was carried out using EZ-FRISK software, developed by Fugro Inc. USA.

As per ICOLD Guidelines, for selecting seismic parameters for large dams (Bulletin 148, 2016), Safety Evaluation Earthquake (SEE) have a return period of 10,000 years. Based on the results of PSHA given in figure 14, the Peak Horizontal Ground Acceleration associated with SSE is 0.52g. This value is close to the seismic design parameters associated with MCE given in NESPAK Report.

CONCLUSION AND RECOMMENDATIONS

Safety inspection and assessment of dams have been a complicated business for developing countries like Pakistan. The current paper presents a case study of Tarbela Dam in Pakistan to elaborate how safety inspections are conducted and what components are usually considered during the safety inspections, and discusses how the seismic hazards are assessed in Pakistan. During inspection, Main Spillway, Auxiliary Spillway, powerhouse, and appurtenant structures were inspected to explore their problems and to assess any arising structural menace from them. Examination of data showed that Main Spillway and Auxiliary Spillway grew in heights by about 45 mm and 37 mm respectively. This growth seems to be attributed to AAR instead of any rock rebound. Four (4 No.) cores may be taken from the piers of the Spillways for petrographic examination and confirmation of AAR activity. Cores can be extracted from the piers at a location above the weir crest in low flow/drawdown conditions.

In the powerhouse, the steel liner of draft tube of Unit No. 11 seemed to be getting damaged progressively. Draft tube flow conditions were particularly violent due to cavitating vortexes across much of the operating head range. The basic problem with the units is the head chosen for best efficiency. Tarbela has a very large operating range and requires a turbine with the point of best efficiency close to maximum head and output. Replacement of the runners by modern engineered runners, designed for the proper head for best efficiency, would provide significant mitigation against future damage. However, lining of the draft tubes must be kept repaired for ample functioning.

The concrete surfaces of the Dal Darra weir show signs of erosion and abrasion damage, accumulated over time due to passage of debris laden flows. While no immediate repairs were required, the Dal Darra weir should be inspected every year and repairs be carried out if the recorded condition of the

weir worsens. At some locations, the joints between the slabs of the weir crest found opened due to erosion damage. Such damages will require to be repaired in near future.

The existing digital seismic network consisting of microseismic stations and accelerographs, installed in 2010 at Tarbela, is presently in excellent working condition and provides real time seismic data with better accuracy due to more number of stations available for processing of earthquake parameters. Analyses/studies of seismic data collected through MSMS of 29 field stations located around Tarbela and critical faults of Northern Pakistan reveal that region is seismically active. Stresses have been accumulating and earthquake energy may be released in the form of large earthquakes in future. Therefore, it is recommended that seismic monitoring of the 29 stations of MSMS be continued for indefinite period. As specified, the PGA associated with SSE is 0.52g. While this value is close to the seismic design parameters assessed in November 1991, it can be conveniently inferred with the analysis of updated seismic data that there is no significant change in seismic hazard.

The seismic safety aspect of existing dams is an imperative issue to deal with, as mostly the contemporary guidelines are targeted for the design of new dams. The design which might have considered safe previously may not considered to be safe forever. Therefore, seismic safety of existing dams must be reassessed using current standards. As an essential requirement, the prevailing seismic hazard at dam sites must be reviewed for compliance with the prevailing design criterions.

AKNOWLEDGEMENTS

This study was sponsored by Water and Power Development Authority (WAPDA), Pakistan, and the cooperation extended by the Tarbela Dam Monitoring Office is highly appreciated and acknowledged.

REFERENCES

Dams Safety Organization, 2018. “Report on Sixth Periodic Inspection – Tarbela Dam Project”. Water and Power Development Authority (WAPDA), Pakistan.

ICOLD, 2003. “World register of dams”. International Commission on Large Dams, Paris.

ICOLD, 1998. “Bulletin 112: Neotectonics and Dams”. Committee on Seismic Aspects of Dam Design, International Commission on Large Dams, Paris.

ICOLD, 2001. “Bulletin 120: Design features of Dams to Effectively Resist Seismic Ground Motion”. Committee on Seismic Aspect of Dam Design, International Commission on Large Dams, Paris.

ICOLD, 2002. “Bulletin 123: Earthquake Design and Evaluation of Structures Appurtenant to Dams”. Committee on Seismic Aspects of Dam Design, International Commission on Large Dams, Paris.

ICOLD, 2011. “Bulletin 137: Reservoirs and Seismicity — State of Knowledge”. Committee on Seismic Aspects of Dam Design, International Commission on Large Dams, Paris.

ICOLD, 2016. “Bulletin 148: Selecting Seismic Parameters for Large Dams, Guidelines”. Committee on Seismic Aspects of Dam Design, International Commission on Large Dams, Paris.

Lemperiere, 2017. “Dams and Floods”. Journal of Engineering, vol. 3, pp. 144-149.

Luo You, Chen Li, Xu Min, Tong Xiaolei, 2012. “Review of Dam-break Research of Earth-rock Dam Combining with Dam Safety Management”. Procedia Engineering, vol. 28, pp. 382-388.

MonaLisa, Khawaja A., Jan Q, 2007. “Seismic Hazard Assessment of the NW Himalayan Fold-and-thrust belt, Pakistan, using probabilistic approach”. Jrnl. of Earthquake Engg, vol. 11, pp. 257-301.

NESPAK 1991. “Seismotectonic Studies-Tarbela Dam”. National Engineering Services of Pakistan.

Poul and Zerva, 2018. “Nonlinear dynamic response of concrete gravity dams considering the deconvolution process”. Soil Dynamics and Earthquake Engineering, vol. 109, pp. 324-338.

Wang JT and Zhang CH, 2018. “Seismic fragility of arch dams based on damage analysis”. Soil Dynamics and Earthquake Engineering, vol. 109, pp. 58-68.

Wieland, 2016. “Safety Aspects of Sustainable Storage Dams and Earthquake Safety of Existing Dams” Journal of Engineering, vol. 2, issue 3, pp. 325-331.

Youngs, R. R., S. J. Chiou, W. J. Silva, and J. R. Humphrey, 1997. “Strong Ground Motion Attenuation Relationships for Subduction Zone Earthquakes”. Seism. Res. Lett. 68, 58–73.

5th International Symposium on Dam Safety

October 27-31, 2018

DAM EXPERT PANEL IN THE FRAMEWORK OF DAM SAFETY MANAGEMENT OF BENER DAM, INDONESIA

Cristina D. YULINING, Tyasamos SANGKA[2]

ABSTRACT

Bener Dam is the highest concrete face rock fill dam in Indonesia with 159 m height (from plinth) and 169 m from the deepest foundation with 712.13 m length and has 90.4 million m^3 total storage on flood water level.

In order to manage Bener Dam safety, dam safety evaluation is still needed to be done by dam expert panel activity which is planned to be done at the beginning of construction. This activity refers to the Minister Regulation of Public Works and Housing No. 27/2015 on Dam that for dams with height of 75 m or more from river base need expert technical advice beyond the advice from Dam Safety Commission.

The important notes to be followed up on the activities of the Dam Experts Panel have been agreed between the stakeholders and the Dam Safety Commission as recommender that the design of the Bener Dam can be constructed.

Keywords: Bener Dam, CFRD, Dam Expert Panel

INTRODUCTION

Bener Dam is a Concrete Face Rock Fill Dam with 159 m height from plinth and 169 m from the deepest foundation with 712.13 m length and has a total storage of 90.4 million m^3 at flood water level.

Spillway is designed as side spillway, located on the left bank with a 90 m long and USBR Type II stilling basin. The diversion channel is designed as circular tunnel with Φ7 m, 763.85 m long and at the Q_{25} design flood elevation. The intake structure is designed as tower (shaft) with 114 m height and very high / extreme hazard level classification. Figure 1 shows the location of the dam.

The purposes of Bener Dam are:
- Irrigation of 1,940 Ha (new) and 15,519 Ha existing.
- Water supply of 1,500 l/s
- Hydro Power Plant of 6 MW

[1] Dam Engineer, Serayu Opak River Basin Unit, Ministry of Public Works and Housing, Indonesia.
e-posta: cristinadwi87@gmail.com
[2] General Manager of Dam Construction, Serayu Opak River Basin Unit, Ministry of Public Works and Housing, Indonesia.
e-posta: bajul.mati@yahoo.com

Figure 1. Location of the Bener Dam

DETAIL DESIGN CRITERIA

General

Dam type was chosen based on topographic, geological and availability of embankment material around the dam location (Figure 2). Based on these considerations, the Bener Dam is designed concrete face rockfill dam (CFRD).

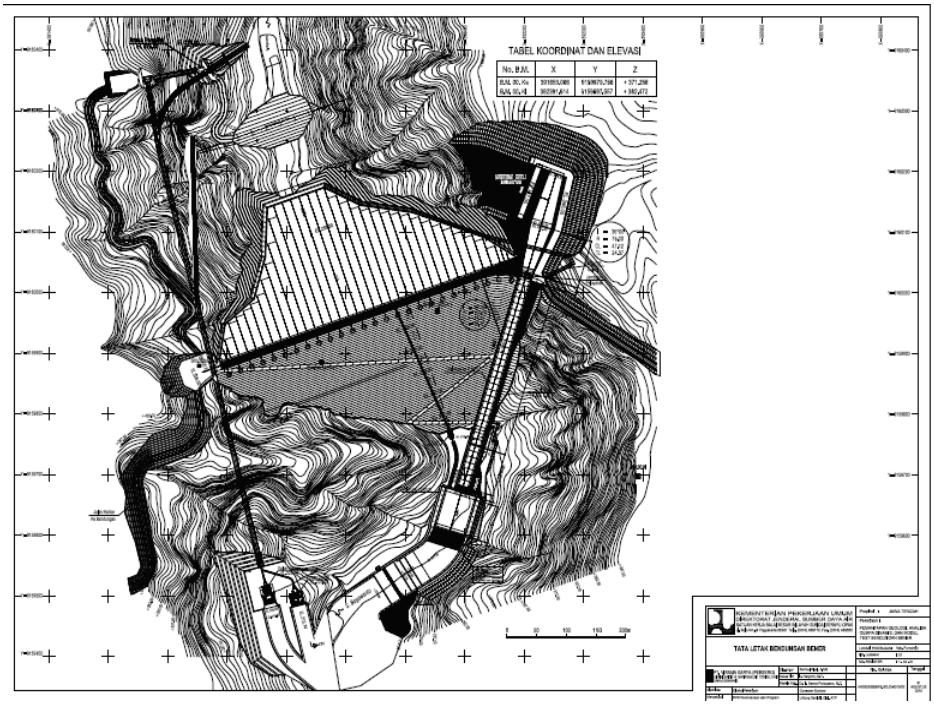

Figure 2. Bener Dam Layout

Dam Zoning

The principle of this dam is material availability from quarry. Zoning is divided based on material sources and requirements, including shear strength, permeability, and compressibility by considering efficiency and economic aspects. Cross section of the dam is given in Figure 3.

Bener Dam zoning design as follows:

Zone 1 Upstream Counterweight
- 1A : silt or fine – coarse non cohessive material < 150 mm,
- 1B : random fine – coarse material

Zone 2 Filter
- 2A fine filter
- 2 B coarse filter (3 m width)

3A as transition

Rockfill embankment zone
- 3B
- 3C

3D : rip rap

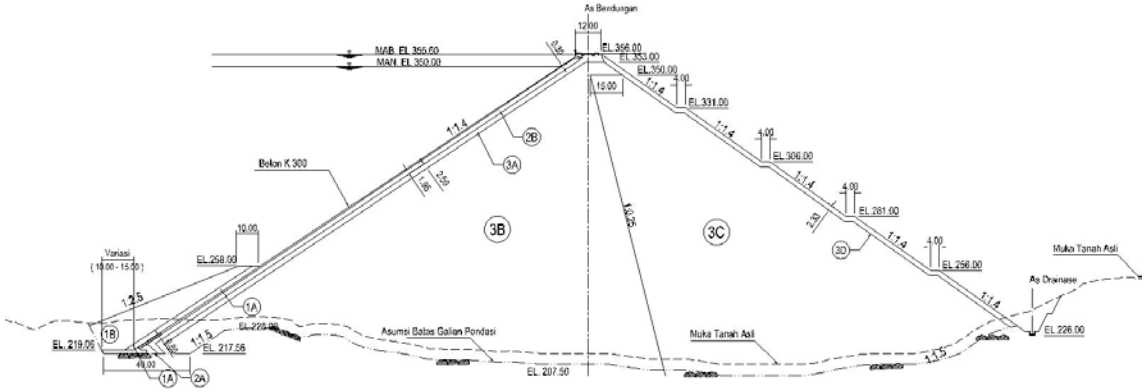

Figure 3. Cross Section of Bener Dam

Plinth

The plinth structure connects the foundation with the slab which are functioned as impermeable layer between the slab and the foundation, grout cap, and initial position of slab slipform equipment (Figure 4).

Determination of the width and thickness of the plinth was based on the hydraulic gradient in the table of Guidelines for Design and Construction of Concrete Face Rockfill Dam where the value taken for the Bener Dam is 20 so that the plinth length is 8.0 m and 1.0 m thickness with K-300 concrete quality.

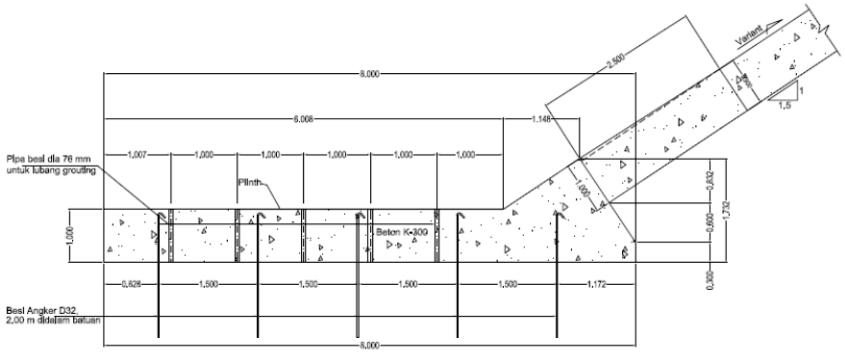

Figure 4. Plinth

Slab

The slab is an impermeable layer on upstream. The determination of the slab segment is based on the body deformation estimation of the dam and construction conditions. The Bener Dam is designed

with 15 m segment width where the distance between vertical joint is usually between 12 ~ 18 m (Figure 5). Thickness of slab designed conservatively with thickness from bottom to top is 1.0 m - 0.5 m with K-250 concrete quality.

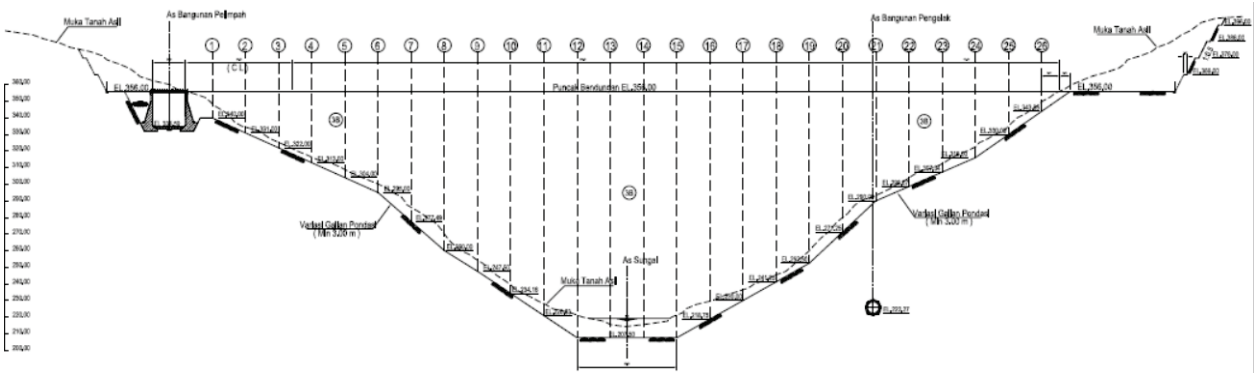

Figure 5. Slab Segment

Spillway

The spillway is designed as side spillway type without gate (overflow) located on the left bank with 90 m long and 113 m long of USBR type II stilling basin where dimensions and types are made followed the results of hydraulic model test. Spillway section is seen in Figure 6.

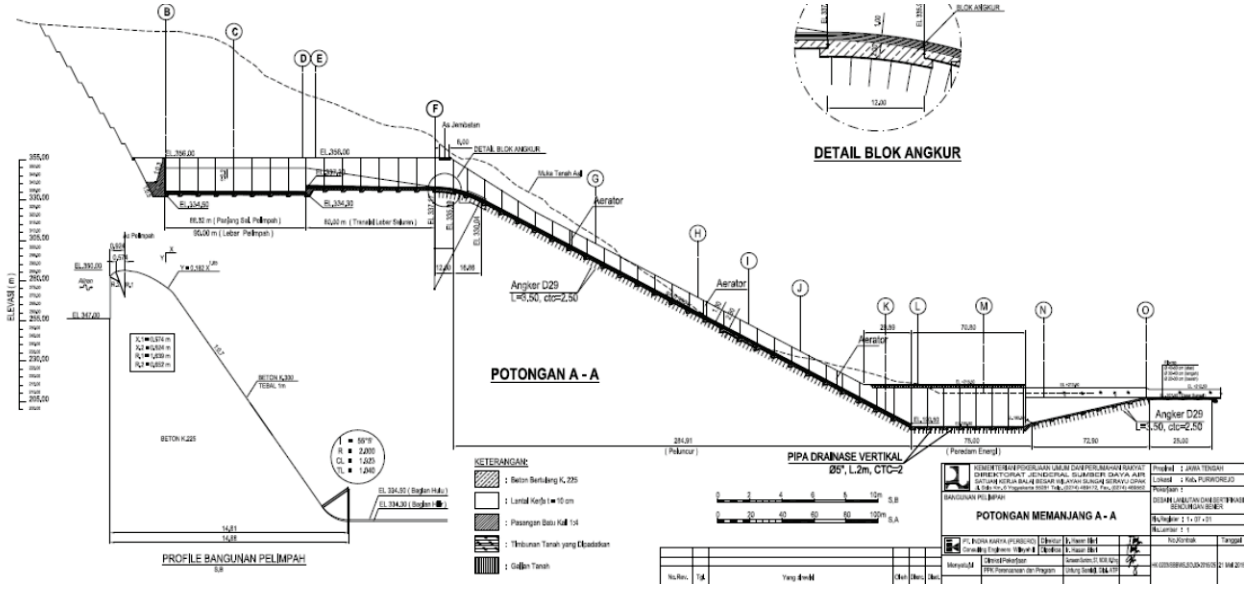

Figure 6. Spillway

Intake

Intake is designed to secure the work site especially the dam body against the Bogowonto river flow when constructed. This intake system consists of cofferdam in the upstream and downstream side of the main dam and diversion channel. Due to dam site topography as narrow river valley, the diversion channel is designed with tunnel of Q_{25} design capacity.

The waterway was planned to diameter 1.4 m from 7.0 m in the downstream section for the purposes of water supply, irrigation, and hydropower whose output will be adjusted to the emergency release opening as seen in Figure 7.

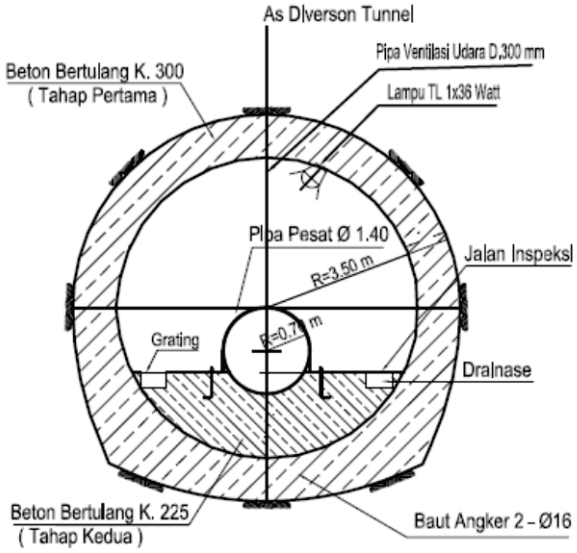

Figure 7. Diameter 7.0 m of Tunnel to 1.4 m of Waterway

DESIGN OPTIMIZATION

Design optimization is carried out in order to manage the dam security more efficiently and effectively. For Bener Dam, the criteria of "Ministry of Public Works and Housing Regulation no. 27/2015 of Dams article no.150 concerning of Dam Panel Expert" must be fulfilled by appointing Dam Panel Expert team, where according to the results of the previous discussion either in the technical meeting or the plenary session of the Dam Safety Commission it is necessary to study in depth, namely:

Bottom Outlet

The proposed structure is intended to empty the reservoir where from the inlet to the deepest reservoir is still about 40 m below.

Gallery on half sides (under plinth on the riverbed until the left side)

This gallery structure was recommended to monitor the possibility of seepage flowing through the slab / plinth.

Zone of 1A and 1B

Based on the guidelines for design and construction of CFRD, it is known that this zone serves to fill cracks that maybe occur at concrete membranes when initial filling. But in the discussion that has been carried out there is a plan to replace this zone with geotextile if the function is as an impermeable zone which the use is in the outer zone of the dam so that if necessary to replace it won't make much failure potential to increase damage to the concrete membrane.

CONCLUSION

Based on the results of the detailed design discussion was carried out that the design of the Dam was recommended for the construction implementation. The important note to be carried out is the activity of the Dam Panel Expert in the early stages of the construction, especially when the excavation of the dam foundation is carried out with the main topics given in the design optimizations.

AKNOWLEDGEMENTS

The authors would like to thank to Dam Safety Unit and Serayu Opak River Basin Unit, Directorate General of Water Resources, Ministry of Public Works and Housing for the authorization to publish the main result of the present study.

REFERENCES

Ministry of Public Works and Housing Regulation no. 27/2015 of Dams.

Ministry of Public Works, 2011. "Guidelines for Design and Construction of CFRD".

Yulinintyas, C. D., 2018. "Dam Safety Management of Bener Dam Design". Paper on Inacold Symposium.

Virama Karya. Ltd and Indra Karya, Ltd, 2015. "Final Report of Bener Dam Design and Certification".

Virama Karya. Ltd and Indra Karya, Ltd, 2015. "Design Drawing of Bener Dam Design and Certification".

5th International Symposium on Dam Safety

October 27-31, 2018

STRUCTURAL BEHAVIOR OF CONCRETE GRAVITY DAMS USING WESTERGAARD, LAGRANGE AND EULER APPROACHES

Ahmet Can ALTUNIŞIK [1], Hasan SESLİ [2], Metin HÜSEM [3], Ebru KALKAN [4]

ABSTRACT

Dams are engineering structures with tasks such as water storage, irrigation, drinking water supply. The earthquake behavior of these constructions is very important for life and property losses. The actual effect of hydrodynamic pressures and water on dams should be reflected more accurately in structural analyzes. In this study, it was aimed to determine the dynamic response of concrete gravity dams using different water modeling approaches such as Westergaard, Lagrange and Euler to calculate the effect of water hydrodynamic pressure on the dam body. Sarıyar Concrete Gravity Dam on the Sakarya River in the northern part of Ankara was chosen as a case study. The finite element model of the dam was constructed by considering the dam-reservoir-foundation interaction using ANSYS software. Linear time history analyzes were carried out using 1992 Erzincan earthquake ground motion recording to determine the structural response of the dam. At the end of the analyzes, dynamic properties, maximum displacements, maximum minimum principal stresses and maximum minimum principal strains were obtained and compared for Westergaard, Lagrange and Euler approaches.

Keywords: Dam-reservoir-foundation interaction, dynamic characteristics, gravity dam

INTRODUCTION

Dams have contributed to the development of civilization for a long time. They will continue to keep their importance in satisfying the ever increasing demand for power, irrigation and drinking water, the protection of man, property and environments from catastrophic floods, and in regulating the flow of rivers (Akköse and Şimşek, 2010). Several factors, which affect the dynamic response during earthquake, can be remarked such as interaction of dam-reservoir interaction and consistencies of the hydrodynamic pressures on dam body. Beside these parameters, hydrodynamic pressures acting on dam faces is one of the most important and influential. So, the calculation of this parameter is very important especially during dynamic loads such as earthquake.

Some papers can be obtained in literature about the static and dynamic behavior of dams considering dam-reservoir-foundation interaction using different water modelling approaches. Westergaard (1933) carried out the first hydrodynamic analysis on the dam-reservoir system. Samii and Lotfi (2007)

[1] Professor, Department of Civil Engineering, Karadeniz Technical University, Trabzon, Turkey, e-posta: ahmetcan8284@hotmail.com
[2] Professor, Department of Civil Engineering, Karadeniz Technical University, Trabzon, Turkey, e-posta: sesli@ktu.edu.tr
[3] Professor, Department of Civil Engineering, Karadeniz Technical University, Trabzon, Turkey, e-posta: mhusem@ktu.edu.tr
[4] Professor, Department of Civil Engineering, Karadeniz Technical University, Trabzon, Turkey, e-posta: ebrukalkan@ktu.edu.tr

performed a study about the comparison of coupled and decoupled modal approaches in seismic analysis for concrete gravity dams. Fathi and Lotfi (2008) investigated the effects of reservoir length on the dynamic analysis of concrete gravity dams. In the analysis, the reservoir is considered by a combination of fluid finite elements and two-dimensional fluid hyper-elements. Bayraktar et al. (2009, 2010) aimed to determine the reservoir length effect on seismic performance of gravity dams subjected to near and far fault ground motions. Akköse and Şimşek. (2010) studied on the nonlinear seismic response of concrete gravity dams subjected to near and far fault ground motions including dam-water-sediment-foundation rock interaction using Lagrangian approach. Wood et al. (2010) offered a computational partitioned coupling strategy for the modelling of large deformation fluid-structure interaction. Gogoi and Maity (2010) produced a unique method to evaluate the hydrodynamic pressure on the upstream face in concrete dams due to seismic excitation. Degroote et al. (2010) performed a stability analysis of Gauss-Seidel coupling iterations for partitioned simulation of fluid-structure interaction. Sevim et al. (2011) presented the water length and height effects on the earthquake behavior of arch dam-reservoir-foundation systems using Lagrangian approach. Heydari and Mansoori (2011) discussed on dam-reservoir interaction modelling approaches using different finite element software's considering dynamics earthquake loads. Shariatmadar and Mirhaj (2011) displayed the dam-reservoir-foundation interaction effects on the modal characteristics of concrete gravity dams. Chen and Yuan (2011) presented a simple approximate formula after hydrodynamic pressure analysis of arch dam. Wang et al. (2012) practiced on the nonlinear seismic analyses of concrete gravity dams using 3D dam model considering hydrodynamic effects of the impounded water. Lin et al. (2012) developed an efficient approach for the hydrodynamic analysis of dam–reservoir systems. Miquel and Bouaanani (2013) proposed a new practical and efficient procedure to investigate the seismic response of gravity dams. Samii and Lotfi (2013) studied on the absorbing boundary conditions for dynamic analysis. Wick (2013) carried out a study about the coupling of fully eulerian and arbitrary lagrangian-eulerian methods for fluid-structure interaction computations. Altunışık and Sesli (2015) determined the dynamic response of dams using different water modelling approaches. Altunışık et al 2018 examined the effects of long-period pulse of near-fault ground motions on the structural performance of concrete gravity dams using Euler approaches. From these studies, it is seen that there are no enough studies about the determination and comparison of dynamic response of gravity dams using different reservoir modelling approaches such as Westergaard, Lagrange and Euler.

This paper presents the dynamic response of concrete gravity dams using different water modelling approaches such as Westergaard, Lagrange and Euler. Sarıyar concrete gravity dam is selected for application. The finite element models of the dam are constituted considering dam-reservoir-foundation interaction. To determine the structural response of the dam, the linear transient analyses are performed using 1992 Erzincan earthquake ground motion record. From the analyses, dynamic characteristics, maximum displacements, maximum-minimum principal stresses and maximum-minimum principal strains are attained and compared with each other for Westergaard, Lagrange and Euler approaches.

NUMERICAL EXAMPLE

The focus of this paper is to determine and compare the structural dynamic behavior of concrete gravity dams including dam-reservoir-foundation interaction using different water modelling approaches such as Westergaard (added masses), Lagrange (displacement-based) and Euler (pressure-based) to imply the hydrodynamic pressure. Sarıyar concrete gravity dam (Figure 1a) is chosen as an application. Sarıyar dam is located on the Sakarya River, 120km to the northeast of Ankara, in Turkey. The dam is constructed to supply the electric power. The crest length and width are 257m and 7m, respectively. Maximum reservoir height is 85m. The dimensions of the dam are given in Figure 1b.

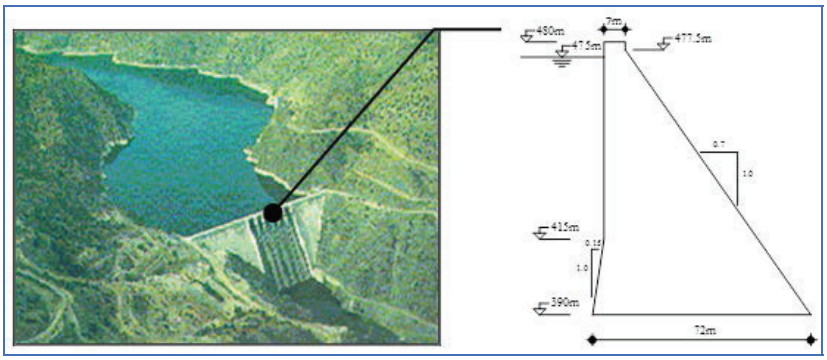

a) b)

Figure 1. Sarıyar concrete gravity dam

The finite element models of the dam including dam-reservoir-foundation interaction using Westergaard, Lagrange and Euler approaches are constituted in ANSYS program and given in Figure 2 (a-c), respectively. In these models, dam body and foundation are represented by solid elements. Reservoir effect is represented by using added masses on dam body for Westergaard approach. But, in the Lagrange and Euler approaches, fluid elements are used to define the reservoir water and its hydrodynamic pressures. In the finite element model, Plane182 element is used for dam body and foundation. Also, MASS21, Fluid79 and Fluid29 (structure absent) elements are selected to represent the reservoir water for Westergaard, Lagrange and Euler Approaches, respectively.

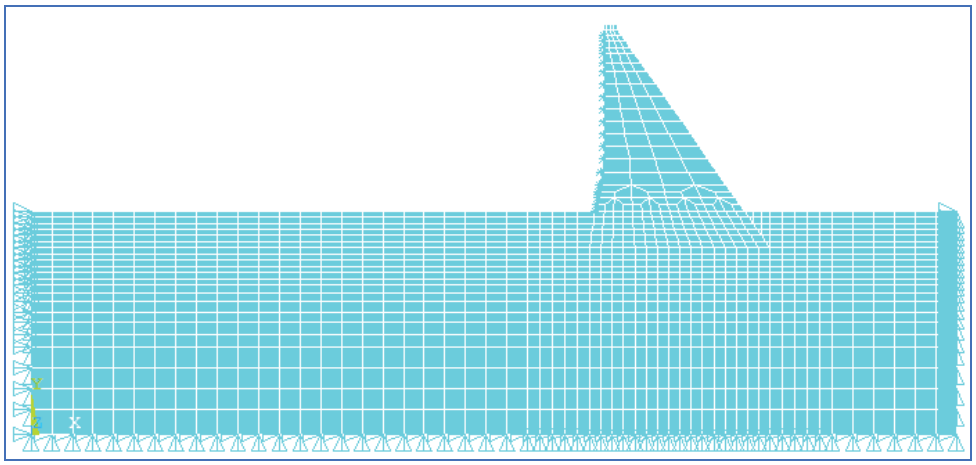

a) Westergaard approach

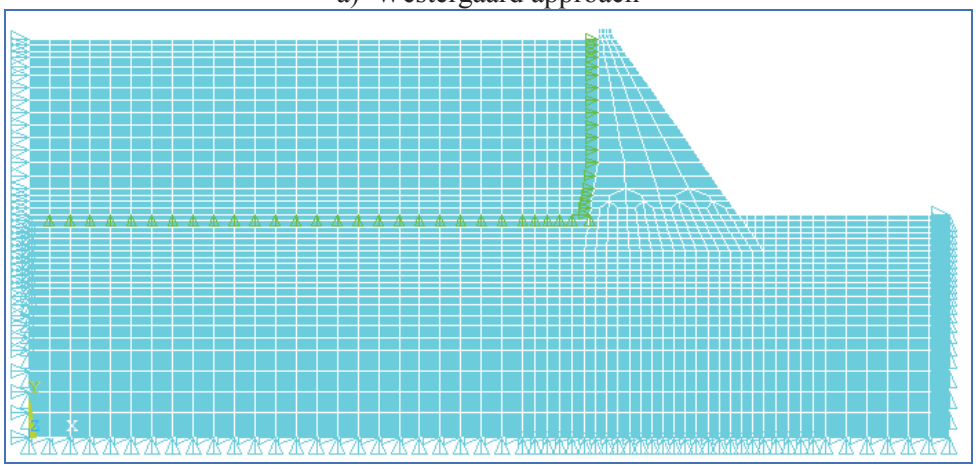

b) Langrange approach

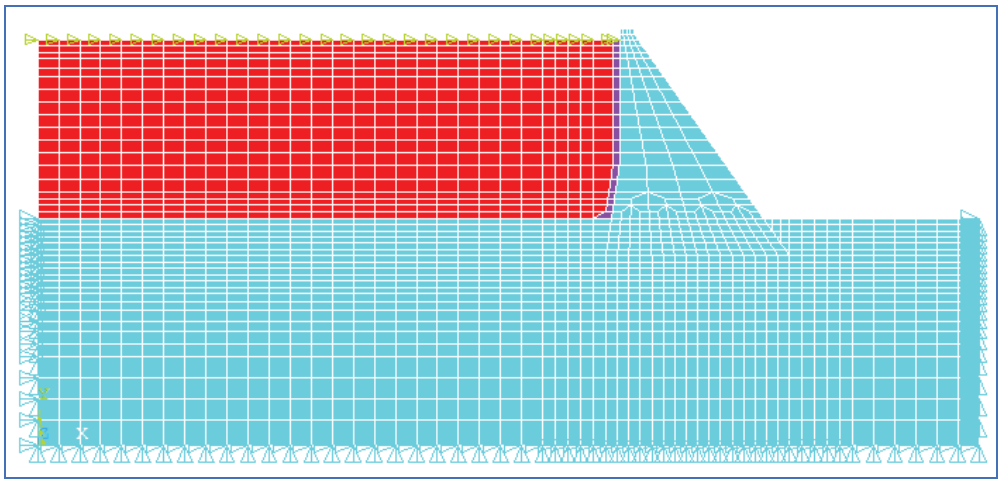

c) Euler approach

Figure 2. Two dimensional finite element models of Sarıyar concrete gravity dam including dam-reservoir-foundation systems using Westergaard, Lagrange and Euler approaches

Massless foundation is used in all dam-reservoir-foundation models. At the dam-reservoir and reservoir-foundation interface, coupling elements with length of 0.001m is used to hold the displacements equal between two reciprocal nodes for Lagrange approach. Between the dam and reservoir faces, the thickness of Fluid 29 element, which shows the hydrodynamic pressures effect on dam body, is chosen as 3.125m for Euler approach. The length of the reservoir in the upstream direction is taken to be as much as three times the dam height in all models. It is assumed that the reservoir has constant depth. In addition, foundation depths are taken into account as much as the dam heights. In the upstream direction, foundation length is considered as the reservoir length and in the downstream direction, foundation length is considered as the dam height. Element matrices are computed using the Gauss numerical integration technique (Bathe, 1996). The Newmark method is used in the solution of the equation of motions. Rayleigh damping is considered in the analyses and damping ratio is selected as 5%.

The material properties used in the analyses is given in Table 1. The ERZIKAN/ERZ-EW component of the Erzincan earthquake occurred on March 13, 1992, Erzincan, Turkey is chosen as strong earthquake ground motion record (Figure 3).

Table 1. The material properties used in the analyses

Material	**Material Properties**		
	Modulus of Elasticity (N/m)	*Poisson's Ratio (-)*	*Mass per unit Vol. (kg/m3)*
Dam (Concrete)	35.0E9	0.15	2400
Foundation	30.0E9	0.20	-
Reservoir	20.7E8	-	1000

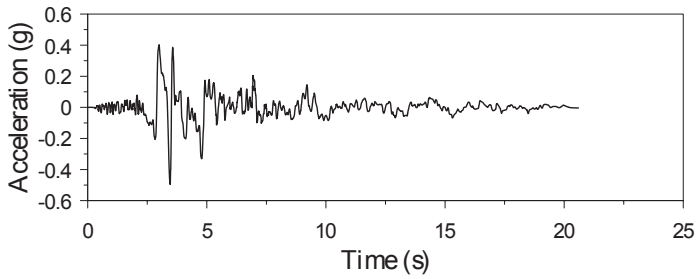

Figure 3. The time history of the 1992 Erzincan earthquake strong ground motion

Displacements

The time histories of the horizontal displacements (upstream-downstream direction) at the crest point of Sarıyar concrete gravity dam obtained from linear transient analysis for three different approaches under ERZIKAN/ERZ-EW component of Erzincan Earthquake (1992) ground motion is presented Figure 4 (a-c). The maximum displacements are attained as 75.61mm, 67.63mm and 35.62 mm for Westergaard, Lagrange and Euler approaches, respectively.

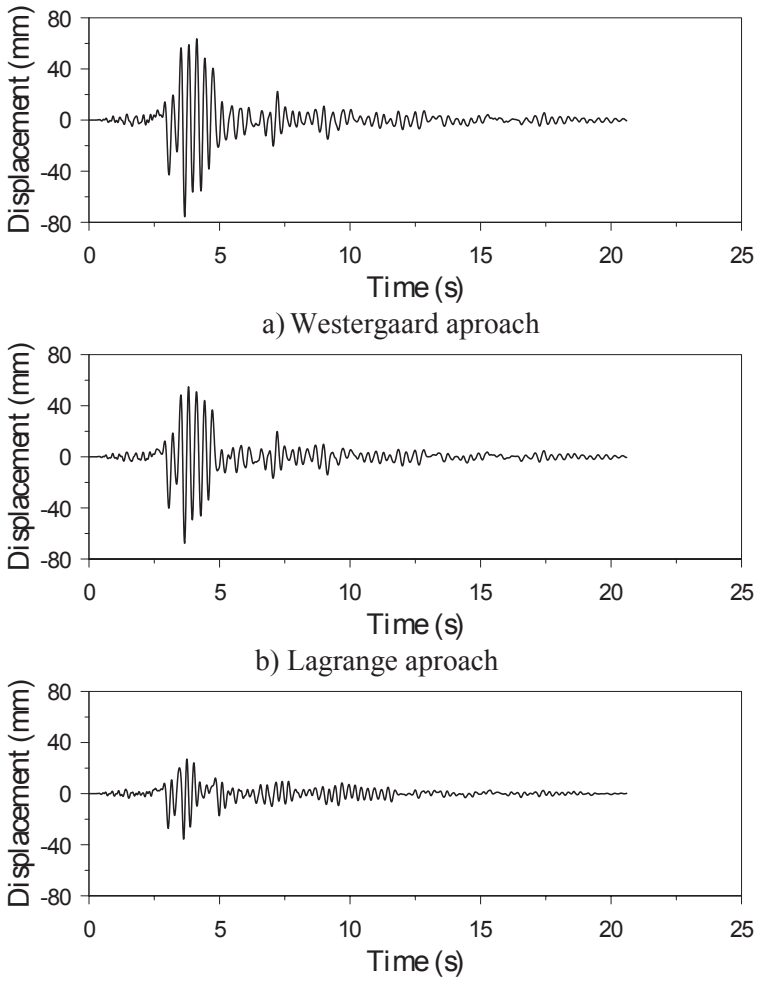

a) Westergaard aproach

b) Lagrange aproach

c) Euler aproach

Figure 4. The time histories of horizontal displacements at the crest point for Westergaard (a), Lagrange (b) and Euler (c) approaches

The changing of maximum displacements by the height of dam body for Westergaard, Lagrange and Euler approaches are given in Figure 5. It is clearly seen from the figure that the displacements increase by height of the dam body for all modelling approaches and maximum displacements attained for Westergaard model. This represents the distribution of the peak values reached by the maximum displacement at each point within the sections.

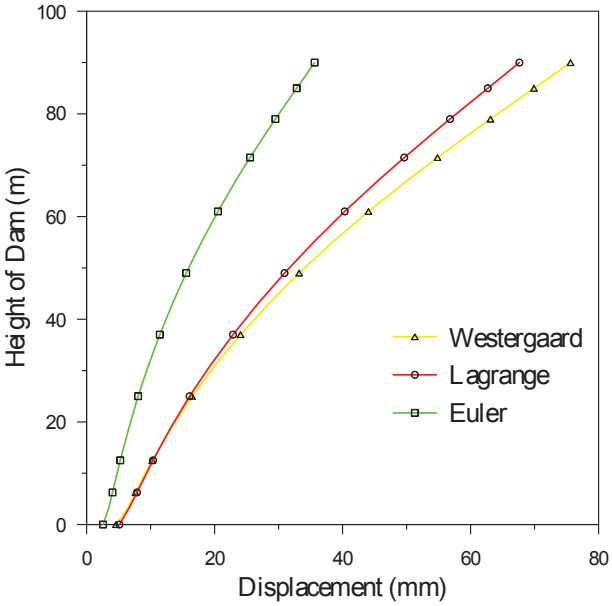

Figure 5. Maximum horizontal displacements by height of Sarıyar concrete gravity dam

Principal Stresses

The changing of maximum compressive and tensile principal stresses by the height of dam body for Westergaard, Lagrange and Euler approaches are given in Figure 6. It is seen from the figure that the maximum values of both principle stresses are attained at 3.215m height from the base point of the dam body. The time histories of the maximum and minimum principal stresses (at 3.125m) for each approaches are plotted in Figure 7 (a-c). The maximum tensile stresses are attained as 12.57MPa, 12.37MPa, 5.30MPa; the maximum compressive stresses are attained as 14.58MPa, 15.50MPa, 6.81MPa for Westergaard, Lagrange and Euler approaches, respectively.

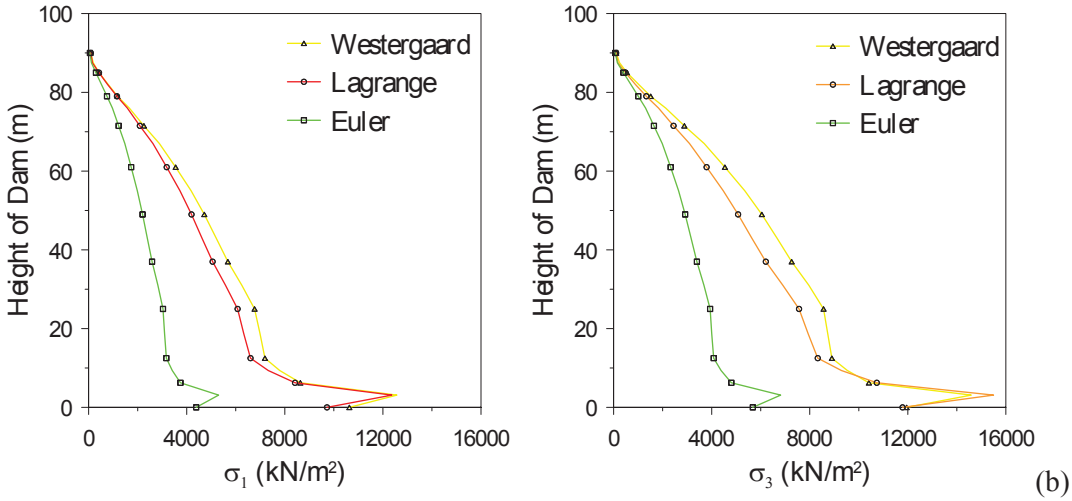

Figure 6. Changing of maximum tensile (a) and compressive (b) principal stresses by height of the changing Sarıyar concrete gravity dam

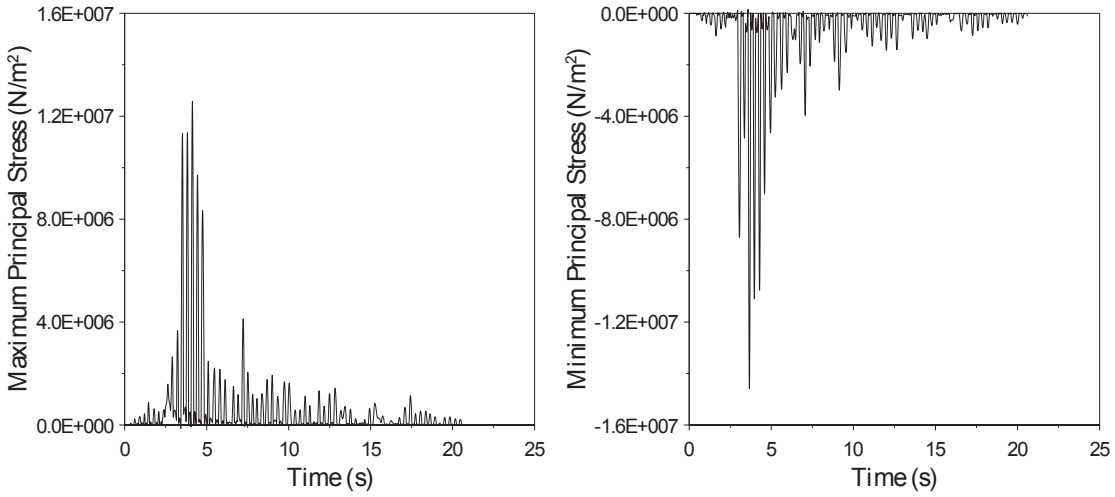

a) Westergaard aproach

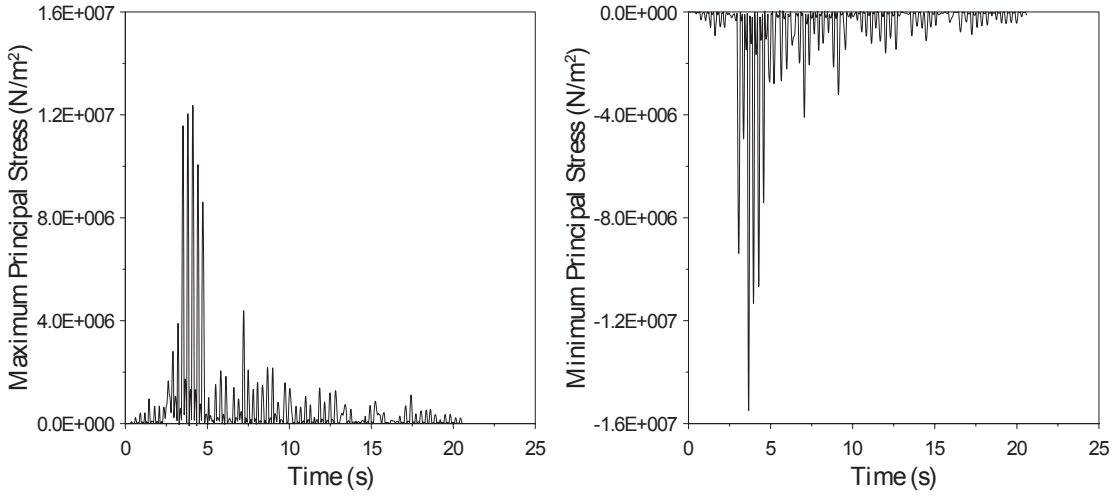

b) Lagrange aproach

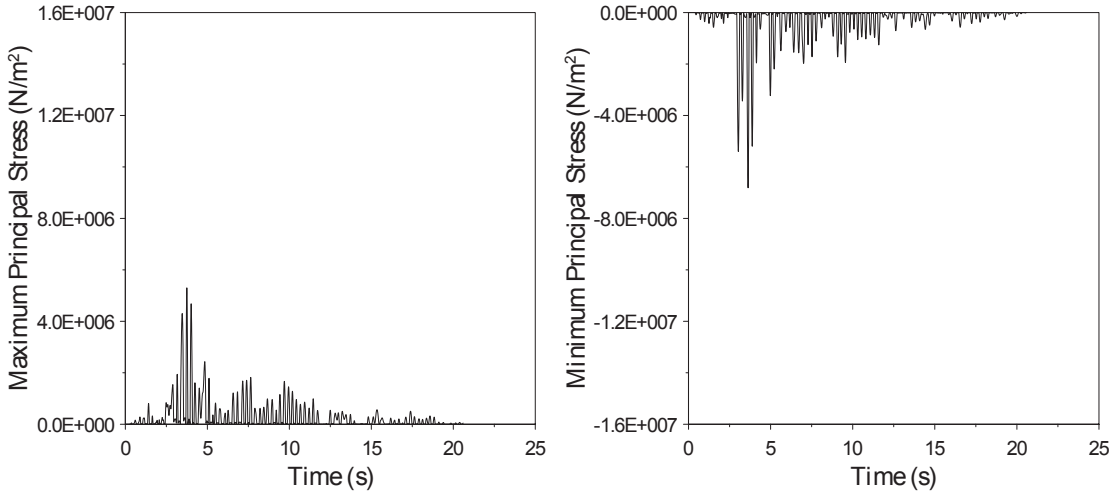

c) Euler aproach

Figure 7. The time histories of maximum and minimum principal stresses at the 3.125m Westergaard (a), Lagrange (b) and Euler (c) approaches

Principal Strains

The changing of maximum compressive and tensile principal strains by the height of dam body for Westergaard, Lagrange and Euler approaches are given in Figure 8. It is seen from the figure that the

maximum values of both principle strains are attained at 3.215m height from the base point of the dam body. The time histories of the maximum and minimum principal strains (at 3.125m) for each approaches are plotted in Figure 9 (a-c). The maximum tensile and compressive strains are attained as 35.47E-5, 35.35E-5, 14.90E-5a; 41.04E-5, 44.13E-5, 19.15E-5 for all approaches, respectively.

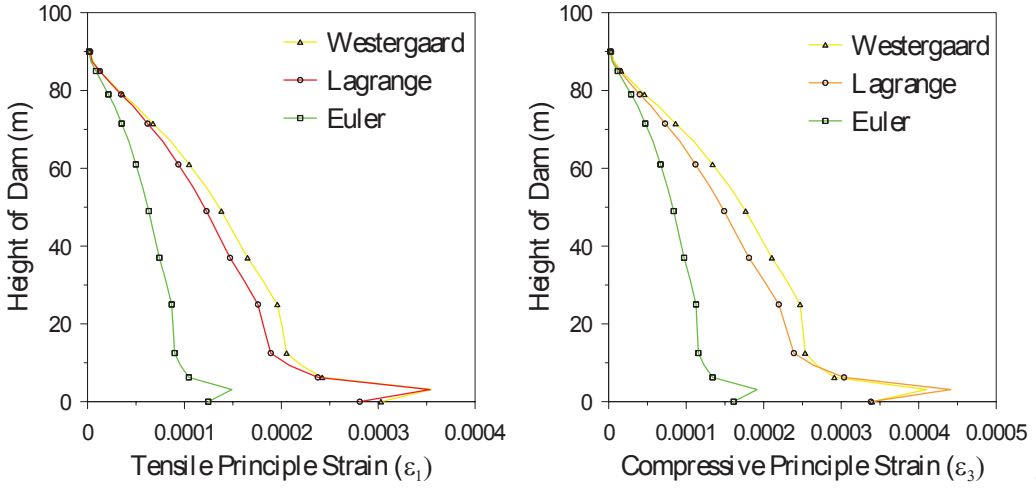

Figure 8. Changing of maximum tensile (a) and compressive (b) principal strains by height of the changing Sarıyar concrete gravity dam.

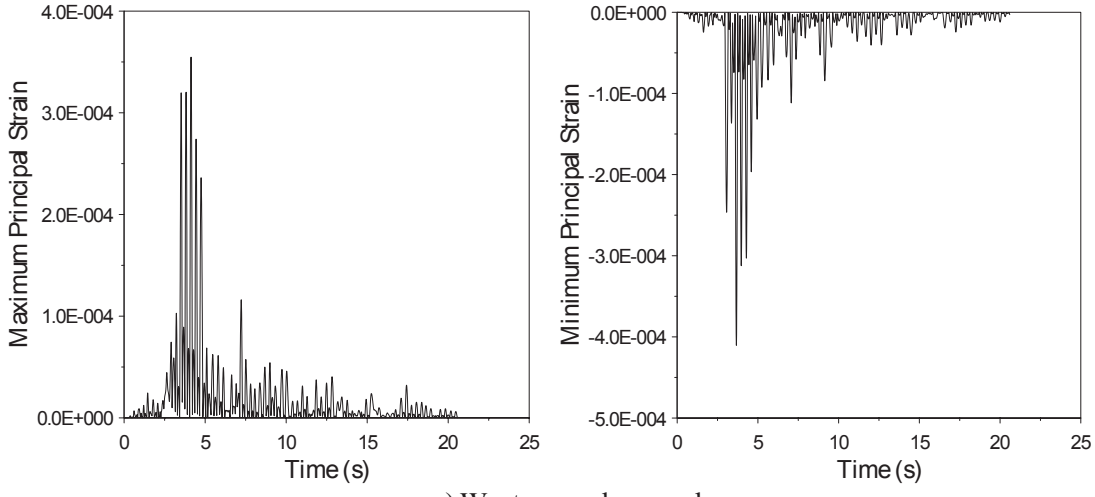

a) Westergaard aproach

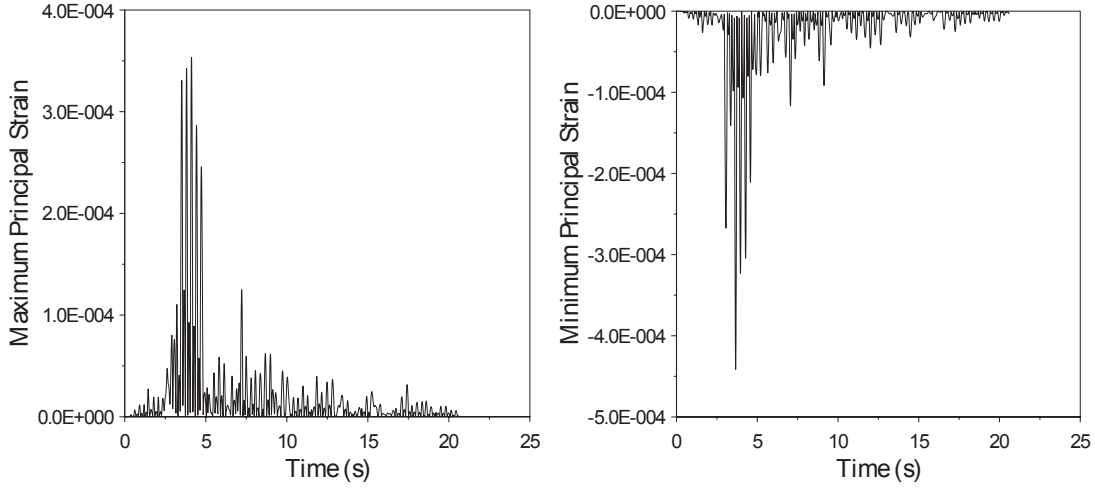

b) Lagrange aproach

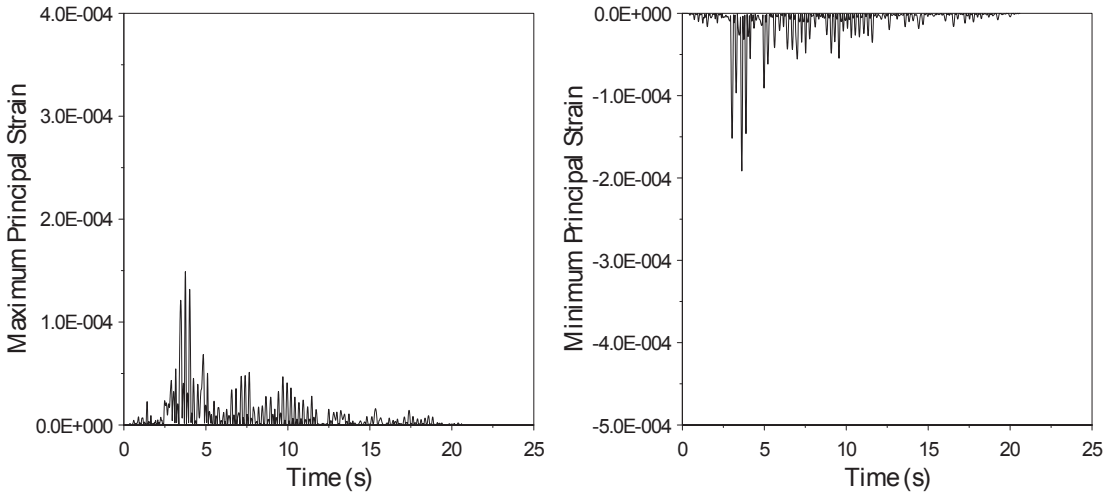

c) Euler aproach

Figure 9. The time histories of maximum and minimum principal strains at the 3.125m Westergaard (a), Lagrange (b) and Euler (c) approaches

CONCLUSION

This paper present the determination and comparison of dynamic response of concrete gravity dams using different water modelling approaches such as Westergaard, Lagrange and Euler. Sarıyar concrete gravity dam located on in Ankara, Turkey, is selected as a case study. The finite element models of the dam are constituted considering dam-reservoir-foundation interaction for all reservoir models. Comparing the results of this study, the following observations can be made:

- The displacements increase by the height of the dam body and maximum displacements occur at crest points for each reservoir modelling approaches. Maximum and minimum displacements are attained from Westergaard and Euler approaches, respectively.
- Maximum compressive and tensile principal stresses and strains have a decreasing trend from the base to crest point of the dam body for all reservoir modelling approaches. Maximum stresses and strains are occurred at the 3.125m height from the base for Westergaard, Lagrange and Euler approaches.
- It is seen that maximum and minimum principal stresses and strains are nearly equal for Westergaard and Lagrange approaches. But, the values attained from Euler approach are different and quite lower than the others.
- MASS21 element type, coupling lines and FLUID29 element using structure present options can be considered to dam-reservoir and reservoir-foundation interaction in Westergaard, Lagrange and Euler approaches, respectively.

REFERENCES

Akköse, M., Şimşek, E., 2010. "Non-linear seismic response of concrete gravity dams to near-fault ground motions including dam-water-sediment-foundation interaction". Applied Mathematical Modelling, Vol. 34, pp. 3685–3700.

Altunışık, A.C., Sesli, H., 2015. "Dynamic response of concrete gravity dams using different water modelling approaches: Westergaard, lagrange and euler". Computers and Concrete, vol. 16, N. 3, pp. 429-448.

Altunışık, A.C., Sesli, H., Hüsem, M., Akköse, M., 2018. "Performance evaluation of gravity dams subjected to near- and far-fault ground motion using euler approaches". Iranian Journal of Science and Technology - Transactions of Civil Engineering, DOI: 10.1007/s40996-018-0142-z.

Bathe, K.J., 1996. “Finite Element Procedures in Engineering Analysis”. Englewood Cliffs, New Jersey, Prentice-Hall.

Bayraktar, A., Altunişik, A.C., Sevim, B., Kartal, M.E., Türker, T., Bilici, Y., 2009. “Comparison of near- and far-fault ground motion effect on the nonlinear response of dam-reservoir-foundation systems”. Nonlinear Dynamics, Vol. 58, N. 4, pp. 655-673.

Bayraktar, A., Türker, T., Akköse, M., Ateş, Ş., 2010. “The effect of reservoir length on seismic performance of gravity dams to near- and far-fault ground motions”. Natural Hazards, Vol. 52, N. 2, pp. 257-275.

Chen, B., Yuan, Y., 2011. “Hydrodynamic Pressures on Arch Dam during Earthquakes”. Journal of Hydraulic Engineering, Vol. 137, pp. 34-44.

Degroote, J., Annerel, S., Vierendeels, J., 2010. “Stability analysis of Gauss–Seidel iterations in a partitioned Simulation of fluid–structure interaction”. Computers and Structures, Vol. 88, N. 5-6, pp. 263-271.

Fathi, A., Lotfi, V., 2008. “Effects of reservoir length on dynamic analysis of concrete gravity dams”. The 14th World Conference on Earthquake Engineering, October 12-17, Beijing, China.

Gogoi, I., Maity, D., 2010. “A novel procedure for determination of hydrodynamic pressure along upstream face of dams due to earthquakes”. Computers and Structures, Vol. 88, pp. 539-548.

Heydari, M.M., Mansoori, A., 2011. “Dynamic Analysis of Dam-Reservoir Interaction in Time Domain”. World Applied Sciences Journal, vol 15, pp. 1403-1408.

Lin, G., Wang, Y., Hu, Z., 2012. “An efficient approach for frequency-domain and time-domain hydrodynamic analysis of dam–reservoir systems”. Earthquake Engineering and structural Dynamics, Vol. 41, N. 13, pp. 1725-1749.

Miquel, B., Bouaanani, N., 2013. “Accounting for Earthquake-Induced Dam-Reservoir Interaction Using Modified Accelerograms”. Journal of Hydraulic Engineering, vol. 139, pp. 1608-1617.

Samii, A., Lotfi, V., 2007. “Comparison of coupled and decoupled modal approaches in seismic analysis of concrete gravity dams in time domain”. Finite Elements in Analysis and Design, Vol. 43, pp. 1003-1012.

Samii, A., Lotfi, V., 2013. “A high-order based boundary condition for dynamic analysis of infinite reservoirs”. Computers and Structures, Vol. 120, pp. 65-76.

Sevim, B., Altunişik, A.C., Bayraktar, A., Akköse, M., Calayir, Y., 2011. “Water length and height effects on the earthquake behavior of arch dam-reservoir-foundation systems”. KSCE Journal of Civil Engineering, Vol. 15, N. 2, pp. 295-303.

Shariatmadar, H., Mirhaj, A., 2011. “Dam-reservoir-foundation interaction effects on the modal characteristic of concrete gravity dams”. Structural Engineering and Mechanics, Vol. 38, N. 1, pp. 65-79.

Wang, H., Feng, M., Yang, H., 2012. “Seismic nonlinear analyses of a concrete gravity dam with 3D full dam model”. Bullettin of Earthquake Engineering, vol. 10, pp. 1959-1977.

Westergaard, H.M., 1933. “Water Pressures on Dams during Earthquakes”. Transactions of the American Society of Civil Engineers, vol. 98, pp. 418–433.

Wick, T., 2013. “Coupling of fully Eulerian and arbitrary Lagrangian-Eulerian methods for fluid-structure interaction computations” Computational Mechanics, Vol. 52, N. 5, pp. 1113–1124.

Wood, C., Gil, A.J., Hassan, O., Bonet, J., 2010. “Partitioned block-Gauss–Seidel coupling for dynamic fluid–structure interaction”. Computers and Structures, vol. 88, pp. 1367-1382.

5th International Symposium on Dam Safety

October 27-31, 2018

FOUNDATION TREATMENT OF POROUS FOUNDATION AT BAJULMATI DAM

Anissa MAYANGSARI [1], Kadek WIDYASARI[2]

ABSTRACT

Bajulmati Dam is located in Banyuwangi, East Java, Indonesia. The type of the dam is impervious earth material at the center supported by rockfill at the outer zone. The height of the dam is 47 meter and the reservoir volume are 10 MCM. The foundation material is sedimentary rock in nearly horizontal strata of varying thicknesses, comprising lapilli tuff, tufaceous sand, laharic gravelly sand and silty tuff. The dam site is also located in Wonogiri groundwater basin. These geological defects have a profound effect on seepage flow beneath dam foundation. The Lugeon value at the riverbed foundation is more than 40 Lu. In the construction, the flow of water through the dam foundation is about 90 – 120 l/s. Due to water tightness problem in dam foundation, some foundation treatments have been proposed from the feasibility study until construction. The foundation treatments are the combination between curtain grouting using neat cement with tube a manchette (TAM) method and chemical grouting. This paper describes the foundation treatment process, the results obtained and the evaluation after construction and impounding of the dam.

Keywords: porous foundation, foundation treatment, curtain grouting, chemical grouting.

INTRODUCTION

Bajulmati dam is located in Banyuwangi, approximately 250 km from Surabaya City, East Java, Indonesia. The main components of Bajumlati Dam consist of a 250 m long and 47 m high rockfill dam with impervious earth material at the center. The dam supply 180 l/s of raw water and irrigated 1,800 ha. The benefit of reservoir also for hydropower and tourism.

The type of main spillway is side spillway with 90 m length. The dam also provides fuse plug emergency spillway. The capacity of spillway is 1,436 m^3/s. The inclined intake with 2 (two) operating gates and 1 (one) flush gate was built at the right abutment. (Figure 1)

[1] Section head of dam analysis, data and information, Dam Safety Unit, Ministry of Public Work and Housing, Indonesia
e-posta: anissamayangsari@gmail.com

[2] Dam planning of commitment making official, Brantas River Basin Agency, Ministry of Public Work and Housing, Indonesia
e-posta: widyasarikadek@gmail.com

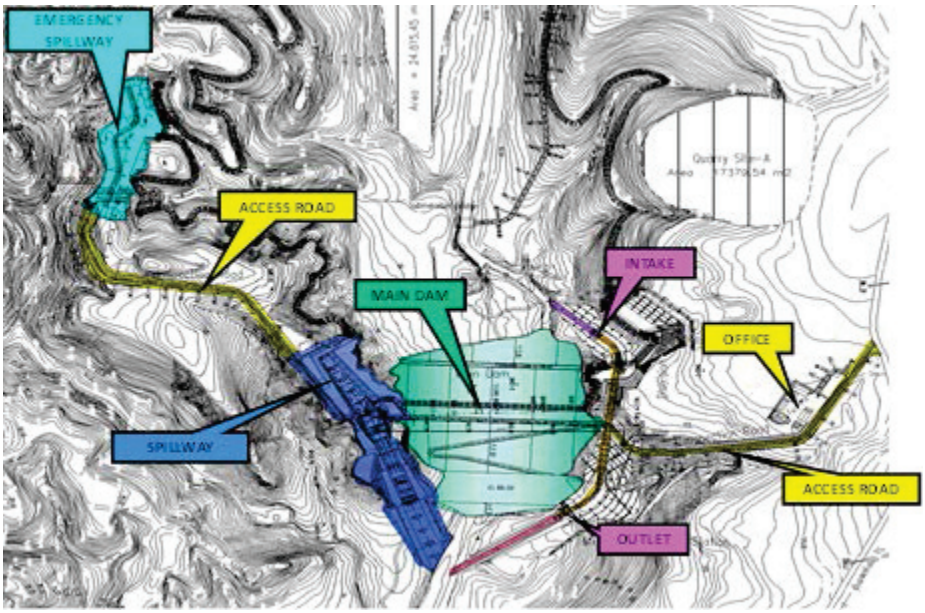

Figure 1 Site plan of Bajulmati Dam

GEOLOGICAL FOUNDATION

Geological foundation at the main dam

Based on investigation study started at 1983 and continued at 2000, 2002 and 2008 and in construction, the geological condition on the main dam were describe in 4 (four) layers.

Overburden consist of:

- *Top soil:* colored ash black, poor strength, weak, highly weathered, non plastis, heterogeneous material, grain size from clay to fine sand, contain root.
- *Terrace deposit*: colored grey, the hardness is very soft to soft (CLL-CL), completely weathered, heterogeneous material, grain size from clay to gravel, slaky, dry, low permeability (9.4 x 10^{-4} m/s).
- *Tallus deposit:* colored dark brown, soft (CL), completely weathered, less plastic, heterogeneous material, grain size from clay to coarse sand, low moisture. In several area, composed by rocks with boulder size, low permeability (1.4 x 10^{-4} m/s).
- *Recent river deposit:* colored dark black, the hardness is very hard, unconsolidated, grain size from gravel to boulder, heterogeneous material, interlocking, composed by andesite-basalt, low permeability (2.6 x 10^{-3} m/s).
- *Sandy clay:* colored reddish, soft (CL), plastic, grain size from clay to fine sand, moist, high permeability (2.3 x 10^{-5} m/s).
- *Old river deposit:* colored dark black, the hardness is very hard, unconsolidated, fresh, grain size from gravel to boulder, heterogeneous material, semi consolidated, poorly cemented, composed by andesite-basalt, low permeability (1,3 x 10^{-3} m/s).

Upper layer consist of:

- *Lapilli tuff:* greyish yellow, rock forming minerals and particles are softened (CL), sandy tuf with andesite fragment, pumice, slaking, moist, semi-impervious with permeability 1.7 x 10^{-4} m/s.
- *Tufaceous sand:* light grey, soft, fresh, sandy tuff with andesite fragment, obsidian, semi-impervious with permeability 6.8 x 10^{-4} m/s.
- *Altered of lapilli tuff:* reddish brown, medium hard (CL-CM), fresh, sandy tuff with andesite fragment, obsidian, massive, several mineral has been change to clay, many sand lenses founded, and impervious material with permeability 7.8 x 10^{-5} m/s.

Middle Layers consist of:

- *Laharic gravelly sand:* dark black, solid, fresh grain size from gravel to cobble, heterogeneous material, poorly cemented, andesite – basalt, pervious with permeability 1.48 x 10^{-3} m/s.

Lower Layers consist of:

- *Lapilli tuff:* light grey, soft (CL), fresh, tufa with andesite which contain pumice, impervious with permeability 7.8 x 10^{-5} m/s.
- *Silty tuff:* light grey, soft (D-CLL), fresh, the rock mass is tufa with pumice fragment, light, slaky, impervious with permeability 5.9 x 10^{-5} m/s.

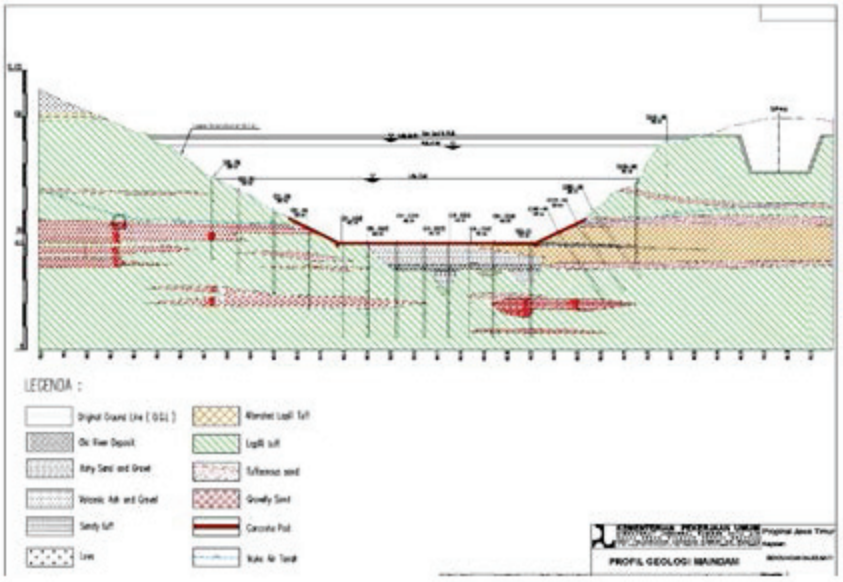

Figure 2 Geological profile of dam site

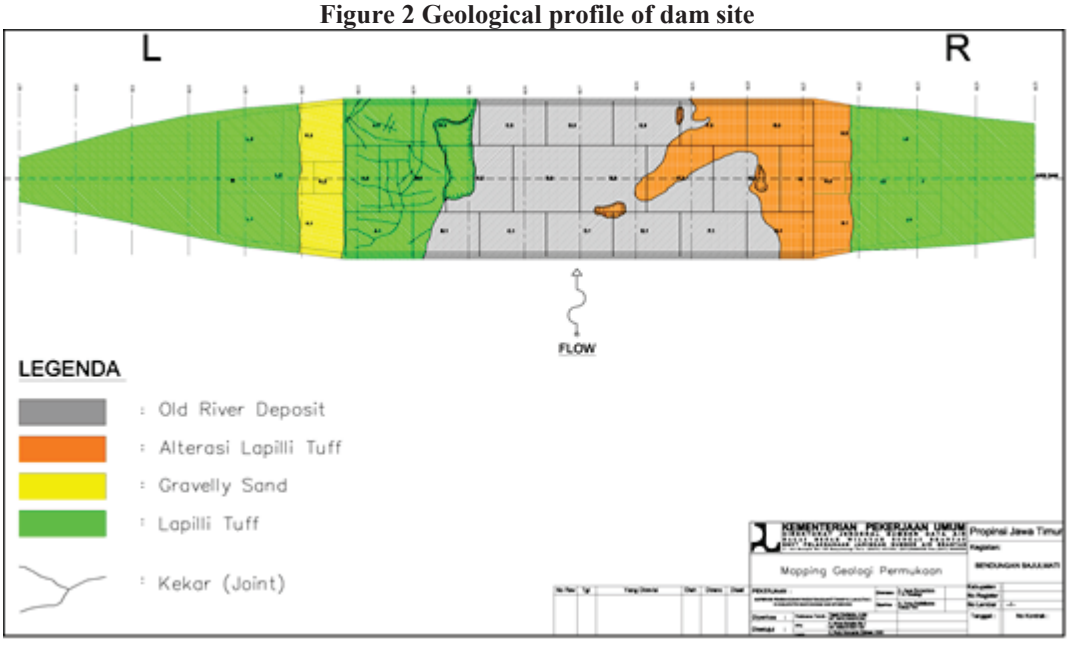

Figure 3 Geological map of dam site

Geological condition at the cut off trench

Based on detail geological map from cut off trench at El +45 m, there are some outcrop at the trench, as follow:

- The rock mass is tufa lapilli at Sta. 11 to Sta. 14+4, compacted, semi-confined seepage through vertical fissure. At the bore hole area, to drainage the water from seepage equipped by pump and gravel ditch.
- Old river deposit consists of sand aggregation, gravel, and boulder. The boulder consists of andesite and basalt which shape are sub-rounded to sub-angular. The boulder being transported to the media in thick cold lava phase. Based on the outcrop at cross section of old river chanel, the pattern of the river was braided. The pattern was because of fluvio-vulcanic sedimentation.

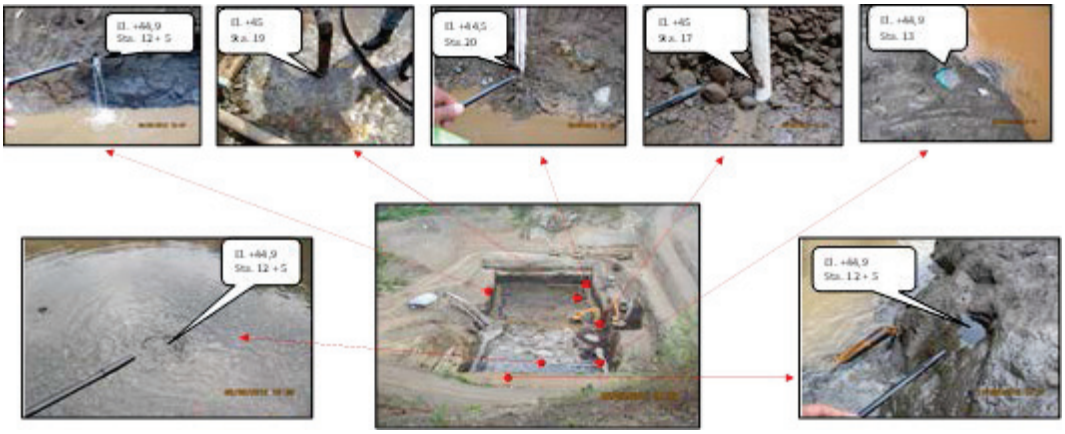

Figure 4 Outcorp at the trench

Altered lapilli tuff with insert of black clay at west side exposed fingered with clay layer. The clay is carbonated, because of combustion effect, as xenolite which is carried by the liquid lava flow and spreads between the turbid flows of cold lava. These materials need to be excavate and replaced with dental concrete.

Geohydrology

The foundation problem of the Bajulmati Dam main shows along with the stages of dam construction. While the foundation excavation process, especially geohydrology in the diversion tunnel, the plunge pool and the river bed. Groundwater sources appear in the invert of the diversion tunnel with a discharge flow ± 50 liter/sec, in the spillway of the discharge overflow ± 50 liter/sec and in the foundation of the main dam ± 40 liters/second.

The big problem is the groundwater that arise, so the method of dewatering should be done properly, including in the cut-off trench.

FOUNDATION TREATMENT AT THE MAIN DAM

Methodology

Due to water tightness problem in dam foundation, some foundation treatments have been proposed from the feasibility study until construction. Basically, the foundation treatments are describe as follows:

- 10 (ten) meters depth of cut off trench combine with curtain grouting using neat cement with tube a manchette (TAM) method with 40-meter depth. The result of these methods is the Lugeon value still vary within range 10 Lu to more than 40 Lu.
- 3 (three) stages of chemical grouting using Portland cement type I and sodium silicate. After the final chemical grouting the Lugeon value vary between less than 5 Lu to 10 Lu.

Cut off trench

At the foundation of the dam, it would be excavated until 10 m depth. The excavation would have some advantages such as cut off trench, removing sand layer, cobble and boulder for 5 m depth and for excavation of construction material which has 30.000 m^3 bank.

The terrain is very steep and irregular at the bottom of the valley where the dam will be placed. To provide a uniform level surface for easier compaction and eliminate the potential for sharp, settlements, a concrete pad can be constructed across the valley floor.

A concrete pad constructed as thick as 1-meter cross to the base of cut off trench. The concrete pad has a function as scaling at the contact between impervious material. With concrete pad the layer of contact clay would be easy to spread, raise the bearing capacity, reduce the differential settlement, and for base in drilling for grouting.

Drilling *Work*

The drilling work use rotary method with hydraulic feed rotary drilling machine. The drilling use metal core bit diameter 66 mm or 73 mm trough the depth of plan. Based on geological condition in various river bed foundation, especially in the layer that has potentially collapse such as gravelly sand, tuffaceous sand, ashy san and gravel, the method of drilling is gradually down stage with the depth of every stage is 2.5 meter. After the drilling has done, the hole was washed by water circulation to clean from slime. The depth measurement of the hole is carried out before installation of packer for water pressure test. After all the drilling was finished, the drilling point would be continuing at another hole after split spacing.

Water Pressure Test

The grouting method need packer in every grout length. The type of packer which is used are air packer type for pervious rock formation or crack or screw expansion packer for compacted rock formation. The installation of good packer was marked with tight sealing and no leakage, so it could reach maximum pressure which has been plan. In order to get good overlap at every grout length, the installation of packer need to raise up around 0.5-meter trough the stage that has been grouting. The measurement on the grouting hole is carried out at the maximum pressure allowed for 10 minutes. The discharge flow read out at every minute.

Table 1 Maximum Pressure in every step of grouting

Step	I (A,B)	II (A,B)	III (A,B)	IV (A,B)	V (A,B)	VI (A,B)
Depth (m)	0 ~ 2.5 2.5 ~ 5	5 ~ 7.5 7.5 ~ 10	10 ~ 12.5 12.5 ~ 15	15 ~ 17.5 17.5 ~ 20	20 ~ 22.5 22.5 ~ 25	25 ~ 27.5 27.5 ~ 30
Maximum Pressure (kg/cm^2)	1.0	2.0	3.0	4.0	5.0	6.0

Tube A Manchette (TAM) Method

The stages of implementing the TAM method (figure 5) are described below:

1. Drilling the hole and installing the casing pipe
2. Install the manchette pipe, pull the casing pipe and pre-grout between the manchette pipe and the drill hole
3. Install the injection pipe after the pre-grout hardens at the depth that will be crushed or grout section and double packer/single packer
4. Break the pre-grout in the grout section through a manchette valve that is temporarily protected with vynil tape
5. Do grouting according to the specifications that apply to the grout section

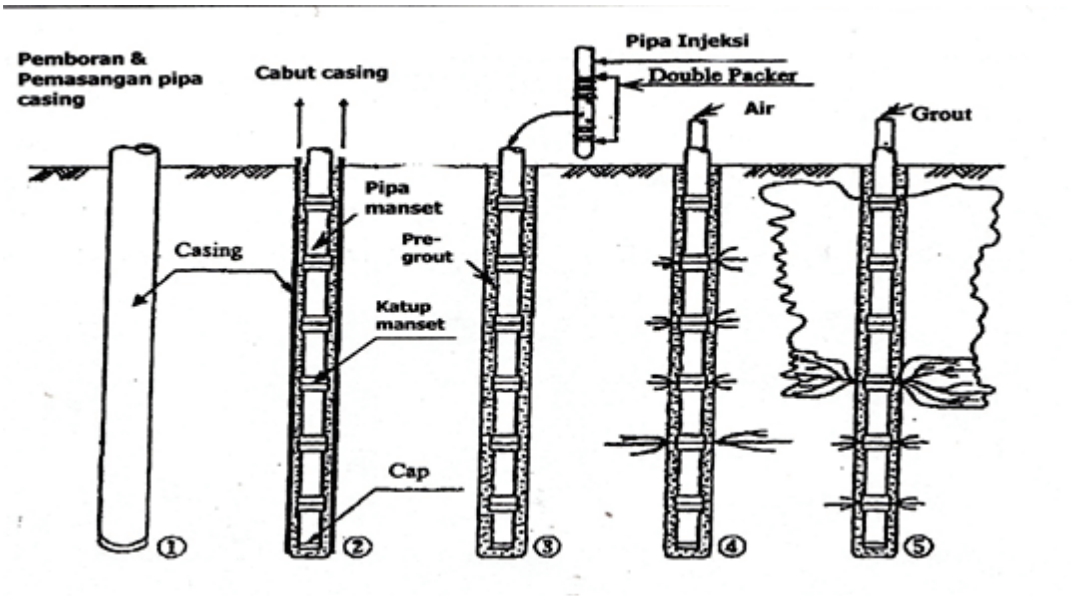

Figure 5 Process of Tube a Manchette Method

Chemical Grouting

The next step after the hole was ready is cementation grouting which cover mixing grouting material and injecting the mixing grouting material. The important thing for grouting in this stage is the setting of grouting pressure in every stage of grout length. The type and overburden depth in every grout length would decide the maximum pressure grouting allowed. The process injection method of chemical grouting is described in figure 6.

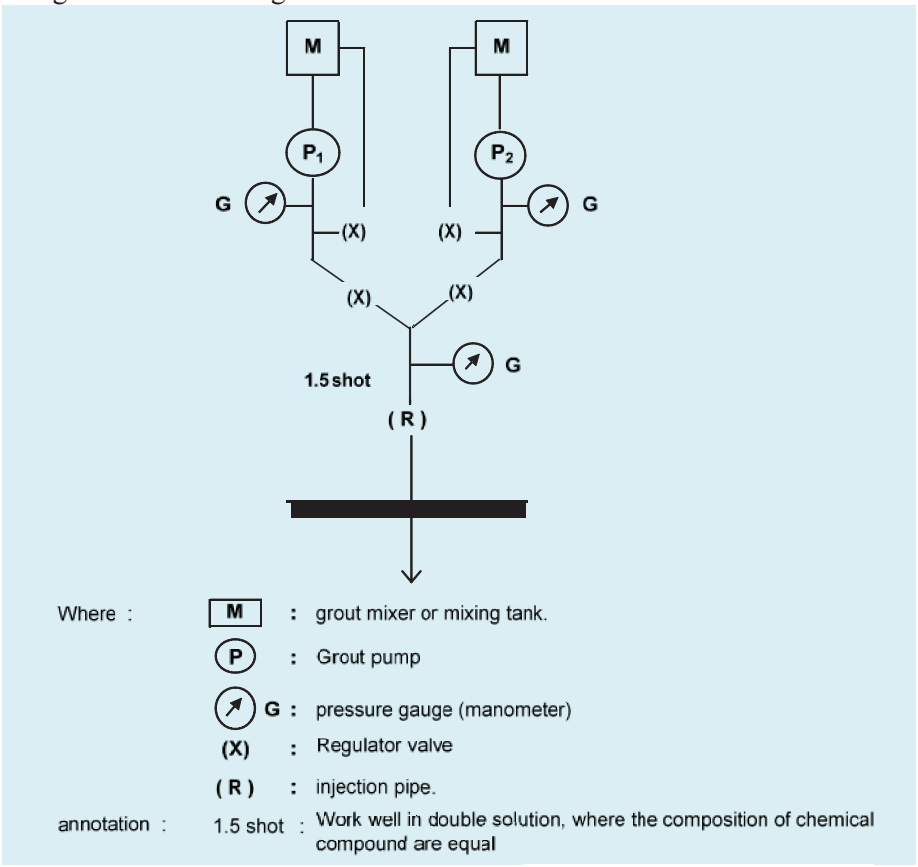

Figure 6 Injection method of chemical grouting

There are several properties of grout material (table 2). The grout material is choose based on the effectivity to grout, the low price, high durability and no toxic. Based on that criteria, the chemical

compound which is used is water glass type (LW) with the composition of mixed material is describe in table 3.

Table 2 Property of grout material

No.	Compound	efectivity	price	durability	toxicity
1.	Portland cement	X	◎	◎	◎
2.	Bentonite	Δ	◎	O	◎
3.	Silicate (LW)	O	O	Δ	O
4.	Resin	O	Δ	X	Δ
5.	Chrom-lignin	O	Δ	X	X
6.	Acrylamide	◎	X	O	X
7.	Polyurethane	◎	X	Δ	O
◎ very good	O good	Δ fair	X poor		

Table 3 Mix proportion of chemical grouting

Mix Proportion of 400 liter quantity			
A - SOLUTION		**B - SOLUTION**	
- Sodium Silicate		- Portland Cement	30 ~ 20 kg
($NaAlSiO_3$)	100 liter	- Water	190 liter
- Water	100 liter		
Total Volume	*200 liter*	*Total Volume*	*200 liter*
Gel time : 3 ~ 4 minutes			

The maximum grouting pressure applied will be modified based on the results of pressure water test, which is shown in table 4.

Table 4 Modified grouting pressure

Step	I (A,B)	II (A,B)	III (A,B)	IV (A,B)	V (A,B)	VI (A,B)
Depth (m)	0 ~ 2.5 2.5 ~ 5	5 ~ 7.5 7.5 ~ 10	10 ~ 12.5 12.5 ~ 15	15 ~ 17.5 17.5 ~ 20	20 ~ 22.5 22.5 ~ 25	25 ~ 27.5 27.5 ~ 30
Maximum Pressure (kg/cm^2)	2.0	3.0	4.0	5.0	6.0	7.0

The application in chemical grouting need some attention which is describe below:

- If the maximum grouting pressure has not been reached and the injection volume of the sodium silicate mixture has reached 800 liters, the grouting must be continued with a neat cement mixture with a weight ratio of W: C = 1: 1.
- If the maximum grouting pressure has been reached, the injection volume is less than 0.2 liters/ minute/meter or the grouting could not penetrate to the foundation, the grouting must be continued at least 10 minutes for saturation.
- Leaks on the surface or in grouting hole needs to be plug (caulking).
- After completing the chemical grouting, the grout hole must be plugged in a 1: 1 mixed mortar to 1: 0.5 to reduce the uplift pressure.

RESULT AND EVALUATION

Based on design criteria the lugeon value at the foundation should reach less than 10 Lu. This criterion has been reached after final foundation treatment by chemical grouting. The total area of grouting zone that reach less than 5Lu is about 78%, and the 32% reach 5 Lu to 10 Lu. After 2 years of impounding the seepage flow through the dam body is 8.3 l/s, which is lower than design calculation 9.7 l/s.

Table 5 Lugeon value before and after grouting

Color	Lugeon Value	Before Grouting (%)	After Grouting (%)	Difference (%)
	≤ 5	-	77.89	+ 77,89
	5 < Lu ≤ 10	-	22.11	+ 22,11
	10 < Lu ≤ 20	52.44	-	- 52,44
	20 < Lu ≤ 40	34.15	-	- 34,15
	Lu ≥ 40	13.41	-	- 13,41
Total		100	100	

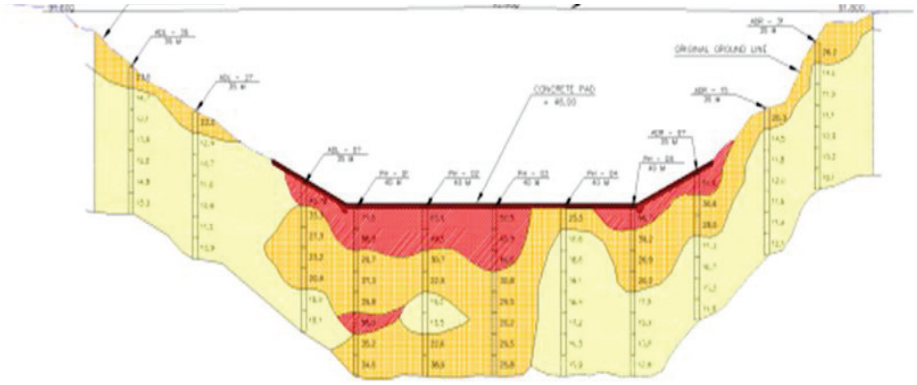

Figure 7. Lugeon value before grouting

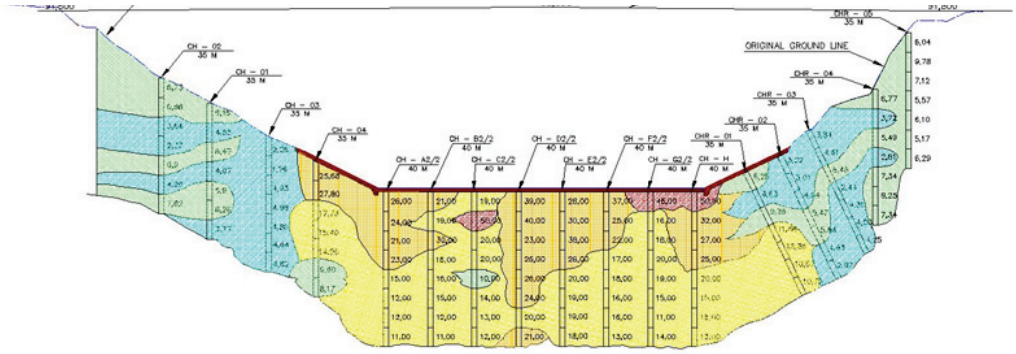

Figure 8. Lugeon value after using Tube A Manchette method

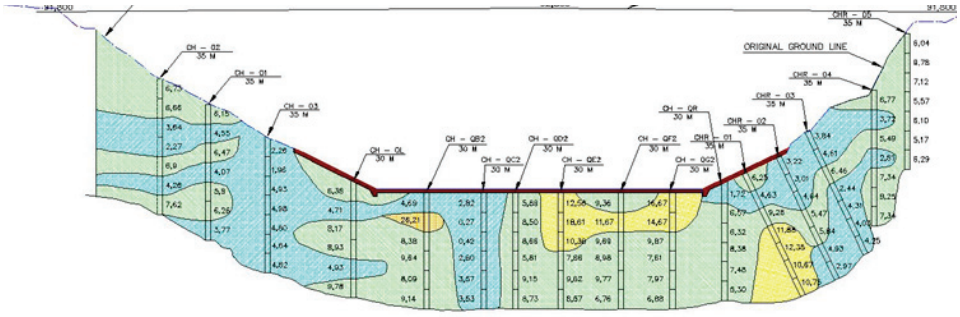

Figure 9. Lugeon value after chemical grouting phase 1

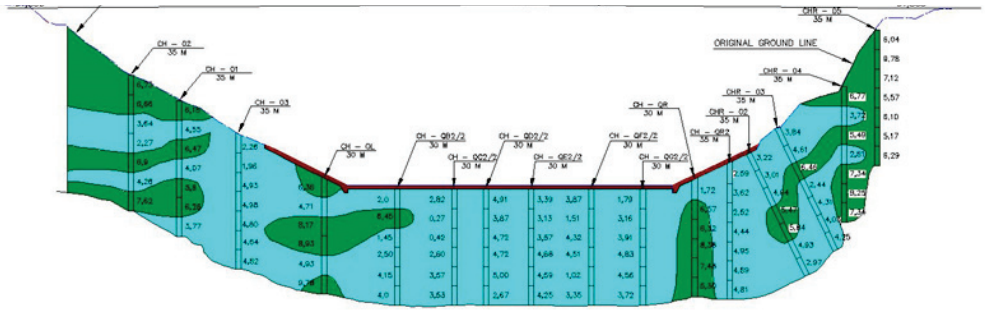

Figure 10. Lugeon value after chemical grouting phase 2

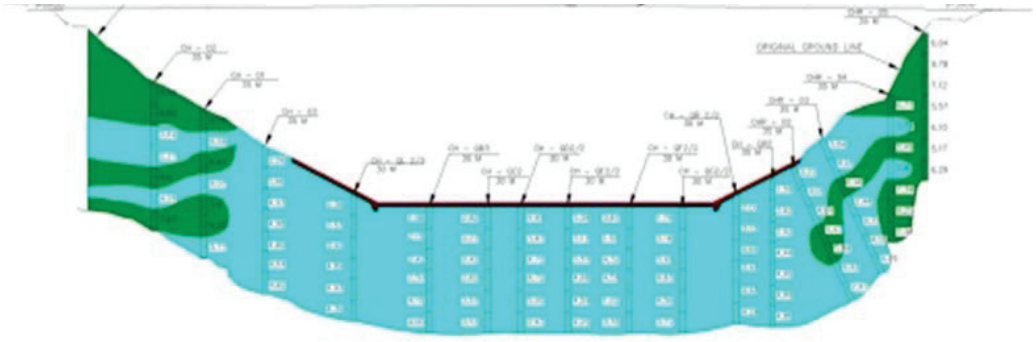

Figure 11. Lugeon value after chemical grouting phase 3

AKNOWLEDGEMENTS

The authors would like to thank Balai Besar Wilayah Sungai Brantas, Directorate General of Water Resources, Ministry of Public Works and Housing for the authorization to publish the main result of the present study. The authors would also like to express their gratitude to PT. Indra Karya as the consultant company who supervise construction of Bajulmati Dam and PT. Brantas Abipraya as the contractor of the dam.

REFERENCES

River, Lake and Reservoir Directorat, 1995. “Guidelines of Dam Grouting”, Department of Public Works.

Karya, PT. Indra, 2015, “Completion report of Bajulmati Dam Construction”, Balai Besar Wilayah Sungai Brantas.

Karya, PT. Indra, 2015, “Geological and Drilling Report of Bajulmati Dam Construction”, Balai Besar Wilayah Sungai Brantas.

5th International Symposium on Dam Safety

October 27-31, 2018

STABILITY ASSESSMENT OF SLOPE FAILURES IN SPILLWAY SITE FOR SEKI DAM-MUĞLA, TURKEY

Halil KUMSAR[1], Ali Rıza ÖZDAMAR[2]

ABSTRACT

Seki dam construction works, carried out by DSI 21st Regional Directorate in Upper Eşen Project, were stopped due to slope failures in the spillway area in the left abutment of the dam site. There are three slope failures took place diagonal and perpendicular to NE-SW trending spillway structure. Failure surfaces of slope failures developed within clayey talus and along the boundary between highly weathered ophiolite and limestone.

In this study, digitized maps of geology, cracks of slope failure and tension, topography, geotechnical borehole locations and their logs, displacement monitoring measurement locations were loaded in SLOPAC computer program written by the first author, and Seki Dam Geological and Geotechnical Information system was formed. Geomechanical parameters of weathered serpentine and clayey talus were determined, and stability assessment of slope failures were carried out by using limiting equilibrium methods. It was obtained that the reasons of slope failures are mainly, weakening of toe of the slope due to slope excavations of spillway construction, damping of excavated material to upper part of the slope, increase of pore water pressure due to groundwater storage within limestone and decrease of shearing strength of weathered serpentine under limestone.

Keywords: Seki dam, geological and geotechnical information system, slope failure, stability assesment

INTRODUCTION

Construction of Seki dam as a part of Upper Eşen Project in Muğla (Turkey) is planned as a rockfill with clay core embankment type of dam. The feasibility works for the dam project started in 1983. The first engineering investigation report of the project was prepared by Özcan Orhun in 1983. The planned spillway structure type is an uncontrolled side channel type. Engineering investigations in the planning stage were completed in 1996. Application stage of engineering studies and reporting were completed in 2014. Geotechnical boreholes were drilled, grouting, derivation tunnel construction, striping of dam foundation overburden was completed. Slope failures took place during the slope excavation in the spillway area in the left abutment of the dam. The spillway construction works were stopped due to slope instability problems. Then, geotechnical investigation of the slope instabilities were performed. In this paper, slope failure modes, factors influenced slope failures were studied and proposed engineering precautions were discussed.

[1]Professor, Pamukkale University, Department of Geological Eng., Denizli, Türkiye
e-posta: kumsarh@gmail.com
[2]Geological engineer, DSİ 21. Regional Directorate, JTH and YAS Department, Aydın, Türkiye
e-posta: arozdamar@hotmail.com

GEOLOGY

Ophiolitic mélange unit, which consists of peridotite, serpenitinite, gabbro, basalt, schist and radiolarite, forms the basement rocks in Seki dam construction site. Thickness of the unit is more than 300 m in the study area (Dallıkavak, 1996). Cretaceous aged limestone blocks were thrusted over the mélange unit (Usta and Topuz, 2016). Peridotite rocks are massive and moderately weathered, serpentinite rocks are moderately and completely decomposed. Peridotite, serpentinite and radiolarite rocks are completely decomposed along the contact zone with groundwater containing limestone blocks.

Ophiolite mélange outcrops in the embankment, cofferdam and spillway construction areas in the dam site. Limestone outcrops in the left abutment area of the dam construction site where spillway structure is located. The thickness of limestone is more than 100m (Dallıkavak, 1996).

Talus formation is composed of loose blocks and gravels of peridotite, serpentinite, radiolarite and limestone rocks. This formation outcrops on the slopes and its thickness was between 0.5m and 7m according to geotechnical borehole logs (Dallıkavak, 1996).

Alluvium is composed of blocks and gravels of peridotite, serpentinite, radiolarite, limestone, sand and silt deposited along the Seki stream.

Earth fill consists of excavated slope material damped on the upper parts of the left abutment area in the dam site (Kumsar, 2017).

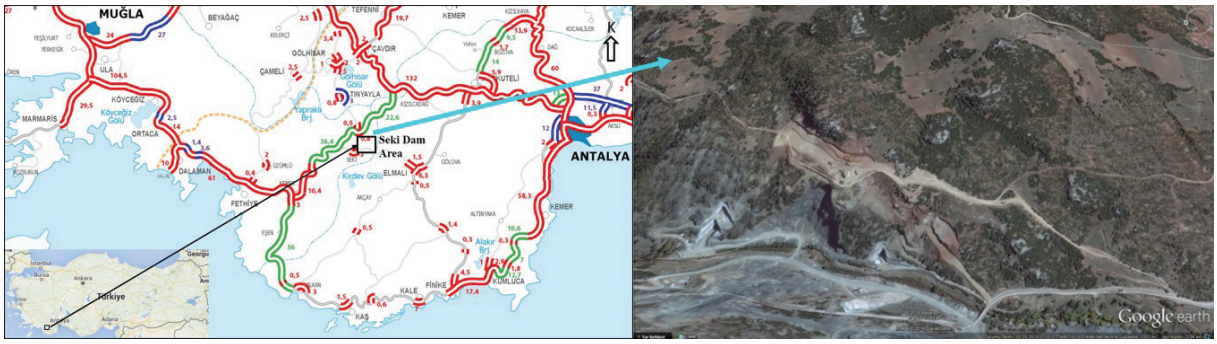

Figure 1. Map of Seki dam site area

ENGINEERING GEOLOGY

Boreholes

There are three boreholes, named as ASK1, ASK2 and ASK3, drilled in planning stage of the dam project. The derivation tunnel was planned in the right abutment of the dam site (Dallıkavak, 1996). TSK1, TSK2, TSK3 and TSK4 named boreholes were drilled along the planned tunnel line (Dallıkavak, 1996). This tunnel was cancelled according to geological structure obtained from borehole data. An alternative tunnel line was chosen by ten State Hydraulic Works of Turkey (DSI) in the right abutment of the dam site and four boreholes, named as UTSK1, UTSK2, UTSK3 and UTSK4, were drilled in the planning stage of the new derivation tunnel (Taner and Karaarslan, 2014). DSK1 and DSK2 named boreholes were drilled in the spillway construction area during the planning stage of the structure (Dallıkavak, 1996). Four boreholes were drilled in the spillway construction area during the construction stage. These boreholes are named as UDSK1, UDSK2, UDSK3 and UDSK4. Slope excavations were carried out during the spillway construction and three slope failures occurred

and affected the spillway construction area. After that, the spillway construction was stopped, slope stability investigation was started, and boreholes (HSK1, HSK2, IHSK3, IHSK4, IHSK5, IHSK6 and IHSK7) were drilled. Core samples were obtained, groundwater level were measured and inclinometer measurements were taken within the boreholes (Usta and Topuz, 2016).

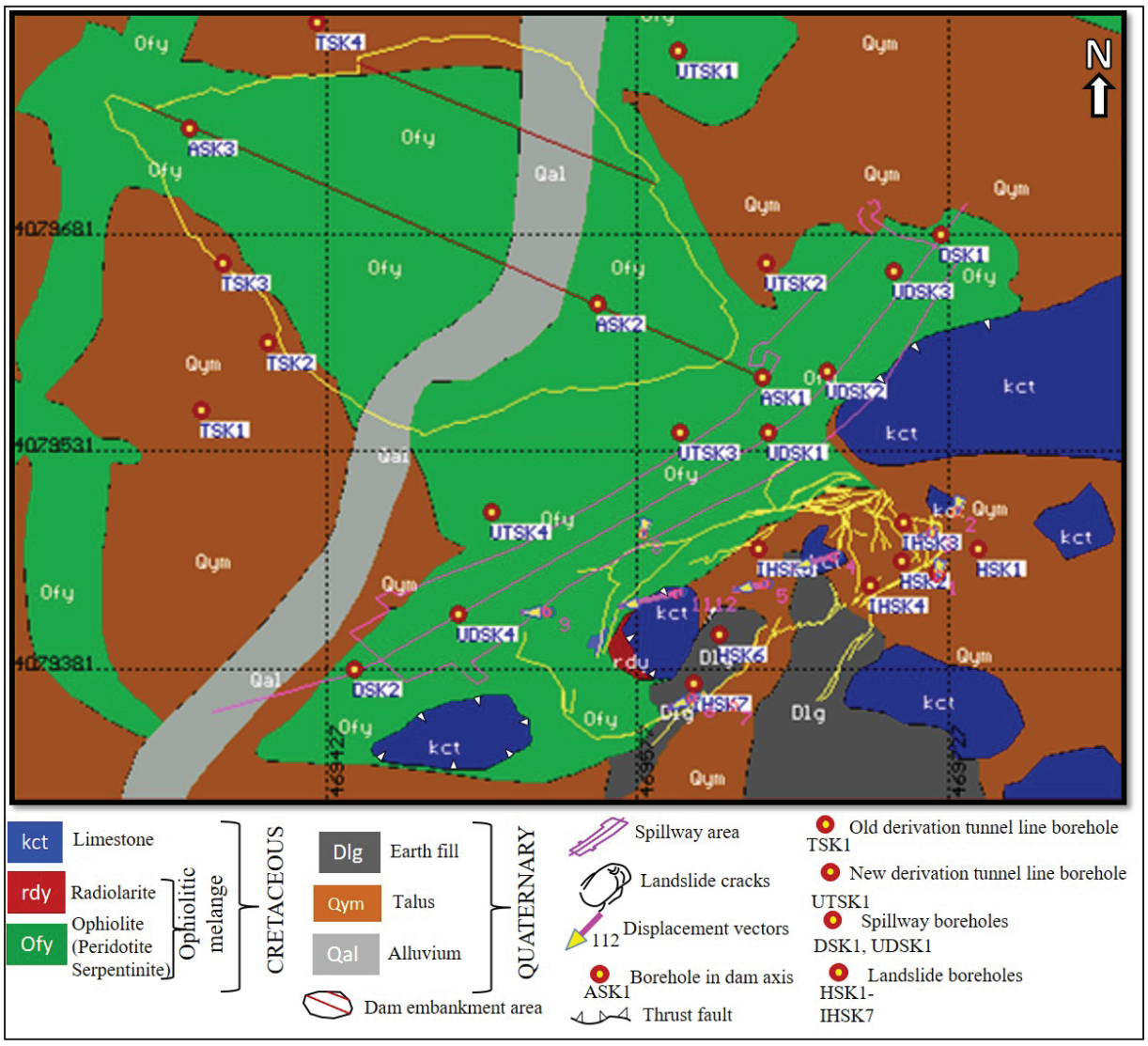

Figure 2. Geological and engineering geological map of Seki dam site (after Orhun 1983; Dallıkavak, 1996; Taner and Karaarslan, 2014; Kumsar, 2017).

Slope Failures

Slope failures took place during spillway slope excavation in the left abutment of the dam site. There are three slope failures, who affected each other, in the spillway construction area. They are named as SLD1, SLD2 and SLD3 as shown in Figure 3. LSD1 slope failure moved from SE to NW direction, LSD2 failure displaced from NE to SW direction and SLD3 failure moved from SE to NW direction (Kumsar, 2017).

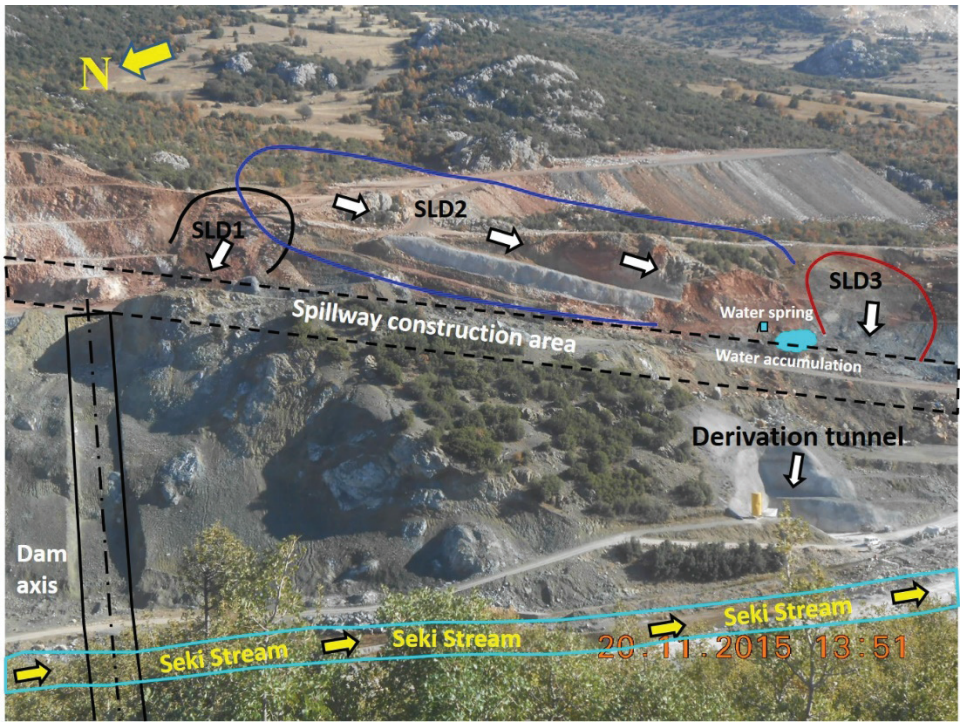

Figure 3. Slope failures took place in spillway construction site in the left abutment area.

SLD1 failure occurred on a circular failure surface within clayey talus formation, SLD2 failure took place along the contact zone between groundwater bearing limestone and underlying completely decomposed ophiolitic zone (Figure 4a, b, c and d). Excavation at the toe of the SLD2 landslide, decomposition of ophiolite due to groundwater, damping of excavated rock on the upper part of the slope had an important influence on the instability of SLD2 slope failure.

SLD3 slope failure took place on a circular failure surface that developed within the decomposed ophiolite under the influence of groundwater. SLD2 is the biggest landslide threatening the construction of the spillway structure (Figure 4).

Displacement measurements

Displacement measurements of 10 different locations in the landslide area were performed by DSI in order to determine main sliding direction and displacement velocity. The measurements were taken weekly in a period of 211 days. Resultant displacement values at 1, 2, 7 and 8 locations are less than 0.25 m. The resultant displacements were measured as 1.078 m at point 3, 2.594 m at point 4, 1.98 m at point 5, 1.99 m at point 6, 1.278 m in point 9, 3.35m in point 1112. Main displacement direction is in from NE to SW direction in the failure direction of SLD2 (Figure 5).

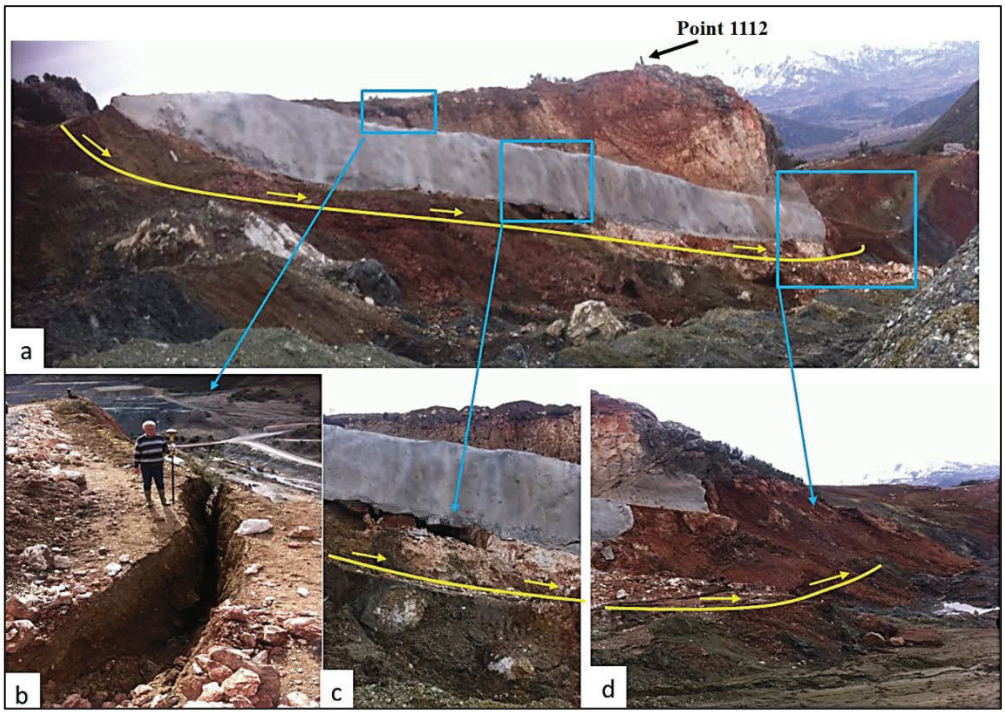

Figure 4. a) View of SLD2 slope failure, b) tension crack of the SLD2 failure, c) water bearing karstic cave within limestone block on radiolarite and ophiolite basement, d) slope excavation in the toe of the SLD2 slope failure and water accumulation.

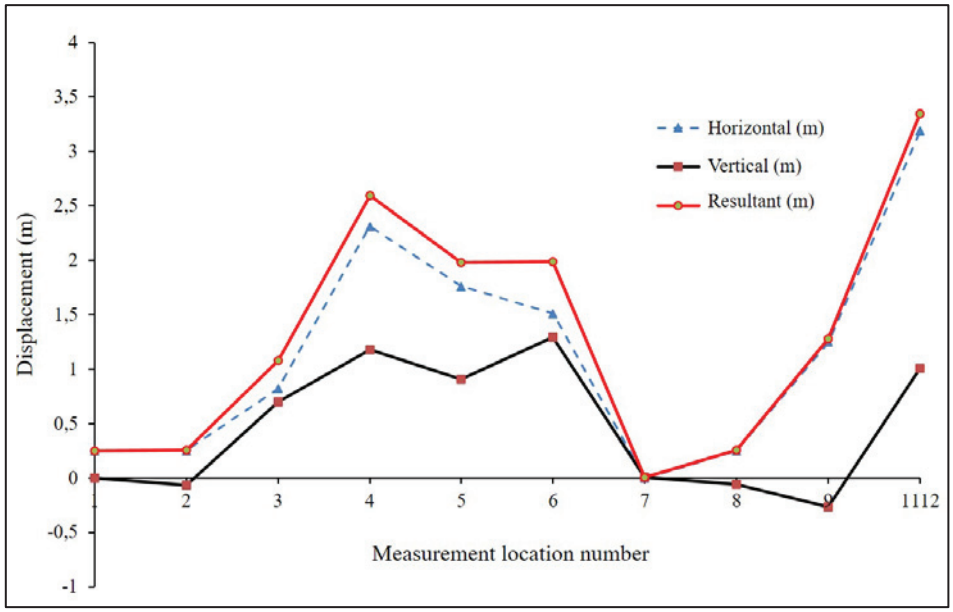

Figure 5. Change of displacement measurements in different locations in the landslide area (Kumsar 2017).

Field sampling and laboratory studies

Field studies were performed and slope failures and their mechanisms were defined. Undisturbed samples from failures surface were taken and their unit weights, water contents, cohesions (c) and internal friction angles (ϕ) were determined by carrying out soil mechanics laboratory experiments.

Table 1: Geomechanical properties of clayey talus and completely decomposed ophiolite.
S1: Clayey talus, S2: Decomposed radiolarite ophiolite mixture, S3: Saturated decomposed ophiolite S3: Semi saturated decomposed ophiolite S5: Low saturated decomposed ophiolite

Sample Name	Water content (%)	Natural unit weight kN/m^3	Dry unit weight kN/m^3	Peak cohesion (c_p) kPa	Peak internal friction angle (ϕ_p) (^{o})	Residual cohesion (c_r) kPa	Residual internal friction angle (ϕ_r) (^{o})
S1	24 - 31	18.9	14.2	45.8	12.57	44.5	10.66
S2	22-27	19.44	15.25	6.22	20.05	4.24	20.05
S3	27-38	19.0	15	39.55	15.45	37	12.45
S4	18.6	19.0	15	48.95	16.43	40.63	15.2
S5	6 - 11	17.6–20.4	13.8-15.8	86.5	43.35	65	34.15

Geological and geotechnical Information of Seki Dam

Various types of data are produced in dam construction projects. Geological and geotechnical data, which covers dam site geology, topographical map, geotechnical boreholes, laboratory experiment results, in-situ tests such as standard penetration, lugeon and pressiyometer tests, rock quality designation and weathering classification of borehole cores,

A geological and geotechnical information system for Seki dam project was written in SLOPAC computer program by Halil Kumsar, and a database mentioned above was set up (Figure 6). In SLOPAC program, a cross section can be taken from a topographical map of the project site before and after the excavations. Borehole logs can be drawn on the cross section. The user choses maximum vertical distance of borehole to the cross section line.

Slope stability analysis of SLD2 slope failure

The biggest slope failure in the spillway construction site in the left abutment area is the SLD2 landslide. This slope failure is about 200 m long and 120 m wide and the failure direction is parallel to the displacement vectors of 1112 of the measured points given in Figure 5. Therefore, its stability assessment was carried out and given in this paper.

As shown in Figure 6, the failure surface is between the basement ophiolite and overlying radiolarite and water bearing limestone blocks. There is water discharge through the failure surface at the toe of the SLD2 failure and the ophiolite in location is completely decomposed.
Undisturbed S2 sample was taken from this location (Figure 6a, b, c, d).

A cross section in H2-H2' direction on the topographical map was taken, geological and geotechnical information and borehole logs were drawn on the cross section in SLOPAC program. Boreholes 30m far from the cross section line were included on the section (Figure 7). Field observation and data were used for defining the failure surface of the SLD2 slope failure. The sliding body was divided into vertical slices (Figure 8) and geomechanical parameters of the S2 sample (i.e., c_p = 6.22 kPa, ϕ_p = 20,05^o) were used for the stability assessment of the slope.

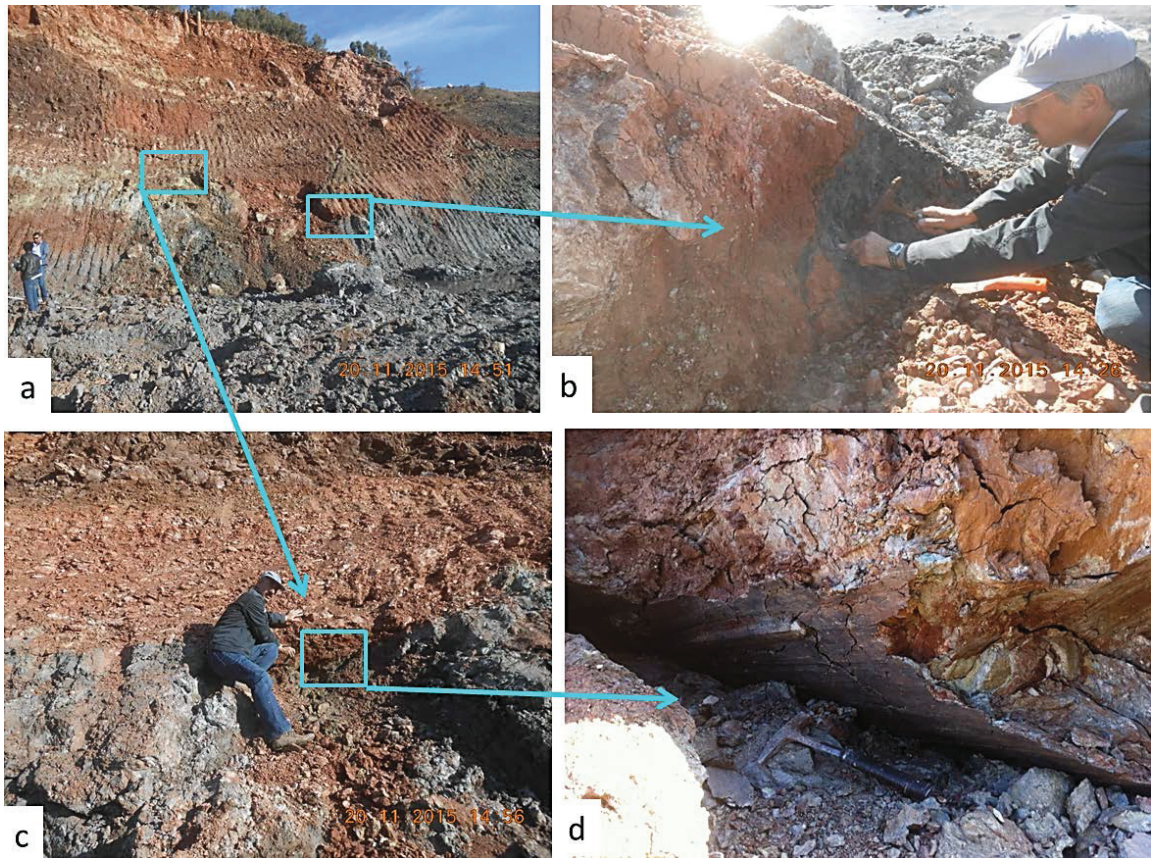

Figure 6. a) Failure surface of SLD2 landslide, b) a close up view, c) undisturbed sampling, d) striation of failure.

The stability assessment of the slope were carried out by means of limiting equilibrium methods programmed in SLOPAC program for different pore pressure ratio (r_u) values. It was found that the LSD2 landslide is stable with the factor of safety (F) 1.45 when if there is no groundwater (r_u = 0). However, there is groundwater accumulation within limestone rocks in the slope, during rainy season, groundwater accumulation and pore water pressure increases within the slope. When the r_u = 0.3-0.31, the F value becomes one, and the slope failure starts (Figure 9).

In order to prevent slope failure, earth material loading at the toe of the slope was considered and the stability assessment of the slope was calculated for different r_u values. Residual geomechanical parameters of the S2 sample (i.e., c_p = 4.24 kPa, ϕ_p = 20,05^o) were used for the stability assessment of the supported slope (Figure 10). It was found that, the stability of the slope increases up to 1.75 after earth material loading at the toe of the slope. The stability assessment of the slope against increasing r_u values depicted out that the slope becomes unstable when r_u= 0.42-0.44 (Figure 11). By considering the seismicity of the area, earth fill at the toe of the slope is not applicable for long-term stability of the slope.

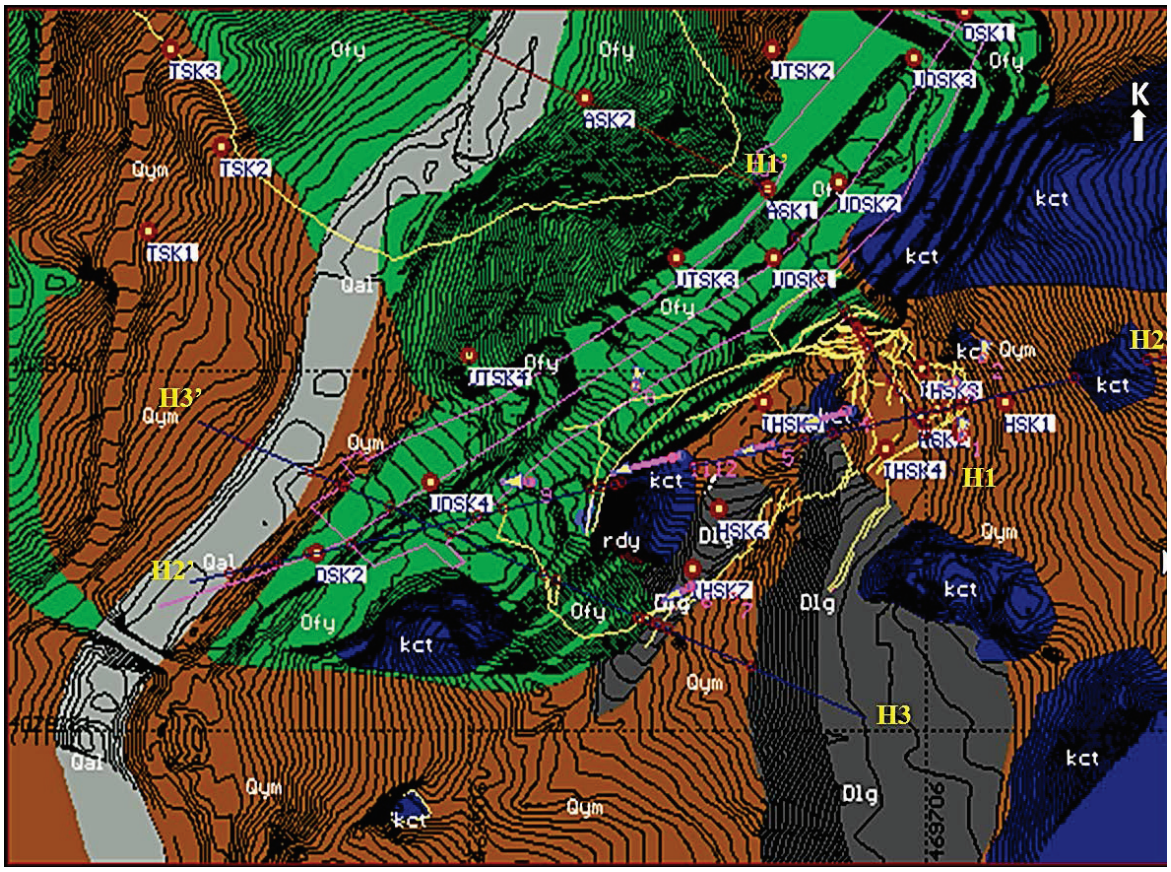

Figure 7. Geological and topographical map of Seki Dam Area and Section lines, borehole locations, displacement vectors and dam structures (for explanation see Figure 2).

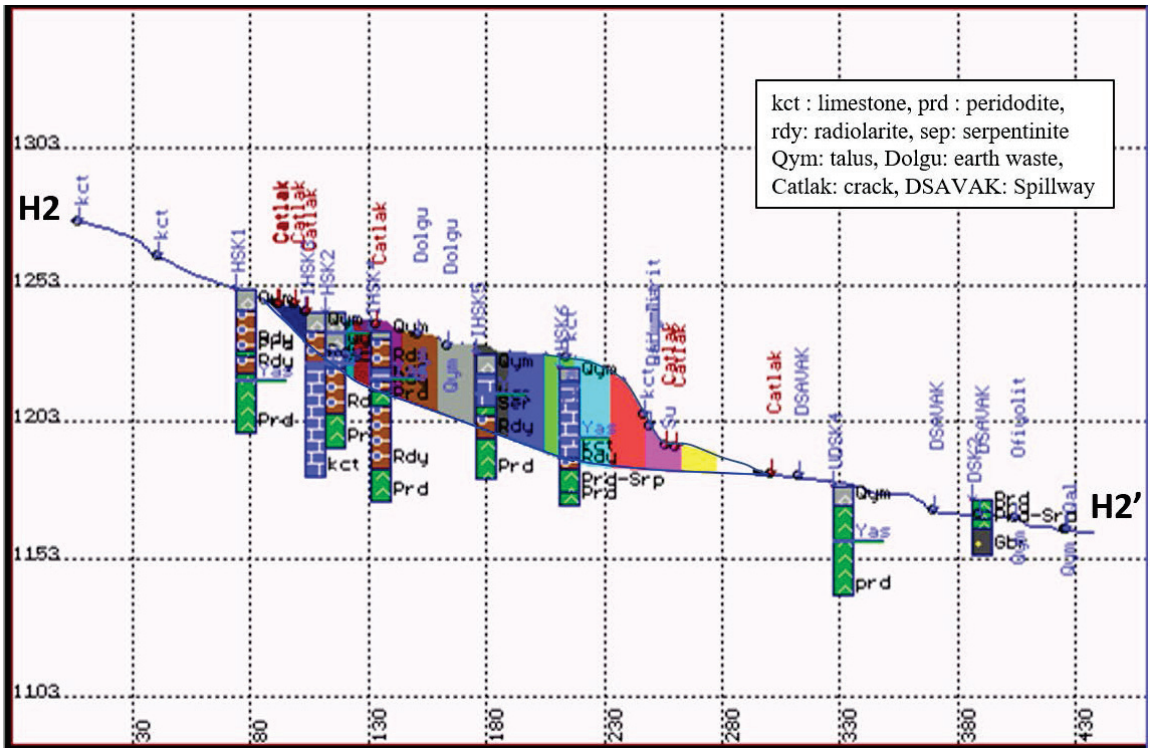

Figure 8. Topographical cross section of H2-H2' direction, borehole logs and traces of geological and construction structures on the section.

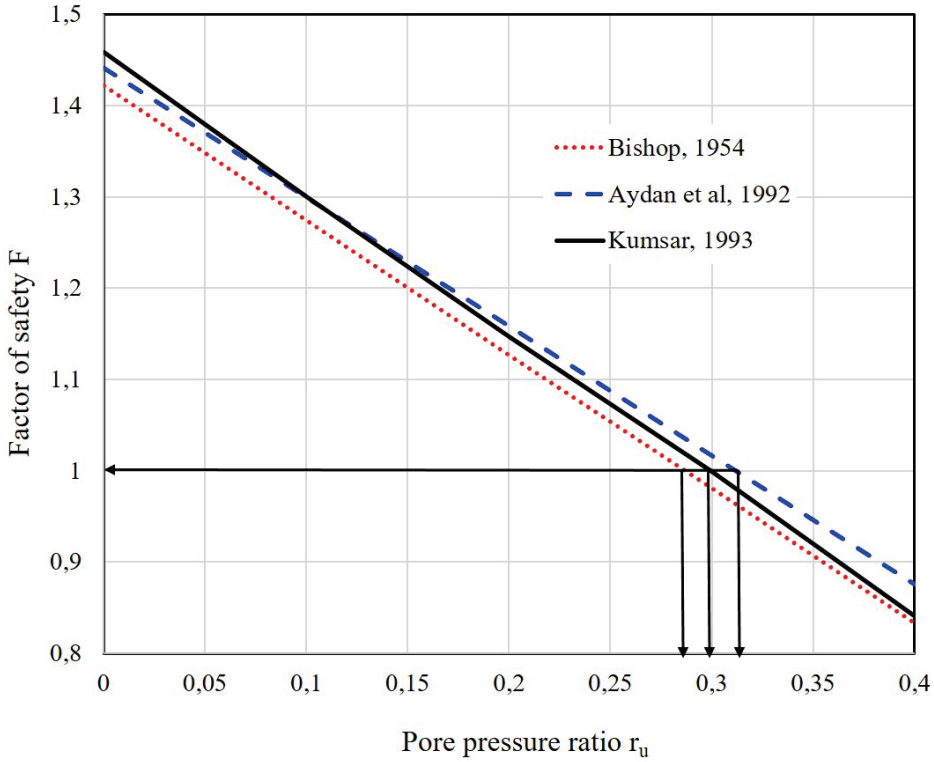

Figure 9. Factor of safety assessment of the slope for changing pore pressure ratio.

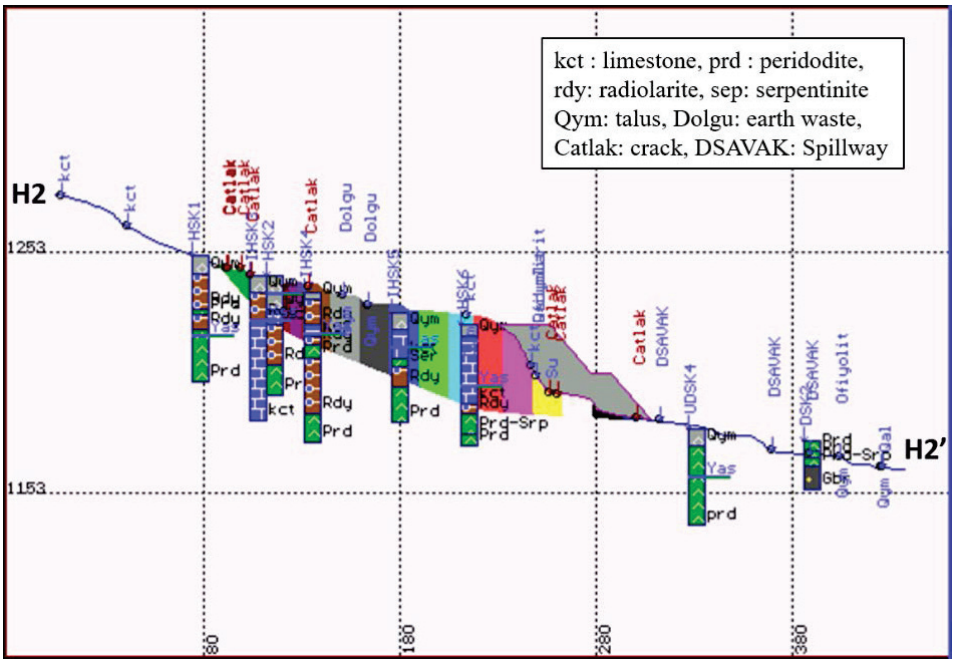

Figure 10. Earth fill support on the toe of the LSD2 slope failure on the cross section.

Terracing application of the unstable slope

Terracing application of the unstable slope was considered for long-term stability of the slope. The failed part of the slope was intented to be removed from the abutment with safe slope design parameters. 16 parallel cross sections were taken in every 20m distance (Figure 12). Slope angle and height were chosen as 30^o and 15m respectively, and bench widths were chosen as 45m, 25m and 20m from toe to upper part of the slope (Figure 13). Total excavation volume of the unstable slope in the

abutment was calculated as 408551.07m^3. Three-dimensional view of the terraced slope is given in Figure 14.

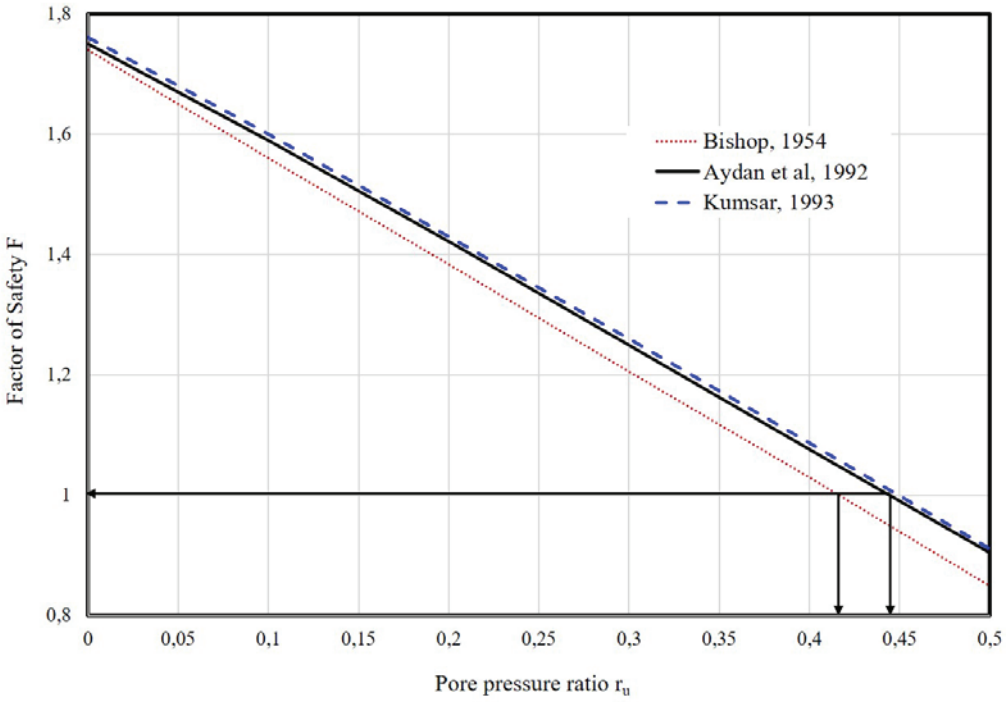

Figure 11. Factor of safety assessment of the slope for changing pore pressure ratio values for earth fill supported toe of the slope.

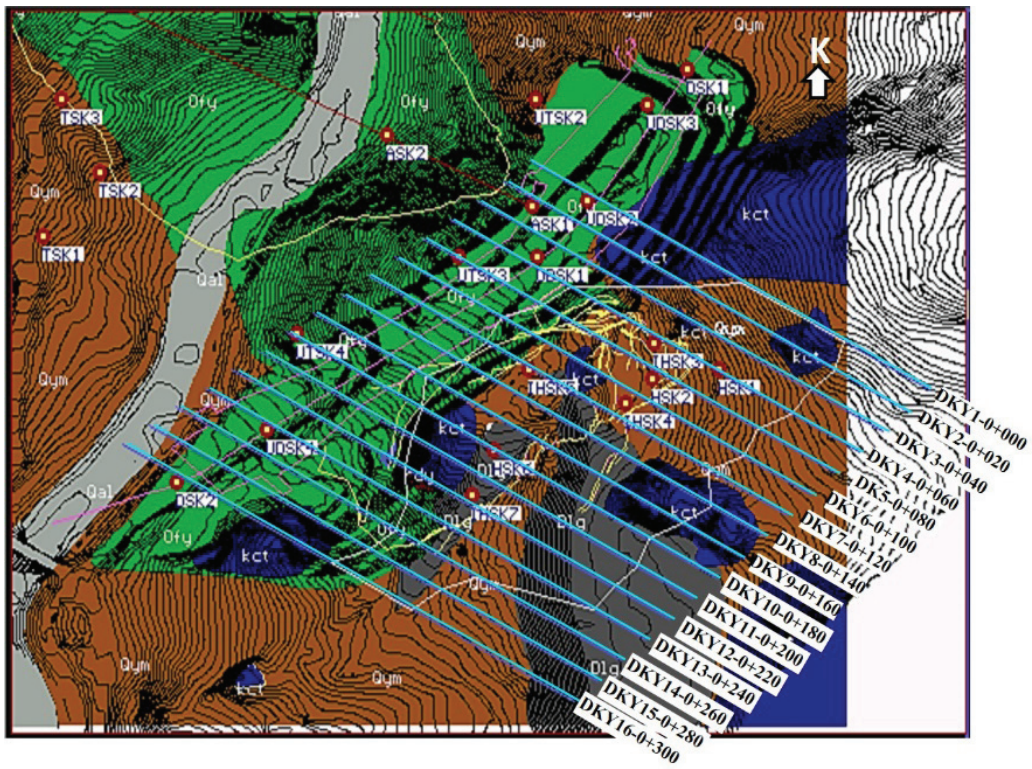

Figure 12. Cross section lines for excavation works in the unstable slope

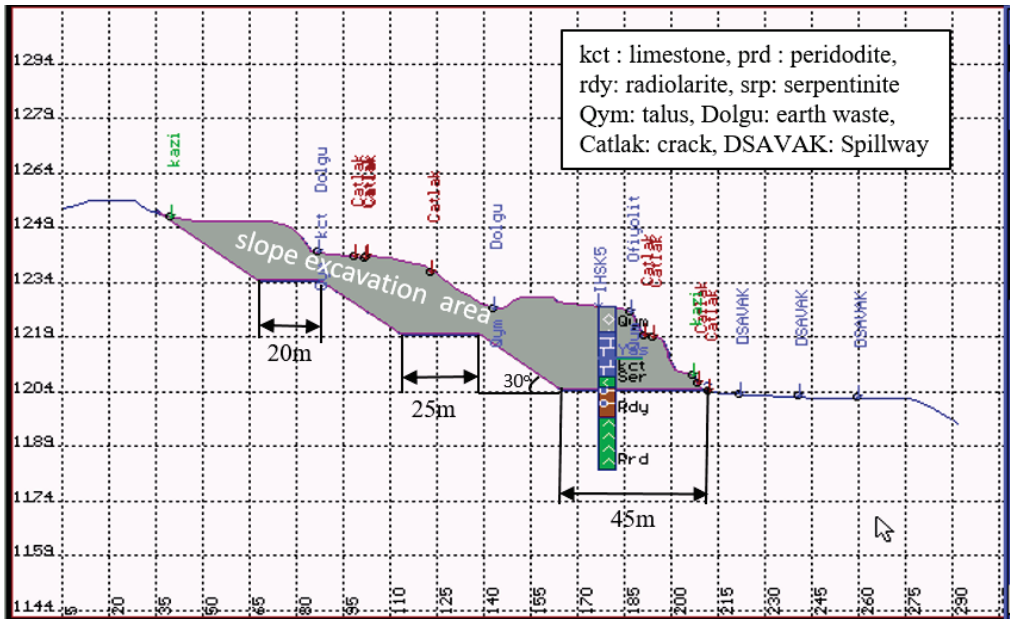

Figure13. Excavation profile of unstable slope on the cross section of DKY8 – 0+140.

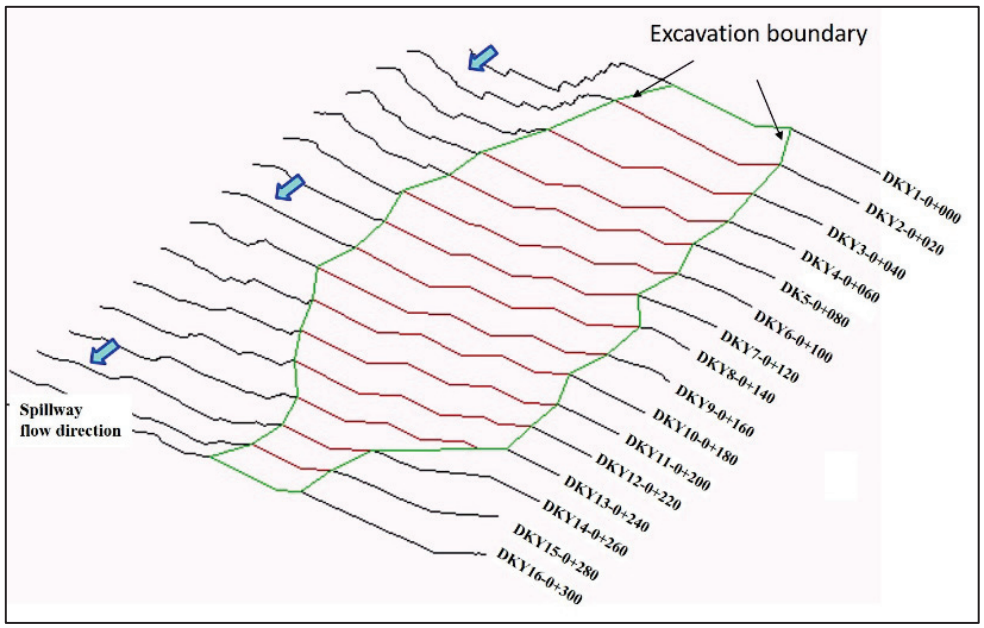

Figure 14. Three-dimensional view of the terraced slope in the spillway construction area.

COLCLUSIONS

Seki dam project was affected by slope failures in the spillway structure construction area of the left abutment of the dam site. There are three slope failures called as SLD1, SLD2 and SLD3. SLD2 failure is the largest slope failure affecting the construction of spillway structure.

Fieldworks and stability analysis of the SLD2 slope failures showed that, the main factors influenced the failure are groundwater, pore pressure within the slope, excavation at the toe of the slope and damping of excavated earth material to the upper part of the slope as a surface loading.

In order to stabilize the slope, failed part of the slope was proposed to be excavated. The total excavation volume of the earth material was calculated as 408551.07m^3.

The shear strength parameters of the ophiolite increase (c = 86.5kPa and $\phi = 65^{o}$) when water content decreases. This means that the stability of the slope increases when the slope is kept dry. Therefore, surface and groundwater drainage is vital for the stability of the slope.

Slope monitoring studies, which include groundwater level, inclinometer and surface displacement measurements, are suggested to be applied in the slope after the excavation works of the slope cut for the long-term stability of the slope.

AKNOWLEDGEMENTS

The authors would like to thank to the General Directorate of State Hydraulics works (DSİ) and Denizli Branch of DSİ for giving technical support, ICC Construction Company for supplying logistic support to the authors.

REFERENCES

Aydan, Ö., Shimizu, Y. and Kawamoto, T., 1992. The stability of slopes against combined shearing and sliding failures and their stabilization. Asian Regional Symposium on Rock Slopes, Oxford & IBH Publ., New Delhi, pp 1105-1117.

Bishop, A.W. 1954. The use of slip circle in the stability analysis of slopes. Geotechnique, Vol 5,pp 7-17.

Dallıkavak, O., 1996. Yukarı Eşen projesi Seki Barajı Planlama Aşaması Mühendislik Jeolojisi Raporu, DSİ 21. Bölge Müdürlüğü, Aydın, (unpublished report in Turkish), 42 p.

Kumsar, H. 1993. Mine Slope Stability Assessment by Uusing Inter-slice Force Transmission, PhD Thesis, Nottingham University, UK., 251 p.

Kumsar, 2017. Seki Barajı Sol Sahil Dolusavak Heyelanlarının Mühendislik Jeolojisi İncelemesi ve Şev Tasarımına İlişkin Jeolojik ve Jeoteknik etüt Raporu, Unpublished technical Report, Pamukkale University Teknokent Project, 42 p.

Orhun, Ö. 1983. Yukarı Eşen Projesi Ön İnceleme Aşaması Mühendislik Jeolojisi Raporu, 6 sayfa, DSİ, Aydın (unpublished report in Turkish).

Taner, O, Karaarslan, N., 2014. Seki Barajı Uygulama Aşaması Jeoteknik Etüt Raporu, Jeodizayn Mühendislik Müşavirlik, DSİ Aydın 21. Bölge Müdürlüğü Projesi, (unpublished report in Turkish), 61 p.

Usta, T. ve Topuz, E. 2016. Yukarı Eşen Projesi Boğalar-Seki barajı Uygulama Aşaması Jeoteknik Etüt Raporu, (unpublished report in Turkish), 146 p.

5 DAM SAFETY
İstanbul Turkey 2018

5th International Symposium on Dam Safety

October 27-31, 2018

ENGINEERING GEOLOGICAL INVESTIGATION OF BEYLERLİ DAM (ÇARDAK-DENİZLİ) SPILLWAY LANDSLIDE IN TERMS OF DAM SAFETY

Halil KUMSAR[1], Ömer AYDAN[2]

ABSTRACT

Beylerli Dam, located in southeast of Çardak district in Denizli, was constructed in 2006. Melange formation, which is made up of weathered schist, basalt, serpentinite, radiolarite, and talus formation, that contains particles and blocks of melange, outcrops in the left abutment area of the dam. Discharge of groundwater through the slope affected alteration degree of melange. There are one fossil landslide and two recent landslides that occurred in 2004 and 2009 respectively. This study covers the investigation of the reasons and mechanism of the landslide that damaged the spillway of the dam in 2009. A circular slope failure took place within weathered melange, and a wedge type of failure occurred at the crest of the circular failure in the slope were observed during field investigation. Undisturbed samples were taken from the weathered melange in which circular failure surface took place. Direct shear tests of samples were carried out under drained and consolidated conditions. Stability of the slope was assessed by using limiting equilibrium methods available on SLOPAC computer program and finite element method. As there is groundwater discharge through slope, the stability assessment of the slope was carried out by considering different values of pore water pressure ratio (r_u), and it was found that slope mass resting on circular failure surface becomes unstable when r_u value is between 0.26-0.3. Talus formation failed on a wedge surface that was formed by intersecting of a normal fault surface and a strike slip fault surface. The wedge failure will continue in the future if the toe of the slope is excavated without taking engineering countermeasures.

Key words: Beylerli dam, spillway landslide, stability analysis, discrete finite element method, dam safety

INTRODUCTION

Stability of adjacent slopes during and after the construction of dams has important influence on safety of dams. Beylerli Dam, which was constructed on Değirmendere brook in Beylerli village of Bozkurt Disrict in Denizli in Turkey (Figure 1), has a clay cored earthfill embankment type of body. Dam construction was completed in 2006. The left abutment of the dam site, where the spillway structure was constructed, suffered from slope instability problems before construction works. During the spill way construction, a circular slope failure occurred in 2004. Another slope failure was occurred in 2009 after the construction of the dam was completed. The last landslide material filled up the spillway channel (Kayahan and Kiremitçioğlu, 2009).Water level in the reservoir was lowered for safety of the dam until the spillway landslide material was removed out from the spillway cahannel and stability of the abutment was ensured (Kumsar et al., 2015).

[1]Professor, Department of Geological Engineerin, Pamukkale University, Denizli, Turkey
e-mail: hkumsar@pau.edu.tr
[2]Professor, Department of Civil Engineering, University of the Ryukyus, Nishihara, Japan
e-mail: aydan@tec.u-ryukyu.ac.jp

In this paper, failure mechanisms and their stability assesment of the spillway landslide were carried out through field and laboratory studies, analyses by limiting equilibrium and discrete finite element method (DFEM).

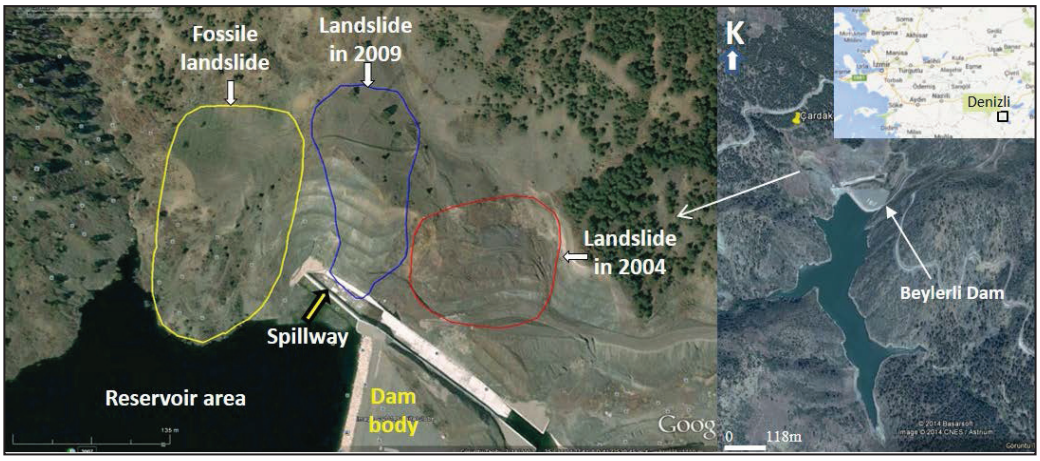

Figure 1. Beylerli dam site and the landslides in the spillway area (Google Earth, 2014)

GEOLOGY

Beylerli dam site is located inbetween the eastern part of Çardak graben and the southwest part of Taurus belt. Geology in Beylerli dam site is generally made up of Marmaris ophiolitic melange which is composed of harzburgite, sepentinite, dunite, peridotite, gabbro, basalt, diorite, limestone, radiolarite and schist blocks (Şenel, 1997; Helvacı vd, 2013). Main tectonic features forming Acigöl basin are Çardak fault, Maymundağı fault and Acıgöl fault (Toker, 2008) (Figure 2). In Beylerli dam area the melange unit contains peridotite, radiolarite, serpentinite, basalt, schist, diorite and their weathered blocks. This unit was situated in the area as a result of overtrusting. Therfore, rock blocks of this unit have too many discontinuities such as cracks, faults and schistosities (Kayahan ve Kiremitçioğlu, 2009).

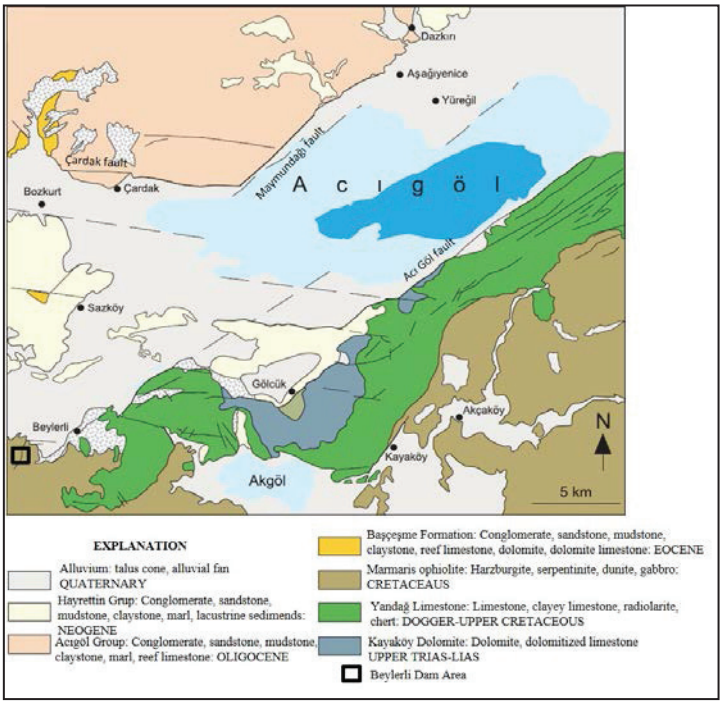

Figure 2. Geological map of Denizli Acigöl basin and Beylerli dam area (Şenel, 1997; Helvacı vd, 2013).

ENGINEERING GEOLOGY

Left abutment area of Beylerli dam site is negatively influenced by slope instabilities. There is a fossile landslide, a landslide ocurred in 2004 during the slope excavation in the abutment, and another lanslide occurred in 2009 after the construction of the dam project. Therefore, a detailed slope stability investigation in the left abutment of the dam site was carried in this study to provide geotechnical suggestions for long term stability of the slopes for the safety of the spillway structure.

Left abutment area of the spillway structure is covered by decomposed serpentinite, weathered radiolarite, basalt, diorite and schist blocks. They are overlaid by talus unit uncomformably. There is groundwater discharge at two different locations in the slope. Trapped groundwater in the slope caused serpentinite, radiolite and schist blocks to decompose and behave like soft clay (Kayahan ve Kiremitçioğlu, 2009). There are normal fault and strike slip fault planes observed in the landslide area. Slope failures ind the spillway abutment area were controlled by these tectonic structures (Kumsar et al, 2015).

A circular slope failure occurred within the decomposed clayey serpentinite and radiolarite. Unstable slope material slided downward into the spillway channel (Figure 5) and made it unusable. After the circular failure, a wedge type failure of talus material took place along the intersection line of the normal fault and strike slip fault in the crest part of the landslide area in the west as shown in Figures 3 and 4 (Kumsar et al., 2015).

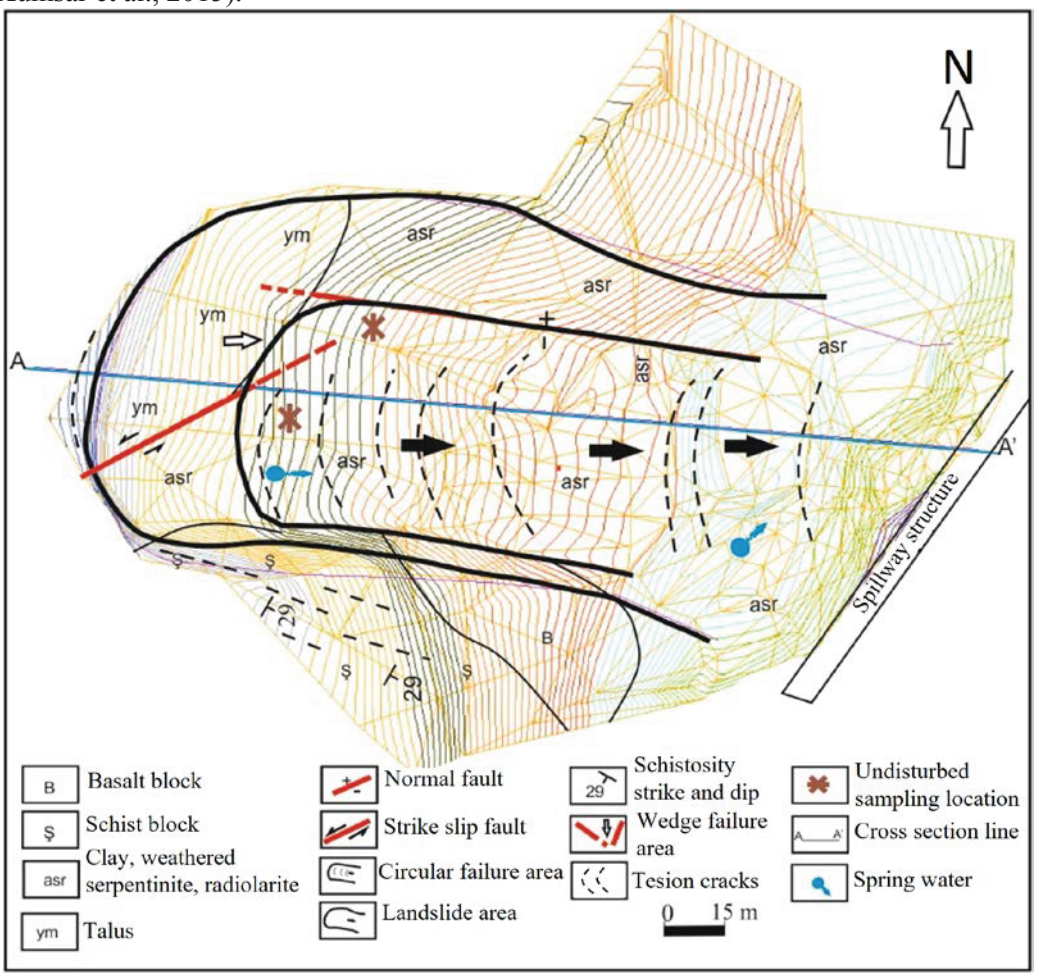

Figure 3. Engineering geology map of spillway land slide area of Beylerli dam (Kumsar et al, 2015).

Figure 4. View of spillway landslide area of Beylerli dam.

Figure 5. Landslide material in spillway structure area

Field investigations and undisturbed sampling were carried out in the landslide area. The undisturbed samples were obtained from the high degree weathered serpentinite (behaves as soft clay) and weathered radiolarite in the melange unit of circular failure area (Figure 6).

Natural unit weights of the samples range between 20,55 kN/m^3 and 22,82 kN/m^3 while saturated unit weights of the samples change between 21,86 kN/m^3 ile 23,46 kN/m^3. Shear strength tests of the undisturbed samples were performed under drained and consolidated conditions for different water contents. Shear strength parameters (cohesion and internal friction angle) of the melange unit increase in relation to the increase of water contents of samples. On the contrary, the same parameters decrease when water content increases. The particule type and size in test samples also effect the shear strength (Table 1).

Table 1. Shear box test results of undisturbed high degree weathered melange unit having different water contents.

Sample Name	Water content (%)	Peak cohesion c_p (kPa)	Peak friction angle ϕ_p (^{o})	Residual cohesion c_r (kPa)	Residual friction angle ϕ_r(^{o})
S1	12.8	32.7	20.44	25.2	21.4
S2	16	40.65	24.56	10	29.98
S3	25.07	0	29.34	0	28.18
S4	25.97	2.68	26.11	2.68	25.45
S5	25.5	8	26.61	2.65	24.41
S6	25.5	15	19.9	9	17.7

Friction angle (ϕ) of schistosity surfaces were found to be ranging between 28° and 35° from in-situ tilting tests (Kumsar et al, 2015).

Stability Assesment

Stability analyses of the spillway landslide was performed in two stages. Firstly, stability assesment of the circular failure was carried out by using limiting equilibrium method and discrete finite element method. Secondly, stability assesment of the wedge failure was done by using kinematic and limiting equilibrium methods.

Circular Failure

A digital topographic map of the slope area before the landslide occurrence was utilized in SLOPAC computer programme developed by the first author and a crossection was taken between A-A' points as shown in Figure 3. A circular failure surface was defined according to field data and, the sliding body was divided into vertical slices (Figure 6). Peak shear strenth parameters of S6 sample (cohesion =15 kPa, friction angle= 19.9^o) were used in the stability assesment. The stability assesment of the slope was performed by using Bishop (1954), Aydan et al (1992) and Kumsar (1993) limiting equilibrium methods for pore pressure ratio values (r_u) changing between 0 and 0.4 (Figure 7). It was obtained that the slope becomes unstable when the r_u value is between 0.23 and 0.26. This result is in a good agrement with the field observation as groundwater discharges were observed in two different location in the landslide area.

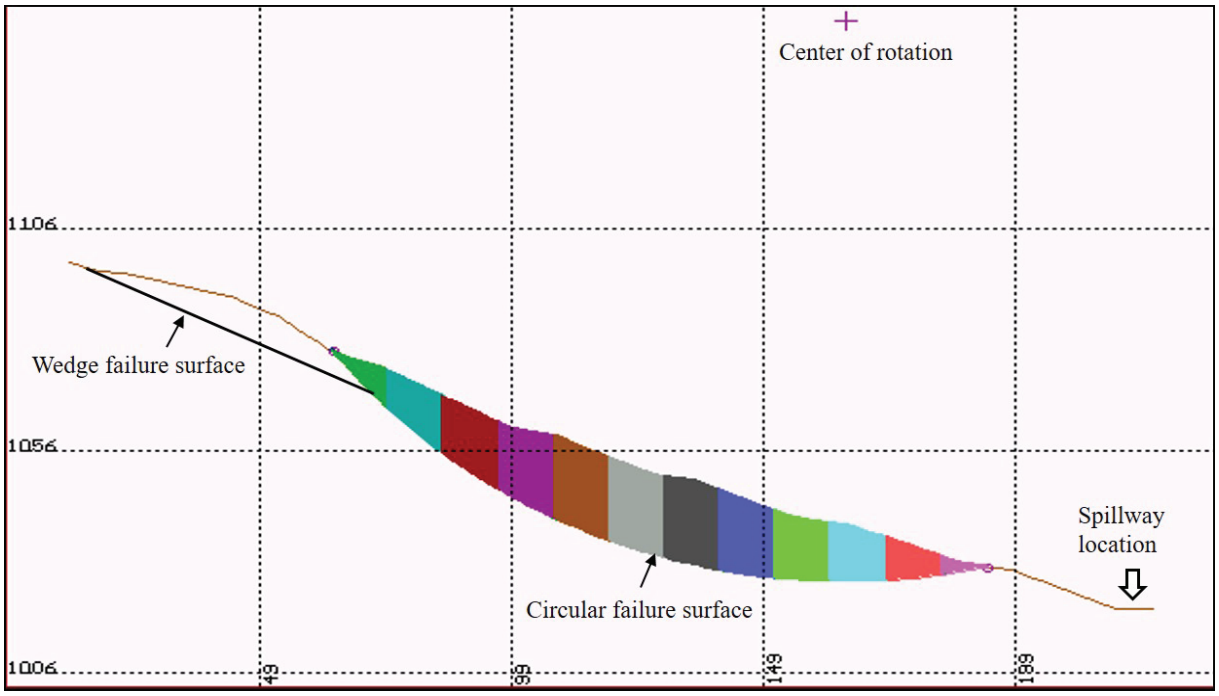

Figure 6. Circular failure surface and wedge failure surface define on the crossection in SLOPAC programme.

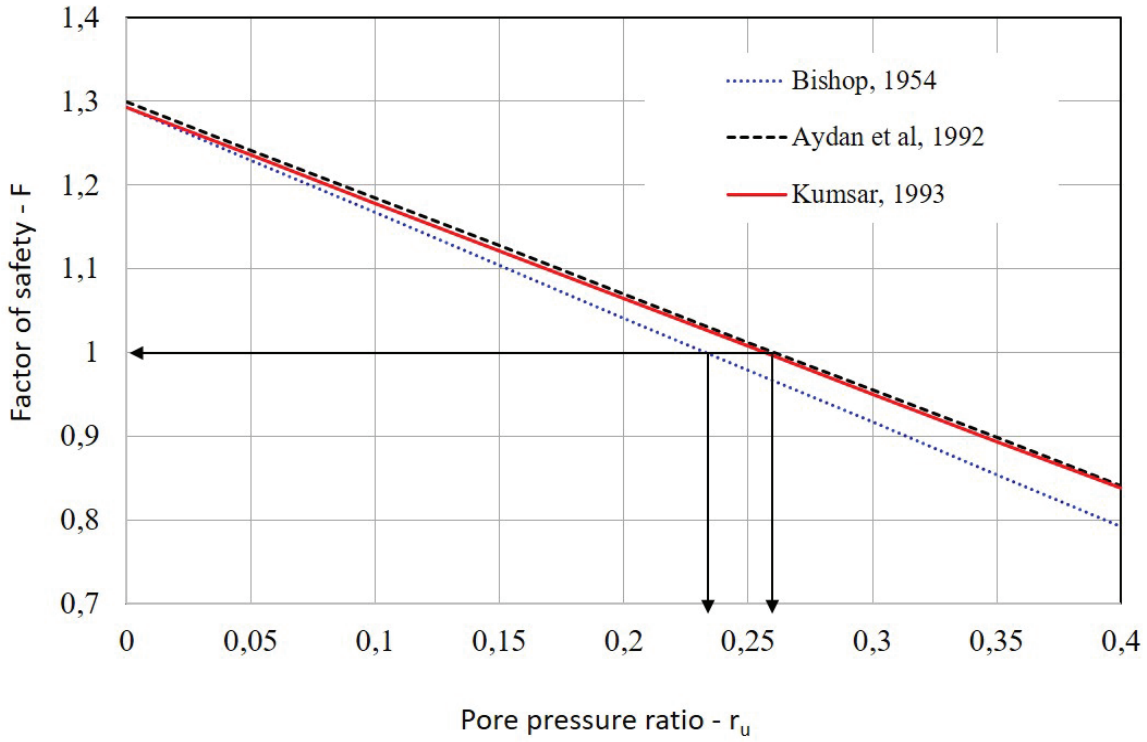

Figure 7. Change of factor of safety against pore pressure ratio whithin the slope.

In limiting equilibrium methods stability state of the sliding mass is assessed. However, deformation of unstable slope has great importance for completed engineering projects. Therefore, analyses by the discrete finite element method (DFEM) for the circular failure was performed by the second author (Aydan et al. 1996). A DFEM mesh was formed for the same circular failure surface and slices of the sliding mass (Figure 8) that was used in the analyses by limiting equilibrium methods shown in Figure 6. In the DFEM analysis, peak shear strenth parameters of S6 sample (cohesion =15 kPa, friction angle= 19.9^o) were used.

DFEM analyses results indicate that yielding does not occur when pore pressure ratio r_u is 0.0. If pore pressure ratio is greater than 0.1, partial yielding occurs. When pore pressure ratio is greater than 0.3, the slope can not remain stable (Figure 9). The results of DFEM analyses are in a good agreement with those of limiting equilibrium analyses as well as observations in the dam site.

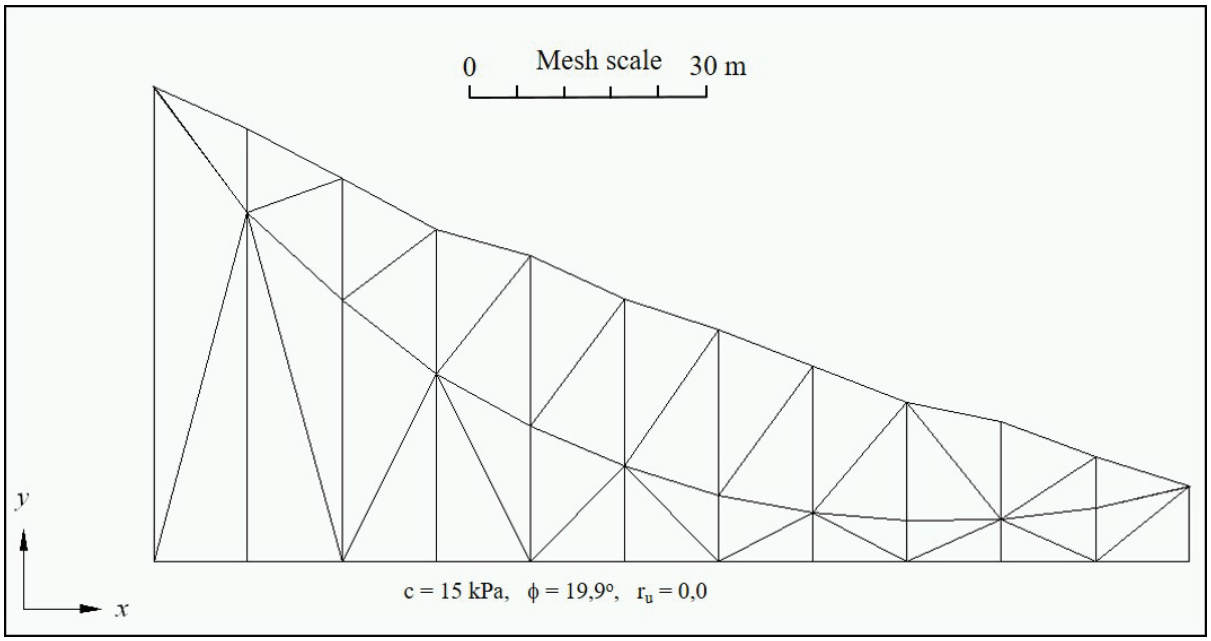

Figure 8. Mesh used for discrete finite element analyses

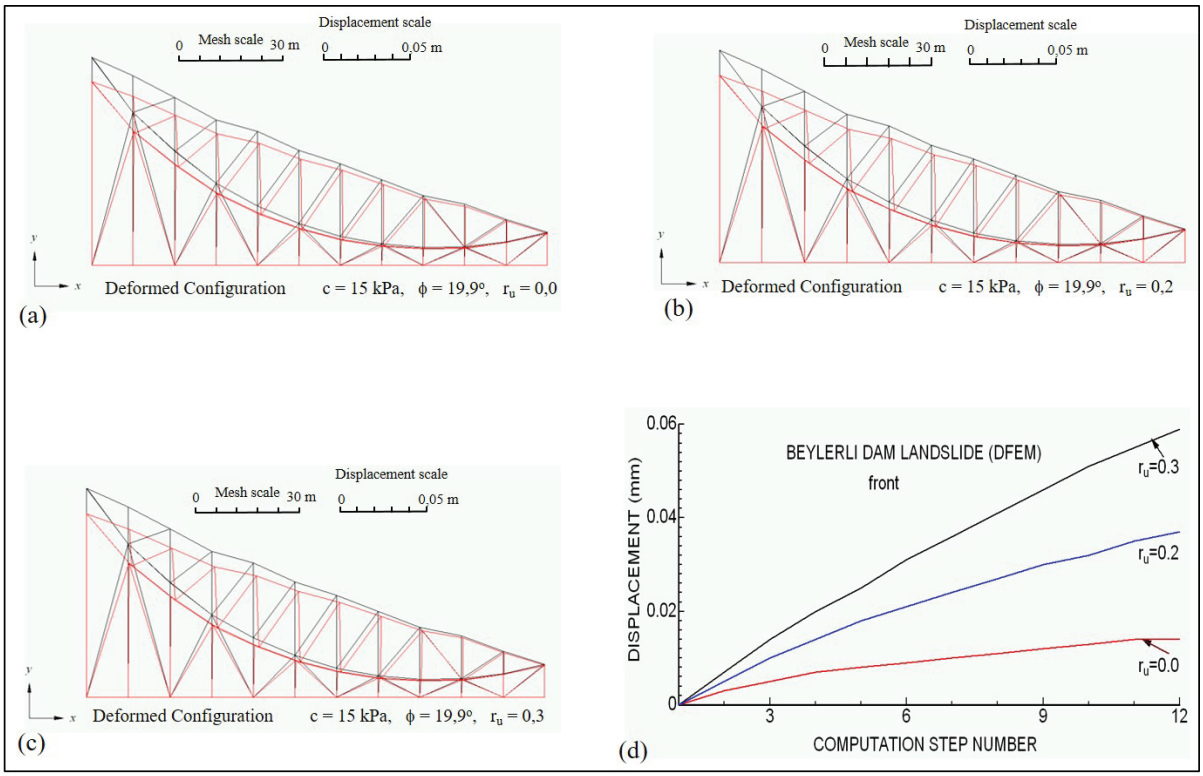

Figure 9. Displacement analyses of the slope by using DFEM for changing pore pressure raito values. a) displacement for r_u = 0.0, b) displacement for r_u = 0.2, c) displacement for r_u = 0.3, d) displacement for different r_u values and computational step numbers.

Wedge Failure

A wedge failure at the crest of the landslide area was developed after the circular failure took place at the lower part of the abutment (Figures 3 and 4). The wedge surface was formed between a normal fault surface (N72E/50NW) and a strike slip fault (N65E/55SE) surface (Figure 10a, b and c). Firm talus sediments deposited on the wedge surface slided after the circular surface took place in the toe of the wedge area. Friction angle (ϕ) of the firm talus sediments rested on the strike slip fault surface was determined as 28^o by using in-situ tilting tests.

Kinematic analysis of the wedge failure was carried out. Incliniation angle (i_a) and dip direction angle (β) of the intersection line were determined as 45.8^o and 110^o respectively (Figure 10d). Stability analysis of the wedge failure was assesed by using Hoek ve Bray (1981), Kovari and Fritz, (1972) and Kumsar et al., (2000) limiting equilibrium methods and the factor of safety of the wedge block was determined as 0.91, 0.80 and 0.80 respectivelty. These results showed that the talus formation on the wedge surface becomes unstable just after the circular slope failure at the toe of the wedge area.

During the field observations in the landslide area, groundwater discharges were observed within the melange unit caused new failures whithin the unstable landslide material. This movement caused additional slope failures in the wedge area and the road connecting villages int the west of the crest of the lanslide was damaged.

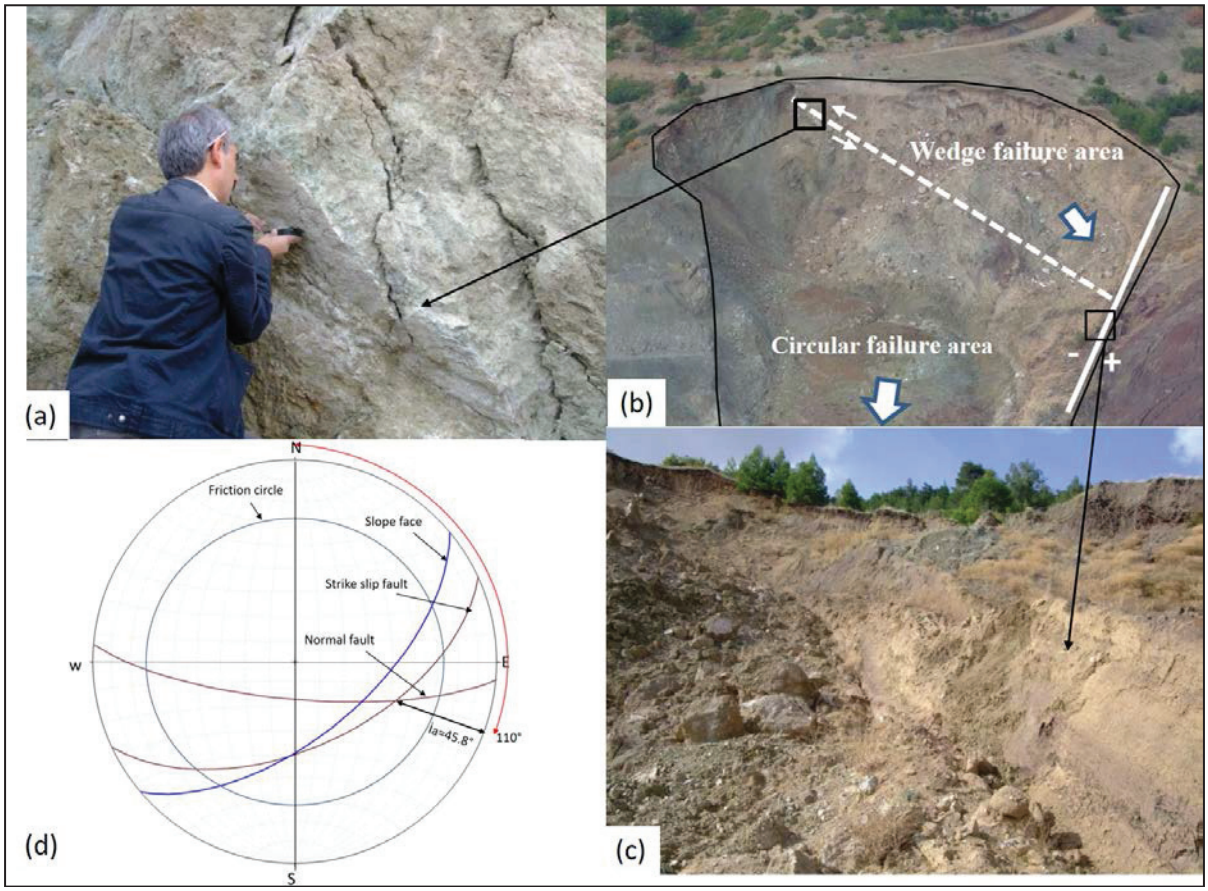

Figure 10. a) Strike slip fault plane, b) wedge failure area at the toe of the landslide, c) normal fault plane, d) kinematic analysis of the wedge failure.

CONCLUSIONS

The left abutment of Beylerli dam, where spillway structure was constructed, had been suffered from land slides before and after the construction of the dam. There were two types of failure surface in the landslide area. The first one was a circular slope failure that moved downward into the spillway

channel and made it unusable. The second failure occurred just after the circular failure at the crest area of the landslide. The main factors that caused the spillway landslide are uncontrolled groundwater discharge within the highly weathered melange unit and slope excavations.

The stability assement of the circular failure showed that the slope should be unstable if the groundwater dicharging within the slope is uncontrolled and undrained. Therefore, a detailed drainage project is urgently necessary and should be implemented in order to keep the slope stable for long term use of the spillway.

AKNOWLEDGEMENTS

The authors would like to thank to the General Directorate of State Hydraulics works (DSİ) and Denizli Branch of DSİ for giving technical support, Doğan Construction Company for supplying logistic support to the authers.

REFERENCES

Aydan, Ö., Shimizu, Y. and Kawamoto, T., 1992. The stability of slopes against combined shearing and sliding failures and their stabilization. Asian Regional Symposium on Rock Slopes, Oxford & IBH Publ., New Delhi, pp 1105-1117.

Aydan, Ö., I.H.P Mamaghani, T. Kawamoto (1996). Application of discrete finite element method (DFEM) to rock engineering structures. *NARMS'96*, 2039-2046.

Bishop, A. W. 1954. The use of slip circle in the stability analysis of slopes. Geotechnique,vol 5, pp 7-17.

Google Earth, 2014. https://maps.google.com/

Helvacı, C. , Alçiçek, M.C., Gündoğan, İ. Gemici, Ü. 2013. Tectonosedimentary development and palaeoenvironmental changes in the Acıgöl shallow-perennial playa-lake basin, SW Anatolia, Turkey, Turkish J Earth Sci., 22, 173-190.

Hoek, E., Bray, J. W. 1981. Rock slope engineering. Inst. Min. and Metall., 3rd edn., London.

Kayahan N., Kiremitçioğlu, İ. H., 2009. Denizli Çardak Beylerli göleti ve sulaması inşaatı dolusavak teknesi ve boşaltım kanalı (palye kazıları) sol yamaçta oluşan heyelan ile ilgili mühendislik jeolojisi raporu, (unpublished report submitted to DSİ), 19 p.

Kovari, K., Fritz, P. 1975. Stability analysis of rock slopes for plane and wedge failure with the aid of a programmable pocket calculator. 16th US Rock Mech. Symp., Minneapolis, USA, 25-33.

Kumsar, H. 1993. Mine Slope Stability Assessment by Uusing Inter-slice Force Transmission, PhD Thesis, Nottingham University, UK., 251 p.

Kumsar, H., Aydan, Ö., Acar, R,Z., Tahracı, Ş., Subaşı, S., Genç, O., 2015. Beylerli Göleti (Çardak-Denizli) Dolusavak Heyelanının Oluşum Mekanizması ve Nedenlerinin İncelenmesi, (*Investigation of Reasons and Mechanisms of Beylerli Dam (Çardak-Denizli) Spillway Landslide*), MUHJEO'2015, Ulusal Mühendislik Jeolojisi Sempozyumu, 3-5 Eylül, Trabzon. Edt. R. Ulusay, M. Ekmekçi, H. Ersoy, A.F. Ersoy, 106-113.

Kumsar, H., Aydan, Ö., Ulusay, R. 2000. Dynamic and static stability of rock slopes against wedge failures. Rock Mechanics and Rock Engineering, Vol.33, No.1, 31-51.

Şenel, M. 1997. Geological maps of Turkey in 1:100.000 scale: Denizli K9 sheet. Mineral Research and Exploration Directorate of Turkey, Ankara, 17 pp.

Toker, E., 2008. Acıgöl Çardak (Denizli) Grabeninin Kuzeyindeki Tersiyer Çökellerinin Tektono-Sedimanter Gelişiminin İncelenmesi. (Doktora Tezi), SDÜ, Fen Bilimleri Enstitüsü, Isparta.

5th International Symposium on Dam Safety

October 27-31, 2018

THE EFFECT OF CLAY CORE SPECIFICATIONS ON THE SEEPAGE BEHAVIOR OF AN EARTHFILL DAM

Pouya ZAHEDİ[1], Hamed Farshbaf AGHAJANİ [2]

ABSTRACT

To ensure the safety of earthfill dam during the operation phase, determining the seepage mechanism and the affecting factors are most important. In this study, the seepage behavior through body of an earthfill dam with different core shapes is investigated by 2D finite element seepage analysis via Geo Studio software. For this end, a model of earthfill dam with different heights and three core types of vertical, inclined and diaphragm is considered. In all of three types of clay cores, the core has different slopes and geometries. Also the effect of anisotropy in the permeability of the clay core and foundation of dam's material are investigated.

Based on the analysis result, seepage discharge and maximum hydraulic gradient in dam with inclined core becomes greater than dam with vertical core. With decreasing the slope of inclined core with constant width, the seepage discharge and maximum hydraulic gradient of core increase. The height of dam has direct influence on the seepage discharge and maximum hydraulic gradient. Also, by increasing anisotropy ratio of core material, seepage discharge through dam body increases and phreatic level in core goes up. By increasing anisotropy ratio of foundation material, seepage discharge and maximum hydraulic gradient of foundation increase. However, it has not significant effect on seepage characteristic through dam body. Furthermore, presence of cutoff wall in foundation of dam decreases seepage discharge from dam body and increases the maximum hydraulic gradient at the junction of core and cutoff wall.

Keywords: core slope; cutoff wall; earth fill dam; seepage discharge; anisotropy; SEEP/W software

INTRODUCTION

In recent years, fast increasing in the world population and urban development increases the need for construction and operation of dams for controlling the water resources. One of the most important aspect in designing process and maintenance of earthfill dams, is to determine the seepage through the body and foundation and identify affecting factors on leakage characteristics. The stability of earth fill dam against leakage is a critical factor in judging its safety. Any leakage through dam body and foundation may cause some unfortunate phenomena such as internal erosion, piping and foundation erosion (Choi, 2016). There are many evidences in world such as Blackman and Teton dam in USA, Mosul dam in Iraq that have been destructed by unexpected seepage phenomenon (Al-Ansari et al., 2015). Regarding to the dam safety against the above problems, the seepage through dam body should be thoroughly explored.

[1] M.Sc student in geotechnical engineering, Department of Civil Engineering, Faculty of Engineering, Azarbaijan Shahid Madani University, Tabriz, Iran, e-posta: pzahadi@ymail.com

[2] Assistance professor, Department of Civil Engineering, Faculty of Engineering, Azarbaijan Shahid Madani University, Tabriz, Iran, e-posta: h.farshbaf@azaruniv.ac.ir

Regarding to the recent development in computer sciences, numerical methods have been widely used in seepage analysis matters. In recent years, extensive studies have been performed about seepage analysis through dam body and its foundation by finite element method. Hassan-Al-Jairy (2010) has modeled and studied two dimensional water flow through a dam body, by finite element software. Asadi and Khazaei (2014) have studied seepage through the body and foundation of earth fill dam using Seep/w and Seep-3D software's. Barzegari and Uromeihy (2007) are investigated the leakage problems and treatment methods in Chaparabad dam. Malkawi and Al-sheriadeh (2000) are studied the leakage problems and treatment methods in Kefrein dam. Aghajani et al (2018) are studied the optimum cutoff wall position for rehabilitation of an inclined core dam. The implementing finite difference method for analyzing seepage in anisotropic and nun-uniform environment carried out by Ramken, Freeze and Vidraspon (Shahrbanozadeh et al., 2010).
In most of the previous studies about seepage analysis of earthfill dam, soil materials are considered isotropic and the effects of anisotropy in permeability of soil on seepage behavior is ignored. However, Fenton and Griffiths (1994), studied the seepage through dam body with considering anisotropy permeability of soil materials. Shakir (2009) is studied theoretically the effect of anisotropy permeability of soil materials on seepage through dam body.
Even though some investigations about seepage modeling of aerthfill dam, there are no comprehensive studies about the effects of core type and its geometry on seepage characteristics through dam body and the effect of anisotropy permeability of core and foundation materials on seepage through dam body. In this study, the effect of core type and its geometry on seepage characteristic through dam body is studied. For this end, an earthfill dam with height 20, 40 and 60 meters, and also with vertical, inclined and diaphragm core is analyzed. The effects of anisotropy permeability of core and foundation materials on seepage characteristics are investigated. Also the effect of presence of cut off wall in foundation of dam on seepage characteristics is studied.

NUMERICAL MODELING

The 2-D finite element analysis is conducted via Geo-Studio software to analyze the seepage through body and foundation of dam. This software is a powerful means to analyze saturated and unsaturated flow in porous media, and is widely used in the seepage analysis of dams (Krahn, 2004). The numerical model consists of a zoned earthfill dam located on the one-layer alluvial foundation. The dam body includes the clay core, shell and filter with thickness of 2 meters.
For investigating the effects of clay core type and slope on the seepage characteristics, an earthfill dam with different heights of 20, 40 and 60 meters is modeled. Besides, three types of core including vertical, inclined and diaphragm shapes are considered for each models. Four values for upstream and downstream slope of vertical and inclined core and three values for width of diaphragm core are selected which are presented in Table 1.

Table 1. The data of numerical models in seepage analysis

Core type	Diaphragm			Inclined				Vertical			
Model name	D1	D2	D4	I1	I2	I3	I4	V1	V2	V4	V5
Upstream core slope	_	_	_	1H:1V	1H:2V	1H:3V	1H:4V	1H:1V	1H:2V	1H:4V	1H:5V
Downstream core slope	_	_	_	1H:2V	1H:3V	1H:4V	1H:5V	-1H:1V	-1H:2V	-1H:4V	-1H:5V
Core width (meters)	1	2	4	_	_	_	_	_	_	_	_

In second series of numerical analysis, an inclined core earthfill dam with height of 60 m is considered which the inclined core has constant width of 4 meters in base and crest and side slope of core is selected variable as shown in Table 2. Moreover, for investigating the effects of cutoff wall on seepage behavior of dam body, the impervious cutoff wall with thickness of 1 meter, has been added to foundation of V4 and I3 models.

Table 2. The data of numerical models of inclined core with equal width in base and crest

Core type	Inclined core t			
Mode name	F1	F2	F3	F4
Upstream core slope	1H:0.5V	1H:1V	1H:2V	1H:4V
Downstream core slope	1H:0.5V	1H:1V	2V:1H	1H:4V

For studying the effects of anisotropic permeability of core materials and foundation, earthfill dam with a height of 40 meters is modeled. Two types of vertical and inclined cores are taken for each model. Various anisotropy ratio is considered for core and foundation materials. The selected values for anisotropy ratio of core and foundation materials are shown in Table 3.

Table 3. The anisotropy ratio of core and foundation in numerical model

	K_y/K_x										
foundation	1/35	1/15	1/10	1/5	1/2	**1**	2	5	10	15	35
core	1/35	1/15	1/10	1/5	1/2	**1**	2	5	10	15	35

For the boundary condition, the hydraulic head equal to reservoir elevation is assigned to upstream face of dam and top surface of upstream blanket. All nodes on the downstream face of the ground have the zero water pressure head. The lower bound and sides of numerical model are closed with the zero flux boundary condition. All analyses are conducted as the steady state 2-D seepage analysis in Geo-studio. The finite element meshing theme of numerical model is shown in Figure 1. The permeability of materials of dam body, foundation and upstream and downstream filters are presented in Table 4.

Table 4. The permeability of materials in numerical model

Materials	filter	shell	core	foundation
Permeability (m/sec)	10^{-2}	10^{-4}	10^{-8}	10^{-6}

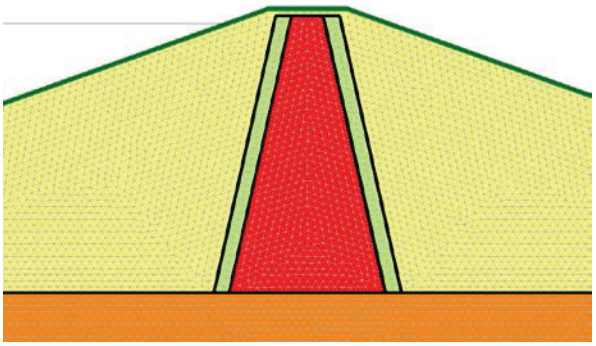

Figure 1. The finite element meshing of numerical model

NUMERICAL ANALYSIS RESULTS

The results of seepage analysis including the phreatic line and equipotential lines in different models are presented in Figure 2, for various types of clay core. The results say that by increasing the core slope, the distance between equipotential lines passed throughout the core are reduced. By decreasing the equipotential lines distance, the number of equipotential drops are reduced, and as a result the phreatic line is located at higher level in the dam body. This fact implies that in earthfill dam with steeper clay core slope, large part of the core goes under saturation and is mostly affected by wetting-drying cycles due to reservoir fluctuation. Thus, probability of cracking in higher core slope is more than in core with low slope. Also by reducing the equipotential lines distance in the core, the drop of water potential per unit width of core increases, and as a result the hydraulic gradient in the core increases.

By comparison the seepage pattern in various types of core, it can be seen that the equipotential lines in inclined core dam are located in close distance rather than vertical core, and as a result the hydraulic gradient in the inclined core is greater than vertical core, and the phreatic level in dam with inclined core is higher than in dam with vertical core. Also by increasing the equipotential lines distance, the number of equipotential drops increases, and as a result the phreatic line will locate at lower level in the dam body.

The effects of diaphragm core width on seepage characteristics are presented in Figure.2. Regarding to the results, the equipotential lines in core with low thickness is closer than the wider core, as a result the hydraulic gradient in the thinner core is greater than wider core, and phreatic level in body of dam is in higher level and large part of the core undergoes to saturation in dam with thinner core.

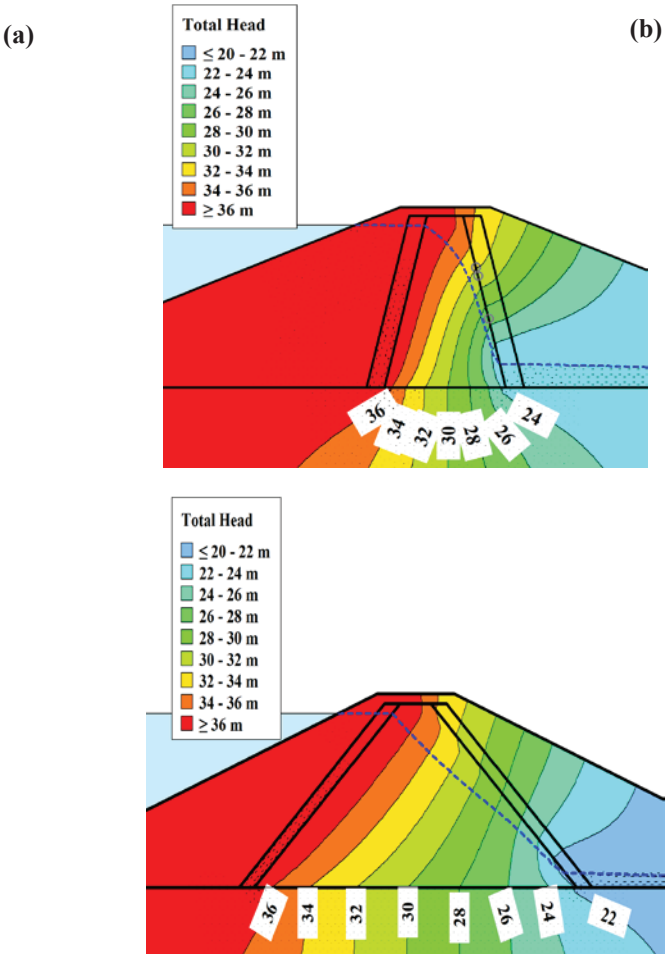

(c)

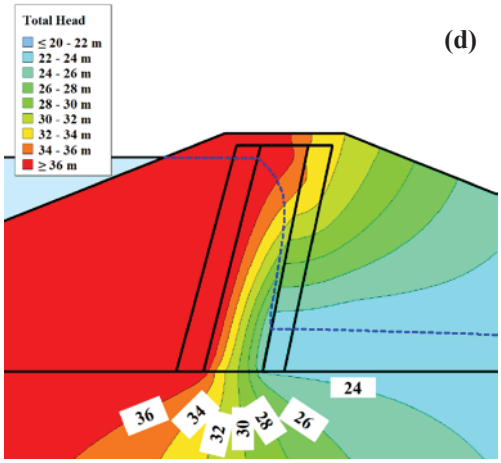

(d)

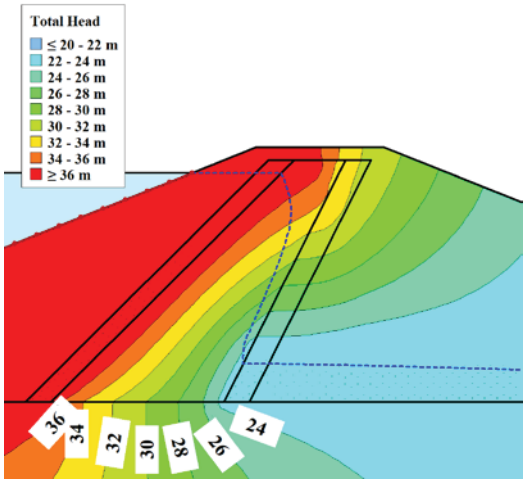

(Continues at the next page)

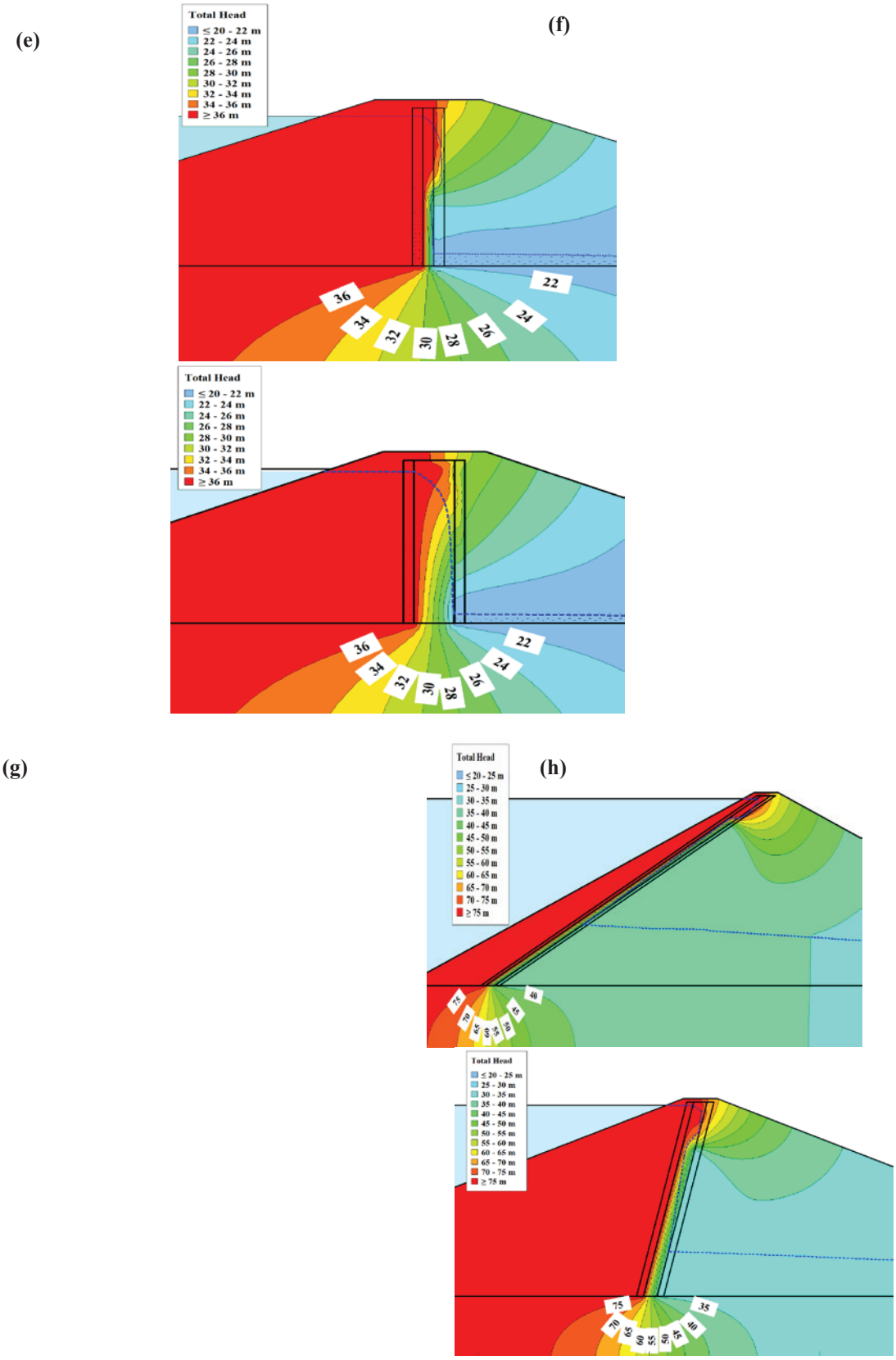

Figure 2. The flow pattern from seepage analysis of dam with height of 20m: a) V1 model, b) V4 model, c) I1 model, d) I4 model, e) D1 model, f) D4 model, g) F1 model, h) F4 model

The effect of anisotropy in permeability of clay materials of both vertical and inclined clay core dams is illustrated in Figure 3. Regarding to the results, by increasing the anisotropy ratio (K_y/K_x) from

isotropic condition (i.e. $K_y/K_x=1$), the higher area of core is affected by reservoir water and the phreatic line is located at the higher level in the core. In turn, by decreasing the anisotropy ratio (K_y/K_x) lower than one, the phreatic line in the core is located at the lower level. However, the pore pressure regime in upstream and downstream shell is not affected by anisotropy. Moreover, by changing the anisotropy ratio from isotropic condition, the equipotential lines distribution in dam body is changed. However, the distribution of equipotential lines in foundation of dam is not affected. Regarding to hydraulic gradient distribution that is presented in Figure 3-f, g, h, by increasing the anisotropy ratio from isotropic condition, the regions of core which have higher hydraulic gradient comparing with other regions, moves toward to downstream regions of core and downstream filter, and by decreasing the anisotropy ratio from isotropic condition, the regions of core which have higher hydraulic gradient comparing with other regions, spreads toward to down regions of core. In fact, by increasing the anisotropy ratio from isotropic condition, the regions with higher hydraulic gradient moves in horizontal direction and by decreasing the anisotropy ratio from isotropic condition, the regions with higher hydraulic gradient expands in vertical direction in the core. Changing in anisotropy ratio of core materials, has not any effect on maximum hydraulic gradient distribution in foundation of dam.

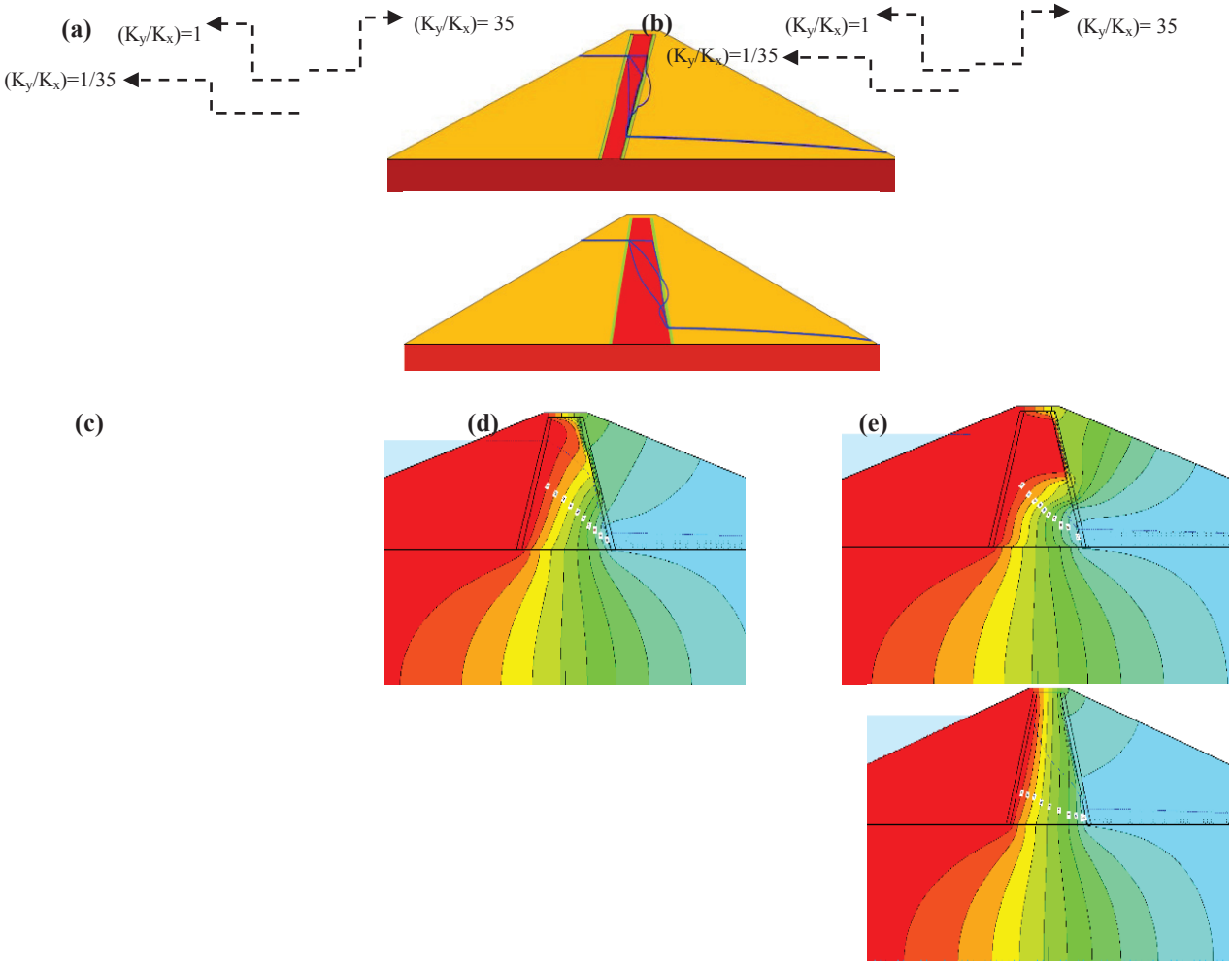

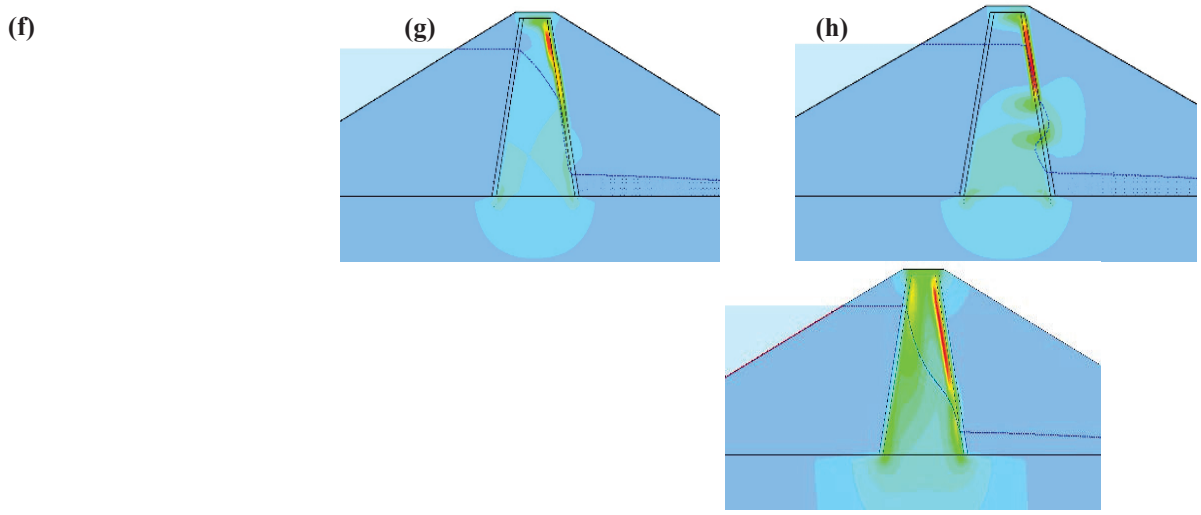

Figure 3 The phreatic line in: a) Vertical core dam, b) Inclined core dam, under various anisotropy ratio of core materials. The equipotential line in body and foundation of dam with: c) (K_y/K_x)=1/35 for core materials , d) (K_y/K_x)=1 for core materials, e) (K_y/K_x)=35 for core materials. Maximum hydraulic gradient in body and foundation of dam with f) with(K_y/K_x)=1/35 for core materials, g) (K_y/K_x)=1 for core materials, h) (K_y/K_x)=35 for core materials.

The seepage behavior in both inclined and vertical core dams with different anisotropy ratio of permeability in foundation material is shown in Figure 4. By increasing the anisotropy ratio (K_y/K_x) from isotropic condition, phreatic level in shell of dam is located at higher level, and by decreasing the anisotropy ratio (K_y/K_x) from isotropic condition, the phreatic level in shell of dam is located at lower level comparing with isotropic condition. However, it did not has any effect on the phreatic level in the core. Also by increasing the anisotropy ratio (K_y/K_x) from isotropic condition, the equipotential line distance in foundation of dam is increased, and by decreasing the anisotropy ratio (K_y/K_x) from isotropic condition, the equipotential line distance in foundation of dam is decreased. However, it has not any effect on equipotential line distribution in dam body. Regarding to the maximum hydraulic gradient distribution, by increasing the anisotropy ratio (K_y/K_x) from isotropic condition, the regions with higher hydraulic gradient in foundation spreads toward to upstream, and by decreasing the anisotropy ratio (K_y/K_x) from isotropic condition, the regions with higher hydraulic gradient in foundation spreads toward to depth of foundation. However, it has not any effect on hydraulic gradient distribution in dam body.

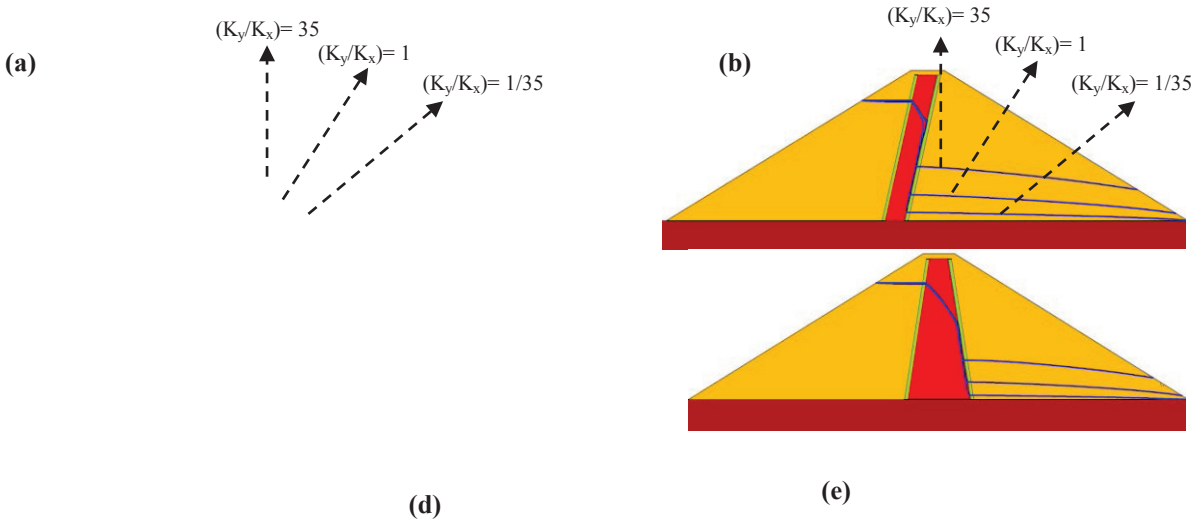

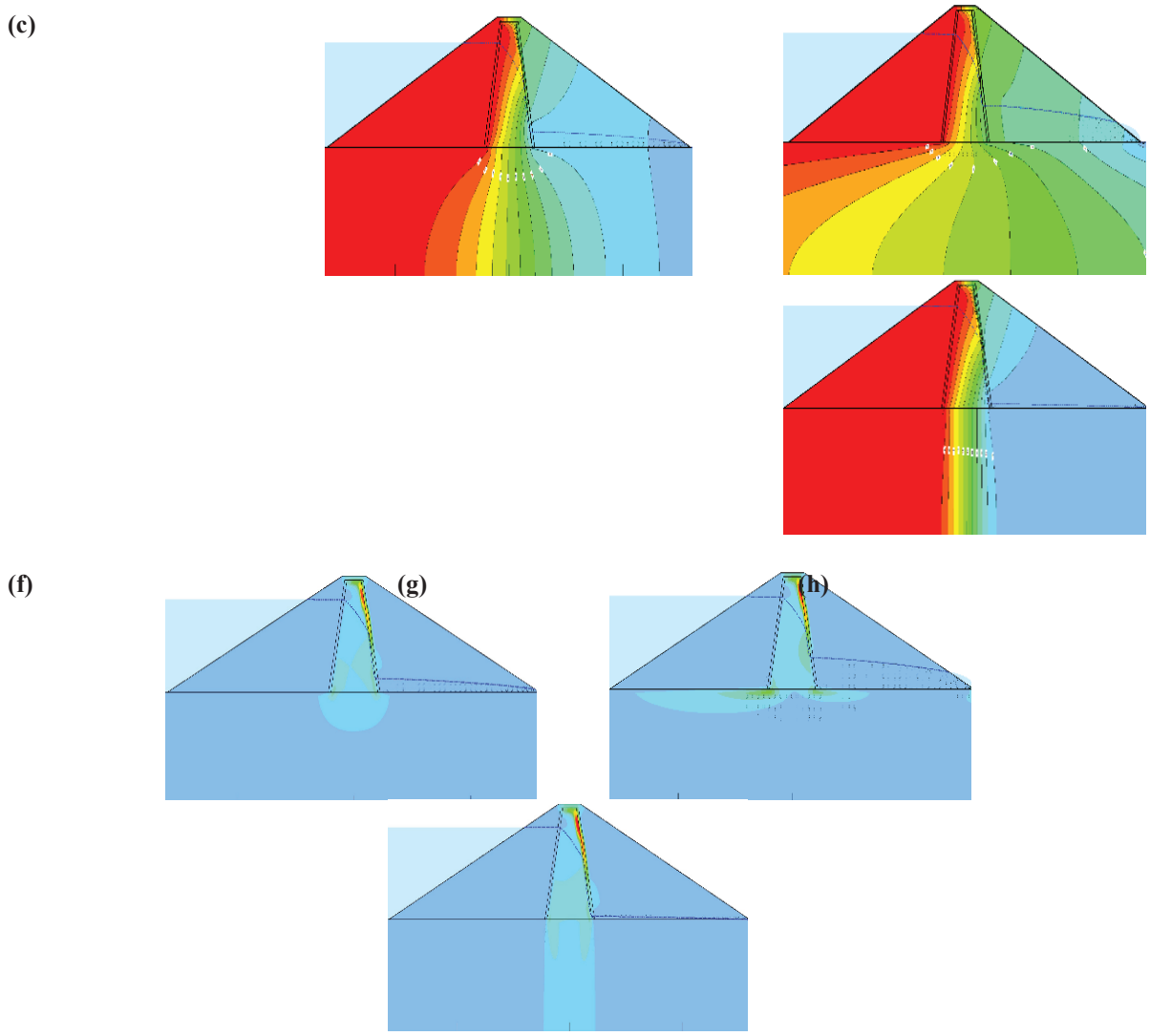

Figure 4. The phreatic line in: a) Vertical core dam, b) Inclined core dam, under various anisotropy ratio of foundation materials. The equipotential line in body and foundation of dam with: c) (K_y/K_x)=1/35 for foundation materials , d) (K_y/K_x)=1 for foundation materials, e) (K_y/K_x)=35 for foundation materials. Maximum hydraulic gradient in body and foundation of dam with f) (K_y/K_x)=1/35 for foundation materials, g) (K_y/K_x)=1 for foundation materials, h) (K_y/K_x)=35 for foundation materials.

EFFECTS OF CORE GEOMETRY ON SEEPAGE CHARACTERISTICS

In this section, the effects of core slope and core type on seepage discharge and maximum hydraulic gradient of flowing water through dam body is studied.

The Effects of Core Slope and Core Type

The graph of seepage discharge and maximum hydraulic gradient versus various core types are presented in Figure 5. As seen, by increasing core slope in both types of vertical and inclined core, seepage discharge through dam body and maximum hydraulic gradient in core tend to increases. Similarly, seepage discharge through dam body and maximum hydraulic gradient of core in models of V1 to V5 is lesser than models I1 to I4. This implies that the seepage discharge through dam body and maximum hydraulic gradient of core in inclined core dam is greater than them in vertical core dam. Increasing the slope of core causes the core width in lower elevations to decrease and, thus the equipotential lines in core lie in closer range. Therefore, the drop of water potential per unit width of

core increases, and as a result the hydraulic gradient in the core increases. According to Darcy law for water velocity through the porous media, water velocity and seepage discharge through dam body increase by increasing maximum hydraulic gradient.

The height of dam has direct influence on seepage discharge and maximum hydraulic gradient of core, and by increasing the height of dam, these two parameters increase. However, in small dam with vertical and inclined cores, the change of core slope has a few effects on the maximum hydraulic gradient of core, and it hasn't any significant effect on seepage discharge through dam body. For instance, in dam with height of 20 meters and both inclined and vertical cores, by increasing core slope from 1H:1V to 1H:4V, the maximum hydraulic gradient of core increases by 75% and 47%, respectively. Also, in this dam, by increasing core slope from 1H:1V to 1H:4V, seepage discharge through dam body increases by 24% and 170% respectively.

By increasing the height of dam, influence of core slope on the seepage discharge and maximum hydraulic gradient is obviously distinguished. In inclined core dam with height of 60 meters, by increasing core slope from upstream core slope, 1H:1V and downstream core slope 1H:2V, (I1 model) to upstream core slope, 1H:4V and downstream core slope 1H:5V, (I4 model), maximum hydraulic gradient of core and seepage discharge increase by 62% and 78%, respectively. However, in vertical core dam with same height, by increasing core slope from upstream core slope 1H:1V and downstream core slope -1H:1V, (V1 model) to upstream core slope, 1H:4V and downstream core slope -1H:4V, (V4 model), the maximum hydraulic gradient of core and seepage discharge increases by 260% and 166% respectively. Regarding to the results, hydraulic gradient rates in high dam with vertical core becomes in same magnitude of inclined core. However, seepage discharge versus various core slopes in vertical core dam is greater than it in inclined core dam.

Hydraulic gradient of core in earthdam is a critical element for ensuring the dam safety. Excessive hydraulic gradient causes to internal erosion and subsequent phenomenon such as piping. Generally, in vertical core dam the effect of core slope on hydraulic gradient is more obvious than the seepage discharge. However, in inclined core dam, seepage through dam body and maximum hydraulic gradient of core significantly dependent on core slope.

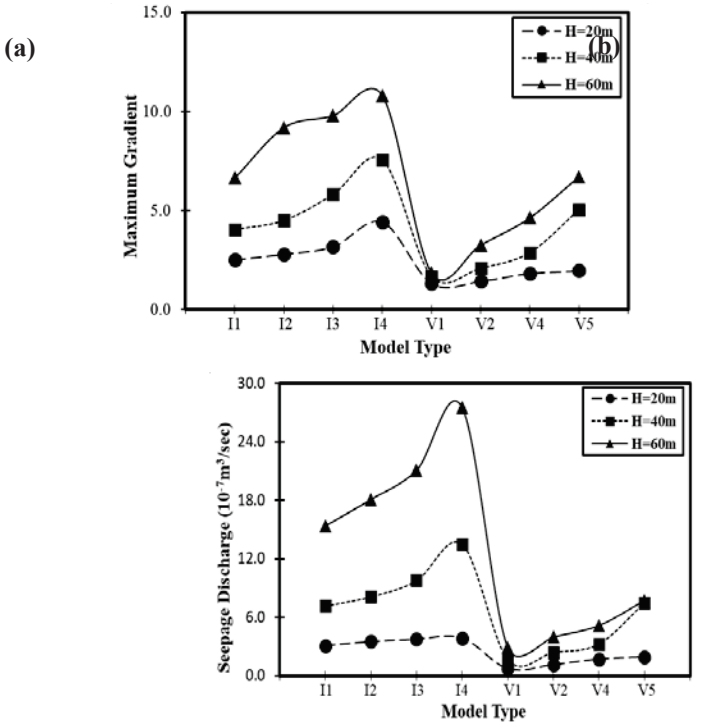

Figure 5. The graph of: a) Seepage discharge from dam body versus core slope, b) Maximum hydraulic gradient of core versus core slope, in dams with different height (H),

The Effects of Slope of Inclined Core with Identical Width at Base and Crest

The graph of seepage discharge and maximum hydraulic gradient of inclined core with identical width at base and crest at various core slopes are presented in Figure 6. As seen, by increasing core slope, seepage discharge and maximum hydraulic gradient of core are decreased. However, the rate of hydraulic gradient changes is much more than the rate of seepage discharge change. Also it can be seen that in earthfill dam with the lowest core slope (i.e. F1 model), seepage discharge gets its maximum value and by increasing core slope (F1model to F4 model) the seepage discharge from dam body is decreased a falls about one-fifth of F1 model. However, for the other models (F2, F3 and F4) the seepage discharge from dam body is close to each other. In other words, increasing core slope has not significant effect on seepage discharge reduction through dam body.
The gradual reduction of maximum hydraulic gradient of core with increasing in core slope is shown in Figure 6-b. As the dams with soil having low plastic limit are more susceptible to internal erosion, it is strongly recommended to avoid using inclined core with lower slope to prevent internal erosion of core material.

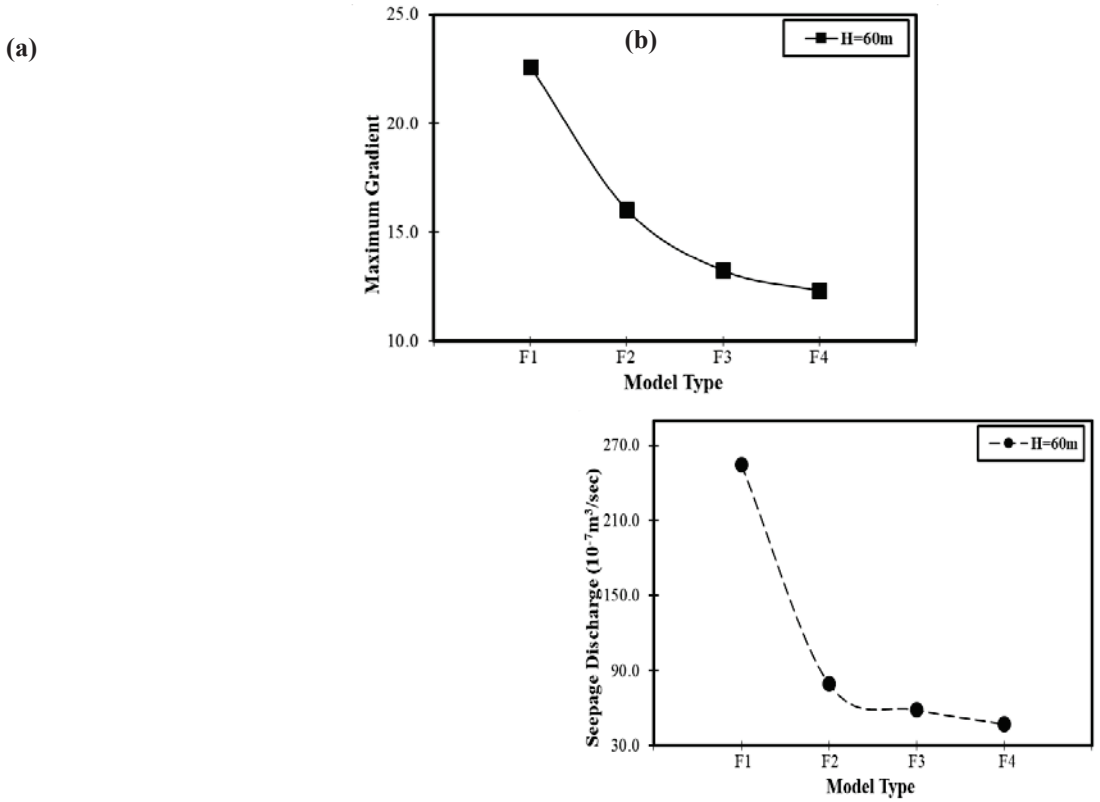

Figure 6. The graph of: a) seepage discharge from body of dam versus core slope, b) Maximum hydraulic gradient of core, versus core slope, in inclined core dams with equal core width at base and crown

The Effects of Diaphragm Core type

The graph of seepage discharge and maximum hydraulic gradient versus various widths of diaphragm type of core are presented in Figure 7. By increasing width of core in base, seepage discharge and maximum hydraulic gradient in dam core increases. However, like vertical and inclined cores, the effect of core width on maximum hydraulic gradient is more distinguished rather than seepage discharge through dam body. In small dam with height of 20 meters, increasing core width from 1 meter to 4 meters reduces seepage discharge and maximum hydraulic gradient about 72%. However, in high dam, by increasing core width from 1 m to 4 m, seepage discharge and maximum hydraulic gradient decreases by 60%. With utilizing cutoff wall, maximum hydraulic gradient reaches to 40. This high hydraulic gradient may cause core erosion and subsequent phenomenon such as piping, then stronger materials must be considered for core materials. By increasing core width up to 4 meters, maximum hydraulic gradient of core decreases more than half and reaches up to 20. However, the

graph of seepage discharge versus core width shows slight rate of change in seepage magnitude. It means that, increasing core width from 2 to 4 meters has not significant effect on seepage discharge from dam body. By decreasing core width, maximum hydraulic gradient of core increases. The main reason of this behavior can be seen in Figure 2-E and 2-F. Regarding to the results, by decreasing core width, the equipotential lines in the core get closer together, so drop of water potential per unit width of core increases, and as a result the hydraulic gradient in the core increases.

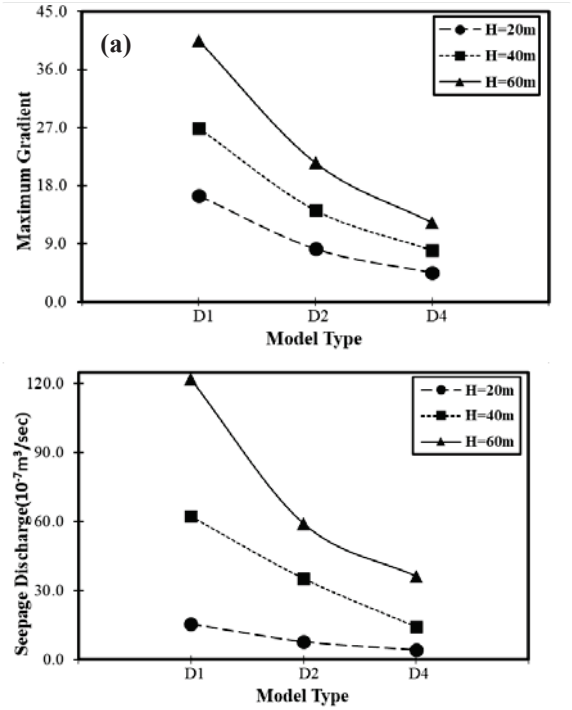

Figure 7. The graph of: a) Seepage discharge from dam body versus core width, b) Maximum hydraulic gradient of core versus core width, in dams with diaphragm core with different height (H),

EFFECTS OF CUTOFF WALL IN DAM FOUNDATION ON SEEPAGE CHARASTERISTICS

For studying the presence of cutoff wall influence on seepage characteristics through dam body, seepage analysis has been conducted with vertical and inclined core dam. The results of seepage analysis are shown in Figure 9. Regarding to the results, by utilizing cutoff wall in dam foundation, seepage discharge through dam body decreases and it doesn't has significant effect on maximum hydraulic gradient of core. However, the presence of cutoff wall causes sharp increase of maximum hydraulic gradient in intersection of core and cutoff wall, that is shown in Figure 8. The cutoff wall as an impervious membrane avoids seepage through dam foundation or by increasing seepage length in foundation of dam, reduces seepage discharge from dam foundation.

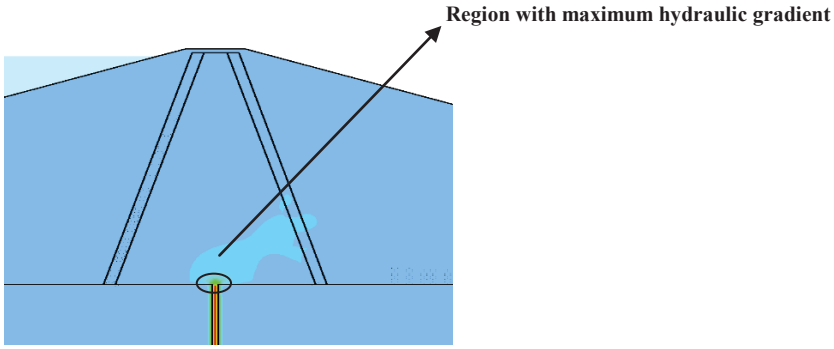

Figure 8. region with maximum hydraulic gradient which located in intersection of core and cutoff wall

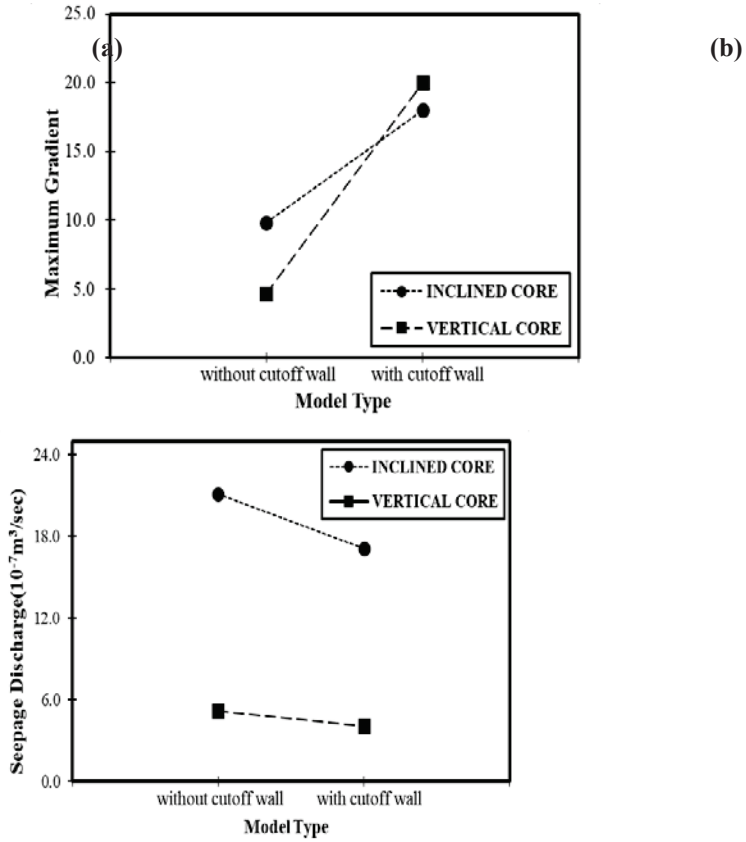

Figure 9. The graph of: a) Seepage discharge from dam body, b) Maximum hydraulic gradient of core, in models with and without cutoff wall

DISCUSION ON THE ANISOTROPIC PERMEABILITY OF CORE AND FOUNDATION MATERIALS

The Effects of Anisotropy Permeability of Core and Foundation Materials on Seepage Characteristics through Dam Body

The anisotropy effects in permeability of core and foundation materials on seepage characteristics are shown in Figure 10. Regarding to the results, by increasing the anisotropy ratio of core materials, from 1/35 to 35, seepage discharge increases. However, the anisotropy in permeability of foundation materials t has not any effect on seepage discharge through dam body. Regarding to the Figure 10, the changes of seepage discharge in case $(K_y/K_x)>1$ is greater than in case $(K_y/K_x)<1$.

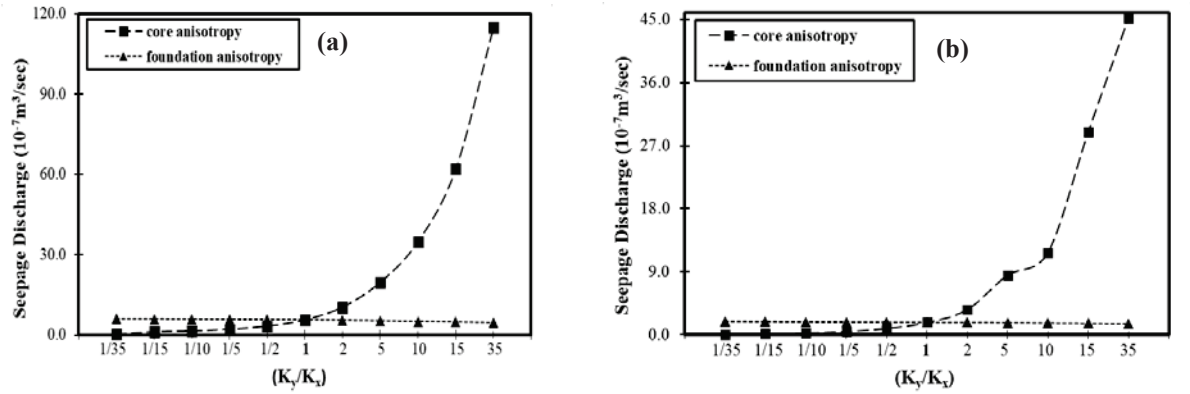

Figure 10. The graph of seepage discharge from dam body versus (K_y/K_x) ratio: a) Inclined core, b) Vertical core

The Effects of Anisotropy Permeability of Core and Foundation Materials on Seepage Characteristics in Foundation of Dam

The effects of anisotropy permeability of core and foundation materials on seepage characteristics in dam foundation are shown in Figure 11. Regarding to the results, by increasing the anisotropy ratio of foundation materials, from 1/35 to 35, the seepage discharge in dam foundation increases. However, However, the anisotropy permeability of core materials doesn't has any effect on seepage discharge in dam foundation. Regarding to the Figure 11, the changes of seepage discharge in case $(K_y/K_x)>1$ is greater than in case $(K_y/K_x)<1$.

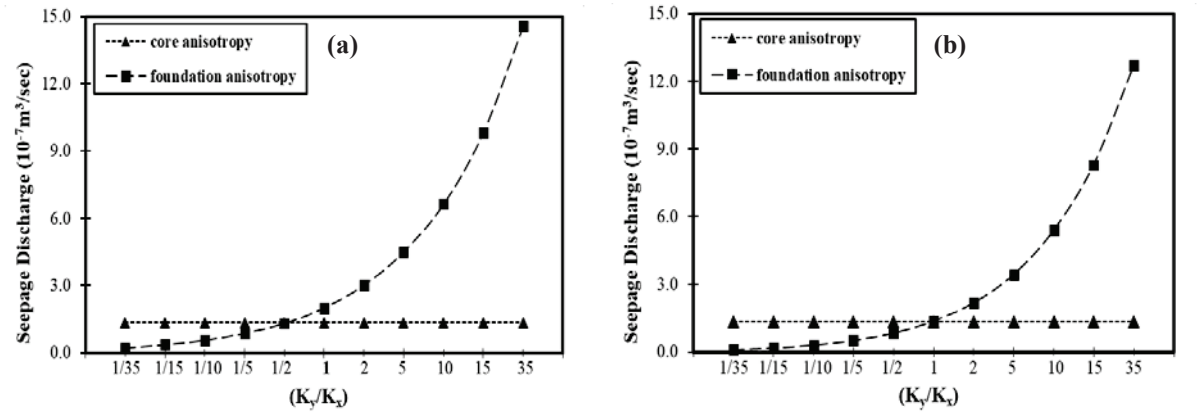

Figure 11. The graph of seepage discharge from dam foundation versus (K_y/K_x) ratio: a) Inclined core, b) Vertical core

CONCLUSION

In this research a 2D finite element method was used to study the effects of core specifications on the seepage characteristics through dam body. The main conclusions of this research can be summarized as following:

1) The seepage discharge and maximum hydraulic gradient of core, in inclined core dam are greater than vertical core dam.

2) With decreasing the slope of inclined core with constant width, the seepage discharge and maximum hydraulic gradient of core increase.

3) the height of dam has direct influence on seepage discharge and maximum hydraulic gradient of core.

4) By increasing anisotropy ratio (Ky/Kx) of core materials, seepage discharge through dam body increases and phreatic level in core goes up.

5) By increasing anisotropy ratio (Ky/Kx) of foundation materials, seepage discharge and maximum hydraulic gradient of foundation increase. However, it has not significant effect on seepage characteristic through dam body.

6) Presence of cutoff wall in foundation of dam decreases seepage discharge from dam body and increases the maximum hydraulic gradient at the junction of core and cutoff wall.

REFERENCES

Aghajani, H.F., Anzabi, M.M., Sheikhi, Z., Shokri, R., 2018. "Selecting Optimum Cutoff Wall Position for Rehabilitation of an Inclined Core Earthfill Dam". In: GeoShanghai 2018 International Conference, China,. Proceedings of GeoShanghai 2018 International Conference: Multi-physics Processes in Soil Mechanics and Advances in Geotechnical Testing. Springer Singapore, pp 252-260. doi:https://doi.org/10.1007/978-981-13-0095-0_29

Asadi, M., Khazaei, J., 2014. "Seepage Analysis in Body and Foundation of Dam Using the Seep/3D and Seep/W". Journal of Science and Today's World, Vol. 3, N. 10, 457-461.

Al-Ansari. N., Adamo. N., Issa. I., Sissakian. V., Knutsson. S., 2015. "Mystery of Mosul Dam the Most Dangerous Dam in the World: Dam Failure and its Consequences". Journal of Earth Sciences and Geotechnical Engineering, Vol. 5, N. 3, 95-111.

Barzegari. G., Uromeihy. A., 2007. "Evaluation and Treatment of Seepage Problems at Chapar-Abad Dam,Iran". Engineering Geology, Vol. 91, N. 2, 219-228.

Choi. B.I., Sin. D. H., Kim. K. Y., Kang. C.K., 2016. "Evaluation of Seepage Quantity of Fill Dam using 3D FEM Analysis". Japanese Geotechnical Society Special Publication, Vol. 2, N. 49, 1703-1707.

Fenton. G., Griffiths. D.V., 1994. "Flow through Earth Dams with Spatially Random Permeability". Geomechanics Research Center, Colorado School of Mines.

Jairy. H. H. A., 2010. "2D-Flow Analysis Through Zoned Earth Dam Using Finite Element Approach". Eng.& Tech. Journal. Vol. 28, N. 21.

Krahn. J., 2004, "Seepage modeling with SEEP/W: An engineering methodology". GEO-SLOPE International Ltd Calgary, Alberta, Canada.

Malkawi. A., Al-sheriadeh. M., 2000. "Evaluation and Rehabilitation of Dam Seepage Problems. A Case Study: Kafrein Dam". Engineering Geology, Vol. 56, N. 3, 335-345.

Sakhmarsi. A.A., Akhbari. H., Naeimi. S. P., Kiapei. A., 2014. "The Effect of the Cutoff Wall Conditions on the Seepage Characteristics of Homogeneous Earth-fill Dams using Seep/w". WALIA journal, Vol. 30, N. S2, 176-182.

Shahrbanozadeh. M. Kermani. Barani. G.A., 2010. "Modelling Seepage through Foundation of Earth-fill Dam using Seep3D. A Case Study: Shahid Abbaspor Dam". The First International Conference on Plant, Water, Soil & Weather Modelling, Shahid Beheshti University of Kerman.

Shakir. R. R., 2009. "Quantity of Flow through a Typical Dam of Anisotropic Permeability". Computational Structural Engineering. Springer Netherlands, 1301-1308.

5th International Symposium on Dam Safety

October 27-31, 2018

A NUMERICAL EVALUATION OF EXCESS PORE PRESSURE DEVELOPMENT IN CLAY-BEARING ROCK UNDER THE UNIAXIAL COMPRESSION

Hasan KARAKUL[1]

ABSTRACT

The negative effect of saturation on geomechanical properties are known and should be considered for design of engineering structures such as dams. One of the geomechanical properties of rocks is uniaxial compressive strength which is an input parameter for failure criterions used for rock masses on which dams are constructed. A great number of the dams (e.g., gravity, arch) are constructed on rock masses which include both intact rock and discontinuities. However, the excess pore pressure development, which can be developed for especially clay-bearing rocks with low permeability, change the effective stresses on rock specimens and drainage condition under which test is performed. In this study, the development of excess pore pressure under uniaxial compression was studied by using numerical analysis. The comparison of experimental and numerical studies showed that the decrement in uniaxial compressive strength due to saturation is mainly stem from development of excess pore pressures during loading. The decrement due to development of excess pore pressure is valid for clay-bearing rock used in this study. However, the interaction between fluid and rock material is also another effective parameter on decrement in uniaxial strength due to saturation.

Keywords: Geomechanical properties, clay-bearing rock, uniaxial compressive strength, excess pore pressure.

INTRODUCTION

The saturation effect on geomechanical properties of rock and soils are primarily important for different rock engineering applications (soil or rock slopes, foundation design, underground openings, dams etc.). Dramatically decreasing trends observed for geomechanical properties of rocks or soils due to saturation attracted the attention of a certain number of investigators (e.g., Vasarhelyi, 2005; Ergüler and Ulusay, 2009; Torok and Vasarhelyi, 2010; Karakul and Ulusay, 2013; Wong et al., 2016). These investigators generally focused on decreasing levels on geomechanical properties (deformability and strength parameters) of rocks by considering the saturation. However these studies did not focus on variation of geomechanical properties under different drainage conditions. The adverse effect of saturation on geomechanical properties of rocks should be considered for design of a great number of engineering structures such as dams. The uniaxial compressive strength which is one of the geomechanical properties of rocks is an input parameter for failure criterions used for rock masses on which dams are constructed. A great number of the dams (e.g., gravity, arch type) are

[1] Associate Professor, Department of Petroleum and Natural Gas Engineering, İzmir Kâtip Çelebi University, İzmir, Turkey,
e-posta: hasan.karakul@ikc.edu.tr

constructed on rock masses consisting of rock material and discontinuities and the variation of strength properties of rock materials has a great importance on design of these types of dams. Therefore in order to predict and prevent to catastrophic failures of rock masses in dam site, reliable determination or estimation of geomechanical properties (deformability and strength properties) are extremely important. However the geomechanical properties of rocks varies under different drainage conditions especially for rock and soils with low permeability. By taking into account the deficiencies in previous studies mentioned above, the variation in geomechanical properties of a clay-bearing rock due to saturation and decrement in uniaxial compressive strength encountered under undrained conditions was investigated by using experimental results and numerical simulations in this study. The main reasons in decrement of geomechanical properties of rocks due to saturation were also mentioned in this study. The occurence of pore pressure development and weakening of rock matrix were also examined by experimental and numerical studies under uniaxial loading conditions. So that the rates of the adverse effects stressed above on uniaxial compressive strength were determined for a clay-bearing rock (claystone) used in this study.

EXPERIMENTAL STUDIES

In order to investigate the effect of saturation and different drainage condition on geomechanical properties of clay-bearing rocks, the claystone which is a sedimentary rock with low permeability was used in this study. The mineral content of claystone was determined by XRD analysis and mineral content and geological age of claystone were given in Table 1. The negative effect of saturation on mechanical properties has been made possible to be observed at higher levels due to the use of rock material with high clay content. On the other hand, some difficulties were also experienced due to low core recovery during sample preparation phase for rock mechanics experiments because of the high clay content. In this study the geomechanical properties of a clay-bearing rock (claystone) was used to evaluate the effect of saturation and drainage conditions on uniaxial compressive strength. Uniaxial and triaxial tests were performed on claystone samples according to suggested method of ISRM (2007). The tests were performed on dry and completely saturated conditions and the saturation was created by considering the suggested method of ISRM (2007) (Figure1). The rock samples were saturated with water which contains 22.8 g/l of bentonite. The physical and geomechanical properties of claystone were given in Table 2.

Table 1. Mineral content of claystone

Rock type	**Age**	**Mineral Content (%)**			
Claystone	Lower Miocene (*)	**Clay (%)**	**Mica (%)**	**Feldspar (%)**	**Quartz (%)**
		72.5	12.2	4	11.3

*Dönmez et al. (2014)

Figure 1. The saturation of core samples by using vacuum saturation equipment

Table 2. The physical and geomechanical properties of claystone.

Rock type	Degree of Saturation	Uniaxial compressive strength (MPa)	Brazilian Tensile Strength (MPa)	Cohesion (MPa)	Internal friction angle (°)	Unit Weight (kN/m^3)	Porosity (%)
Claystone	Dry	10,31	1,37	1,97	42,20	21,68	20
	Saturated	6,93	0,86	1,94	36,73		

The experimental results show that the saturation creates adverse effect on strength properties of claystone. The levels of this adverse effect are 32.8% for uniaxial compressive strength, 37.2% for Brazilian tensile strength and 13% for internal friction angle of claystone. However, the decrement in cohesion due to saturation was determined too limited according to experimental results. The decrement in internal friction angle of rock material is most likely due to the effect of lubrication observed after saturation. However, there are a few parameters that can be effective on decrement in strength properties of rock such as pore pressure, weakening of rock matrix. In order to determine the level of possible development of excess pore pressure, numerical simulations were carried out within the content of this study.

NUMERICAL SIMULATIONS

In order to clarify the possible effects of pore pressures on decrement of geomechanical properties of rocks due to saturation during to uniaxial compressive test numerical simulations were carried out by PLAXIS 2D which is two-dimensional finite element software. The mesh and boundary conditions of the model were given in Figure 2.

Figure 2. Finite element model and mesh used for numerical simulations

In order to explain two different saturation conditions (dry and saturated), two different simulations were performed. While an axial loading was applied to upper edge of rock specimen, top and side edges did not fix in the model. 618 triangle elements were used in the model. The rock specimen with diameter of 5.4 cm and with height 14 cm (L/D ratio is equal to 2.5) on which uniaxial compressive tests were performed was simulated in 2D finite element model. The rock behaviour was modelled with linear elastic perfectly plastic Mohr Coulomb Model. The geomechanical properties of claystone used in finite element model are as follows: cohesion and internal friction angle are 1.97 MPa and 42.20˚, respectively; tensile strength is 1.37 MPa, Biot's pore pressure coefficient is 0.19; Young's modulus is 1.6 GPa and Poisson's ratio is 0.3 (Gerçek, 2007), respectively.

In the simulations performed for different saturation conditions, the principal stress and strain relationships which were obtained in the plastic region were compared. The duration of uniaxial compressive strength tests performed on rocks are generally 5-10 minutes as stated in standards or suggested methods. By considering the low permeability values of rocks (no matter which porosity values have), this time is generally not enough for completely drainage of water within the rock sample during the loading. So, the behaviour of saturated rocks tested under loading is generally not completely drained. So, the effective stresses should be calculated to obtain strength properties. Karakul and Ulusay (2013) stated that strength properties of saturated rocks are vulnerable to pore pressure and weakening of matrix material by interaction between water and rock minerals (especially clay minerals). So, in order to consider the effect level of excess pore pressures induced during uniaxial loading the undrained analysis was also carried out in this study. In undrained analysis of Plaxis 2D the excess pore pressures were also calculated besides other stress components.

Numerical analysis indicates that rock material (claystone) fails with 8.8 and 7.8 MPa axial stresses under drained and undrained conditions, respectively (Figure 3 and Figure 4). As it is clear from Figure 5 that the difference is mainly due to development of excess pore pressure under undrained loading condition. It can be also stated that while the material behaviour obtained under drained condition was brittle, ductile type of material behaviour observed under undrained condition. On the other hand, the experimental compressive strength values determined for dry and completely saturated conditions are 10.31 and 6.93 MPa, respectively. While the decrement level of uniaxial compressive strength is 11.4% for numerical analysis, this value is close to 32.8% by considering the experimental values. However, the weakening of rock matrix as a result of interaction between water and clay minerals could not be considered in numerical simulations. So why the experimental values are higher

than the values found by numerical simulations refers to another parameter which controls the weakening of rock matrix and is effective on this decrement due to saturation. Karakul and Ulusay (2013) defined this parameter as Effective Clay Content-ECC which is a product of porosity and clay content of rocks. So, it can be expressed that the 21.4% of 32.8% is due to weakening of rock matrix as a result of interaction between fluid and clay minerals. The occurrence of excess pore pressure is also mainly deal with the volumetric strain developed in rock sample. Excess pore pressure values are close to 2.9 MPa at some points within the modelled rock sample on which volumetric strain values are high. Figure 5 shows that while the values of excess pore pressure are low around the plastic regions in test specimen, these values increase close to elastic region. Excess pore pressure values contribute on decrement of both effective stresses and strength properties of rock sample. The effect of Biot's pore pressure coefficient on excess pore pressure was also studied within the content of this study. In addition to original value (0.19) of α, 0.3 and 0.6 values of α were also used in numerical simulations. The excess pore pressure distribution obtained for 0.3 and 0.6 values of α were given in Figure 6. It can be inferred from Figure 6 that maximum excess pore pressure values (3.49 and 4.03 MPa) increase due to increment in Biot's pore pressure coefficient. It means that increment in elastic strains creates higher excess pore pressure development.

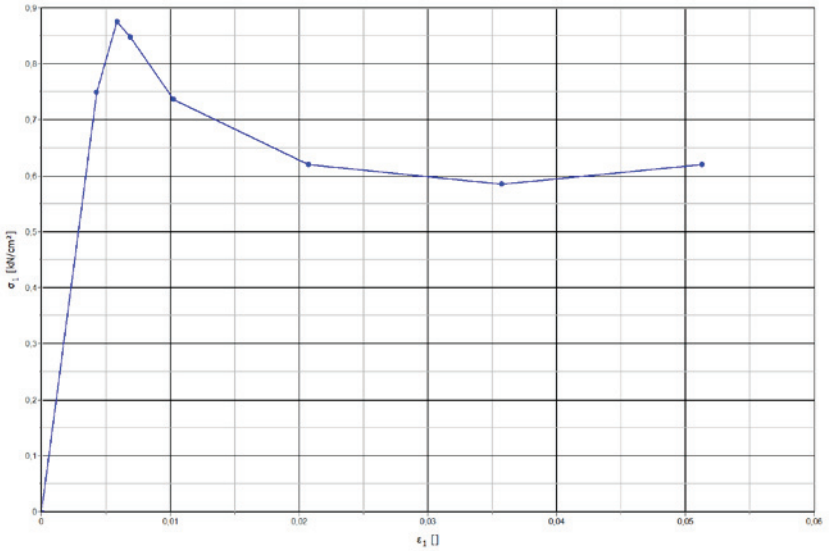

Figure 3. Principal stress-strain relationship obtained for undrained analysis of claystone.

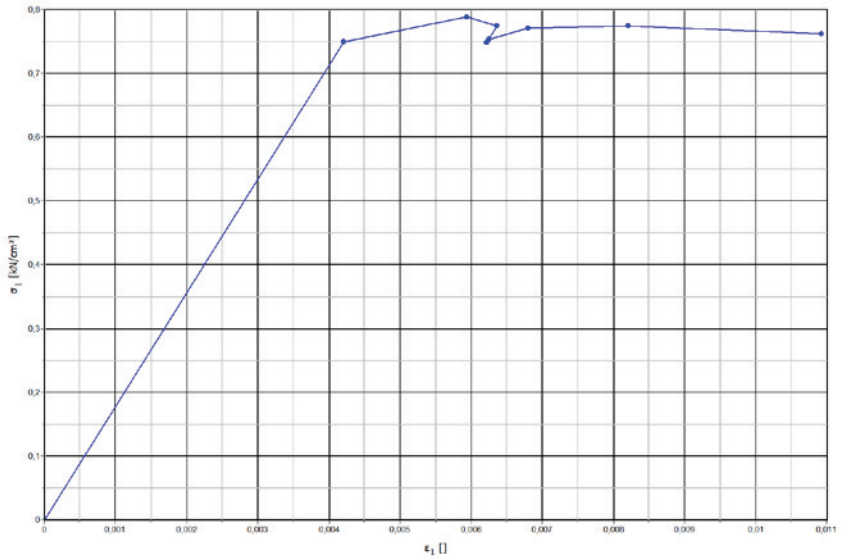

Figure 4. Principal stress-strain relationship obtained for drained analysis of claystone.

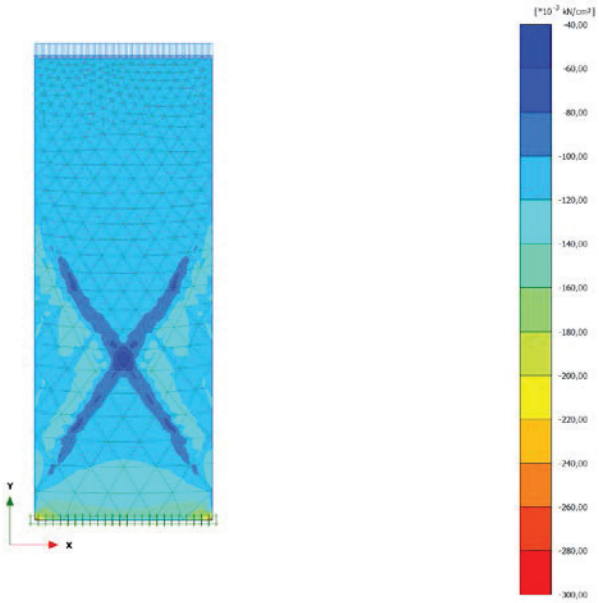

Figure 5. The distribution of values of excess pore pressure for undrained analysis of claystone.

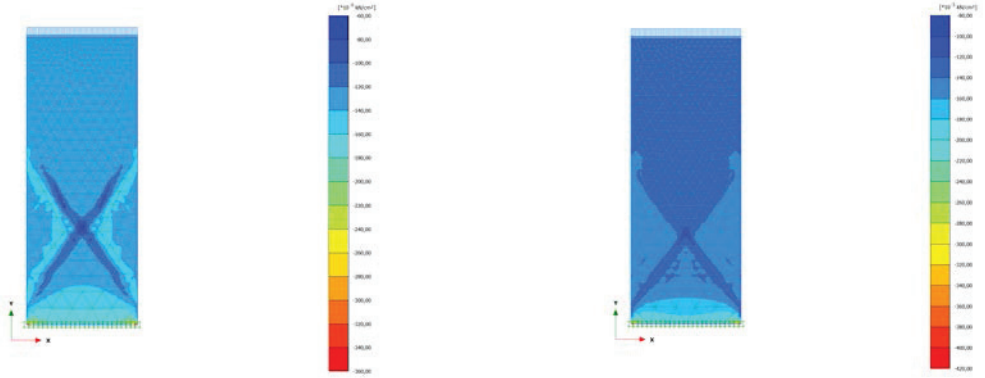

Figure 6. The distribution of values of excess pore pressure for undrained analysis of claystone for 0.3 and 0.6 values of α.

CONCLUSIONS

The vulnerability of geomechanical properties to saturation was investigated in this study. The test results referred that the decreasing trends due to saturation are valid for strength properties of claystone. By considering the low permeability of clay-bearing rocks, uniaxial loading was investigated under undrained and drained conditions by using numerical simulations. The results of numerical simulations showed that the development of excess pore pressure is considerable on uniaxial loading of claystone. However, the adverse effect observed due to excess pore pressure development determined by numerical simulations is not at the experimentally determined level. So the decrement in uniaxial compressive strength is not only related to development of excess pore pressure but also to interaction between fluid and clay minerals. While occurrence of excess pore pressure decreases the effective stresses, the interaction between fluid and clay minerals make rock matrix weaker. The effect of Biot's pore pressure coefficient on excess pore pressure was also investigated in this study. By considering the results of numerical simulations, it was understood that excess pore pressures induced during uniaxial loading increase as a result of increment in Biot's pore pressure coefficient. So the rocks which have high values of Biot's pore pressure coefficient are more suitable for excess pore pressure development

ACKNOWLEDGMENTS

This study was supported by the Scientific Research Project Coordination Unit (Project No. 2016-GAP-MÜMF-0004) of İzmir Kâtip Çelebi University. The author thanks to Assistant Professor Ali Ettehadi, Osman Ünal (Research assistant) and Naci Sertuğ Şenol (Graduate student) for their kind help in the study.

REFERENCES

Dönmez M, Akçay AA and Türkecan A (2014), İzmir-K 18 Paftası, 1:100.000 Ölçekli Türkiye Jeoloji Haritaları, No:213, MTA Jeoloji Etütleri Dairesi, Ankara

Ergüler Z.A.& Ulusay R., 2009. Water-induced variations in mechanical properties of clay-bearing rocks, International Journal of Rock Mechanics and Mining Sciences, vol.46, 355–370.

Gerçek, H. (2007). Poisson's ratio values for rocks. International Journal of Rock Mechanics and Mining Sciences, 44 (1), 1-13.

ISRM, 2007. The complete ISRM suggested methods for rock characterization, testing and monitoring: 1974–2006. Suggested methods prepared by the commission on testing methods. In: Ulusay R, Hudson JA (eds) Compilation arranged by the ISRM Turkish National Group. ISRM, Ankara.

Karakul H. and Ulusay R., 2013. Empirical correlations for predicting strength properties of rocks from P-wave velocity under different degrees of saturation, Rock Mechanics and Rock Engineering, vol. 46, 981–999.

Torok A.& Vasarhelyi B., 2010. The influence of fabric and water content on selected rock mechanical parameters of travertine, examples from Hungary, Engineering Geology, vol. 115, 237–245.

Vasarhelyi B., 2005. Statistical analysis of the influence of water content on the strength of the Miocene limestone, Rock Mechanics and Rock Engineering, vol.38, 69–76.

Wong, LNY, Maruvanchery, V, Liu, G. (2016). Water effects on rock strength and stiffness degradation. Acta Geotechnica, 11 (4), 713-737.

5 DAM SAFETY İstanbul Turkey 2018

5th International Symposium on Dam Safety

October 27-31, 2018

MAINTENANCE OF DAMS: FAST AND DURABLE REPAIR WITH POLYMERIC GEOMEMBRANES

Marco Bacchelli [1], Giovanna Lilliu[2], Alberto Scuero[3], Gabriella Vaschetti[4]

ABSTRACT

Maintenance is important to keep dams in safe operating conditions and ensure their long functional life. Deterioration, and consequent seepage, may require repair. Even when safety of the dam is not threatened, deterioration can cause economic loss, and reflect negatively on public opinion. Inadequate design, construction or operation, exceptional loading such as an earthquake, or just ageing can be the cause of deterioration. Permanent repair of dams can be done in a short time, requiring minimum equipment, by using polymeric geomembranes. Since their introduction in the late 1950s for constructing new embankment dams, polymeric geomembranes have been used in the rehabilitation of any type of dam. Methods have been developed for installing polymeric geomembranes also underwater, with minimum disruption of operation. In newly constructed dams, polymeric geomembranes are increasingly being selected in alternative to more traditional linings, showing to be a safe and financially beneficial solution. Performance properties of the geomembrane sealing system depend on the physical and mechanical characteristic of the waterproofing geomembrane, but also on the design and installation of the whole system. A geomembrane with potential optimal characteristics will still perform faulty if the geomembrane sealing system is not properly designed and installed. To this purpose, ICOLD has issued dedicated Bulletins (ICOLD 1991, 2010) that contain guidelines for designing geomembrane sealing systems according to the best practice. The company to whom the authors of this paper are affiliated, has worked in more than 150 dams since the 1970s and largely contributed to editing the latest of these Bulletins (ICOLD, 2010). Since 1980s, Concrete Face Rockfill dams (CFRDs) and Roller Compacted Concrete dams (RCCs) have increasingly been selected in Turkey and worldwide because of their considerable potential economic benefit. This paper is dedicated to describing a few rehabilitation projects with SIBELON® geomembrane sealing systems (Carpi patent) of RCCs and CFRDs, underwater and in the dry.

Keywords: Maintenance, repair, CFRD, RCC, geomembrane, SIBELON®.

INTRODUCTION

Maintenance of dams is an ongoing process that, at some stage, can entail repair. Deterioration, and consequent seepage, can have a negative impact on the public opinion, if not affect negatively operation of the dam and cause economical loss. The worst case can be loss of stability and potential

[1] Sales Manager at Carpi Tech
e-posta: marco.bacchelli@carpitech.com
[2] Marketing Manager at Carpi Tech
e-posta: giovanna.lilliu@carpitech.com
[3] Managing Director at Carpi Tech
e-posta: alberto.scuero@carpitech.com
[4] Vice President at Carpi Tech
e-posta: gabriella.vaschetti@carpitech.com

failure, with related hazardous conditions to downstream residents and properties. Need for repair can be related not only to quality of the design, of the construction and operation, but also to the natural ageing process of the structure. Exceptional loading conditions can also contribute to accelerate structural deterioration, such as earthquakes. Apparently small investments in partial or temporary repairs can result, in the long term, counter-productive because of the frequency they are needed: besides the hard costs of the repairs also costs for limited operation of the dam or its complete shut down must be considered.

This paper describes some case studies of dams where seepage has been remarkably mitigated, or cancelled, after installation of a customized geomembrane sealing system. The projects considered are: Platanovryssi RCC dam, Greece (underwater repair of a localized crack), Grindstone Canyon RCC dam, USA (repair in the dry of the most critical section), Turimiquire CFRD, Venezuela (underwater repair of the most critical sections), Pecineagu CFRD, Romania (staged repair in the dry).

RCCs and CFRDs have increasingly been selected in alternative to traditional concrete or embankment dams, because of their considerable potential economic benefits.

RCCs are mainly of the gravity type, with relatively small stresses in most parts, which allow use of low strength concrete. Speed of construction and low unit costs of RCC are major economic advantages of RCCs. In fact, RCC can be placed in large volumes; to limit heat of hydration, part of the cement content can be replaced with pozzolan or fly-ash. Watertightness is the major disadvantage of RCCs: the dam is built in thin horizontal layers that require special treatment to prevent water percolation through the horizontal lift joints. Leakage can also occur from defective contraction joints or from cracks that develop due to mechanical or thermal loading.

CFRDs consist of a zoned rockfill embankment with concrete slabs lining the upstream face and transition and filter zones beneath the concrete slab. CFRDs have several advantages compared to rockfill dams with an inner core: they can be built with steeper slopes, with reduction of the fill volume and, therefore, of the time required for its placement and thus the construction costs; fill placement is independent of weather conditions and can start before construction of the grout curtain is completed; they are inherently more stable, as the whole body of the dam resists to the water thrust; they also better resist to earthquakes because the rockfill is potentially dry, without development of excess of pore pressures. Critical aspects of CFRDs are the vulnerability of the perimeter joint, deformations in the fill, which may eventually result in excessive displacement of the concrete slabs and rupture of the joints, formation of cracks in the concrete slabs and, in general, ageing of the concrete forming the upstream lining.

The geomembrane sealing systems adopted in the projects described in this paper are patents of Carpi and use SIBELON® geocomposites and geomembranes as waterproofing material. These systems have been applied since the 1970s in more than 150 dams worldwide. The first projects were gravity and arch dams. Their use has been extended to all types of dams, not only for rehabilitation, but also in new construction. At Miel I RCC dam, in Colombia, the original design of an upstream face made of slip formed reinforced concrete was changed to a SIBELON® drained exposed geomembrane sealing system for meeting the contractual schedule. At the time of the project, in 2002, with its 188 m of height Miel I was the highest RCC dam in the world. More recently, in 2015, a SIBELON® drained exposed geomembrane sealing system has been installed at Susu dam, the 90 m high RCC dam that is part of Ulu Jelai Hydroelectric project, in Malaysia. This dam was originally conceived with a geomembrane attached to pre-cast concrete panels used as formwork to place the RCC. The original mix design considered 100 kg/m^3 cement content and 80 kg/m^3 fly ash. Adopting a SIBELON® exposed geomembrane sealing system has allowed reduction of the cement content to 95 kg/m^3 and removal of the fly ash from the mix design. Nam Ou VI rockfill dam, 88 m of height, in Lao PDR, is an example of design change from CFRD to Geomembrane Face Rockfill Dam (GFRD) with SIBELON® exposed geomembrane sealing system. Here, the reason for the change in design was the inability of the concrete slabs to accommodate the large displacements predicted for the fill.

SIBELON® GEOMEMBRANE SEALING SYSTEMS FOR REPAIR OF RCCS AND CFRDS

SIBELON® is the trademark for polymeric geomembranes produced exclusively for Carpi. SIBELON® geocomposites are obtained heat-bonding an impervious SIBELON® PVC geomembrane, which has a permeability lower than 10^{-6} $m^3/m^2/day$ as from EN 14150, to a non-woven needle-punched virgin fibre geotextile. Thickness of the geomembrane and of the geotextile, usually in the range 2.5÷4.0 mm, and 500÷700 g/m^2, respectively, depend on the specific project. The geocomposite has the function of enhancing resistance of the geomembrane against puncturing and its thermal stability. Furthermore, the backing geotextile provides the geocomposite with a superior tensile strength than the geomembrane alone. Main mechanical characteristics of SIBELON® geocomposites are their flexibility and their extreme elongation capability, which exceeds 250%. These, together with the typical monotonically increasing tension-elongation diagram, positively affect behaviour in the field. The material is stable on the slopes, is not prone to develop large wrinkles, and is not subject to localized straining, which can reduce the functional life of a geomembrane system. In addition, SIBELON® geocomposites can bridge large discontinuities in the subgrade and differential displacements, and resist impact loads. SIBELON® geomembranes are formulated for providing a high resistance to UV radiation. Monitoring of SIBELON® geomembrane sealing systems installed in dams at high altitudes in the Italian Alps in the years 1985-1997 (Cazzuffi, 2014), shows that these geomembrane sealing systems are still functional. Analytical processing with the Arrhenius method of accelerated aging tests performed in the laboratory, indicate that a 3 mm thick SIBELON® geomembrane can have a functional life of 100 years, when left exposed to UV radiation and at temperature comparable to those in Panama (Giroud, 2013).

Performance properties of a geomembrane sealing system depend on the physical and mechanical characteristic of the geomembrane, but also on its design and installation. A waterproofing material with potential optimal characteristics will still perform faulty if the geomembrane sealing system is not properly designed and installed. To this purpose, ICOLD Bulletin 135 (ICOLD, 2010) provides guidelines for designing geomembrane sealing systems. Carpi has largely collaborated to edition of this Bulletin, which includes several of the systems patented by Carpi. The following figure is an excerpt from Bulletin 135, showing the typical scheme of an exposed geomembrane sealing system and a detail of the tensioning profiles (Carpi patent) for anchorage of the waterproofing geomembrane to the dam face.

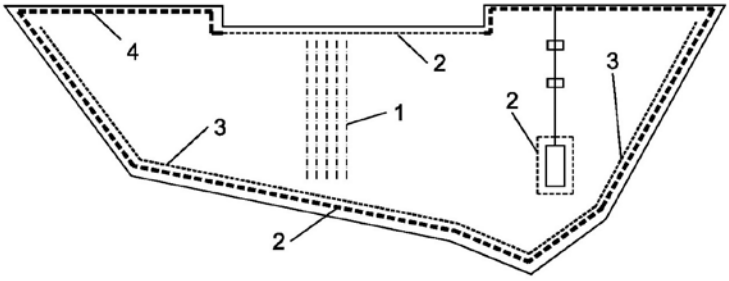

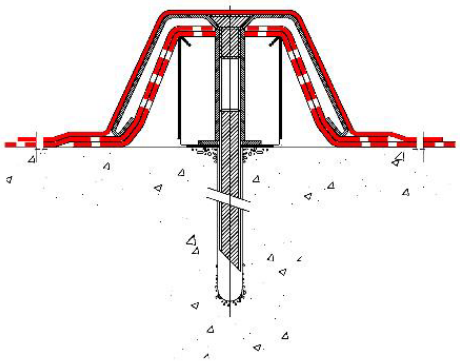

2. Watertight submersible perimeter seal
3. Drainage water collection
4. Watertight NON submersible perimeter seal

Figure 1. (Left) Typical scheme for exposed geomembranes. (Right) Tensioning profiles for anchorage of the waterproofing geomembrane to the dam face (Carpi patent). Excerpt from ICOLD Bulletin 135.

In the geomembrane sealing systems adopted in the projects described in this paper, the waterproofing geocomposite is fastened to the dam face along vertical lines. Primary scope of the face anchorage is to resist the uplift force of winds. The other scope is to tension the geocomposite liner between the anchorage lines, creating a taut system across the upstream face. The system (Carpi patent) considered

in this paper consists of couples of stainless steel profiles. The internal profile is fixed directly onto the upstream face. The type of anchors, chemical or mechanical, short or long, depend on the characteristics and strength of the subgrade. Once the geocomposite has been installed over the internal profile, the external profile is coupled to the internal profile, so tensioning the geocomposite between the anchorage lines. Then, a geomembrane cover strip is heat seamed over the external profile, producing a watertight seal over each profile line.

Along the perimeter of the geomembrane sealing system is a seal that can be either submersible or non-submersible, depending on the location. The submersible seal consists of stainless steel batten strips, with different dimensions, depending on the water head (standard dimensions are 80x8 mm or 60x6 mm). The stainless steel batten strips compress the geocomposite against the subgrade and are fastened with anchors spaced at 15 cm (again, type and length of the anchors depend on the characteristics of the subgrade). A rubber gasket placed beneath the stainless steel batten strip ensures even distribution of stresses and a two-part epoxy resin placed underneath the geocomposite creates a smooth surface against the subgrade and removes possible voids. Submersible seals have been designed and tested by Carpi for water heads higher than 850 m (Avila et al., 2018). The non-submersible seal must resist only water not in pressure, such as rain water, or snow melt, or waves; it consists of more flexible stainless steel batten strips than those used for the submersible seals, fastened to the subgrade with expansion anchors spaced at 20 cm. A neoprene gasket placed beneath the geocomposite provides watertightness against water not in pressure.

Draining the geomembrane sealing system is very important for its good performance. Scope of the drainage system is to prevent that water filtrating through the geomembrane stagnates behind it or penetrates the dam body. In case of rapid drawdown, water in pressure behind the geomembrane can eventually produce large stresses in the geomembrane and in its anchoring system. The drainage system can also be used to monitor performance of the geomembrane. The water, after travelling by gravity in the gap between the waterproofing geocomposite and dam face, is collected at the bottom and discharged (usually in the drainage gallery or downstream). The internal profiles that form the face anchoring system are also part of the drainage system, since they work as vertical water collectors. Depending on the required drainage capability, a high transmissivity geonet can be placed all over the surface of the dam or on portions of it.

Exposed geomembrane sealing systems as those discussed further in this paper have several benefits: one benefit is the possibility of being easily inspected, and, in case of damage, of being easily repaired. In the unlikely case of damage, the waterproofing geocomposite can be repaired by patch work: the portion of damaged material is cut out, and a patch of new material is heat-seamed or fixed with stainless steel profiles to the rest of the lining, so to restore its continuity. Components and installation procedures of the geomembrane sealing systems discussed so far have been adapted to underwater installations, which bring the additional benefit of minimizing or eliminating at all costs due to operation disruption during repair.

REPAIR OF RCC DAMS UNDERWATER AND IN THE DRY

Platanovryssi - underwater repair of a localized crack

Platanovryssi is a 95 m high, 305 m long RCC dam on the river Nestos in Greece, owned by Public Power Corporation. It is the middle of three hydroelectric power stations, which include Thysavros and Temenos plants (the last, not yet constructed). Its purpose is hydropower and irrigation. Upstream and downstream facings consist both of slip-formed/extruded elements, with 0.10H:1V and 0.75H:1V slope, respectively. The RCC forming the dam body has a content of 50 kg/m^3 cement and 225 kg/m^3 high-lyme fly ash (ASTM Class C). Its placement was completed in 50 working weeks between October 1995 and March 1997, with a planned summer close-down between mid-June and early November 1996.

The contraction joints, spaced at 25 m, were obtained by cutting a slot and placing a drain/crack inducer in the upstream facing elements, and by vibrating galvanized-steel crack inducer in the RCC bulk material. In 1998, an external waterstop (Carpi patent), designed to accommodate 25 mm opening due to thermal loading, was installed on these joints. The external waterstop consists of a 400 mm wide band of SIBELON CNT® 5050 geocomposite (3.5 mm thick SIBELON® PVC geomembrane + 500 g/m^2 geotextile) anchored along the perimeter with a submersible seal. The waterproofing layer was placed on a support consisting of two layers of the same SIBELON® geocomposite and one layer of 2,000 g/m^2 geotextile, anchored with impact anchors. In the fluctuation section, the external waterstop is protected against floating debris and wilful damage by means of corrugated stainless steel plates. These plates are conceived to accommodate openings of the joints under the maximum hydrostatic head.

Impounding of the reservoir began on 17th September 1998 and the pool level was reached on 14th November 1998. Initially, the total measured seepage was even lower than expected, but it eventually increased to 21 l/s in May 2000 and to 30.56 l/s in October of the same year. A crack that developed in one of the shorter dam monoliths, on the left abutment, was the cause of this anomalous seepage. The crack, with a maximum opening of 25 mm, produced leakage both in the gallery and through to the downstream face. An underwater inspection revealed that the crack extended from elevation 228.6 m down to elevation 209.8 m and, in the lower section, it divided into two cracks running nearly 2 m apart from each other. Faster rate of cooling of the monolith, which has a relatively large width and small volume, was considered a possible cause of the crack. Being quite an isolated phenomenon, it was concluded that formation of the crack was not generally related to properties and quality of the RCC material, but more to construction practices or detailed design (Papadopoulos, 2002).

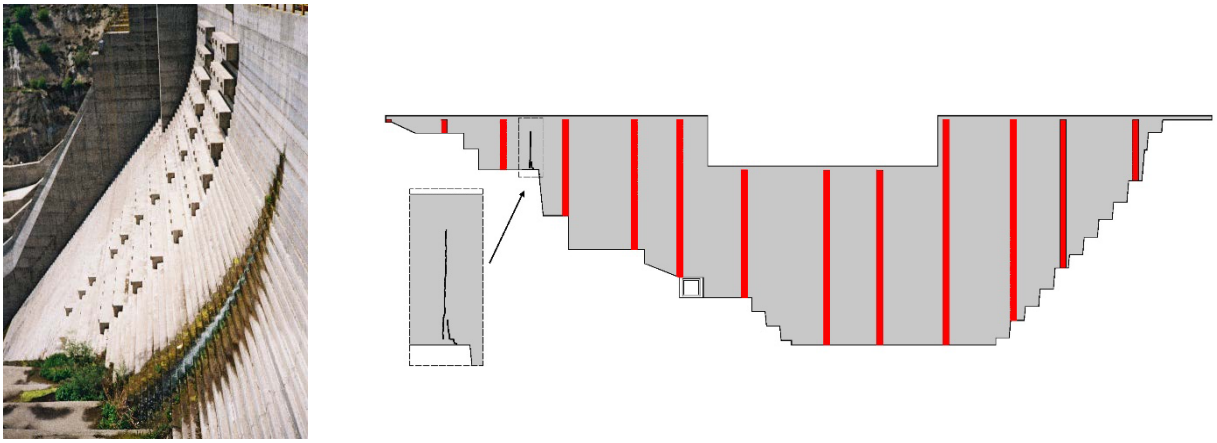

Figure 2. (Left) Leakage through to the downstream face of Platanovryssi dam, due to a crack that formed on the left abutment. (Right) Layout of the upstream face of the dam: the vertical lines indicate the contraction joints sealed with a Carpi external waterstop system in 1998. The insert indicates location of the crack that developed in one of the monoliths on the left abutment.

Based on the good performance of the external waterstop installed on the contraction joints in 1998, it was decided to adopt a similar system also for repairing the crack, properly adapted for being installed underwater. In fact, Platanovryssi reservoir serves as lower reservoir of Thysavros pumped storage and lowering the level of water would have affected operation of the whole scheme.

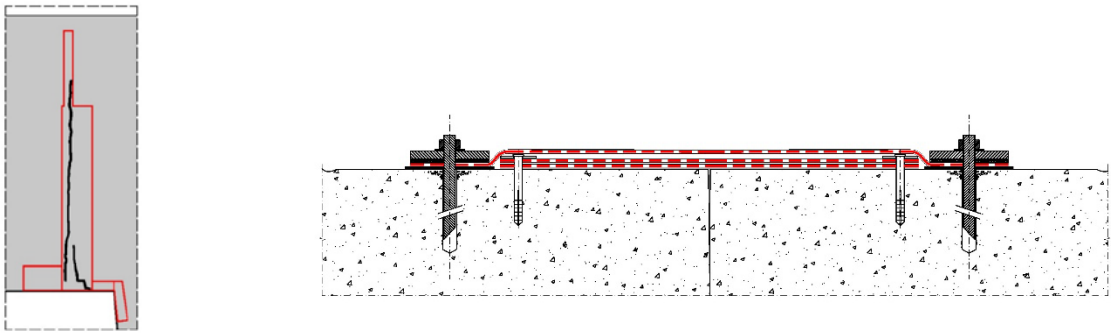

Figure 3. Layout of the Carpi external waterstop sealing the crack that developed on the left abutment.

The external waterstop was designed with a geometry such to follow path of the crack and consists of a band of SIBELON CNT® 3750 geocomposite (2.5 mm thick SIBELON® PVC geomembrane + 500 g/m^2 geotextile) supported by a double layer of the same geocomposite material. Widths of the bands of geocomposite were adjusted to cover the whole cracked section. Because of the smaller water load, components of the external waterstop sealing the crack are thinner than the components of the external waterstops sealing the contraction joints.

For performing the underwater installation, shutting of the turbines was first agreed with the owner, so to allow safe operation of the divers. The major equipment used for the installation was a truck boom at crest of the dam and a pontoon moored in the reservoir. To optimize installation, the SIBELON® geocomposite was cut and pre-assembled at site to form panels of the proper shape and dimensions to cover the whole section; furthermore, the two layers of geocomposite forming the supporting layer were previously glued together. Installation was executed with the assistance of a frame that was used first as template for drilling the holes in correspondence of the perimeter seal and then for correct positioning of the supporting layer and of the waterproofing layer.

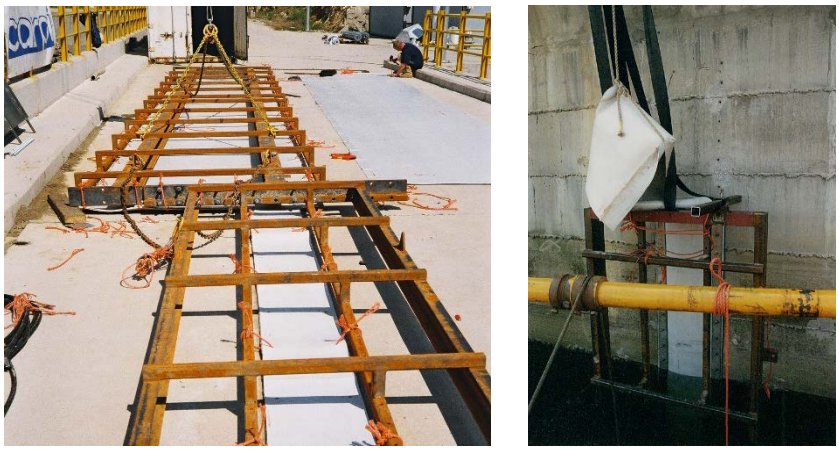

Figure 4. Frame used as template for drilling holes and for correct positioning of the supporting and waterproofing layer forming the Carpi external waterstop.

The perimeter seal, consisting of stiff stainless steel batten strips fastened with threaded anchors was made watertight against water in pressure by means of a neoprene gasket placed on the dam face, beneath the geocomposite, and of a rubber gasket placed beneath the batten strip. Surface of the dam was grinded by the divers in correspondence of the perimeter seal for eliminating any roughness that could endanger watertigthness of the seal. The works started on April 22, 2002 and were completed on May 23, 2002. The downstream face practically dried up immediately after completion of the waterproofing works.

Figure 5. (Left) Downstream face dried up immediately after completion of the waterproofing works and (right) during an inspection in 2006.

Grindstone Canyon- repair in the dry of the most critical section

Grindstone Canyon is a 43 m high RCC dam owned by the Village of Ruidoso in New Mexico, USA. The dam, which provides raw water supply for residents of the Village of Ruidoso and is also used for recreational fishing, was built in 1986. The upstream face of the dam is vertical and the downstream stepped face has a slope of 0.75H:1V. The RCC forming the dam body, with 76 kg/m^3 cement content, was lined with a conventional concrete layer, distinguished by a grid of vertical and horizontal rustication joints. The vertical joints, 8 cm deep and spaced at approximately 5 m, were intended to accommodate expansion and contraction of the concrete. The horizontal joints, 4 cm deep and spaced every 0.60 m or 1.20 m, depending on the elevation, were likely intended to give the dam an aged appearance.

Figure 6. (Left) Upstream face of Grindstone Canyon RCC dam before the waterproofing works. (Right) Detail of the rustication joints in the conventional concrete facing.

The dam had a history of high seepage since its first filling. Several repair projects were conducted in 1989, 1996, 2002 and 2009, including filling the rustication joints with sealant and placement of a bentonite blanket along the upstream foundation contact. These interventions had a limited success and seepage generally increased, leading to a stability study. Already in 2010 the New Mexico Office of State Engineer had restricted use of the reservoir to only 11% of its capacity. The stability study, completed in 2013, concluded that seepage was caused by porous zones of partially cemented aggregate and/or transverse thermal cracking, and recommended lining the upstream face of the dam 20 m down from the crest. In this manner uplift forces on the lift joints could be reduced and stability significantly increased, especially in case of an earthquake. Lining the whole upstream face of the dam was not considered because the reservoir could not be drained completely, so to meet the water demand by the Village of Ruidoso, and the option of an underwater installation was excluded because of budgetary constraints.

The geomembrane sealing system installed at Grindstone Canyon dam is composed of a SIBELON® CNT 4400 (3 mm thick SIBELON® PCV geomembrane + 500 g/m^2 geotextile) placed on top of a 2,000 g/m^2 geotextile, which prevents intrusion of the geocomposite in the rustication joints and, although limited, provides some drainage capability. Fastening of the waterproofing geocopmposite to the dam face is with the system of tensioning profiles at 5.70 m spacing, and along the perimeter with submersible or non-submersible seals, depending on the location. Where the seals cross the rustication joints, these were filled with a special low-modulus epoxy joint-filling compound, formulated with

ceramic microspheres to reduce shrinkage. To prevent water by-passing the bottom perimeter seal, a hydrophobic polyurethane chemical grout was injected behind the concrete facing in the immediate vicinity of the bottom seal between the abutments. At the abutments, only the vertical rustication joints were grouted, below and slightly above the bottom seal. The face was inspected for visible cracks and these, once found, were also grouted.

The drainage system consists of a band of drainage geonet placed at the bottom of the geomembrane sealing system. The drainage geonet conveys the water drained from the geomembrane sealing system towards three discharge points. The drained water is discharged downstream, in a stilling basin, through the same stainless steel core barrels that were used for drilling the dam body from upstream to downstream, which were left in place after the drilling. These pipes, after daylighting on the downstream face, were buried to prevent freezing.

Figure 7. (Left) Installation of the SIBELON® geomembrane sealing system. (Middle) Detail in correspondence of the bottom seal. (Right) Stainless steel water collectors protruding from the downstream face and placed in a trench, before backfilling.

Installation of the geomembrane sealing system started on March 4, 2015 and was completed by June 20, 2015, for a total of 5,435 m^2 surface lined. The total amount of water drained by the three geomembrane drains is less than 4 l/min.

Figure 8. Upstream face of Grindstone Canyon RCC dam after completion of the waterproofing works.

REPAIR OF CONCRETE FACE ROCKFILL DAMS UNDERWATER AND IN THE DRY

Turimiquire dam- underwater repair of the most critical sections

Las Canalitas CFRD dam in Venezuela, better known as Turimiquire, owned by the Ministerio del Poder Popular para el Ambiente, was built between 1976 and 1983. The dam has a height of 113 m; the crest is at elevation 335 m, and maximum water level is at elevation 328 m. The dam forms a reservoir that supplies water to some 1,000,000 people in the northeast of the country. The dam body is made of a quarry random fill that was placed in compacted lifts of 1.4 m height. A 5 m thick transition zone (grading 6.5 to 180 mm) was placed upstream of the main rockfill in lifts of 0.5 m

height. The upstream face of the dam is formed by 33 reinforced concrete slabs, mostly 15 m wide and 12.15 m high, with thickness varying from 30 cm at crest to 100 cm at foundation. The construction joints are reinforced and have a double 9-in rubber waterstop.

The dam, impounded in 1988, already in July 1989 had a leakage of 300 l/s. It was decided then to lower the water level and place clay material, which reduced leakage to 60 l/s. In 1994 leakage had increased up to 2500 l/s, and a second repair was made by filling with material of two different sizes, which reduced leakage to 674 l/s. However, also this solution showed to be only temporary, because in 1996 leakage became 3,173 l/s. In this case, a landslide worked out as a "natural repair", reducing leakage to 1,255 l/s. In September 1999 leakage of 6,500 l/s required another repair, which was made by filling with material of four different sizes. In 2000 a further repair was made over an area of 450 m^2, with granular material plus an impervious geomembrane type XR5. The result of this repair was very poor, and leakage eventually rose to 9,800 l/s. Extensive investigation with sonar multi-beam scanning carried out by the owner showed that leakage was not at the plinth, contrary to what was originally believed, but there were two epicentres: a crater of 4.1 m^2 area in slab 24 and another crater at 270 m elevation in slab 9. Further investigation showed an extensive zone with cracks randomly oriented and up to 7 m length, that were presumably caused by settlements at the crest. The concrete slabs were exhibiting a honeycomb texture due to loss of cementitious material in several locations, and erosion at 275-285 m elevation. Also, insufficient anchorage had caused local displacement and folding of the membrane installed in 2000, and, therefore, a large permeable area below it. Part of the perimeter anchorage had also been displaced. Sediments and debris up to 6 m height were detected at the toe. Inspections and analysis provided unquestionable evidence of the deterioration of the face, and of the very poor outcome of all repair interventions until then.

In July 2008, Carpi was awarded a first contract for lining the most critical sections of the dam face, with a target seepage of 3,000 l/s. The original plan was to line a total surface of 14,930 m^2. Effectively, as consequence of the unexpected rising of the water level in the reservoir, caused by rains, and of budgetary constraints, only 10,105 m^2 were lined. This corresponds to only 20% of the total surface. The sections lined with the SIBELON® geomembrane sealing system are shown in the following figure. Section 4, from elevation 304 m down to elevation 295.93 m, is the only area were works were executed out of water (corresponding to an area of 1,345 m^2).

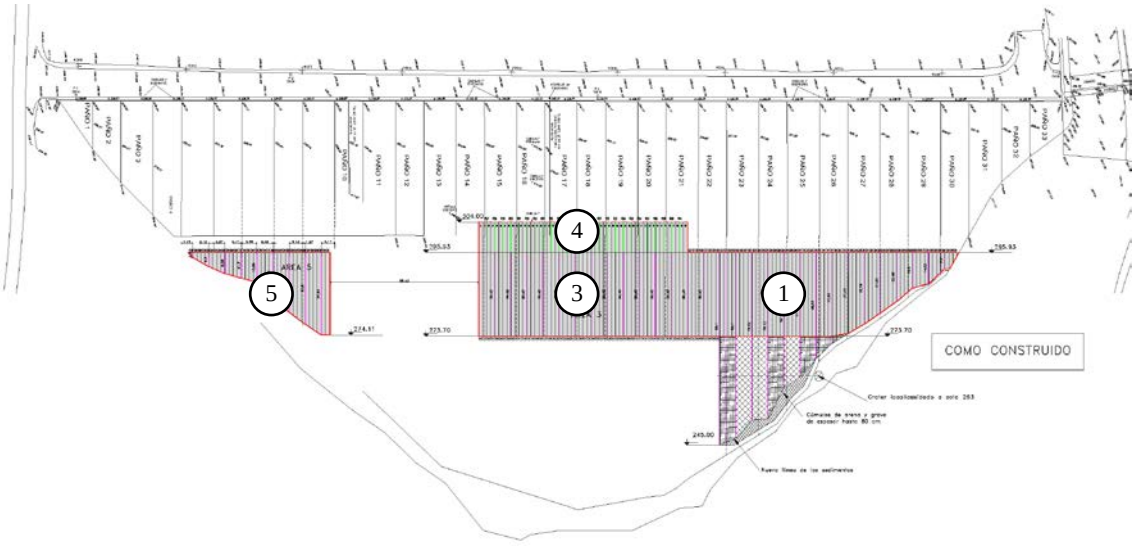

Figure 9. Layout of the upstream face of Turimiquire CFRD. The numbers identify the critical sections where a SIBELON® geomembrane sealing system was installed in 2009-2011.

Minimizing sediment removal, and conceiving design so to allow installation in stages were among the requirements of the geomembrane sealing system. Also, due to the underwater installation environment, minimising surface preparation was mandatory. To this purpose, extensive use of

synthetic materials was made. A support layer made of a high-strength geogrid was placed on top of the concrete surface so to provide support over discontinuities, and a 2,000 g/m^2 geotextile was installed on top of the geogrid to provide protection against puncturing of the waterproofing liner. In the zones of the craters, cavities were filled with sand bags to avoid that the waterproofing liner would be sucked into the crater during operation. The waterproofing geocomposite is a SIBELON® CNT 4600 geocomposite (3 mm thick SIBELON® PVC geomembrane + 700 g/m^2 geotextile), selected to resist high water heads. The sheets of SIBELON® geocomposite, of 2.10 m width, were heat-seamed at site to form prefabricated panels of 7.7 m width, so to optimize the underwater installation. Fastening of the waterproofing geocomposite to the dam face is with the system of tensioning profiles (customized so to be suitable for underwater installation), spaced at 3.4 m in the sections above water, and at 7.4 m in the sections permanently under water. Along the perimeter, the seal is of the submersible type.

Figure 10. (Left) Detail of the tensioning profiles, customized for underwater installation. (Right) Geogrid installed between the tensioning profiles for supporting the waterproofing geocomposite.

Figure 11. (Left) Prefabricated panel of SIBELON® geocomposite, obtained heat-seaming four sheets, each with width of 2.10 m. (Right) Lowering of the pre-fabricated panel of SIBELON® geocomposite in the water.

Divers' crew mobilized on November 1, 2009; works were completed on June 30, 2009. Leakage measured after the waterproofing works was less than 2,400 l/s, well below the target leakage. Following this successful result, a new budget was approved for continuing the waterproofing works but, due to the financial and political situation in the country, works could be continued only in June 2017. The sections waterproofed in 2017 include an area from elevation 277.82 m down to elevation

271.80 m next to the plinth, in the right abutment, and the area between sections 3 and 5, from elevation 295.93 m down to elevation 273.70 m, for a total of 2,718.50 m^2.

Pecineagu-staged repair in the dry

Pecineagu is a 105 m high CFRD in Romania, owned by Apele Române, Scope of the dam is multiple: supply of drinking and industrial water to the capital city, Bucharest, flood control and power production. The upstream face, with a slope of 1.72H:1V, was lined with 271 concrete slabs of varying size and thickness. The joints between concrete slabs were waterproofed with PVC waterstops and copper waterstops or elasto-plastic bituminous mastic poured in place. To enhance watertightness of the concrete face, the upper part was treated with epoxy resin; the lower part, up to 20 m from the bottom, was covered with argillaceous material. Construction started in 1975 and was completed in 1984. Filling was gradual, reaching the maximum level between 1994 and 1997. The dam is in a rather harsh environment, with temperatures ranging from a minimum of -21.5°C and a maximum of +42°C, snow up to 100 cm thickness and ice up to 50 cm thickness.

Pecineagu dam has a history of repeated repair works, in 1993, 1999 and 2003, aimed to mitigate seepage; none of them showed to be efficient longer than 2÷3 years. During the various inspections conducted upon de-watering, it was established that most of the infiltration occurred through the concrete facing and through deteriorated joints between the concrete slabs. Moreover, over time, the peripheral slabs had significantly rotated due to settlements of the dam body. Therefore, joints had opened exceeding the elongation capacity of the waterproofing materials and were locally destroyed. An increase in time of the flow rates indicated that this was an evolutionary phenomenon, difficult to control with isolated interventions, but requiring a radical intervention.

Figure 12. (Left) The upstream face of Pecineagu CFRD before installation of the SIBELON® geomembrane sealing system. (Right) Effect on concrete slabs and joints of the settlements in the dam body.

A safety project was made, which involved installation of an exposed geomembrane sealing system in two stages. In stage 1, works were conducted on the lower 36 m of the dam, starting from elevation 1,060 m, on a surface of 6,635 m^2. Water was diverted so to execute the works completely in the dry. In stage 2, works were conducted from elevation 1,095 m down to elevation 1,060 m, on a surface of 13,041 m^2. In stage 2, works were executed with a partially impounded reservoir. The upper 22 m of the dam remained unlined. Total duration of the waterproofing works was of 106 calendar days: stage 1 started on September 26, 2011 and was completed on November 16, 2011. Stage 2 started on September 9, 2012 and was completed on November 3, 2012. Surface of the concrete slabs was

preliminarily prepared by cleaning it from sediments and debris; joints were cleaned and filled with mortar so to obtain a relatively smooth surface. Finally, an anti-puncturing 2,000 g/m^2 geotextile was placed on the concrete slabs. The waterproofing layer is a SIBELON® geocomposite of different thickness, depending on the water head. In the lower section (stage 1), the geocomposite is a SIBELON® CNT 4400 (3 mm thick SIBELON® PVC geomembrane + 500 g/m^2 geotextile). In the upper section (stage 2), the geocomposite is a SIBELON® CNT 3750 (2.5 mm thick SIBELON® PVC geomembrane + 500 g/m^2 geotextile). The waterproofing geocomposite is fastened to the dam face with the system of tensioning profiles and along the perimeter with a submersible or not submersible seal, depending on the location.

The waterproofing geocomposite installed during stage 1 was fastened to the dam face with a temporary, non-submersible seal. This consists of 50x3 mm stainless steel batten strips fastened with expansion anchors, with a neoprene gasket placed between concrete and geocomposite to prevent filtration of rain water, water from snow melt or waves. Continuity at the periphery between the geomembrane sealing system installed in stage 1 and the one installed in stage 2 was obtained overlapping and heat-seaming the two geocomposites and placing an additional band of geomembrane on top of this junction. The geomembrane sealing system is drained. The drainage system consists of bands of drainage geonet along the perimeter; the water drained from the geomembrane sealing system is discharged in the inspection gallery at the upstream toe through 5 discharge points. To enable flow of the drained water from the upper (stage 2) to the lower section (stage 1), the upper perimeter seal installed during stage 1 was removed for some extension at both sides of the tensioning profiles and replaced with bands of drainage geonet. Following the successful performance of the geomembrane sealing systems installed in 2011 and in 2012, the owner is now considering extending the lining also to the upper part of the dam.

Figure 13. Waterproofing works ongoing during stage 1 (left) and stage 2 (right).

FINAL REMARKS

Maintenance of dams may require repair. Traditional, partial or temporary repairs can result very expensive in the long term, because of the frequency they are needed. Polymeric geomembrane sealing systems can be a fast and durable repair system, if they are designed according to the best practice. The paper analyses a few projects where a SIBELON® geomembrane sealing system, installed in the dry or underwater, has strongly mitigated or practically cancelled seepage in RCC and CFR dams.

REFERENCES

Avila, R., McManus, R., Yu, A. and Wilkes, J., 2018. “Helms Pump Storage Penstock Access Tunnel Rehabilitation: Waterproofing a Hydraulic Tunnel under 1,800+ Feet (550+ m) of Static Pressure”, Proceedings of HydroVision International 2018, Charlotte, USA, June 26-28, 2018.

Cazzuffi, D., 2014. “Long-time Behavior of Exposed Geomembranes used for the Upstream Face Rehabilitation of Dams in Northern Italy”, Proceedings of the 10th International Conference on Geosynthetics, Berlin, Germany, September 21-25, 2014.

Giroud, J.P., 2013. “Functional Service Life of SIBELON® Geomembrane for Panama Canal WSB”, Memorandum.

ICOLD, 1991. “Watertight Geomembranes for Dams-State of the Art”. ICOLD Bulletin 78.

ICOLD, 2010. “Geomembrane Sealing Systems for Dams”. ICOLD Bulletin 135.

Papadopoulos, D., 2002 “Seepage evolution and underwater repairs at Platanovryssi”, Hydropower & Dams, Issue 6.

5th International Symposium on Dam Safety

October 27-31, 2018

TAILINGS DAMS AND THEIR RISK ASSESSMENT

Nihat ATAMAN [1]

ABSTRACT

Failure of tailings dams has had serious and negative impacts on public health and safety, economic life and environment. Rate of failures of tailings dams that is recorded during last century is 1.2 %. This rate is 1200 times higher than that of water retention dams. This situation puts forward the need to focus on safety of tailings dams. Although the studies on the risk assessment of water retention dams date back to 1976, research on the risk assessment of tailings dam is relatively new.

In this paper, types of tailings dams, differences between tailings dams and water retention dams, causes and occurrences of tailings dam failures, classification of tailings dams, situation in Turkey, and a literature survey on the risk assessment of tailings dams are presented.

Keywords: Tailings dam, failure, risk, assessment

TAILINGS DAMS

Tailings dams are dams constructed of mill tailings, mine wastes or earth of rock fill for the retention of tailings slurry or slurry water for reclamation (ICOLD, 1982). The construction of tailings dam can be either (1) upstream; (2) centerline; (3) downstream; (4) a variation of water-retention dam; or (5) a combination of any of the previous methods.

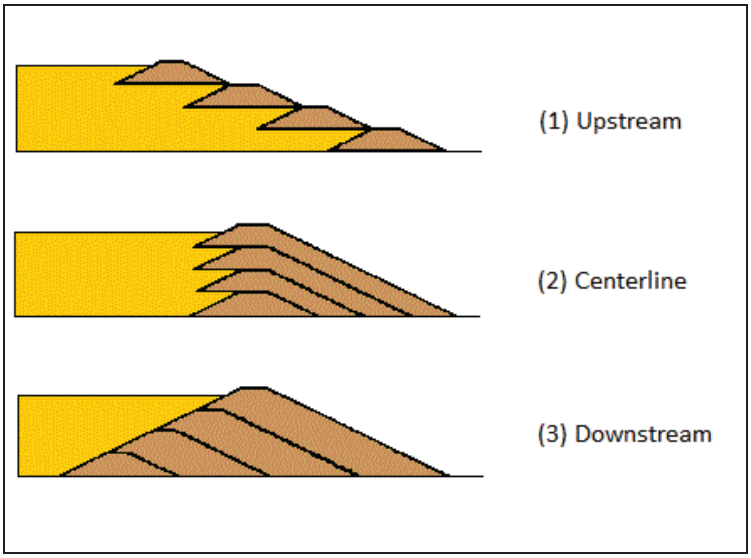

Figure 1. Types of sequentially raised tailings dams (reproduced from Vick, 1990)

[1] Mining Engineer, MSc., State Hydraulics Works (DSİ), Ankara, Turkey
e-posta: nihata@dsi.gov.tr

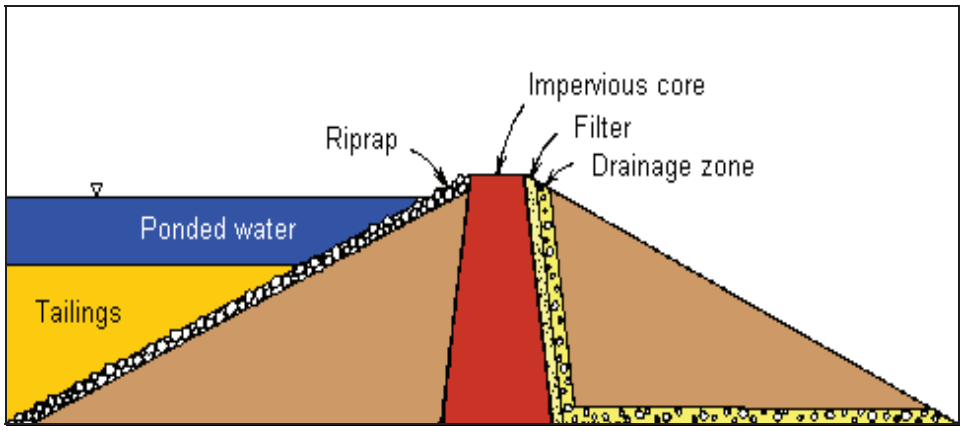

Figure 2. Water-retention type dam for tailings storage (Vick, 1990)

Design methods for tailings dams vary a lot as it is affected by (Benckert & Eurenius, 2001);

- Tailings characteristics and mill output
- Site characteristics as; topography, hydrology, geology, groundwater, seismicity and available material
- Disposal methods

Design, construction, operation, and closure of tailing dams have some fundamental differences when compared to conventional water storage dams (see Table 1). Some of these differences work to the benefit of the dam designer, and some increase the complexity and difficulty (McLeod & Murray, 2003).

Table 1. Differences between tailings and water dams (Benckert & Eurenius, 2001)

	Tailings Dam	**Water Dam**
Design Objectives	Contain wastes from mineral processing (tailings) and some water (or saturated tailings) in a safe, stable and environmentally acceptable manner.	Safely contain and control water for any purpose.
Engineering design criteria	Static and seismic stability. Hydrology based on downstream flood, environmental risk and process needs.	Static and seismic stability. Hydrology based on downstream risk.
Environmental criteria	Minimize environmental impact to an acceptable level throughout construction, operation and closure and minimize emissions to the surrounding environment throughout operation and after closure.	Minimize environmental impact.
Construction	Staged construction during operation to suit storage requirements.	Single construction phase
Operation	Ongoing design, construction and storage control to meet waste disposal, environmental and flood control requirements.	Reservoir level operation.
Closure	Closure when mineral extraction/processing ceases to create a safe and stable structure, and an environmentally sustainable closure solution for thousands of years.	No specific closure requirements, unless breaching is required for environmental reasons.

Types of tailings dams also differ from each other in many aspects (see Table 2). In addition, Every tailings dam is unique due to a variety of factors including the nature both of the land and the tailings themselves (Van Niekerk & Viljoen, 2005).

Table 2. Comparison of tailings dam types (Vick, 1990).

	Water Retention	Upstream	Downstream	Centerline
Mill Tailings Requirements	Suitable for any type of tailings	At least 40-60% sand in whole tailings. Low pulp density desirable to promote grain-size segregation	Suitable for any type of tailings	Sands or low-plasticity slimes
Discharge Requirements	Any discharge procedure suitable	Peripheral discharge and well-controlled beach necessary	Varies according to design details	Peripheral discharge of at least nominal beach necessary
Water Storage Suitability	Good	Not suitable for significant water storage	Good	Not recommended for permanent storage. Temporary flood storage acceptable with proper design
Seismic Resistance	Good	Poor in high seismic areas	Good	Acceptable
Raising Rate Restrictions	Entire embankment constructed initially	Less than 4.5 - 9 m/yr most desirable. Greater than 15 m/yr can be hazardous	None	Height restrictions for individual raises may apply
Embankment Fill Requirements	Natural soil borrow	Natural soil, sand tailings, or mine waste	Sand tailings or mine waste if production rates are sufficient, or natural soil	Sand tailings or mine waste if production rates are sufficient, or natural soil
Relative Embankment Cost	High	Low	High	Moderate

TAILINGS DAM FAILURES

A number of particular characteristics make tailings dams more vulnerable to failure than water storage dams (Rico, Benito, & Diez-Herrero, 2008):

(1) Embankments formed by locally derived fills (soil, coarse waste, overburden from mining operations and tailings)
(2) Multi-stage raising of the dam to cope with the increase in solid material stored and effluent (plus runoff from precipitation) released;
(3) The lack of regulations on specific design criteria;
(4) Dam stability requiring a continuous monitoring and control during emplacement, construction and operation of the dam;

(5) The high cost of remediation works following the closure of mining activities.

Geotechnical knowledge with engineering experience can enable safe tailings dams to be designed and constructed, but the current rate of tailings dam failures that have averaged 1.7 a year during the past 30 years shows that this knowledge and experience has not been applied in every case (Penman, 2001).

Tailings dams have failed at a rate that is significantly higher than the failure rate for water supply reservoir dams (Cambers and Higman, 2011). Broadly, 2 to 5 out of the 3,500 tailings dams in the world experience major failure each year (Lemphers, 2010).The failure rate of tailings dams over the last one hundred years is estimated to be 1.2% (Azam & Li, 2010). This is more than two orders of magnitude higher than the failure rate of conventional water retention dams that is reported to be 0.01% (ICOLD & UNEP, 2001).

The ICOLD study (2001) on dangerous occurrences of tailings dam revealed that the three leading causes for tailings dam incidents are “overtopping”, “slope stability”, and “earthquakes”.

Rico et al. (2008) differentiated 11 “cause of failure” categories (see Figure 3) and stated that the major fraction of incidents relates to meteorological causes (e.g. unusual rainfall events/periods and snow), accounting for 25% of worldwide cases and 35% in Europe.

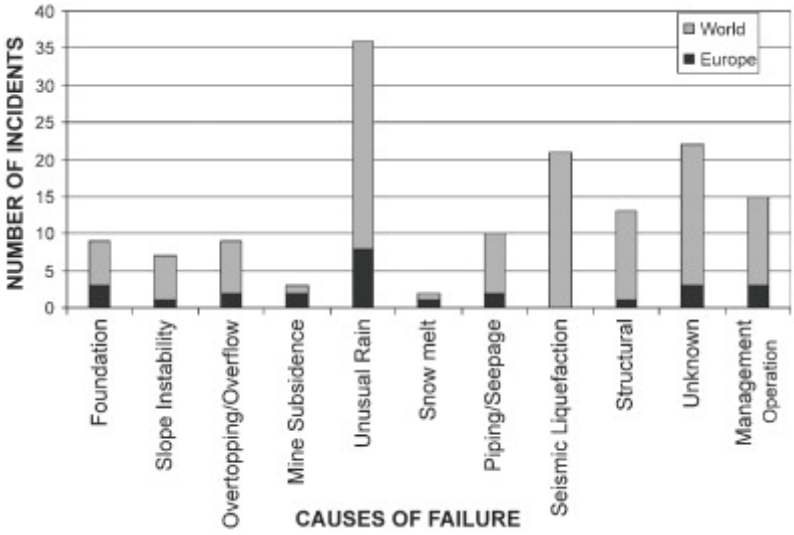

Figure 3. Distribution of the number of incidents according to cause in the world and in Europe (Rico, Benito, Salgueiro, Diez-Herrero, & Pereira, 2008)

Xin et al. (2011) state that main factors affecting the deformation and stability of the tailings dam in china as the tailings dam material composition; physical-mechanical properties and the geometric parameters of dam (dam height, inside and outside slope ratio, dry beach length, warehouse inner water level, groundwater level elevation and earthquake). They categorized tailings dam failure modes into flood overtopping and the dam structural failure. They added that structural failure mode can be divided into seepage failure, slope instability failure and seismic failure; and seismic failure mode can be further divided into seismic liquefaction failure and seismic instability failure (Xin, Xiaohu, Kaili, 2011).

The reports on tailings dam failures are incomplete and heavily biased. There is no (complete) worldwide database of all historical failures. The majority of tailings dam incidents remain unreported, especially in developing countries. In cases where a known accident did occur it is often

difficult to access basic information regarding the tailings dam and its condition prior to the incident (e.g., dam height, tailings storage volume, tailings thickness, water content, etc.). To date, 250 cases of tailings dam failures in the world have been compiled (Rico et al., 2008).

Tailings dam failures result from a variety of causal mechanisms spilling out polluted water and tailings with a variety of textural and physical–chemical properties, which may impact over the downstream socio-economic activities and ecological systems (Rico et al., 2008).

The failure of a tailings dam and the uncontrolled release of the impounded waste may have serious consequences for the public safety, the environment and the Owner or Operator. Some of the types of consequences can include the following (ICOLD & UNEP, 2001):

- Economic Consequences: Included under this heading are the costs of repair or reconstruction of the dam and impoundment and the effects on the operator of the facility of a temporary lack of storage for waste.
- Public Safety: Public attention has increasingly focused on matters relating to safety and a hazard which may affect a large number of people in a single catastrophe is less acceptable than every day hazards which may in aggregate cause far more deaths but in each incident affect only one or two individuals. An imposed and involuntary exposure due to living close to some hazard is much less acceptable than a voluntary exposure to a high risk activity.
- Environmental Damage: The release of a substantial quantity of waste material which then flows over a large area of surrounding ground may cause massive environmental damage, particularly if the waste is toxic. There are also risks associated with incremental events over a longer term such as dust dispersion, groundwater contamination, landslide or ground instability.

Following table gives some examples of tailings dam disasters occurred since 2000.

Table 3. Selected Tailings Dam Disasters (Adopted from www.wise-uranium.org/mdaf.html, Retrieved, 18-8-2018)

Date	Location	Ore type	Type of Incident	Impacts
June 4, 2018	Chihuahua, Mexico	gold, silver	Tailings dam failure	Dam failure results in tailings release travelling 29 km downstream; most of the tailings have been deposited along the course of the Cañitas River. Three workers were killed, two wounded, and four are reported missing.
June 30, 2017	Mishor Rotem, Israel	phosphate	phosphogypsum dam failure	The toxic wastewater surged through the dry Ashalim riverbed and left a wake of ecological destruction more than 20 km long
Aug. 8, 2016	Luoyang, Henan province, China	bauxite	Failure of a tailings dam holding about 2 million cubic metres of red mud	village totally submerged in red mud, around 300 villagers evacuated, many farm and domestic animals killed
Nov. 5, 2015	Minas Gerais, Brazil	iron	Insufficient drainage, leading to liquefaction of the tailings sands shortly after a small earthquake.	slurry wave flooded town of Bento Rodrigues, destroying 158 homes, at least 17 persons killed and 2 reported missing; slurry pollutes North Gualaxo River, Carmel River and Rio Doce over 663 km, destroying 15 square kilometers of land along the rivers and cutting residents off from potable water supply

Aug. 4, 2014	British Columbia, Canada	copper, gold	Tailings dam failure due to foundation failure	tailings flowing into adjacent Polley Lake and, through Hazeltine Creek, into Quesnel Lake (Mitchell Bay)
Oct. 4, 2010	Kolontár, Hungary	Bauxite	Tailings dam failure	Several towns flooded, 10 people killed, approx. 120 people injured, 8 square kilometers flooded
Aug. 29, 2009	Karamken, Magadan region, Russia	Gold	Tailings dam failure after heavy rain	Eleven homes were carried away by the mudflow; at least one person was killed
Dec. 22, 2008	Kingston fossil plant, Harriman, Tennessee, USA	Coal ash	Retention wall failure	The ash slide covered 1.6 square kilometers. The wave of ash and mud toppled power lines, covered Swan Pond Road and ruptured a gas line. It damaged 12 homes, and one person had to be rescued
Sep. 8, 2008	Xiangfen county, Shanxi province, China	Iron	Collapse of a waste-product reservoir at an illegal mine during rainfall	A mudslide several meters high buried a market, several homes and a three-storey building. At least 254 people are dead and 35 injured.
April 30, 2006	Shangluo, Shaanxi Province, China	Gold	Tailings dam failure during sixth upraising of dam	The landslide buried about 40 rooms of nine households, leaving 17 residents missing. Five injured people were taken to hospital. More than 130 local residents have been evacuated. Toxic potassium cyanide was released into the Huashui river, contaminating it approx. 5 km downstream.
2004, Nov. 30	British Columbia, Canada	Mercury	Tailings dam collapses during reclamation work	Tailings spilled into 5,500 ha Pinchi Lake
2002, Aug. 27 / Sep. 11	San Marcelino, Zambales, Philippines	Mercury (?)	Overflow and spillway failure of two abandoned tailings dams after heavy rain	Tailings spilled into Mapanuepe Lake and eventually into the Sto. Tomas River, low lying villages flooded with mine waste; 250 families evacuated;
2001, Jun. 22	Nova Lima district, Minas Gerais, Brazil	Iron	Mine waste dam failure	Tailings wave traveled at least 6 km, killing at least two mine workers, three more workers are missing
2000, Jan. 30	Baia Mare, Romania	Gold recovery from old tailings	Tailings dam crest failure after overflow caused from heavy rain and melting snow	Contamination of the Somes/Szamos stream, tributary of the Tisza River, killing tonnes of fish and poisoning the drinking water of more than 2 million people in Hungary

TAILINGS DAM CLASSIFICATION

European Union classifies mining waste facilities in Category A/not Category A in accordance with the provisions in Annex III of Directive 2006/21/EC of 15 March 2006 on the management of waste from the extractive industries and which states that:

"A waste facility shall be classified under category A, if:

a) a failure or incorrect operation, e.g. the collapse of a heap or the bursting of a dam, could give rise to a major accident, on the basis of a risk assessment taking into account factors such as the present or future size, the location and the environmental impact of the facility; or
b) it contains waste classified as hazardous under Directive 91/689/EEC above a certain threshold; or
c) it contains substances or preparations classified as dangerous under Directives 67/548/EEC or 1999/45/EC above a certain threshold."

European Commission adopted a decision (2009/337/EC) on the definition of the criteria for the classification of waste facilities. The Decision explains the details of classification system. The Decision states that (EC, 2009):

A waste facility shall be classified under Category A in accordance with 2006/21/EC if the predicted consequences in the short or the long term of a failure due to loss of structural integrity, or due to incorrect operation of a waste facility could lead to (Article 1)*:*

(a) non-negligible potential for loss of life;
(b) serious danger to human health;
(c) *serious danger to the environment.*

According to the Decision, the potential for loss of life or danger to human health is considered to be negligible or not serious if people other than workers operating the facility that might be affected are not expected to be present permanently or for prolonged periods in the potentially affected area. Injuries leading to disability or prolonged states of ill-health shall count as serious dangers to human health. The potential danger for the environment is considered to be not serious if:

(a) the intensity of the potential contaminant source strength is decreasing significantly within a short time;
(b) the failure does not lead to any permanent or long-lasting environmental damage;
(c) the affected environment can be restored through minor clean-up and restoration efforts

Department of Minerals and Energy (DME) of Western Australia published a guideline in 1999 - *Guidelines on the safe design and operating standards for tailing storages* - using a hazard rating system for the categorization of tailings storage facilities (TSFs). The guideline classifies the TSFs using a hazard rating that recognizes the potential impact on the environment and any life, property, or mine infrastructure as a result of possible uncontrolled leakage or failure of the embankment.

The hazard rating is derived by considering (DME, 1999):

- the potential impact in terms of safety on any nearby community infrastructure and/or mining developments (including the TSF operator) in the event of either controlled or uncontrolled escape of material, seepage and/or abrupt failure of the TSF embankment at any stage in its life; and
- the potential environmental impact in the event of either controlled or uncontrolled escape of material, seepage and/or abrupt failure of the storage embankment at any stage in its life;
- the potential impact in terms of economics on any nearby community infrastructure and/or mining developments (including the TSF operator) in the event of either controlled or uncontrolled escape of material, seepage and/or abrupt failure of the TSF embankment at any stage in its life; such economic impacts should also consider the impact on the mining operation due to the temporary loss of the TSF resulting from the failure or uncontrolled escape of tailings from the facility.

DME guideline uses the hazard rating system together with the size of the facility to define three categories of TSF for which varying levels of detailed study and justification of design, operating

procedures and rehabilitation measures are required. The matrix for defining the three categories of TSFs is shown in Table 4.

Table 4. Hazard Rating/Height Matrix to Derive TSF Categories (reproduced from DME, 1999)

TSF Categories				
Hazard Rating*		High	Significant	Low
Maximum Embankment Height**	>15 m	1	1	1
	5 - 15 m	1	2	2
	< 5 m	1	2	3
*All cross-valley facilities, or facilities which block or significantly impede the flow in natural drainage lines, are to be considered as Category 1 TSF regardless of embankment height.				
** In-pit TSFs are to be classified assuming an embankment height of less than 5m.				

SITUATION IN TURKEY

Recently failures of two tailings dams have drawn public attention in Turkey. On September, 2009 Melet River, major drinking water source of Ordu province, was polluted by tailings from metallic ore processing plant due to tailings dam break after a heavy rain. On May, 2011 an intermediate dike of a tailings dam containing silver leach tailings failed and all the tailings held back by the outer perimeter dike in Kütahya province. These cases highlighted risks induced by tailings storage facilities.

Figure 4. Tailings dam break in Ordu Province

The Regulation on Mining Waste was published in Official Gazette numbered 29417 on 15 July 2015. In line with Directive 2006/21/EC, this regulation has been completely harmonized with EU. It classifies mining waste facilities in Category A and Category B in accordance with the provisions in Annex 5.

RISK ASSESSMENT OF TAILINGS DAMS

Risk-based analysis was first used in 1976 to analyze the failure of the Teton dam in the United States. The Australian National Committee on Large Dams (ANCOLD) created risk assessment guidelines in 1994; it then made new guidelines in 2003. The International Commission on Large Dams (ICOLD) also proposed risk assessment guidelines in 1998, which provided a technical basis for risk-based analysis in dam safety assessment (Zhong, Sun, & Li, 2011). Before this, some experts and researchers thought that the tailings dam could not be treated as a real dam because of its simple

design, long time of construction, and inability to store water. Later, serious disasters caused by accidents related to large tailings ponds gradually have aroused attention and awareness (Wang et al., 2011).

Several studies have been conducted to compile data on tailings dam failures, isolate the causes of these failures and identify trends (Azam & Li, 2010; Rico et al., 2008; UNEP, 1996; USCOLD, 1994). No single legislative body, however, records tailings dam statistics. Furthermore, the data do not allow comparisons between the number of tailings dam failures and the total number of tailings dams built in any given area or time period (ICME & UNEP, 1998).

Failure mechanism of tailings dams, consequences of failures have been investigated by many researches (Benito et al., 2001; Blight, 1997; Blight & Fourie, 2005; Fourie, Papageorgiou, & Blight, 2000; Gallart et al., 1999; Jeyapalan, Duncan, & Seed, 1983; Krausmann & Mushtaq, 2008; Neuhold & Nachtnebel, 2011; Pastor et al., 2002; Van Niekerk & Viljoen, 2005).

Jeyapalan et al. (1983) applied a Bingham plastic model (TFLOW computer program) for analyses of flow failures in more highly viscous tailings which undergo laminar flow. They stated that analyses of potential inundation zones likely to result from very fluid tailings, such as phosphate tailings and the mixture of water and coal waste can be modeled as turbulent flows (Jeyapalan et al., 1983).

Lucia et al. (1981) proposed a method to estimate the potential mine waste run-out distance based on historical tailings dam failures and using the value of the residual strength of liquefied tailings. Their procedure is based on the failures where liquefied tailings became stable after flowing over slopes of less than 4^0. They emphasized that steeper slopes may require different analyses and they also indicate that it appears unlikely that tailings material will come to rest on slopes steeper than about 9^0. In such case it should be expected that flow will continue until a flatter area or body of water is reached (Lucia, Duncan, & Seed, 1981). Their model requires some detailed geotechnical data of the material contained in the tailings ponds as well as on the geometry of the downstream valley.

Apart from complex hydraulic calculations applied to specific case studies, more simple estimations can be performed based on generic empirical relationships. Rico et al. (2008) compiled the information on historic tailings dam failures with the purpose to establish simple correlations between tailings ponds geometric parameters and the hydraulic characteristics of floods resulting from released tailing. In their study, researchers plotted "tailings dam" factor ($H \times V_F$) versus the outflow run-outdistance (D_{max}) and created a regression line and formula as following (Rico, Benito, & Diez-Herrero, 2008):

$$D_{\max} = 1.61 \times (HV_F)^{0.66},\ r^2 = 0.57 \quad (1)$$

where H is dam height in meters and V_F is waste outflow volume in $10^6 \times m^3$

Rico and her colleagues pointed out that a major limitation to the application of this equation to risk analysis of standing tailings dams consists of the uncertainty of potential tailings outflow volume (V_F) in the case of failure. They found another empirical relationship between the tailings storage volume and the tailings released at the incidents, which has the equation:

$$V_F = 0.354 \times V_T^{1.01},\ r^2 = 0.86 \quad (2)$$

The above equation shows, that in average, one-third of the tailings and water at the decant pond is released during dam failures. V_T is the maximum tailings volume that can be released in the most extreme situation in which pond volume was emptied following the dam break (Rico et al., 2008).

Mara et al. (2007) developed a methodology to assess the hazards associated with mine waste tailings dams which is based on quantifying the hazardous components and assigning a hazard value, using a system of criteria, indexes, and notes.

The hazard associated to a dam is appreciated by the RB index, $RB = CA/(\alpha \times BA + \beta \times CB)$. Other indexes used by the researchers in the evaluation are:

- The BA index is determined by the characteristics of dam or deposit (dimensions, type, discharge, importance class), its location (the nature of the ground and seismicity), and the condition of the lake or waste deposit;
- The CB index is determined by the situation of the dam, the sophistication of the operational controls and monitoring system(s), the level of maintenance, the dam's behavior over time, the conditions of the accumulation lake, and the level of site-specific knowledge;
- The CA index quantifies the consequences of damage to the dam/deposit, taking into consideration: the possibility of loss of lives, potential effects on the environment, potential social-economic effects, etc.
- α and β are the weight coefficients.

Mara et al. (2007) defined the risk of tailing dams to surface waters as $Risk = RB \times WRI$, where WRI (Water Risk Indexes) quantify the vulnerability of the environment to pollution due to possible accidents at the tailing dams. WRI = log (∑WRC), where WRC is Water Risk Class and determined according to Annex III of European Union Directive 67/548/EEC: *Nature of special risks attributed to dangerous substances and preparations.*

Risk of tailing dams to surface waters is determined by $Risk=[CA/(\alpha \times BA + \beta \times CB)] \times \log (\sum WRC)$.

Recently Mei (2011) studied on a quantitative assessment method based on weakness theory of dam failure risks in tailings dam. They calculated effectiveness-losing probability of dam failure in tailings dam using volume weight, internal friction angle and cohesion as random variables and adopting Monte-Carlo model. They established a flow model of tailings after dam failure based on hydrology, hydrodynamics and movement theory of non-Newtonian fluid to compute submergence range due to the failure. Loss ratio of dam failure is calculated through computation of loss of life, financial and environmental loss after dam failure (Mei, 2011). Loss level (V) of submergence range is constituted by weight method of multi-stress: $V= W_1H+W_2P_E+W_3S$; where H, P, S is loss of life, economic loss and influences on social environment, respectively, and W_1, W_2, W_3 refer to weight of each factor derived through expert evaluation and analytic hierarchy process.

Xin et al. (2011) studied on risk assessment of the tailings dam break. They analyzed the cases of tailings dam accident worldwide, established a tailings dam stability evaluation index system. The theory of set pair analysis is used to assess the tailings dam break possibility.

The routing and movement of tailing flow in the downstream after tailings dam break is simulated using DAMBRK model and the distributions of personnel and structures in the influence range is investigated. They use a comprehensive factor weighted method to construct consequence evaluation model. Their model considered the tailings dam scale, loss of life, economic losses and social environment impact. Following equation is used to evaluate the consequences (C) of tailings dam failure: $C=W_1D+W_2H+W_3P+W_4S$; where D, H, P, S are tailings dam scale, loss of life, economic losses and social environment influence, respectively, and W_1, W_2, W_3, W_4 are the four factors weight. Risk assessment of tailings dam is finally given in matrix form as integrated risk classification given in Table 6 (Xin et al., 2011).

Table 2: Tailings dam integrated risk classification

Tailings dam integrated risk classification		Dam break severity classification			
		Extreme effect (4)	High effect (3)	Moderate effect (2)	Low Effect (1)
Tailings dam break probability	Tailings dam break at any time (4)	16	12	8	4
	Safety facilities exist serious hidden trouble, if not timely treatment will lead to tailings dam break (3)	12	9	6	3
	Tailings dam meet the basic conditions for safe production (2)	8	6	4	2
	Tailings dam fully equipped with the conditions for safe production (1)	4	3	2	1

REFERENCES

Azam, S. and Li, Q. (2010). Tailings dam failures: A review of the last one hundred years. Geotechnical News, 28, 50-53.

Benckert, A., Eurenius, J., 2001. Tailings dam constructions. In Seminar on safe tailings dam constructions (pp. 30-36). Gallivare: Swedish Mining Association, Natur Vards Verket, European Commission.

Benito, G., Benito-Calvo, A., Gallart, F., Martin-Vide, J. P., Regues, D., & Blade, E., 2001. Hydrological and geomorphological criteria to evaluate the dispersion risk of waste sludge generated by the Aznalcollar mine spill (SW Spain). Environmental Geology, 40, 417-428.

Blight, G. E., 1997. Destructive mudflows as a consequence of tailings dyke failures. Proceedings of the Institution of Civil Engineers: Geotechnical Engineering, 125, 9-18.

Blight, G. E., Fourie, A. B., 2005. Catastrophe revisited-disastrous flow failures of mine and municipal solid waste. Geotechnical and Geological Engineering, 23, 219-248.

Cambers, D., Higman, B., 2011. Long Term Risks of Tailings Dam Failures. http://www.csp2.org/reports.htm Retrieved, 1-2-2012

DME (1999). Guidelines on the safe design and operating standards for tailing storages Department of Minerals and Energy, Government of Western Australia.

EC., 22-4-2009. Commision Desion on the definition of the criteria for the classification of waste facilities in accordance with Annex III. 2009/337/EC.

Fourie, A. B., Papageorgiou, G., Blight, G. E., 2000. Static liquefaction as an explanation for two catastrophic tailings dam failures in South Africa. Tailings and mine waste '00.Proceedings of the 7th international conference, Fort Collins, January 2000., 149-158.

Gallart, F., Benito, G., Martin-Vide, J. P., Benito, A., Prio, J. M., Regues, D., 1999. Fluvial geomorphology and hydrology in the dispersal and fate of pyrite mud particles released by the Aznalcollar mine tailings spill. Science of The Total Environment, 242, 13-26.

ICME & UNEP (1998). Case studies on tailings management International Council on Metals and the Environment (ICME) and United Nations Environment Programme (UNEP).

ICOLD, 1982. Manual on Tailings Dam (Rep. No. Bulletin 45). International Commission on Large Dams.

ICOLD & UNEP, 2001. Tailings Dams - Risk of Dangerous Occurrences, Lessons learnt from practical experiences (Rep. No. Bulletin 121).

Jeyapalan, J. K., Duncan, J. M., Seed, H. B., 1983. Investigation of Flow Failures of Tailings Dams. Journal of Geotechnical Engineering, 109, 172-189.

Krausmann, E., Mushtaq, F., 2008. A qualitative Natech damage scale for the impact of floods on selected industrial facilities. Natural Hazards, 46, 179-197.

Lemphers, N., 12-10-2010. Could the Hungarian tailings dam tragedy happen in Alberta? Retrieved, 13-3-2012 from http://www.pembina.org/blog/417.

Lucia, P. C., Duncan, J. M., Seed, H. B., 1981. Summary of Research on Case Histories of Flow Failures of Mine Tailings Impoundments. In Mine Waste Disposal Technology.

Mara, S., Tanasescu, M., Ozunu, A., Vlad, S. N., 2007. Criteria for Identifying the Major Risks Associated with Tailings Ponds in Romania. Mine Water and the Environment 26:256–263

McLeod, H., Murray, L., 2003. Tailings Dam versus a Water Dam, What is the Design Difference? In ICOLD Symposium on Major Challenges in Tailings Dams .

Mei, G. (2011). Quantitative Assessment Method Study Based on Weakness Theory of Dam Failure Risks in Tailings Dam. Procedia Engineering, 26, 1827-1834.

Neuhold, C., Nachtnebel, H. 2011. Assessing flood risk associated with waste disposals: methodology, application and uncertainties. Natural Hazards, 56, 359-370.

Pastor, M., Quecedo, M., Fernandez Merodo, J. A., Herrores, M. I., Gonzalez, E., & Mira, P. (2002). Modelling tailings dams and mine waste dumps failures. Geotechnique, 52, 579-591.

Penman, A. D. M. (2001). Risk analyses of tailings dam constructions. In Seminar on safe tailings dam constructions (pp. 37-53). Gallivare: Swedish Mining Association, Natur Vards Verket, European Commission.

Rico, M., Benito, G., Diez-Herrero, A., 2008. Floods from tailings dam failures. Journal of Hazardous Materials, 154, 79-87.

UNEP, 1996. Environmental and safety incidents concerning tailings dams at mines: results of a survey for 1980-1996 United Nations Environment Programme.

USCOLD, 1994. Tailings Dam Incidents United States Commission On Large Dams .

Van Niekerk, H. J. & Viljoen, M. J., 2005. Causes and consequences of the Merriespruit and other tailings-dam failures. Land Degradation & Development, 16, 201-212.

Vick, S. G., 1990. Planning, Design, and Analysis of Tailings Dams. Richmond B.C., Canada: BiTech Publishers Ltd.

Wang, T., Zhou, Y., Lv, Q., Zhu, Y., Jiang, C., 2011. A safety assessment of the new Xiangyun phosphogypsum tailings pond. Minerals Engineering, 24, 1084-1090.

Xin, Z., Xiaohu, X., Kaili, X., 2011. Study on the Risk Assessment of the Tailings Dam Break. Procedia Engineering, 26, 2261-2269.

Zhong, D., Sun, Y., & Li, M., 2011. Dam break threshold value and risk probability assessment for an earth dam. Natural Hazards, 59, 129-147.

5th International Symposium on Dam Safety

October 27-31, 2018

MOSUL DAM, IRAQ: MAINTENANCE GROUTING WORKS FOR THE DAM SAFETY

Raffaella GRANATA[1], Carlo CRIPPA[2]

ABSTRACT

The Mosul Dam is an earthfill dam located on the Tigris river, about 60km North of Mosul (Iraq), about 200 km South of Turkish border (Siirt Şırnak Yolu). It was built in the first half of the 1980s as a multipurpose project conceived for irrigation, flood control, water supply and hydropower generation. Over the years, the structural integrity of the dam and its operational capacity were cause for concerns, principally because of the phenomena of dissolution of gypsum and anhydrite layers, occurred in the bedrock foundation. The deteriorating foundation of the dam poses a risk that, if not fully addressed, could result in catastrophic events, loss of life, economic damage, and geopolitical instability. In October 2015 the Iraqi Government issued an international invitation to tender for the emergency maintenance and safety of the dam. Trevi S.p.A. was awarded the tender (March 2016). The contract included works for the repair of manufactured structures in relation to the bottom outlet, the grout injections aimed at repairing the grout curtain, and the supply and sale of all the equipment necessary to execute the intervention. This paper focuses on the drilling-and-grouting activities implemented for the refurbishment of the grout curtain along the axis of the dam.

Keywords: Dam safety, drilling and grouting, refurbishment, monitoring and instrumentation

INTRODUCTION

The Mosul Dam is located on the Tigris River about 60 km north-west from the city of Mosul (Fig.1).

Figure 1. Mosul Dam - Location Map

[1] Senior Technical Advisor at Design, Research & Development Department, Trevi S.p.A., Cesena, Italy
e-mail: rgranata@trevispa.com
[2] Area Manager and Project Director at the International Department, Trevi S.p.A., Cesena, Italy
e-mail ccrippa@trevispa.com

The Dam was built in the first half of the 1980s as a multipurpose project conceived for irrigation, flood control, water supply and hydropower generation. It is a zoned embankment dam, which includes a 5-gate service spillway, a hydropower facility rated to 750 MW and features a bottom outlet structure with two gates and an emergency spillway. The Dam is 3500 m long and 113 m high, with the crest at El.+343 m above the sea level. The design maximum water level in the reservoir is at El.+335.0 m, the minimum operating level is at El.+300 m. The reservoir storage capacity is an estimated 11.1 billion cubic meters. Mosul Dam is the largest dam within Iraq and the 4th largest in the Middle East. The typical cross section is shown in Figure 2. The construction of the Dam was completed in 1984, and the impounding started at the end of the following winter season.

BACKGROUND

Geological setting

At the Mosul Dam site, the geological setting includes Pleistocene to recent alluvial deposits overlying rocks of Miocene age. The lower terraces along the Tigris River comprise the sandy and clayey silt that was used to create the core of the dam.

The foundation rocks beneath the dam are predominantly of the Late Miocene-age Fatha Formation and were deposited in lagoon and arid to semiarid supratidal ("sabkha") environments (Jassim et al. 1997). Original deposition of the Fatha Formation followed the usual cyclic pattern of sabkhas and resulted in alternating layers of marl, gypsum, and carbonate. In the area, the Fatha Formation is up to 350 m thick and comprises two members (Upper Fars and Lower Fars Groups). In the foundation, the Lower Fars Group is the predominant group of rocks. It comprises gypsum and anhydrite layers interbedded with marls, limestones and claystones, and can be further divided into the Upper and Lower Marl Series, with the F-bed Limestone in between (Jassim et al. 1999).

The F-bed Limestone consists of both highly fractured, brecciated limestone beds and interbedded marls and limestones; the main part of the spillway was constructed on the F-bed Limestone. The historical records report that the F-bed Limestone was one of the problem areas taking large quantities of grout in the spillway area, at the time of the construction of the dam.

The Lower Marl Series is approximately 180 m thick and consists of interbedded layers of anhydrite/gypsum, marls, and limestones (Figure 2).

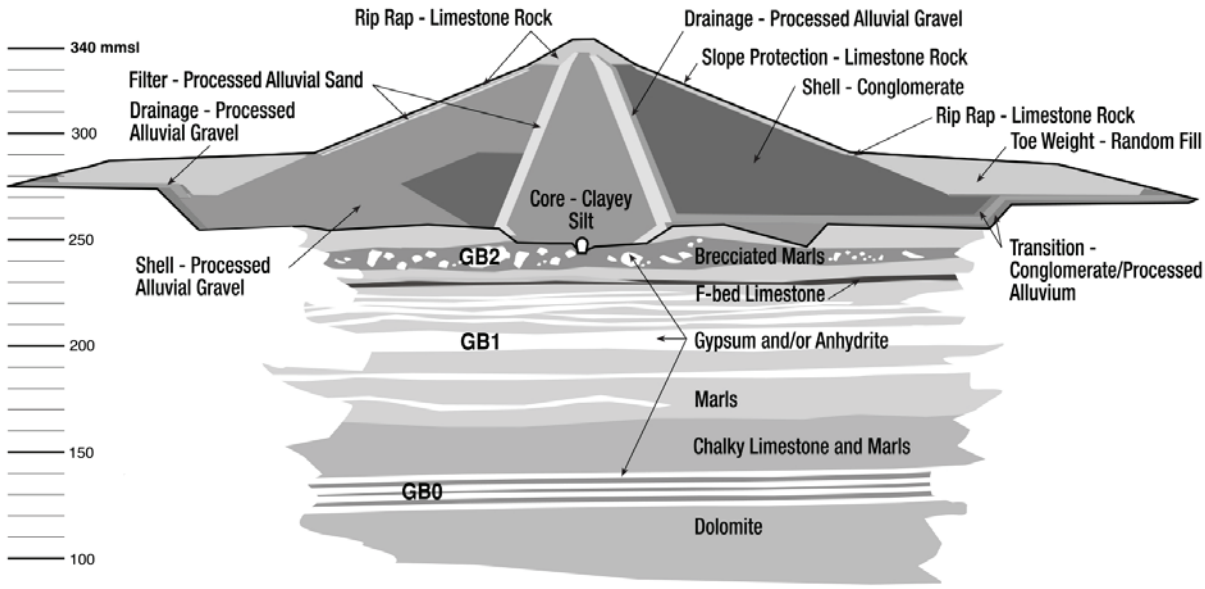

Figure 2. Mosul Dam - Typical Cross Section and Geological Setting (Station 2400 circa)

Four dominant anhydrite/gypsum breccia layers have been identified as marker beds; they are designated (from upper to lower) GB3, GB2, GB1, and GB0. The base of the GB0 is the bottom boundary of the Lower Fatha Formation (Kelley et al. 2007), which rests on the dolomite of the Jeribe formation.

The local geology is affected by the presence of karstic limestone and solution cavities within the gypsum and the anhydrite layers. The erosion and dissolution rates in gypsum are related to the seepage velocities and hydraulic gradient. Dissolution phenomena result in the formation of fissures and voids that, due to the strong hydraulic gradient, allow considerable water percolation. These flows favor further dissolution phenomena, in a vicious circle. These dynamics may result in the collapsing of limestone and marls layers into the underneath cavities, forming beds of "Gypsum Breccia", which contain fragments, clasts or blocks of limestone, marls, or larger pieces of insoluble rocks of collapsed material (Figure 3).

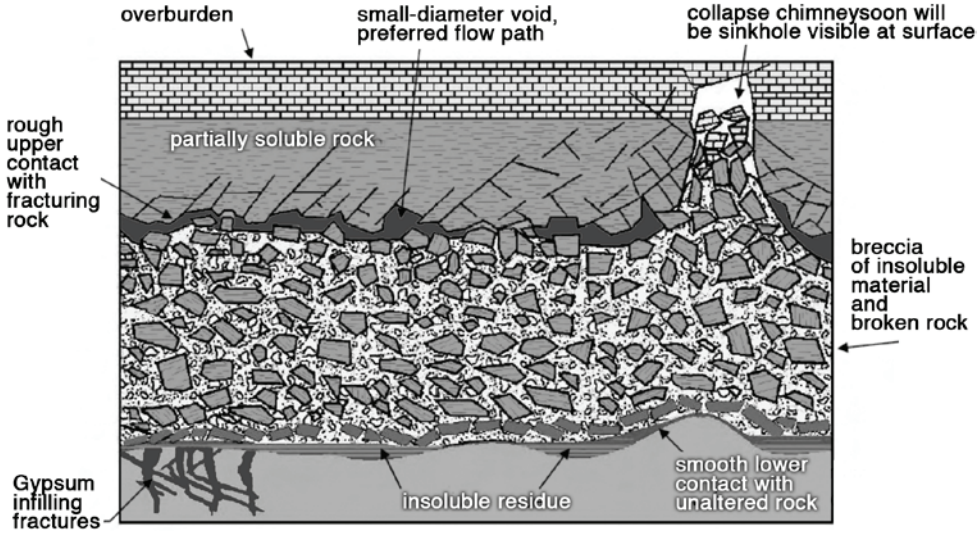

Figure 3. Development of breccia within a layer of gypsum (Kelley et Al. 2007, after Warren, 2006).

Dam Design and Construction

Concern for the dissolution of gypsum in the foundation was raised at the time of the original design of the dam, when the four gypsum units, varying in thickness from 8 to 16 m, were identified. It was recognized from the beginning of the feasibility studies that the foundation geology was an issue. The presence of karst phenomena, down to a depth of over 100 m below the foundation of the dam, was confirmed by further investigation and excavation carried out during the dam construction.

Actions were taken to face the problematic geological setting, in an attempt to mitigating the possible outcomes. A grout blanket was installed beneath the dam core to a depth of 25 m. A deep grout curtain was designed to be installed all along the dam centerline. In addition, a grouting gallery was constructed at the base of the embankment dam, on top of the foundation rock, from the spillway on the east abutment to the west abutment. The gallery was specifically designed to deal with the considerable challenges posed by the karst foundation and to allow repeated grouting efforts to continue over the lifetime of the dam. As per the design, the original Italian-German specialized subcontractor initiated an aggressive grouting program in 1984; but due to political pressures, the impoundment of the reservoir began whilst the installation of the deep curtain grouting was in progress. Afterward, the Iraqi Ministry of Water Resources (MoWR) has continued grouting ever since 1989, using the equipment and technique left by the subcontractor.

Safety Risk-Assessment

In spite of the actions taken, over the years the structural integrity of the dam and its operational capacity were cause for concerns, principally because of evident phenomena of dissolution of the gypsum and anhydrite layers. The rate of subsurface dissolution was increased by the presence of the reservoir. Seepage flows have appeared as springs in the downstream riverbank and in the riverbed since reservoir impoundment in 1985. In the '90s small sinkholes have reached the surface downstream of the dam. Above a pool elevation of 318 m, the rate of subsurface dissolution increased markedly, leading to the recommendation that the pool not be raised above this level. The low reservoir level obviously impacted the power generation and the agricultural irrigation.

In addition, the geopolitical instability in northern Iraq almost interrupted the maintenance grouting operations between 2014 and 2015, and it is believed to have further impacted the condition of the Dam foundation.

In 2015-2016, the USACE Risk Assessment Team performed a risk-assessment analysis and identified 24 Potential Failure Modes. It is worth noting that Mosul Dam serves as a flood control structure protecting more than one million people residing in the flood plain. The risk-based study considered the likelihood of dam failure due to various PFMs related to the foundation conditions combined with the predicted loss of life if the dam were to fail. When shown on the USACE standard risk chart, the risks for Mosul Dam were classified as very high: if the risks were not addressed, failure could result in catastrophic loss of life, economic damage, and geopolitical instability (Paul et Al., 2018).

The Tender for the Maintenance Grouting and Rehabilitation of the Bottom Outlet

In consideration of the critical situation characterizing the dam, at the end of 2015 the Iraqi Government issued an international invitation to tender with an emergency procedure for the maintenance and safety of the Dam, and requested that the US Army Corps of Engineers (USACE) serve as the Engineer for these efforts.

In March 2016, the Iraqi Ministry of Water Resource (MoWR) awarded the Mosul Dam Rehabilitation Project to Trevi, while the design and the supervision of the works was entrusted to the USACE, acting as Engineer for the project. The contract included all the activities aimed at repairing the grout curtain, with the supply of all the equipment and materials necessary to execute the drilling and grouting intervention.

The contract included as well the works for the repair and maintenance of structures and plants associated with the bottom outlet tunnels, through operations on the electromechanical parts. These works required the intervention of divers and specialized sub-contractors, and were conducted by a dedicated staff in parallel with the grouting activities.

REHABILITATION GROUTING

Site Preparation and Infrastructure Upgrading

Immediately after the award, the Trevi mobilization promptly started. Mobilization and site preparation faced logistic problems related to the site location being about 20 km from the firing-line of the conflict against Isis in the city of Mosul.

The setting up of the site began in early summer, with the construction of a secure base camp facility to provide living and working accommodations for the approximately 1000 people on site. Also, the construction of six new office buildings, a new repair-maintenance shop and the grout and mortar mixing plants began. Concurrently, activities were started for the replacement of the entire grouting infrastructure and for the construction of new electrical, ventilation, communication /internet and water/wastewater systems.

The electrical upgrade included removal of over 3000 m of old cables and installation of 170,000 m of new cables, cable trays, transformers and generators to supply power for the gallery and crest of the dam. New lighting systems were installed in the gallery and along the crest, to grant safer and more effective operations. A new ventilation system was designed and installed to draw fresh air in through the right access gallery, circulate it throughout the gallery and then out through the left access gallery.

The entire gallery and crest were equipped with a Local Area Network (LAN) using the 2500 m of fiber optic cable newly installed. Wireless hotspots with internet connection were setup across the entire dam to enable communication among teams working simultaneously throughout the dam and the offices.

New submersible pumps were installed to circulate fresh water through the 3.4 km dam. Over 4500 m of new pipelines were installed (and 2000 m relocated) to carry fresh water/wastewater in and out of the gallery. New sump pumps were also installed to carry the wastewater from the sumps to the siltation tanks outside the gallery. Over 15,000 m of new pipeline were installed to deliver the bentonite slurry and the grouting mix to the gallery and crest (see below).

Overall, more than 200,000 m of cables and pipes were installed and relocated in the first 8 months, always without interrupting the drilling and grouting activities when/where they were already in progress.

Drilling and Grouting Works

The grouting activity for the Dam refurbishment started at the end of October (2016). The end purpose of the emergency grouting program was to install a double line grout curtain along the full length of the grouting gallery and connecting curtains from the crest of the dam east of the spillway (saddle dam) and west abutment.

Accordingly, the drilling and grouting activities had to be carried out both from the dam crest and from the grouting gallery, with the goal of injecting mixes able to intercept and plug the fissures and voids, mainly derived from dissolution and karst phenomena. Because of the stratigraphy and design considerations, it was necessary to drill and inject holes to a depth of 150 m and over. Due to the lake water level, the gallery activities were further complicated by the need to operate in the presence of a significant water-head. This required the use of a blow-out preventers, necessary for the performance of almost all the drilling and grouting activities.

Drilling and Grouting Equipment

In relation to the main dam, injections were executed from the 2200 m long gallery, resting on the foundation rock at the base of the impervious core. The small dimensions of this horseshoe shaped gallery, 3.7 m high and 3.0 m wide, with slopes up to 41%, obviously had a considerable impact on the time required for carrying out the intervention. These features entailed the use of small-size rigs and grouting units and posed significant challenges in terms of equipment configuration and maneuvering requirements. In addition, since the grouting gallery is accessible only from two long and small access galleries (located at its two ends), special techniques and logistical arrangements were needed to transport the grouting material to the boreholes to be injected.

Given the limited space constraints in the gallery, the grouting system was designed to prepare a “Base Mix” at the outdoor mixing plants (outside the gallery) and use a conveyance system to bring the grout into the gallery, in a continuous loop. Additional conveyance lines were installed to deliver bentonite slurry and fresh water through the gallery. In the gallery nearby each injection hole, a batching and grouting unit (BGU) draws Base Mix, water and bentonite slurry from the conveyance system, and prepares one of the required design grouts by dosing and mixing the components in the appropriate proportions. The additives are automatically added as well, when required by the specific mix design.

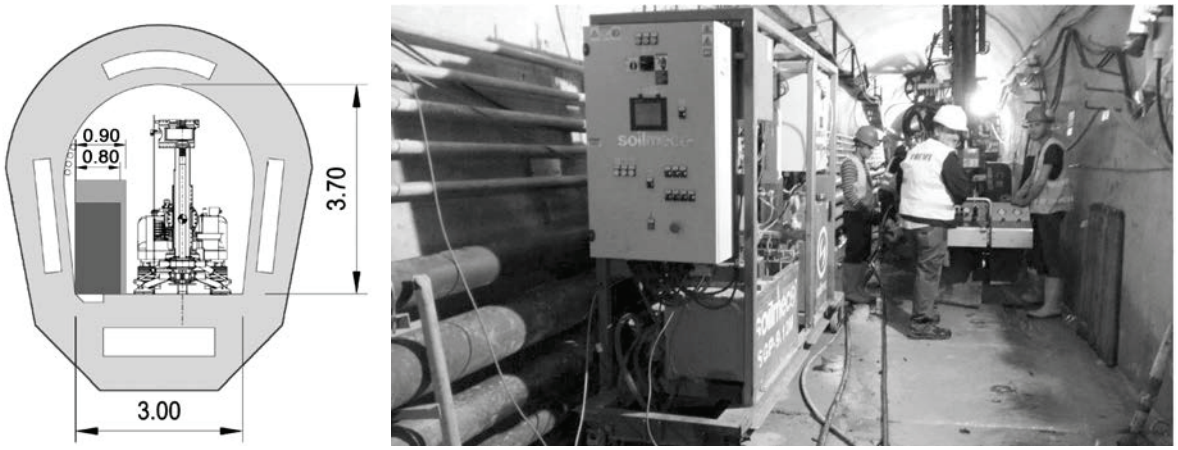

Figure 4. Drilling and Grouting equipment inside the Grouting Gallery (Drill Rig SM5 and BGU)

The BGUs were custom designed to fit within the limited available space in the gallery and on the dam crest (Figure 4). Each BGU is equipped with a piston-pump, directly fed by the batcher. The piston pump was designed to operate at high pressures and flow rates, when needed. The BGUs are automated to communicate with computer-based monitoring systems and to be remotely managed by the grouting software (see below). The same system was adopted at the crest of the Dam, to deliver/prepare the grout mixes and to manage the grouting process.

The magnitude of the project and the need to comply with the schedule required the use of 13 drill rigs, 3 outdoor "Main Mixing Plants" and 20 BGUs (batching and grouting units).

Six small Soilmec SM-5 electric crawler-mounted rigs were supplied for the drilling works inside the gallery (Figure 5). A small Ripamonti Birdie E250 was supplied to work in the 100 m long stretch of gallery under the spillway, characterized by a furtherly reduced section (2 m wide, 3 m high).

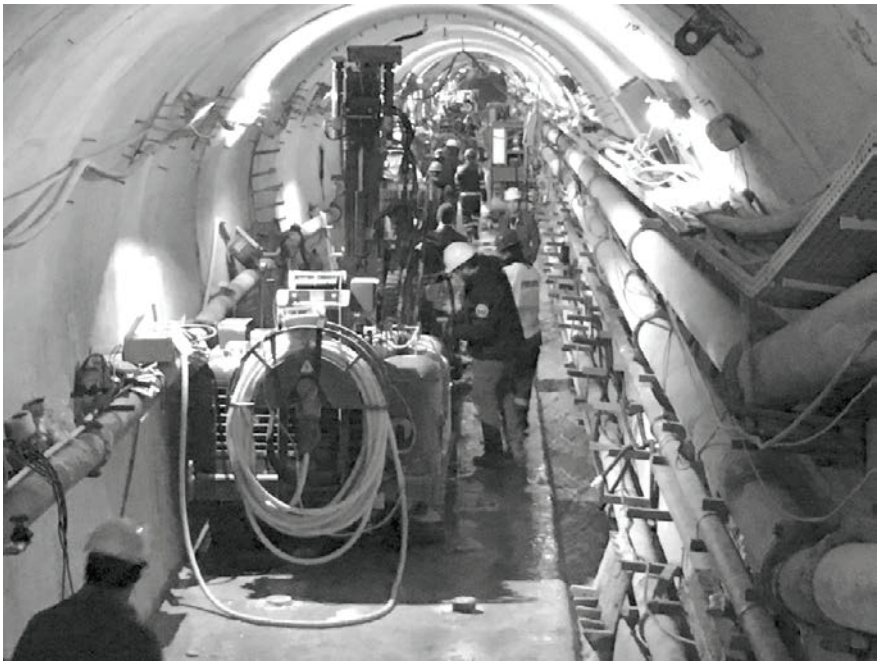

Figure 5. Drilling equipment in the Grouting Gallery (Drill Rig SM5)

Two double-rotary, long mast SM-16 diesel crawler rigs where supplied for the outdoor drilling works (Figure 6). Both rig types are capable of drilling holes to a maximum depth of 300 m, by rotary or coring (or roto-percussion if required). The SM-16 rigs where equipped with a powerful double rotary, to allow the simultaneous driving of auger rods and steel casing while drilling the embankment. All the rigs were equipped with a drilling parameter recording (DPR) device, to collect the various parameters (i.e. penetration and rotation speed, thrust and torque pressure, fluid pressure, specific energy) for analysis.

Figure 6. Drilling Equipment at the East Left Bank (Drill Rig SM16)

The three "Main Mixing Plants" were installed in separate locations over the length of the dam, and conveniently close to the gallery adits. These plants operate on weight-based batching; they are equipped with silos to store cement, dry bentonite, bentonite slurry and water (Figure 7). They have a capacity of 1500 liters/batch and are capable to produce 30 m3 of grout per hour. Each plant is equipped with a group of pumps used to deliver and keep in continuous circulation the mix in the rout-line circuit (3000 m long). As said, the conveyance system feeds the 20 small batching and grouting units (BGUs), which can be conveniently located along both the gallery and the crest, nearby the borehole to be grouted.

Mortar mixes can be prepared by a small mortar batching plant. The mortar can be delivered via larger pipes installed throughout the gallery, or from the crest of the dam to the gallery via three existing vertical service holes established through the embankment.

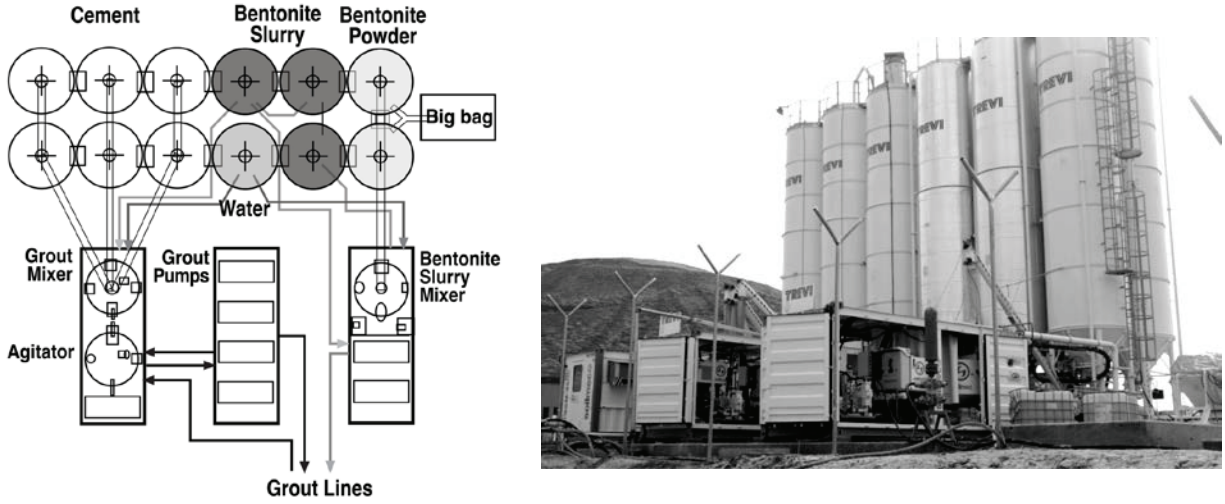

Figure 7. One of the three Outdoor Main Mixing Plant (MMP-3, above) and its configuration (below)

Drilling and Grouting Method

According with the analysis, studies and outcomes of the mentioned Risk Assessment Findings (2016), the Dam's foundation was divided into "Critical Areas", which defined the grouting priorities. The drilling and grouting methods were based on a "flexible approach", since the rock conditions vary significantly within very short distances and depths. These variable conditions include solution features of different sizes and orientations, joints and widened joints, irregular slopping, rock fissures, irregular top of rock, and varying combinations of these features. The presence of flowing water under artesian pressures was typically encountered when drilling and grouting from the gallery.

The upstage method (5 m long stages), was the most applied grouting method. The downstage and downstage-zone methods were also used based on field observations and geology. For all cases, each borehole was pressure grouted using a single packer, lowered in the hole at top of the stage to be grouted.

Drilling through the foundation rock was always performed by rotary system (by PDC drilling bits or core barrels with core recovery), using water as the flushing system. Most of the drilled boreholes were vertical or subvertical. However, there are seven water supply tunnels in the foundation beneath the grouting gallery, associated with the outlet structures, the power plant and a nearby pump storage facility. Therefore, several boreholes were to be drilled in inclined array, to allow the closure of the curtain also under these structures. Further inclined boreholes were drilled and grouted to connect the curtain installed from the East bank to the one under the spillway concrete structure. Each borehole in the gallery was equipped with a steel standpipe to allow for the installation of the blowout preventer. The standpipes were cut at the floor level, to prevent the trip hazard and difficulties related with the movement of the equipment (with the standpipe protrusion). They were cemented using a special grout, designed and tested to resist against the pull-out, and fitted with a flush treated joint at the top-end for the connection to the BOP (Figure 8).

Figure 8. Gallery with Standpipes Cut Flush to Surface (left) and installation of packer through the preventer (right)

The boreholes bored from the crest of the dam involved the drilling of the embankment and core. While drilling through the embankment the use of any drilling fluid (air or water) was forbidden, to prevent possible hydraulic/pneumatic fracturing of the embankment and re-molding of the dam-core. Accordingly, the drilling was performed by auger and temporary casing, down to 1.0 m into the bedrock underneath clay-core (Figure 9). Afterward, a permanent plastic casing was cemented inside the borehole, to avoid any risk of fracturing and damaging the dam core during the upcoming drilling and grouting of the foundation rock.

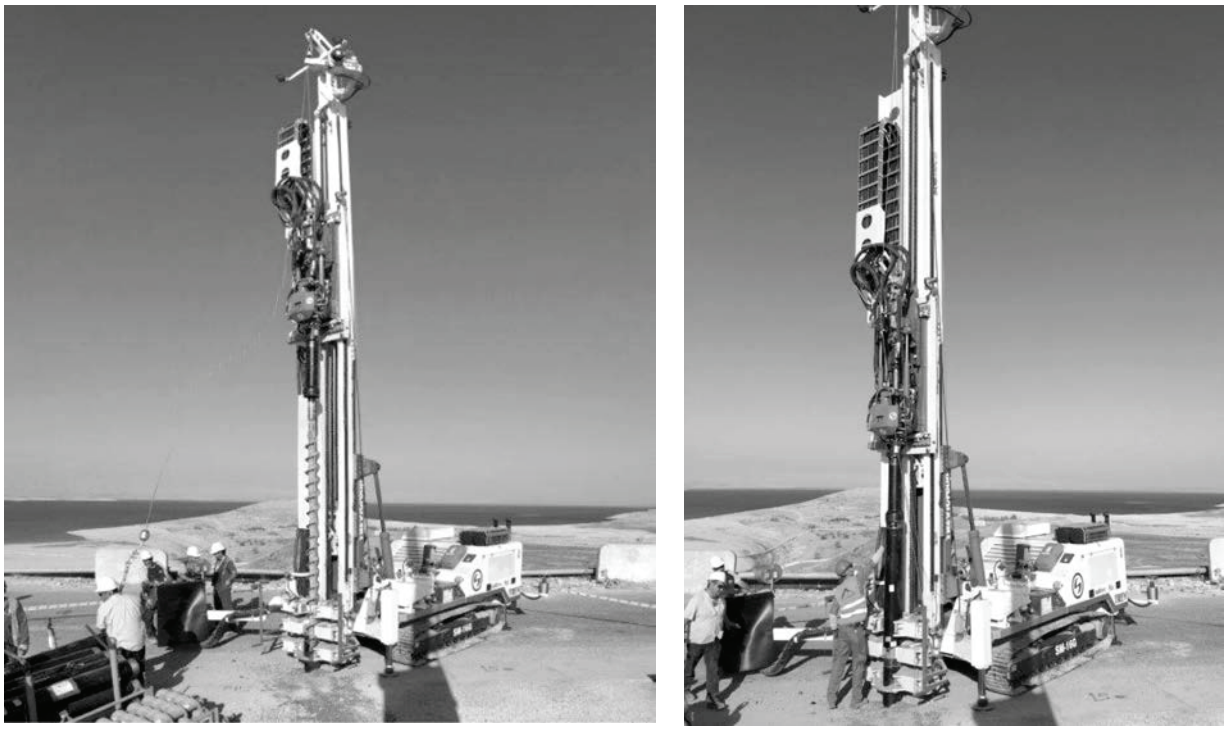

Figure 9. Drilling through the Dam embankment (auger and steel casing)

The mix design of the grouts was started at Trevi main offices in Italy prior to mobilization, using the components being considered for the project. This effort continued in the new laboratory installed at site for the project. A series of stable grout mixes, characterized by different cement content, viscosity and setting time were designed and grouted.

As a rule, the grouting of each stage was started with a thin grout (both in density and viscosity), and continued with thicker grouts, with high cement content and setting fastener (or sand), as needed. The grouting volume for each type of mix was directed by a flowchart defining the relationship between the effective pressure recorded during grouting and the volume of mix being injected. The grouting pressure and methodology varied along the dam, based on encountered geology and observed issues while drilling. The maximum effective pressure to be used in each borehole, at the different depths, was determined by the Engineer, on the basis of specific considerations to get the best penetration while limiting the risk of rock hydro-fracturing. As such, the closure criteria for each stage was based on the refusal pressure and flowrate (less than 1 lit/min), which had to be reached and maintained constant for a prefixed period of time (at least 2 minutes).

Electronic equipment was extensively used to investigate the conditions of the rock, before and/or after grouting. The borehole optical televiewer (OPTV), capable of creating a high-resolution photographic image of the full circumference of the borehole, is a very useful instrument to provide reliable information on the state of the rock (and borehole deviation) in lieu of the time-consuming traditional coring (Figure 10). The use of the high-resolution acoustic televiewer (HRAT) allowed the surveying of borehole in the presence of turbid water. The closed-circuit television camera (CCTV) was used to generate electronic high-resolution video of boreholes above the groundwater level.

The high-resolution impeller flowmeter (HRIF) was used to measure the artesian flow rate encountered in the boreholes at various depths. Lugeon water pressure tests were carried out upon Engineer request, mainly after having grouted a stretch of curtain.

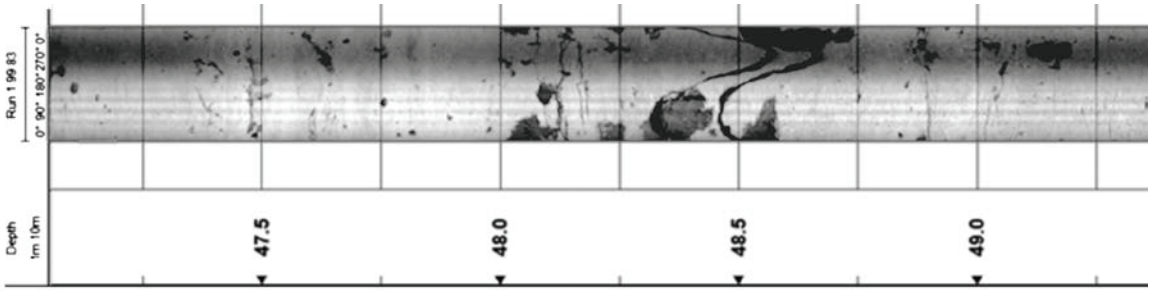

Figure 10. OPTV Record in a check hole. It is worth noting the grouted fissures

Automated Grout Monitoring System

At Mosul Dam Project all the grouting operations are controlled, monitored and managed by "T-Grout", a proprietary and copyrighted Automated Control System of the Grouting Process (Figure **11**).

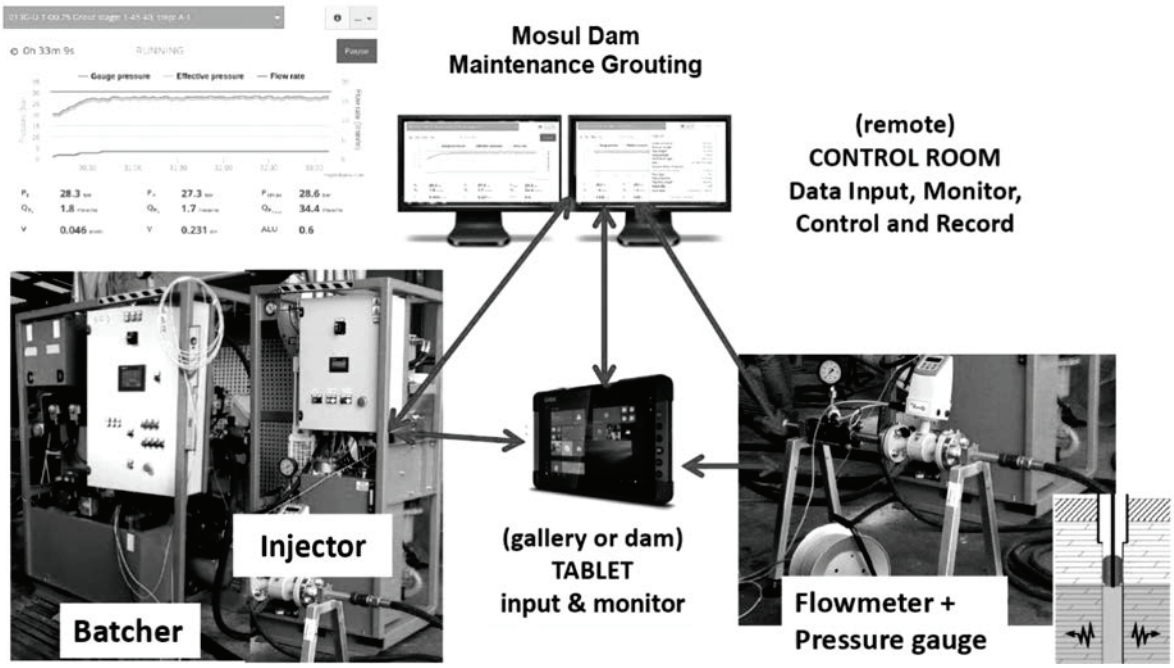

Figure 11. Computerized Grouting Control System: Structure of the System

Electronic data acquisition devices are set up near each injection hole (flowmeter and pressure gauge at the grout header) and the grout pump, to gather pressure and flow data. All the collected data are transmitted to the grouting software, which in turn regulates the pump pressure and flow-rate to maintain their values within the required limits. The software automatically computes the effective pressure, correcting the "raw value" measured at the borehole collar, taking into consideration all the dynamic and static head losses/gains. The grouting software directly governs the whole grouting process and triggers mix changes based on pre-set criteria for pressures or volumes within the bounds of the refusal criteria.

A centralized control room is setup to manage and monitor the grouting operations across the dam from a single location (Figure 12). At the grouting location, technical operators are allowed to check all the parameters and the grouting behavior through tablets (through optical fibers and wi-fi), directly connected to the "grout header" and the "control room". A verbal and written messaging system

allows the direct communication between the operators in the gallery and the “control room”.

Figure 12. Activity in the “Control Room”

The gathered grouting data and process behavior are recorded, analyzed and archived by the software in the database. The software produces “in-real-time” reports for each stage and summary of the main grouting data for each borehole, and updates the database for the whole site, including grout takes (volumes and solids) and grouted length (with number of stages and boreholes). Likewise, the software creates (and automatically updates) the drawings representing position and detailed grout take of every stage of each hole, along the grout curtain profile. SQL Code skilled operators can query the database to receive and combine any kind of information for further analyses.

Also, the drill rigs can be connected to the T-Grout, to automatically transfer the drilling parameter data to the database. T-Grout computer monitoring system is integrated with GIS and with the information management system developed by the USACE on SIMDAMS platform (Bateman et Al., 2018).

PERFORMED QUANTITIES

Trevi workforce reached a peak of more than 700 personnel, with Italian management and supervision, third country national staff and local personnel, for a total of 11 different nationalities. Through mid-August 2018, about 5.5 million man-hours were worked without recordable incidents.

Through mid-August 2018, the downstream line of grouting boreholes (1.5 m spaced) was completed along the entire length of the dam, and the upstream line installation is in progress. More than 34,600 m3 of grout (22,700 tons of cement) were injected, in more than 54,000 grouting stages, most of which were 5 m long. Of the 2910 grouted holes, 766 were on the crest and the others inside the grouting gallery. For technical and scheduling reasons, all the drilling and grouting works have been performed 24 hours per day, 6 days a week.

Besides the drilling and grouting works, activities were performed to install and renew the inclinometer and piezometer array, both downstream of the dam and into the gallery. As mentioned, part of the works on the electromechanical parts of the bottom outlet structure were carried out with the involvement of divers and specialized sub-contractors.

The equipment and grouting methods employed at the site are heavily dependent on electronic systems and grouting software for communication, and data gathering, processing and reporting. Drilling rigs, mixing plants and BGUs incorporate electronic controls that are relatively new to MoWR staff. Under the Contract, Trevi has trained MoWR staff and technicians on the operation, maintenance and repair of the equipment and mixing plants. However, MoWR-USACE-Trevi team

has further extended the training concept to include the integration of MoWR personnel into the Contractor's crews with the objective of bringing MoWR work force to directly execute the work on their own with the new techniques being implemented. The objective is to have approximately 250 MoWR workers integrated during the course of the works.

CONCLUSIONS

As of mid-August 2018, over 306,000 m of boreholes have been grouted with a total of approximately 34,600 m3 of grout.

Considerable improvements have been attained in a year and half of activity, and a pre-draft version of a revised risk analysis downgraded the risk to a level significantly lower than the one evaluated in 2016 (as per USACE standard risk chart). During the last flooding season, the water level flow was raised to El. +321 m, i.e. 3 m higher than the level used in the recent years. The general safe conditions of the Dam allowed for the water to rise again at levels of 2005, and to reopen the spillway after 12 years.

At the time of this writing, the activities at Mosul Dam continue, since the Government of Iraq signed the extension of the contract for a further year of grouting, until August 2019.

AKNOWLEDGEMENTS

The Authors would like to sincerely thank the representatives of the Ministry of Water Resources, Government of Iraq, and the US Army Corp of Engineers, for the great cooperation established among MoWR, USACE and Trevi that made working in this difficult environment not only possible but also successful.

REFERENCES

Bateman, V.C., Worsham, B.M., Blackman, L.E., Williams, N.D., Sells, B.S., 2018, "Mosul Dam – Building 2D & 3D Project Information Systems for Construction Monitoring and Risk Assessments", DFI & EFFC Proceedings, International Conference on Deep Foundations and Ground Improvement, Rome, Italy, June 6-8.

Grana

Jassim, S.Z., Jabril, A.S., Numan N.M.S., 1997, "Gypsum karstification in the Middle Miocene Fatha Formation, Mosul area, Northern Iraq". Geomorphology, 18, pp. 137-149.

Jassim, S.Z., Raiswell, R., Bottrell, S.H., 1999, "Genesis of the Middle Miocene strata bound sulphur deposits of northern Iraq". Journal of the Geological Society, London 156: 25-39.

Kelley, J.R., Wakeley, L.D., Seth, W.B, Monte, L.P., McGrath, C.J., McGill, T.E., Jorgeson, J.D., Talbot, C.A., 2007, "Geologic setting of Mosul dam and its engineering implications", USACE ERDC TR-07-10, pp.1-60.

Paul, D., Vargas, J., Malayla, N., Granata, R., 2018. "Mosul Dam: An Extraordinary Year of Rehabilitation to Address Dam Safety Issues", Geotechnical News, Vol.36, N.1, pp.42-49.

Warren, J.K., 2006, "Evaporites: Sediments, resources and hydrocarbons". New York: Springer-Verlag.

5th International Symposium on Dam Safety

October 27-31, 2018

DEFORMATION ANALYSIS OF CONCRETE FACED AYDIN KARACASU DAM AND COMPARISON OF THEORETICAL RESULTS WITH MEASUREMENTS

Tuğçe Tütüncübaşi TOSUN[1], M. Yener ÖZKAN [2] , Gülru Saadet YILDIZ[3], Erdal ÇOKÇA[4]

ABSTRACT

The improvement in design technologies has enhanced the use of different fill materials in construction of the embankment dams. Rockfill is one of the most preferred fill material for embankment dam. Also, use of different fill material such as sand-gravel has been preferred in recent years. Previous studies on concrete faced sand-gravel fill dam (CFSGD), results of the laboratory experiments and in-situ testing analysis display that using sand-gravel as a fill material is not only cost-effective but also safe and provides high quality natural construction material. In this study, settlement of Karacasu Dam, which is the first concrete faced sand-gravel fill dam in Turkey, is examined for "end of construction" and "reservoir impoundment" loading conditions. Deformations are determined by computing two dimensional finite element analyses. Hardening soil model is utilized to obtain non-linear, stress dependent and inelastic behavior of the sand-gravel fill material. Deformations which are calculated by finite element analyses, are compared with the data observed by General Directorate of State Hydraulic Works (DSİ) for both end of the construction and reservoir impoundment periods. The comparison of the results indicates that calculated deformations are generally compatible with the observed ones.

Keywords: CFSGD, deformation, 2D FEM, hardening soil model, sand-gravel fill.

INTRODUCTION

With technological development and increased perfection in dam engineering, concrete face sand-gravel dams (CFSGD) are widely used in today's world. Due to economic aspects, the application of sand-gravel fill materials, mostly alluvial deposits, is gaining more and more relevance as fill a fill material. Safety of CFSGDs is based on construction, appropriate design, and observation of actual behavior during construction and operation of the structure. The most important problems encountered at CFSGDs is cracking of impervious face due to deformation behavior of dam body causing leakage (Haselsteiner and Ersoy, 2011).

The main objective of this study is to determine the deformation behavior of the Karacasu Dam, the first concrete faced sand-gravel dam in Turkey. In this study, deformations are calculated for both construction and water impoundment periods with the computer program Plaxis v8.2. The results taken from finite element analysis and observed data, obtained from General Directorate of State Hydraulic Works (DSİ, 2011), are compared. Hardening soil model is used to represent sand-gravel

[1] İn.Y.Müh, KGM Ankara Türkiye,
e-posta: tosun0tugce@gmail.com
[2], [4] Prof. Dr., İnşaat Mühendisliği Bölümü, ODTÜ, Ankara Türkiye,
e-posta: myozkan@metu.edu.tr; ecokca@metu.edu.tr
[3] İnş.Y.Müh, öğr.gör., İnşaat Mühendisliği Bölümü, ODTÜ, Ankara Türkiye,
e-posta: saadetgulruyildiz@gmail.com

material behavior in Plaxis v8.2 during analyses since hardening soil model is a nonlinear and inelastic model.

CONCRETE FACED AYDIN KARACASU DAM

Karacasu Dam was designed as a concrete faced sand-gravel fill dam (CFSGD) and construction of the Karacasu Dam was completed in 2012. (DSİ, 2011) Catchment area of the dam is 537 km^2. Reservoir area is 1,07 km^2 with 17,20 hm^3 total reservoir capacity and active storage volume of the dam is 13,70 hm^3.Total fill volume used in the design is 2.320.000 m^3. A view of the general layout of Karacasu Dam is shown in *Figure 1*.

Figure 1. A general layout of Karacasu Dam (DSİ, 2011)

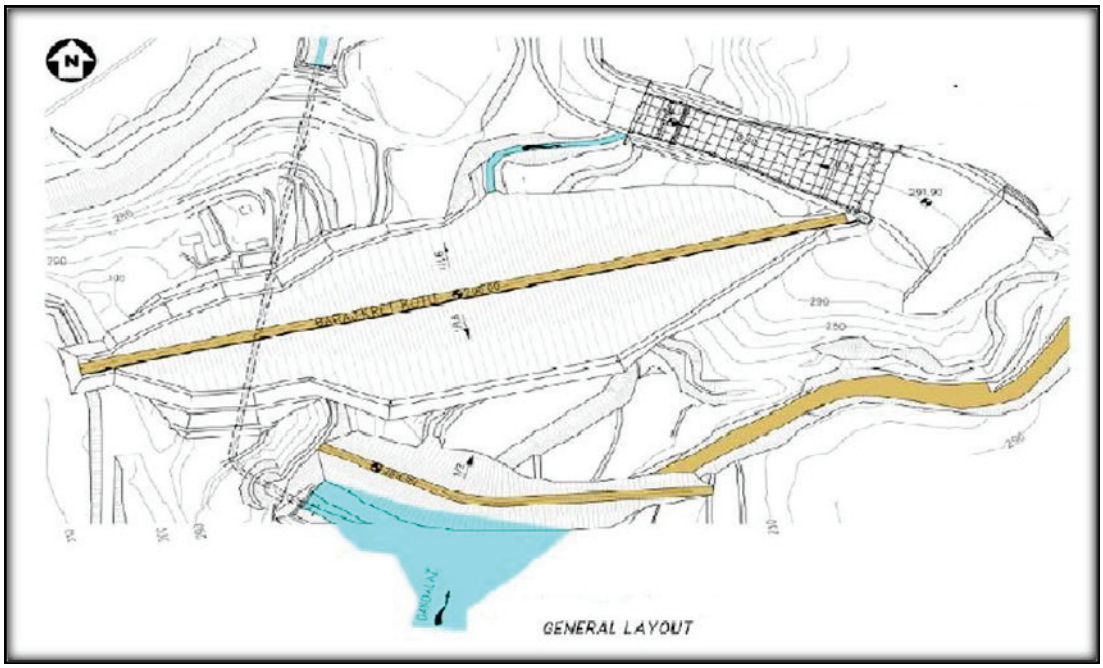

Crest level of the dam is 298.50 m and crest length is 649.4 m. Height of the dam is 60 m from foundation and 53.5 m from the river bed. Normal water level of the dam is 293.50 m. Spillway of Karacasu Dam is uncontrolled. Discharge capacity of the spillway is 1.389 m^3/s. A view of the maximum cross section and material zoning of Karacasu Dam are given in the *Figure 2*.

Figure 2. The cross-section of Karacasu Dam (DSİ, 2011)

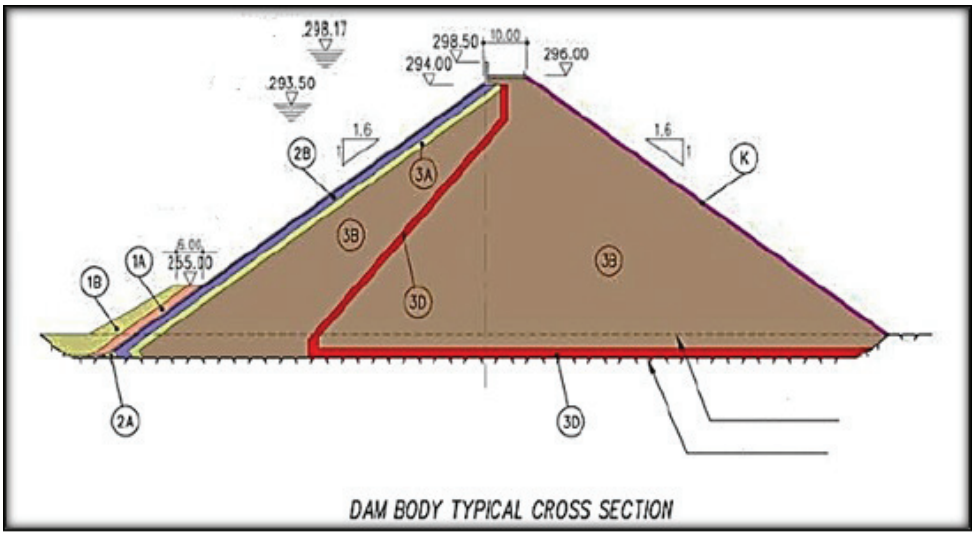

In *Figure 2*,"Zone 1A" represents the cohesionless fill; "Zone1B" shows the random fill, perimetric joint filter zone is shown by the symbol; "2A" and "Zone2B" represents the cushion zone under concrete slab; "Zone3A" shows the filter zone; "Zone3B" displays the permeable sand-gravel fill; "Zone3D" shows the drainage zone or filter zone (clear gravel) and "K" represents surface protection material. As can be seen in the Figure 2 above, the main construction material of Karacasu is sand-gravel (Zone3B).

Karacasu Dam is a moderate-sized dam. After the completion of main dam body, construction of concrete slab started. Concrete slab provides the impermeability and helps to decrease the leakage. Thickness of the concrete slab of Karacasu Dam is 30 cm and constant throughout the dam body.

According to results of petrographic analysis, the basic geologic formations at the Karacasu Dam site are denominated as marl, calcareous marl, limestone, clayey-sandy lignite, clayey lignite. Among these geologic formations, limestone has spongy configuration due to dissolution of rock and it is formed from microcrystalline, little clay and feldspar fragments. Few amounts of Clayey-sandy lignite, quartz, feldspar fragments, calcium carbonate and gypsum are seen in the sample. Base rock of the Aydın Karacasu Dam comprises of old neogene sediments (Foundation Boreholes of Aydın Karacasu Dam DSİ, 2011).

Instrumentation of Aydın Karacasu Dam

The main purposes of dam instrumentation are to develop a better understanding of its behavior and to control the design concepts (Singh and Varshney, 1995). An instrumentation system is designed at Aydın Karacasu Dam.

30 hydraulic settlement gauge (ZDÖ) were installed in the Karacasu Dam body. Instruments were located at three different cross-sections Km 0+250.00 m, Km 0+300.00 m, Km 0+350.00 m, respectively. The maximum cross-section of the dam body is the section located at Km 0+300.00 m. Thus, instruments of Km 0+300.00 m are examined in this study.

Observed Settlement Behavior of Aydın Karacasu Dam

According to the general schedule of the Aydın Karacasu Project, dam construction has started in December 2009 and the main body has filled to El. 296m in February 2012 (20.02.2012). Reservoir impounding has officially started in September 2012; however, it is said that the reservoir has begun to rise two months after official impounding date. During these periods, the performance of the dam has been observed by instrumentation devices located at different elevations and cross-sections. The settlements, which occur in the foundation and occur in the dam body, have been recorded respectively by hydraulic settlement devices. Hydraulic settlement devices are installed in three different cross-section of the dam body (Km 0+250.00m, Km 0+300.00m, Km 0+350.00m). Settlement devices are represented with a symbol of "ZDÖ" in this study. Location of these devices can be seen from *Figure 3*.

Figure 3. Location of the hydraulic settlement devices of Aydın Karacasu Dam at Km 0+300.00m (DSİ, 2011)

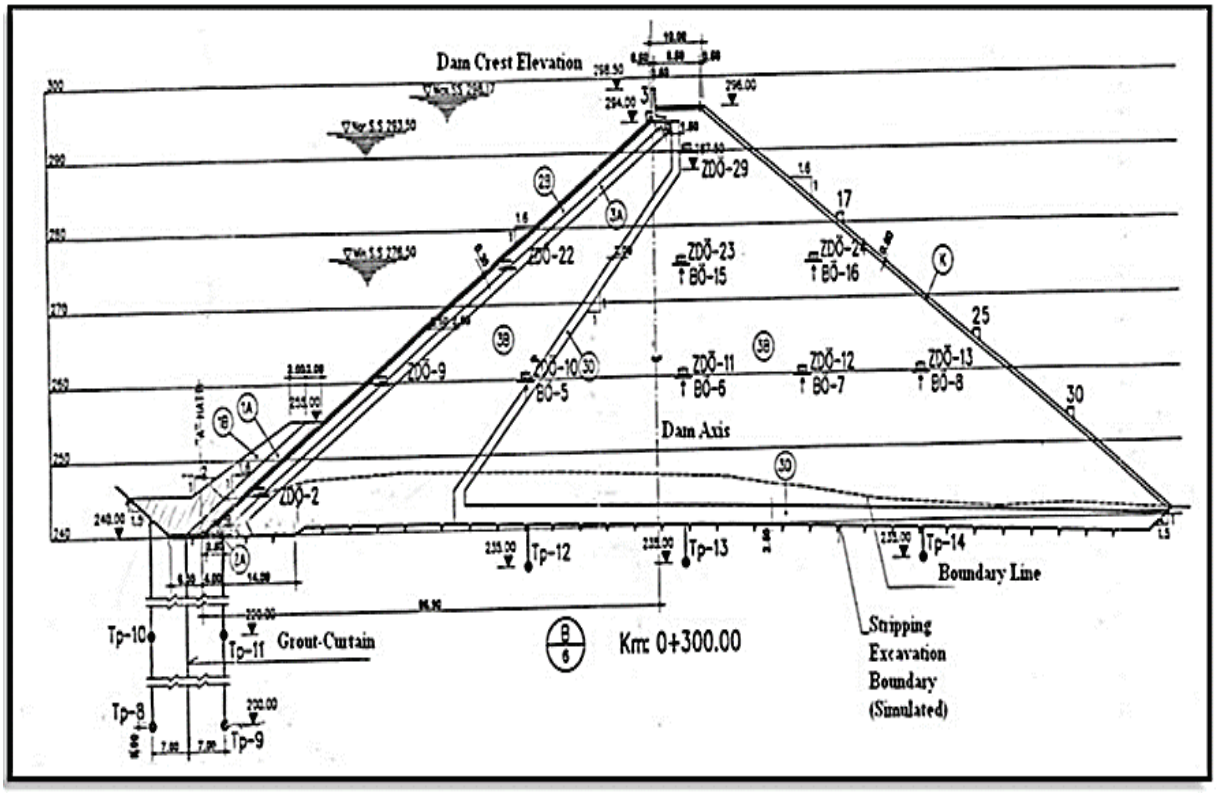

The maximum cross-section of the dam body is Km 0+300.00m. Maximum settlements occur at the maximum cross-section of the dam body, as expected (Özkuzukıran, 2005). According to the data taken from DSİ, recorded values of hydraulic settlement devices located at Km 0+300.00m are larger than the settlements values recorded on other cross-sections as expected. Hence, in this study, instrumentation devices installed in Km 0+300.00m are taken into account. Figure 3 shows the location of the hydraulic settlement device installed in Km 0+300.00m. They are installed at four different elevation El 245, El 260, El 275, El 290 at Km 0+300.00m.

Deformation behavior of the dam is studied for end of construction (EOC) and reservoir impoundment (RI) conditions. Observed settlement values, provided by DSİ, are displayed in the *Table 1.*

Table 1. Observed Settlements for End of Construction Condition of Aydın Karacasu Dam (DSİ, 2011)

OBSERVED VERTICAL SETTLEMENTS AT MAX. CROSS SECTİON OF KARACASU DAM (Km 0+300.00m)				
Settlement Features				
Hydraulic Settlement Gauge	Elevation (m)	Horizontal Distance From Upstream Toe (m)	Max. Settlement Observed by General Directorate of State Hydraulic Works EOC (cm)	Max. Settlement Observed by General Directorate of State Hydraulic Works RI (cm)
ZDÖ2	245.00	19.50	-32.00	-42.00
ZDÖ9	260.00	43.00	-36.00	-44.00
ZDÖ10	260.00	70.00	-22.00	-32.00
ZDÖ11	260.00	100.00	-23.00	-27.50
ZDÖ12	260.00	132.50	-27.00	-40.00
ZDÖ13	260.00	155.00	-28.00	-41.00
ZDÖ22	275.00	67.00	-28.00	-41.00
ZDÖ23	275.00	100.00	-37.50	-45.50
ZDÖ24	275.00	135.00	-32.00	-42.00
ZDÖ29	290.00	102.00	-32.00	-44.00

Preliminary Analysis of Aydın Karacasu Dam

Material Model

Two dimensional Finite element method is utilized to perform settlements analysis of Karacasu Dam. Firstly, appropriate material model is determined to examine the stress-strain behavior of the fill material. Material is assumed non-linear, inelastic and stress dependent. Soil behavior is represented by utilizing frequently hyperbolic model that was improved by Duncan and Chang (1970).

The soil hardening model is formulated in a system of complicated theory based on plasticity rather than elasticity (Schanz et. al., 1999). By virtue of the plastic shear and strain properties, soil hardening model is thought to be isotropic. Finite element software Plaxis v8.2 is utilized with the hardening soil model to compute the deformations more realistically.

Material Model Parameters

Material Model Parameters used in the analysis are presented in Tables 2-4.

Mesh Model

In Plaxis v8.2 program, settlements are calculated at nodes. Finite element system is formed with 6-node triangle mesh elements or 15-node triangle mesh elements. In this study, 15-node triangle element model is used to model Aydın Karacasu Dam.

The model comprises of 8125 nodes, 990 Soil Elements, 11880 Global Stress Points. The model is shown in the *Figure 4.*

Table 2. Parameters used in hyperbolic models for sand-gravel fill material of Aydın Karacasu Dam

Triaxial Stiffness E_{50}^{ref} (kPa)	Triaxial Unloading Stiffness E_{ur}^{ref} (kPa)	Oedometer Loading Stiffness E_{oed}^{ref} (kPa)	Unit weight (γ) (kN/m^3)	c (kN/m^2)	ϕ
30000	90000	30000	17.2	2	38^o

Table 3. Parameters used in hyperbolic models for bedrock material of Aydın Karacasu Dam

Elasticity Modulus	Unit weight γ	c (kN/m^2)	ϕ
600000 KPa	22 kN/m^3	25	40^o

Table 4. Parameters used in hyperbolic models for concrete slab of Aydın Karacasu Dam

EA (kN/m)	EI (kNm^2/m)	*d (m)*	*v*
8550000	64125	0.30	0.20

Figure 4. Connectivity in mesh analysis of Aydın Karacasu Dam (Plaxis v8.2)

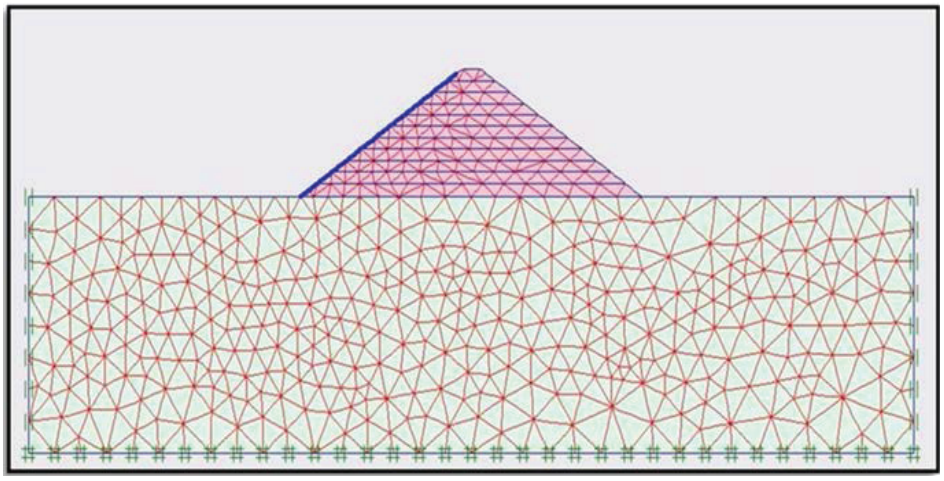

Analysis Method

Analysis of the dam is carried out by stage construction method, recalling that embankment is formed in layers. Stage construction affects stress dispersion and deformations occurred in vertical or horizontal direction (Clough and Woodward, 1967). Layer thickness affects the analysis results. Analyses conducted by smaller layer thicknesses, is more accurate. However, it takes too much computation time (Özkuzukıran, 2005).

In this study, imaginary axes are defined at the maximum cross-section of the dam to show locations of instrumentation devices. Imaginary axes are shown in the *Figure 5*. Hydraulic settlement devices are located in six different axes of the dam body. As seen in the *Figure 5,* ZDÖ2 is located in axis X_1-X_1, ZDÖ9 is located in axis X_2-X_2, ZDÖ10 and ZDÖ22 are located in axis X_3-X_3, ZDÖ11, ZDÖ23 and ZDÖ29 are located in axis X_4-X_4, ZDÖ12 and ZDÖ24 are located in axis X_5-X_5 and ZDÖ13 is located in axis X_6-X_6.

As stated above, two dimensional deformation analyses are carried out for the end of construction (EOC) and the reservoir impoundment (RI) stages. for the maximum cross-section, Km 0+300.00 m of the dam. Sand-gravel fill material deforms under only its own weight for end of construction condition. However, water load causes additional deformation in the embankment for reservoir impoundment condition (RI).

Settlement calculations are made in stages starting from the foundation level and advancing upwards layer by layer. For each layer settlements are calculated at specific points where hydraulic settlement devices are located. At the end of each layer, recorded settlements are reset to zero and intermediate steps are deleted. Then, calculated settlements are superposed to find the total settlements at specific points for EOC and RI conditions.

Figure 5. Location of imaginary axes and instrumentation devices at maximum cross-section (Km: 0+300.00 m) of Aydın Karacasu Dam

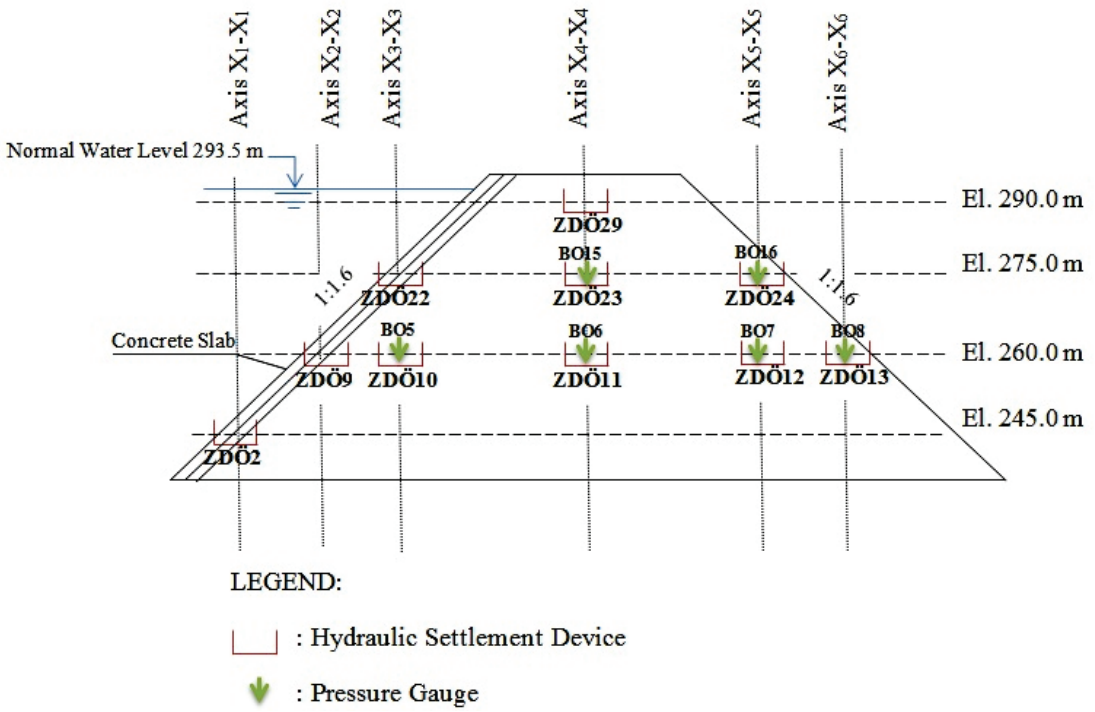

In the analyses, it is assumed that, the rock foundation of the Aydın Karacasu Dam is infinitely rigid. It is also assumed that there is a perfect bond between concrete slab and sand-gravel fill. It is decided to utilize 5 m layers in the analyses.

RESULTS OF ANALYSES

End of Construction Analyses (EOC)

Embankment is formed by sand-gravel material prior to impounding. Results of analyses for end of construction condition are presented in *Table 5.*

Table 5. Results of Analyses of Aydın Karacasu Dam at Max. Cross-Section (Km 0+300.00 m) for EOC

Axes	X_2-X_2	X_3-X_3		X_4-X_4			X_5-X_5		X_6-X_6
Instrument	ZDÖ9	ZDÖ10	ZDÖ22	ZDÖ11	ZDÖ23	ZDÖ29	ZDÖ12	ZDÖ24	ZDÖ13
Elevation (m)	260.00	260.00	275.00	260.00	275.00	290.00	260.00	275.00	260.00
Vertical Settlement Observed by DSİ (cm)	-36.0	-22.0	-28.0	-23.0	-37.5	-32.0	-27.0	-32.0	-28.0
Calculated Vertical Settlement by Plaxis v8.2 (cm)	-15.0	-27.9	-23.0	-32.5	-35.5	-21.6	-26.2	-18.8	-16.5
Difference between Observed Settlement and Plaxis v8.2 Results (cm)	-21.0	5.9	-5.0	9.5	-2.0	-10.4	-0.8	-13.2	-11.5
% Difference between Observed Settlement and Plaxis v8.2 Results	58.4	26.6	17.7	41.4	5.3	32.4	2.9	41.1	41.1

(*) In the Table "-" settlement value shows compression.

Reservoir Impoundment (RI)

A large part of post-construction deformations occur during reservoir impoundment. Settlements increase by the rising water level. Large settlements may cause cracks in the concrete slab and leakage problems may emerge as a result of these cracks in the concrete slab.

In Aydın Karacasu Dam, reservoir impounding started in 07.09.2012. Water level reached El. 293.50 m in a short time and then ultimately reached El. 298.17m. After end of construction of the dam body, majority of the deformations occur during first impounding so, first impounding is a critical condition that should be analyzed (Özkuzukıran, 2005). Thus, El. 293.50 m is considered as a critical condition to be considered in calculations.

Concrete slab is presumed as uncracked and impervious in the finite element analyses and water load is assumed as acting in a perpendicular direction to the concrete slab and calculated as a triangle-shaped distributed load as shown in the *Figure 6* below.

Figure 1. Water Load Acting on the Concrete Membrane of the Dam

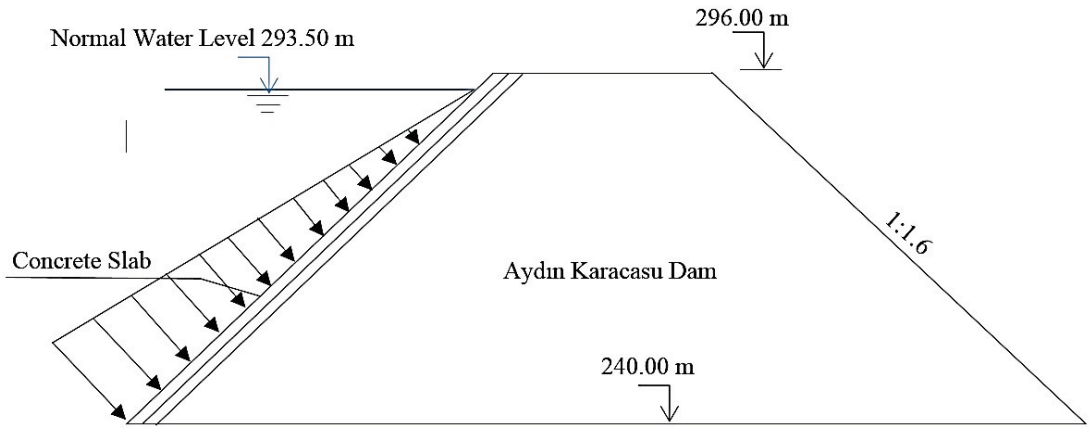

The maximum water load (at El 240.00 m) is 524,835 kN/m^2. It decreases with increasing elevations. Reservoir impounding analyses are conducted at five imaginary axis defined above. Results of the analyses for reservoir impounding condition are shown in *Table 6.*

It can be observed from Table 6 Maximum observed settlement recorded as 45,50 cm on axis X_4-X_4 for RI, which is measured by device ZDÖ23 located at 62.5 % of the height of the dam above the bottom. Maximum vertical settlement is calculated as 39,30 cm at El. 271 m at 55,00% of the dam height.

Table 6. Results of analyses of Aydın Karacasu Dam at max. Cross-section (Km 0+300.00 m) for RI Condition

Axis	X_2-X_2	X_3-X_3		X_4-X_4			X_5-X_5		X_6-X_6
Instrument	ZDÖ9	ZDÖ10	ZDÖ22	ZDÖ11	ZDÖ23	ZDÖ29	ZDÖ12	ZDÖ24	ZDÖ13
Elevation (m)	260.00	260.00	275.00	260.00	275.00	290.00	260.00	275.00	260.00
Settlement Observed by DSİ (cm)	-44,0	-32,0	-41,0	-40,0	-45,5	-44,0	-40,0	-42,0	-41,0
Calculated Settlement by Plaxis v8.2 (cm)	-23,5	-31,6	-28,7	-35,1	-38,8	-25,3	-28,1	-21,4	-17,6
Difference between Settlement Observed by DSİ and Settlement Calculated by Plaxis v8.2 (cm)	-20,5	-0,4	-12,3	-4,9	-6,7	-18,7	-11,9	-20,6	-23,4
% Difference between Observed Settlement and Calculated Settlement by Plaxis v8.2	46,5	1,1	30,0	12,3	14,7	42,5	29,9	49,0	57,0

(*) In the Table "-" settlement values shows compression.

Tables 7, 8 show the impact of water loading on vertical settlements, recorded by DSİ and calculated by finite element analyses. EOC settlements are not included in these values, which are indicated in the following tables in order to show the reservoir impounding effect on the deformation behavior of the dam body. Therefore, vertical settlement values observed at the end of construction are subtracted from the ones observed when reservoir impounding reaches El 293,50 m.

Table 7. Effect of reservoir impounding on vertical settlements as measured by DSİ

Axis	X_2-X_2	X_3-X_3		X_4-X_4			X_5-X_5		X_6-X_6
Instrument	ZDÖ9	ZDÖ10	ZDÖ22	ZDÖ11	ZDÖ23	ZDÖ29	ZDÖ12	ZDÖ24	ZDÖ13
Elevation (m)	260.00	260.00	275.00	260.00	275.00	290.00	260.00	275.00	260.00
Settlement Observed by DSİ for EOC (cm)	-36,0	-22,0	-28,0	-23,0	-37,5	-32,0	-27,0	-32,0	-28,0
Settlement Observed by DSİ for RI (cm)	-44,0	-32,0	-41,0	-40,0	-45,5	-44,0	-40,0	-42,0	-41,0
Effect of Reservoir İmpounding (cm)	-8,0	-10,0	-13,0	-17,0	-8,0	-12,0	-13,0	-10,0	-13,0

Table 8. Effect of reservoir impounding on vertical settlements calculated by Plaxis v8.2

Axes	X_2-X_2	X_3-X_3		X_4-X_4			X_5-X_5		X_6-X_6
Instrument	ZDÖ9	ZDÖ10	ZDÖ22	ZDÖ11	ZDÖ23	ZDÖ29	ZDÖ12	ZDÖ24	ZDÖ13
Elevation (m)	260.00	260.00	275.00	260.00	275.00	290.00	260.00	275.00	260.00
Settlements Calculated by Plaxis v8.2 for EOC (cm)	-15,0	-27,9	-23,0	-32,5	-35,5	-21,6	-26,2	-18,8	-16,5
Settlements Calculated by Plaxis v8.2 for RI (cm)	-23,5	-31,6	-28,7	-35,1	-38,8	-25,3	-28,1	-21,4	-17,6
Effect of Reservoir İmpounding (cm)	-8,5	-3,7	-5,7	-2,6	-3,3	-3,7	-1,9	-2,6	-1,1

CONCLUSIONS

In this study; settlement analyses of Aydın Karacasu Dam, the first concrete faced sand-gravel dam of Turkey, are conducted by using two dimensional Plaxis v8.2 finite element program. Results of analyses, are compared with observed ones recorded by DSİ. Following conclusions may be drawn from this study:

- Difference between the calculated and observed ones decreases with increasing elevations, nevertheless, the observed and calculated settlement are in general agreement .Poor quality of compaction or irregular readings taken from instrumentation devices during end of construction and reservoir impoundment may be the cause of those differences between observed and calculated vertical displacements.
- For the end of construction condition, majority of the calculated values obtained from both finite element program results are compatible with observed settlement values. Maximum vertical settlement is found as 36,20 cm which corresponds to about 55% of the total dam height from the foundation base by Plaxis v8.2. These results ~~indicate~~ that compressibility of the fill material decreases with increasing elevations.
- In the reservoir full condition, analyses results indicate that most of the calculated settlements are somewhat smaller than the observed ones; except settlements calculated in axis X_4-X_4. In axis X_4-X_4, maximum calculated vertical settlement is found as 39,30 cm which corresponds to about 55% of the total dam height above the base. Results of analyses X_3-X_3 and X_4-X_4 are compatible with observed values. Results of RI analyses show that reservoir impounding has significant effect on regions closer to upstream membrane.
- A few number of observed values which were out of practical range indicating malfunctioning of the devices were eliminated. It may be concluded that soil deformations, under loading and unloading conditions, during end of construction and reservoir impoundment periods can be estimated reasonable accuracy by two dimensional FEM analysis. It is suggested that, for future studies, 3D finite element analyses may be utilized to compare the observed and calculated settlements in order to derive more reliable conclusions.

REFERENCES

Clough, R. W., Woodward, R. J. (1967). "Analysis of Embankment Stresses and Deformations". *Journ. SMFD, ASCE*, vol. 93, no. SM4.

Duncan, J. M., Chang, C. Y., (1970). "Nonlinear Analysis of Stress and Strains in Soils", *Journ. SMFD, ASCE*, 96 (SM5): 1629-1653.

Haselsteiner, R., Ersoy, B., (2011). "Seepage Control of Concrete Faced Dams with Respect to Surface Slab Cracking", 6th International Conference on Dam Engineering, Lisbon, Portugal.

Hydraulic State Works (2011), DSİ Report on Aydın Karacasu Dam.

Özkuzukıran, R S, (2005). "Settlement Behavior of Concrete Faced RockFill Dams, A Case Study, Msc. Thesis, METU, Ankara.

Plaxis ver. 8.2, Material Model Manual, 2010 and 2013.

Schanz, T., Vermeer, P. A., Bonnier, P. G., (1999). "The Hardening Soil Model: Formulation and Verification", Beyond 2000 in Computational Geotechnics-10 Years of Plaxis, Balkema, Rotterdam.

Singh, B., Varshney, R. S., (1995). "Engineering For Embankment Dams", A.A. Balkema Publishers, Brookfield.

5th International Symposium on Dam Safety

October 27-31, 2018

DYNAMIC ANALYSES FOR SMALL EMBANKMENT DAMS AND A CASE STUDY

Turgut Vatan TOSUN[1] Hasan TOSUN[2]

ABSTRACT

Ground motion induced at the dam site by an earthquake located at some distance from the dam can result damages to dams and their appurtenant facilities. There are so many examples about this phenomenon. Direct fault movement across the dam foundation can create displacements, which result to more serious problems for embankments and their appurtenant structures. Especially active faults on or near dam sites can cause to damaging deformation of the embankment. Therefore, meaningful seismic parameters are needed to perform a satisfactory evaluation of dam structure. It is possible to make design with low factor of safety for the dams with low total risk. For this study Ayanlar dam, which has an earth fill embankment having a 30.0 m height from foundation, was selected as a case study. A seismic evaluation of dam site was performed in detail. For the dam site, the dynamic analysis of 2-D finite element model of dam-foundation system shows that the maximum value of vertical displacement is 39.8 cm on the crest under the loading of Maximum Design Earthquake (MDE).

Keywords: earthquake, dams, seismic hazard analysis, stability analysis

INTRODUCTION

Earthquake safety of dams is an important phenomenon in dam engineering and requires more comprehensive seismic studies for understanding the seismic behavior of dams subjected to severe earthquakes. It is a well-known phenomenon that earthquakes can result damages and failures for dams and their appurtenant structures. Tosun et al (2007) stated that safety concerns for embankment dams subjected to earthquakes involve either the loss of stability due to a loss of strength of the embankment and foundation materials or excessive deformations such as slumping, settlement, cracking and planer or rotational slope failures. Safety requirements for concrete dams subjected to dynamic loadings should involve evaluation of the overall stability of the structure, such as verifying its ability to resist induced lateral forces and moments and preventing excessive cracking of the concrete (Jansen, 1988).

In the world there are some important cases, which subjected to damages and failures after earthquake,. Lower San Fernando Dam in USA is first example failed as a result of liquefaction phenomenon under the earthquake loading conditions. In case of the May 12, 2008 Wenchuan earthquake in China many dams and reservoirs had been subjected to strong ground shaking. So many

[1] Civil engineer, TVT Hydrotech Bureau, Ahmet Mithat Efendi sok. 40/12 Cankaya, Ankara, Turkey, e-posta: barajproje@gmail.com

[2] Full Professor, Eskisehir Osmnagazi University, Batı Meselik, 26480Turkey, e-posta: hasantosun26@gmail.com

dams and hydropower plants were damaged. During the 2001 Bhuj earthquake in Gujarat, India, 245 dams had been affected and rehabilitated or strengthened after the earthquake. Also, in the case of the March 11, 2011Tohoku earthquake in Japan, damages were observed about 400 dams and the 18 m high embankment dam failed and 8 people lost their live (Tosun, 2015).

In general, strong ground shaking can result in the instability of the embankment and loss of strength at the foundations However, embankment dams, which are well compacted according to the specification, are suitable type for regions having high seismic activity. Well-compacted embankment dam can withstand moderate earthquake shaking, with peak accelerations of 0.2g and more, with no detrimental effects (Seed et al, 1978; Seed, 1979). According to recent studies, the well-compacted modern dams can withstand substantial earthquake shaking with no detrimental effects. Performance of well-compacted embankment dams have also been good in general after the 1999-Kocaeli earthquake, Turkey. Recently we have seen from some cases that active faults, which are very close to the foundation of dams, have the potential to cause damaging displacement of the structure.

In this study main principles of seismic hazard, pseudo-static and dynamic analyses, adopted in Turkey, were summarized and evaluated as based on case study.

METHODS OF ANALYSES

The deterministic and probabilistic seismic hazard analyses are commonly used to relieve the seismic activity for a dam site in Turkey. Same procedures are considered for both small and large dams. The deterministic seismic hazard analysis considers a seismic scenario and includes four-step process. It is very simple procedure and gives rational solutions for large dams because of providing a straightforward framework for evaluation of worst ground motions. The probabilistic seismic hazard analysis is widely used and considers uncertainties in size, location and recurrence rate of earthquakes.

ICOLD (2016) states that the Maximum Credible Earthquake (MCE) is the largest reasonably conceivable earthquake magnitude that is considered possible along a recognized fault or within a geographically defined tectonic province. In Turkey, earthquake definitions given by FEMA (2005) are generally considered for seismic hazard analyses even if there are some regulations prepared by some state organization. Most of large dams in Turkey were analyzed by using these definitions in past.

The probabilistic hazard calculation is performed to obtain 5 percent damped elastic hazard pseudo-acceleration spectra and to generate the response spectrum compatible acceleration time histories for time domain analyses. The elastic hazard acceleration spectra on the basis of Boore et al (1997) are obtained. For generating the acceleration time histories, a software program such as TARSCTHS is commonly used (Papageorgiou et al, 2000). Pseudo static analysis is performed for all embankment dams. A 2-D finite element model for the maximum section of the dam and soil profile including bedrock is needed for dynamic analysis. Physical and mechanical properties of materials used in the embankment are selected from literature.

For this study deterministic and probabilistic seismic hazard analyses were used to relieve the seismic activity for the dam site. the Maximum Credible Earthquake (MCE), Operational Based Earthquake (OBE) and Maximum Design Earthquake (MDE) are defined. A elastic hazard acceleration spectra on the basis of different approximations was obtained and 2-dimentional numerical model was developed by Plaxis software (2008) for the dynamic analysis. Once the model was defined to represent the layered construction technique, then it was modified for dynamic loading conditions. Standard fixity elements were considered along the base and vertical sides of the model. It was assumed that the ground motion acts uniformly along the fixed boundaries.

CASE STUDY-AYANLAR DAM

Ayanlar dam is an earthfill dam, which is situated at the western part of Turkey. The main section of the dam is 40.17 m high from river level and 181.2 m long. The embankment cross section includes a central core zone flanked on both side by rock shell zones. The outer slopes of dam are inclined at 2.5:1 (horizontal: vertical) for upstream and 2.25:1 for downstream. The cross section includes a transition filter zone between core and rock material zone on both sides and a blanket drain system on downstream to collect seepage through the dam and foundation. It rests on the hard bed rock. The alluvium soil on river bed is removed before beginning to embankment constructions

Table 1. Properties of Bebekli Dam

Properties	Value
Location	West of Turkey
Type	Rockfill with central core
River	Kunduz
Volume of embankment	317 439 m^3
Beginning to construction	2012
Completion of construction	2015
Crest elevation	833.17 m
Crest length	181.20 m
Height from foundation	40.17 m
Geological formation of foundation	Fresh rock
Maximum Water Level	832.48 m
Minimum water level	812.36 m
Reservoir capacity at Max.W.L *	5.3 hm^3

(*) Max.W.L means the maximum water level in operation stage.

Seismic Hazard Analyses

The seismic hazard parameters were obtained from the magnitude-frequency relation of Gutenberg-Richter for two different linear seismic zone (DSİ, 2011). The seismic hazard analysis was performed for the dam by means of two separate methods. The deterministic seismic hazard analysis shows that the PGA values for 50 percentile range from 0.151 to 0.201 while those for 84 percentile they are between 0.244 and 0.360. They average to 0.174 for 50 percentile and 0.288 for 84 percentile. These PGA values are high. Because the fault is very close to the dam site. Its distances to the main Holosen fault is 20.5 km. The seismo-tectonic model used for this study is given Figure 1.

The results of probabilistic seismic hazard analysis indicate that peak ground acceleration (PGA) changes within a wide range for all earthquakes levels. For OBE, MDE and SEE, the PGA value averages to 0.251 g, 0.327g and 0.5469, respectively. These values mainly depend to the predictive relationships. In this study six separate relationships were considered for determining horizontal peak ground acceleration (DSI, 2011).

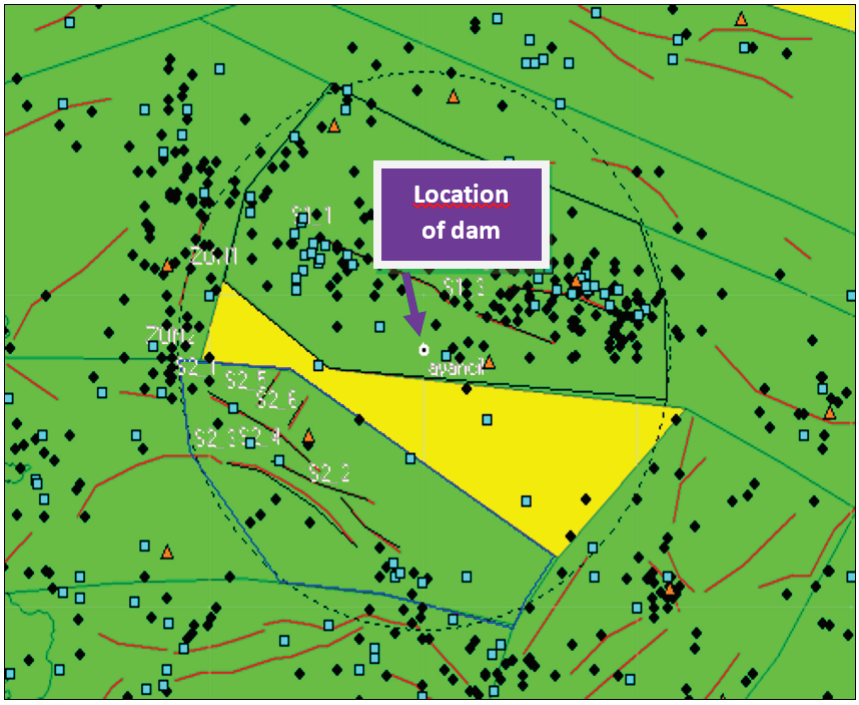

Figure 1. Seismo-tectonic model used for Ayanlar dam

For the dam site, Total Risk Factor (TRF) value is calculated as 89.5 and it is identified as risk class of II of Bureau (2003) method . It means that it has moderate risk potential for downstream life and structures. According to the risk classification adopted by DSI (2012), It is categorized as class III with high risk. The seismic hazard analyses performed throughout this study indicates that Ayanlar dam is one of the most critical dams within the basin when considered downstream life.

Analytical and Numerical Analyses

For this study, the slopes stability of earth fill of Ayanlar dam have been determined as defining a factor of safety for different loading condition by means of pseudo-static analysis (Table 2). At the beginning of this study, seismic coefficient was determined for pseudo-static analysis as based on the approach given in DSI specification. According to this approach seismic coefficient ranges from 0.15 to 0.20. For this study, it was selected as 0.20. Analyses have been executed by means of a software, namely GSTABIL7. The safety factors were calculated by the Modified Bishop Method. The value of seismic coefficient (k) was determined as 0.35 for limit equilibrium condition (F_S= 1.0). An example from analyses is introduced in Figure 2.

The parameters of dynamic analysis were selected after defining the OBE and MDE values for the dam site. The probabilistic hazard calculation was performed to obtain 5 percent damped elastic hazard pseudo-acceleration spectra and to generate the response spectrum compatible acceleration time histories for time domain analyses. For generating the acceleration time histories, a software program TARSCTHS was used. The output of time history record of dam site for OBE level is given in Figure 3.

Table 2. Safety factors of pseudo-static analysis for separate loading conditions

Case	Description	Slope	Factor of Safety	
			Required	Calculated
I	End-of Construction	Downstream Upstream	1.3	2.26 2.74
II	Rapid drawdown	Upstream	1.1-1.3	2.32
III	Operation	Downstream Upstream	1.4-1.5	2.18 2.32
IV	Earthquake	End-of Construction Downstream Upstream Operation Downstream Upstream	1.0	1.41 1.67 1.31 1.34

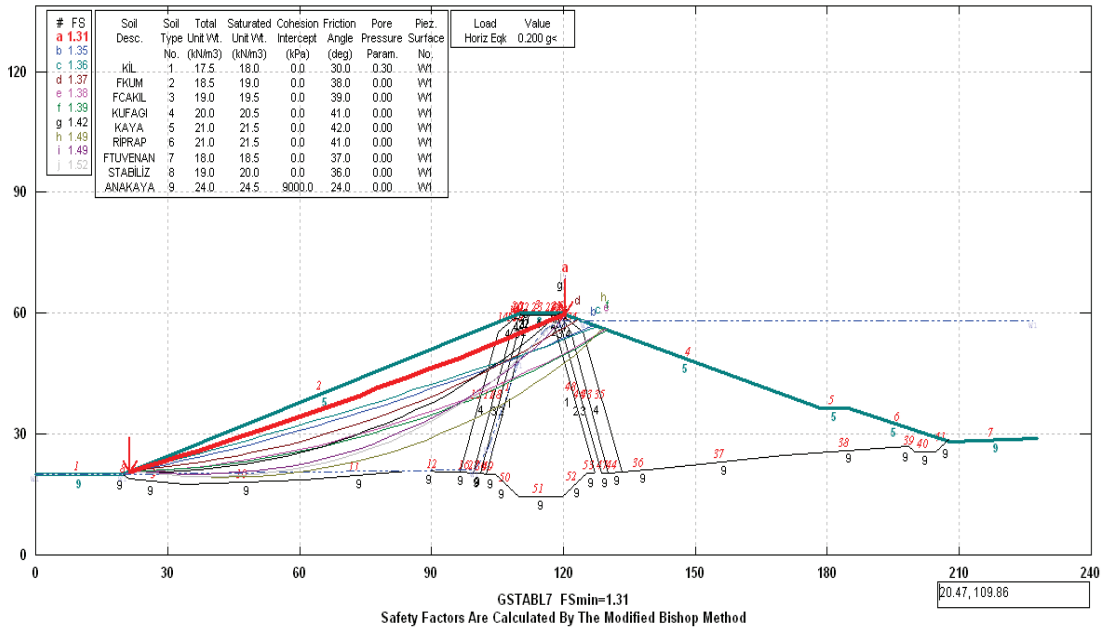

Figure 2. An example of slope stability analyses for Ayanlar dam embankment

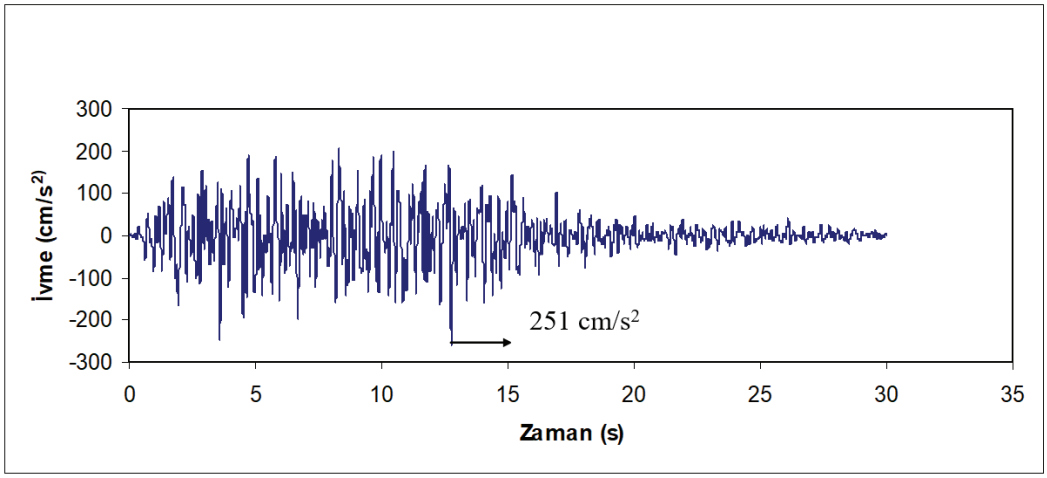

Figure 3. Synthetic acceleration-time history of OBE plot for input motions used in the dynamic analysis of Ayanlar dam

The 2-D finite element model for the maximum section of the dam and soil profile including bedrock and alluvial soil is given in Figure 3. The model consisted of 8887 nodel points and 1020 six-node plane-strain elements. Standard fixity elements were considered along the base and vertical sides of the model. It was assumed that the ground motion acts uniformly along the fixed boundaries. The hardening soil model was selected to define soil properties for all models discussed here.

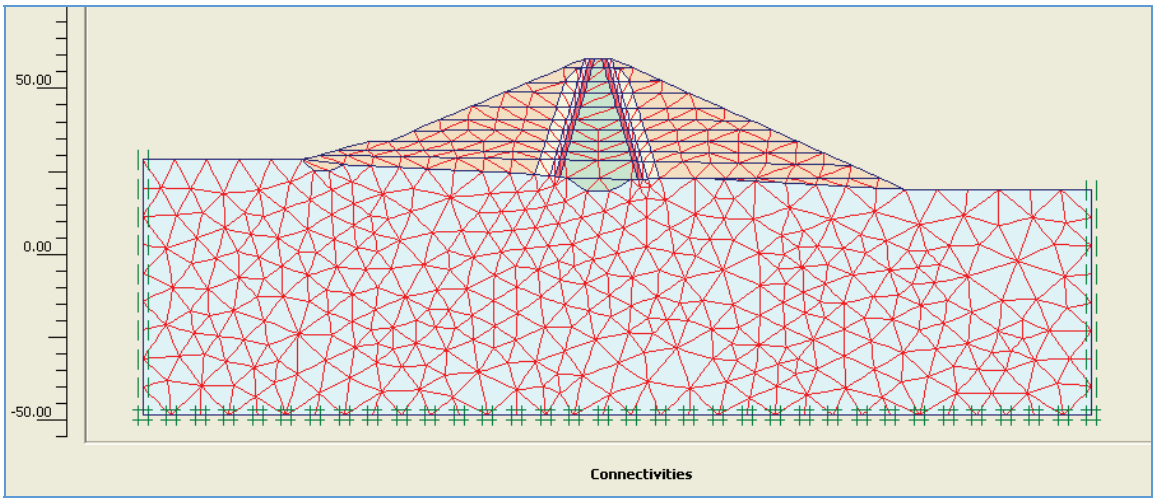

Figure 4. The finite element model of the embankment

The finite element model used in this study is composed of five different materials including the diaphragm wall. The bedrock is also considered as a rigid element with high deformation modulus. The parameters used in the model were considered from the laboratory tests and the literature survey (Seed et al, 1984; Hunter and Fell, 2003; Brenner et al, 2005). For the analysis, the deformation moduli of impervious zone and pervious zone were taken into account as 40 000 and 80 000 kPa, respectively.

As a result of this analysis, maximum vertical settlement was predicted as 40 cm for dynamic loading of MDE level (Figure 4). The horizontal displacements are little greater than vertical displacements. Figure 5 introduces the distribution of horizontal displacement on the model during the dynamic time.

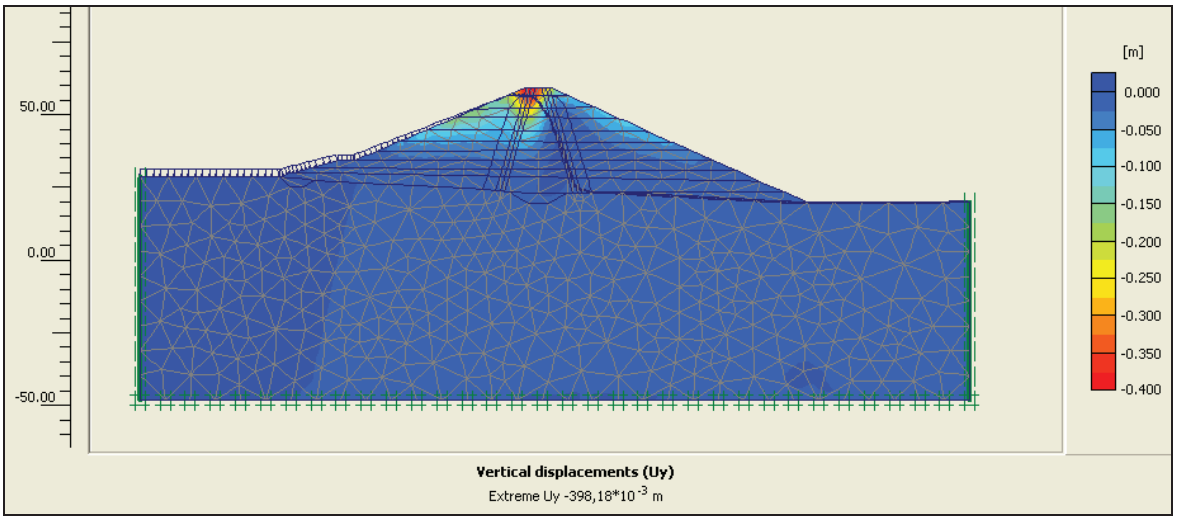

Figure 4. Distribution of vertical displacement for MDE loading condition

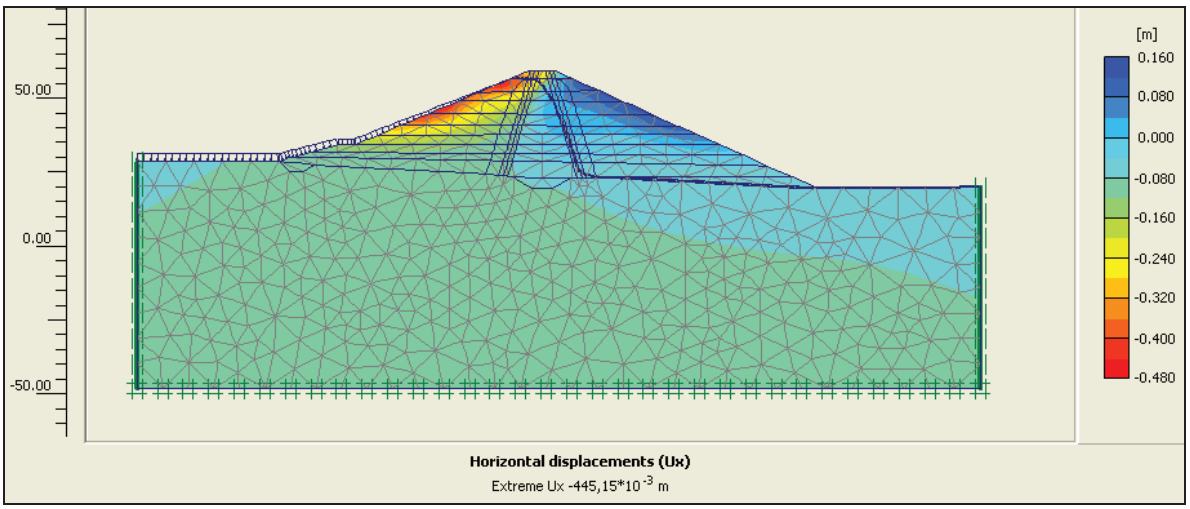

Figure 5. Distribution of Horizontal displacement for MDE loading condition

Results and Discussion

The pseudo-static analysis indicates that both slopes of embankment are safe. The value of seismic coefficient was obtained as 0.35 for limit equilibrium condition. As a result of numerical analysis, maximum vertical settlement was predicted as 39.8 cm for dynamic loading of MDE level, while it obtains as 44.5 cm for horizontal section. The vertical and horizontal displacements are given in table 3 for OBE and MDE conditions.

Table 3. Summary of displacements for different loading conditions

Loading conditions	Vertical Displacement (m)	Horizontal Displacement (m)
OBE	0.194	0.152
MDE	0.398	0.445

As a result of finite element analysis, the horizontal component of acceleration was obtained for different level of embankment. Figure 6 introduces the horizontal acceleration on dam crest with input ground motion. In this figure, red line represents horizontal peak ground acceleration on the base rock, while blue line represents same parameter on the crest of dam, but both for MDE.

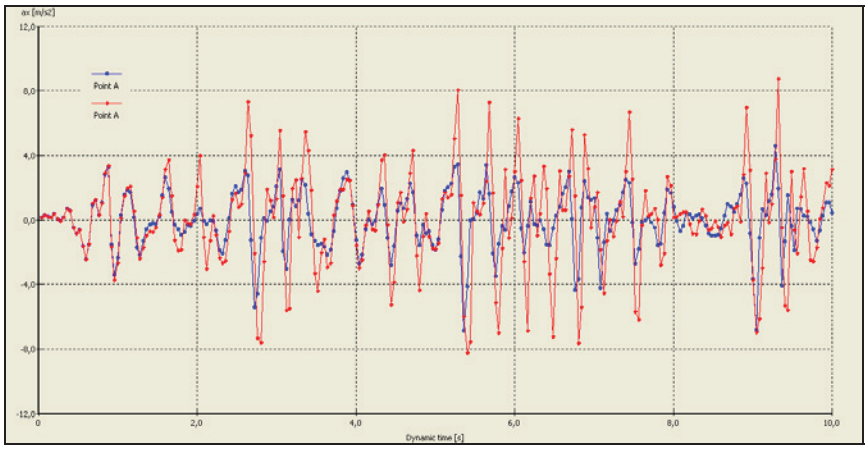

Figure 6. Horizontal acceleration on crest of embankment for MDE.

The critical slip surfaces are generally passing through toe of embankment when executed analyses for total and effective stress conditions. Peak ground acceleration on crest (a_{maks}) was obtained as 0.80g (figure 6). The maximum seismic coefficient (k_{maks}) was determined as 0.35 from pseudo-static analysis. Their ratio (a_{maks}/ k_{maks}) was calculated as 0.44. According to Makdisi and Seed (1978), displacement ranges from 5 to 13 cm. These values obtained from empirical approximation confirm data given by numerical methods. The displacement values obtained from numerical methods provides the limitations given in literature (FEMA, 2005; Makadisi and Seed, 1978).

CONCLUSIONS

Ayanlar dam site is located on very active seismic region of Turkey. According to the updated seismic data, it is under near field motion. The slopes of embankment are safe when considered the pseudo analyses. The dynamic analysis of 2-D finite element model of dam-foundation system indicates that the maximum value of displacement is only 44.5 cm on the crest under the loading of Maximum Design Earthquake. The permanent deformation for this model was obtained between 5 and 13 cm by means of semi-empirical methods. These results indicate that only local sliding problem can be seen during the loading of MDE condition, not failure of dam. In other words, its embankment is rather safe, when well compacted during construction.

REFERENCES

Boore, D.M., Joyner, W.B., and Fumal, T.E. 1997. Equations for estimating horizontal response spectra and peak acceleration from Western North American earthquakes: A summary of recent work. *Seismological Research Letters,* 68, 128-153.

Brenner, R.P., Wieland, M. and Malla, S. Large-diameter cyclic triaxial tests for seismic safety assessment. 16 th ICSMGE, 2005, Osaka.

Bureau, GJ (2003). *Dams and Appurtenant Facilities in Earthquake Engineering Handbook edited by Chenh, W.F and Scawthorn,C.* CRS press, Bora Raton 26.1-26.47.

DSİ, (2011).Seismic Hazard Analysis of Ayanlar Dam. State Hydraulic Works, Ankara (in Turkish).

DSİ (2012). *Selection of Seismic Parameters for Dam Design.* State Hydraulic Works, Ankara, 29 p (in Turkish).

FEMA, (2005). Federal Guidelines for Dam Safety-Earthquake Analyses and Design of Dams.

Hunter, G. and Fell, R. Rockfill modulus and settlement of concrete faced rockfill dams. J. Geotech. and Geoenvir. Engrg. 129, 2003.

ICOLD (2016). *Selecting Seismic Parameters for Large Dams-Guidelines*. ICOLD, Bulletin 148.

Jansen, R.B., (ed.) 1988. Advanced Dam Engineering for Design, Construction and Rehabilitation. Van Noswtrand Reinhold, New York, 884p.

Makadisi, F.I anad Seed, H.B. (1978). Simplified procedure for estimating dam and embankment earthquake-induced deformations. J. Geotech. Eng. Div. ASCE 104(7): 849–867.

Papageorgiou, A., Halldorsson, B. and Dong, G. (2000) Target Acceleration Spectra Compatible Time Histories. University of Buffalo, Dept. of Civil, Structural and Environmental Engrg., NY.

Parish, Y. and Abadi, F.N. (2009). Dynamic Behaviour of Earth Dams for Variation of Earth Material Stiffness, International Scholarly and Scientific Research & Innovation 3(2) 446-451.

Plaxis, (2008) Plaxis V8 Professional Version-User Manual (Edited By Brinkgreve, R.B.J., Broere, W., And Waterman, D.), Netherlands.

Seed, H. B and Makdisi, F. I. and De Alba,P. (1978). Performance of Earth Dams During Earthquakes, Journal of Geotechnical Engineering, American Society of Civil Engineers, Vol, 104, No. GT7, pp. 967-994.

Seed, H.B. (1979) Considerations in the Earthquake-Resistant Design of Earth and Rockfill Dams, 19th Rankine Lecture of the British Geotechnical Society, Geotechnique, Vol XXIX, No. 3, pp. 215-263.

Seed, H.B., Wong, R.T., Idriss, J.M. and Tokimatsu, K. Moduli and damping factors for dynamic analysis of cohesionless soils. Report No: UCD/EERC-84-14, Earthquake Engineering Center, University of California, 1984.

Tosun, H (2015). *Earthquakes and Dams.* Earthquake Engineering-Seismology to Optimal seismic design of engineering structures (edited by A.Moustafa), Intec Publication ISBN 978-953-51-2039-1.

Tosun, H., Zorluer, I., Orhan, A., Seyrek, E., Savaş, H. and Türköz, M. (2007). *Seismic Hazard and Total Risk Analyses for Large Dams in Euphrates Basin,* Turkey. Engineering Geology, 89, 155-170.

5th International Symposium on Dam Safety

October 27-31, 2018

AN ARTIFICIAL INTELLIGENCE BASED APPROACH FOR INVESTIGATING SLOPE STABILITY OF EARTH DAMS

Yılmaz Emre SARIÇİÇEK [1], Onur PEKCAN[2]

ABSTRACT

The structure of this study is formed upon developing an approach that makes limit equilibrium based slope stability calculations of earth dams in an easy and fast way. For this purpose, a database consisting of various earth dam scenarios and their safety factors against failure was formed using a limit equilibrium software frequently used in industry. The variations in the database included the slope of the upstream/downstream, height of the dam, crest width, shear strength properties of both homogenous fill and its foundation, unit weight of the fill and the water level in the upstream. Stability investigations were interpreted with common methods in the literature. The database including the abovementioned variations and the analysis results were divided into two portions, namely training and testing data. In order to eliminate time consuming work for software input, the first part of database was trained by a machine learning method called Support Vector Machines (SVM) and following the training part, the success of the method was tested in predicting the remaining safety factors for testing data. The results indicated that SVM is providing an accurate and sufficient approach within the boundaries of the above variations. Additionally, an independent dataset was formed for investigating the behavior beyond the limitations given in the training.

Keywords: Earth dams, slope stability, support vector machines

INTRODUCTION

Dams are among the most significant engineering structures in many countries worldwide as people construct them for various purposes such as irrigation, hydropower, water supply, flood control and management. Therefore, especially in the developed and developing countries, many dams have been constructed mainly in the last century. Numbers based on ICOLD (International Comission on Large Dams) data indicate that by 1949, around 5000 large dams had been constructed and 75% of them were in industrialized countries. The number had increased significantly by the turn of the century reaching up to 45000 large dams in more than 150 countries (Altinbilek, 2002).

Along with construction works, scarcity of proper dam sites, design or construction improperness, material defects etc. may result in problems during the construction and service life of dams. Zhang et al. (2009) handled the failure of earth dams with a statistical approach. Accordingly, in their study, earth dams were classified into four broad categories as homogenous earthfill dams, zoned earthfill

[1] Research Assistant, Department of Civil Engineering, Middle East Technical University, Ankara, Turkey, e-mail: yilmazs@metu.edu.tr
[2] Assistant Professor, Department of Civil Engineering, Middle East Technical University, Ankara, Turkey, e-mail: opekcan@metu.edu.tr

dams, earthfill dams with corewalls and concrete faced earthfill dams. In the next step, dam failure reasons were summarized as overtopping, quality problems, poor management, disasters etc. Further details regarding quality problems revealed that spillway quality, piping around spillway, piping in dam body or foundation and sliding of dam body or foundation formed the sub-category of quality problems.

Out of many possible dam and failure types, this study focuses on homogenous type of earthfill dams and their slope stability computations. The main structure of the study is based upon investigating the applicability of a machine learning method in prediction of slope stability factor of safeties calculated via limit equilibrium methods. For this purpose, an artificial case dataset regarding the factor of safeties of earth dam slopes was formed and tested in Slide®, Rocscience software. In the next step, Support Vector Machines (SVM), a well-known computational learning technique, was utilized for training the dataset based on the input variables and their outcomes, and further predicting the results that were already given by the software. Thus, in the study, the success of prediction in our model was compared with the software data. Also, relatively greater database was used in the process compared to similar works in the literature. Following sections summarizes the basics of SVM, main work and conclusions respectively.

LITERATURE & SUPPORT VECTOR MACHINES

The field of machine learning, a sub-category of artificial intelligence, has attracted the attention of the researchers over the last decades. The intriguing side of machine learning is its capability of making predictions without any prior information about the data relationships. Machine learning algorithms learn the background of the data while being trained. There are many machine learning techniques including, but not limited to, support vector machines, neural networks, decision trees, random forests, genetic programming, self-organizing map etc. that implement various algorithms (Lary et al., 2016).

Researchers have investigated for possible solutions to the dam and slope stability/landslide problems and utilized various machine learning problems. Depending on the complexity of the problem, accuracy expectations for solutions, availability and applicability of the software, diversity of machine learning algorithms have been presented in the literature.

For example, Lin et al. (2010) used support vector machines in order to forecast long term discharge in a dam site which was stated to be important for hydropower reservoir management. Mata (2011) investigated the dam behavior with the help of artificial neural networks in terms of crest displacements. Ranković et al. (2014) similarly worked on the dam safety by forecasting dam displacements, which is a function of hydrostatic pressure, temperature and various other causes. The study of Fisher et al. (2017) focused on piping and crack detection that are vital for internal erosion in earth dams. Geophysical data was processed with support vector machines.

In addition to the above studies, Sakellariou and Ferentinou (2005) performed slope stability safety estimations using neural networks for case studies. Similarly, Samui (2008) carried out the investigation of these case studies with support vector classification and regression analyses. Manouchehrian et al. (2014) also worked on real case slope stability studies together with genetic algorithms.

The applicability and power of some of the machine learning algorithms have been compared in some of the essays. Salazar et al. (2015) compared the success of random forests, boosted regression trees, neural networks, support vector machines and multivariate adaptive regression splines in terms of dam behavior prediction. Suman et al. (2016) focused on functional networks, multivariate adaptive

regression splines and multigene genetic programming whereas Lin et al. (2018) referred to gravitational search algorithm, random forest, support vector machines and naive Bayes for slope stability predictions.

The progress of the research studies ended up having hybridization of the algorithms. Zhao (2008) aimed at combining first-order second-moment method with support vector machine for slope stability reliability analyses. Samui and Kothari (2011) examined whether the least square support vector machines could be an alternative for support vector machines using slope stability cases. Xue et al. (2014) investigated hybrid use of support vector machine and particle swarm optimization. Likewise, Hoang and Pham (2016) worked on slope stability issue integrating Firefly Algorithm and Least Squares Support Vector Classification.

More specific readings on SVMs gives details of the background principles of the predictions. Accordingly, SVMs can be utilized both for classification and regression purposes. Initially, the algorithm worked on classification of linearly separable input data as given in Figure 1. In the figure, possible separation planes were given and the algorithm tries to find the plane that had maximum distances from each group.

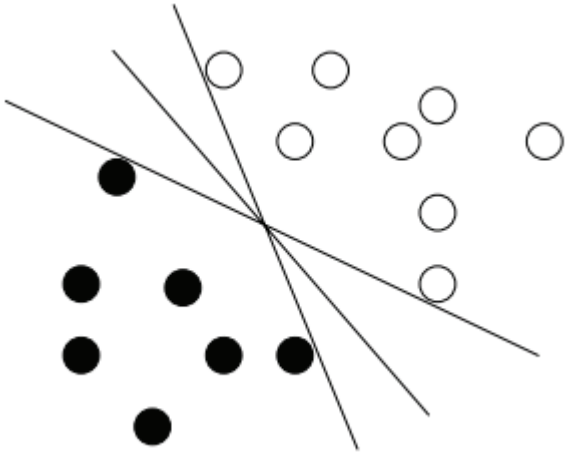

Figure 1. Possible Separation Planes (Goh and Goh, 2007)

Whenever complex and noisy data exist, SVM can adopt more flexible approach by assigning some variables and cost parameters. For linearly inseparable inputs, an operation called mapping, which uses functions called kernel functions, makes data available for SVM application.

Support vector regression approach, on the other hand, depends on prediction of the values rather than classification. For instance, epsilon insensitive support vector regression model predicts the values within the epsilon distance from the optimum separation plane. Variables denoted with ζ letter helps predictions to become more flexible (Figure 2.).

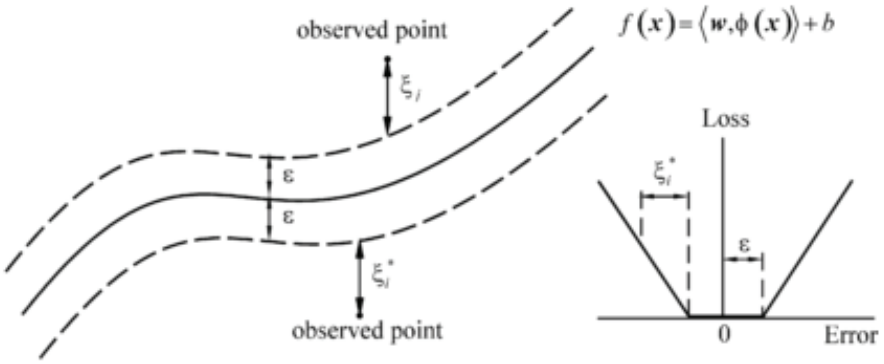

Figure 2. Epsilon insensitive support vector regression model (Ranković et al., 2014)

MAIN WORK

This part is dealing with main work of the research study. Various slope stability of artificial earth dam scenarios was tested via Slide®, Rocscience software, the details of which are presented in Table 1. In these scenarios, the slope of the upstream/downstream, height of the dam, crest width, shear strength properties of both the homogenous fill and foundation, unit weight of the fill and the water level in the upstream were chosen to be variables. Diverse combinations of these variables extended the scope of this work up to 420 separate cases.

As previously stated, some of the outstanding research studies also focused on similar issue. Sakellariou and Ferentinou (2005), Samui (2008), Manouchehrian et al. (2014), Xue et al. (2014), Hoang and Pahm (2016) and Lin et al. (2018) opted to use real case slope stabilities and unit weight of soil, cohesion, internal friction angle, slope angle, slope height and pore water pressure ratio were their research variables. Differences in variables, data source (real / artificial) and number of cases exist in this study.

Material strength types were chosen to be Mohr – Coulomb. Non-circular surface search optimization was performed with Particle Swarm Search option. Factor of safety values were determined with Bishop, Janbu Corrected, General Limit Equilibrium (GLE) / Morgenstern-Price and Sarma methods.

Table 1. Earth Dam Scenarios Technical Properties

Slope (V:H)	**Dam Height (m)**	**Crest Width (m)**
0.33 – 0.4 – 0.5	Max: 58	Max: 60
	Min: 10	Min: 30
c (kPa) – Fill	**Φ (º) - Fill**	**γ (kN/m^3) - Fill**
0	Max: 42	Max: 22
	Min: 26	Min: 17
Water Height (m)	**c (kPa) – Foundation**	**Φ (º) - Foundation**
Max: 50	Max: 58	Max: 58
Min: 0	Min: 10	Min: 10

Regarding artificial intelligence part, a MATLAB code that uses embedded sub-codes available in library called LIBSVM (Chang and Lin, 2001) was prepared for the solution of these scenarios. The library provides users chances to make either support vector classification or support vector regression. Also, various kernel functions, namely, linear, polynomial, radial basis and sigmoid, are available in the library package.

Step by step, the procedure can be summarized as follows:

- Initially, whole dataset is randomly separated into two as training and test parts. Out of 420 rows of data, 350 rows of them were chosen to be as training data and the remaining as test data. Each row consisted of abovementioned variables and a single factor of safety. In other words, each method of slope stability determination was treated independently.
- Following the minor details regarding the software related issues (scaling, data format preparation, data reading etc.), the code worked on finding a relation between variables and factor of safety.
- At that point, some major details were implemented to the code: Radial basis kernel function was used in the system. Bui et al. (2012) mentioned in their research about details of kernel functions and stated that linear kernel functions could be a specific type of radial basis function and sigmoid kernel functions could behave like radial basis ones for some certain parameters. Also, trial and errors in this study revealed radial basis functions to be optimum solution in our study.
- In order to detect possible cost and other required parameter in solution that optimize the regression, cross validation approach was adopted. In other words, best parameters were found by dividing the training dataset into subgroups and comparing them with each other in terms of optimum solution parameters.
- Parameters obtained in the training part were then used in the test part for making predictions. The next section provides the results of test dataset predictions.

RESULTS

For detection of success, root mean square error (RMSE) and the mean absolute percentage error (MAPE) were selected to be indicators. In overall, data prediction worked with similar efficiency in each slope stability method probably due to already close results in each method. Maximum RMSE of 0.06 and MAPE of 3.09 % indicated high efficiency. Figures 3, 4, 5 and 6 show software results versus prediction results.

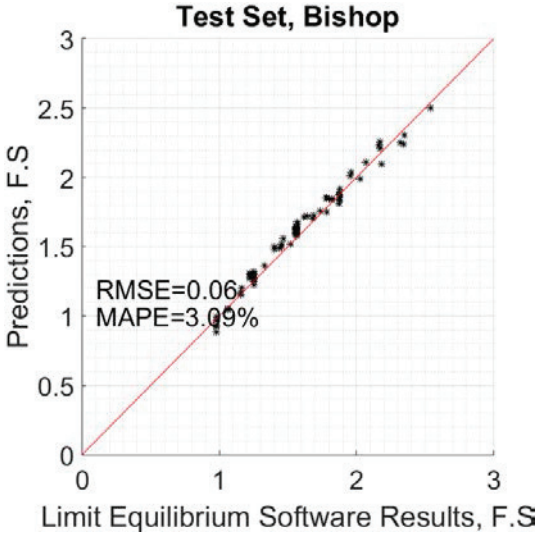

Figure 3. Predictions vs Software Results- Bishop Method

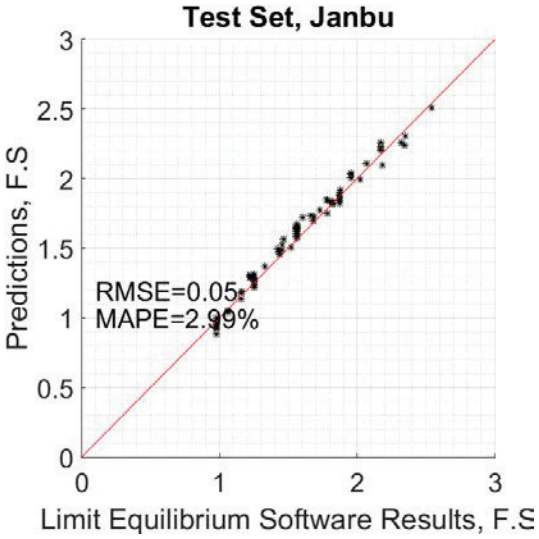

Figure 4. Predictions vs Software Results- Janbu Corrected Method

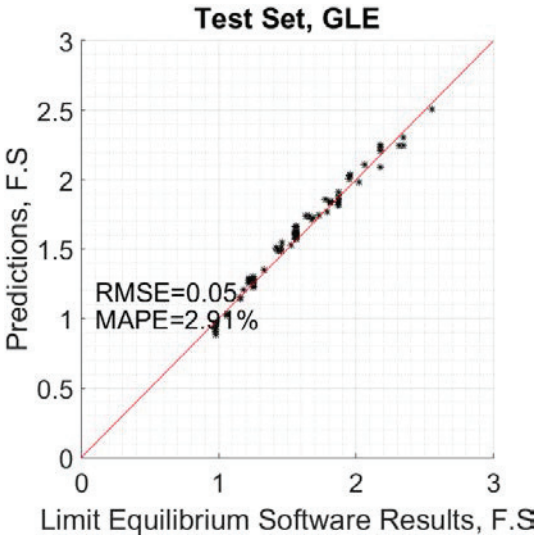

Figure 5. Predictions vs Software Results- GLE Method

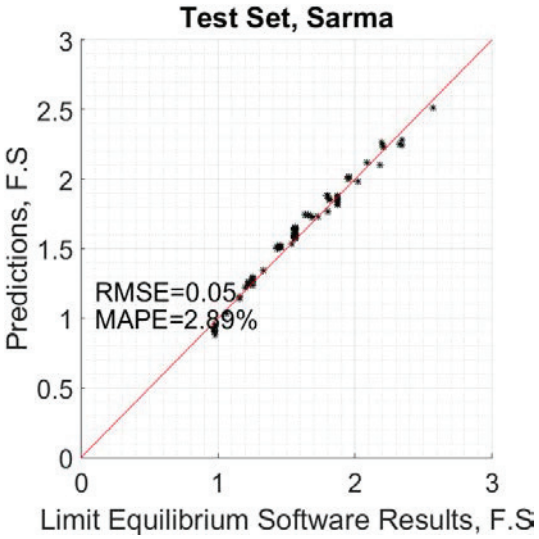

Figure 6. Predictions vs Software Results- Sarma Method

Additionally, in order to check whether the code is successful enough for detection of the factor of safety of cases that had features beyond the training set, the following variables were tested with the previously trained dataset. Most of the variables in this independent dataset extended the boundaries variables in the training. 15 cases, the details of which were given in Table 2, were determined. The results were given in Figures 7, 8, 9 and 10. Accordingly, maximum RMSE of 0.75 and MAPE of 20.68 % were obtained that could be considered as promising for the system for unfamiliar dataset. The main deviations seemed to happen after factor of safety of 2.5, which was the maximum value observed in training dataset.

Table 2. Independent Earth Dam Features

Slope (V:H)	Dam Height (m)	Crest Width (m)	c (kPa) – Fill	Φ (°) - Fill	Water Height (m)	γ (kN/m^3) - Fill	c (kPa) – Foundation	Φ (º) - Foundation
0,28	70	200	0	45	60	23	20	38
0,25	75	150	0	44	50	24	23	37
0,28	80	140	0	43	40	23	18	39
0,28	75	180	0	24	0	16	16	38
0,25	60	180	0	24	0	16	25	37
0,45	75	80	0	36	60	22	20	20
0,45	85	150	0	26	30	18	0	36
0,28	60	100	0	34	15	19	26	30
0,45	65	185	0	36	20	17	25	38
0,25	60	80	0	38	20	22	17	37
0,28	50	75	0	42	30	22	0	36
0,28	65	100	0	25	0	18	16	38
0,45	65	100	0	25	0	18	0	24
0,45	80	120	0	42	70	21	0	39
0,45	80	120	0	25	40	17	16	20

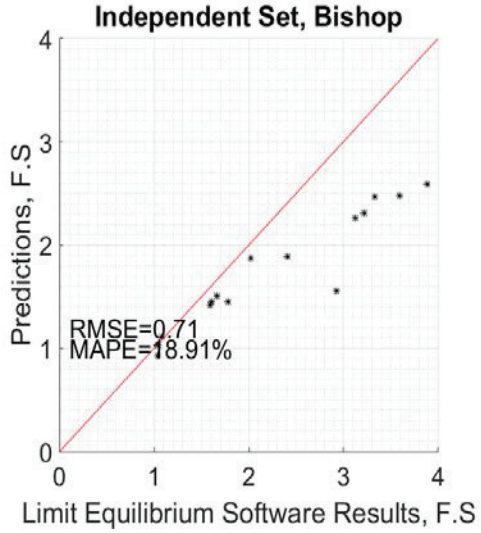

Figure 7. Independent Predictions vs Software Results- Bishop Method

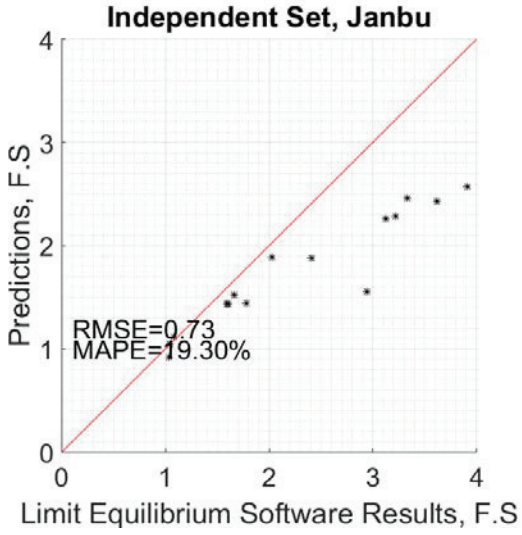

Figure 8. Independent Predictions vs Software Results- Janbu Method

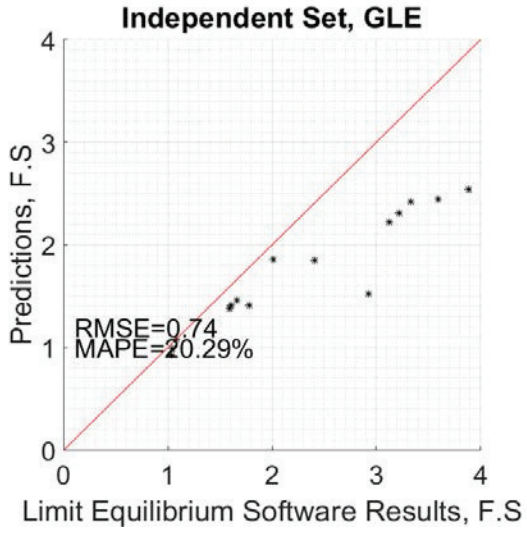

Figure 9. Independent Predictions vs Software Results- GLE Method

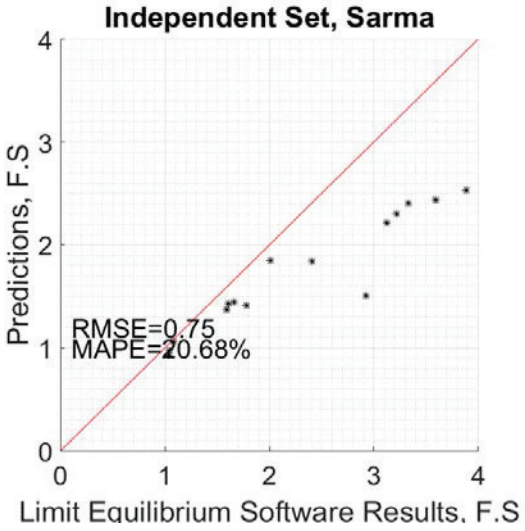

Figure 10. Independent Predictions vs Software Results- Sarma Method

CONCLUSIONS

In this paper we checked the applicability of limit equilibrium factor of safety software data prediction and had successful results. The variables included some foundation data and excluded the pore pressure ratio compared to other prominent studies. Within the boundaries of the variables that were introduced to the system, the results were highly promising. Trials that extend the training provided results that were less accurate (MAPE around 20%) but still promising.

The most critical surfaces obtained via software mainly happened to occur around the surface which would change with cohesive fills. However, in this research, we assumed the fill to be cohesionless that resembled coarse grained materials. Use of large clay core or fill materials with cohesion could be considered in future studies. Also, pore pressure ratio, which could be vital for earth dams, can be other important part that is the another issue in future works. More complex geometries, more material properties etc. offer numerous possible working areas in this subject.

REFERENCES

Altinbilek, D. (2002) The Role of Dams in Development, International Journal of Water Resources Development, 18:1, 9-24,doi: 10.1080/07900620220121620

Bui, D. T., Pradhan, B., Lofman, O., & Revhaug, I. (2012). Landslide Susceptibility Assessment in Vietnam Using Support Vector Machines, Decision Tree, and Naïve Bayes Models. Mathematical Problems in Engineering,2012, 1-26. doi:10.1155/2012/974638

Chang, C.-C., & Lin, C.-J. (2001). LIBSVM: a library for support vector machines. http://www.csie.ntu.edu.tw/~cjlin/libsvm.

Fisher, W. D., Camp, T. K., & Krzhizhanovskaya, V. V. (2017). Anomaly detection in earth dam and levee passive seismic data using support vector machines and automatic feature selection. Journal of Computational Science,20, 143-153. doi:10.1016/j.jocs.2016.11.016

Goh, A. T., & Goh, S. (2007). Support vector machines: Their use in geotechnical engineering as illustrated using seismic liquefaction data. Computers and Geotechnics,34(5), 410-421. doi:10.1016/j.compgeo.2007.06.001

Hoang, N., & Pham, A. (2016). Hybrid artificial intelligence approach based on metaheuristic and machine learning for slope stability assessment: A multinational data analysis. Expert Systems with Applications,46, 60-68. doi:10.1016/j.eswa.2015.10.020

Lary, D. J., Alavi, A. H., Gandomi, A. H., & Walker, A. L. (2016). Machine learning in geosciences and remote sensing. Geoscience Frontiers,7(1), 3-10. doi:10.1016/j.gsf.2015.07.003

Lin, J., Cheng, C., & Chau, K. (2006). Using support vector machines for long-term discharge prediction. Hydrological Sciences Journal,51(4), 599-612. doi:10.1623/hysj.51.4.599

Lin, Y., Zhou, K., & Li, J. (2018). Prediction of Slope Stability Using Four Supervised Learning Methods. IEEE Access,6, 31169-31179. doi:10.1109/access.2018.2843787

Manouchehrian, A., Gholamnejad, J., & Sharifzadeh, M. (2013). Development of a model for analysis of slope stability for circular mode failure using genetic algorithm. Environmental Earth Sciences,71(3), 1267-1277. doi:10.1007/s12665-013-2531-8

Mata, J. (2011). Interpretation of concrete dam behaviour with artificial neural network and multiple linear regression models. Engineering Structures,33(3), 903-910. doi:10.1016/j.engstruct.2010.12.011

Ranković, V., Grujović, N., Divac, D., & Milivojević, N. (2014). Development of support vector regression identification model for prediction of dam structural behaviour. Structural Safety,48, 33-39. doi:10.1016/j.strusafe.2014.02.004

Sakellariou, M. G., & Ferentinou, M. D. (2005). A study of slope stability prediction using neural networks. Geotechnical and Geological Engineering,23(4), 419-445. doi:10.1007/s10706-004-8680-5

Salazar, F., Toledo, M., Oñate, E., & Morán, R. (2015). An empirical comparison of machine learning techniques for dam behaviour modelling. Structural Safety,56, 9-17. doi:10.1016/j.strusafe.2015.05.001

Samui, P., & Kothari, D. (2011). Utilization of a least square support vector machine (LSSVM) for slope stability analysis. Scientia Iranica,18(1), 53-58. doi:10.1016/j.scient.2011.03.007

Samui, P. (2008). Slope stability analysis: A support vector machine approach. Environmental Geology,56(2), 255-267. doi:10.1007/s00254-007-1161-4

Suman, S., Khan, S. Z., Das, S. K., & Chand, S. K. (2016). Slope stability analysis using artificial intelligence techniques. Natural Hazards,84(2), 727-748. doi:10.1007/s11069-016-2454-2

Xue, X., Yang, X., & Chen, X. (2014). Application of a support vector machine for prediction of slope stability. Science China Technological Sciences,57(12), 2379-2386. doi:10.1007/s11431-014-5699-6

Zhang, L., Xu, Y., & Jia, J. (2009). Analysis of earth dam failures: A database approach. Georisk: Assessment and Management of Risk for Engineered Systems and Geohazards,3(3), 184-189. doi:10.1080/17499510902831759

Zhao, H. (2008). Slope reliability analysis using a support vector machine. Computers and Geotechnics,35(3), 459-467. doi:10.1016/j.compgeo.2007.08.002

5th International Symposium on Dam Safety

October 27-31, 2018

SAFETY EVALUATION IN SOFT FOUNDATION SOILS DURING FILL CONSTRUCTION

Zülal AKBAY ARAMA [1], S. Feyza ÇİNİCİOĞLU[2]

ABSTRACT

In this study a new and original design method for shallow embankments such as cofferdams or levees located on soft clays is proposed. The method is a limit state method combined with stress evaluations. This property enables the designer to apply a stage construction method as well as computing for a one-stage application. Moreover, limit state approach is linked to the mobilized stress states at a regional basis and hence a more realistic calculation for any stage can be made. The proposed method is based on lower bound plasticity theory for finding the varying stress states along the possible slip surfaces beneath the embankment. The method is combined with a limit equilibrium approach specifically developed for the earth embankment problem constructed on soft soils. The method is applicable for all types of embankments including dams, levees and cofferdams. In this paper the context is restricted to the undrained construction phase of cofferdams.

Keywords: Cofferdam, levee, safety, soil plasticity, limit equilibrium.

INTRODUCTION

In the context of embankment construction for dams and levees the main and important objective is to ensure system stability because of the possibility of hazard due to flooding, slope instability and foundation collapse. Safety conditions require that every component of fill shall be of suitable design and construction sufficiency, adequate strength and capacity for the aim of usage (Chirapuntu and Duncan, 1976). Depending on an envisaged dam construction case, fills can be made up from different materials to supply safety requirements such as earth-fill, rock-fill, single-walled, double-walled, braced or cellular types due to the project necessities, foundation soil conditions, fluctuations in the water level, excavation area sizes and the available material at the site for construction. This study tackles the cofferdam construction problem through the instrument of foundation collapse mechanism for evaluating the safe and fast design of an envisaged temporary earth-fill cofferdam project built on soft foundation soils. Earth-fill cofferdams are preferred to be constructed at places that the height of water level is less than three meters and at the section that the flow velocity is low (Department of Primary Industries and Water, 2008). They are usually built by using the local available material in the field such as fine sand, clay or whatever (Hanna and Meyerhof, 1974). The height of the coffer body is kept a meter more than the potential maximum water level not to cause failure because of possible flooding risk. In order to solve the slope stability problems inclination of slopes are given as 1:1 or 1:2 depending on the material used in the construction of coffer. With the elimination of flooding and slope instability risks, the only problem for the design and construction of cofferdams has to be the adequateness of foundation soil bearing capacity. Soft foundation soil media

[1] Dr., Department of Civil Engineering, Istanbul University-Cerrahpasa, Istanbul, Turkey, e-posta: zakbay@istanbul.edu.tr

[2] Professor, Department of Civil Engineering, Ozyegin University, Istanbul, Turkey, e-posta: feyzacinicioglu@gmail.com

creates an unsafe brace for structures due to their material characteristics. Soft soils response to applied loads is generally critical due to their high deformability and low shear strength (Florkiewicz, 1989). So that in order to build small dams like coffers or levees on soft soils, soft soil behavior should be carefully followed in terms of preventing failure (Santhosh et al., 2014)

In this study a new design method developed by Akbay Arama (2016) for embankments built on soft foundation soils is described and applied by taking cofferdam construction details into consideration. The new method utilizes lower bound limit analysis (soil plasticity theory) for evaluating varying stress states along the identified slip surfaces underneath the coffer and at the foundation soil side (Chen, 1975). The identified slip surfaces are zoned by using the stress fans and thereby changing stress states can be evaluated along the considered slip plane. Soft foundation soil media can be scanned by considering various slip planes at different depths. Limit equilibrium logic, which is defined as the static equilibrium of horizontal and vertical forces and moment in a selected system, is used with integration of the mass created by slip fans. This integrated limit equilibrium and limit analysis method is capable of taking into consideration the static equilibrium conditions at different regions throughout the foundation soils. Thus the method scans the whole width of cofferdam beginning from the toe of the slope to the centerline of the symmetrical structure. This application is repeated for various depths of foundation soils, the choice of depth intervals relies on the desired sensitivity level. The aim is to evaluate the depth of failure surface and to find the propagation of stresses under a cofferdam of a specified height. Due to the use of equilibrium equations the rate of slip resistant and verifier forces can be obtained to evaluate safety levels of all envisaged slip zones in the foundation soils. The new design method has a significant advantage of integrating limit analysis lower bound calculations with static limit equilibrium theory. With the use of this combined procedure it will be possible to determine all the stress states at different locations and adapt them into the developed limit equilibrium equations. By this way, the calculations can be used for further phases of load application followed by stress state changes due to the loading and consolidation steps, in case stage construction method is preferred. Besides all these, the method is unique because of taking into consideration the initial stress conditions which are not evaluated in conventional limit equilibrium calculations. The application of the method is made for a number of hypothesized cases of cofferdam construction and a verification work has been conducted by using a commercial two dimensional finite element program, Plaxis. The results of the analysis showed that the design procedure is applicable for cofferdam construction cases.

APPLICATION OF THE PROPOSED METHOD

A new method for evaluating the behavior of soft foundation soils under a specified embankment in terms of available safety levels at different depths has been developed by Akbay Arama (2016). The proposed method is appropriate for modeling cofferdams. In this section the application procedures of the method are presented in detail and verified by numerical calculations.

As undrained loading conditions are critical for soft soils, construction stages are taken into account to evaluate the possibility of failure or the safety level available. The new design method is applied either for evaluating the maximum construction height of embankments under sudden loading conditions or to define safety levels of foundation soils under an embankment of a specific height. To achieve this purpose, foundation soil is divided into a mesh of elements as fine as it is necessitated by the required sensitivity of the analysis. Local failure mechanisms are evaluated by drawing slip surfaces with segments of circular shape for each depth scanned starting from the ground surface. Evaluating the static equilibrium of each local failure mechanism and solving the integrated moment equation of the whole system gives the representative failure surface in terms of limit equilibrium. This surface brings the level of system safety to the limit conditions and restricts the foundation soils which is affected by the loading stage of embankment and generated the failure surface. The application phases of the proposed method is presented below in detail.

Evaluation of General Failure Mechanism: Geometrical Limits and Stress Distribution

With the aim of evaluating general failure mechanisms of a cofferdam-soft foundation soils interaction system an embankment with a specific construction height (h_d) has been considered. Figure 1 shows the symmetrical embankment and it is assumed that the failure mechanism starts at the toe of the embankment and it is extended due to the increasing depth by circular shaped failure surfaces centering at the toe. The acquired general failure mechanism involves a triangular shaped active zone which extends over the embankment base. The slip zone is made up of circular shaped slices that are centered at the toe of the embankment. The limits of active-slip-passive zones are determined from limit analysis lower bound theorem by using stress fans. At the same time, a sliding surface resistance is activated which tries to stop the movements by passive forces created under the slip zone.

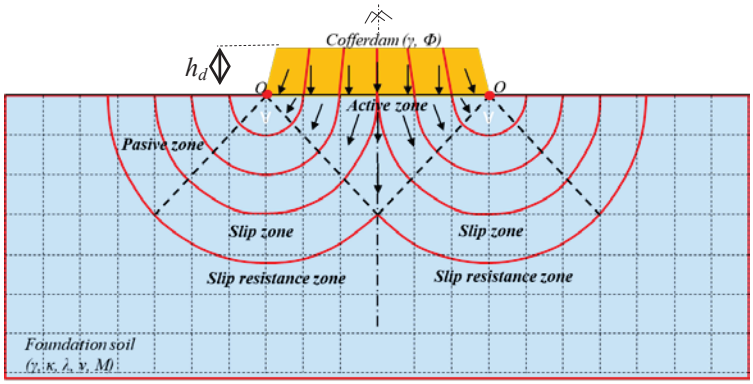

Figure 1. Envisaged general failure mechanism (Akbay Arama, 2016)

The limits of stress zones depend on the location of discontinuity planes. Limit analyses lower bound theorem helps to find these locations by the contribution of loading conditions, soil material properties and the number of selected discontinuity plane number (Atkinson, 1981). The equations that are used to evaluate the geometrical limits of the general failure mechanism is shown in Figure 2.

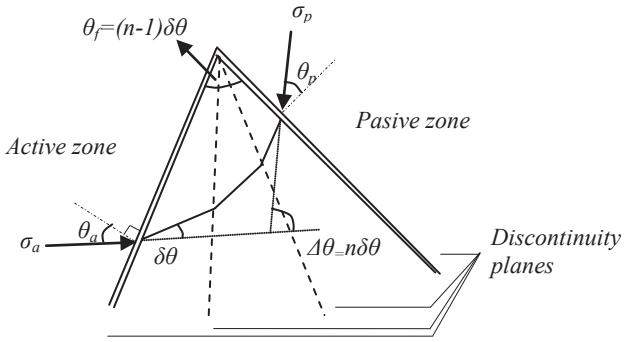

Figure 2. The angular rotations between discontinuity planes (Atkinson, 1981)

There are discontinuous slip planes between active and passive zones given in Figure 2. The angular rotation δθ is the stress rotation amount in the direction of major principle stresses in the stress fan consisted of discontinuity planes. The total amount of angular rotation between active and passive zone is "Δθ=n.δθ" and the value of "n" represents the number of slip planes selected by the researcher. The principal stresses are mobilized at the axis passing through the center of the embankment. The principal stresses are transferred from the center of the embankment to the passive zone. The rotation angle between active and passive zone is 90°. The stress change within "n" numbered discontinuous plane is "$\Delta s=n\ (2.\ c_u.\ \sin\delta\theta)$".

Adaptation of Limit Analysis and Limit Equilibrium Calculations to the New Design Method

The foundation soil can be scanned by the introduction of a grid system with vertical and horizontal lines starting from the toe of the embankment. By means of the generated grid system, the slip planes at different depths can be integrated into the mechanism and the location of the possible failure plane can be investigated. The active forces are transmitted to the passive zone that tries to maintain the system stability though slip zones defined as rigid local slip slices. As can be seen in Figure 3, the analyses begin from the smallest rigid slip slice and the slices enlarge as the considered depth increases.

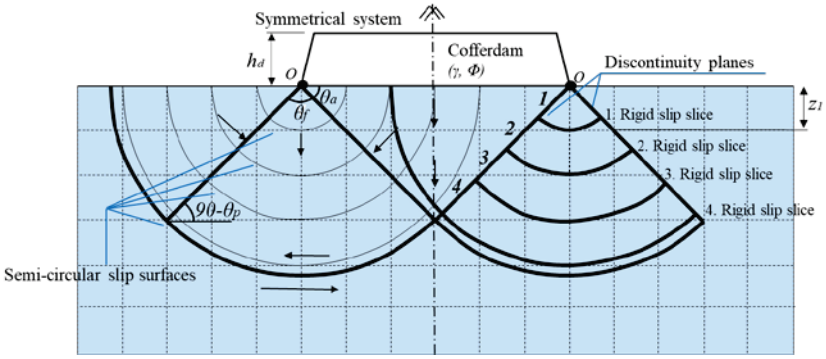

Figure 3. Failure grid and failure mechanism mobilization

The static equilibrium of the stresses on each rigid slip slice is based on the equilibrium of forces in the vertical and horizontal directions and the moment of the system with respect to the toe. The analyses are repeated depending on the fineness of the failure grid for all the defined depths. Equilibrium condition is controlled using the values of active and passive forces to identify the safety level of the embankment-soil interaction system. Figure 4 shows the rigid wedge of the failure mechanism.

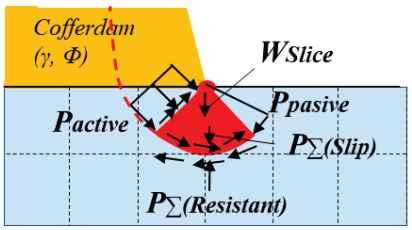

Figure 4. The forces acting on the rigid sliding block of wedge shape

The efficiency of the force-balance system shown in Figure 4 is evaluated according to the vertical and horizontal force and moment equilibrium. The first depth which gives equilibrium equations (FoS=1) is selected as the failure surface for the specified loading condition. The forces $P_{a\sigma}$ and $P_{a\tau}$ shown in Figure 4 stand for the active normal and shear forces respectively. These forces result from the self-weight of the embankment. The vertical stress distribution and stress decrements based on depth can be calculated by the well-known stress distribution methods (2/1 method, Boussinesq method, Newmark method etc.). The horizontal distribution and variation of stresses are obtained by the use of stress fans. The details of stress distribution and variation of stress ratios are described in detail in the PhD thesis by Akbay Arama (2016). $P_{\sum\sigma(slip)}$ and $P_{\sum\tau(slip)}$ are given as the normal and shear forces which trigger the failure throughout the slip surface boundary and they can be calculated by Eqn. 1.

$$P_{\sum\sigma(slip)} = \sum_{i=2}^{n}\left[\sigma_{za(i)}.L_{a(i-1)}\right] \qquad P_{\sum\tau(slip)} \sum_{i=2}^{n}\left[\tau_{xa(i)}.L_{a(i-1)}\right] \tag{1}$$

where W_{slice} is the weight of the soil mass which remains within the selected rigid slip slice and evaluation of its value is a classical geometry calculation. The simple equation to obtain W_{slice} is given in Eqn. 2

$$W_{slice}=(\theta_f.\ \pi.\ z^2.\ \gamma_z)\ /\ 360° \tag{2}$$

By the use of Eqn. 2, it can be inferred that, the total passive force available at any depth can determine the amount of embankment loading that can be carried by the foundation soils based on the available shear strength parameters. P_p is defined as the passive resistance force that is activated by the self-weight of soil mass. P_p increases linearly with depth and can be calculated by Equation 3.

$$P_p=(\sigma_{1p2}+\sigma_{3p2})0,5.z \tag{3}$$

In the proposed method, the slip plane forced to fail under the influence of $P_{\Sigma\sigma\ (slip)}$ and $P_{\Sigma\tau\ (slip)}$. But as a reaction to these forces a resistance system is mobilized by the passive stresses at the slip plane boundary. The resistive forces are called $P_{\Sigma\sigma\ (resistant)}$ and $P_{\Sigma\tau\ (resistant)}$ and they can be calculated by using the rigid sliding fan. The geometrical characteristics of the fan is same for calculations of both disturbing and resisting forces. In this context, the force and moment equilibrium equations can be written. In addition to this the safety ratios of all envisaged rigid slip slices can be obtained by using the sliding and resistive forces and moments ratios. The minimum value of the safety numbers calculated by the given equations below shows the safety levels for a slice.

$$GS_{HorizontalDirection} = \frac{P_{p(h)} + P_{\Sigma\tau(resis\tan t)}}{P_{a\sigma(h)} + P_{a\tau(h)} + P_{\Sigma\tau(slip)}} \tag{4}$$

$$GS_{VerticalDirection} = \frac{P_{p(v)} + P_{\Sigma\sigma(resis\tan t)}}{W_{slice} + P_{a\sigma(v)} + P_{a\tau(v)} + P_{\Sigma\sigma(slip)}} \tag{5}$$

$$GS_{Moment} = \frac{P_p \dfrac{2}{3} + P_{\Sigma\tau(resis\tan t)}}{P_{a\sigma}.\dfrac{1}{2} + P_{\Sigma\tau(slip)}} \tag{6}$$

THE NUMERICAL APPLICATION OF THE PROPOSED METHOD TO COFFERDAM CONSTRUCTION

Numerical applications are carried out to evaluate the applicability of the proposed method for cofferdam construction and results are compared with the results of a commercial geotechnical engineering program Slope/W. The considered cofferdam geometry and soil parameters are shown in Figure 5. Cofferdam height (h_d) is the main variable that is changing between 1 to 5 meters. The foundation width (B) and platform width (C) are the fixed values of the cofferdam and they are 24 meters and 20 meters respectively. The cofferdam consists of granular materials which has a unit weight of 21 kN/m^3 and a friction angle of 35°. Cofferdam material properties affected the loading conditions and the loading magnitude. Foundation soil is soft and unit weight of the material is 14.2 kN/m^3 and critical state parameters are given in Figure 5.

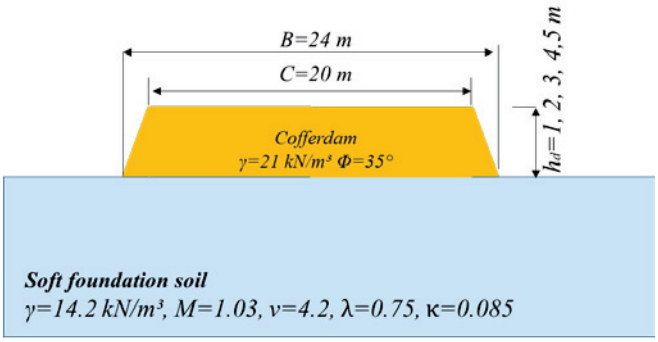

Figure 5. A cofferdam example (geometry and variable characteristics)

Analyses are repeated for five different heights (1, 2, 3, 4, 5 meters) for the symmetrical cofferdam. Discontinuity plane number (n) is selected as two and the failure grid is drawn by 1 meter sensitivity (Figure 6). Due to the fixed values of cofferdam foundation width, the location of stress fan is the same for all selected cases. Only the case of 1 meter cofferdam loading is exemplified in the context of this paper because of the limited space. The geometrical limits of stress fans are evaluated from equations given above. For two discontinuity planes case the angle θ_a is calculated as 67.5° and the angle of fan is calculated as 45°. The mobilized stresses within the foundation soil under undrained loading conditions is calculated by the 2/1 method throughout the depth and distributed by stress fans through the width of the encountered possible failure plane at all depths. According to the calculated stress values, the forces acting on the first rigid slip slice are evaluated for all the given slices.

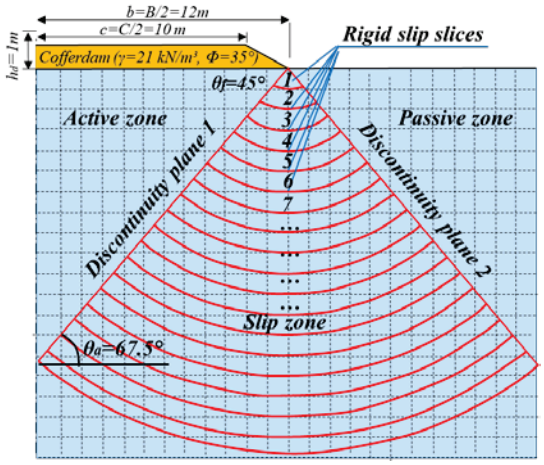

Figure 6. Failure grid and rigid slip slices of selected cofferdam construction cases

Limit equilibrium equations are written separately for each rigid slip slice and the calculations are started from the slip slice which is closest to the cofferdam toe in the drawn metric grid depending on the desired sensitivity ratio. With the use of equations (4), (5), (6) the safety numbers of each slice due to the horizontal, vertical forces and moment equilibrium are calculated for 1 meter height cofferdam and given in Table 1. The value of the safety factor obtained as a result of the horizontal equilibrium for the rigid slip slice passing through one meter depth is 0.61, the vertical equilibrium result is 0.67 and the moment equilibrium result is 0.69. These results show that the slice fails and one meter depth is not the depth representing the critical equilibrium denoted by FoS of one. Therefore failure surface scanning followed up by 2 meter depth. The number of safety obtained as a result of the horizontal equilibrium written for the rigid slip slice passing through 2 meter depth is 0.99, the vertical equilibrium result is 1.05 and the moment equilibrium result is 1.12. The results show that the slice is nearly in equilibrium. However, in order to satisfy the safety requirements the depths which

give a FoS greater than one can be considered as the safe depths. The research continues with applying the same procedure to greater depths in order to evaluate the safety conditions all through the foundation soils. The minimum value from the calculated safety numbers is selected to show the slices security amount.

Table 1. The results of proposed method for 1 meter height cofferdam

h_d=1 meter	1 meter depth	2 meter depth	2.8 meter depth
Horizontal equilibrium $(FoS)_h$	0.61	0.99	1.39
Vertical equilibrium $(FoS)_v$	0.67	1.05	**1.27**
Moment equilibrium $(FoS)_m$	0.69	1.12	1.57

This procedure is repeated for all cofferdam heights and the results of minimum safety factor values are given in Table 2 for 2 meter height cofferdam, Table 3 for 3 meter height cofferdam, Table 4 for 4 meter height cofferdam, Table 5 for 5 meter height cofferdam.

Table 2. The results of proposed method for 2 meter height cofferdam

Depth (m)	1	2	3	4	4.10
FoS	0.33	0.61	0.78	0.99	1

Table 3. The results of proposed method for 3 meter height cofferdam

Depth (m)	1	2	3	4	5	5.9
FoS	0.24	0.50	0.70	0.92	0.96	1

Table 4. The results of proposed method for 4 meter height cofferdam

Depth (m)	1	2	3	4	5	6	6.7
FoS	0.19	0.42	0.64	0.86	0.92	0.97	1

Table 5. The results of proposed method for 5 meter height cofferdam

Depth (m)	1	2	3	4	5	6	7	8	8.9
FoS	0.16	0.36	0.59	0.80	0.88	0.94	0.95	0.98	1

The limit safety number is evaluated at the 4.10 meter, 5.9 meter, 6.7 meter and 8.9 meter depth for 2 meter, 3 meter, 4 meter, 5 meter cofferdam height respectively. It can be seen that increasing cofferdam height results increasing failure depth. The considered cofferdam construction cases are modelled by using the commercial limit equilibrium program Slope/W with the use of Morgestern Price method. The acquired values of safety factors are shown at Table 6. Results show that the proposed method gives satisfactory results for designing cofferdams in undrained loading conditions.

Table 6. Comparison of purposed method with Slope/W analyses

h_d (m)	1	2	3	4	5
Purposed method	2.8	4.2	5.9	6.7	8.9
Slope/W analyses	3	5	5.9	6.8	8.7

RESULTS

Within the scope of this paper, a new approach has been proposed for the interpretation of the failure behavior under undrained conditions. The theoretical basis of the proposed method is based on limit analysis and limit equilibrium methods. The unique aspect of the proposed method compared to the existing limit equilibrium design methods is to identify a network that determines the safety levels of foundation media by scanning the initial stress states of the soil zones. With the proposed method, the boundaries of the affected foundation soils can be determined for the cofferdam constructed at a certain height. Besides this the opposite perspective can be used and the maximum cofferdam height

which can be constructed on a certain foundation profile can be obtained. The method is applicable to staged construction technique because of its stress state-based approach.

REFERENCES

Akbay Arama, Z. 2016. "Yumuşak Zeminler Üzerinde Yer Alan Genişletilmiş Yol Dolgularınn Teorik ve Nümerik Analizi". PhD Thesis, Istanbul University, Istanbul (in Turkish).

Atkinson, J.H. 1981. "Foundations and Slopes: An Introduction to Applications of Critical State Soil Mechanics". Mc Graw-Hill Book Company.

Chen, W.F. 1975. "Limit Analysis and Soil Plasticity". Elsevier Scientific Publishing Company, New York.

Chirapuntu, S., Duncan, J. M. 1976. "The Role of Fill in the Stability of Embankments on Soft Clay Foundations". Geotechnical Engineering Report No. TE 75-3, University of California, Berkeley.

Department of Primary Industries and Water. 2008. "Guidelines for the Construction of Earth-fill Dams". Tasmania.

Florkiewicz, A. 1989. "Upper Bound to Bearing Capacity of Layered Soils". Canadian Geotechnical Journal, Vol. 26, pp. 730-736.

Hanna, A.M., Meyerhof, G.G. 1974. "Ultimate Bearing Capacity of Foundations on a Three Layer Soil with Special Reference to Layered Sand". Canadian Geotechnical Journal, Vol. 16, pp. 412-414.

Santhosh, H. P., Swamy, H. M., Prabharaka, D. L. 2014, "Construction of Cofferdam-A Case Study". IOSR Journal of Mechanical and Civil Engineering, pp 45-50.

5th International Symposium on Dam Safety

October 27-31, 2018

RAPID AND SLOW DRAWDOWN EFFECTS ON THE STABILITY OF CLAY CORE DAMS

Zülal AKBAY ARAMA [1]

ABSTRACT

In this study, the stability of clay cored earth fill dams are investigated under conditions of rapid and slow drawdown with performing multivariate parametrical analysis using a commercial finite element program in two dimensional space. Fast reduction of the water level at the upstream of dams lead to instability of interacted fill-foundation system due to the sudden increase of excess pore water pressures that confined inside the dam fill body. Besides this situation slow reduction of the water level at the upstream of dams allows pore water pressures to dissipate and damp. In situations like this transient groundwater flow analyses are required for performing the calculations with finite element method. Within the scope of this application process, pore pressures are evaluated by using groundwater flow analysis, transferred to the deformation analysis and used for stability calculations respectively. This research presented in this paper is focused on the modeling details of the flow conditions that can be encountered in the design of dams by taking into account the effects of material properties of fill, core and subsoil to the stability of interacted fill-foundation system due to the change of water level at the upstream of dam body by performing randomly fictionalized cases.

Keywords: Clay core dam, Rapid drawdown, Slow drawdown, Transient groundwater flow, Stability.

INTRODUCTION

Earth fill dams are huge and complicated engineering structures that are storing water with the resistance of large soil masses. The design and construction stages of these water structures are different than other conventional geotechnical engineering structures due to their huge volume, variable structure material properties and water force effects. The prediction of the stability and evolution of deformations of any earth fill-foundation soil system always plays a key role due to the complex and interacted behavior characteristics (Athani et al., 2015). Sudden loading of the fill stages during construction, transmitting this additional loads to the foundation media and applying envisaged water forces to the whole system respectively, generates excessive pore water pressures and creates the deformations throughout the foundation media and into the earth fill. This rapid application composition leads to the mobilization of fractures, tensile cracks and probable collapse (Özçoban et al., 2007). Therefore, evaluating the stress-strain characteristics and actual stability situation of earth fills and auxiliary facilities during and after the construction is the major design consideration to obtain both a secure stable system and to provide sustainable usage of structures (İlter and Yılmaz, 2016). To provide sustainable usage of dams and auxiliary structures, all the situations that can be encountered at the expected life of the system have to be taken into account at the design step. Staged construction method has also being preferred more than sudden loading method to control the rate of

[1] Dr., Department of Civil Engineering, Istanbul University-Cerrahpasa, Istanbul, Turkey,
e-posta: zakbay@istanbul.edu.tr

loads not to cause collapse at the construction of fill body (Al-Homoud and Tanash, 2001). Construction stage thicknesses are identified due to the geotechnical characteristics of foundation soil and geometrical properties of structures. Besides these, the stability of earth fill and foundation soil under critical conditions such as earthquake and flood have to be supplied. Considering the reservoir storage conditions which are varied between full and empty charge situations, the control of seepage and overtopping have to be checked by safety analysis. Various analysis techniques and computation methods have been implemented beginning from the first phase of construction to long term usage due to the in-situ measuring, statistical mathematics and numerical solutions. Finite element method is a numerical technique which can lead to reach approximate results to a wide variety of geotechnical problems. Equilibrium of forces, compatibility of displacements, continuity of flow, evaluation of material constitutive properties and taking into account the boundary conditions brings the success of the method.

In this study, an arbitrary fictionalized clay core dam is selected to perform stability analysis of interacted fill-foundation system. It is assumed that the dam was constructed by staged construction technique and the dam-foundation system satisfied adequate safety in empty reservoir condition. Multivariate parametrical analyses are done for this arbitrary fictionalized clay core dam by taking into account the changeability of material properties of fill, clay core and the foundation soil. According to the changes in material characteristics, the effect rate of reservoir water storage condition with respect to time is also investigated by performing coupled finite element analysis by a commercial finite element program called Plaxis2D.2017. The details and variables of analyses are given below with detailed information.

NUMERICAL ANALYSES: PARAMETRIC ASSUMPTION AND EVALUATION

Plaxis 2D is one of the most preferred two dimensional finite element program, that is developed for the analysis of stability, deformation and groundwater flow in geotechnical engineering. Geotechnical applications require advanced material constitutive models to simulate the non-linear, time-dependent and anisotropic behavior of soils. In addition, since soil is a multi-phase material, special procedures and applications are required to deal with hydrostatic and non-hydrostatic pore pressures in the soil. Although the modeling of the soil itself is an important issue, many geotechnical projects involve the modeling of structures and the interaction between the structures and the soil (Brinkgreve et al., 2017). Depending on these informations it can be said that dams and auxiliary structures design and construction process is a multivariate and interacted geotechnical problem due to the soil-based structural components. Plaxis 2D finite element program seems suitable to reflect the behavior characteristics of whole system from construction beginning to long term usage. To perform interacted system analysis with finite element method by the use of Plaxis 2D.2017, a systematic procedure have to be followed with the use of five tabs. Firstly the soil layers are defined by means of boreholes at the “soil” tab with choosing appropriate constitutive model for relevant soils. Then structural elements are modeled by “structures” tab. “Mesh” is generated for the whole system with different element distribution options. The geometry of model is discretized and transformed to a finite element mesh. Water levels with their change due to the times function can be defined by “flow condition” tab. “Staged construction” tab characterizes calculation mode. Parts of the model geometry can be activated or/and deactivated and material properties can be modified at this tab.

In the scope of this research following the given instructions above, a clay cored earth fill dam is modeled using this finite element software. The geometry of the model is obtained from Plaxis.2D tutorial manual that is shown in Figure 1. The modelled clay core dam is modeled with 30 meter height, 172.5 meter foundation and 5 meter platform width respectively. Clay core of the dam is surrounded by a well graded fill at both sides. This core has 5 meter width at the top and 20 meter width at the base. Foundation soil is homogenous cohesionless material and rested limitless throughout the depth.

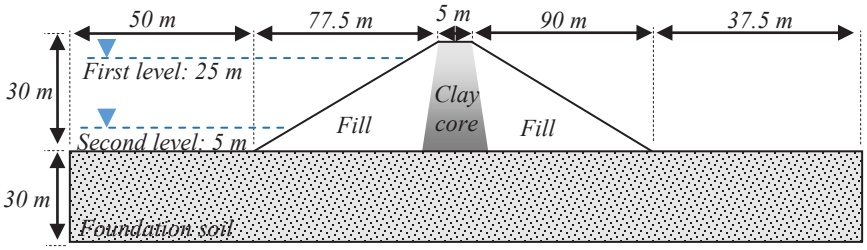

Figure 1. Geometry of the selected dam (Plaxis, 2017)

The reservoir storage at the upstream of the dam is assumed 25 meter (first level in Fig.1) from the ground surface at normal (steady state) conditions. The water storage height is reduced to 5 meter (second level at Fig. 1) to innerve an exception for flow conditions due to the fictionalized case. The aim of this application is to define flow functions due to the time dependent hydraulic conditions and to form transient flow conditions using different water storage heights to unfold modeling the extraordinary situations at the design of dams. The material properties are given in Table 1 for clay core, dam fill and foundation soil. All the materials are modeled by using Mohr Coulomb (MC) material model which represents linear elastic-perfectly plastic behavior. The model requires a total of five parameter, which are generally familiar to most geotechnical engineers and can be evaluated from basic laboratory or/and field tests on soil samples. The main properties needed to identify Mohr Coulomb model is saturated and unsaturated unit weight, Young modulus, Poisson ratio, shear strength parameters (in this study, effective cohesion and friction angle is used for drained analyses and undrained shear strength is used for undrained B analyses), permeability coefficients in both directions. Identified parameters can be either effective or undrained depending on the selected drainage type. Reference analyses are done to compare material property effects in the behavior of clay cored dams. The parametrical analyses are evaluated by varying material properties such as Young modulus, permeability coefficient and friction angle of dam fill, undrained shear strength and permeability of clay core and friction angle and permeability of foundation soil. The dam fill material properties are selected from literature to represent semi-permeable and permeable materials. Clay core and foundation soil material properties are selected from Brinkgreve et al. (2017). The unit weight of fill layers, Poisson ratio and Young modulus values are selected from Bowles (1996), friction angle is taken from Striegler and Werner (1969), the permeability characteristics are selected from Selvi (2012). Figure 2 shows the dam-foundation system structural components that are classified as clay core, embankment fill and foundation soil. The figure also expresses the fictionalized parametrical analysis with their terminations and variables. Subsoil (Figure 3a) and dam geotechnical properties (Figure 3b) are defined at the soil and structures tabs then mesh is evaluated by generating mesh with fine element distribution option including 378 element and 3189 nodes (Figure 3c).

Table 1. Geotechnical properties of clay core, dam fill and foundation soil for performing reference analysis

Parameter	*Clay core*	*Semi-permeable fill*	*Permeable fill*	*Foundation soil*
γ_{unsat} *(kN/m^3)*	16	17	17	17
γ_{sat} *(kN/m^3)*	18	20	21	21
E' (kPa)	1500	30000	50000	50000
ν'	0.35	0.33	0.33	0.3
Φ' (°)	-	30-32-34	34-36	35
c' (kPa)	-	5	5	5
s_u *(kPa)*	5	-	-	-
Ψ (°)	-	0-4	3-6	5
$k_x=k_y$ *(m/s)*	10^{-4}	10^{-2}-10^{-1}	10^{-1}-1	10^{-2}

Dam-foundation interacted system: Structural Components		
Clay core	**Embankment fill**	**Foundation soil (subsoil)**
Core 1: s_u=5 kPa $k_x=k_y=10^{-4}$ m/s ***Core 2:*** s_u=10 kPa $k_x=k_y=10^{-4}$ m/s ***Core 3:*** s_u= 20 kPa $k_x=k_y=10^{-4}$ m/s ***Core 4:*** s_u=5 kPa $k_x=k_y=10^{-2}$ m/s ***Core 5:*** s_u=5 kPa $k_x=k_y=10^{-6}$ m/s	***A. Semi-permeable fill*** ***Fill 1:*** ϕ=30° $k_x=k_y=10^{-2}$ m/s ***Fill 2:*** ϕ=30° $k_x=k_y=10^{-1}$ m/s ***Fill 3:*** ϕ=32° $k_x=k_y=10^{-2}$ m/s ***Fill 4:*** ϕ=32° $k_x=k_y=10^{-1}$ m/s ***Fill 5:*** ϕ=34° $k_x=k_y=10^{-2}$ m/s ***Fill 6:*** ϕ=34° $k_x=k_y=10^{-1}$ m/s ***B. Permeable fill*** ***Fill 7:*** ϕ=34° $k_x=k_y=10^{-1}$ m/s ***Fill 8:*** ϕ=34° $k_x=k_y=1$ m/s ***Fill 9:*** ϕ=36° $k_x=k_y=10^{-1}$ m/s ***Fill 10:*** ϕ=36° $k_x=k_y=1$ m/s	***Subsoil 1:*** ϕ=35° $k_x=k_y=10^{-2}$ m/s ***Subsoil 2:*** ϕ=28° $k_x=k_y=10^{-2}$ m/s ***Subsoil 3:*** ϕ=30° $k_x=k_y=10^{-2}$ m/s ***Subsoil 4:*** ϕ=32° $k_x=k_y=10^{-2}$ m/s ***Subsoil 5:*** ϕ=36° $k_x=k_y=10^{-2}$ m/s ***Subsoil 6:*** ϕ=35° $k_x=k_y=10^{-3}$ m/s ***Subsoil 7:*** ϕ=35° $k_x=k_y=10^{-1}$ m/s ***Subsoil 8:*** ϕ=35° $k_x=k_y=10^{-4}$ m/s

Figure 2. Analysis variables

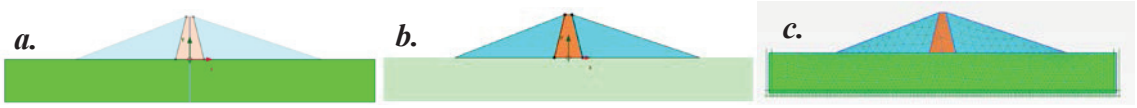

Figure 3. Soil-Structure-Mesh tab images from Plaxis 2D modelling

In dam-foundation soil interacted system it is very important to define flow conditions to reflect the real problematic condition. The scenario details that was introduced to the model the unexpected storage conditions during sustainable usage of dam has been modelled at the flow conditions tab. The phases inserted to define the water level change is given below:

1. Long term condition with 25 meter water level-High reservoir storage (HRSV)
2. Rapid drawdown of water level to 5 meter in 5 days duration (RDSV)
3. Slow drawdown of water level to 5 meter in 50 days duration (SDSV)
4. Long term condition with 5 meter water level-Low reservoir storage (LRSV)

The calculation process consists of eight phases including safety determinations defined after the phases given above. All the defined analysis phases are given at Figure 4. Gravity loading condition is used to form normal working conditions of dam to evaluate initial stresses and pore water pressure conditions (initial phase). The calculations are done by using steady state groundwater flow calculation to evaluate pore water pressure distribution. Rapid drawdown (first phase) and slow drawdown (second phase) situations both started from initial phase. In these cases excess pore water pressures are evaluated by transient water flow calculation.

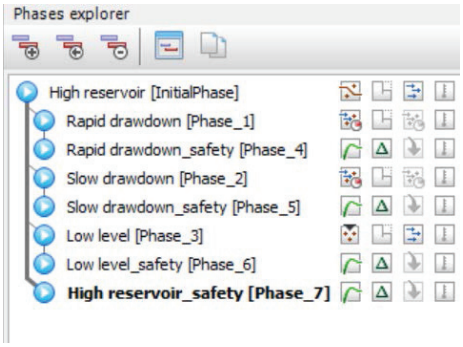

Figure 4. The phases that are described in the Plaxis analysis

The behaviour of the water levels can be described by specifying flow functions. Flow functions are defined for different speeds of water level reduction by using time interval. Low level calculation phase is the third phase that also starts from initial condition. This phase describes long term behaviour of dam under 5 meter reservoir level. The ground water flow calculations are done by steady state groundwater flow situation. The focus point of the all analyses is the variation of safety factor of dam for different water levels. At the end of analysis for all of the water situations, safety factor of the whole system is calculated by phi-c reduction method. The geometry of the model never changes during the phases (Brinkgreve et al., 2017).

RESULTS AND DISCUSSION

At this section of the paper, the results of analysis are given according to the safety evaluations and pore water pressure distribution diagrams of different phases and cases. The results of analysis that are obtained due to changes in embankment fill properties are given in Table 2, the results obtained due to changes in clay core properties are given in Table 3 and the results obtained due to the changes in subsoil properties are given Table 4. All the tables mentioned above are arranged according to the reservoir storage conditions. “k” symbol describes permeability coefficients and the subscripts consisted of numbers characterizes the values of 0.01, 0.1, 1 respectively. Geotechnical parameters of semi-permeable and permeable fill layers are selected according to the changes in friction angle, Young modulus, unit weight and permeability coefficient. Four different water level change cases, which are described in previous section, are integrated for these fictionalized situations. According to the Table 2, using constant friction angle with the increase of permeability coefficient causes to improve the system stability (except the situation of low reservoir condition). On the contrary situation (constant permeability with increasing friction angle) the safety value of the whole system increases in all phases. At the same permeability value and the same friction angle condition (for Fill 6 and Fill 7) the variance of system causes by the change of Young modulus. The permeable fill layer has greater modulus value than semi-permeable fill layer. At this condition the safety value of permeable layer is likewise greater than semi-permeable layer. In other words the raise of Young modulus of embankment fill causes the increment of safety value. The high water level condition (25 meter) at steady state situation always leads to lower safety value than low water level condition (5 meter) at steady state situation. The critical condition of the dam stability always occurs at the rapid drawdown of water level in all cases with the use of various geotechnical properties. The decrease of water level according to the flow function based on time avoids probable failure and ensures the decrement of safety level to occur gradually. In Table 3, the effects of geotechnical parameter change for clay core is investigated by taking into account the fill layers properties (ϕ32° and k_x=k_y=0.1 m/s) and subsoil properties (given in Table 1) at constant values. The cases and geotechnical properties are selected not to cause collapse in any phase to evaluate the level of safety degrees change and to obtain the rate of effectiveness of parameters. At the cases named Core 1, Core 2 and Core 3 the

permeability coefficient is constant at the value of 10^{-4} m/s and the undrained shear strength is selected 5, 10, 20 kPa respectively. The increase of undrained shear strength raises the values of safety.

Table 2. Analysis results obtained due to changes in embankment fill properties

	Name of fill	Different fill properties	$FoS_{(RDSV)}$ **R**apid **D**rawdown **S**afety **V**alue	$FoS_{(SDSV)}$ **S**low **D**rawdown **S**afety **V**alue	$FoS_{(LRSV)}$ **L**ow **R**eservoir **S**afety **V**alue	$FoS_{(HRSV)}$ **H**igh **R**eservoir **S**afety **V**alue
Semi-permeable fill	Fill 1	ϕ30°k1	0,9000	0,9709	1,6510	1,6280
	Fill 2	ϕ30°k2	0,9624	1,0690	1,6140	1,7020
	Fill 3	ϕ32°k1	0,9067	1,0660	1,7710	1,7190
	Fill 4	ϕ32°k2	1,0090	1,1670	1,7280	1,8100
	Fill 5	ϕ34°k1	0,9311	1,1240	1,8740	1,8030
	Fill 6	ϕ34°k2	1,0610	1,1840	1,8280	1,7700
Permeable fill	Fill 7	ϕ34°k2	1,1260	1,2610	1,8490	1,7900
	Fill 8	ϕ34°k3	1,2140	1,6080	1,8290	1,9310
	Fill 9	ϕ36°k2	1,1470	1,3070	1,9620	1,8350
	Fill 10	ϕ36°k3	1,2650	1,6630	1,9390	2,0390

The cases Core 4 and Core 5 are defined at constant undrained shear strength with 5 kPa value. The system difference comes from the changes in permeability coefficient. The decrease in the permeability coefficient value of clay core layer increases system stability by limiting the infiltration process. The safety change of dam system based on the different levels of water is ranged $FoS_{(HRSV)}>FoS_{(LRSV)}>FoS_{(SDSV)}>FoS_{(RDSV)}$ respectively. At this gradation "FoS" represents the values of safety.

Table 3. Analysis results obtained due to changes in clay core properties

Clay Core Property	$FoS_{(RDSV)}$ **R**apid **D**rawdown **S**afety **V**alue	$FoS_{(SDSV)}$ **S**low **D**rawdown **S**afety **V**alue	$FoS_{(LRSV)}$ **L**ow **R**eservoir **S**afety **V**alue	$FoS_{(HRSV)}$ **H**igh **R**eservoir **S**afety **V**alue
Core 1	1,0090	1,1670	1,7280	1,8100
Core 2	1,0120	1,1560	1,7430	1,7370
Core 3	1,3160	1,3640	1,5370	1,6880
Core 4	1,1970	1,2800	1,5090	1,5130
Core 5	1,3170	1,3850	1,5310	1,6800

The results of the analyses based on the change in foundation soil (subsoil) properties are given in Table 4. The embankment fill (ϕ32° and $k_x=k_y=0.1$ m/s) and clay core (given in Table 1) geotechnical properties are remained at constant values.

Table 4. Analysis results obtained due to changes in subsoil properties

Subsoil Property	$FoS_{(RDSV)}$ **R**apid **D**rawdown **S**afety **V**alue	$FoS_{(SDSV)}$ **S**low **D**rawdown **S**afety **V**alue	$FoS_{(LRSV)}$ **L**ow **R**eservoir **S**afety **V**alue	$FoS_{(HRSV)}$ **H**igh **R**eservoir **S**afety **V**alue
Subsoil 1	1,0090	1,1670	1,7280	1,8100
Subsoil 2	0,8738	1,0110	1,6080	1,4750
Subsoil 3	0,9315	1,0430	1,6590	1,5450
Subsoil 4	0,9422	1,0740	1,6810	1,6160
Subsoil 5	1,0050	1,1360	1,7390	1,8280
Subsoil 6	0,9544	1,1250	1,7110	1,8070
Subsoil 7	1,0650	1,2870	1,7700	1,7270
Subsoil 8	-	-	-	-

The variables of analysis are friction angle and permeability coefficients of subsoil for these cases. The permeability coefficient value is 10^{-2} m/s in all the cases named Subsoil 1, Subsoil 2, Subsoil 3, Subsoil 4 and Subsoil 5. The friction angle value changes between 28°-36°. The graduation of friction angles is given as $\phi_{subsoil2}=28° < \phi_{subsoil3}=30° < \phi_{subsoil4}=32° < \phi_{subsoil1}=35° < \phi_{subsoil5}=36°$. In the cases Subsoil 6, Subsoil 7, Subsoil 8 the friction angle remains constant with the value of 35° and the permeability coefficients are changed gradually as $k_{subsoil8}=10^{-4}$ m/s< $k_{subsoil6}=10^{-3}$ m/s< $k_{subsoil1}=10^{-2}$ m/s< $k_{subsoil7}=10^{-1}$ m/s. The increase of friction angle causes the raise of safety levels and effects the system stability rather than permeability coefficient change. However, when the coefficient of permeability takes the value of 10^{-4} m/s, the initial phase of the dam system cannot be calculated by the finite element program. This situation supports the application of permeable filter layer at the base of dam foundation level to create an infiltration zone for the drainage of excess water pressures. The smaller permeability values causes to confine water pressures above the ground level and disallows these pressures to spread and damp in the foundation media within a short time period. The excess pressures presses the body of the dam and induces to occur failure. In Figure 5 all the analysis results are given with order to clarify the differences of safety behavior under various storage conditions. Vertical axes defines safety of the system and the horizontal axes defines number of phases. The horizontal axes doesn't have any numerical meaning. When the graphs given in Figure 5 are examined, it can be seen that the highest safety condition is reached at low steady state water level. The most critical condition is the sudden drawdown in water level. However the reduction in water level due to time can also result in safety decrease that can lead to fail. The conditions mentioned above are valid except for one exception between the cases evaluated within the concept of this paper. This exception arises from two of the cases identified according to the fill properties. In this exception condition, the permeability value is 1 m/s and the friction angle of the fill material is 34-36°. At these cases the higher safety value is reached at low and high steady state water level conditions in both. This situation arises in all other variable changes for Fill 8 and Fill 10. It is believed that this condition happens because of the equalizer effects of water forces at the upstream side of the dam. From all above mentioned informations, it can be seen that the significant change of safety condition occurs during the rapid drawdown of water at the upstream side of the dam. While rapid drawdown, the equalizer effect of the water forces on the upstream side of the dam is suddenly lost but the excess pore water pressures within the dam may already remain at high values due to the permeability characteristics of material. Highly permeable soils can drain quickly and also water pressures are damped quickly too. But it will be take a long time for low permeable materials to dissipate and damp water pressures. Because of the significant effect of water storage levels on the stability of dams, active pore pressures are controlled for the four phase of analysis. The active water pressure changes are represented by shadings at the figures given below. Only specific reference cases can be selected according to the allowed limits of paper to show water pressures. Figure 6 represents the active pore water pressure distribution phases of Fill 3 and Fill 4 cases. This condition searches the effects of permeability coefficient change of fill material at the same friction angle value. It can be seen from Figure 6 that according to the decile decrease of permeability coefficient the water flow condition only changes at the rapid and slow drawdown phases. The active pore pressure values are evaluated for the toe point of upstream slope from Plaxis for all the phases threated. Active pore water pressure is defined as the multiplication of pore water pressure with effective saturation parameter. Pore water pressures are differentiated from active pore pressures when the saturation degree is less than unity. The utilization of the active pore water pressures evinces that the maximum value of pressure is reached at the high reservoir condition by the self-weight of water level. Low reservoir level induces minimum pressures on the toe point of slope. The forces acting on the toe point is less than full reservoir condition than drawdown conditions. Figure 7 represents the flow condition differences with the evaluation of active pore pressure dissipation diagrams for Core 1, Core 4 and Core 5 cases. The difference between these selected cases is the permeability coefficient values. Undrained shear strength value is constant at 5 kPa. Decrease of clay cores permeability coefficient value leads water flow to follow a route close to the base of core or in other words close to the relative permeable subsoil. Looking into the active pore pressures, it can be said that the decrease of permeability decreases equalizer water forces on the upstream side slope.

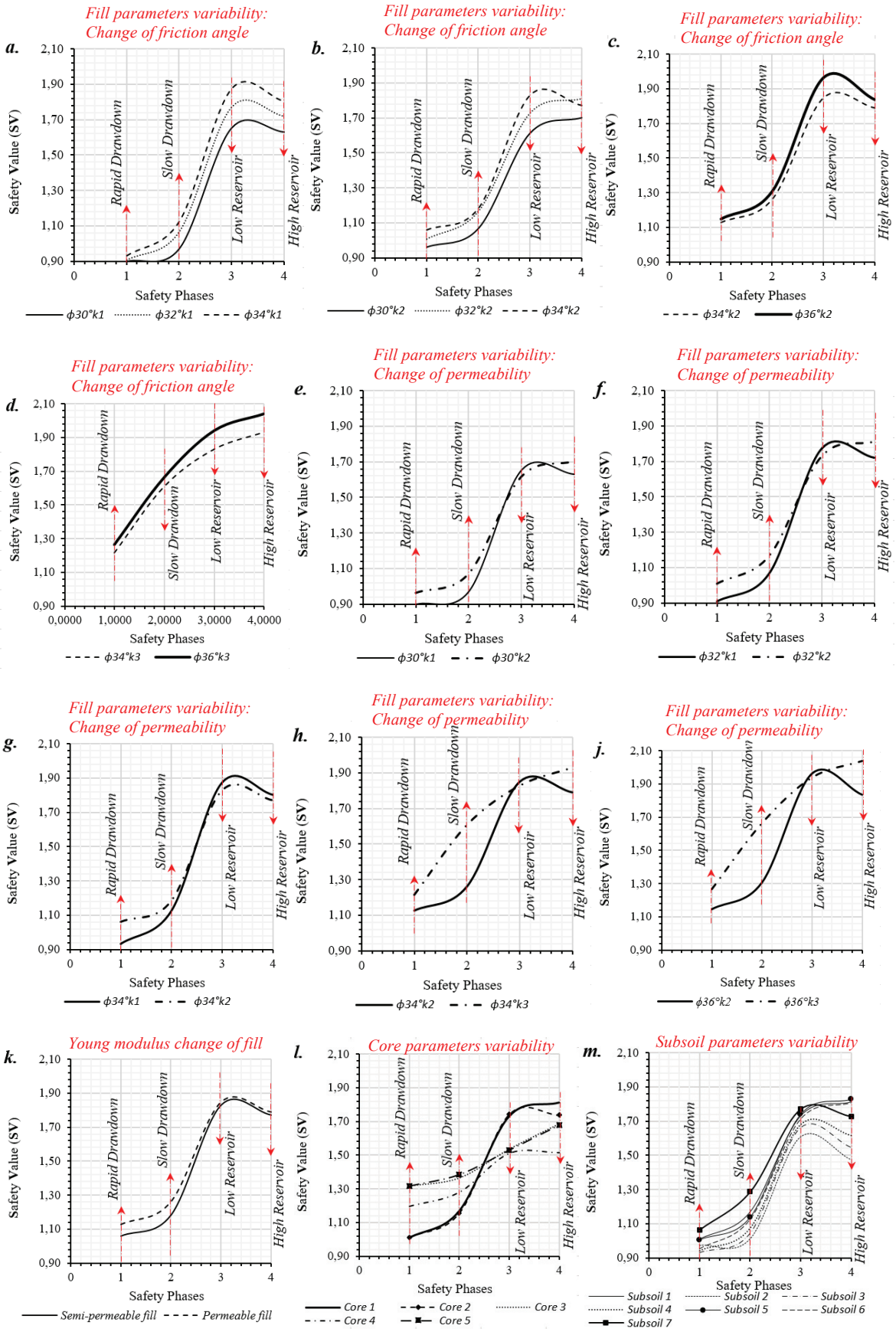

Figure 5. Numerical analyses results obtained from Plaxis 2D

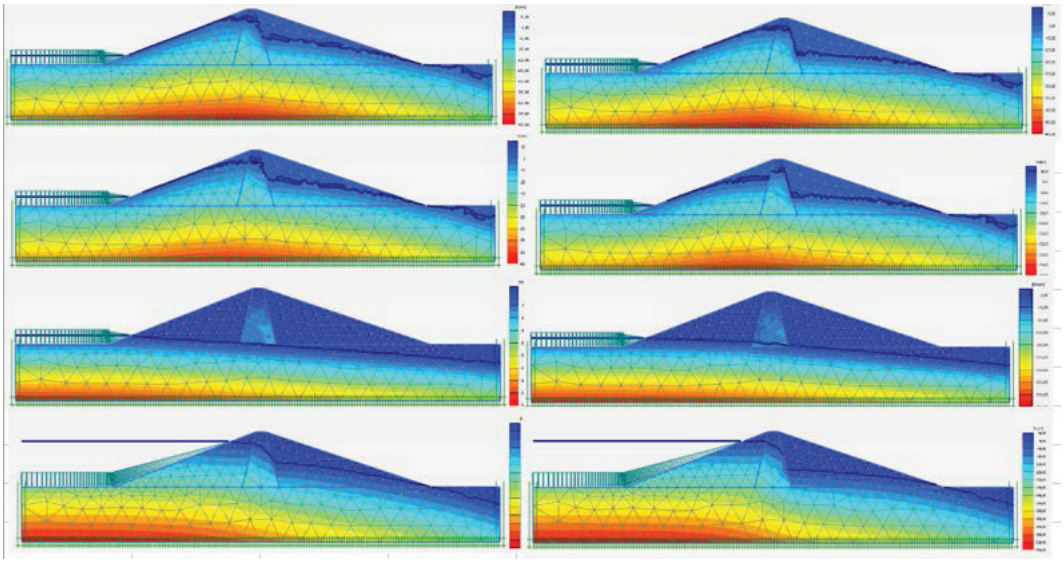

Figure 6. Comparison of P_{active} pressures activated in the cases of Fill 3 and Fill 4

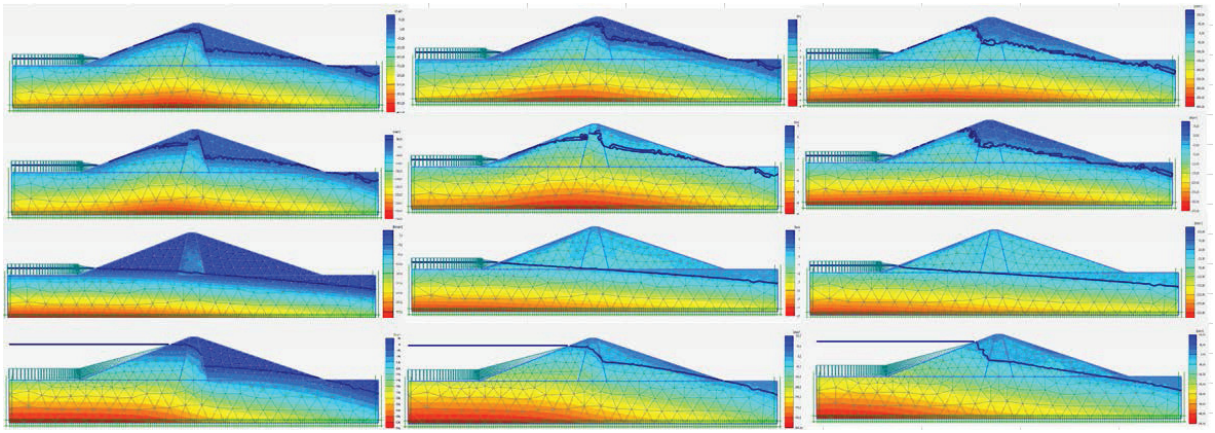

Figure 7. Comparison of P_{active} pressures activated in the cases of Core 1, Core 4 and Core 5

Figure 8 represents the behavior characteristics of Fill 9 and Fill 10. The difference between these cases comes from the permeability property variability.

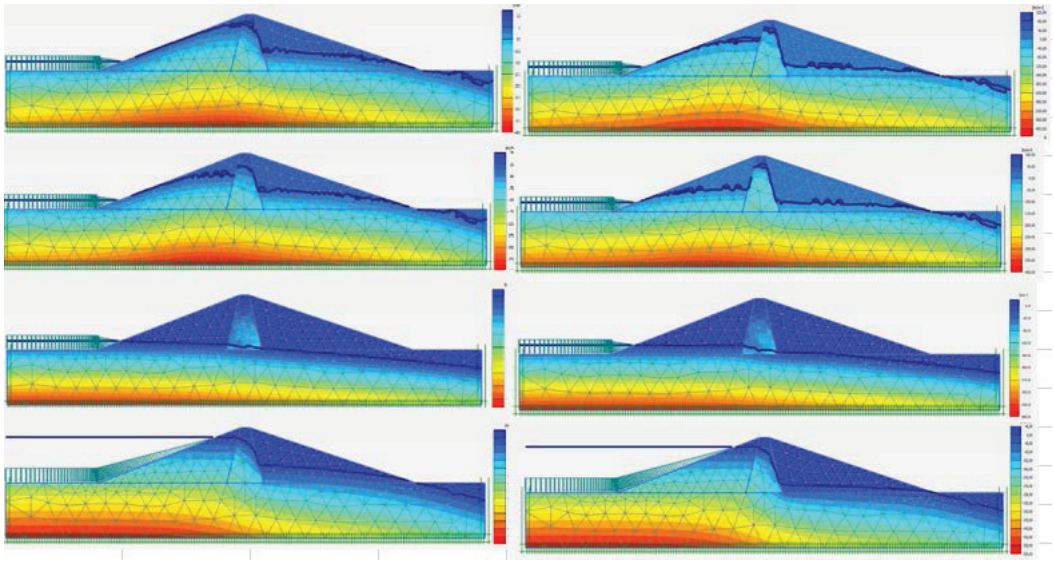

Figure 8. Comparison of P_{active} pressures activated in the cases of Fill 9 and Fill 10

Friction angle remains at constant value at 36° but the permeability coefficient is 0.1 m/s for the case of Fill 9 and 1 m/s for the case of Fill 10. Increase of permeability of fill layer seemed to decrease water forces effected the toe. But similar trend is captured for the active pore pressure dissipation. Subsoil 2 and Subsoil 2 cases are compared at Figure 9. The difference between cases is the friction angle change. Subsoil 1 has 35°and Subsoil 2 has 28° friction but the permeability coefficient of soils is the same. The trend of flow not changed due to the differentiation of friction. As a result the conspicuous parameter is permeability coefficient for the design of dams. The values given in Table 5 approves this attitude.

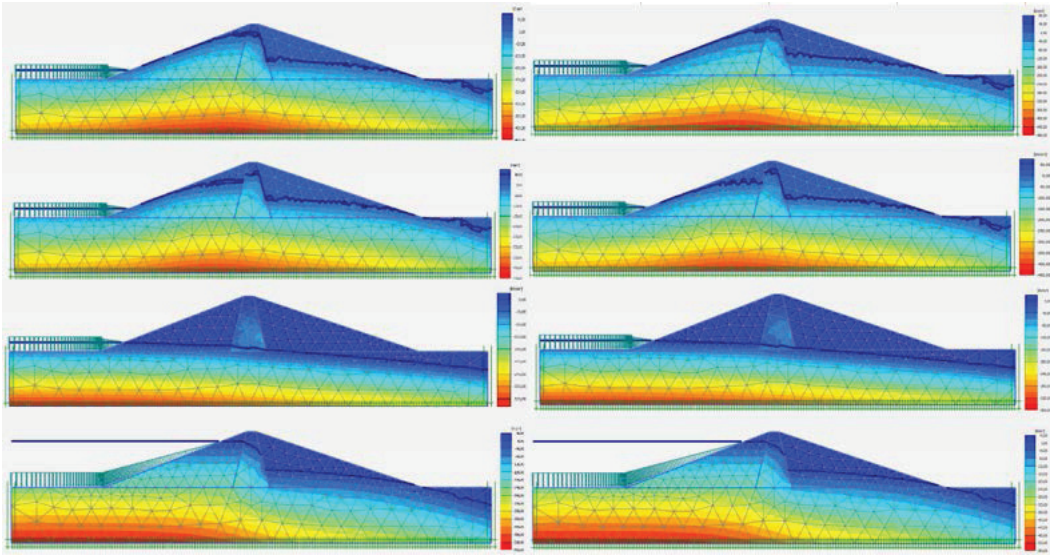

Figure 9. Comparison of P_{active} pressures activated in the cases of Subsoil 1 and Subsoil 2

Table 5. Values of P_{active} pressures at the toe of upstream slope for different cases

P_{active} (kPa)	Fill 3	Fill 4	Core 4	Core 5	Fill 9	Fill 10	Subsoil 2
$P_{active\text{-}Rapid\ Drawdown}$	189.505	190.815	191.310	166.941	188.974	177.852	189.960
$P_{active\text{-}Slow\ Drawdown}$	191.893	192.617	191.851	166.830	191.807	181.628	191.967
$P_{active\text{-}Low\ Reservoir}$	141.379	136.252	136.228	133.961	141.379	147.011	141.379
$P_{active\text{-}High\ Reservoir}$	193.106	194.234	194.200	170.314	193.130	183.328	193.106

CONCLUSION

The rapid drawdown of the water level at the upstream side may be the critical condition for dams under the general loading effects. This unexpected condition can be encountered at the flood retarding dams after overflow disasters. The water level at the upstream side of the flood retarding dams after overflow may remain stable at the maximum level for a while. In the meantime, steady state water flow condition almost occurs within the dam body and the upstream side of the dam maintains stability with a relative safety factor (Fattah et al., 2015). But at the retreatment time the water level suddenly drops. Under this circumstances, the excess water pressures are kept for some time despite the fact that decrease of reservoir storage condition (Çalamak et al., 2015). It takes time to dissipate and decrease excess pore water pressures due to the permeability characteristics of materials. This time (velocity) is too short for dams constructed with low permeable materials. In other words the relative difference between the excess pore water pressure decrease and storage velocity drawdown

speed will cause to fail the slope of the upstream side of dam. Failure of the dam occurs by collecting plastic shear strains over time with the decrease of shear strength in these plastic zones (Stark and Duncan, 1991). Plaxis is a well-equipped program taking into consideration these circumstances with fully coupled flow deformation analysis and stability analysis can be done by applying shear strength method (Khalilzah et al., 2015). In this paper, fully coupled deformation analysis and stability analysis are performed respectively for rapid and slow drawdown conditions according to arbitrary fictionalized cases. The cases are constituted with constant geometric dimensions but various material properties. The variability of geotechnical parameters like friction angle, undrained shear strength, permeability coefficient and Young modulus are examined in the finite element analysis. The analysis are conducted for rapid drawdown, slow drawdown, low storage and high storage condition to control the safety situations for unexpected situations that can be encountered within the lifetime of a dam. It is believed that the results obtained from analysis will guide practitioners in the case of rapid reservoir discharge condition occurred in a dam for modeling with finite element method. The study shows performing details of fully coupled analysis with finite element method and reveals the effective parameters of materials on the safety behaviour of dam-foundation interacted system. It has seen from the results that the most critical condition occurs at rapid drawdown of upstream but the failure can be prevented at this condition by using different material properties for dam body. Using a core material with appropriate undrained shear strength at the center of the dam leads to protect skeleton of the dam. Changing the permeability coefficient of clay core causes to change the way of seepage activated within the body of the dam. Highly permeable core materials brings the system stability approximately failure condition. Decreasing the permeability coefficient makes system more stable and reduces the active pore pressure forces acting on the toe of the upstream slope. The embankment fill material and its properties are also the other effective factor of safety but not effective as core material properties for the situations treated in this study. Embankment fill materials with permeable properties brings the interacted system to higher values of safety. The permeability coefficient of fill material becomes the second most effective parameter of the design. The foundation layer investigated in this study consists of frictional materials. The efficient parameters selected to research the rate of influence on the stability condition is selected friction angle and permeability coefficient of subsoil. Friction angle plays an important role to ensure stability of overall system. The increase of friction angle rises safety values. Besides friction angle, the effect of permeability incontrovertibly effective on the behavior. The decrease of permeability causes the water not to be transmitted to the foundation layers. Water stores above the ground level and this undamped water pressure forces the dam body.

REFERENCES

Al-Homoud, A.S., Tanash, N., 2001. “Monitoring and Analysis of Settlement and Stability of an Embankment Dam Constructed in Stages on Sort Ground”, Bull. Eng. Geol. Env., vol. 59, pp. 259-284.

Athani, S.S., Shivamonth, Solanki, C.H., Dodagoudar, G.R., 2015. “Seepage and Stability Analysis of Earthdam Using Finite Element Method”, Aquatic Procedia, Vol. 4, pp. 876-883.

Bowles, J.E., 1996. Foundation Analysis and Design. 5th edition, Mc Graham Hill.

Streigler, W., Werner, D., 1969. “Dammbau in Theorie und Praxis”, Springer, Vienna-New York, pp. 462 .

Brinkgreve, R.B.J., Kumarswamy, S., Swolfs, W.M., 2017. “Plaxis Essential for Geotechnical Professionals”.

Çalamak, M., Selamoğlu, M., Yanmaz, A.M., 2015. “Toprak Dolgu Barajlarda Hazne Seviyesindeki Ani Düşmenin Şev Stabilitesine Etkilerinin Değerlendirilmesi”, 4. Su Yapıları Sempozyumu, pp. 278-287.

Fattah, M.Y., Omran, H.A., Hassan, M.A., 2015. “Behavior of an Earth Dam During Rapid Drawdown of Water Reservoir-Case Study”, International Journal of Advanced Research, Vol. 3(10), pp. 110- 122.

İlter, G., Yılmaz, Y., 2016. "Toprak Dolgu Bir Baraj Altındaki Olası Zayıf Lokal Bir Bölgenin Barajın Oturma-Gerilme Davranışına Etkisi".

Khalilzad, M., Gabr, M.A., Hynes, M.E., 2015. "Deformation-Based Limit State Analysis of Embankment Dams Including Geometry and Water Level Effects", International Journal of Geomechanics, Vol. 15(5):04014086.

Özçoban, Ş., Berilgen, M.M., Kılıç, H., Edil, T.B., Özaydın, İ.K., 2007. "Staged Construction and Settlement of a Dam Founded on Soft Clay", Journal of Geotechnical and Geoenvironmental Engineering, doi: 10.1061/(ASCE)1090-0241(2007)133:8(1003).

Selvi, M., 2012. "Dolgu Barajlar Tasarım Rehberi", 1. Barajlar Kongresi.

Stark, T.D., Duncan, J.M., 1991. "Mechanisms of Strength Loss in Stiff Clays", Journal of Geotechnical Engineering, doi: 10.1061/(AASCE)0733-9410(1991)117:1(139), 139-154.

5th International Symposium on Dam Safety

October 27-31, 2018

DAM AND PUBLIC SAFETY DURING OPERATION PERIOD

Ali Rıza ÖÇ

ABSTRACT

In this article summary of international approach and explanation on the recommendations of ICOLD on Dam safety and Public safety shall be made.

In order to explain the approach, the possible hazards generally mentioned in the ICOLD bulletins as well as failure mechanisms and possible response of the dams against above mentioned hazards and failure mechanisms are explained.

Risk criteria as recommended by ICOLD are explained in the text as well. What should be made against the dam failure and the public safety against the adverse results of the dam failure has been tried to be explained through cascade dams which are still operational in the Middle Asia Country.

After the explanation to the safety criteria and Risk Factors, the extreme critical conditions are considered and precautions as well as organizations to eliminate the adverse results of those conditions or to mitigate them are recommended.

Keywords: Public, Dam, Safety, ICOLD, Criteria.

INTRODUCTION

Dams generally are constructed to withstand the water accumulated in the reservoir while it is under;

- Dead load of the structures
- Hydraulic load from the water accumulated in the reservoir
- Seismic load

Based on the importance of the structures with respect to loses expected to be happened after the failure of the structures (Dams) the international critical conditions are defined and the current conditions of the dams are compared with them to define the safety levels of the structures.

Beside of the design conditions of the dams, the external factors that may affect the safety conditions are also observed and investigated in order to define under which conditions they may be agent to threaten the safety of the structures.

The defined safety conditions with respect to the importance of the structures must be fulfilled during the whole life of the structures. In order to check the current safety levels of the structures (Dams), dam instrumentation system must also be followed up and periodically must be reported.

In addition to the interpretation of dam instrumentation, observation as well as necessary investigation if required must be made on the structures and foundations and evaluations based on their results must be compared with the criteria specified for the safety of the structures.

In this text, information about international criteria for the safety of the Dams and Public safety shall be given first, and later the study on the structures which are still operational shall be explained.

INTERNATIONAL CRITERIA FOR SAFETY OF DAMS & PUBLIC SAFETY

Prior to start explaining the criteria recommended by ICOLD, the possible hazards which will affect the safety of the Dams given in the ICOLD are listed below:

- . Storm
- . Earthquake
- . Design Flood Exceeded
- . Improper operations
- . Sabotage
- . Inadequate design Control
- . Inadequate Hydraulic Assessment
- . Inadequate Site Investigations
- . Chemical attack
- . Prolonged dry weather
- . Outlet Gate Failure
- . Inadequate wave wall
- . Flood
- . Reservoir Land Slide
- . Design Earthquake Exceeded
- . Incorrect Parameters Assumed
- . Vandalism
- . Inadequate Construction Control
- . Burrowing Annimals
- . Debris Inflow
- . Tree and Plant Growth
- . Changed Design Criteria
- . Lightening Strike
- . Inadequate Rip Rap
- . Upstream Dam Failure
- . Power Supply Failure
- . Operator Error
- . Rapid Draw Down
- . Incompetent Inspection
- . Construction Delays
- . Deterioration and Aging
- . Tree removal
- . Missile Impact
- . Calcification

Possible failure mechanisms which are caused by the effect (or effects) of one or more above hazards are listed below:

- . Overtopping
- . Hydrofracturing
- . Earth slippage
- . Cracking
- . Gate inoperable
- . Pore pressure rise
- . Rise in pool level
- . Drain blockage
- . Piping
- . Differential settlement
- . Sink holes
- . Undermining
- . Uplift
- . Excessive wave action
- . Spillway blockage
- . Cavitation
- . Gates jamming
- . Dry tensile cracks
- . Loss of cohesion
- . Excessive seepage

The dam will respond with one or more of below, to the possible above failure mechanisms;

- . Breach
- . Sliding failure
- . Foundation failure
- . Structural failure
- . Progressive erosion
- . Overturning failure
- . Liquefaction
- . Slope failure
- . Floatation
- . Dynamic Failure

Based on the design, observations and monitoring, the dam behavior can be assessed. As conclusion of this, possible critical Hazards that will cause one or more failure mechanisms listed above can be defined. Then, by comparing with the safety criteria, the level of safety of the structures can be decided.

At this stage of the study, the potential risks associated with the dams which are consisting of structural components and socio-economic components as explained in ICOLD bulletin 72, shall be mentioned.

Since potential downstream consequences are mostly proportional to the storage capacity and height of the Dam, the structural components of potential risk depend mostly on them.

Socio-economic risks can be expressed by a number of persons who need to be evacuated in case of danger and potential downstream damage.

It is possible to rate the potential risk by weighting with respect to the mentioned components, associating a larger weighting factor to dams with larger storages, posing larger evacuation requirements and entailing larger potential downstream damage. In this way a risk rating can be formulated and subdivided into different classes, ranging from low to extreme.

It is emphasized that the above mentioned weighting of risk components, and especially the socio economic risk components, are assessments based on judgement and reflect the impact of the socio-economic risk contribution to suit the prevailing circumstances. The foregoing considerations can be used as general guidance in this respect.

The tables-1 and 2 are showing the rate of risk associated with dams. Four risk factors are separately weighted as low, moderate, high and extreme. The table -1 is recommended to be used as general guidance.

Table - 1: Risk associated with dams

Risk factor	Extreme	High	Moderate	Low
Contribution to Risk (Weighting points)				
Reservoir Capacity (Hm3)	>120	120 - 1	1 - 0,1	< 0,1
weighting Points	6	4	2	0
Height (m)	>45	45 - 30	30 - 15	<15
weighting Points	6	4	2	0
Evacuation Requirements (Nos. Of Persons)	>1 000	1 000 - 100	100 - 1	none
weighting Points	12	8	4	0
Potential Downstream Damage	High	Moderate	Low	none
weighting Points	12	8	4	0
Total	36	24	12	0

Total risk factors of the dams can be calculated by summing the weighting points of each of the four risk factors to provide the Total Risk Factor as;

Total Risk Factor = Risk factor coming from the Reservoir Capacity
+ Risk factor coming from the Dam Height
+ Risk factor coming from Evacuation Requirements
+ Risk factor coming from Potential Downstream Damage

The Risk Class of a dam based on the Computed Total Risk Factor, can be found in table - 2.

Table – 2: Risk Class of the Dams

Total Risk Factor	Risk Class
(0-6)	I (Low)
(7-18)	II (Moerate)
(19-30)	III (High)
(31-36)	IV (Extreme)

In addition to the above, as it is defined in the ICOLD, in case of existing dam, other factors such as;

- the availability or lack of construction and maintenance records,
- processed instrumentation and surveillance records,
- the level of effort expended in previous safety evaluations, and
- new planned downstream development,

may affect the risk associated with a particular structure. Such other factors, however, cannot be easily quantified and should be considered case by case.

Many existing dams have been analyzed with relatively low accelerations, using pseudostatic analyses. Re-evaluation of the structural safety using dynamic analyses may be necessary if high PGA (say about 0,25 g) are found to apply to these locations. **This may specifically be the case if greater magnitude event occurs in the area than considered in the design.**

SAFETY CONDITION OF DAMS ALONG NARYN RIVER

Following the international safety criteria given above, the safety conditions of the cascade projects along the Naryn River will be explained. Prior to start, some information about the design characteristics of the Projects as well as our assignment which has already been completed, are given below.

Table 3 is showing the design characteristics of the projects along the Naryn River.

Table – 3: Design Characteristics of the Project along the Naryn River.

Designation	Unit	Toktogul	Kurpsai	Tash-Kumyr	Shamaldy-Say	Uch-Kurgan
Installed capacity	MW	4x300	4x200	3x150	3x80	4x45
Mean annual generation	10^6 kWh	4100	2630	1555	902	820
Full Supply Level	m a.s.l.	900	724	628	572	539.5
Dead Storage level (DSL)	m a.s.l.	837	721.6	627.2	569.9	538.5
Maximum Head	m	180	101	59.5	31	36
Rated Head	m	140	91.5	53	26	29
Minimum Head	m	110	90.5	40	23.8	18.5
Reservoir Surface Area	km^2	284.3	12.0	7.8	2.4	4.0
Total reservoir volume	10^6 m^3	19500	370	144	40,87	52,5 установленная 16,4 фактическая
Live storage volume	10^6 m^3	14,000	35	5.9	5.66	20.9 установленная 3,153 фактическая
Dam type		Concrete gravity	Concrete gravity	Concrete gravity	Rockfill	Concrete earth fill
Storage		Annual	Weekly	Weekly	Weekly	Daily
Rated unit discharge	m^3/sec	240	243	319	345	190
Total rated discharge	m^3/sec	960	972	957	1035	760
Total Spillway Capacity:	m^3/sec	3500	2537	3293	3090	3250
Bottom outlet Discharge	m^3/sec	2340	1037	2093	3090	2296
Spillway Discharge	m^3/sec	1160	1500	1200	-	954
Commissioning Dates Unit # 1		14.01.75	21.02.81	22.12.85	01.07.92	30.12.61
Unit # 2		27.11.75	19.12.81	30.08.86	12.02.94	03.06.62
Unit # 3		10.01.76	15.04.82	30.09.87	30.12.95	07.09.62
Unit # 4		10.01.76	04.11.82	-	-	05.11.62

In this cascade, the last one in the table-3, name of it is Uch Kurgan was the first project that the operation of the reservoir had been started on 30.12.1961.

The next project that had been completed after Uch Kurgan, was Toktogul which is the biggest project among the others. Reservoir capacity of Toktogul is about 19.5 billion m^3 and commissioning of the first unit was made on 14.01.1975. The other projects followed Toktogul and each other from upstream to downstream (see table-3).

At this occasion, I would like to give following information; the Uch Kurgan reservoir was subjected to all sedimentation brought by Naryn River during 14 years until construction of Toktogul Dam was completed and started impounding. As consequence of this, total reservoir capacity of Uch Kurgan was drop from quantity of 52,5 million m^3 to 16,4 million m^3 because of the sedimentation brought by Naryn River. As result of this sedimentation, three bottom outlet gates out of eight are blocked. Therefore, total discharge capacity of Uch Kurgan has decreased (Rehabilitation of Uch-Kurgan Dam is considered in a separate project Funded by ADB – Asian Development Bank).

As it is seen from table - 3 reservoir capacities of downstream four projects are much less than the reservoir of Toktogul Dam. As natural consequence of this all four projects at downstream are operated from the maximum operation level and are controlled from Toktogul.

All above information was taken into the consideration during the safety studies for all dams individually and for all cascades as integrated.

Below information is about the summary of assignment and activities made during the assignment.

The objective of the assignment was to conduct dam safety assessment that assessed the condition of the five dams on the Naryn cascade with necessary remedial measures identified.

Tasks for the assignment were including the followings:

- investigating the current condition and performance of the five dams, reservoirs and auxiliary facilities on the Naryn Cascade,
- carrying out the dam safety assessments for dams in Naryn Cascade
- determining the required scope of rehabilitation and improving the monitoring systems as well as the hydro-systems for safe and smooth operation,
- developing effective risk management strategies and emergency procedures for safety of the dams for ongoing operations.

In order to complete the assignment, below activities and studies were made;

Data Collection and Review of Documents collected:

- Hydrologic and Seismic data
- Design reports and drawings
- Monitoring reports
- Investigation reports
- Reports from External Experts
- International reports

Observations and measurements made during assignment

- Observations of the structures and their foundations
- Observations of hydro-mechanical and mechanical equipment.
- Observations of instrumentations
- Observations of reservoir rims
- Observations of underwater sections of the structures

Based on the documents and observations and measurements listed above, reports below were prepared.

Reports prepared during assignment

- Inception report
- Annual Inspection Reports
- Periodical Inspection Reports
- Final Report

- Quarterly Reports
- Underwater Investigation Report
- Technical Report for an existing Bridge in Uch Kurgan

To prepare the reports mentioned above, supporting reports below were prepared with updated data obtained during observations and measurements;

- Hydrological Report (Prepared for cascade)
- Stability Analyses for all dams
- Seismic Hazard Analyses (Prepared for cascade)
- Deformation Analyses for all dams
- Dynamic Analyses for all dams

Table-4 is showing the risk classes evaluated for the Dams in Naryn Cascade. This table has been prepared by utilizing the tables 1, 2 and 3. While preparing this table the information of high potential downstream damage of the Dams and high evacuation requirements were taken into the considerations.

Table-4: Risk Class Table of the Dams in Naryn Cascade

Dams	RC	Height	ER	PDD	Total Risk Grade	Risk Class
Toktogul	6	6	12	12	36	Extreme
Kurpsai	6	6	12	12	36	Extreme
Tashkumyr	6	6	12	12	36	Extreme
Shamaldy Sai	4	4	12	12	32	Extreme
Uch Kurgan	4	0	12	12	28	High
RC	Reservoir Capacity					
ER	Evacuation Requirement					
PDD	Potential Downstream Damage					

Based on the ICOLD Recommendations, the safety levels of the Dam/Dams with Risk Classes as stated in table-4 must be considered at the highest level as specified in the International Criteria.

Therefore, below statements must always be taken into the considerations when safety evaluations are reviewed:

- **Hydrological conditions** of the Structures must always be considered with respect to PMF (Probable Maximum Flood)

- **Structural conditions** must fulfil the international criteria with respect to the current Parameters of foundation and concrete and the current condition of uplift that is major factor affecting the stability.

- **The external factors** those may possibly affect the stability and / or operation of the structures temporarily or permanent.

Safety assessments include examination of the critical components of the dams that are accessible by obtaining the opinions of the Operator's engineers and site staff, and reviewing all available design reports, drawings, inspection reports and monitoring measurements. Results obtained from the monitoring instrumentation, where available, have also been taken into account in the safety analysis.

The design of the principal features of the dam has been reviewed and findings are compared with the design criteria in order to compare with the current international practice for both static and seismic loading conditions.

The studies have also covered the capacity calculations of spillways and bottom outlets in order to state the level of safeties with respect to the critical floods estimated; based on these evaluations, recommendations were made for rehabilitation works to enhance the long-term safety and performances of the dams.

The methodology to complete detailed investigation and analysis of the structural conditions of Dams and to prepare recommendations for remedial works that may be required to rehabilitate the structures has been prepared. This methodology includes also guideline; first for assessing the current conditions of the dams on the Naryn Cascade System including appurtenant structures and the second is to define a way to improve the safety of the hydro-system by performing detailed and scrutinized investigations, by analysing their stabilities, evaluating the structural integrity and safety conditions.

This period of the assignment also covers determining the required scope of rehabilitation and remedial works that may be required for enhancing the safety and improving the smooth operation of the cascade, developing effective risk management strategies and emergency procedures for ongoing dam safety and operations.

In this text the method for the assessment of safety and safety level of the Toktogul Dam shall be explained. When it is said 'safety' malfunctioning of the system will also be considered.

Malfunctioning of the system as well as the failure of the Dam have been considered to be occurred due to the failure of one or more sub-systems and / or due to hazards which are listed below:

- Foundation and abutment
- Discharge Units (Bottom Outlet & Surface Spillway)
- Turbines
- Behaviour of the Dam Body
- Uplift
- Excess seepage
- Hydrology
- Overtopping
- Earthquake
- Falling dawn rock masses on the structures

These hazards and sub-systems had been studied in the reports mentioned above. Following to the studies, the critical conditions with respect to the safety of the structures had been defined. Then, the necessary improvements had also been defined to enhance the safety of the structure. In addition to these, the financial conditions of the improvements to enhance the safety of the structures had also roughly been estimated.

At this stage of the text, some interesting conclusions related with the safety conditions mentioned above will be given below:

Hydrological conditions of the Structures (recommendations are given only for PMF - Probable Maximum Flood here)

As it was studied in the reports received during the assignment there were temporary constraints on the discharge capacities of spillway and bottom outlet specified by the Management of Joint Stock Company based on the report prepared by Kyrgyz Slavic University in Kyrgyzstan.

Due to the temporary limitations on discharging capacities of Bottom Outlet and Spillway, in order to prevent overtopping possibilities over the Dam Crest the freeboard arrangements were considered necessary with respect to the international criteria for the risk evaluation against floods prior to entering to the flood seasons.

For the Toktogul Reservoir this arrangement were made for two conditions:

1) Short term arrangement of freeboard that is before discharging capacities of Spillway and Bottom outlet are reinstated (based on existing condition).

2) Long term arrangement that is after the discharge capacities of Spillway as well as Bottom Outlet are reinstated (including the rehabilitations and also reinstated the discharge capacities of the Dams at the downstream of Toktogul).

Conditions for floods evaluated based on the updated hydrological data were studied in the reports and the most critical conditions when the structure is subjected to the PMF (Probable Maximum Flood) are mentioned here.

The graphs in Figure 1 are showing the variation of lake level with respect to the inflow representing the PMF (Probable Maximum Flood) and discharges from turbines and Bottom Outlet and Spillway. Under the conditions in the figure lake is reaching to maximum 904,35 m a.s.l. which is slightly lower than the crest. The initial lake level when entering to the flood season is considered as 885 m a.s.l.

Figure 1. Reservoir elevation with respect to inflow PMF and the existing discharge capacities. Initial lake level is about 885 m a.s.l.

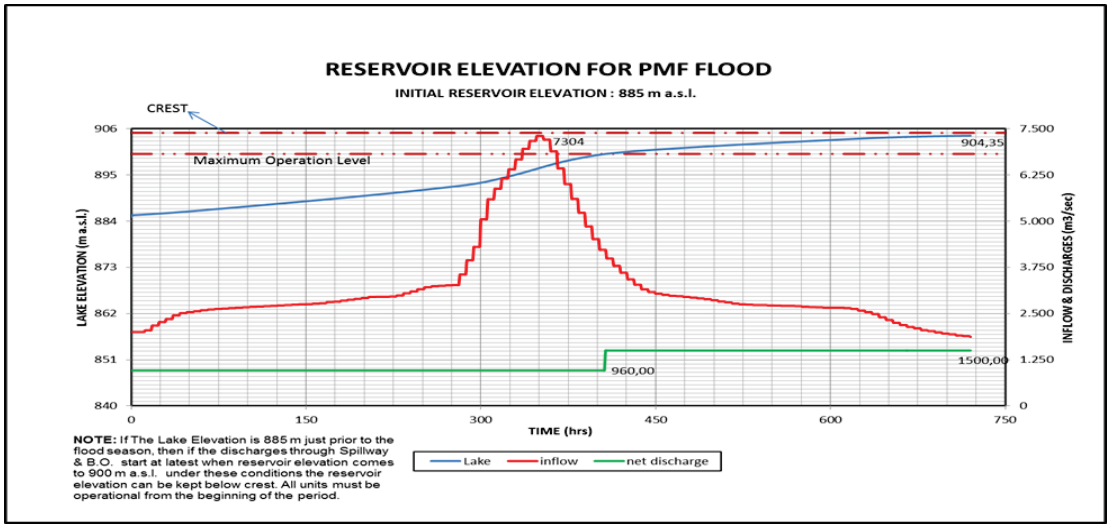

The graphs in Figure 2 are showing the variation of lake level with respect to the inflow which is representing PMF (Probable Maximum Flood) and discharges from the turbines and Bottom Outlet and Spillway for Long term condition. Long term condition stands for the discharge conditions of all dams in the cascade after they are rehabilitated to their original discharging capacities.

Figure 2. Total discharges from Toktogul for safe operation of Kurpsai is 3 023 m3/sec

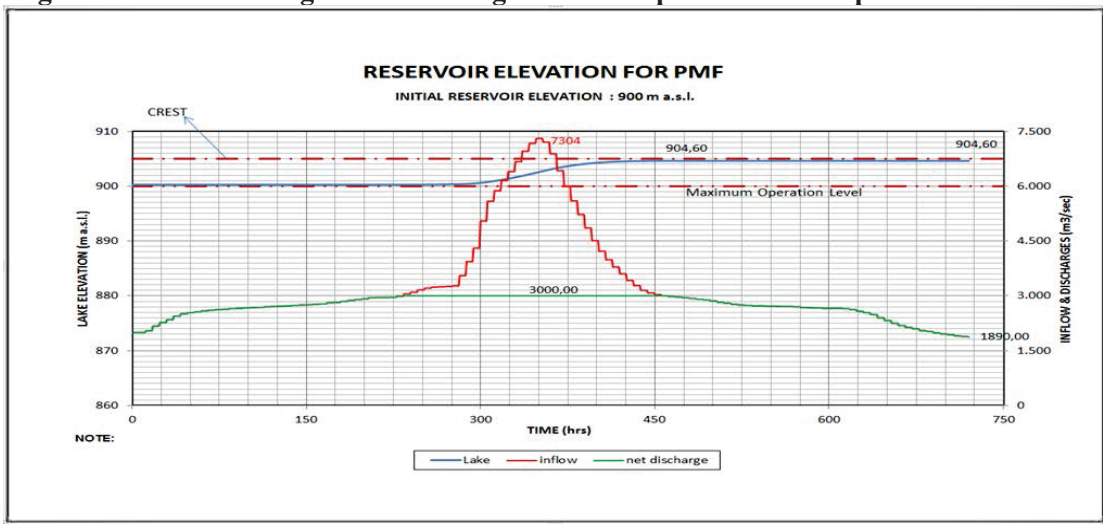

Even the lake level is at maximum crest elevation of Toktogul Dam, the Toktogul Dam itself as well as all dams in the cascade are safe when it is subjected to PMF if it is operated as in the figure 2.

Structural conditions (must fulfil the international criteria with respect to the current Parameters of foundation and concrete and the current condition of uplift that is major factor affecting the stability)

Structural conditions based on the updated and evaluated foundation and concrete properties had been checked and found safe when they are compared with the international criteria. Prior to making analysis the field observation on the foundation rock as well as on the concrete had been made. Additionally current concrete strength were tried to be measured by destructive and non-destructive field tests.

At this section of the text, although the dam body is safe in all structural conditions (dynamic analysis had also been made), below graphs are considered interesting which are showing the horizontal deflections of the dam body measured with pendulums in flow directions.

The deflections on the sections were very small and measured when the reservoir elevation was close to minimum and close to maximum. When reservoir elevation was close to maximum the deflection of the crest measured by pendulum was towards downstream and when close to minimum lake level the relative deflection turns towards upstream. This oscillation of the deflections had been continued from the beginning in this way. This behaviour is also confirmed by the geodetic measurements and also by static calculations. Those deflections had been measured with respect to the point fixed in the foundation rock. In this occasion, I would like to congratulate the Operators team of Toktogul, who are following up the monitoring and observations of the dam and appurtenant structures in a very sensitive way from the beginning.

Figure 3. Deflection of crest when reservoir is close to minimum operation level

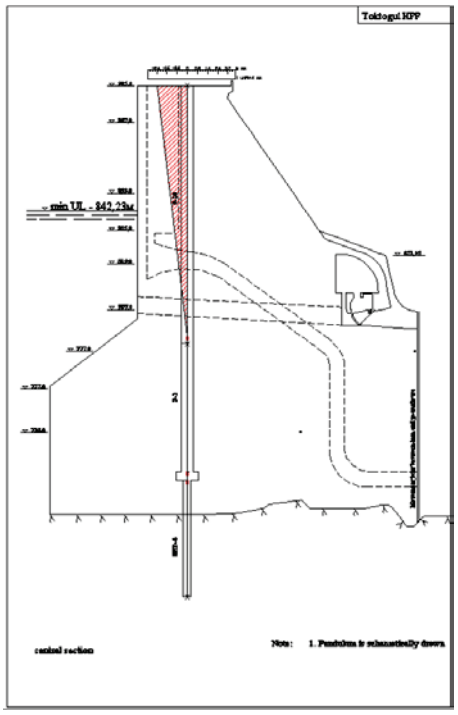

Figure 4. Deflection of crest when reservoir is close to maximum operation level

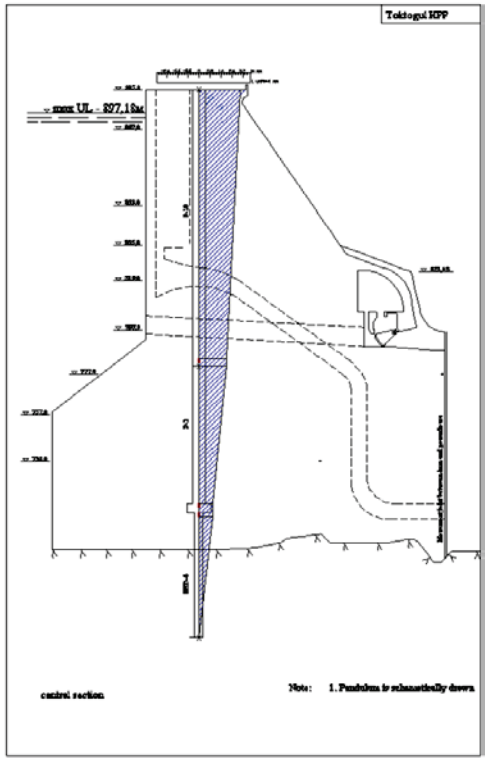

The external factors (those may possibly affect the stability and / or operation of the structures temporarily or permanent)

The factors affecting the structures externally have been studied and mainly below agents are found critical:

Overtopping Possibility due to landslide
Observation results for potential landslides have been studied and included in safety reports. Below information are taken from those reports.

- Large scale debris flows on Right bank-Tamgaterek Mountain Slope (see picture 1)
- Active landslide on left bank –Sarykamish Site (see picture 2)

Since the Toktogul dam is located in seismically active region and close to the Talas-Fergana fault which is the longest active fault of Kyrgyzstan, below recommendations were made in the report.

Tamgaterek debris flow and Sarykamısh landslide, which are identified in the reservoir, are close to each other. Large earthquakes may probably trigger these two landslides synchronously and they both can slide suddenly into the reservoir as large masses. These two potential landslides are at a distance of 7-10 km to the dam axis. It is possible that sudden mass fall into the reservoir will create waves. Waves created by this way may have a risk of overflow above the dam crest.

In order to assess the overflow risk, a serial geological-geotechnical investigation of mentioned landslides should be conducted and the risk assessment should be performed based on the results of the investigation and reservoir geometry.

Picture 1: Debris Channels on southern slope of Mount Tamgaterek

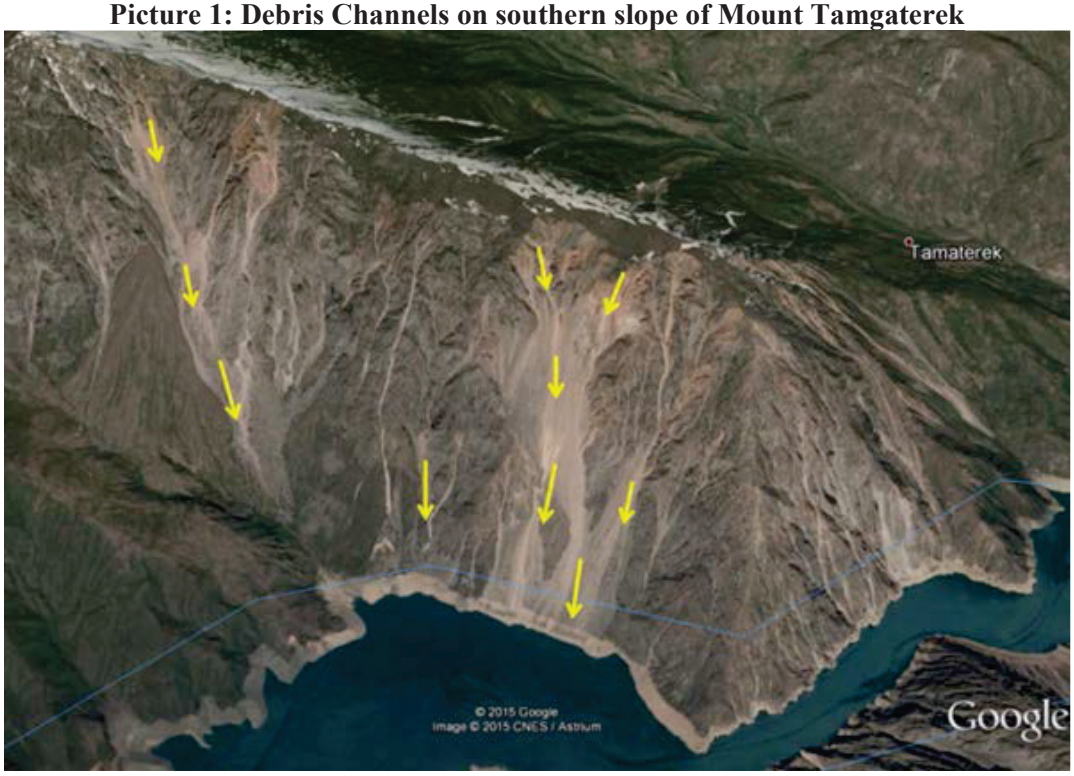

Picture 2: Sarykamısh Landslide

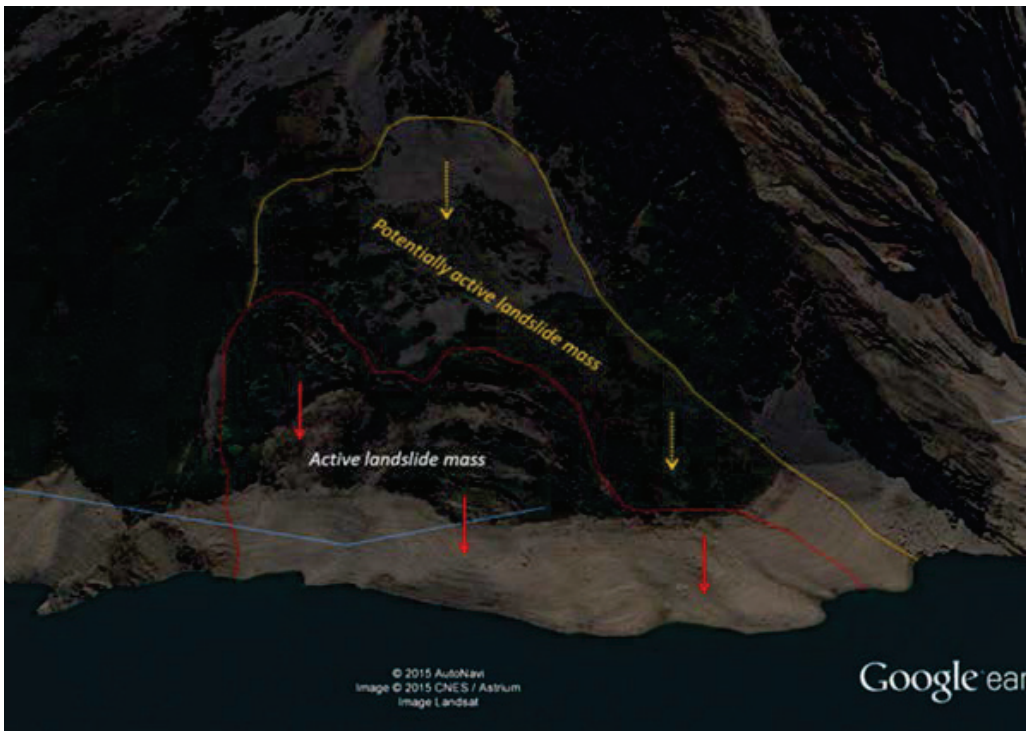

For the risk assessment of the overflow possibility above the crest, geological as well as geotechnical studies are recommended to be conducted to find out:

- Maximum mass that can possibly be triggered by earthquake
- Analysing possible generated wave/waves due to the mass which suddenly fall into the reservoir
- When this wave is generated what can be the critical lake elevation that overtopping from the crest of the dam can occur
- What can be the effects and results of such waves to the dam.

Falling Down Rock Masses on the Structure

Measurements as well as criteria for instability of the rock masses have been studied and comments made in the reports.

Since the removing possibility of the rock seems difficult, we have made below recommendation to increase the stability of the rock mass.

This proposal has already been applied in some projects in Turkey and the method schematically been shown on instable Rock mass in the Toktogul Right Bank in picture 3.

Picture 3. Proposal to increase the stability of the Rock mass.

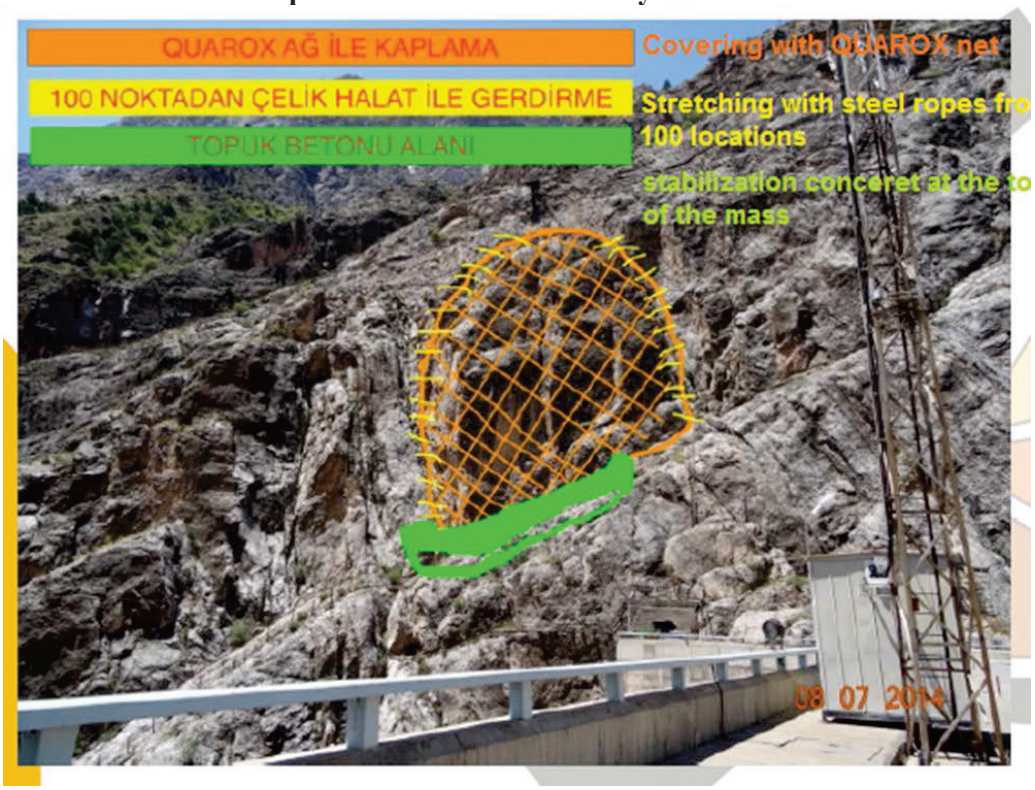

Further to the above, a scenario on the failure of Toktogul Dam was considered in order to see the effects of the failure of Dam to the Downstream of the Toktogul.

At the end of the assignment, an Emergency Action Plan (EAP) was strongly recommended to be prepared with respect to the findings and a guide report with the minimum requirements as based on the international rule had been prepared and given to the Client.

As mentioned in the report, followings are recommended to be included in the EAP:

- The items which should be made available at each plant site (since it is cascade consisting 5 different projects)
- Team for the First responders and duty and structure of the Team
- Engineers who will follow up the Engineering inspections
- List of the Potential failure modes defined as result of the assignment
- List of inspection places and the structures with the priority order, obtained as result of the studies above.
- The responsibilities and the actions to be taken by the responders, Engineers etc. after the critical conditions are defined in the report.

After the inspections and studies above, one of the ‘emergency conditions’ given below may have to be considered. These conditions were studied in detail in the reports submitted to the Client:

EMERGENCY CONDITION

There may be three emergency conditions with respect to the condition of the dam after the earthquake shaking. These are;

1) Overflow

2) Impending failure

3) Failure

1) Overflow

After the earthquake, depending on the level of damages occurred on discharge structures and energy units, there may be possibility of overflow from the crest although the condition of the dam is stable.

This condition can be considered in three levels.

i) Discharging structures and energy units may be affected partially

In this case the current discharging rate must be compared with the inflow and depending on the differences followings have to be applied;

As long as inflow to the reservoir is less than the current discharge there will not be any problem. However, the discharging capacity must immediately be brought to the level earlier than event.

If current discharging quantity is less than the inflow, then the reservoir elevation must be controlled. Until the reserve capacity of the reservoir is completed, the discharge capacities must be increased. Otherwise overtopping will be unavoidable.

ii) All gates of discharging units are jammed

In this case (the condition that all gates of discharging units including turbines are jammed) necessary precautions depending on the flow over the dam to the downstream must be taken into the considerations for the downstream part of the dam and also for the downstream projects.

iii) Overflow due to landslide

The overflow due to the landslide occurred at the upstream reservoir of the Toktogul will most likely affect the downstream part of the Toktogul (This must be confirmed by the evaluations explained above).

2) Impending failure

If the inspections made following earthquake indicate a potentially imminent failure then, failure procedure as listed below must be applied;

- Decreasing the reservoir load by discharging water in the reservoir as much as possible (by decreasing water in the reservoir total failure of the dam can be prevented).
- Giving alarm to the settlement areas at the downstream which will be evacuated from the areas where possibly be underwater.
- Inundation plan attached to the inundation report will help to choose locations for collecting people with some goods that the people can take with them,

This failure and the actions to be taken must be announced to the people who will be affected. The responsibility for such warning varies between different countries. They can be dam owners, states etc. Therefore, the responsibilities should clearly be defined in official EAP.

3) Failure

In case of sudden failure happen or potentially imminent failure seems unavoidable, then the authorized team (mentioned in previous paragraph) must give alarm, especially to the downstream plants and the settlement areas for evacuation. As soon as this announcement is received all people must immediately be ready to move outside of the boundary where the higher than the inundation area.

REFERENCES

ICOLD Bulletin 72
ICOLD Bulletin 62a
REPORTS for the Safety of Dams in Naryn Cascade issued between years 2014 and 2016 by TEMELSU

- Inception report
- Annual Inspection Reports
- Periodical Inspection Reports
- Final Report
- Quarterly Reports
- Underwater Investigation Report
- Technical Report for an existing Bridge in Uch Kurgan
- Hydrological Report (Prepared for cascade)
- Stability Analyses for all dams
- Seismic Hazard Analyses (Prepared for cascade)
- Deformation Analyses for all dams
- Dynamic Analyses for all dams

5th International Symposium on Dam Safety

October 27-31, 2018

FAILURE MECHANISM OF EMBANKMENT DAMS AND QUALITATIVE RISK ASSESSMENT METHOD

Uğur Şafak ÇAVUŞ [1], Murat KİLİT[2]

ABSTRACT

Consequences of dam failures are usually severe and catastrophic since loss of lives and properties may occur and remedial measures are also quite costly. Therefore, correct design and proper construction of dam structures have vital importance. In addition, forecasting damage mechanisms, failure risks and their consequences of dam structures have vital importance. Failure risks of embankment dams are much more comparing to concrete dams. Embankment dams are constructed by using earth materials and usually located on river alluviums which are vulnerable against seepage, internal erosion, piping and liquefaction due to earthquake or heaving due to high seepage forces. Sometime, embankment dams are constructed on soft soils which undergo large settlements for long times and bearing capacity losses. This study first reviews and also classifies embankment dam failure mechanisms depending on types of embankment dams. In addition, the study provides a general qualitative risk assessment table developed for the engineers who deal with dam design and responsible for the evaluation of future safety and performance of the dam structures. This developed method is also applied on a dam case to assess its failure risks and consequences.

Keywords: Embankment dams, Classification, failure mechanisms, Qualitative Risk Assessment

INTRODUCTION

Dams are constructed for irrigation, energy production, supply domestic water and prevent flooding. Construction of dams and other related structures such as spillways, conduits or derivation tunnels as weel as power plants are costly and require big investment. In addition, any type of failure and damages are so costly and sometime heavy life and property losses may occur. Therefore, the proper and careful design and providing post construction safety are essential. Depending on the dam type, site geoleogy, material characteristics, failure risk of the dam structures varies from project to project. In general, failure risks of embankment dams are much more comparing to concrete dams. Since, embankment dams are constructed by earth materials and usually located on river alluviums instead of foundation rock. Thus, they are vulnerable seepage type failures, internal erosion, piping, heaving and soil liquefaction due to earthquake. In addition, embankment dams constructed on soft soils may undergo large settlements along long time periods and bearing capacity losses may also occur.

[1] Assistant Professor, Department of Civil Engineering, University of Applied Science, Isparta, Turkey
e-posta: ugurcavus@sdu.edu.tr

[2] Assistant Professor, Department of Civil Engineering, Afyon Kocatepe University, Afyonkarahisar, Turkey,
e-mail: : mkilit@aku.edu.tr

Failures may probably happen along operation life time of any dams. However, catastrophic failures mostly occur at high storage levels. The probability of failure is much lower when reservoir levels are much lesser than the normal water levels.

This study first classifies and reviews embankment dam failure mechanisms depending on types of embankment dams. In addition, the study provides a general qualitative risk assessment table.

POTENTIAL FAILURE MODES OF EMBANKMENT AND ROCKFILL DAMS

There are different failure modes of dams. For embankment dams, in general, the most common failure modes are slope sliding, subsiding, overtopping, internal erosion and piping, liquefaction of embankment and its foundation due to earthquake shaking, equipment malfunction and foundation bearing capacity failure and leakage related other types of failures such as sinkholes. However, for the gravity type of dams, the most common failures are sliding along the base of the dam, overturning, foundation bearing capacity failure, cracks due to overstressing. For embankment dams, if overtopping happens, erosion and/or sliding of the slopes of the dam body and its abutments may lead to partial or complete failure of the dam. Therefore adequate spillway discharge capacity, proper design of spillway structure dimension and freeboard allowance have vital importance in embankment dams. In addition, use of improper soil materials such as dispersive clays and poor seepage measures such as improper filter and drainage well constructions and improper compaction may cause internal erosion, hydraulic fracturing and piping in embankment dams and their foundations. Moreover, Performance of a dam may also be threatened by natural events and such as earthquake ground motion, excessive rainfall and floods, abutment slides abd rock falls. Furthermore, malfunction of bottom outlets and spillway gates may cause excess seepage forces and flooding (Badenhorst, 2005).

Possible failure modes of earthfill and rockfill dams may be categorized basically as those:

- Homogeneous clayfill earthfill dams located on either alluvium or rock foundations
- Bearing capacity failure of the foundation alluvium
- Lateral spreading
- Excessive settlement
- Overtopping of reservoir wave
- Hydraulic fracturing,
- Internal erosion and piping
- Heave occurrence at the downstream toe of the embankment
- Sinkhole occrences
- Slope sliding and
- Liquefaction of alluvium
- Cracks on the embankment material

- Zoned earthfill (sand fill or gravel fill) dams located on alluvium foundations
- Bearing capacity failure of the foundation alluvium
- Excessive settlement
- Overtopping of reservoir wave
- Liquefaction of alluvium and sandfill zones of the dam
- Slope sliding
- Heave occurrence at the downstream toe of the embankment
- Internal erosion and piping
- Lateral spreading
- Cracks on the embankment material

- Zoned earthfill (sand fill or gravel fill) dams located on rock foundations

- Settlement of embankment
- Overtopping of reservoir wave
- Liquefaction of sandfill zones of the dam
- Slope sliding
- Heave occurrence at the downstream toe of the embankment in pervious rocks
- Internal erosion and piping
- Cracks on the embankment material

- Zoned earthfill (sand fill or gravel fill) dams located on rock foundations
- Settlement of embankment
- Overtopping of reservoir wave
- Liquefaction of sandfill zones of the dam
- Slope sliding
- Heave occurrence at the downstream toe of the embankment in pervious rocks
- Internal erosion and piping
- Cracks on the embankment material

- Rockfill dams (usually located on rock foundations)
- Settlement of the dam
- Overtopping
- Slope sliding
- Heave occurrence at the downstream toe of the embankment in pervious rocks

In general, spillway structures should be designed for either catastrophic flooding or 10000 year of flooding if there is some population located on dam downstream. Cofferdams for large dams should be designed for 50 year of flooding or 25 year of flooding together with some freeboard allowance. Structural malfunctions such as concrete deterioration of bottom outlet, poor welding of steel outlet pipes, damages on the valves, damages on the spillway gates and their mechanical parts may also cause failures of dams.

QUALITATIVE RISK ASSESSMENT OF DAM STRUCTURES

In this section, Probabillity and Impact Matrix (Table 1) method is used to determine risk potential of dam structures. Basic risk factors affecting dam safety are determined as dam type, dam height, reservoir capacity, reservoir maximum water height, type of spillway structure and discharge capacity, hydrological and hydraulic data period, earthquake magnitude, duration and fault distance to the site, life loss risk and downstream property damage risk. A questionnaire was prepared to perform qualitative risk assesment and some questions were asked to the experts on the dam failure risks (Table 2).

In Table 2, there are 12 predetermined risk factors for dam failure probability rates and impact rates if failure occurs. Dam failure probability rates vary from 1 to 5 representing rare, unlikely, moderate, likely and very likely. Impact rates vary also from 1 to 5 representing trivial, minor, moderate, major and extreme.

Later, those numbers from 1 to 5 are then assigned to Impact and failure probability matrix such as for Trivial, 2 for Minor, 3 for moderate, 4 for Major and 5 for Extreme for the impact row. Numbers from 1 to 5 are also assigned for failure probablity column values such as 1 for Rare, 2 for Unlikely, 3 for Moderate, 4 for Likely and 5 for very Likely. Later, each corresponding cell Risk value in the Probablity and Impact matrix are found by multiplying failure and probability rates (Risk value= Probability x Impact) such as cell value is 6 (2x3) for the cell matcing failure probability of unlikely with the Moderate impact (Table 3).

As seen in table 3, minimum risk value is 1 and maximum risk value is 25. Therefore, risk groups are determined using Tables 1 and 3 together (Table 4). So, risk values from 1 to 3 in Table 4 represents low risk (see green area in Table 1), from 4 to 14 represents Moderate risk (yellow area in Table 1) and from 15 to 25 represents High risk (red area in Table 1).

Finally risks assigned by each expert for each subgroups in the questionnaire were added and then divided to the number of predetermined risk factors (12) in order to determine risk groups Risk value of each risk factor (depend upon experts' opinion) = {∑(Risk value assigned by each expert for each risk factor = Probability x Impact}/ (number of risk factors which is 12) to obtain final Qualitative risk assessment table for determining risk of dam structures (Table 5).

Table 1. Probability and Impact Matrix

		Impact				
		Trivial	Minor	Moderate	Major	Extreme
Probability	Rare	Low	Low	Low	Medium	Medium
	Unlikely	Low	Low	Medium	Medium	Medium
	Moderate	Low	Medium	Medium	Medium	High
	Likely	Medium	Medium	Medium	High	High
	Very likely	Medium	Medium	High	High	High

Table 2. Questionnaire for expert opinion to perform qualitative risk assessment

Dam Type	**Failure probability (risk)**					**Impact risk**				
Dam type	**Failure probability (risk)**					**Impact risk**				
I-Homogeneous	5	4	3	2	1	5	4	3	2	1
II-Zoned (sand and gravel fill) earthfill with clay core	5	4	3	2	1	5	4	3	2	1
III-Rockfill with clay core	5	4	3	2	1	5	4	3	2	1
IV-Concrete or Asphalt faced rockfill	5	4	3	2	1	5	4	3	2	1
V-Gravity dam or arched dam	5	4	3	2	1	5	4	3	2	1
Dam height	**Failure probability (risk)**					**Impact risk**				
>100m	5	4	3	2	1	5	4	3	2	1
100-50m	5	4	3	2	1	5	4	3	2	1
50-30m	5	4	3	2	1	5	4	3	2	1
30-15m	5	4	3	2	1	5	4	3	2	1
<15m	5	4	3	2	1	5	4	3	2	1
Foundation Type (rock/soil)	**Failure probability (risk)**					**Impact risk**				
I-Soft alluvium with silty sand, clayey sand, soft clay	5	4	3	2	1	5	4	3	2	1
II-Medium to stiff alluvium (sand, gravel, silt and clay)	5	4	3	2	1	5	4	3	2	1
III-Weak, weathered, heavily cracked impervious or pervious rock (RQD<50)	5	4	3	2	1	5	4	3	2	1
IV-Rock with medium strength, medium weathered, less cracked impervious or pervious rock (RQD 50-75)	5	4	3	2	1	5	4	3	2	1
V-Strong impervious or pervious rock with high compressive strength kayaç (RQD≥75)	5	4	3	2	1	5	4	3	2	1

Table 2. Questionnaire for expert opinion to perform qualitative risk assessment (continue)

Reservoir capacity	**Failure probability (risk)**					**Impact risk**				
>1x10^{9}m^3	5	4	3	2	1	5	4	3	2	1
1x106m3-1x109m3	5	4	3	2	1	5	4	3	2	1
5x105m3-1x106m3	5	4	3	2	1	5	4	3	2	1
1x105m3-5x105m^3	5	4	3	2	1	5	4	3	2	1
<1x10^{5}m^3	5	4	3	2	1	5	4	3	2	1
Reservoir water level	**Failure probability (risk)**					**Impact risk**				
Maximum storage	5	4	3	2	1	5	4	3	2	1
Normal storage level	5	4	3	2	1	5	4	3	2	1
Storage level between NSS and Mininimum water levels	5	4	3	2	1	5	4	3	2	1
Minimum Storage	5	4	3	2	1	5	4	3	2	1
Below minimum storage	5	4	3	2	1	5	4	3	2	1
Spillway type	**Failure probability (risk)**					**Impact risk**				
Controlled with gates >6	5	4	3	2	1	5	4	3	2	1
Controlled with gates between 6 and 4	5	4	3	2	1	5	4	3	2	1
Controlled with gates between 4 and 2	5	4	3	2	1	5	4	3	2	1
Controlled with gates <2	5	4	3	2	1	5	4	3	2	1
Kontrolsüz serbest akışlı	5	4	3	2	1	5	4	3	2	1
Hydraulic data up to date	**Failure probability (risk)**					**Impact risk**				
≥30 years	5	4	3	2	1	5	4	3	2	1
Between 15-30	5	4	3	2	1	5	4	3	2	1
Between 5-15	5	4	3	2	1	5	4	3	2	1
Between 1-5	5	4	3	2	1	5	4	3	2	1
Less than 1 year	5	4	3	2	1	5	4	3	2	1
Earthquake fault distance to dam site	**Failure probability (risk)**					**Impact risk**				
D < 25 km	5	4	3	2	1	5	4	3	2	1
D = 25 - 50 km	5	4	3	2	1	5	4	3	2	1
D = 50 - 100 km	5	4	3	2	1	5	4	3	2	1
D = 100- 200 km	5	4	3	2	1	5	4	3	2	1
D > 200 km	5	4	3	2	1	5	4	3	2	1
Maksimum probable earthquake acceleration	**Failure probability (risk)**					**Impact risk**				
amax > 0,4g	5	4	3	2	1	5	4	3	2	1
amax = 0,3g - 0,4g	5	4	3	2	1	5	4	3	2	1
amax = 0,2g - 0,3g	5	4	3	2	1	5	4	3	2	1
amax = 0,1g - 0,2g	5	4	3	2	1	5	4	3	2	1
amax < 0,1g	5	4	3	2	1	5	4	3	2	1
Earthquake moment magnitude and duration	**Failure probability (risk)**					**Impact risk**				
Mw > 7,5 ve/veya T = 20s	5	4	3	2	1	5	4	3	2	1
Mw = 7 – 7,5 ve/veya T = 15-20s	5	4	3	2	1	5	4	3	2	1
Mw = 6,0 - 7,0 ve/veya T = 10-15s	5	4	3	2	1	5	4	3	2	1
Mw= 5,0- 6,0 ve/veya T = 10-15s	5	4	3	2	1	5	4	3	2	1
Mw < 5,0 ve/veya T < 10s	5	4	3	2	1	5	4	3	2	1
Life loss risk	5		4		3	2		1		
Property damage risk	5		4		3	2		1		

Table 3. Assigned risk numbers (1 to 5) and calculated cell Risk values

P (↓) – I (→)	Trivial (1)	Minor (2)	Moderate (3)	Major(4)	Extreme(5)
Rare (1)	1	2	3	4	5
Unlikely (2)	2	4	6	8	10
Moderate (3)	3	6	9	12	15
Likely (4)	4	8	12	16	20
Very likely (5)	5	10	15	20	25

Table 4. Risk groups according to probability and Impact Matrix

Risk value	Risk group
(1-3)	**I-** Low (green)
(4-14)	**II-** Medium (yellow)
(15-25)	**III-** High (red)

.

Table 5. Qualitative risk assessment table

Risk Factor	Very High	High	Medium	Low	Very Low
Dam Type	I- **(17)**	II-**(14)**	III- **(10)**	IV- **(8)**	V-**(8)**
Dam height	> 100 m **(17)**	100-50 m **(12)**	50-30 m **(7)**	29-15 m**(4)**	< 15 m **(2)**
Foundation Type (rock/soil)	I- **(10)**	II- **(8)**	II- **(6)**	IV-**(4)**	V- **(2)**
Reservoir capacity	> $1x10^9m^3$**(15)**	$1x10^6m^3$ - $1x10^9m^3$ **(12)**	$1x10^6m^3$-$5x10^5m^3$ **(10)**	$1x10^5m^3$- $5x10^5m^3$ **(7)**	< $1x10^5m^3$**(4)**
Reservoil water level	Maxsimum **(18)**	NSS **(16)**	Between NSS and Minimum**(10)**	Minimum storage**(4)**	Below minimum **(1)**
Spillway type	Controlled gates adedi ≥ 6 **(11)**	Controlled gates: 4-6 **(10)**	Controlled gates:2-4 **(9)**	Controlled gates < 2 **(8)**	Uncontrolled free flow **(3)**
Hydraulic data up to date	>= 30 yıl **(1)**	15-30 yıldan az **(3)**	5-15 yıldan az **(5)**	1-5 yıldan az **(8)**	1 yıldan az **(12)**
Earthquake fault distance to dam site	D < 25 km **(17)**	D = 25 - 100 km **(12)**	D = 100-200km **(8)**	D = 200 - 500 km **(5)**	D > 500 km **(2)**
Maksimum probable earthquake acceleration	a_{max}> 0.4g **(17)**	a_{max} = 0.4g - 0.3g **(12)**	a_{max} =0.3g -0.2g **(8)**	a_{max} = 0.2g-0.1g **(5)**	a_{max}< 0.1g**(2)**
Earthquake moment magnitude and duration	Mw>7.5 ve/veya T > 20s **(17)**	M_w = 7-7.5 ve/ veya T = 15-20s **(12)**	M_w = 6.0-7.0 ve/ veya T = 10-15s **(8)**	M_w = 4.0-6.0 ve/ veya T = 10-15s **(5)**	Mw<4.0 ve/veya T <10s **(2)**
Life loss risk	Very high **(25)**	High **(16)**	Medium **(9)**	Low **(4)**	None **(1)**
Property damage risk	Very high **(25)**	High **(16)**	Medium **(9)**	Low **(4)**	None **(1)**

QUALITATIVE RISK ASSESSMENT OF CAY DAM

Cay dam is located on highly populated Cay province of Afyonkarahisar in Turkey Fig.5). It is 105. 5 meter heigh concrete face rockfill dam and very close to the active fault. Reservoir capacity is 16.5 million cubic meter. Foundation alluvium has 30 meter depth and foundation rock has RQD value less than 50. Spillway is uncontrolled structure. Maximum earthquake acceleration is 0.23g. Hydraulic data is 30 years old. Earthquake magnitude is 6.3. fault distance to the site is less than 25 km.

Fig. 1. Location of Cay dam

Given those parameters calculated risk values are:

For dam type	: 8
For dam height	: 17
For foundation type	: 6
For reservoir capacity:	: 12
For reservoir level	: 16
For spillway type	: 3
For hydraulic data year	: 1
For fault distance	: 17
For earthquake acceleration	: 8
Fort he magnitude of earthquake	: 8
Life loss risk	:25
Property damage risk	:25

Total risk value = 146 / 12 (number of risks) = 12.17

So, Cay dam risk is II which is medium.

CONCLUSION

This study first reviews and also classifies embankment dam failure mechanisms depending on types of embankment dams. In addition, the study provides a general qualitative risk assessment table developed for the engineers who deal with dam design and responsible for the evaluation of future safety and performance of the dam structures. This developed method is also applied on a dam case to assess its failure risks and consequences.

REFERENCES

Badenhorst, D., 2005. "The Design of Earthfill Dams", SANCOLD, a Presentation at the University of Stellenbosch.

Mattsson, H., Helström, J.G.I. and Lundström, T.S., 2008. "On Internal Erosion in Embankment Dams" Research Report, Lulea University of Technology,Department of Civil, Mining and Environmental Engineering, Division of Mining and Geotechnical Enginnering, ISSN:1402-1528.

US Army Corps of Engineers, 2003. "Identification of Visiual Dam Safety Deficiencies" TADS Workbook, ER 1110-2-1156.

5th International Symposium on Dam Safety

October 27-31, 2018

GUIDELINES ON THE STABILITY AND DESIGN OF GEOMEMBRANE FACED EMBANKMENT DAMS LOCATED ON PERVIOUS FOUNDATIONS

Uğur Şafak ÇAVUŞ [1] , Murat KİLİT [2] , İsmail Zorluer[3]

ABSTRACT

The number of constructions of geomembrane faced embankment dams with large reservoirs have been increased due to lack of availability of proper earth core materials in economical distances for some locations to provide impervious seepage barrier of the dam structures. However, if they are located on pervious rock or alluvium soils, some proper design measures have to be considered against any possible heave or seepage loss at the downstream toe of the dam due to high seepage forces in the foundation if geomembrane tears or damages. This study discusses some important risks and measures for the stability of the geomembrane faced embankment dams located especially on pervious rocks or soils. In addition, this study provides some guidelines for stability analyses of those dam structures as well as seepage measures if any failure or damage of the geomembrane occurs.

Keywords: Geomembranes, Embankment dams, Stability, Design, Guidelines

INTRODUCTION

Dam structures constructed for different purposes such as energy production, irrigation, flood protection and domestic water and store large amount of water. If any dam fails, heavy property damages and life losses may occur. Therefore, well planning, careful design and use of right construction methods are always important to prevent any type of failure and to provide structural, environmental and public safety as well.

The stability of embankment dams is affected by various factors. Strength of embankment and foundation soil or rock material characteristics, compaction degree of the embankment, filter and drainage system of the dam are main properties for the stability (Pak and Nabipour, 2017). Internal erosion and piping phenomena may also occur in embankment dams. If internal erosion or piping occurs, this may cause embankment slopes to slide and even a complete breach failure of the dam.

Failure due to piping occurs almost for 43% of embankment dams and is observed 54% for dams constructed after 1950. Almost 40% of those failures occurred in the embankment and foundation soil (Foster et al. 1998, 2000a, b). Piping and internal erosion risk is usually low for geomembrane faced embankment dams. However, if geomembrane tears for sand fill dams located on pervious foundation soils, then, high seepage forces may occur in the dam and its foundation. This situation may cause internal erosion or slope stability problems. It is, therefore, substantial to assess safety against seepage considering that geomembrane liners may damage and leaks may occur (Bhowmiki et al., 2017).

[1] Assistant Professor, Department of Civil Engineering, University of Applied Science, Isparta, Turkey
e-posta: ugurcavus@sdu.edu.tr

[2] Assistant Professor, Department of Civil Engineering, Afyon Kocatepe University, Afyonkarahisar, Turkey,
e-mail: : mkilit@aku.edu.tr

[3] Associated Professor, Department of Civil Engineering, Afyon Kocatepe University, Afyonkarahisar, Turkey,
e-mail: izorluer@aku.edu.tr

Geomembrane faced embankment dams are actually in limited number in the world and mostly constructed in recent years. High geomembrane faced rockfill dams with large reservoir capacities are also rarely constructed on the earth. There are 183 earthfill and rockfill dams with geomembranes in the world (Koerner and Wilkes, 2012). Most of those dams are located on low population density areas (ICOLD, 2010).

This study basically discusses some important risks and measures for the stability of the geomembrane faced embankment dams located on pervious rocks or soils. Study also provides a guideline for stability analyses and seepage measures of those dam structures.

GEOMEMBRANE BARRIERS FOR EMBANKMENT DAMS

Basically two different geomembrane use as water barriers are available. One is internal geomembrane diaphragm, the other is external seepage barrier (Fig. 1.) There is superiority of external geomembrane barriers over internal diaphragms: External membranes allow steeper embankment slopes than internal membranes since external membranes increase sliding safety factor of slide surfaces. Embankments with internal membrane are much more affected from earthquake since upstream side of the membrane will completely be saturated and shear strength of the embankment material is reduced. Connection of zigzag internal membrane to straight grouting line is difficult. However, external diaphragm allows easy gouting and construction. External diaphragms allow easy access for inspection and repair. On the contrast, inspection and emergency repair of internal diaphragms is not easily possible.

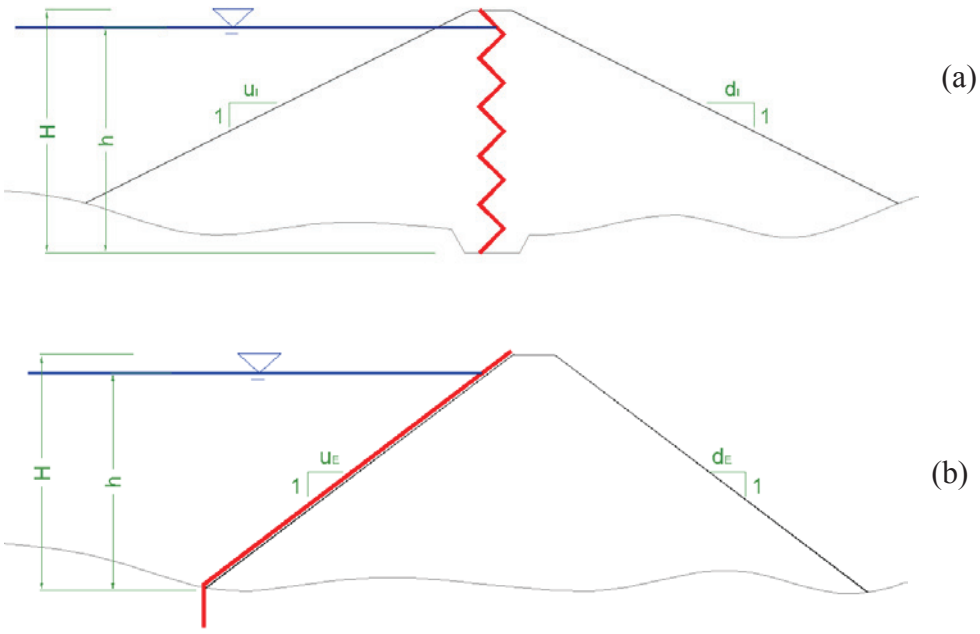

Fig. 1. Geomembrane water barrier types for embankment dan rockfill dams (a) Internal diaphragm (b) External diaphragm (DSİ and Coyne & Bellier, 2007)

EVALUATIONS AND GUIDELINES FOR STABILITY ANALYSES

For embankment dams with geomembrane liners piping is not usually an issue since an increase of pore water pressure within the embankment during or after construction is not possible due to use of pervious cohesionless embankment material (sand, gravel or rock) (if there is no hole or tear on the liner).

In terms of slope stability, the most critical case is not the end of construction or even full storage case (if geomembrane is not damaged). However, minimum storage case is the most critical case. Reservoir water pressure acting on the external upstream geomembrane liner results in an increase in normal soil pressure on sliding surfaces which also increases the shear strength of the failure surface. Therefore, low storage levels cause lower water pressure on sliding surfaces and results in lower sliding safety factors than those for full storage condition. Table 1 summarizes the critical loading and stability cases.

Table 1. Critical loading and stability check cases for embankment dams with geomembrane liners

Upstream Slope	Downstream Slope
Full storage case	Full storage case
Minimum storage case	Minimum storage case

In Turkey, there is a regulation of State Hydraulic Works for the minimum acceptable safety factors when static and pseudo static slope stability analysis is performed for all type of embankment dams (Table 2). This regulation should also be applied for the embankment dams with geomembrane liners.

Table 2. Minimum required safety factors for embankment dam slopes (Çavuş, 2015)

Upstream slope		Downstream slope	
End of construction		End of construction	
Without Earthquake (1.5)	With Earthquake (1.2)	Without Earthquake (1.5)	With Earthquake (1.2)
Sudden drawndown or min reservoir level		Full storage case	
Without Earthquake (1.0)	With Earthquake (1.0)	Without Earthquake (1.5)	With Earthquake (1.2)

Possible slopes to be chosen for the design are 3H/1V, 2.5H/1V or 2H/1V for the upstream slope and 2.5H/1V or 2H/1V for the downstream slope. Steeper upstream slope than the 2H/1V is not considered for sandy gravel earthfill material due to the risk of the segregation and construction difficulties of the geomembrane placement. For rockfill dams, the design slope of 2H:1 V for the upstream slope of rockfill embankments is too steep due to the low interface shear strength of HDPE geomembrane liner on the sandy soil overlain rockfill as bedding layer (Girard et al., 1990; Wu et al., 2008). As an example, Fig.2 and 3 provides a geomebrane faced embankment dam stability analyses result.

Geomembrane liners is possible to tear or damage. Thereby, in the stability analyses of the geomembrane lined embankment slopes, seepage pressure effects have to be taken into account in case of tearing of geomembrane liners. The most critical loading condition for upstream and downstream slope stability analyses of geomembrane faced rockfill dams is the occurrence of a rupture on the geomembrane at the maximum water level. Performing transient numerical seepage

analyses to see development of seepage path and seepage pressure variation within the embankment especially for pervious rock and soil conditions are important. Seepage paths, water pressures and amount of seepage at the downstream toe of the embankment depending on the geomembrane liner tear locations and tear dimensions have to be determined by numerical seepage analyses since embankment water pressures developed because of tears of the liners are used in the stability calculations of the dam slopes. In addition, calculated water pressures at the toe level of the embankment have to be used in heave risk calculations if foundation soil or rock is pervious in order to assess whether any seepage measure is needed.

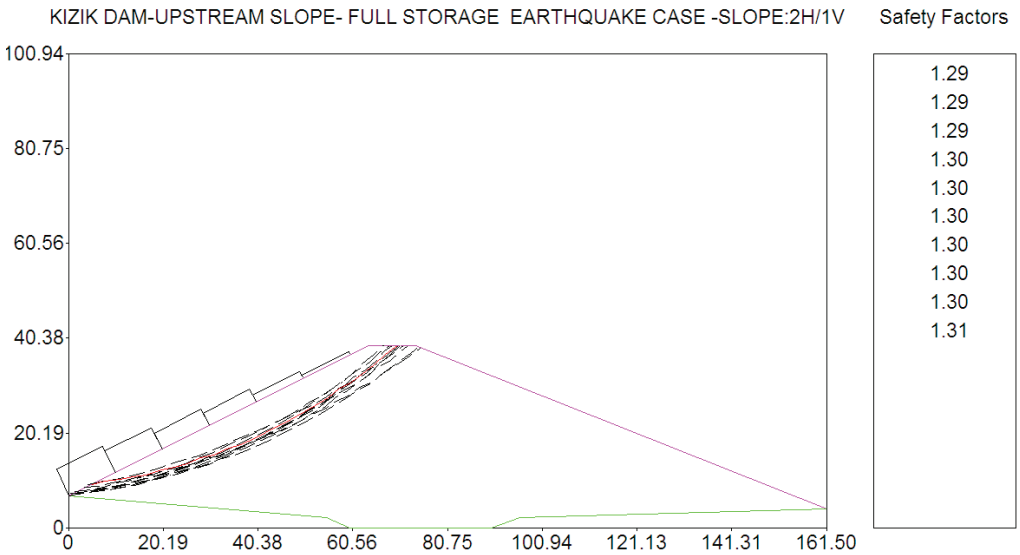

Fig.2. Minimum safety factors of 10 most critical sliding surfaces for the evaluation of upstream slope of Kızık dam (Full storage case with 0.2g earthquake coefficient) (Çavuş, 2015)

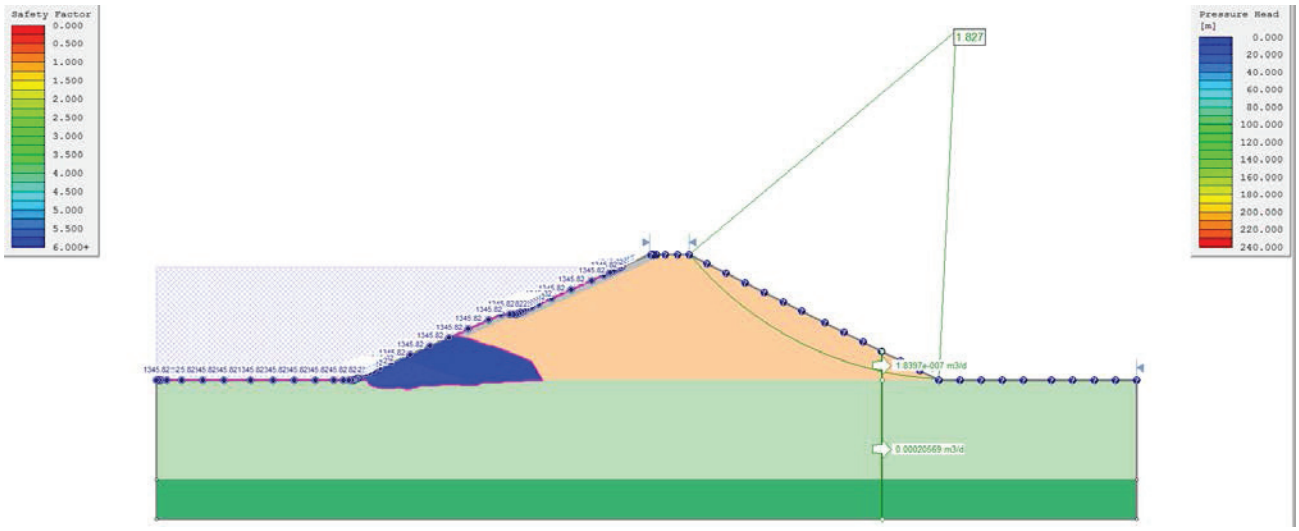

Fig. 3. Flow lines, pressure heads, seepage amount and safety factor of downstream slope in case of a geomembrane rupture at the upstream toe level of the dam when the reservoir is in its maximum level (First time step: Beginning of leakage)

CONCLUSION

✓ Running transient numerical seepage analyses is important to find the critical leak elevation for different bedrock or foundation soil permeability conditions.

✓ The highest seepage pressures occur on sliding surfaces and reduce the safety factors of slopes in case a rockfill dam having pervious bedrock or foundation soil conditions. It is also recommended that a downstream toe drain or a relief well be designed for this particular dam to prevent the risk of occurrence of heave at the dam toe or to eliminate any instability in the toe of the rockfill dam due to the generation of high foundation seepage pressures at the downstream toe of the dam.

✓ In case of any tear on the geomembrane liner, some seepage measures against any heave or instability such as internal erosion or piping have to be considered in the design stage of embankment dams with geomembrane liners for pervious rock and soil conditions.

REFERENCES

Pak, A., Nabipour, M., 2017. "Numerical Study of the Effects of Drainage Systems on Saturated/Unsaturated Seepage and Stability of Tailings Dams." Mine Water Environ DOI 10.1007/s10230-017-0468, Springer-Verlag GmbH Germany 2017.

Foster, M. A., Fell, R., and Spannagle, M. 2000. ''The statistics of embankment dam failures and accidents.'' Can. Geotech. J., 37~5, 1000–1024.

Foster, M. A., Fell, R., and Spannagle, M. 2000 ''A method for estimating the relative likelihood of failure of embankment dams by internal erosion and piping.'' Can. Geotech. J., 37~5, 1025–1061.

Bhowmik, R., Shahu, J.T., Datta, M. 2017. Failure analysis of a geomembrane lined reservoir embankment. Geotextiles and Geomembranes, vol. 46, p. 52–65.

Koerner, R. M. and Wilkes, J. A. (2012), 2010 ICOLD Bulletin on Geomembrane Sealing Systems for Dams, Geosynthetics, April 2001.

ICOLD, 2010. Geomembrane Sealing Systems for Dams - Design Principles and Return of Experience. International Commission on Large Dams, Bulletin 135, Paris, France.

DSİ and Coyne & Bellier, 2007. "Configuration of Kırca Rockfill Dam."

5th International Symposium on Dam Safety

October 27-31, 2018

TWO DIMENSIONAL DAM BREAK ANALYSIS OF BERDAN DAM WITH HEC-RAS 5.0.3

Çağla Irmak ÜNAL [1] and Zafer BOZKUŞ[2]

ABSTRACT

Dam break analysis of Berdan Dam was carried out in order to determine the potential risk areas of floodplain and to help preparation of emergency action plans. Flow hydrograph obtained from flood routing, digital elevation model created from bathymetric maps and Manning's roughness coefficient value calculated from land maps were integrated into Hec-RAS 2-D model. Breach formation geometry and dependent variables were decided. Breach parameters were specified for certain boundary conditions and an initial condition for unsteady flow. When all hydraulic and hydrological parameters were specified depending on variables and selected method of solution, flood inundation maps were obtained. As a result of the analysis, distributions of the maximum velocity profile and maximum water surface elevation of the flood were obtained from inundation maps on which flood areas near the dam body were identified as high-risk areas. These risk areas were visualized on digital elevation model with the help of RAS-Mapper in terms of water surface elevation, velocity and depth of the water in the terrain of the project.

Keywords: Dam break analysis, Hec-RAS, 2-D model, inundation mapping

2-D DAM BREAK MODEL

The study area is located in the sub-basin of the Berdan River which is in the East Mediterranean Basin and represents general features of this basin.

The Berdan Dam is located within the borders of Tarsus district. The water flowing from the Berdan Dam merges with river tributaries and then flows into the Mediterranean Sea from the Berdan River through the main channel.

Two-dimensional dam break analysis was found appropriate to perform since floodplain is expected to spread over a wide area which requires precision, accuracy, and visualization of simulations in the worst case flood scenarios, whereas one-dimensional model are sufficient to analyze floods of rivers and easy to implement. (Gharbi et al., 2016)

Dam Break Analysis Methods

Dam break analysis methods, which are related to regression relationship between the types of dam breaks and maximum possible flows that are produced due to dam breaks, were produced depending on the differences of main material of dam body. These methods are based on reservoir volume, depth of water, the geometry of breach formation and height of dam or joint evaluation of some of these parameters. (Bureau of Reclamation, 1988; MacDonald and Landridge-Monopolis, 1984; Costa, 1985; Wahl, 1998, 2004; Von Thun and Gillette, 1990; Froehlich, 1995a,b, 2008).

These parameters may vary from dam to dam or may vary at different times for the same dam. The most critical parameters of dam break are breach formation time and final bottom width of the breach.

[1] Çağla Irmak ÜNAL, Civil Engineering Department, Middle East Technical University, Ankara, Turkey, e-mail: irmak.unal@metu.edu.tr

[2] Prof. Dr. Zafer Bozkuş, Civil Engineering Department, Middle East Technical University, Ankara, Turkey, e-mail: bozkus@metu.edu.tr

Basic empirical formulations for these parameters represented in Table 1.

Table 1: Comparison of basic methods of the dam break

Formulation	Equation	Cases	Average Error of Estimation (log scale)	Uncertainty Interval (log scale)
Average Width of Final Breach (m)				
Bureau of Reclamation (1988)	$B_{avg}=3h_w$	70	−0.09	**±0.43**
MacDonald and Langridge-Monopolis (1984)	$B_{avg}=V_{er}/(h_b*W_{avg})$	58	−0.01	**±0.82**
Von Thun and Gillette (1990)	$B_{avg}=2.5h_w+C_b$	70	+0.09	**±0.35**
Froehlich (1995a)	$B_{avg}=0.1803K_oV^{0.32}h^{0.19}$	75	+0.01	**±0.39**
Breach Formation Time (hour)				
MacDonald and Langridge-Monopolis (1984)	$t_f=0.0179V^{0.364}$	35	−0.21	**±0.83**
Von Thun and Gillette (1990)	$t_f=0.015h_w$ highly erodible	34	−0.64	**±0.95**
	$t_f=0.020h_w+0.25$ erosion resistant			
Von Thun and Gillette (1990)	$t_f=B_{avg}/(4h_w+61)$ highly erodible	35	−0.38	**±0.84**
	$t_f=B_{avg}/(4h_w)$ erosion resistant			
Froehlich (1995a)	$t_f=0.00254(V_w)^{0.53}h^{-0.9}$	33	−0.22	**±0.64**
Bureau of Reclamation (1988)	$t_f=0.011(B_{avg})$	39	−0.40	**±1.02**

As it can be seen from the above table, MacDonald and Langridge-Monopolis and Froehlich methods can be preferred when the average bottom width of the final breach and breach formation time are considered.

However, Froehlich formulation yields more accurate and precise results. Furthermore, this formulation is commonly used for earth fill dams as in the dam break scenario of the Berdan Dam. In addition to previous case studies, Froehlich also examined 74 more earth fill dams in 2008.

Dam break analysis of the Berdan Dam were carried out on the basis of Froehlich formulation as earth fill dams which were analyzed with Froehlich formulation reflect the characteristics of the Berdan Dam better than the above-mentioned methods.

2-D Dam Break Model in Hec-RAS

Two-dimensional dam break analysis of the Berdan Dam was accomplished with the help of hydraulic modeling and dam break parameters in Hec-RAS.

Preparation of digital elevation model, flood hydrology studies and determination of Manning's roughness coefficient are crucial inputs to determine in dam break analysis.

Integration of Geometric Data with Hec-RAS Model

The map, which was obtained from field studies and compiled from 1/1000 scale maps, digitalized in ArcGIS environment and digital elevation model was created. Then, digital elevation model (DEM) was converted to triangulated irregular network (TIN) map with the help of the Hec-GeoRAS add-in in ArcGIS so that geometric information of terrain can be imported to Hec-RAS and can be converted to a grid system.

U.S. Army Corps of Engineers (2016) indicated that storage area, 2-D flow area and boundary condition lines should be defined on the TIN map in the geometric data editor. Therefore, these areas were created after TIN map was imported as geometrical data in Hec-RAS.

Elevation-area-volume graph of reservoir volume was used to define the storage area. Dam characteristics, Froehlich 2008 dam break model and piping failure data were entered in order to create breach model.

Triangulated irregular network and riverbeds on terrain can be seen from Figure 1.

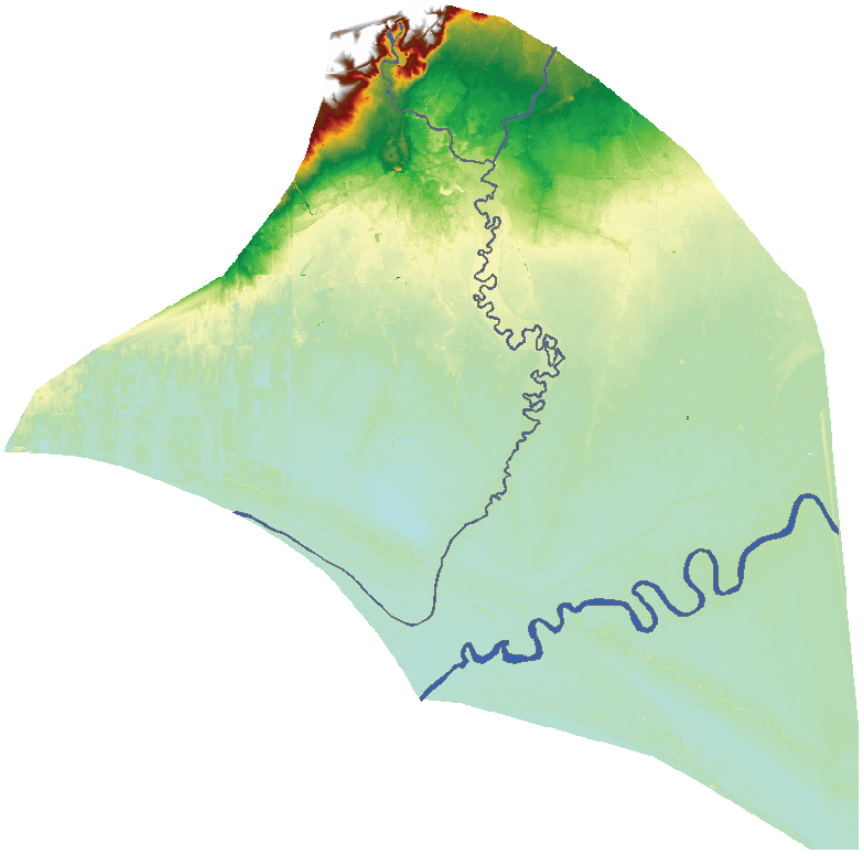

Figure 1: Triangulated irregular network (TIN) and riverbeds

Determination of Manning's Roughness Coefficient of Terrain
The roughness coefficient varies depending on such factors as grain size distribution of bed material, geometric properties of riverbeds and floodplain areas, the amount of vegetation cover and flow rate change.

2-D flow area was studied in six regions by taking into consideration these factors in Figure 2.

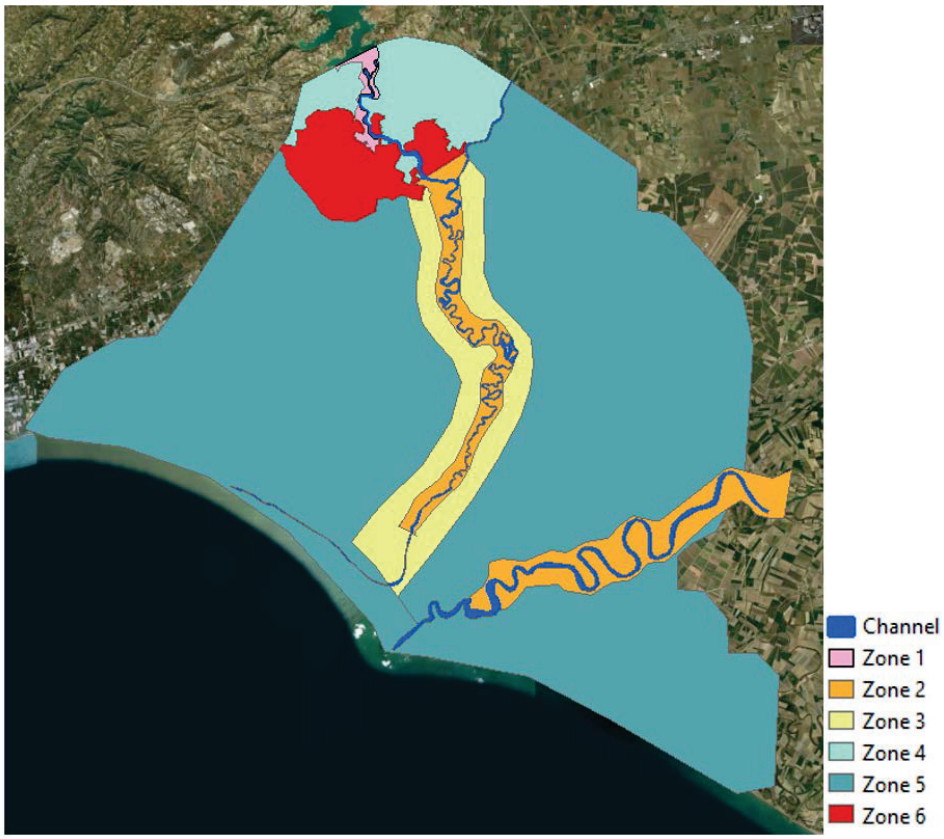

Figure 2: Zones for different Manning's roughness coefficient values

Cowan (1956) introduced a formulation (Equation 1) as;

$$n = (n_0 + n_1 + n_2 + n_3 + n_4) \times m \qquad (1)$$

where n_0 is roughness coefficient that depends on channel properties, n_1 coefficient includes effects of channel irregularity, n_2 coefficient covers the degree of change in shape and size of channel cross-section, n_3 coefficient contains the effects of existing barriers in the channel, n_4 correction factor covers vegetation cover and flow conditions and m is meander coefficient.

Cowan formulation was used with n values which were read by Cowan tables and U.S. Geological Survey tables which were evaluated by Costa (1985). Calculated n values were given in Table 2.

Table 2: Zones for different Manning's roughness coefficient values

Area	Description of Area	Manning's Roughness Coefficient
1	Inside levees (between Berdan Dam and highway D400)	0.045
2	Inside levees (between the Mediterranean Sea and highway D400)	0.052
3	Floodplain within levee vicinity	0.060
4	Outside levee vicinity (between Berdan Dam and highway D400)	0.041
5	Outside levee vicinity (between the Mediterranean Sea and highway D400)	0.040
6	Residential Area	0.010

However, evaluating the analysis for 0.06 as Manning's roughness coefficient value in 2-D flow area will be useful to be able to investigate more realistic values of hydraulic conditions which may occur in the river channel and flood inundation area during a catastrophic flood.

Calculation of Flow Rates of Berdan Dam

In dam break analyses, catastrophic discharges are required rather than flood frequency studies in order to display the worst case scenario. Catastrophic discharges were taken from planning reports which were obtained from DSİ 6. Regional Directorate and studies under the project of engineering services of "Determination of Flood Risk Areas of Mersin-Tarsus-Berdan River and Their Tributaries" carried out by Suiş Proje. Then, flood routing operations were accomplished in order to obtain outflow data for boundary condition between the storage area and two-dimensional flow area in Hec-RAS.

For flood routing, average inflow and outflow should be considered with the change in storage. Chow (1951) indicated that a change in storage can be considered with instantaneous rates of discharges which are produced between two reservoir routing period to enhance flood predictions.
Chow (1951) introduced simplified reservoir routing equation (Equation 2) as;

$$\frac{S_1}{T} - O_1 + I_1 + I_2 = \frac{S_2}{T} + O_2 \qquad (2)$$

where,
I_1, O_1 = Instantaneous inflow and outflow rates at the beginning of the first routing period, m^3/sec
I_2, O_2 = Instantaneous inflow and outflow rates at the end of the first period or at the beginning of the second period of routing, m^3/sec
S_1 = Storage at the beginning of the first routing period, m^3
S_2 = Storage at the end of the first period or at the beginning of the second period of routing, m^3
T = Time interval of routing period, hour

After reservoir routing operations were completed according to Equation 2, outflow hydrograph was used as a boundary condition that represents the dam body. Inflow and outflow hydrograph can be seen from Figure 3.

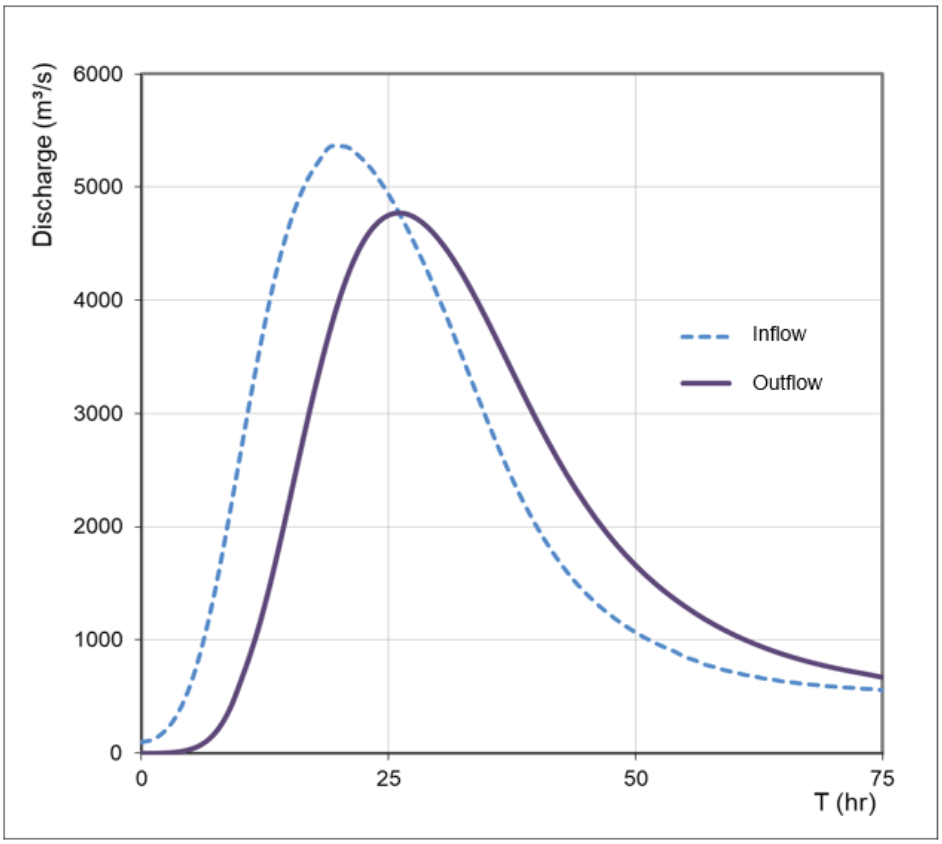

Figure 3: Inflow and outflow hydrographs

Xu & Zhang (2009) indicated that an empirical relation should be provided between breach formation geometry (such as average breach width, depth and top width of the breach) and variables of the reservoir (such as dam type, failure mode and dam erodiblity) in order to establish a nonlinear breach model.

Breach formulations should be used under unsteady flow analysis options in order to define the dam break phenomenon in a model in Hec-RAS. Dam body was determined as a boundary condition to introduce the outflow hydrograph of Berdan Reservoir so that boundary condition line can state a connection between the storage area and 2-D flow area. Thus, breaching of connection means breaching of the dam body in the dam break model.

A connection breach between the reservoir and 2-D flow area was introduced as shown in Figure 4.

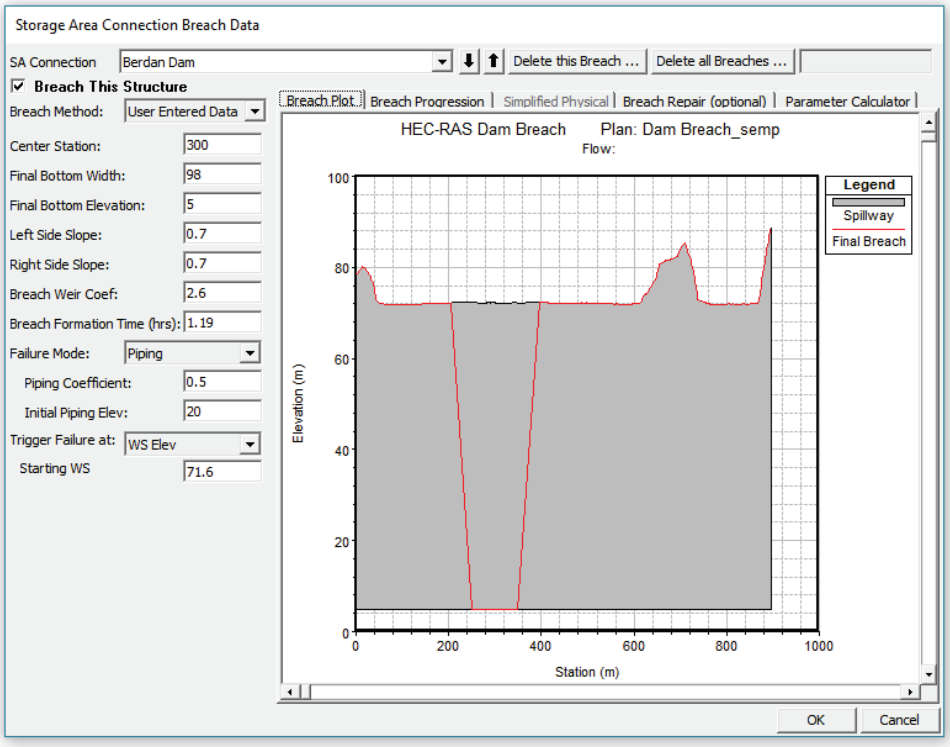

Figure 4: Storage area connection breach geometry

Connection breach data editor provides to determine the breach geometry and breach parameter calculation according to the selected breach formulation, i.e, Froehlich 2008 as shown in Figure 5.

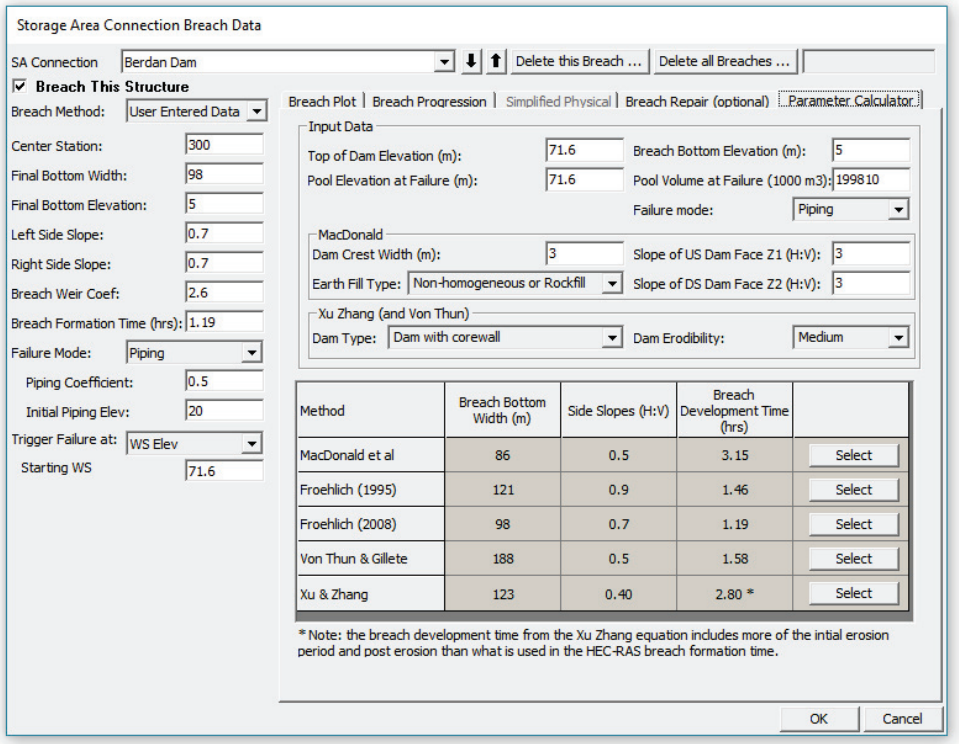

Figure 5: Calculation of connection breach parameter

Results of 2-D Dam Break Analysis in Hec-RAS

After all geometric, hydrologic and hydraulic inputs were entered in Hec-RAS, property tables were computed on 2-D flow area in RAS-Mapper to associate 2-D flow area to the terrain. Finally, the dam break analysis was carried out by using a hydrodynamic model in Hec-RAS. Results of the analysis can be viewed from output maps which were visualized on digital elevation model with the help of RAS-Mapper in terms of water surface elevation, velocity and depth of water and flood arrival time.

Tarsus settlement is located approximately 6 kilometers away from Berdan Dam. Hence, it is expected to reach the flood to the settlement center within half an hour according to the analysis. It is also expected that settlement area is affected by the maximum possible flood severely since it is close to the dam body.

The maximum velocity of water was found as 113 m/s in 200 meters away from the dam body. The maximum velocity values ranged from 1.5 m/s to 5 m/s in the settlement area which are beyond the tolerable limits when considering together with the maximum depth of water in the flow area. The average value of velocity was found as 1 m/s in the terrain which means that there will be less risk due to factors that are caused by velocity like drag, accumulation and erosion of materials in the floodplain. Figure 6 shows the distribution of maximum velocity values in terrain.

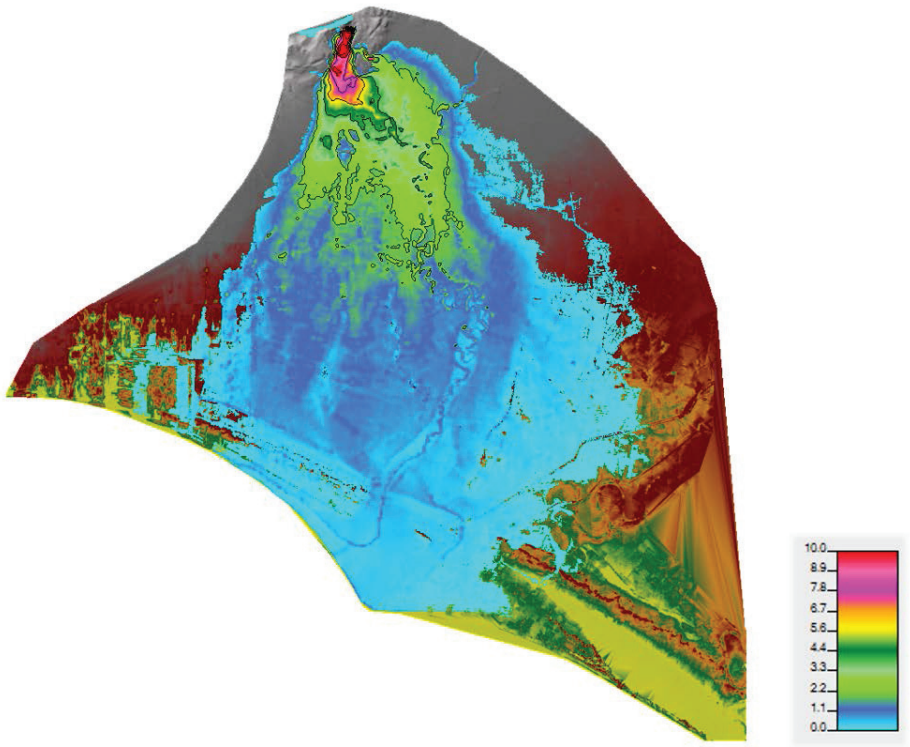

Figure 6: Distribution of maximum velocity of water

The maximum depth of water was observed as 33 meters at approximately 200 meters away from the dam body. The depth of water was found to be decreasing from upstream to downstream of flow area as expected, yet the water depth value remains over 2 meters on a very wide area in the terrain. Furthermore, prolonged exposure to high depths of water may lead to even worse damages during catastrophic floods.

The average depth of water values ranged from 2 to 6 meters in the settlement area as shown in Figure 7.

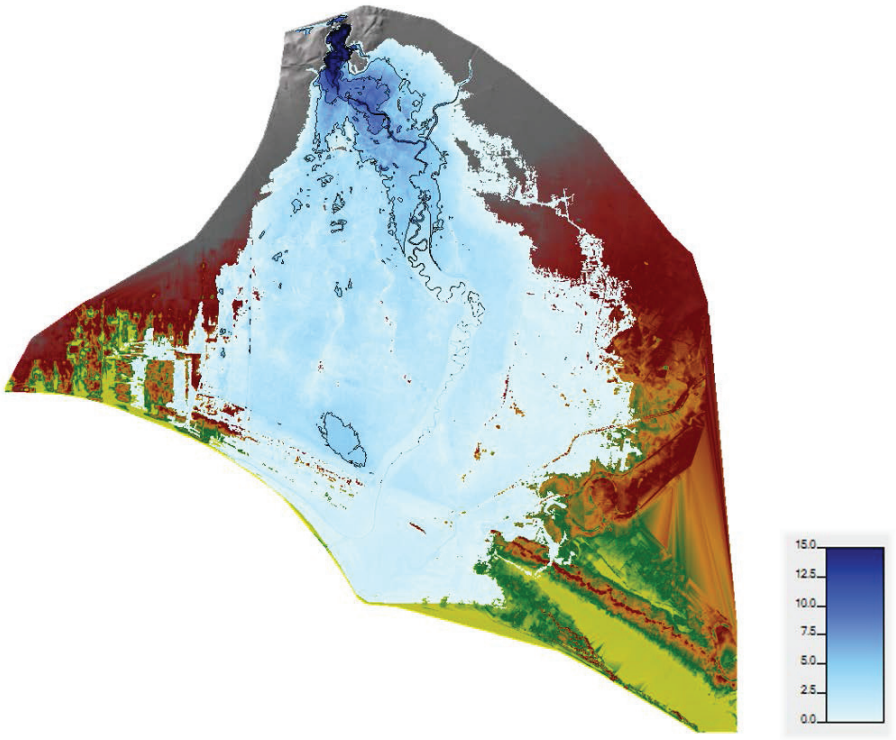

Figure 7: Distribution of maximum depth of water

The maximum water surface elevation was found as 71.6 meters at the dam body since it was the determined initial condition at reservoir volume. The average value of water surface elevation in the terrain was found as 8 meters. Water surface elevation values varied between 20 and 25 meters in Tarsus settlement as it can be seen from Figure 8.

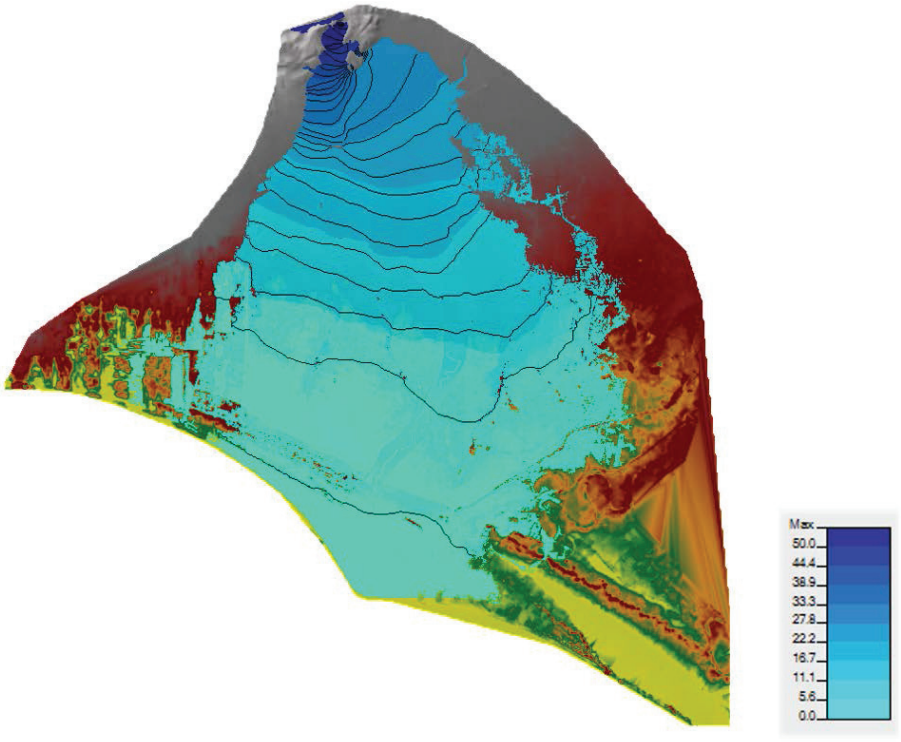

Figure 8: Distribution of maximum water surface elevation

In addition, distribution of maximum flood arrival time in terrain was displayed in Figure 9. It was determined that flood arrival time varied between 8 and 8.5 hours in Tarsus settlement.

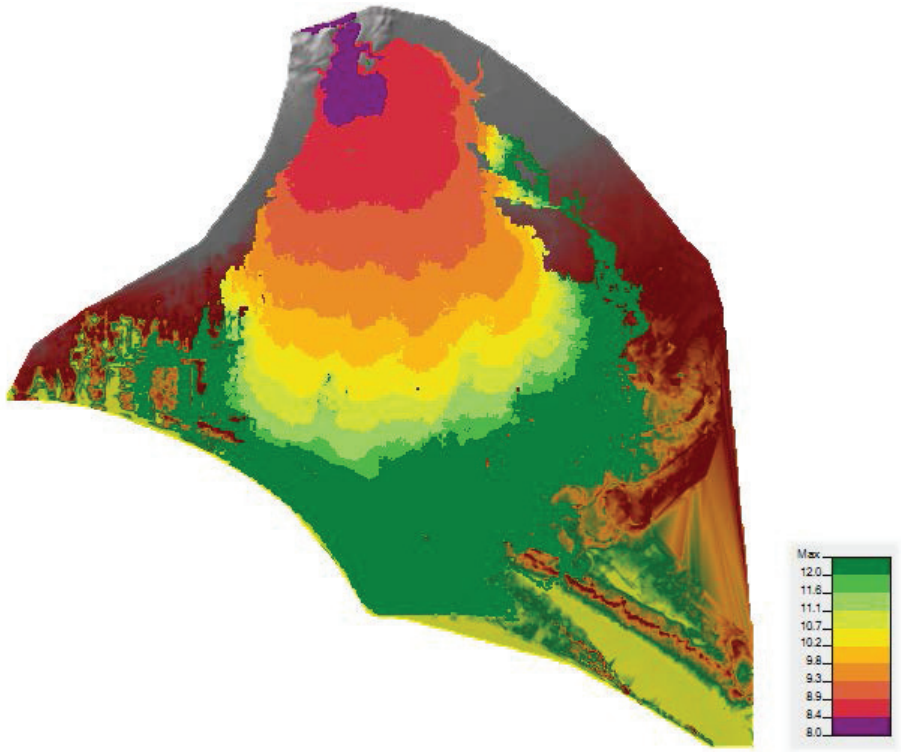

Figure 9: Distribution of flood arrival time

Discussion of Results

Froehlich (2008) formulation identified the breach formation time as 1.19 hours. Therefore, the breach formation time of Berdan Dam is 1.19 hours. Completion of the dam breach period was found as approximately 8 hours according to the map layers of results. In other words, the flood which is caused by dam break started to propagate at the 8th hour of the analysis.

However, it is crucial to determine the flood arrival time of the settlement area. After the dam breach occurred, the maximum flood reached the settlement center of Tarsus in between half an hour to forty minutes.

During the dam break analysis, dam body of Berdan Dam where two-dimensional flow area and reservoir volume were connected, the maximum velocity of water was found as 113 m/s, maximum depth of water and maximum water surface elevation were found as 33 meters and 71.6 meters, respectively.

Probable damages should be determined according to these values which are obtained from dam break analysis. When dam break analysis are evaluated by considering only the loss of human life, determination of population in settlement centers and preparation of evacuation plans for that population should be the first step in establishing emergency action plans.

All in all, Tarsus settlement, which is close to the Berdan Dam, has a high risk of inundation. Measures should be taken according to the flood arrival time, maximum depth and maximum velocity of water in terrain. With the preparation of emergency action plans by the authorities which are in charge of public safety, the loss of life can be prevented in the event of a probable flood on this scale.

ACKNOWLEDGMENTS

First and foremost, I would like to express my gratitude to my precious mentor and advisor Prof. Dr. Zafer Bozkuş who provided a unique support from the beginning to the end of this study. He changed my point of view with his constructive criticism and made a great contribution by finding solutions to the difficulties that I encountered.

I would like to thank Suiş Proje team for their valuable contributions to this study. Numerical data of basic inputs were provided by them.

I would also like to thank my esteemed colleague Okan Çağrı Bozkurt who has always encouraged me to continue. He shared all of his engineering knowledge and experience with me throughout this study.

APPENDIX A

n = Manning's roughness coefficient
B_{avg} = Average width of the final trapezoidal breach, m
h_w = Maximum water depth on the final breach bottom at the time of failure, m
V_w = Water volume on the breach, m^3
V_{er} = Eroded volume at dam body, m^3
h_b = Maximum height of the final trapezoidal breach, m
h_d = Height of dam, m
W_{avg} = Average width of embankment, m
t_f = Breach formation time, hr
K_o = Multiplier in Froehlich breach width formulation, unitless, 1.0 for piping
C_b = Determined value based on reservoir width, m
I_1, O_1 = Instantaneous inflow and outflow rates at the beginning of the first routing period, m^3/sec
I_2, O_2 = Instantaneous inflow and outflow rates at the end of the first period or at the beginning of the second period of routing, m^3/sec
S_1 = Storage at the beginning of the first routing period, m^3
S_2 = Storage at the end of the first period or at the beginning of the second period of routing, m^3
T = Time interval of routing period, hr

REFERENCES

Chow, V. T. (1951). A practical procedure of flood routing. *Civ. Eng. And Public Works Rev., 46*(542), 586–588.

Costa, J. E. (1985). U.S. Geological Survey Open-File Report: *Vol. 85-560. Floods from Dam Failures*. Denver, Colorado.

Cowan, W. L. (1956). Estimating hydraulic roughness coefficients. *Agricultural Engineering, 37*(7), 473–475.

Froehlich, D. C. (1995a). Peak outflow from breached embankment dam. *Journal of Water Resources Planning and Management, 121*(1), 90–97. https://doi.org/10.1061/(ASCE)0733-9496(1995)121:1(90)

Froehlich, David C., 1995b. Embankment dam breach parameters revisited. In Water Resources Engineering, Proceedings of the 1995 ASCE Conference on Water Resources Engineering, San Antonio, Texas, August 14-18, 1995, p. 887-891.

Froehlich, D. C. (2008). Embankment dam breach parameters and their uncertainties. *Journal of Hydraulic Engineering, 134*(12), 1708–1721. https://doi.org/10.1061/(ASCE)0733-9429(2008)134:12(1708)

Gharbi, M., Soualmia, A., Dartus, D., & Masbernat, L. (2016). Floods effects on rivers morphological changes application to the Medjerda River in Tunisia. *Journal of Hydrology and Hydromechanics, 64*(1), 56–66. https://doi.org/10.1515/johh-2016-0004

MacDonald, T. C., & Langridge-Monopolis, J. (1984). Breaching Characteristics of Dam Failures. *Journal of Hydraulic Engineering, 110*(5), 567–586. https://doi.org/10.1061/(ASCE)0733-9429(1984)110:5(567)

U.S. Army Corps of Engineers, 2016. HEC-RAS River Analysis System, User's Manual, Version 5.0.3, CPD 68.

Von Thun, J. Lawrence, and David R. Gillette, 1990, Guidance on Breach Parameters, unpublished internal document, U.S. Bureau of Reclamation, Denver, Colorado, March 13, 1990, 17 p.

Wahl, T.L., 1998. Prediction of Embankment Dam Breach Parameters: A Literature Review and Needs Assessment Denver, Colorado, July 1998., Dam Safety Research Report DSO-98-004, U.S. Dept. of the Interior, Bureau of Reclamation

Wahl, T. L. (2004). Uncertainty of predictions of embankment dam breach parameters. *Journal of Hydraulic Engineering, 130*(5), 389–397. https://doi.org/10.1061/(ASCE)0733-9429(2004)130:5(389)

Xu, Y., & Zhang, L. M. (2009). Breaching parameters for earth and rockfill dams. *Journal of Geotechnical and Geoenvironmental Engineering, 135*(12), 1957–1970. https://doi.org/10.1061/(ASCE)GT.1943-5606.0000162

5th International Symposium on Dam Safety

October 27-31, 2018

NUMERICAL MODELING OF SUBMERGED HYDRAULIC JUMP UNDER A SLUICE GATE, COMPARISON OF NUMERICAL AND PHYSICAL MODELS

Ali YILDIZ [1], Ali İhsan MARTI[2], Şerife Yurdagül KUMCU

ABSTRACT

The flow passing under a sluice gate can be in two states, free flow and submerged flow. If the regime of the flow changes from subcritical to supercritical then a submerged hydraulic jump can occur near the gate. Due to the strong turbulence forces inside submerged hydraulic jump, it will be difficult to determine flow heights and velocities by using analytical methods. In this study, an open channel system containing a sluice gate and a step was used in the experiments. By the aid of the step, the flow regime was changed and a submerged hydraulic jump was obtained. The numerical model of the physical model was generated in the same size with the same initial condition by Flow-3D working with VOF method. The numerical analysis was made for two different gate openings and 10 different flow rates. Also, 4 different turbulence models were used in the numerical analysis to determine which turbulence model gives the best result for estimating the behavior of the submerged hydraulic jump. The flow depths and water surface profiles of the models were compared. According to the results, the numerical tools were found to be sufficiently advanced to simulate a submerged hydraulic jump.

Keywords: Computational Fluid Dynamics (CFD), Flow-3D, Numerical Modeling, Sluice Gate, Submerged Hydraulic Jump

INTRODUCTION

Sluice gates are commonly used in open channels and rivers for controlling discharge, flow depths and capturing floating objects on water. The regime of flow passing under a sluice gate is supercritical and this flow may produce hydraulic jump after gate. Hydraulic jump occurs when flow regime is changed supercritical to subcritical in hydraulic structures such as spillways, weirs and sluice gates. An uncontrolled hydraulic jump can be dangerous for hydraulic structures such as river bad. The main aim of producing a hydraulic jump is to dissipate energy. In some cases baffle blocks and steps are used for producing submerged hydraulic in order to improve energy dissipation (Peterka, 1984).

Hydraulic design of the sluice gates is done with some graphical and analytical methods. In some cases design of the sluice gates made with physical models. At design stage of hydraulic structures, the small-scaled physical models are constructed to observe the behavior of water and determine the problems that may be encountered. However, preparing physical tests models requires professional labor work. Moreover, experimental studies may be more expensive, take longer time and have scale effect. Although the main reason for the need for gates don not vary past to today, significant steps

[1] Res. Asist., Department of Civil Engineering, Konya Teknik University, Konya, Turkey, e-posta: aliyildiz@selcuk.edu.tr
[2] Dr., Department of Civil Engineering, Konya Teknik University, Konya, Turkey, e-posta: alihsan@selcuk.edu.tr
[3] Dr., Department of Civil Engineering, Necmettin Erbakan University, Konya, Turkey, e-posta: yurdagulkumcu@gmail.com

were achieved by progressive engineering techniques and computer technologies. Computational Fluid Dynamics (CFD) is a type of numerical modeling technique developed to solve fluid mechanics problems. CFD investigates fluid-fluid and fluid-solid interactions behavior. Applicability of CFD to spillway design is great advantage of hydraulic engineering due to its features (Cederstorm 1998). Although solution of numerical models take a long time in the computer, results such as free surface profile, velocity and discharge which cannot be obtained from one and two dimensional models can be easily examined in 3-Dimensional models. CFD can be used in many areas where fluid flow is present. Mostly, the results of the numerical model and the physical model are compared to determine the reliability of the results obtained by the numerical model. Besides the accuracy test of the numerical model, these comparisons are also used for the calibration of the numerical model. During the comparison process between the numerical and physical models, they must be evaluated in terms of hydraulic engineering judgment.

In this study, present a numerical and experimental study of the turbulent flow in a hydraulic jump. Then, a numerical model of the sluice gate was built using Flow-3D computer program widely used in CFD researches. Finally, the results of the numerical and physical models were compared and discussed with each other.

MATERIAL AND METHOD

Sluice Gates and Hydraulic Jump

Sluice gates are used in controlled spillways. Sluice gates provide that the water in reservoir remains at the maximum level and drains the water fro the reservoir when necessary. In addition, sluice gates capture floating objects such as ice, wood and prevent floods passing to downstream. Discharge and flow speed of water should be determined depending on the opening of the gate. The flow under sluice gates is investigated in two condition; free flow and submerged flow. In the case of free flow, the flow passing through is supercritical flow and opened the atmosphere. The flow depth is smaller than the gate opening. The flow may be subjected to hydraulic jump but this jump occurs away from the gate. In the case of submerged flow, a submerged hydraulic jump occurs adjacent to gate. The flow depth is higher than the gate opening and flow is not opened atmosphere directly. Turbulence forces and backflows are greater therefore large forces are formed in submerged flow. Free flow and submerged flow conditions can be seen in Figure 1.

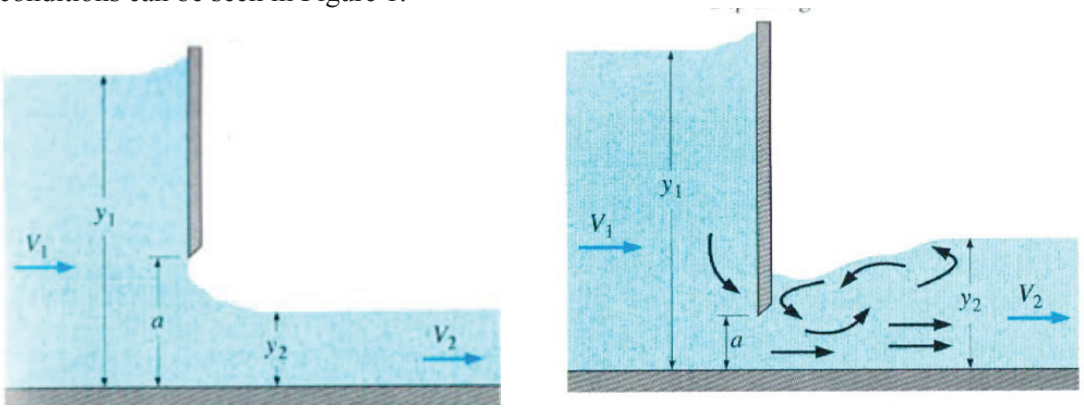

Figure 1. Free and submerged flow under a sluice gate

Discharge value of flow passing under gate is determined by formula;

$$Q = C_d * a * b * \sqrt{2 * g * y_1} \quad (1)$$

Where;
Q : Discharge (m^3/sn)
C_d : Discharge Coefficient
a : Gate opening (m)
b : Gate width (m)

y_1 : Upstream flow depth (m)
Discharge coefficient, C_d is determined from Figure 2. below.

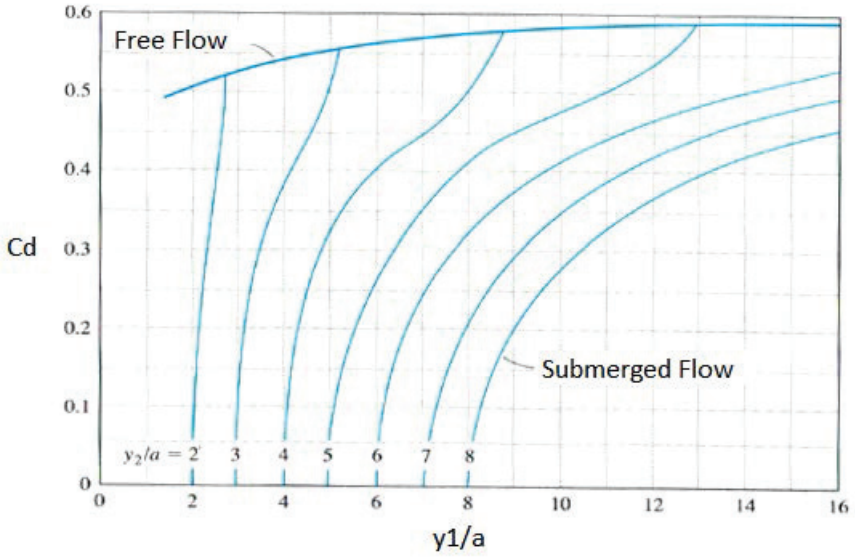

Figure 2. Determining discharge coefficient depending on type of flow

Hydraulic Jump occurs in two type which are free hydraulic jump and submerged hydraulic jump. Although many problems related to free hydraulic jumps have been solved, submerged hydraulic jumps are not fully understood yet. The amount of energy to be broken in submerged hydraulic jump cannot be calculated by the formulas used in free jump. The calculations of submerged hydraulic jumps are usually carried out with experimental and numerical studies. The scale effect is has a great importance in these studies. It is not obvious that results of the experiments in the model will give same results in the prototype because of scale effect.

Numerical Modeling-Flow-3D

The flow over the spillway was modeled by Flow-3D VOF-based CFD program and uses finite-volume approach to solve the Reynolds Averaged Navier Stokes (RANS) equations (Flow Science, 2002). The program evaluates the location of the flow obstacles by implementing a cell porosity technique called as the fractional area/volume obstacle representation of FAVOR method. The computational domain is subdivided using Cartesian coordinates into a grid of variable-sized hexahedral cells. The general governing RANS (3) and the continuity equations (2) for an incompressible flow, including the FAVOR variables, are given by

$$\frac{\partial}{\partial x_i}(u_i A_i) = 0 \tag{2}$$

$$\frac{\partial u_i}{\partial t} + \frac{1}{V_F}\left(u_j A_j \frac{\partial u_i}{\partial x_j}\right) = -\frac{1}{\rho}\frac{\partial p}{\partial x_i} + g_i + f_i \tag{3}$$

Where u_i is the velocities in x-y-z direction, t is time, A_i is fractional areas open to flow, V_F is volume fraction of fluid in each cell, ρ is density of fluid, p is hydrostatic pressure, g_i is gravitational forces, f_i represent the Reynolds stresses.

Boundary conditions are determined in accordance with real experiments to represent physical model accurately in numerical model. There are six different (+X, -X, +Y, -Y, +Z, -Z) boundaries on the main grid system because of flow domain is defined as a hexahedron. The upstream boundary condition (-X), where water is supplied to channel and behave as reservoir, is defined hydrostatic pressure. This hydrostatic pressure is entered to Flow-3D as a height and it creates a total head over the ogee spillway. Therefore, varying total heads over the ogee spillway is provided by changing hydrostatic pressure value at (-X). Downstream boundary condition (-X), in other words end of the

channel is defined as output. On the top boundary (+Z) defined as atmospheric pressure and the bottom boundary (-Z) defined as wall. Side walls (-Y, +Y) is defined symmetric.

In the numerical analysis two different mesh plane system were used. Firstly a mesh plane is generated to cover all system which have same dimensions with real physical model. The cell size of the mesh is chosen as $\Delta x=\Delta y=\Delta z=0{,}01$ m. Total number of the cells was calculated as 1085000. Analysis duration of numerical model takes too long time, when effect of the turbulence flow and total mesh number are considered. In experimental study, measurements are conducted for 10 different total heads and discharge values. One analysis takes 3.5 hour to complete and get steady-state solution. Therefore, mesh plane is contracted to middle of channel to make a solution with lower number of cells. However there are two questions arises "Will side walls affect the flow characteristic?" and "Will contracted mesh plane affect turbulent forces. To answer these questions, analyses conducted with two different mesh plane on model as seen Figure 3.

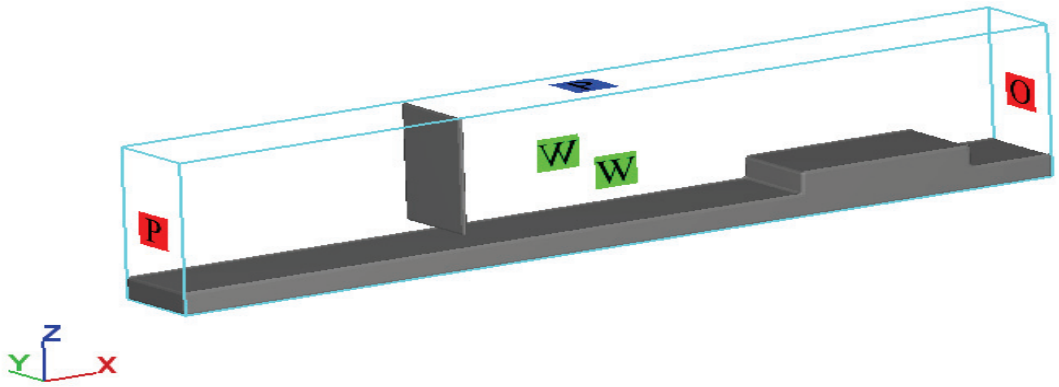

a) Mesh solution-1 having 0,3 m width same as channel width

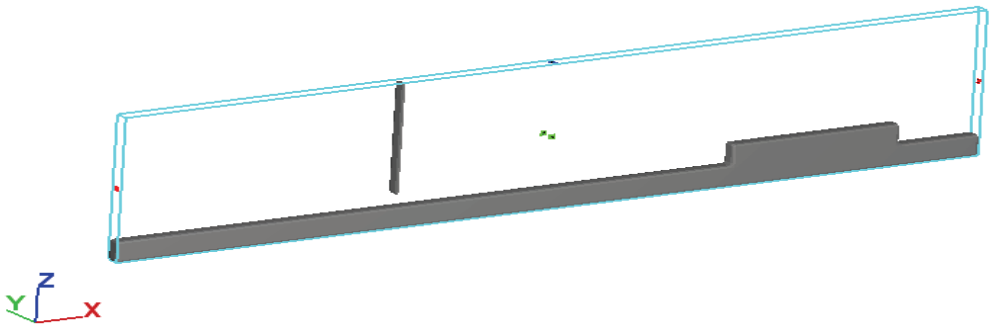

b) Mesh solution-2 having 0,05 m width

Figure 3. Two different mesh solutions

Second mesh plane is generated as cover middle section of channel. With of the second mesh plane is set 0,05 width, 0,25 m smaller than first mesh plane which has 0,3 m. The total number of cells in second mesh plane was calculated as 108500. However side walls conditions (-Y, +Y) is defined different from first mesh. Side wall conditions defined as Symmetry to remove effect of wall frictions on fluid flow.

Experimental Setup

A physical model of a typical sluice gate was fabricated from plexiglas and placed in open channel. The open channel which made of tempered glass is 6 m long, 0,6 m wide and 0,5 m height with zero tangential slope. The open channel is contracted to 0,3 m in a certain region, to get higher heads behind the sluice gate. The open channel has a closed water loop system and flow to the channel is supplied from reservoir by pump. Pumps send water from one reservoir to another by pipes and water passes to channel. Discharges values are measured by Ultrasonic flow meter which placed on pipe coming from pumps. Total heads behind sluice gate are determined with limnimetre. In experiments a

step which 1,2 m far from gate is placed to channel. This step turns flow regime from subcritical to supercritical and causes submerged hydraulic jump near the gate (Figure 4.).

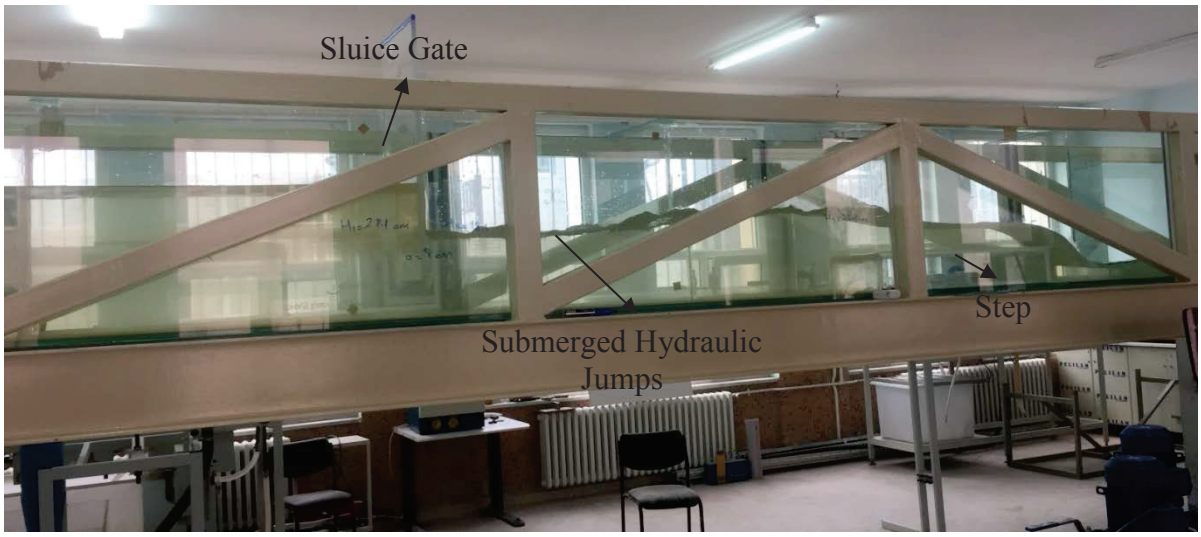

Figure 4. Physical experiment setup

RESULTS

The physical model carried out in the laboratory and the numerical model analyzed by Flow-3D were compared and discussed in terms of total heads (H_e), 3 measurement points and corresponding discharges (Q). Measurement points and general scheme of physical experimental setup can be seen in Figure 5.

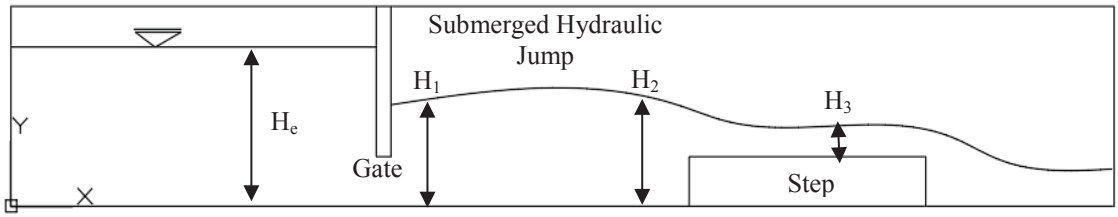

Figure 5. General scheme of physical system and position of measurement points

The main objective of the comparison of the physical model with the numerical model was to determine how much numerical model is successful for predicting flow rate under effect of submerged flow. Firstly, performances of two meshes systems are evaluated. According to results there is no significant difference between mesh systems in terms of flow depths and discharge values. By using contracted mesh planes, analysis time is shortened from 3,5 hours to 0,3 hours. This study showed that the numerical tools using RANS equations are sufficiently advanced to simulate a flow passing through a sluice gate. As seen from Figure 6, the physical model and the numerical model are similar to each other.

Figure 6. Comparison of numerical and physical model

In numerical analysis 4 different turbulence models which are Prandti mixing length, Two-equation(k-e) model, Renormalized group (RNG) model and Large eddy simulation model were used. Best performance and consistency was got with Renormalized group (RNG) turbulence model. Also that was seen that using a contracted mesh plane instead of full size mesh does not affect the turbulence forces in analysis.

Results get from numerical and physical model can be seen on Table 1. For 2 different gate openings and 10 different discharge values physical experiments and numerical analysis are conducted. Numerical model gives highly consistent results especially where not turbulent flow such as Total head, measurement points 2-3. To compare discharge values of numerical model with physical model, discharge values of numerical model multiplied with 6 because mesh plane used in analysis six times smaller than real channel width. Although using a contracted mesh plane, numerical model gives good discharge results. Also graphical comparison of flow depths gets from numerical and physical model can be seen Appendix-A.

Table 1. Results get from numerical and physical models

Physical Experiment (a=0,058 m, b=0,3 m)					Numerical Model (a=0,058 m, b=0,3 m)				
H_e	H_1	H_2	H_3	$Q(m^3/sn)$	H_e	H_1	H_2	H_3	$Q(m^3/sn)$
0,183	0,157	0,170	0,044	0,00858	0,182	0,162	0,168	0,042	0,00842
0,210	0,163	0,183	0,051	0,01109	0,208	0,170	0,183	0,049	0,01140
0,272	0,168	0,205	0,062	0,01596	0,271	0,185	0,204	0,061	0,01634
0,340	0,165	0,225	0,069	0,02047	0,338	0,191	0,228	0,073	0,02114
Physical Experiment (a=0,08 m, b=0,3 m)					Numerical Model (a=0,08 m, b=0,3 m)				
H_e	H_1	H_2	H_3	$Q(m^3/sn)$	H_e	H_1	H_2	H_3	$Q(m^3/sn)$
0,168	0,163	0,168	0,041	0,00885	0,167	0,160	0,163	0,040	0,00812
0,200	0,175	0,189	0,050	0,01255	0,198	0,177	0,185	0,050	0,01224
0,240	0,185	0,210	0,060	0,01728	0,237	0,190	0,208	0,061	0,01710
0,245	0,186	0,212	0,061	0,01795	0,243	0,192	0,210	0,063	0,01752
0,281	0,186	0,225	0,068	0,02158	0,281	0,202	0,227	0,071	0,02162
0,287	0,186	0,228	0,068	0,02250	0,285	0,200	0,226	0,073	0,02220

The flow depth measurements taken from the physical model were affected from the waves, since especially the water passing under sluice gate. Some small differences obtained between the flows depths obtained by the physical and numerical model especially where submerged hydraulic jump occur. An experimental and numerical study of flow under sluice gate with submerged hydraulic jump was conducted. Results obtained experiments showed that the discharge values obtained by Flow-3D were good agreement with physical model. This study showed that the numerical tools using RANS equations are sufficiently advanced to simulate a flow under a sluice gate.

APPENDIX A

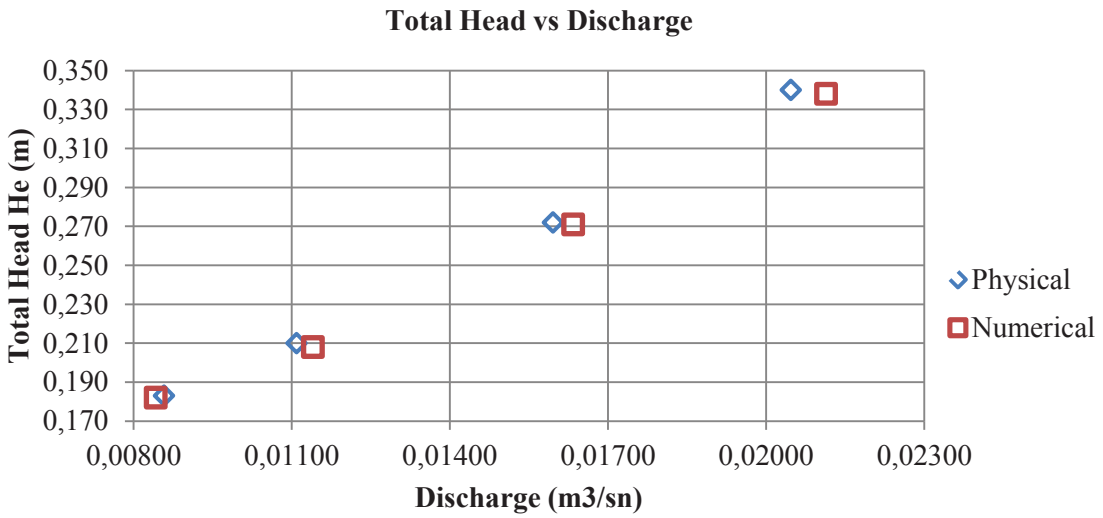

Figure 7. Comparison of Total Head (H_e) gets from physical and numerical model for gate opening a=0,058 m.

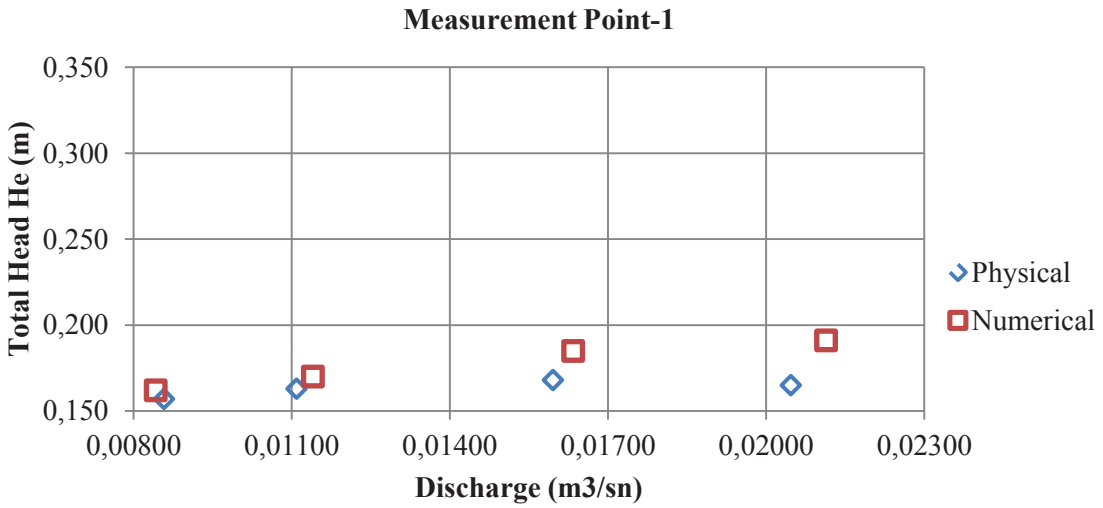

Figure 8. Comparison of flow depths (H_1) at measurement point-1 gets from physical and numerical model

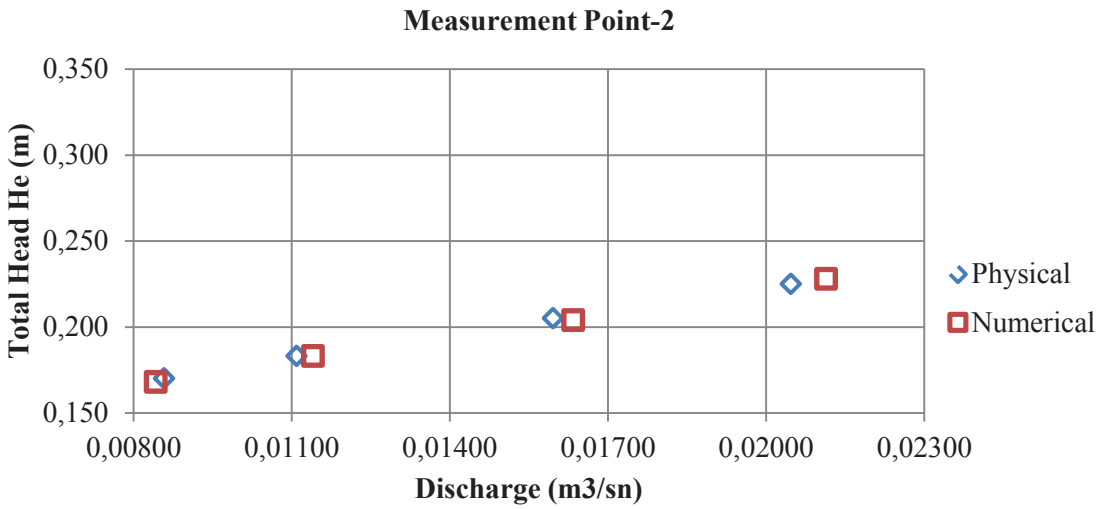

Figure 9. Comparison of flow depths (H_3) at measurement point-2 gets from physical and numerical model

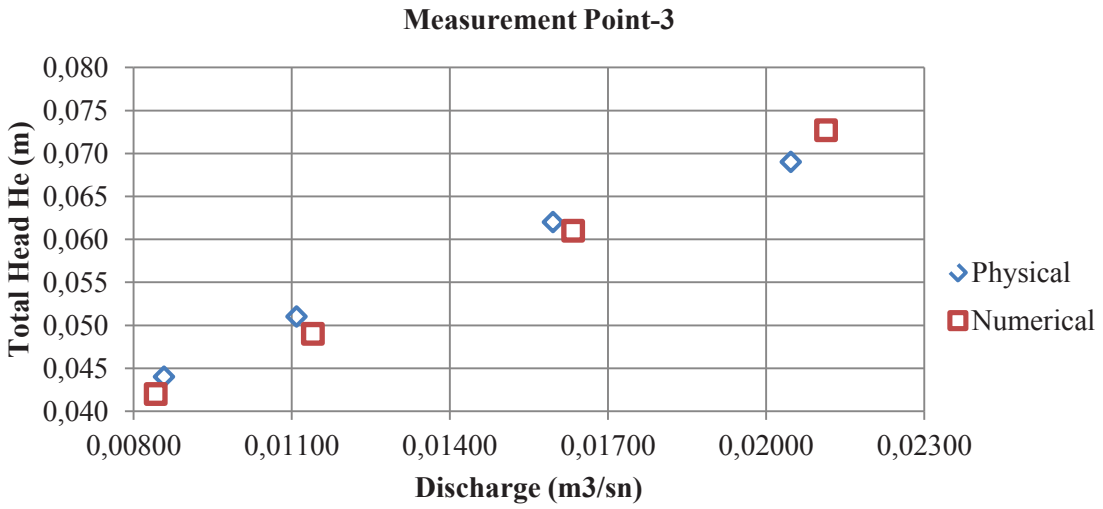

Figure 10. Comparison of flow depths (H_2) at measurement point-2 gets from physical and numerical model

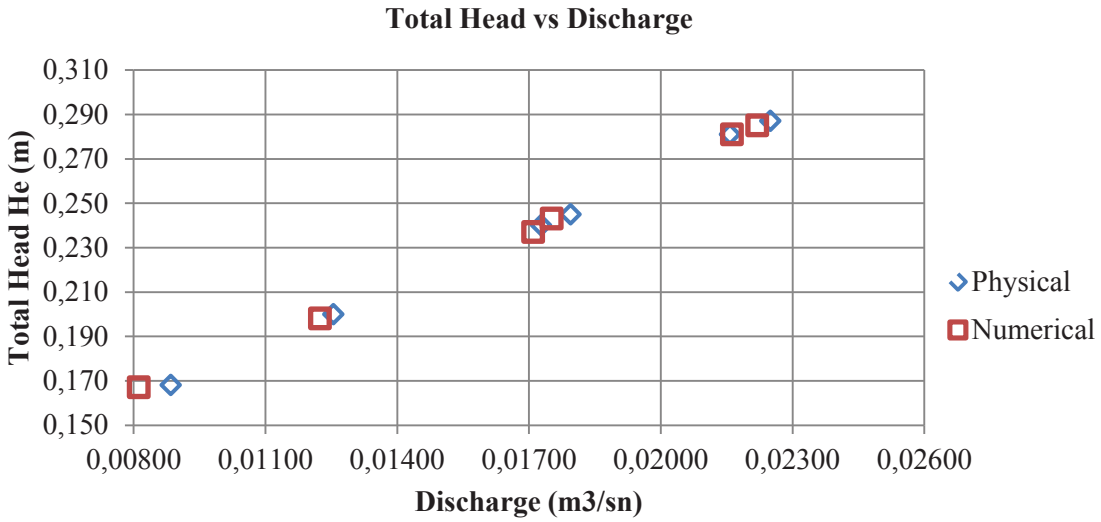

Figure 7. Comparison of Total Head (H_e) gets from physical and numerical model

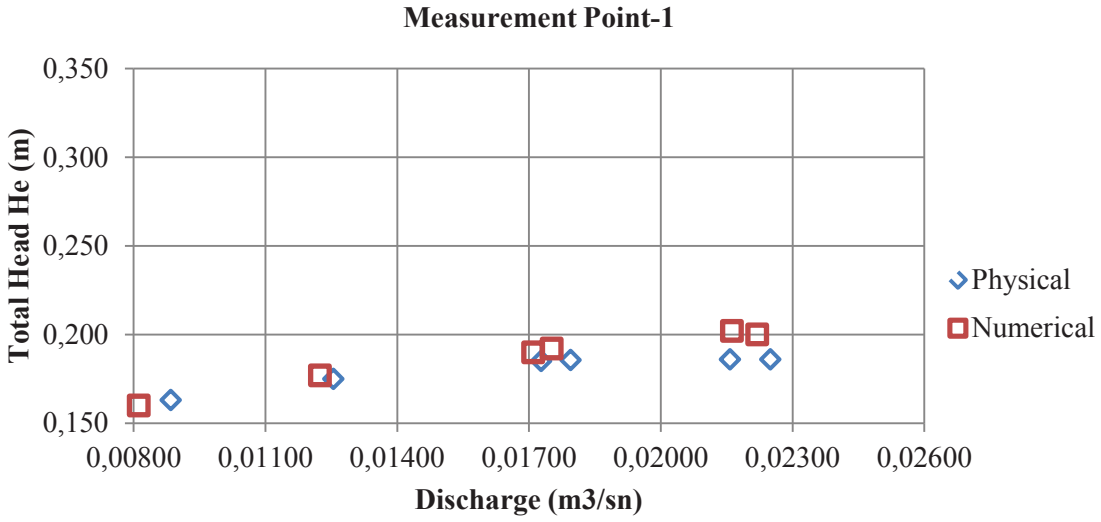

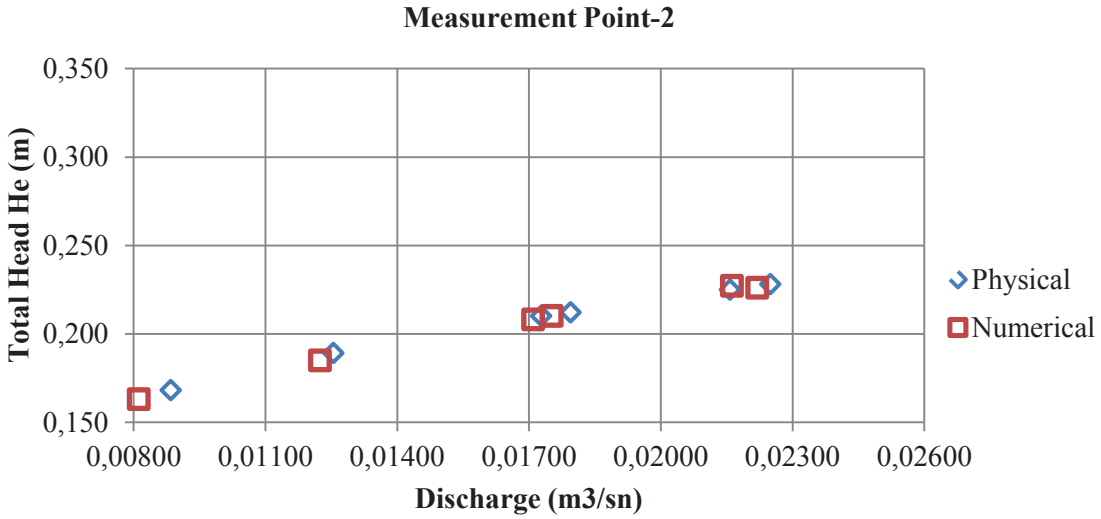

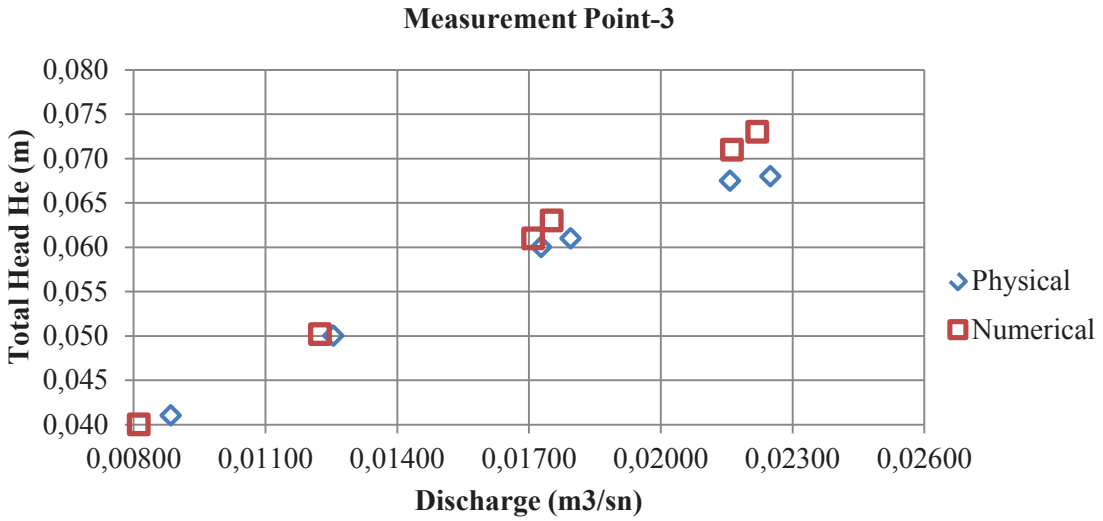

REFERENCES

Cederstorm, M 1998, 'CFD modeling of spillway capacity- A comparison between hydraulic and mathematical models', *Dam Safety*, Balkema, Rotterdam.

Flow Science 2002, Theory manual of Flow3-D, Flow Science, Los Alamos, NM

Peterka, A. J., 1984. Hydraulic design of stilling basins and energy dissipators, 8th Ed. Engineering Monograph No. 25, U.S. Bureau of Reclamation, Denver.

5th International Symposium on Dam Safety

October 27-31, 2018

WATER QUALITY ASSESMENT OF KIRKLARELI DAM LAKES (NORTHERN SECTION OF THE ERGENE RIVER BASIN)

Cem TOKATLI [1]

ABSTRACT

Kayalıköy and Kırklareli Dam Lakes are located in the Kırklareli Province in the north part of Ergene River Basin, which is known as one of the most contaminated river basin of Turkey. In this study water quality of Kayalıköy and Kırklareli Dam Lakes were investigated by determining a total of 16 water quality parameters including temperature, dissolved oxygen, oxygen saturation, pH, electrical conductivity, total dissolved solids, salinity, turbidity, nitrate, nitrite, phosphate, sulfate, fluorine, biological oxygen demand, chemical oxygen demand, fecal coliform. Water samples were collected from the input and output locations of the reservoirs in spring season of 2018 and 3 stations were selected for each dam lakes.

According to data observed, Kayalıköy Dam Lake has I. – II. Class water quality in terms of temperature, dissolved oxygen, oxygen saturation, EC, TDS, nitrate, phosphate, sulphate, fluorine and COD parameters, and III. Class water quality in terms of nitrite, BOD, FC and pH parameters; and Kırklareli Dam Lake has I. – II. Class water quality in terms of temperature, dissolved oxygen, oxygen saturation, EC, TDS, nitrate, phosphate, sulphate, fluorine, nitrite and COD parameters, and III. Class water quality in terms of FC, BOD and pH parameters in general.

Keywords: Ergene River Basin, Dam Lakes of Kırklareli, Water Quality.

INTRODUCTION

One of the most contaminated parts of environment is of course freshwater resources. Contamination caused by especially agricultural and industrial activities reduces the quality of the limited freshwater resources of the world (Tokatlı, 2015). Only about 2.8% of water is suitable and fresh for human consumption, and a large part of this water is found in the glaciers and underground (Gupta, 1997). It is known that dam lakes are one of the most significant sources of potable and domestic water supply for numbers of villages, districts and provinces. But unfortunately many organic and inorganic pollutants sourced have been identified as strong contaminants found in these water (Hudak, 1999; Tokatlı, 2014). Therefore monitoring water quality has an importance both for human health and ecosystem health especially in rural areas.

Kayalıköy and Kırklareli Dam Lakes, which have an irrigation area of 14716 ha and 9050 ha respectively, are located in the Kırklareli Province (http://www2.dsi.gov.tr/). There are very large agricultural lands because of contained rich soil and many freshwater resources in Kırklareli. Therefore agricultural pressure is a significant pollution factor for the region. The Ergene River is the most important river basin of the Thrace Region and it is known to be exposed to a great industrial

[1] Associated Professor, Department of Laboratory Technology, Trakya University, İpsala, Edirne, Turkey, e-posta: tokatlicem@gmail.com

pressure (Tokatlı, 2015; 2017; Tokatlı and Baştatlı, 2016). Kayalıköy and Kırklareli Dam Lakes, which are located on the northern section of Ergene River Basin, are the most important reservoirs of Kırklareli Province. The reservoirs were constructed by DSİ (State Water Works) with body fill type of rock in order to provide irrigation and drinking water and flood protection. The body volumes of the the reservoirs stated by DSİ as 1528 dam3 for Kayalıköy Dam Lake and 1838 dam3 for Kırklareli Dam Lake. Kayalıköy Dam Lake, which has a volume of 150 hm^3 at normal water elevation and lake area of 10 km^2 at the normal water level, was constructed between the dates of 1975 – 1986 by DSİ on the Teke Stream (http://www2.dsi.gov.tr/). Kırklareli Dam Lake, which has a volume of 112 hm^3 at normal water elevation and lake area of 6 km^2 at the normal water level, was constructed between the dates of 1985 – 1997 by DSİ on the Şeytandere Stream (http://www2.dsi.gov.tr/). They were constructed to provide irrigation and drinking water to the local people and flood protection, but as many freshwater ecosystems, these reservoirs are being effected from agricultural and domestic pressure.

The aim of this study was to evaluate the water quality of Kayalıköy and Kırklareli Dam Lakes by determining some limnologic parameters including temperature, dissolved oxygen (DO), oxygen saturation (%O2), pH, electrical conductivity (EC), total dissolved solids (TDS), salinity, turbidity, nitrate (NO3), nitrite (NO2), phosphate (PO4), sulfate (SO4), fluorine (F), biological oxygen demand (BOD), chemical oxygen demand (COD), fecal coliform (FC).

MATERIALS AND METHODS

Study Area and Collection of Samples

Kayalıköy Dam Lake and selected stations on the reservoir are given in Figure 1. Water samples were collected in spring season of 2018 and one water sample was taken from each selected stations on the dam lake.

Physicochemical Analysis

Temperature, dissolved oxygen, oxygen saturation, pH, EC, TDS and salinity parameters were determined by using “Hach Lange HQ40D Multiparameter” device during the field studies; turbidity parameter was determined by using “Hach Lange 2100Q Portable Turbiditymeter” device during the field studies; nitrate, nitrite, phosphate, sulphate, fluorine and COD parameters were determined by using “Hach Lange DR3900 Spectrophotometer” device during the laboratory studies; BOD parameter was determined by using “Hach Lange BOD Trak II” device during the laboratory studies.

Microbiological Analysis

Microbiological analysis was carried out using membrane filtration technique. All water samples were filtered with membrane filtration technique and the membrane filter was placed in coliform chromogenic m-FC Agar. All growth mediums were left to incubate for 24 hours at 44.5 ± 0.2 0C and counted by automatic colony counter.

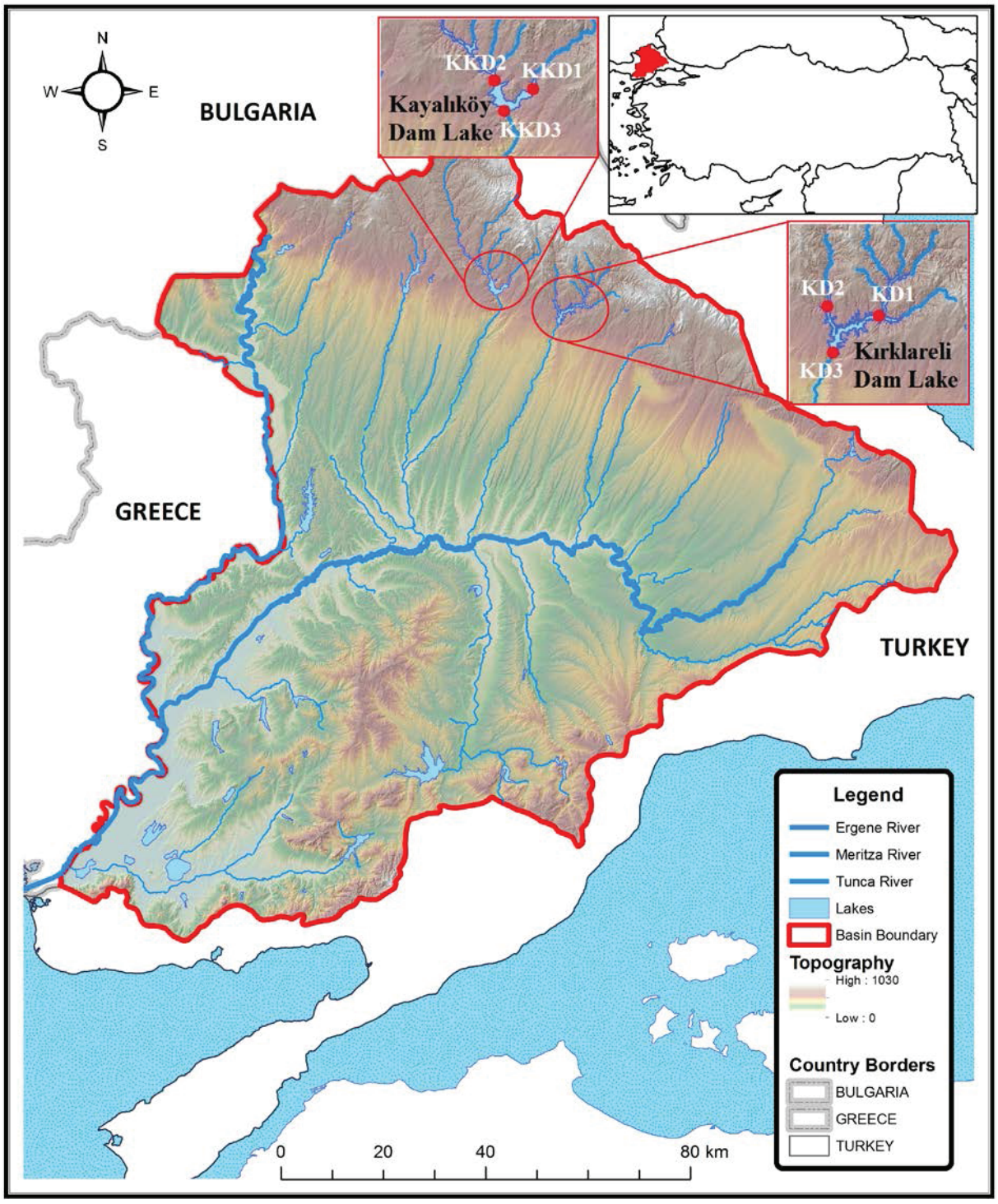

Figure 1. Ergene River Basin and Kayalıköy and Kırklareli Dam Lakes

RESULT AND DISCUSSION

The detected water quality parameters in Kayalıköy and Kırklareli Dam Lakes and some national – international limit values are given in Table 1.

According to the Water Pollution Control Regulation criteria in Turkey (2004; 2012), Kayalıköy Dam Lake has I. Class water quality in terms of temperature, dissolved oxygen, oxygen saturation, EC, TDS, nitrate, phosphate, sulphate and fluorine parameters; II. Class water quality in terms of COD

parameter; and III. Class water quality in terms of nitrite, BOD and FC parameters. It was also determined that KKD1 has I. Class, KKD2 and KKD3 have III. Class water quality in terms of pH parameter. In a study performed in dam lakes of Edirne Province in Ergene River Basin, water quality of Sultanköy (İpsala District), Altınyazı (Uzunköprü District), Süloğlu (Süloğlu District), and Kadıköy (Keşan District) Dam Lakes were investigated. According to the results of this study, as similar to the present study, the investigated reservoirs were found to be as III. Class water quality in terms of nitrite parameter in general (Tokatlı et al., 2017). The main sources of nitrogen compounds in water are anthropogenic activities including mainly; nitrogen rich fertilizers that is commonly being used around the reservoirs, animal feedlots that is also common in the region; and municipal wastewater, sludge and septic tanks that are being used at everywhere in the region (Self and Waskom, 2013; Tokatlı, 2014).

According to the Water Pollution Control Regulation criteria in Turkey (2004; 2012), Kırklareli Dam Lake has I. Class water quality in terms of temperature, dissolved oxygen, oxygen saturation, EC, TDS, nitrate, phosphate (KD1 is II. Class), sulphate and fluorine parameters; II. Class water quality in terms of nitrite and COD (KD1 is I. Class) parameters; and III. Class water quality in terms of FC and pH (KD1 is I. Class) parameters. It was also determined that KD1 has II. Class, KD2 has III. Class and KD3 has I. Class water quality in terms of BOD parameter. Changes in pH values in surface water ecosystems can be indicative of an industrial pollutant, photosynthesis or the respiration of algae, which is feeding on a contaminant. Most ecosystems are sensitive to changes in pH and the monitoring of pH has been incorporated into the environmental laws of most industrialized countries (Ugwu and Wakawa, 2012). In a macroscopic point of view, pH values were recorded in quite high levels in Kırklareli Dam Lake and it has an alkaline water characteristic.

CONCLUSION

In this study, water quality of Kayalıköy and Kırklareli Dam Lakes located in the Kırklareli Province were evaluated by investigating some psychochemical and microbiological water quality parameters. According to data observed, organic contents in water of almost all the stations were detected in quite high levels and the reservoirs have alkaline water characteristic. As a result of this study, it can be concluded that Kayalıköy and Kırklareli Dam Lakes are being affected from agricultural activities, they have especially III. Class water quality in terms of nitrite, BOD and FC parameters in general. In order to provide the sustainability of these reservoirs, organic contents originated from agricultural and domestic applications have to be reduced.

Table 1. Results of detected parameters and some limit values

Limit Values andthe Results of Present Study		Parameters															
		Temp. (C^0)	**DO** (mg/L)	**%O_2**	**pH**	**EC** (mS/cm)	**[a]TDS** (mg/L)	**Salinity** (‰)	**Tur** (NTU)	**NO_3** (mg/L)	**NO_2** (mg/L)	**[b]PO_4** (mg/L)	**SO_4** (mg/L)	**F** (mg/L)	**COD** (mg/L)	**BOD** (mg/L)	**FC** (cfu/100mL)
***Turkish Regulations Water Quality Classes** (2012)	**I. Class**	25	8	90	6.5-8.5	400	500	-	-	5	0.002	0.02	200	1	25	4	10
	II. Class	25	6	70	6.5-8.5	1000	1500	-	-	10	0.01	0.16	200	1.5	50	8	200
	III. Class	30	3	40	6.0-9.0	3000	5000	-	-	20	0.05	0.65	400	2	70	20	2000
	IV. Class	>30	<3	<40	Out of 6.0-9.0	>3000	>5000	-	-	>20	>0.05	>0.65	>400	>2	>70	>20	>2000
Drinking Water Standards	**TS266** (2005)	-	-	-	6.5-9.5	2500	-	-	5	50	0.5	-	250	1.5	-	-	-
	EC (2007)	-	-	-	6.5-9.5	2500	-	-	-	50	0.5	-	250	1.5	-	-	-
	WHO (2011)	-	-	-	-	-	-	-	-	50	0.2	-	-	1.5	-	-	-
Kayalıköy Dam Lake	**KKD1**	19.3 I. Class	12.3 I. Class	137 I. Class	8.84 I. Class	227 I. Class	124 I. Class	0.12	4.58	1.240 I. Class	0.017 **III. Class**	0.012 I. Class	24.9 I. Class	0.229 I. Class	30.0 II. Class	8.7 **III. Class**	252 **III. Class**
	KKD2	24.7 I. Class	17.4 I. Class	215 I. Class	9.07 **III. Class**	286 I. Class	135 I. Class	0.13	5.64	0.519 I. Class	0.038 **III. Class**	0.009 I. Class	27.0 I. Class	0.237 I. Class	26.1 II. Class	12.0 **III. Class**	344 **III. Class**
	KKD3	20.5 I. Class	12.1 I. Class	138 I. Class	9.10 **III. Class**	230 I. Class	118 I. Class	0.12	6.95	1.150 I. Class	0.020 **III. Class**	0.003 I. Class	26.2 I. Class	0.223 I. Class	30.7 II. Class	9.1 **III. Class**	370 **III. Class**
Kırklareli Dam Lake	**KD1**	20.8 I. Class	11.9 I. Class	136 I. Class	8.31 I. Class	319 I. Class	170 I. Class	0.17	4.05	0.246 I. Class	0.008 II. Class	0.031 II. Class	17.0 I. Class	0.088 I. Class	21.2 I. Class	7.5 II. Class	222 **III. Class**
	KD2	20.8 I. Class	11.6 I. Class	132 I. Class	8.85 **III. Class**	251 I. Class	129 I. Class	0.13	3.88	0.255 I. Class	0.007 II. Class	0.004 I. Class	19.1 I. Class	0.152 I. Class	29.1 II. Class	9.7 **III. Class**	224 **III. Class**
	KD3	19.9 I. Class	10.0 I. Class	112 I. Class	8.92 **III. Class**	256 I. Class	136 I. Class	0.14	2.34	0.206 I. Class	0.007 II. Class	0.005 I. Class	18.6 I. Class	0.141 I. Class	29.0 II. Class	2.6 I. Class	338 **III. Class**

[a]Turkish Regulations. 2004; [b]Uslu and Türkman. 1987; *III. – IV. Class water qualities are given in bold

TS266 – Turkish Standards Institute; EC – European Communities; WHO – World Health Organization

AKNOWLEDGEMENTS

The author would like to thank for the financial and technical supports supplied by Trakya University, Turkey. This investigation has been supported by the project numbered as 2017/211 accepted by Trakya University, Commission of Scientific Research Projects.

REFERENCES

EC (European Communities), 2006. EC of the European Parliament and of the council of 6 September 2006 on the quality of fresh waters needing protection or improvement in order to support fish life. Directive 2006/44.

Gupta, A. D., 1997. "Importance of groundwater as water resource". Proceedings of Seminar and Training on Groundwater Contaminated by Hazardous Substances, Bangkok, January 20–21.

http://www2.dsi.gov.tr/

Hudak, P. F., 1999. "Chloride and Nitrate Distributions in the Hickory Aquifer, Central Texas, USA". Environment International 25 (4), 393–401.

Self, J. R., Waskom, R. M. (2013). "Nitrates in Drinking Water". Colorado State University Extension. 7/95. Revised 11/13.

TS 266, 2005. Sular-İnsani tüketim amaçlı sular. Türk Standartları Enstitüsü. ICS 13.060.20.

Tokatlı, C., 2014. "Drinking Water Quality of a Rice Land in Turkey by a Statistical and GIS Perspective: İpsala District". Polish Journal of Environmental Studies, 23 (6): 2247-2258.

Tokatlı, C., 2015. "Assessment of the Water Quality in The Meriç River: As an Element of the Ecosystem in the Thrace Region of Turkey". Polish Journal of Environmental Studies. 24 (5): 2205-2211.

Tokatlı, C., 2017. "Bio – Ecological and Statistical Risk Assessment of Toxic Metals in Sediments of a Worldwide Important Wetland: Gala Lake National Park (Turkey)". Archives of Environmental Protection, 43 (1): 34-47.

Tokatlı, C., Baştatlı, Y., 2016. "Trace and Toxic Element Levels in River Sediments". Polish Journal of Environmental Studies, 25 (4): 1715-1720.

Tokatlı, C., Baştatlı, Y., Elipek, B., 2017. "Water Quality Assessment of Dam Lakes Located in Edirne Province (Turkey)". Sigma Journal of Engineering and Natural Sciences, 35 (4): 743-750.

Turkish Regulations, 2004. Yüzeysel Su Kalitesi Yönetimi Yönetmeliği. 31 Aralık Cuma tarihli Resmi Gazete. Sayı: 25687. http://suyonetimiormansu.gov.tr.

Turkish Regulations, 2012. Yüzeysel Su Kalitesi Yönetimi Yönetmeliği. 30 Kasım 2012 tarihli Resmi Gazete. Sayı: 28483. http://suyonetimiormansu.gov.tr.

Ugwu, A.I. and Wakawa, R. J., 2012. "A study of seasonal physicochemical parameters in River Usma". American Journal of Environmental Science, 2012, 8 (5): 569-576.

WHO (World Health Organization), 2011. Guidelines for Drinking-water Quality. World Health Organization Library Cataloguing-in-Publication Data. NLM classification: WA 675.

WATER QUALITY ASSESMENT OF EDIRNE DAM LAKES (WESTERN SECTION OF THE ERGENE RIVER BASIN)

Cem TOKATLI [1]

ABSTRACT

Altınyazı, Sultanköy and Süloğu Dam Lakes are located in the Edirne Province in the west part of Ergene River Basin. In this study water quality of these reservoirs were investigated by determining a total of 16 limnologic parameters (temperature, dissolved oxygen, oxygen saturation, pH, electrical conductivity, total dissolved solids, salinity, turbidity, nitrate, nitrite, phosphate, sulfate, fluorine, biological oxygen demand, chemical oxygen demand, fecal coliform).

According to detected data, Altınyazı Dam Lake has I. – II. Class water quality in terms of temperature, dissolved oxygen, oxygen saturation, pH, TDS, nitrate, phosphate, sulphate, fluorine, COD, EC and BOD parameters, and III. Class water quality in terms of nitrite and FC parameters; Sultanköy Dam Lake has I. – II. Class water quality in terms of temperature, dissolved oxygen, oxygen saturation, pH, TDS, nitrate, sulphate, fluorine, EC, phosphate and COD parameters, and III. – IV. Class water quality in terms of BOD, nitrite and FC parameters; and Süloğlu Dam Lake has I. – II. Class water quality in terms of temperature, dissolved oxygen, oxygen saturation, pH, EC, TDS, nitrate, sulphate, fluorine, phosphate and COD parameters, and III. Class water quality in terms of nitrite, BOD and FC parameters in general.

Keywords: Ergene River Basin, Dam Lakes of Edirne, Water Quality.

INTRODUCTION

Rapid growth of world population and the developments of industry and lack of environmental awareness in society cause many environmental problems and decrease the limited freshwater quality of the world. Water pollution has nearly become a limiting factor for the mankind and it is on the top of attention all over the globe. It is known that assessment of a large number of lymnological water quality data is a significant requirement for an effective contamination control and water management (Tokatlı, 2014; 2015; Köse et al., 2014; Tokatlı et al., 2014).

Altınyazı, Sultanköy and Süloğu Dam Lakes, which have irrigation areas of 7730 ha, 7773 ha and 3986 ha respectively, are located in the Edirne Province (http://www2.dsi.gov.tr/). There are very large agricultural lands because of contained rich soil and many freshwater resources in Edirne. Therefore agricultural pressure is a significant pollution factor for the region. The Ergene River is the most important river basin of the Thrace Region and it is known to be exposed to a great industrial pressure (Tokatlı, 2015; 2017; Tokatlı and Baştatlı, 2016). Altınyazı, Sultanköy and Süloğlu Dam Lakes, which are located on the western section of Ergene River Basin, are the most important reservoirs of Edirne Province. The reservoirs were constructed by DSİ (State Water Works) with body

[1] Associated Professor, Department of Laboratory Technology, Trakya University, İpsala, Edirne, Turkey, e-posta: tokatlicem@gmail.com

fill types of soil (Altınyazı and Sultanköy Dam Lakes) and rock (Süloğlu Dam Lake) in order to provide irrigation and drinking water and flood protection. The body volumes of the reservoirs stated by DSİ as 524 dam3 for Altınyazı Dam Lake, 1762 dam3 for Sultanköy Dam Lake and 1320 dam3 for Süloğlu Dam Lake. Altınyazı Dam Lake, which has a volume of 31 hm^3 at normal water elevation and lake area of 4 km^2 at the normal water level, was constructed in 1970 by DSİ on the Basamaklar Stream (http://www2.dsi.gov.tr/). Sultanköy Dam Lake, which has a volume of 26 hm^3 at normal water elevation and lake area of 3 km^2 at the normal water level, was constructed in 1996 by DSİ on the Manastır Stream (http://www2.dsi.gov.tr/). Süloğlu Dam Lake, which has a volume of 33 hm^3 at normal water elevation and lake area of 3 km^2 at the normal water level, was constructed in 1981 by DSİ on the Süloğlu Stream (http://www2.dsi.gov.tr/). They were constructed to provide irrigation and drinking water to the local people and flood protection, but as many freshwater ecosystems, these reservoirs are being effected from agricultural and domestic pressure.

The aim of this study was to evaluate the water quality of Altınyazı, Sultanköy and Süloğlu Dam Lakes by determining some limnologic parameters including temperature, dissolved oxygen (DO), oxygen saturation (%O2), pH, electrical conductivity (EC), total dissolved solids (TDS), salinity, turbidity, nitrate (NO3), nitrite (NO2), phosphate (PO4), sulfate (SO4), fluorine (F), biological oxygen demand (BOD), chemical oxygen demand (COD), fecal coliform (FC).

MATERIALS AND METHODS

Study Area and Collection of Samples

Altınyazı, Sultanköy and Süloğlu Dam Lakes and selected stations on the reservoir are given in Figure 1. Water samples were collected in spring season of 2018 and one water sample was taken from each selected stations on the dam lake.

Water Quality Analysis

Temperature, dissolved oxygen, oxygen saturation, pH, EC, TDS and salinity parameters were determined by using “Hach Lange HQ40D Multiparameter” device during the field studies; turbidity parameter was determined by using “Hach Lange 2100Q Portable Turbiditymeter” device during the field studies; nitrate, nitrite, phosphate, sulphate, fluorine and COD parameters were determined by using “Hach Lange DR3900 Spectrophotometer” device during the laboratory studies; BOD parameter was determined by using “Hach Lange BOD Trak II” device during the laboratory studies.

Microbiological analysis was carried out using membrane filtration technique. All water samples were filtered with membrane filtration technique and the membrane filter was placed in coliform chromogenic m-FC Agar. All growth mediums were left to incubate for 24 hours at 44.5 ± 0.2 0C and counted by automatic colony counter.

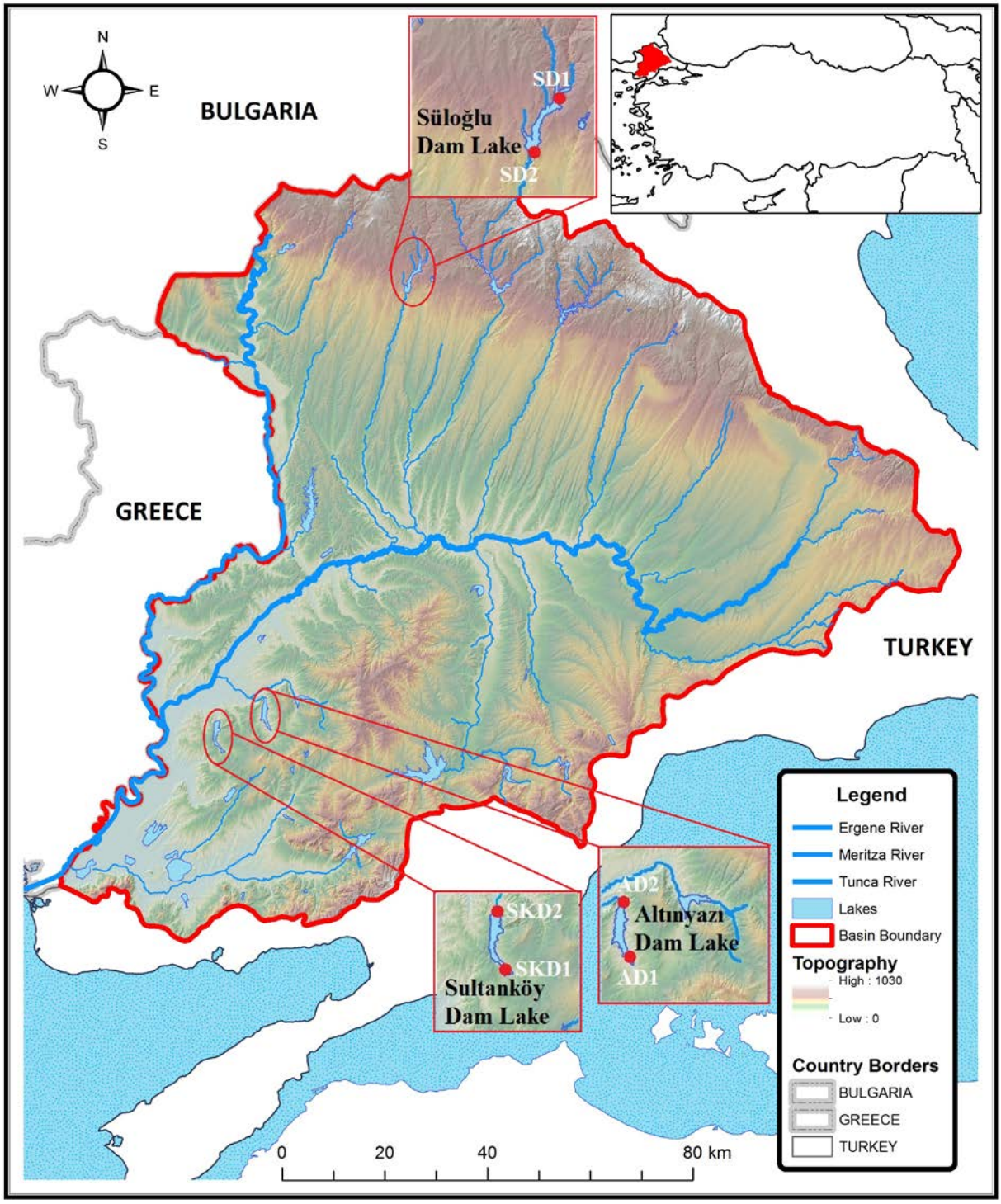

Figure 1. Ergene River Basin and Altınyazı, Sultanköy and Süloğlu Dam Lakes

RESULT AND DISCUSSION

The detected water quality parameters in Altınyazı Dam Lake and some national – international limit values are given in Table 1.

According to the Water Pollution Control Regulation criteria in Turkey (2004; 2012). Altınyazı Dam Lake has I. Class water quality in terms of temperature, dissolved oxygen, oxygen saturation, pH, TDS, nitrate, phosphate (AD1 is II. Class), sulphate, fluorine and COD parameters; II. Class water quality in terms of EC and BOD parameters; and III. Class water quality in terms of nitrite parameter. It was also determined that AD1 has III. Class and AD2 has II. Class water quality in terms of FC parameter. It is clearly known that organic and inorganic fertilizers used in agricultural activities increase the level of nitrogen compounds in water and soil especially in rural areas (Wetzel, 2001; Manahan, 2011).

According to the Water Pollution Control Regulation criteria in Turkey (2004; 2012). Sultanköy Dam Lake has I. Class water quality in terms of temperature, dissolved oxygen, oxygen saturation, pH, TDS, nitrate, sulphate and fluorine parameters; II. Class water quality in terms of EC, phosphate, COD and FC (SKD1 is III. Class) parameters; III. Class water quality in terms of BOD parameter; and IV. Class water quality in terms of nitrite parameter. It is clearly known that organic and inorganic fertilizers used in agricultural activities increase the level of nitrogen compounds in water and soil especially in rural areas (Wetzel, 2001; Manahan, 2011). In a study performed in dam lakes of Edirne Province in Ergene River Basin, water quality of Sultanköy (İpsala District), Altınyazı (Uzunköprü District), Süloğlu (Süloğlu District), and Kadıköy (Keşan District) Dam Lakes were investigated. According to the results of this study, as similar to the present study, the investigated reservoirs were found to be as highly contaminated by nitrite parameter in general (Tokatlı et al., 2017).

According to the Water Pollution Control Regulation criteria in Turkey (2004; 2012), Süloğlu Dam Lake has I. Class water quality in terms of temperature, dissolved oxygen, oxygen saturation, pH, EC, TDS, nitrate, sulphate and fluorine parameters; II. Class water quality in terms of phosphate and COD parameters; and III. Class water quality in terms of nitrite and FC parameters. It was also determined that SD1 has III. Class and SD2 has II. Class water quality in terms of BOD parameter. Nitrite is an intermediate product in the biological oxidation process reaching from ammonium to nitrate. It can reach to high concentrations in organically contaminated water. Fertilizers using intensively in agricultural activities, municipal wastewater discharges from settlement areas are significantly contaminating the freshwater bodies organically and they are known as the most important factors on increasing the amount of nitrite in water (Wetzel, 2001; Manahan, 2011).

CONCLUSION

In this study, water quality of Altınyazı, Sultanköy and Süloğlu Dam Lakes located in the Edirne Province were evaluated by investigating some psychochemical and microbiological water quality parameters. According to data observed, organic contents in water of almost all the stations were detected in quite high levels. As a result of this study, it can be concluded that Altınyazı, Sultanköy and Süloğlu Dam Lakes are being affected from agricultural activities, they have especially III. – IV. Class water quality in terms of nitrite parameter. In conclusion, rice and sunflower are the main crops produced in Edirne City, where is known as the most important region on rice production in Turkey. The water leached through from these paddy and sunflower fields are contaminated by pesticides and fertilizers, which are being used intensively in almost all the districts of Edirne Province in order to reduce the effects of monoculture farming ongoing for many years.

Table 1. Results of detected parameters and some limit values

Limit Values andthe Results of Present Study		Parameters															
		Temp. (C^0)	**DO** (mg/L)	**%O_2**	**pH**	**EC** (mS/cm)	**[a]TDS** (mg/L)	**Salinity** (‰)	**Tur** (NTU)	**NO_3** (mg/L)	**NO_2** (mg/L)	**[b]PO_4** (mg/L)	**SO_4** (mg/L)	**F** (mg/L)	**COD** (mg/L)	**BOD** (mg/L)	**FC** (cfu/100mL)
***Turkish Regulations Water Quality Classes** (2012)	**I. Class**	25	8	90	6.5-8.5	400	500	-	-	5	0.002	0.02	200	1	25	4	10
	II. Class	25	6	70	6.5-8.5	1000	1500	-	-	10	0.01	0.16	200	1.5	50	8	200
	III. Class	30	3	40	6.0-9.0	3000	5000	-	-	20	0.05	0.65	400	2	70	20	2000
	IV. Class	>30	<3	<40	Out of 6.0-9.0	>3000	>5000	-	-	>20	>0.05	>0.65	>400	>2	>70	>20	>2000
Drinking Water Standards	**TS266** (2005)	-	-	-	6.5-9.5	2500	-	-	5	50	0.5	-	250	1.5	-	-	-
	EC (2007)	-	-	-	6.5-9.5	2500	-	-	-	50	0.5	-	250	1.5	-	-	-
	WHO (2011)	-	-	-	-	-	-	-	-	50	0.2	-	-	1.5	-	-	-
Altınyazı Dam Lake	**AD1**	19.4 I. Class	13.0 I. Class	139 I. Class	8.35 I. Class	581 II. Class	282 I. Class	0.28	2.05	2.99 I. Class	0.049 **III. Class**	0.050 II. Class	98.4 I. Class	0.282 I. Class	24.0 I. Class	4.6 II. Class	246 **III. Class**
	AD2	18.6 I. Class	12.1 I. Class	128 I. Class	8.20 I. Class	590 II. Class	287 I. Class	0.29	2.29	3.01 I. Class	0.048 **III. Class**	0.011 I. Class	96.7 I. Class	0.290 I. Class	18.3 I. Class	7.6 II. Class	164 II. Class
Sultanköy Dam Lake	**SKD1**	19.1 I. Class	16.6 I. Class	179 I. Class	8.07 I. Class	537 II. Class	260 I. Class	0.26	3.44	2.01 I. Class	0.082 **IV. Class**	0.050 II. Class	61.8 I. Class	0.280 I. Class	47.0 II. Class	9.1 **III. Class**	208 **III. Class**
	SKD2	17.5 I. Class	18.4 I. Class	192 I. Class	8.24 I. Class	550 II. Class	267 I. Class	0.27	2.60	1.88 I. Class	0.113 **IV. Class**	0.052 II. Class	64.5 I. Class	0.298 I. Class	39.9 II. Class	8.4 **III. Class**	166 II. Class
Süloğlu Dam Lake	**SD1**	24.1 I. Class	9.7 I. Class	118 I. Class	8.21 I. Class	213 I. Class	103 I. Class	0.10	10.10	1.21 I. Class	0.021 **III. Class**	0.076 II. Class	28.4 I. Class	0.214 I. Class	37.7 II. Class	9.2 **III. Class**	264 **III. Class**
	SD2	21.1 I. Class	9.8 I. Class	112 I. Class	8.04 I. Class	247 I. Class	130 I. Class	0.13	7.60	1.29 I. Class	0.016 **III. Class**	0.078 II. Class	24.8 I. Class	0.188 I. Class	29.1 II. Class	7.3 II. Class	350 **III. Class**

[a]Turkish Regulations. 2004; [b]Uslu and Türkman. 1987; *III. – IV. Class water qualities are given in bold

TS266 – Turkish Standards Institute; EC – European Communities; WHO – World Health Organization

AKNOWLEDGEMENTS

The author would like to thank for the financial and technical supports supplied by Trakya University, Turkey. This investigation has been supported by the project numbered as 2017/211 accepted by Trakya University, Commission of Scientific Research Projects.

REFERENCES

EC (European Communities), 2006. EC of the European Parliament and of the council of 6 September 2006 on the quality of fresh waters needing protection or improvement in order to support fish life. Directive 2006/44.

http://www2.dsi.gov.tr/

Köse, E., Tokatlı, C., Çıçek, A., 2014. "Monitoring Stream Water Quality: A Statistical Evaluation". Polish Journal of Environmental Studies, 23 (5): 1637-1647.

Manahan, S. E., 2011. "Water Chemistry: Green Science and Technology of Nature's Most Renewable Resource". Taylor & Francis Group, CRC Press, 398 pages.

TS 266, 2005. Sular-İnsani tüketim amaçlı sular. Türk Standartları Enstitüsü. ICS 13.060.20.

Tokatlı, C., 2014. "Drinking Water Quality of a Rice Land in Turkey by a Statistical and GIS Perspective: Ipsala District". Polish Journal of Environmental Studies, 23 (6): 2247-2258.

Tokatlı, C., 2015. "Assessment of the Water Quality in The Meriç River: As an Element of the Ecosystem in the Thrace Region of Turkey". Polish Journal of Environmental Studies. 24 (5): 2205-2211.

Tokatlı, C., 2017. "Bio – Ecological and Statistical Risk Assessment of Toxic Metals in Sediments of a Worldwide Important Wetland: Gala Lake National Park (Turkey)". Archives of Environmental Protection, 43 (1): 34-47.

Tokatlı, C., Baştatlı, Y., 2016. "Trace and Toxic Element Levels in River Sediments". Polish Journal of Environmental Studies, 25 (4): 1715-1720.

Tokatlı, C., Baştatlı, Y., Elipek, B., 2017. "Water Quality Assessment of Dam Lakes Located in Edirne Province (Turkey)". Sigma Journal of Engineering and Natural Sciences, 35 (4): 743-750.

Tokatlı, C., Köse, E., Çıçek, A., 2014. "Assessment of the Effects of Large Borate Deposits on Surface Water Quality by Multi Statistical Approaches: A Case Study Of The Seydisuyu Stream (Turkey)". Polish Journal of Environmental Studies, 23 (5): 1741-1751.

Turkish Regulations, 2004. Yüzeysel Su Kalitesi Yönetimi Yönetmeliği. 31 Aralık Cuma tarihli Resmi Gazete. Sayı: 25687. http://suyonetimiormansu.gov.tr.

Turkish Regulations, 2012. Yüzeysel Su Kalitesi Yönetimi Yönetmeliği. 30 Kasım 2012 tarihli Resmi Gazete. Sayı: 28483. http://suyonetimiormansu.gov.tr.

Wetzel, R. G., 2001. "Limnology: Lake and River Ecosystems". Elsevier Academic Press, 1006 pages.

WHO (World Health Organization), 2011. Guidelines for Drinking-water Quality. World Health Organization Library Cataloguing-in-Publication Data. NLM classification: WA 675.

5th International Symposium on Dam Safety

October 27-31, 2018

AFFECT TO RUNOFFS OF HYDROLOGICAL SIMILARITIES OF TWO AGRICULTURAL SUBWATERSHEDS WHICH ARE LOCATED IN MERİÇ BASIN

Fatih BAKANOĞULLARI [1], Cantekin KIVRAK[2]

ABSTRACT

In this study, hydrological characteristics of two sub watersheds, which are located in Meriç river basin, have been given. In between 1985 and 2006 years, the annual average rainfall, the annual average and maximum runoff and the annual average water yield have been calculated, respectively for two watersheds.
These sub watersheds of some hydrological characteristics such as area, aspect, shape, slope, curve number and long term precipitation values of similarities with runoff values has been investigated.
Finally, long term average annual runoff value of Kumdere watershed 2.5 times bigger than long term average annual runoff value of Vize creek has been calculated. This result has been affected by curve number difference which relates plant coverage and land using.

Keywords: Kumdere, Vize Creek, Hydrological Similarities, Martiza Basin, Runoff

INTRODUCTION

Although there are many water resources in our country, the precipitation and runoff regimes are very irregular. The rainfall regime is a natural phenomenon and cannot be intervened. However, by technically interfering with runoff events, it is possible to keep the raindrops falling to the soil to the ground or to store the rainwater flowing to the stream, through various tillage techniques and various storage facilities. In this case, the purpose is to harvest the water in a very long period of time and search for ways to use it properly when there is less. It is very difficult to transfer research into nature elsewhere because there are many factors that affect the event. Finding their analogies is quite difficult Leave one blank line after the paragraph heading to begin the paper text. Paper text should be written in 11 point Times New Roman font.

The robustness and reliability of hydraulic structures depend on large-scale hydrological observations and investigations. Topraksu, which has been closed, and the Village Services which have been established in its place, and the State Hydraulic Works, which is currently actively working, are doing these activities in different regions of the country. However, these studies are not sufficient for each investment area. The main reasons for this are the fact that our country is under the influence of different climates, and also the vegetation shows significant differences in topography, soil and geological features. Rainfall and runoff observations are absolutely necessary for the planning and designing of these constructions. As a result of these observations, the amount of precipitation falling in the pond and the amount of runoff based on precipitation through the pond will be determined and

[1] Dr,, ATATÜRK Soil,Water and Agricultural Meteorology Research Institute Kırklareli, Turkey, e-posta: fbakanogullari@gmail.com
[2] Agri. Engineer ,ATATÜRK Soil,Water and Agricultural Meteorology Research Institute Kırklareli Turkey, e-posta: cantekin070@gmail.com

the amount of water coming from the pond will be determined, as well as the accumulation pattern in the storage facility will be identified. As a result of this determination, any kind of sizing on the facilities will be done in good health.

On the other hand, observation and research in every area is never a goal and it is both costly and impossible.The hydrological data obtained in this study and all hydrological structures to be constructed in this and similar basins will be projected more reliably and economically.

MATERIAL

Kumdere and Vize Creek Basin, where the research is applied, are representing the collecting water basins.

General information about the research basin
The Kumdere basin is located about 10 km northwest of Edirne and 10 km away from the central county. It is within the borders of Musabeyli, Hırağa and Karayusuf villages. The basin area is 4.40 km2. When the 1/25000 topographic map of the basin is examined, the waterways are being poured directly into the Meriç River as a branch of Kumdere in 3rd order. The basin exit is at 41^0 40 '59' 'North latitude, 26^0 40' 09 " East longitudes and 115 m high from the sea-level. (Bakanoğulları and Baran, 2006)

The Vize River basin is located within the boundaries of Topçu village, 11 km south of Vize county of Kırklareli province. The basin area is 4.64 km2. When the 1/25000 topographic map of the basin is examined, the Vize River is poured into the Meriç River as a branch from the 5th order. The watershed exit is at 41^0 30 '53' 'North latitude, 27^0 41' 20 " East longitudes and the height from the sea-level is 185 m. (Bakanoğulları and Baran, 2006)

Precipitation and runoff observation stations
There are 3 rainfall stations in the Kumdere watershed and very close to the watershed, and 1 runoff measuring watershed is installed at the exit of the watershed to measure the runoff.
The R-1 precipitation station (1 pluviometer and electronic pluviograph) 115 m high at the watershed exit, the R-2 station (1 pluviometer) at the center of the watershed at 145 m height and the R-3 precipitation station at the 150 m high (1 pluviometer and monthly diagram pluviograph, siphon type) are used to monitor the local and temporal distribution of rainfall.

At the exit of the watershed for runoff observations, a 1/5 tapered triangular weir was built at 115 meters of elevation. Limnigraph, which is connected with a canal near the construction of the weir, measures the temporal distribution of the runoff, through the creek bed with the help of the weir.

There are 3 rainfall stations in the Vize Creek watershed and very close to the watershed, and 1 runoff measuring watershed is installed at the exit of the watershed to measure the runoff.
The R-1 precipitation station (1 pluviometer and electronic pluviograph) at a height of 185 meters at the watershed exit, R-2 station (1 pluviometer) of 222 meters near the western border of the watershed and 233 meters of R- 3 rainfall stations (1 pluviometer and monthly diagram pluviograph, siphon type) are placed to monitor the local and temporal distribution of rainfall.

At the exit of the watershed for runoff observations, a 1/5 tapered triangular weir was built at 185 meters level. Limnigraph, which is connected with a canal near the construction of the weir, measures the temporal distribution of the flow, through the creek bed with the help of the weir.

Kumdere and Vize watersheds of precipitation and runoff stations, water ways, and topographic maps are shown at figure. 1

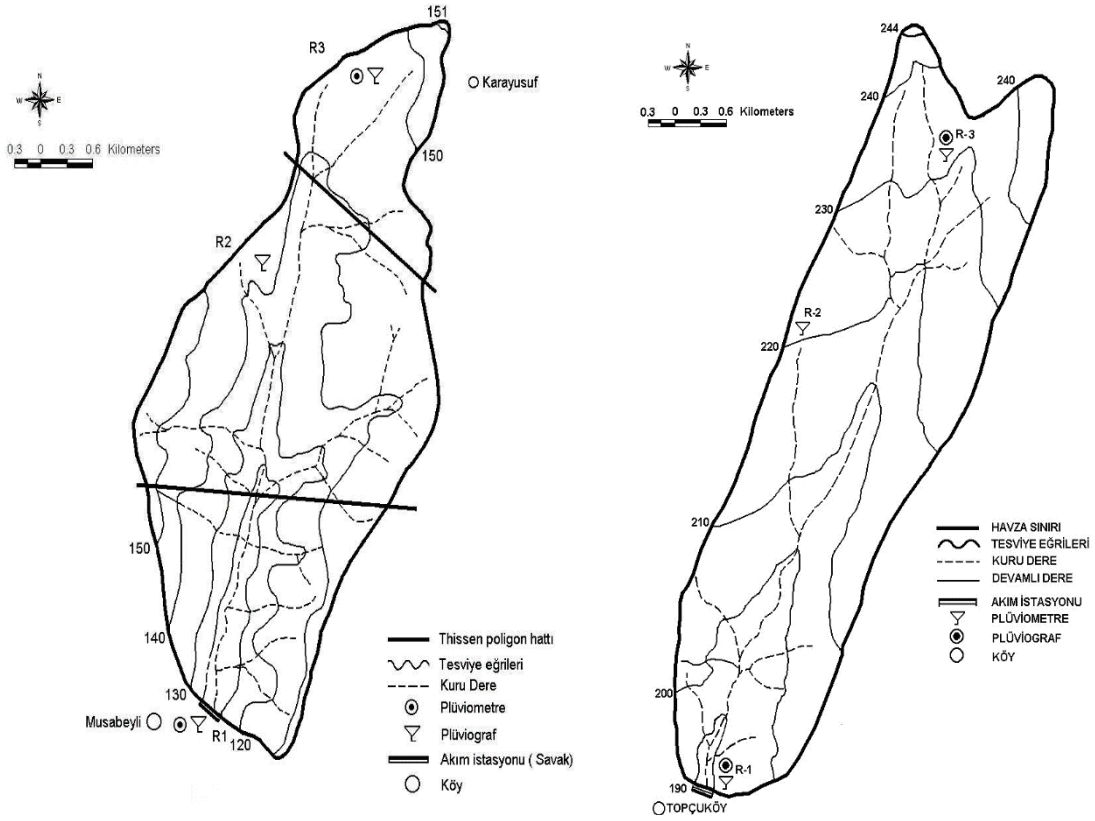

Figure1. Kumdere Watershed and Vize Deresi Watershed Topographic Maps

Soil, geological and hydrogeological properties of watersheds

Detailed soil survey of Kumdere watershed taken from the report of Marmara Watershed fields published in the closed TOPRAKSU General Directorate is explained below.

U5.1-NIIe; the large soil group of this land of 4.378 km2, which constitutes a large part of the total catchment area, is calcareous brown soil. There is medium soil, topography and drainage deficiency which restricts agriculture.

V5.1-N-II_s; Vertisol soil is a large soil group of this land of 0.021 km2 which is a small part of the total watershed area. There is medium soil, topography and drainage deficiency which restricts agriculture.

U9.2-M-IIIe; A very small fraction of the total watershed area, 0.001 km2, is a large soil group, calcareous brown soil. It is in the middle slope, deep, medium erosive soil (TOPRAKSU, 1980).

The watershed consists of two formations in terms of geological structure. The Ergene formation (N1, 3-6) formed by units of white sand, clay, gravel and lacquered is dominant in the watershed. Ergene formation is Upper Miocene old.

The other formation is Sinanlı formation (N1 - N2) formed by limestone clay and marl layers observed around. The other formation is Sinanlı formation (N1 - N2) formed by limestone clay and marl layers observed around Hızır hill in the north of the watershed. This formation is Pliocene.

The detailed soil survey of the Vize River watershed taken from the report of the Marmara Watershed fields published in the closed TOPRAKSU general directorate is explained below.

The large soil group in the 27.4 ha section of the watershed is deciduous brown forest soil. They have A, B, C profiles and offer a well-developed body. It is possible to find the original horizon in this soil which is covered with forest and shrubbery close to the half. There are obviously the decomposed 01 and 02 horizons at various degrees brought by the leaves and stalks in a few centimeters thick on the

mineral section. The thickness of A horizon is approximately 22 cm. There is moderately some structures built up. A horizon does not bloom in acid treatment. The root distribution in this horizon is very large.
The average thickness of the B horizon, known as the bottom soil, is 40 cm. Because of the accumulation of clay in this horizon, it is generally incised from A horizon. It is dominated by silty loamy clay, loamy clay, loamy sandy and fine and medium structures.
The characteristic structure of B horizon is block and formation level is strong. Only in the lower parts of the horizon, that is the C horizon, the structure is weakened.
CaCO3 is not found in the B-horizon, so it is uncreated.
The C horizon is mainly the third time sedimentary mass and unconverted products of metamorphic and volcanic rocks such as gneiss, mixist, basalt, andesite and tuffs. It is usually 75 cm deep. The main material is calcareous clay stones.
In the rest of 19 hectares, the large soil group is the undeclared brown forest land. This dividing feature is near dry, deeply, with little or no erosion, and is already a rare dry agricultural land. It is suitable for all kinds of agriculture.
The watershed geological structure is dominated by the pliocene deviated terrestrial formation, and occasionally clay, sand and pebbles of the Miocene period are encountered. The Istranca massif is based on limestone masses that follow from the south.
All of the watershed forms a crater - top formation (N2 - O1). The Ergene is at the top of the group, age is pliocene. The ergene group generally consists of white yellowish colored cross-layered clay and loose gravel with gravel. Below the Yarma hill formation, there are the upper Miocene aged formation in the same group and formed by river taracas (Umut et al., 1994).

RESULTS AND DISCUSSION

Both watershed which are Kumdere and Vize some physiographic and hydrologic characteristics have been measured and calculated and given at the Table.1

Table 1. Physiographic and hydrologic characteristics of watershed

Watershed name		Kumdere	Vize
Watershed Area	A	4.40 km^2	4.64 km^2
Watershed Perimeter	P	9.50 km	10.55 km
Watershed length	(L_H)	3.45 km	4.45 km
Watershed width	(W_H)	1.28 km	1.03 km
Watershed max. heights	($h_{max.}$)	154 m	244 m
Watershed min. heights	(h_{min})	115 m	185 m
Watershed Reliance	(r)	39	59
Watershed Relative Relief	(r_n)	% 0.041	% 0.56
Watershed direction		North South	Northeast-southwest
Average elevation of the watershed	(h_{or})	139.5 m.	215 m.
Median height of watershed	(h_m)	135 m	212 m
Watershed mean slope	(S_H)	% 4.0	% 3.0
Watershed shape indices			
Index connected to the main waterway	(S_1)	2.71	4.32
Index dependent on watershed length	(S_2)	2.86	4.36

Circularity ratio	(S_3)	0.61	0.52
Condensation index	K_c	1.27	1.37
Watershed rectangular equivalent	L_a L_b	3.49 km 1.26	4.14 km 1.12 km
Slope index to the watershed rectangular equivalent	I_p	% 3.25	% 3.66
Hydrological soil cover no.		80.15	72.15
Main waterway length	(L_s)	3.55 km	4.50 km
Total waterways length	(L_u)	12.50 km	10.25 km
The distance of the watershed center of gravity to the watershed exit of the projection on the main waterway	(L_c)	1.85 km	2.475km
Main waterway profile and slope	S_s	% 0.9	% 1.3
Harmonic slope of main waterway	S	% 0.936	% 0.587
Average annual precipitation of watershed		576.6 mm	548.1 mm
Annual maximum rainfall in watershed		895.7 mm (1999)	848.7 mm (1998)
Watershed average flow		16.22 mm	6.64 mm
Instantaneous maximum flow rate		12760.9 L/s (1985)	6365.22 (1998)
Average unit hydrograph duration		1.00 hour	1.00 hour
Average Unit Hydrograph peak		599.7 L/s	354.63 L/s
Average Unit Hydrograph Time to reach peak		1.3 hours	1.63 hours
Average Unit Hydrograph base time		8.2	14.43 hours
Effective precipitation duration		0.07-2.0 saat	0.1–3.0 hours
Average annual flow coefficient	%	2.8	1.2

Land use and vegetation status of the watershed

Most of the Kumdere Watershed lands (90.9%) is applied fry agriculture. The dominant product is the wheat-sunflower rotation system and both watershed land use is given at table 2. and table 3.

Table 2. Kumdere watershed land use

Vegetations	Covered area km2	% Area
Cereals	2.701	61.4
Sunflower	1.298	29,5

Pasture	0.400	9.1

Table 3. Vize creek watershed land use

Vegetations	Covered area km2	% Area
Shrubbery	2.74	59.05
Cereals	1.88	40.52
Cereals, Vegetables	0.02	.43

The 22-year precipitation and runoff data of two small sub-catchment watersheds located within the province of Kırklareli and Edirne provinces of Meriç watershed are given in tables 4 and 5 respectively. When examined in terms of features and similarities of watersheds, the first factor affecting the runoff is average annual precipitation. The second factor is the average slope of the watershed, which has a significant effect on infiltration, surface runoff, soil moisture and groundwater distribution. The third factor is the surface runoff curve number, which is an indicator of soil and vegetation cover and is used to determine how much of the rainfall will flow to the surface.

These two watersheds seem to have close to each other for a long time in terms of annual rainfall averages. However, when the surface runoffs and subsurface runoffs of the other components of runoffs and the annual total runoff are examined, the average values of Kumdere watershed are 2.5 times higher than those of the Vize Creek watershed. When the average slopes of the watershed are examined, the slopes are close to each other and are located within the same group (slight gradient 2-6%). They differ from surface runoff curve numbers (CN) when examined. It is thought that the biggest factor in this difference is related to the vegetation state. Dry farming without fallowing (Wheat-Sunflower) is carried out in both watersheds. This ratio is 90.9% in Kumdere watershed and 40.52% in Vize river watershed. It is forested in the form of shrubbery at the rate of 59.05% in the Vize River watershed. This land use situation has resulted in a great deal of influence on the runoff in the Vize Creek watershed.

Table 3. Edirne-Kumdere Watershed Precipitation and Runoff Data

YEARS	PRECIPITATION	TOTAL FLOW	SURFACE FLOW	S.SURFACE FLOW	BASE FLOW
1985	460,2	31,89	21,57	8,83	1,48
1986	454,6	11,56	5,29	0,29	5,99
1987	562,2	0,00	0,00	0,00	0,00
1988	668,5	4,77	3,78	0,99	0,00
1989	686,7	11,88	7,40	4,48	0,00
1990	526,5	1,66	1,66	0,00	0,00
1991	537,0	18,82	15,83	2,99	0,00
1992	470,6	1,20	1,09	0,11	0,00
1993	438,0	2,33	1,99	0,34	0,00
1994	504,7	1,22	0,98	0,24	0,00
1995	864,8	28,71	24,42	0,52	3,77
1996	635,1	42,80	25,60	16,80	0,40
1997	558,8	2,49	1,67	0,81	0,00
1998	880,9	30,09	26,79	1,04	2,26
1999	895,7	130,04	89,59	32,60	7,85
2000	396,1	0,06	0,00	0,00	0,06
2001	455,4	0,00	0,00	0,00	0,00
2002	422,2	7,17	0,62	0,00	6,39
2003	505,7	9,48	4,27	0,00	5,20
2004	494,7	1,95	1,70	0,00	0,25
2005	632,4	9,75	3,94	1,86	3,95
2006	634,6	9,00	7,08	0,00	1,92
ORT	576,6	16,22	11,15	3,27	1,80

Table 3. Kırklareli-Vize Deresi Watershed Precipitation and Runoff Data

YEARS	PRECIPITATION	TOTAL FLOW	SURFACE FLOW	S.SURFACE FLOW	BASE FLOW
1985	553,7	0,66	0,56	0,09	0,00
1986	798,9	21,11	1,51	0,01	19,60
1987	678,0	0,80	0,80	0,00	0,00
1988	610,9	0,12	0,11	0,02	0,00
1989	684,4	0,62	0,46	0,16	0,00
1990	555,4	0,00	0,00	0,00	0,00
1991	426,2	0,05	0,05	0,00	0,00
1992	343,9	0,00	0,00	0,00	0,00
1993	266,5	1,12	0,91	0,21	0,00
1994	119,5	0,00	0,00	0,00	0,00
1995	538,7	2,63	0,80	0,66	1,17
1996	412,9	3,78	2,41	1,37	0,00
1997	404,7	3,11	1,44	0,87	0,80
1998	848,7	27,96	17,53	4,06	6,37
1999	789,3	37,26	28,36	5,32	0,00
2000	624,3	7,12	5,00	4,76	0,96
2001	503,6	10,71	0,00	0,00	0,00
2002	675,4	3,77	1,85	0,00	0,00
2003	536,9	19,68	15,60	0,00	4,01
2004	557,7	2,09	1,69	0,00	0,41
2005	450,4	0,39	0,20	0,00	0,19
2006	677,7	3,048	1,71	0,00	1,33
ORT	548,1	6,64	3,68	0,80	1,58

Despite similar characteristics of these two small rural watersheds taking into account the runoffs they have created, which are being investigated by the Ataturk Soil, Water and Agricultural Meteorology

Research Institute, they will contribute to the approaches to be made in the segregation of hydrological regions and to the project engineers.

REFERENCES

Bakanoğulları, F., Baran, M..F, 2006. Edirne-Merkez Kumdere havzası yağış ve akım karakteristikleri Tarım ve Köyişleri Bakanlığı Tarımsal Araştırmalar Genel Müdürlüğü, TAGEM-BB-TOPRAKSU-2006/25, KIRKLARELİ-TURKEY

KIRKLARELİBakanoğulları, F., Baran, M..F, 2006. Kırklareli-Vize deresi havzası yağış ve akım karakteristikleri Tarım ve Köyişleri Bakanlığı Tarımsal Araştırmalar Genel Müdürlüğü, TAGEM-BB-TOPRAKSU-2006/26, KIRKLARELİ-TURKEY

Dizdar, M. Y., 1984 Küçük Havzalarda Yüzey Akışı Eğri Numarasının Tayini. Tarım ve Köyişleri Bakanlığı Topraksu Genel Müdürlüğü Yayınları, Yayın no. 749 ANKARA-TURKEY

Sevinç, A. N., Demirkıran, O., 1995 Terme Çayı Havzalarının Benzerliklerinin İncelenmesi. Köy Hizmetleri Ankara Araştırma Enstitüsü. Basılmamış –ANKARA-TURKEY

TOPRAKSU, 1980. Marmara havzası toprakları, T.C. Köyişleri ve Kooperatifler Bakanlığı, TOPRAKSU Genel Müdürlüğü Yayınları No: 309, Raporlar serisi No: 91, ANKARA-TURKEY

UMUT, M. ve ark. 1994. Edirne ili-Kırklareli ili- Lüleburgaz, Uzunköprü civarının jeolojisi, MTA derleme No: 7064, ANKARA-TURKEY

5th International Symposium on Dam Safety

October 27-31, 2018

EXPERIMENTAL INVESTIGATION OF THE EFFECT OF VEGETATION ON THE WATER DEPTH AND VELOCITY VALUES DUE TO DAM BREAK FOR SUDDEN FAILURE

Ayşegül ÖZGENÇ AKSOY [1], Semire OĞUZHAN[1], Görkem TANIR[1], Mustafa DOĞAN[1], Mehmet Şükrü GÜNEY[2]

ABSTRACT

In this study, the effects of the vegetations on the water depth and velocity values in the case of dam break were investigated experimentally by using the distorted physical model of Ürkmez Dam Lake and its downstream residential area. The horizontal and vertical scales of this distorted physical model are 1/150 and 1/30, respectively. The residential area and the Seferihisar-Kuşadası highway were reflected in the model. The vegetation configuration of the studied area was determined from the related maps and in situ inspections. The vegetation configuration, simulated by plastic sink brushes, was located by taking into consideration the model scales. The sudden failure was simulated by means of a rotating vertical gate. The time dependent water depths in the lake and at downstream part were measured by using Ultrasonic Level Sensors (ULS). The velocities at specified locations were recorded in terms of time by Acoustic Doppler Velocity meter (ADV). The so obtained water depth and velocity values were compared with those obtained from the experiments at which the vegetation configuration was not reflected.

Keywords: Distorted physical model, dam break, vegetation effect, Ürkmez dam

INTRODUCTION

Since dam failures can cause immense damage and loss of lives, this subject attracts the attention of the hydraulic researchers. Dam break experiments are usually carried out in rectangular channels by lifting a gate (Leal et al., 2002; Vasquez and Leal, 2006; Cagatay and Kocaman, 2008; Kocaman and Cagatay, 2009; Hooshyaripor and Tahershamsi, 2015). Morris et al. (2008) investigated dam break by using a 6 m high fill dam constructed in the field.

In this study, the effects of the vegetations on the flood wave propagation in the case of sudden dam break were investigated experimentally by using the distorted physical model of Ürkmez Dam. The horizontal and vertical scales of the distorted physical model are 1/150 and 1/30, respectively. The vegetation configuration, simulated by plastic sink brushes, was located by taking into consideration the model scales. The locations of the plastic sink brushes were determined by using the satellite images of the prototype. The sudden failure was simulated by means of a rotating vertical gate. Time variations of the water depths and velocities were determined during the experiments. The so obtained water level and velocity values were compared with those obtained from experiments of TÜBİTAK 110M240 project at which the vegetation configuration was not reflected.

[1] Department of Civil Engineering, Dokuz Eylul University, Izmir, Turkey
[2] Department of Civil Engineering, İzmir Economics University, Izmir, Turkey

MEASUREMENTS AND EXPERIMENTS

The experiments were performed by using the distorted physical model of Ürkmez Dam which was designed and constructed in the Hydraulic Laboratory of Civil Engineering Department within Dokuz Eylul University. The pictures of the physical model without and with vegetation are given in the Figure 1 and Figure 2, respectively.

Figure 1. Physical model of Ürkmez Dam lake and downstream region without vegetation

Figure 2. Physical model of Ürkmez Dam lake and downstream region with vegetation

The characteristics of the prototype and physical model of Ürkmez Dam are given in Table 1.

The sudden failure scenario is achieved by means of a rotating vertical gate. The clamp is lifted up by a motor and the gate is opened by toppling suddenly. The photos of the sudden failure mechanism are given in Figure 3.

Table 1. The characteristics of the prototype and physical model

Characteristic	Prototype	Model
High of dam (m)	32	1.07
Crest length (m)	426	2.84
Crest Width (m)	12	0.08
Reservoir volume for minimum level (m^3)	375000	0.556
Reservoir volume for maximum level (m^3)	8625000	12.78
Reservoir volume for normal level (m^3)	7950000	11.78
Active capacity (m^3)	7575000	11.22

Figure 3. Sudden failure mechanism

During the experiments temporal variations of water depths were measured by using UltraLab ULS (Ultrasonic level sensor) 80-D device and USS20130 sensors (Figure 4). ULS 80-D has 8 different channels so the water depths were measured simultaneously from 8 different measurement points.

The temporal velocity values were determined by using the Sontek MicroADV which is used to measure water velocity in a wide range of environments such as laboratories, rivers, etc. The device is given in Figure 5.

Figure 4. ULS 80D and USS20130 sensors.

Figure 5. Sontek MicroADV device.

During the experiments water levels were measured at eight different points and velocity was measured at one point. The locations of the measurement points are shown in Figure 6.

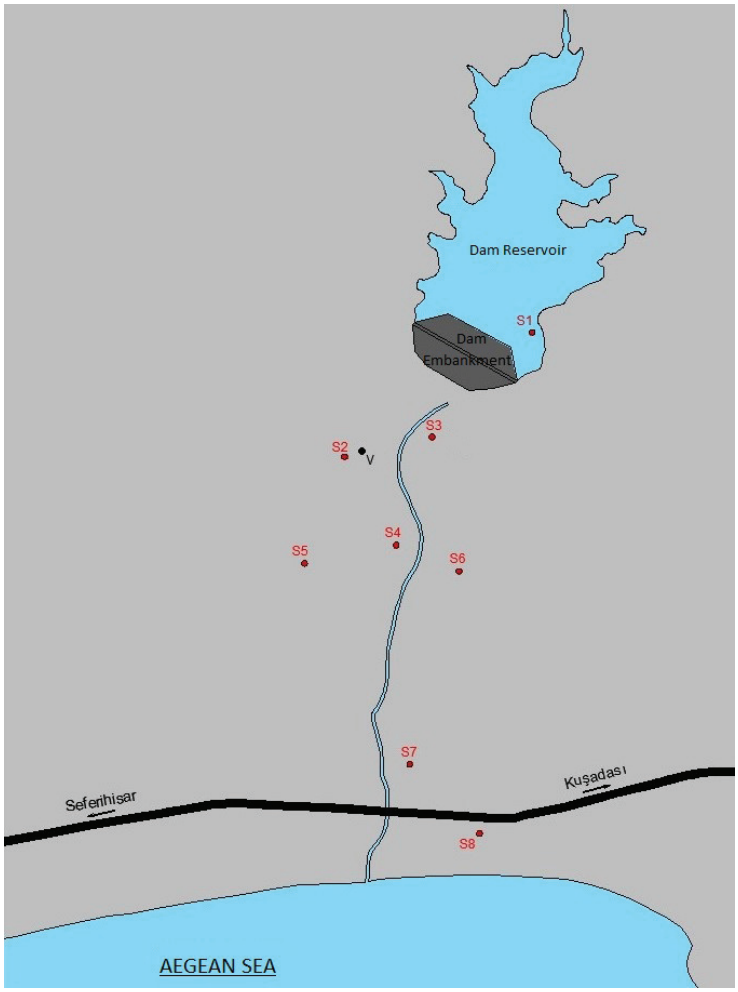

Figure 6. The locations of the measurement points on the physical model.

Kaolin clay was used as suspended solid materials to increase the accuracy of the velocity measurements. Before the experiment dam reservoir was filled up to the maximum level. The output hydrographs related to the experiments with and without vegetation are given in Figure 7. These hydrographs were obtained by means of the model reservoir water depth – volume curve. The water depth-volume curve was generated from the calibration performed previously. Figure 8 depicts time dependent changes of the reservoir level during the experiments. Temporal water levels measured during the experiments are given in Figure 9, 10, 11, 12, 13 and 14.

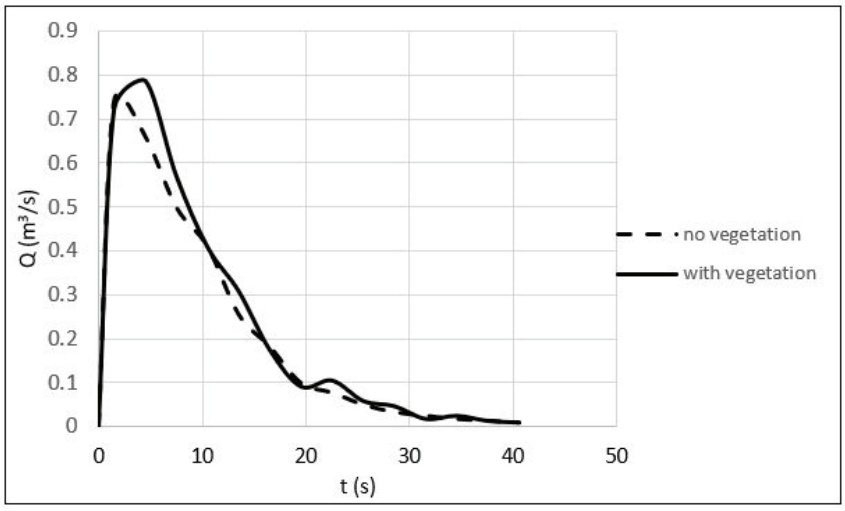

Figure 7. Output hydrographs.

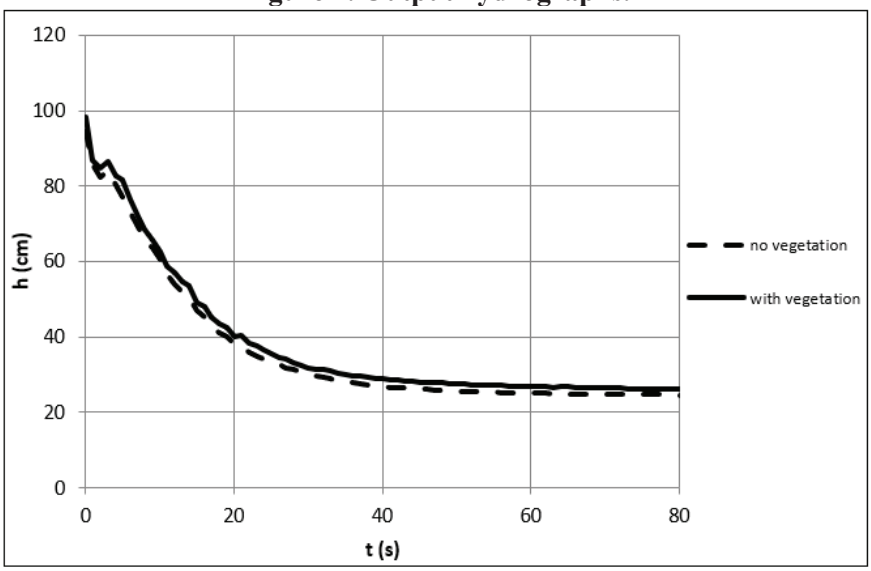

Figure 8. Time dependent variation of the reservoir level.

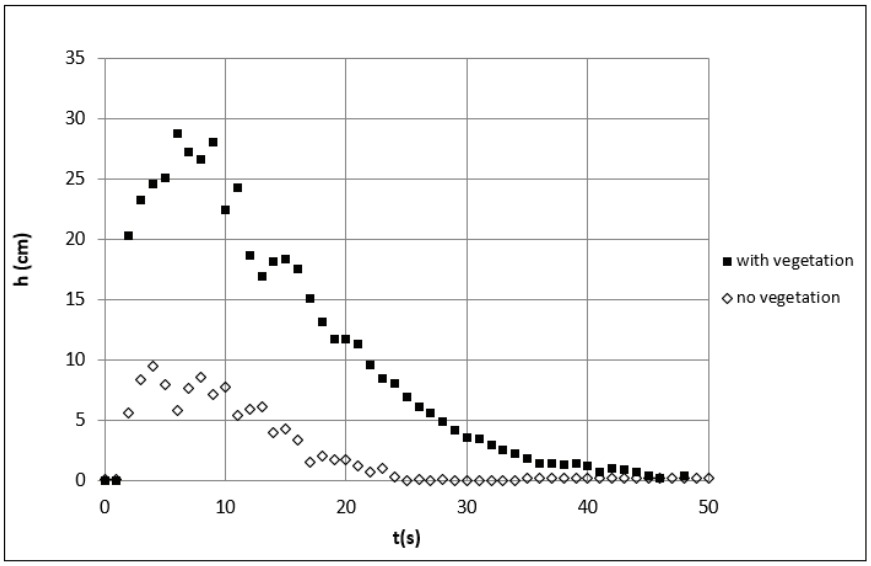

Figure 9. Temporal variation of the water depths measured at S2 point.

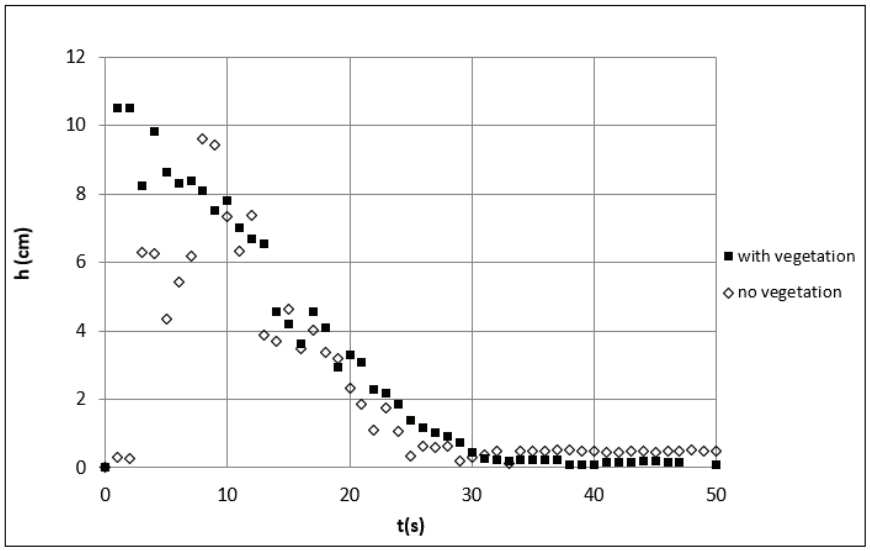

Figure 10. Temporal variation of the water depths measured at S3 point.

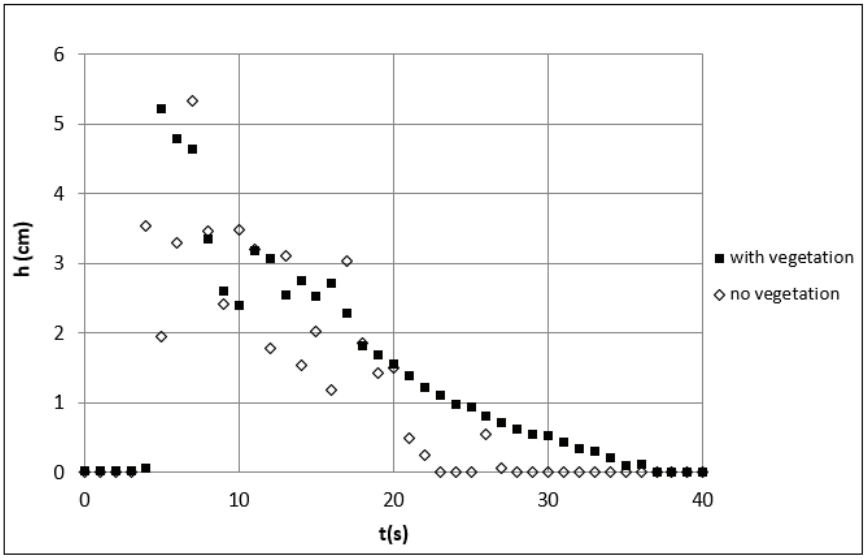

Figure 11. Temporal variation of the water depths measured at S4 point.

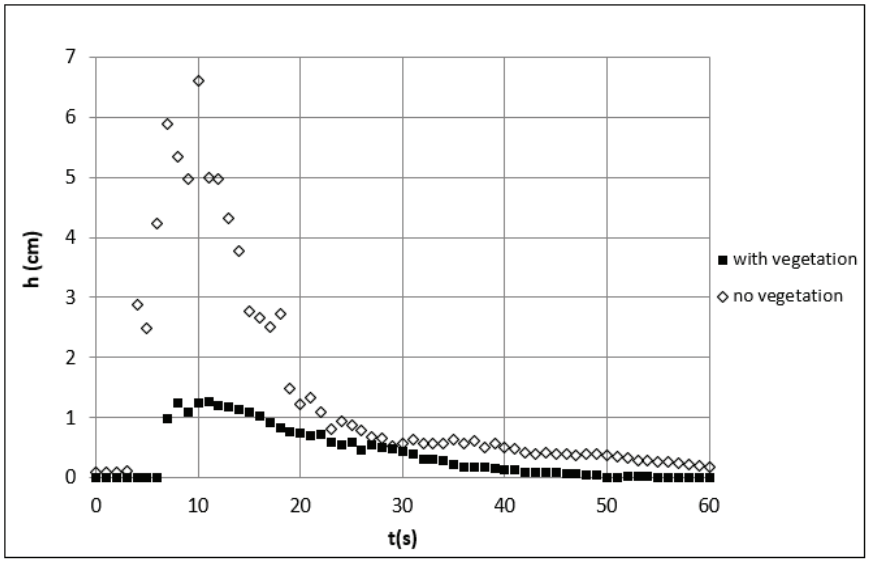

Figure 12. Temporal variation of the water depths measured at S5 point.

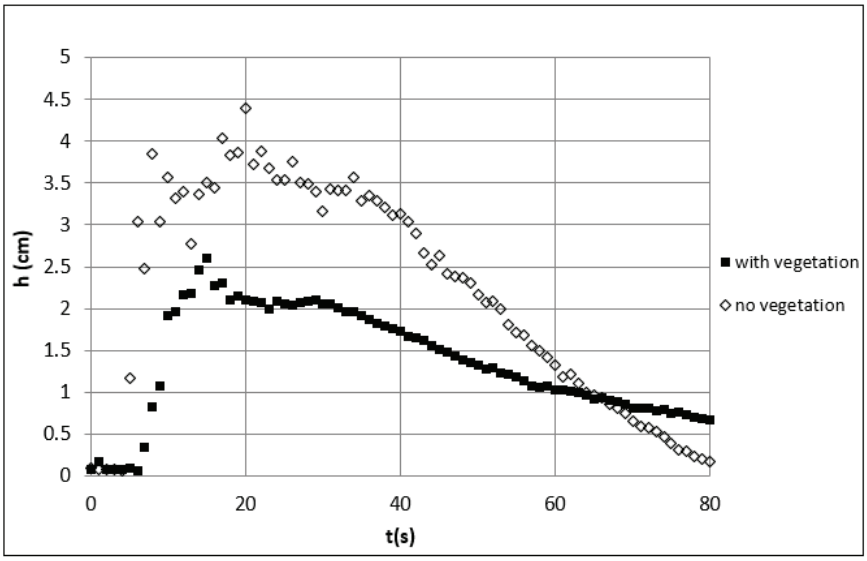

Figure 13. Temporal variation of the water depths measured at S6 point.

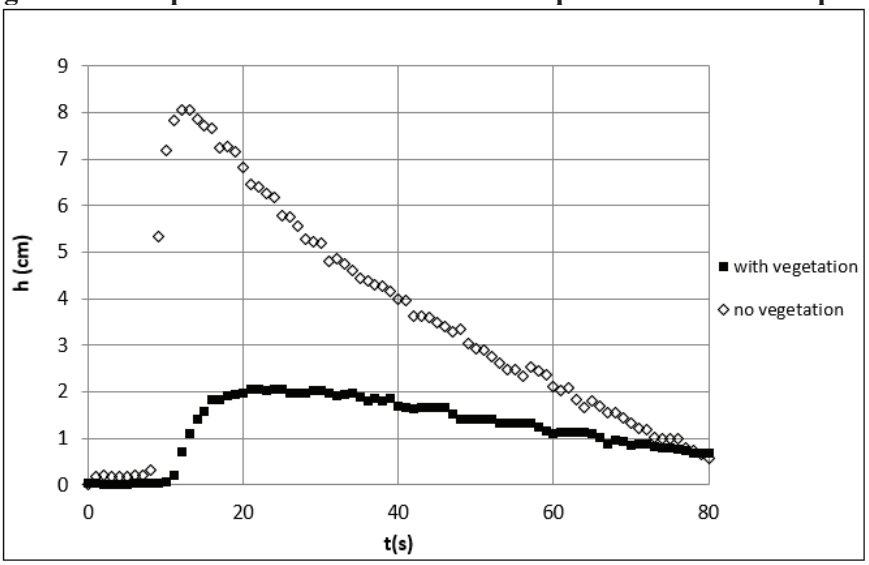

Figure 14. Temporal variation of the at S8 point.

According to the experimental results higher water depths were observed where the vegetation exists intensively, as expected. However, flood wave reaches later and with lower depths the downstream part of the area compared to the without vegetation case.

Time dependent velocities measured during the experiments are presented in Figure 15. The velocity values obtained from the experiment performed with vegetation are smaller than those obtained from the experiments without vegetation.

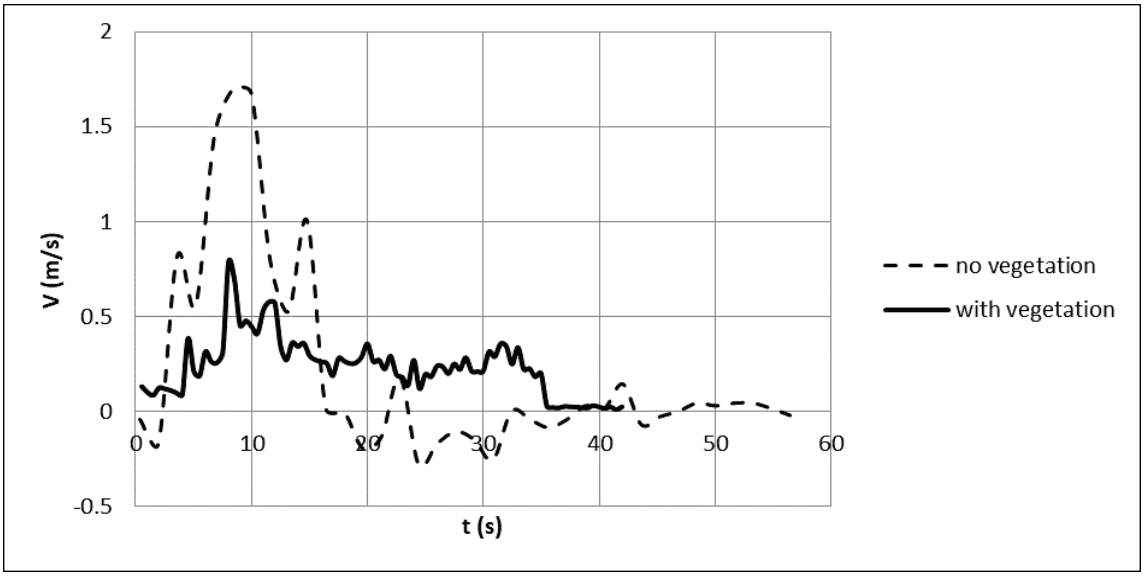

Figure 15. Temporal variations of the velocity measured at point V.

CONCLUSION

In this study, the effects of the vegetations on the water depth and velocity values in the case of dam break were investigated experimentally by using the distorted physical model of Ürkmez Dam Lake and its downstream residential area. According to the experimental results, the presence of the vegetation induced an increase in water depths and a decrease in velocity values. The vegetation also caused the mitigation of the flood wave and so its effect decreased through the downstream part of the studied area.

ACKNOWLEDGEMENT

This study is financially supported by TUBITAK through the 116M237 project.

REFERENCES

Çağatay, H. And Kocaman, S. (2008). "Experimental study of tailwater level effects on dam break flood wave propagation", In Altinakar, Kökpınar, Aydın, ÇokgörveKırkgöz (Eds) Riverflow2008, Volume 1, 635-644, Kubaba, ISBN 978-605-60136-1-4.

Hooshyaripor F., Tahershamsi A. (2015). "Effect of reservoir side slopes on dam-break flood waves" Engineering Applications of Computational Fluid Mechanics, 9:1, 458–468.

Kocaman, S. Ve Çağatay, H. (2009). 'Baraj yıkılması akımının analitik ve deneysel karşılaştırılması. IV. Ulusal Su Mühendisliği Sempozyumu, Orhantepe, İstanbul, 77-87.

Leal, J.G.A.B., Ferreira, R.M.L., Franco, A.B. and Cardoso, A.H. (2002). 'Dam-break waves on movable beds.' In Bousmar&Zech (eds) Riverflow 2002, Volume 2, 981-990.

Morris, M. W., Hassan, M. A. A. M., and Samuels, P. G. (2008). "Development of the HR BREACH model for predicting breach growth through flood embankments and embankment dams." Riverflow2008, Vol. 1, M. S. Altinakar, M. A. Kökpınar, I. Aydın, S. Çokgör, and S. Kırkgöz, eds., Kubaba, Ankara, Turkey, 679–687.

TÜBİTAK 110M240. Final report, Tayfur G., Guney M.S., Haltas İ., Elci S., Bombar G. (2013). "Baraj Yıkılması Sonucu Oluşan Taşkının Deneysel ve Nümerik Metodlar ile Araştırılması— Gerçek Barajlara CBS Ortamında Uygulanması". TÜBİTAK.

Vasquez, J.A. and Leal, J.G.B. (2006). Two-dimensional dam-break simulation over movable beds with an unstructured mesh.In Ferreira, Alves, Leal ve Cardoso (Eds) Riverflow 2006, Portugal, Taylor&Francis, Volume I, 1483-1491. ISBN: 0-415-40815-6.

5th International Symposium on Dam Safety

October 27-31, 2018

PREDICTING OF BEHAVIOR OF MEASUREMENT POINT AT DAM'S

Slavko MILEVSKI [1]

ABSTRACT

The basic element in any construction or infrastructure project is safety. Dams as objects of great significance and the consequences that can cause them should constantly be monitored. The monitoring of dams is performed visually and through embedded instruments in the body and terrain around the dam in order to constantly monitor the safety of the dam. Predicting the behaviour of the measuring points in the future is important for assessing the safety of the dam and timely undertaking any remedial measures. The proceeding will show the application of the method of statistical correlation in predicting the behavior of the measuring points in the future in Electro Power company of Macedonia (ELEM).

Keywords: Dam, accumulation, monitoring, reliability, prediction, statistical correlation

INTRODUCTION

The basic element in any construction or infrastructure project is reliability. The basic element for forming the accumulation is the dam. Dams as objects of great significance and the consequences that can cause them should constantly be monitored. The monitoring of dams is performed visually and through embedded instruments in the body and terrain around the dam in order to constantly monitor the safety of the dam.

The analysis of the data from the technical observation is an important factor for determining the behavior of the dam, for the purpose of assessing the reliability of the dam and the timely undertaking of possible remedial measures. In recent years, there has been increased knowledge that leads to the discovery of analytical methods that use the data from technical observation to obtain better results in predicting the behavior of the dam.

Deterministic and statistical methods are used for the behavior of the dams. The International Committee for Large Dams (ICOLD) recommends using deterministic methods during the design, construction, first filling and the first 5 years of exploitation, while using statistical methods in the case of lateral exploitation of dams. This is because during a longer exploitation, a good foundation of measured data is formed that realistically depicts the state of the dam with the environment. In view of this, the results of analyzes with statistical methods are more reliable. The most commonly used statistical method is the statistical correlation method.

[1] M.Sc.Civ.Eng. Section manager, Technical monitoring and maintenance at dams and other civil objects , JSC "Macedonian Power Plants", Branch HEC "Crn Drim", Struga, R. Macedonia
e-mail: slavko.milevski@elem.com.mk

DAM'S IN ELEM

JSC Macedonian Power Plants (ELEM) owns and operates eight hydropower plants in the Republic of Macedonia, located in south-eastern Europe, with a total installed capacity of 528 MW. The hydropower assets include the five clay core embankment dams of Mavrovo, Spilje, Globocica, Tikves and Kozjak, as well as, the Sveta Petka arch dam. A location map of the dams is given in Figure 1; salient features of the dams are summarized in Table 1.

Figure 1. Location map of the dams belonging to JSC Macedonian Power Plants (ELEM)

Table 1. Salient features of the dams belonging to JSC Macedonian Power Plants (ELEM)

	Name	Type	Year completed	Height [m]	Crest length [m]	Dam volume [103 m3]	Reservoir volume [10^6 m3]
1	Mavrovo	EF	1952	54	210	777	357
2	Spilje	RF	1969	101	330	2'699	520
3	Globocica	RF	1965	83	196	998	58
4	Tikves	RF	1968	104	338	2'722	475
5	Kozjak	RF	2004	114	300	3'340	550
6	Sv. Petka	AR	2011	69	118	27	9

ER – earthfill dam; RF – rock-fill dam; AR – arch dam;

MONITORING OF DAM'S IN ELEM

The monitoring instrumentation in the first four dams is, to a large extent, the same as originally installed more than 40 years ago and due to careful maintenance most of the instruments are still in good condition. However, some components, such as the readouts for the cells measuring the pore and

total pressures in the dam bodies and the seismic monitoring equipment, were outdated. ELEM therefore brought under way a project for the rehabilitation of the dam monitoring instrumentation. At the same time a comprehensive program for the automation of the monitoring instrumentation and transmission of the monitoring data to a central auscultation center for all dams under ELEM's responsibility was initiated. This transmission of the monitoring data also included the more recent dams of Kozjak (commissioned in 2004) and Sveta Petka (commissioned in 2012), which already had local systems for automatic dam monitoring.
The following sections describe the systems installed.

AUTOMATIC MONITORING SYSTEMS INSTALLED

For each dam site a local Automated Data Acquisition System (ADAS) was established. The automation of the dam instrumentation comprised, as far as practicable, all the existing measuring systems, and among others the following:

- Open piezometer pipes were equipped with vented pressure transducers;
- Manometers for measuring piezometers under pressure were complemented with vibrating wire pressure transducer. Such piezometers are mainly located in the dam galleries but also in the abutments;
- Seepage and leakage water measurement locations were outfitted with pressure transducers;
- The reservoir water level measurements were automated by mean of vented pressure transducers, for which installation required a specialized diver.

The local Data Processing Centers are connected to the Central Control Station forming a client/server architecture that provides the services of recording, processing, visualization and analysis of the monitoring data. In particular, the local Data Processing Centers:

- allow elaboration of the data from the individual instruments or from instrument groups in graphic and numeric form;
- summarize data from the individual instruments or of instrument groups in long term graphs or numeric tables;
- allow the display of alarms when readings from selected instruments reach specified values;
- allow the manual input of data and the download of data from the handheld field computer, used for manual readings, and from the portable data logger.

Automatic monitoring produces many data and therefore the methodology of data processing and analysis is very important for interpreting data and predicting the behavior of the measurement points in the future.
One of the methods for behavior analysis at the metering point is the method of statistical correlation.

METHOD OF STATISTICAL CORRELATION

For the analysis of the data from the monitoring of the dams from the French electricity industry under the name "global seasonal analytical method" (Methode d'analysis globale). This method is also known as the "hydrostatic-season-time HST" (hydrostatic-season-time HST). This method significantly improved the analysis of the behavior of the dams. This method represents the French standard in technical observation and is accepted worldwide.
The HST model is based on the following:
It is assumed that the measuring size can be written in the following form:

$$y_i = F(t) + F(h) + F(s) \tag{1}$$

The three components are:

$F(t)$: influence of time (irreversible effect consisting of a linear combination of positive and negative exponential functions;

$F(h)$: hydrostatic impact (the effect of hydrostatic pressure on the upstream side of the dam, consisting of fourth-degree polynomials)

$F(s)$: impact of the season (season effect, which is a sum of four sine functions with a one-year and six month period);

The analysis is carried out as follows. The period of data for which the analysis is made is selected. For this data set an incomplete system of linear equations is formed. By solving the system, the coefficients of the polynomial are obtained. It is important to note that there should be at least 40 data and over 5 years of data measurement. A table with values for the behavior of the measuring point for a period in the future will be formed with this obtained polynomial.

The HST method is also used by the service for technical observation of dams and other buildings in JSC ELEM for assessment of the behavior of the instruments in the future. An own application has been made that uses measured data from the instruments in the past period. In the following text is a description of several examples of the analysis and assessment of the behavior of the measuring points in bulk and concrete concrete dam.

The analysis is carried out as follows. The period of data for which the analysis is made is selected. For this data set an incomplete system of linear equations is formed. By solving the system, the coefficients of the polynomial are obtained. It is important to note that there should be at least 40 data and over 5 years of data measurement. A table with values for the behavior of the measuring point for a period in the future will be formed with this obtained polynomial.

The HST method is also used by the service for technical observation of dams and other buildings in JSC ELEM for assessment of the behavior of the instruments in the future. An own application has been made that uses measured data from the instruments in the past period. In the following text is a description of several examples of the analysis and assessment of the behavior of the measuring points installed downstream of dam's.

EXAMPLES FOR THE USE OF THE METHOD OF STATISTICAL CORRELATION

In order to illustrate the practical application of the method of statistical correlation, there are several examples for analyzing the values of open piezometer's downstream of dam that are dependent on the level of the accumulation.

Following charts present more realistic examples from piezometers monitoring on a dam. HST model of measurements comparing and forecast values is applied on these piezometers.

The measurements from 1970 to 2002 are taken into account. At each figure, the top chart is graph of precipitation, the middle one is graph of water level in accumulation and bottom chart is graph of measurement point (full line) and forecasting value at measurement point (with HST methodology).

At Figures 2, 3, 4 are given an example's of measurement point (piezometer) where statistical correlation is applied to a measuring point that has a trend of increasing of values over time, decreasing of values over time and no trending. In all cases there is good adaptability of the acquired polynomial with the HST methodology (dot's) and measured values (line).

At Figure 5 is given an example where measurement data are missing in a certain period and their interpolation with the HST methodology

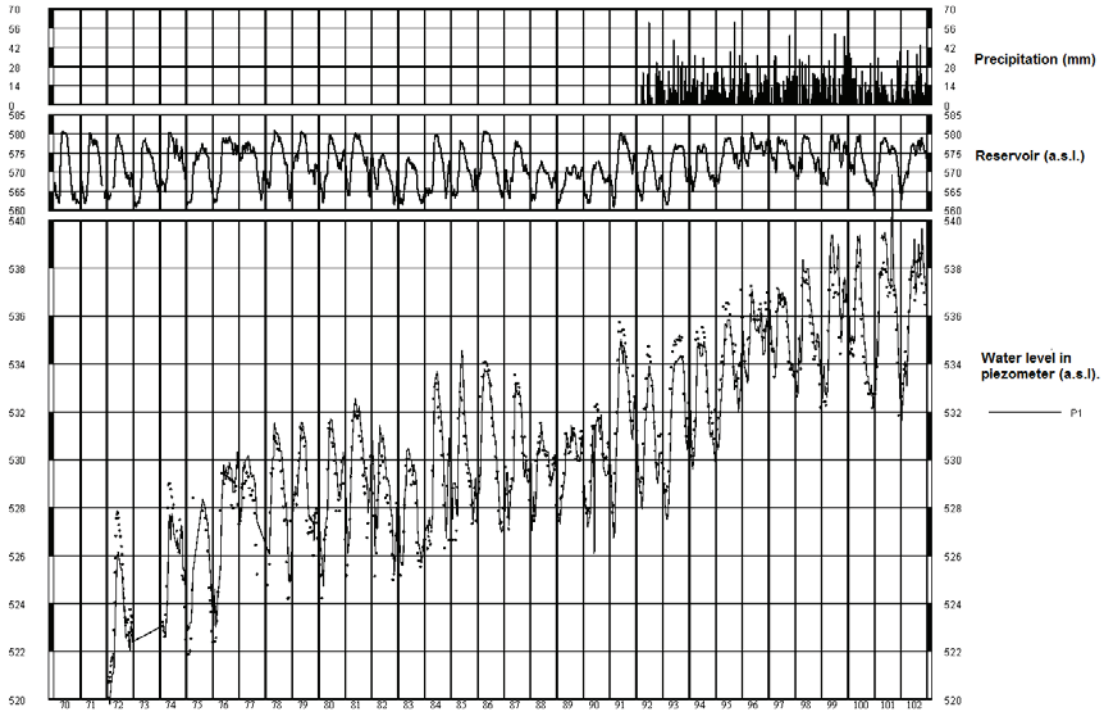

Figure 2. Graphical view of gathered data from dam monitoring where trend of measured values is increasing in time (line) with piezometer's trend prognosis by model (dots);

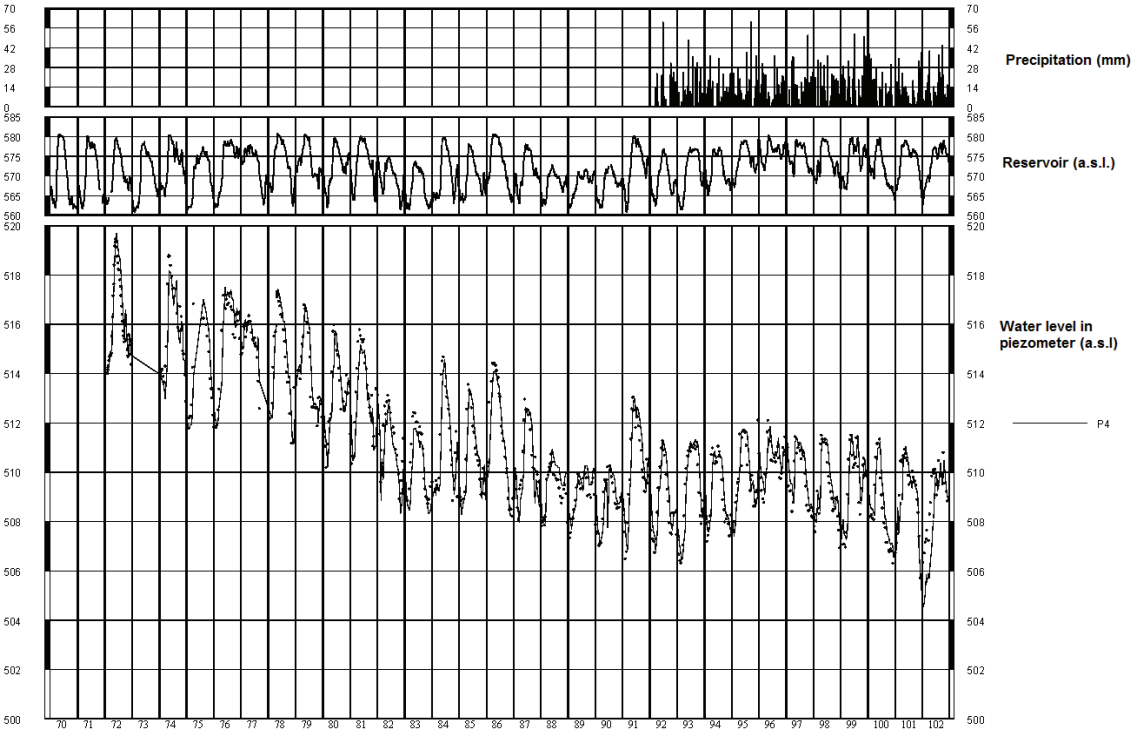

Figure 3. Graphical view of gathered data from dam monitoring where trend of measured values is decreasing in time (line) with piezometer's trend prognosis by model (dots)

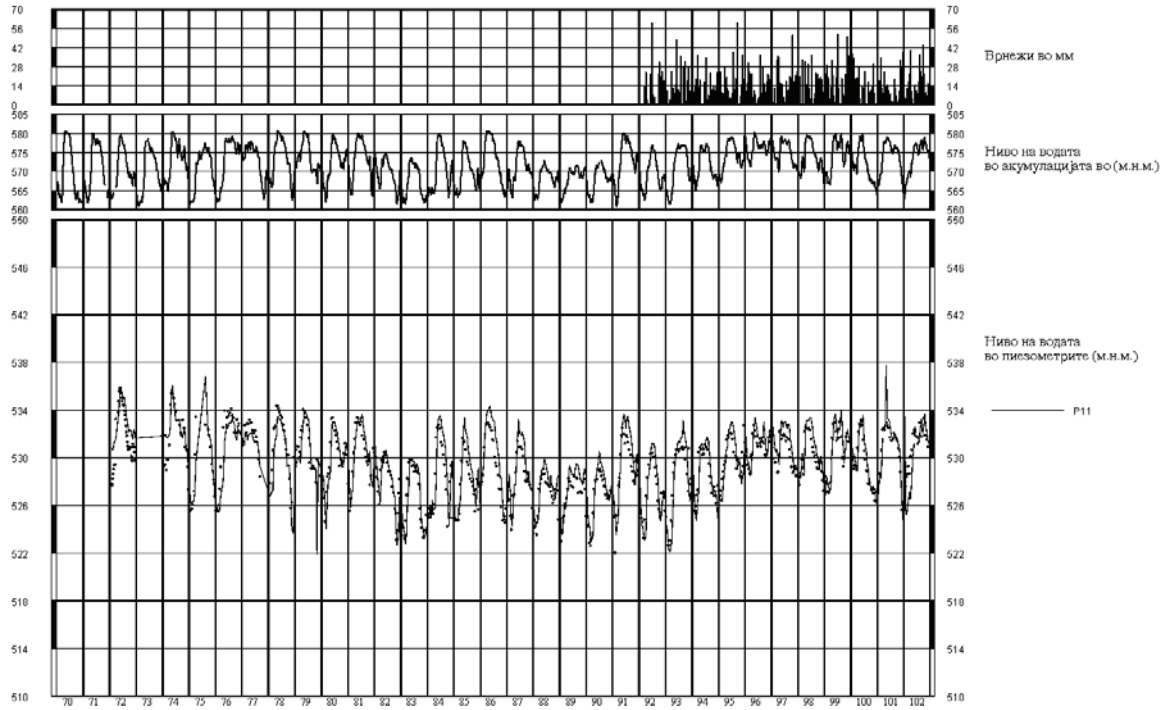

Figure 4. Graphical view of gathered data from dam monitoring where there is no trending during the given time frame (line) with piezometer's trend prognosis by model (dots)

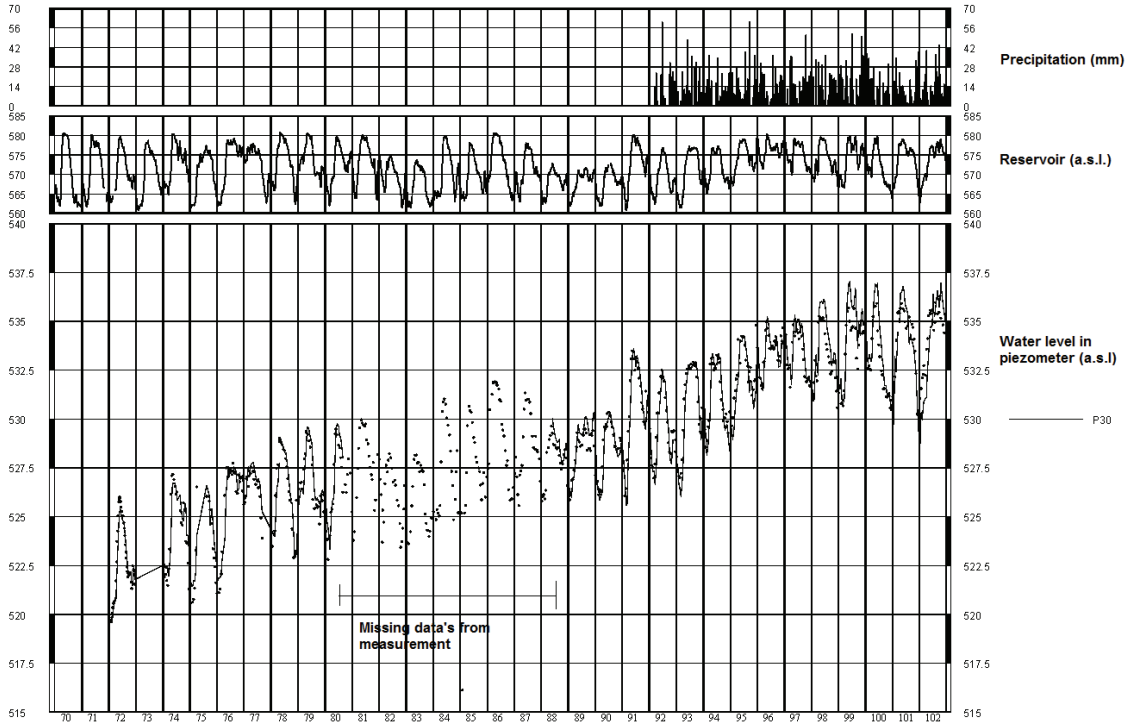

Figure 5. Graphical view of gathered data from dam monitoring where there is no data for period of 8 years (line) with piezometer's trend prognosis by model (dots)

EXAMPLES FOR THE USE OF THE METHOD OF STATISTICAL CORRELATION FOR PREDICTION OF VALUE IN THE FUTURE

Following charts present use of statistical correlation method for prediction fo values of measurement point in future. At figure 6 is given chart of precipitation, reservoir and measurement point with applied HST method (pink box). From chart is seen than polinom calculated with HST methodology is very good. T values obtained by the HST methodology are almost glued to the measured values.
At figures 7 and 8 is presents graphic and tabular displays of expected minimum, maximum and average values at the measuring point for the corresponding minimum, maximum and average reservoir values in 2025 to 2030 year.

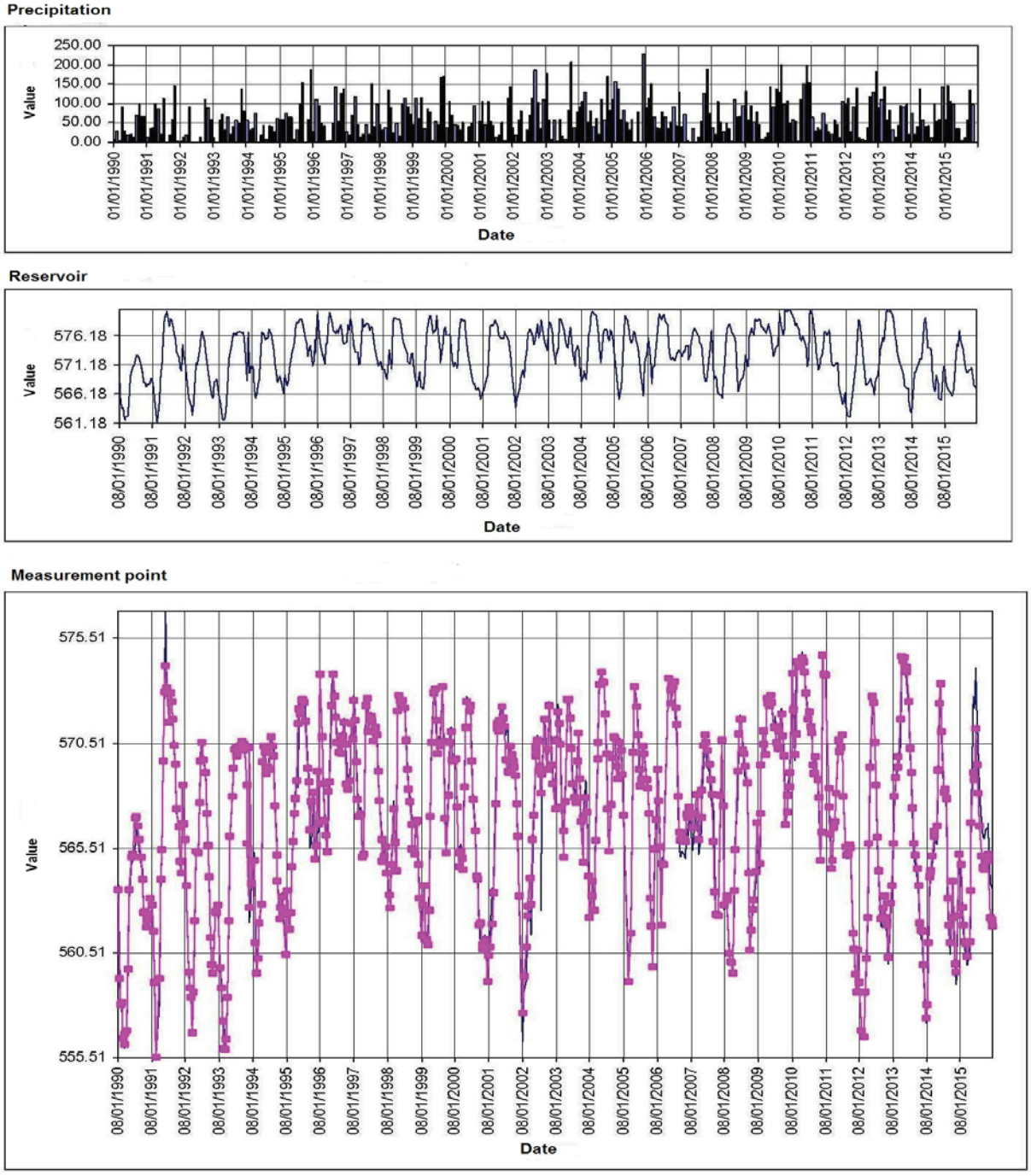

Figure 6. Chart of precipitation, reservoir and measurement point with

applied HST method (pink box)

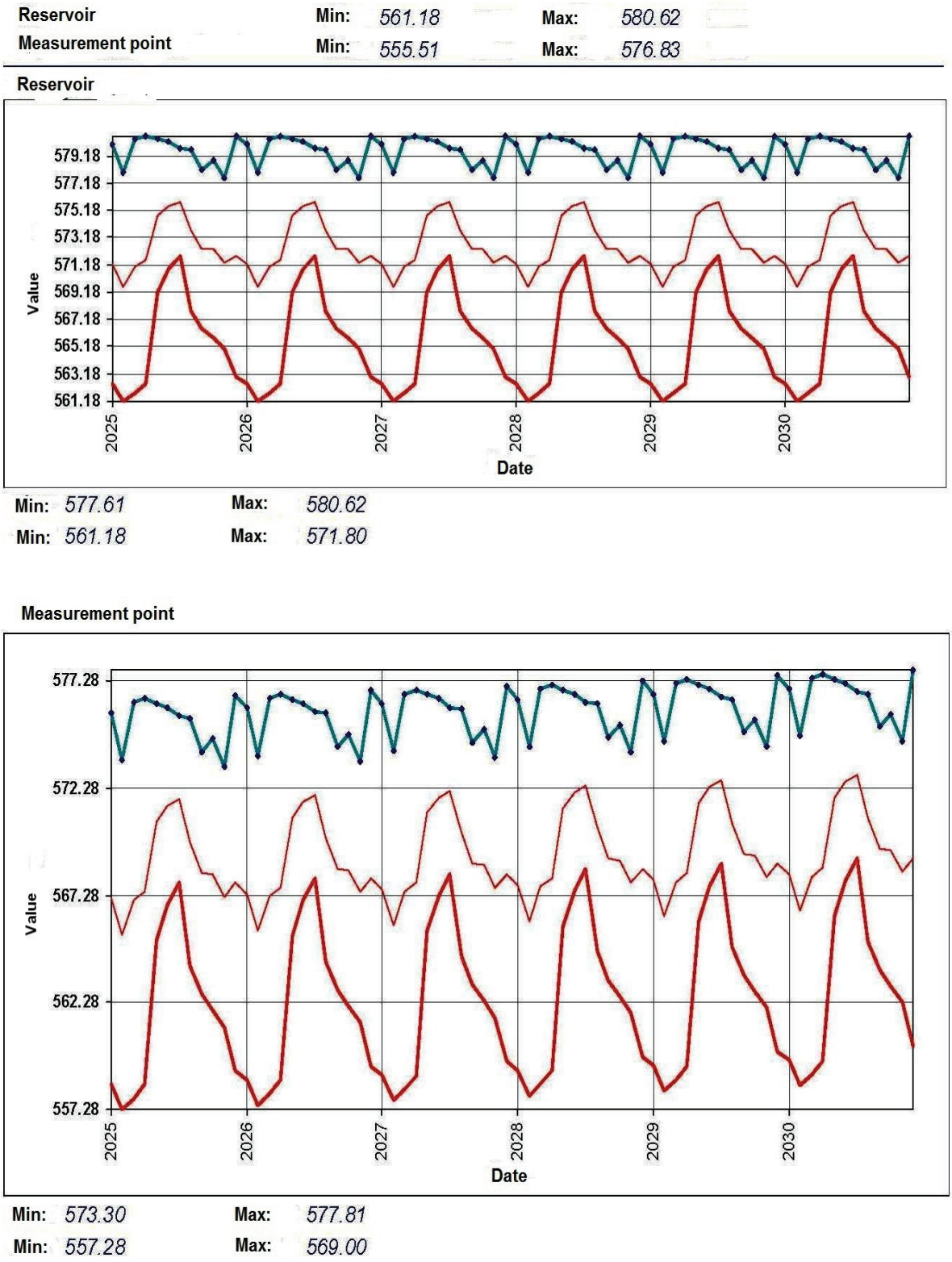

Figure 7. Predicted minimum, maximum and average value of measurement points in 2025 to 2030 year (graphic)

Reservoir	**Min**	*561.18*	**Max**	*580.62*
Measurement point	**Min**	*555.51*	**Max**	*576.83*

Reservoir, max. value

Year	Month 01	02	03	04	05	06	07	08	09	10	11	12
2025	580.05	577.98	580.41	580.59	580.40	580.18	579.76	579.63	578.20	578.82	577.61	580.62
2026	580.05	577.98	580.41	580.59	580.40	580.18	579.76	579.63	578.20	578.82	577.61	580.62
2027	580.05	577.98	580.41	580.59	580.40	580.18	579.76	579.63	578.20	578.82	577.61	580.62
2028	580.05	577.98	580.41	580.59	580.40	580.18	579.76	579.63	578.20	578.82	577.61	580.62
2029	580.05	577.98	580.41	580.59	580.40	580.18	579.76	579.63	578.20	578.82	577.61	580.62
2030	580.05	577.98	580.41	580.59	580.40	580.18	579.76	579.63	578.20	578.82	577.61	580.62

Reservoir, min. value

Year	Month 01	02	03	04	05	06	07	08	09	10	11	12
2025	562.50	561.18	561.76	562.46	569.20	570.82	571.80	567.78	566.48	565.80	565.06	562.98
2026	562.50	561.18	561.76	562.46	569.20	570.82	571.80	567.78	566.48	565.80	565.06	562.98
2027	562.50	561.18	561.76	562.46	569.20	570.82	571.80	567.78	566.48	565.80	565.06	562.98
2028	562.50	561.18	561.76	562.46	569.20	570.82	571.80	567.78	566.48	565.80	565.06	562.98
2029	562.50	561.18	561.76	562.46	569.20	570.82	571.80	567.78	566.48	565.80	565.06	562.98
2030	562.50	561.18	561.76	562.46	569.20	570.82	571.80	567.78	566.48	565.80	565.06	562.98

Reservoir, aver. value

Year	Month 01	02	03	04	05	06	07	08	09	10	11	12
2025	571.28	569.58	571.08	571.53	574.80	575.50	575.78	573.71	572.34	572.31	571.33	571.80
2026	571.28	569.58	571.08	571.53	574.80	575.50	575.78	573.71	572.34	572.31	571.33	571.80
2027	571.28	569.58	571.08	571.53	574.80	575.50	575.78	573.71	572.34	572.31	571.33	571.80
2028	571.28	569.58	571.08	571.53	574.80	575.50	575.78	573.71	572.34	572.31	571.33	571.80
2029	571.28	569.58	571.08	571.53	574.80	575.50	575.78	573.71	572.34	572.31	571.33	571.80
2030	571.28	569.58	571.08	571.53	574.80	575.50	575.78	573.71	572.34	572.31	571.33	571.80

Measurement point, max. value

Year	Month 01	02	03	04	05	06	07	08	09	10	11	12
2025	575.82	573.60	576.28	576.47	576.25	576.05	575.66	575.56	573.99	574.59	573.30	576.64
2026	576.02	573.80	576.48	576.67	576.45	576.26	575.86	575.77	574.20	574.80	573.51	576.85
2027	576.23	574.02	576.70	576.89	576.66	576.47	576.08	575.99	574.42	575.02	573.73	577.07
2028	576.45	574.24	576.92	577.11	576.89	576.70	576.31	576.21	574.65	575.25	573.96	577.31
2029	576.69	574.47	577.15	577.35	577.13	576.94	576.55	576.45	574.89	575.49	574.20	577.55
2030	576.93	574.72	577.40	577.60	577.38	577.19	576.80	576.71	575.14	575.74	574.46	577.81

Measurement point, min. value

Год.	Month 01	02	03	04	05	06	07	08	09	10	11	12
2025	567.15	565.44	567.04	567.46	570.72	571.45	571.76	569.78	568.33	568.26	567.22	567.86
2026	567.35	565.64	567.24	567.66	570.93	571.65	571.96	569.99	568.54	568.46	567.43	568.07
2027	567.56	565.85	567.46	567.87	571.14	571.86	572.18	570.21	568.76	568.68	567.65	568.29
2028	567.78	566.08	567.68	568.10	571.37	572.09	572.41	570.44	568.99	568.91	567.88	568.53
2029	568.02	566.31	567.92	568.33	571.61	572.33	572.65	570.68	569.23	569.16	568.12	568.77
2030	568.26	566.56	568.16	568.58	571.85	572.58	572.90	570.93	569.48	569.41	568.38	569.03

Measurement point, aver. value

Year	Month 01	02	03	04	05	06	07	08	09	10	11	12
2025	558.48	557.28	557.80	558.44	565.20	566.84	567.86	564.01	562.67	561.92	561.14	559.08
2026	558.68	557.48	558.01	558.64	565.40	567.04	568.06	564.21	562.88	562.13	561.35	559.29
2027	558.89	557.69	558.22	558.86	565.62	567.26	568.28	564.43	563.10	562.35	561.57	559.51
2028	559.11	557.91	558.44	559.08	565.85	567.49	568.51	564.66	563.33	562.58	561.80	559.74
2029	559.34	558.15	558.68	559.32	566.08	567.72	568.75	564.90	563.57	562.82	562.04	559.99
2030	559.59	558.40	558.92	559.57	566.33	567.97	569.00	565.15	563.82	563.08	562.30	560.24

Figure 8. Predicted minimum, maximum and average value of measurement points in 2025 to 2030 year (table's)

CONCLUSION

In well managed Dam's contemporary approach of dam surveillance is combination of HST statistical models and finite-element geo-mechanical models. Usage of statistical methods is first step towards full appraisal of the dam's condition. Macedonian Power plant's department for technical monitoring and maintenance of dams and other civil objects is utilizing the analytical method to forecast the values and trends at the measurement points which are covered by the long period dams surveillance at given reservoir water levels. These methods can't be used to discover why certain parameters changed, but only to acknowledge that the actual change occurred and for successful practical utilization of these models, minimum 5 years of previously measured values are needed. With usage of these methods, the engineers can make predictions on eventual developments that can potentially jeopardize the dam security in future.

REFERENCES

HPP "Globochica", Struga Report's for dam monitoring in Electro Power Company of Macedonia.
HPP "Globochica", Struga, "Project documentation from investigation, building and maintenance of dam's in Electro Power Company of Macedonia

5th International Symposium on Dam Safety

October 27-31, 2018

THE EUPHRATES-TIGRIS RIVERS AND THE DETERMINATION OF TURKEY

Selami OĞUZ

ABSTRACT

The Euphrates and Tigris Rivers are two transboundary bodies of water that spring from eastern Turkey and flow into the Persian Gulf. The total amount of water that originates in Turkey and carried by these two rivers to the border is 48-50 billion m3/year, and this constitutes approximately 60% of the water carried by Shatt-al Arab. Turkey has started working on the Euphrates and Tigris Rivers in 1930s to produce energy and to irrigate land and has produced 30 billion kWh of energy and opened 420 thousand hectare of agricultural land to irrigation to-date. Turkey pays extreme attention to the water rights of its downstream countries. Turkey wishes these waters to bring peace to her neighbors, and for this, has proposed to develop common scientific and technology-based strategies in a three-phase plan to Syria and Iraq. The three countries, sharing a common religion, culture and several hundred years of common history should be able to also share peacefully the waters of the two rivers. This paper, which was prepared by a engineer who worked actively on the largest structure on Euphrates, the Ataturk Dam and the hydroelectric power plant, presents how the people of the three countries sharing the resources of the Euphrates and Tigris can collaborate with good will for their mutual future benefit.

Keywords: Euphrates, Tigris, Transboundary Rivers, Water resources

INTRODUCTION

The Euphrates and Tigris Rivers are two transboundary bodies of water that spring from eastern Turkey and flow into the Persian Gulf. The Euphrates River springs from high mountain ranges in northern parts of the East Anatolian Region in Turkey in two tributaries. These tributaries join after 400-500 km to form what is called Euphrates. The river flows within Turkey a distance of 500 km from its spring site until the Syria-Turkey border and then enters Iraq through Syria to join the Tigris. The Tigris River springs out from the highlands of the southern part of East Anatolian Region, flows through a distance of around 530 km within Turkey and joins the Euphrates River in Iraq. The point where these two rivers join is called Shatt-al Arab, and this single water body discharges into the Persian Gulf after a distance of about 100-150 km. In terms of the water load, the Euphrates and Tigris rivers are the two largest rivers in Turkey. The annual water load the Euphrates carries from Turkey into Syria is 30– 31 m3/year, whereas the Tigris has an annual water flow load into Iraq of 18-19 m3/year. The total amount of water these two rivers carry outside Turkish borders is 48-50 m3/year;

considering the total water capacity of Shatt-al Arab being 85 billion m3/ year, we estimate that almost 60% of the water flowing in these two rivers should spring from Turkey.

HISTORY

Flowing for centuries, these rivers have given life to the Lower Mesopotamia region where the first civilizations in history have flourished. The Euphrates and Tigris Rivers springing from the highlands of East Anatolian Region of Turkey have caused erosion for centuries as they have flown through high slopes in Turkey and formed vast alluvium plains in Iraq where the land has developed lower slopes with the sediments. As a result of such natural flows, Turkey has faced severe erosion and desertification, whereas Iraq and Syria have made use of fertile plains rich in alluvium.

Works on the Euphrates River

Works of Turkey on the Euphrates River to make use of the river with the advantages provided by technology date back to 1930s. These works have commenced with hydrology and geology research necessary for energy production tasks. Those tasks were carried out by experts invited from technologically more advanced countries at that time and these initiatives by Turkey to generate energy on the Euphrates River has continuously been hindered by foreign experts and powers behind them with a number of excuses.

Manifesting the decisiveness on the Euphrates River in 1960s and constructing Keban Dam and Hydroelectric Plant, Turkey managed generation of 6 billion Kwh of energy upon the completion of Keban Dam in 1974. This is the first serious and strong step in Turkey's struggle on utilizing the Euphrates River. Turkey re-shaped planning and project tasks commenced under the name of Lower Euphrates Project together with the country's own technical ability upon including the Tigris River into the process in the 70s under the name of Southeastern Anatolia Project (GAP) thus, has manifested its commitment to utilize the capacity of these rivers in prevention of floods, generation of energy and irrigation. The very first product of this commitment is the Karakaya Dam and Hydroelectric Plant constructed after Keban Dam on the Euphrates River, which commenced operation in 1987 with an annual capacity of 7.5 Kwh.

The biggest step in GAP is the construction of Atatürk Dam and Hydroelectric Plant. Foreign assistance was used only for the electromechanical devices of energy generation; the rest of the project was financed completely by national resources. While the project, construction and technical maintenance for Keban and Karakaya

Dams were conducted by foreign companies, the project and maintenance of Atatürk Dam was a joint work of Turkish and foreign companies, construction by Turkish firms, and production as well as mounting of the electromechanical systems were made by foreign companies.

Atatürk Dam and Hydroelectric Plant have great importance in the history of Turkish engineering. That importance can be seen as follows: The construction work of this world-scale dam was conducted completely by Turkish technical labor. Turkey gained a respectable position within the World Dams League by constructing this dam of 169 m in height and 83 million m3 in volume in a period of only 10 years. The real important feature of this project is that it made possible for the first time in history to transfer Euphrates waters to the plains of Upper Mesopotamia through Şanlıurfa irrigation pipes of 2 x 26.4 km long, that were also constructed by Turkish labor. Other dams constructed on the main tributary of the Euphrates River are Birecik and Karkamış Dams and Hydroelectric Plants, which provide 2.8 + 0.652 =

3.452 billion Kwh energy annually. With the completion of these dams, the overall dam construction on the Euphrates River is complete. Facilities that need to be constructed on the tributaries of the river are planned and constructed within the framework of a plan and program and with the use of national sources and labor. Turkey has progressed far in its struggle to develop the watershed of Euphrates. The installed capacity and annual energy generation rates of the plants and facilities built on the main tributary of Euphrates River are presented in Table 1. The use of the river for irrigation will be presented under the title of GAP.

Table 1. Installed Capacity, Annual Generation and Generation-to-date of the Plants and the Facilities Built on the Main Tributary of Euphrates River

Dam	Installed Capacity (MW)	Annual Generation (kWh/year)	Generation-to-date (kWh)
Keban	1330	6 billion	204 billion
Karakaya	1800	7,5 billion	158 billion
Atatürk	2400	8,9 billion	128 billion
Birecik	672	2,83 billion	25 billion
Karkamış	189	0,65 billion	6 billion
TOTAL	6391	25,88 billion	519 billion

Works on the Tigris River

Works that commenced on the Tigris River during 1970-80s have failed to be completed on schedule due to financial challenges and primarily the separatist terror acts.
Kralkızı, Dicle, and Batman Dam and Hydroelectric Plants on the main tributary of Tigres River has been completed. The most important construction of Ilısu Dam and Hydroelectric Plant has commenced in 2006.

After long and challenging struggles, foreign credit was made available for the project. The counselor of the project is a Turkish-foreign partnership and the construction work is conducted by Turkish companies.Electromechanical system will be established by foreign companies.
There have been strong oppositions as to the construction of Ilısu Dam and Hydroelectric Plant, especially from abroad. This author believes that Turkish public knows the actual intentions for blocking this project by claims, such as human rights, environmental status, resettlement of the communities and protection of historical heritage. This author believes that Turkey is determined to take the Ilısu Dam that will provide generation of 3.83 Kwh of energy annually, into operation by 2013.

Credit companies delayed the credit of Ilısu Dam at the beginning of the project. Credit aggreement was cancelled because of latency of the foreign credit companies. Ilısu Dam construction project started in 2009 by Turkish Government budget financial ownership. Ilısu Dam will be completed in 2019.
*Detailed imformation will be covered in Ilısu Dam and Hydroelectric Plant Section.

The installed capacity and annual energy generation rates of the plants and facilities built on the main tributary of the Tigris River are presented in Table 2. The information for the hydroelectric plants planned for the future is presented in Table 3.

Table 2. Dicle nehri üzerindeki tesislerin kurulu güçleri, yıllık enerji üretimleri ve bugüne kadar ürettikleri enerji miktarları

Dam	Installed Capacity (MW)	Annual Generation (kWh/year)	Generation-to-date (kWh)
Kralkızı	204	444 million	4,4 billion
Dicle	110	146 million	1,3 billion
Batman	198	483 million	2,4 billion
TOTAL	512	1073 million	8,1 billion

Table 3. Planned Hydroelectric Plants

Dam	Kurulu Güç MW	Yıllık Üretim Kwh/yıl
Ilısu	1200	3,833 billion
Cizre	240	1,280 billion

WATER STRUCTURES

Rivers can be used for irrigation, provision of drinking and industrial water, energy generation, tourism, fishery, transportation, etc. Certain structures can be built on rivers to facilitate their use, the most important of these being dams and regulators, as water collection structures. Thousands of dams were and are still being built all over the world in various sizes and heights in order to collect and store water. This enables hydroelectric generation through the energy generated by flowing water, and the water stored is used for irrigation during periods of need. Dams also have quite a number of disadvantages. The benefits and disadvantages of dams can be summarized as in Table 4. Before the construction of a dam, first an income-loss analysis is conducted, in general, to decide on its feasibility. Areas downstream usually benefit from the construction of a dam whereas areas upstream are usually harmed.

Table 4. The Benefits and Disadvantages of Dams

Advantages	Disadvantages
Prevents floods *Regulates the flow regime* *Provides hydropower generation* *Provides irrigation water* *Decreases drought impacts* *Provides drinking, municipal, industrial water for residential areas* *Creates new tourism alternatives* *Increases transportation options* *Creates new ecosystems, new fauna and floras*	*Areas under the reservoir destroy flora, such areas can't be utilized for other purposes* *Historical remnants remain under water* *Local people are forced to resettle, causing humanitarian problems* *They change downstream flow, forming new ecosystems*

The Effects of Dams Constructed by Turkey on the Euphrates and Tigris Rivers on Downstream Countries Syria and Iraq

Do dams constructed on Euphrates by Turkey have any benefits to downstream countries?

Yes, they have. Annual flow regimes of rivers are regulated with the dams constructed, and the river downstream receives relatively steady amounts of water according to the season of the year. Therefore, countries downstream of the river:

• are prevented from damages of floods
• are prevented from droughts
• their hydropower capacity will increase by receiving steady flow for their hydropower plants and dams
• their water projects become more affordable since they work on steady flows

The flow rate of the Euphrates River before the construction of the dams used to fall as low as 150 m3/second in summer, and go up to over 3000 m3/second. Upon the completion of the dams, the flow rate averaged at about 500-700 m3/second.

Do dams constructed on Euphrates by Turkey have any disadvantages to downstream countries ?

Yes, they might have. Benefiting from the floods is over. Since the flow of sediments stops, the expansion of alluvium plains halts as well. Yet the cleaner and steady flow of water into these plains should have positive effects on the wetland ecosystems.

Furthermore, the amount of water downstream of the river decreases while water is stored upstream during the water collection phase. The amount of the water released downstream during water collection phase should be sufficient to meet the demands of the countries downstream. These demand figures are determined among those countries. For instance, Turkey and Syria have agreed on releasing at least 500 m^3/second during water collection phase of Atatürk Dam, and this amount was maintained during the period of 23 November 1989 until 26 July 1992 – the date when energy generation commenced.

It should be mentioned that Syria experienced energy losses from its dams on the Euphrates River during this period of 2.5 years. However, since 1992, namely for 26 years now, Syria gained excess power from these plants and this excess will continue to increase in the future. Therefore, when one mentioning of the losses, one should also present the gains, to put things into perspective. Another potential problem for downstream countries could be the deterioration of water quality due to the returned irrigation water upstream. However, it was measured that water reaching Syria after receiving irrigation drainage at Şanlıurfa-Harran Plain had salinity below 0.75 dss, namely acceptable quality for further irrigation.

To sum up, Turkey has provided more benefit than harm to the countries downstream the rivers with the dams it constructed in Southern Anatolia. While doing this, Turkey lost considerable areas from its own territories to reservoir lakes. In return for the labor and expenditures made for these dams, Turkey asks for nothing from the countries downstream. With this fact so clear, the squalls of these countries stating they are damaged by GAP are unacceptable. This is an improper act, against all humanity and moral values. We consider such acts of accusations from countries, which we have considered as friends, but which we understand were never so friendly, as unfair and wrong. Turkish people do not have any intention to do injustice to anyone on making use of the Euphrates and Tigris Rivers.

Now let us focus on the main aspects of Southeastern Anatolia Project GAP which is a global scale regional development project, having great importance for not only Turkey but also all humanity.

SOUTHEASTERN ANATOLIA PROJECT (GAP)

As seen in Figure 1, GAP, which is an integrated development project, aims at developing the region on a socio-economical basis in sectors of urban-rural infrastructure, agricultural infrastructure, transportation, industry, education, health, accommodation and tourism. It is being constructed solely with national resources in order to generate 27,378 Gwh with an installed capacity of 7,490 MW and to irrigate 1,820,358 ha of agricultural land.

The hydroelectric potential of GAP constitutes 25 % of the total hydraulic energy potential in Turkey, whereas the irrigation potential of the project constitutes 20 % of the total irrigable land in Turkey. These rates show the importance of the project for Turkey. The actualization rate of the project in energy generation in 2008 has been 74%, whereas the same rate for irrigation has been 15%. Turkey is committed to complete the GAP Project by 2023. This will bring along food, work, social security, peace and welfare to the people of the region, and will provide a self-respecting life standard for the Turkish citizens living in the region.

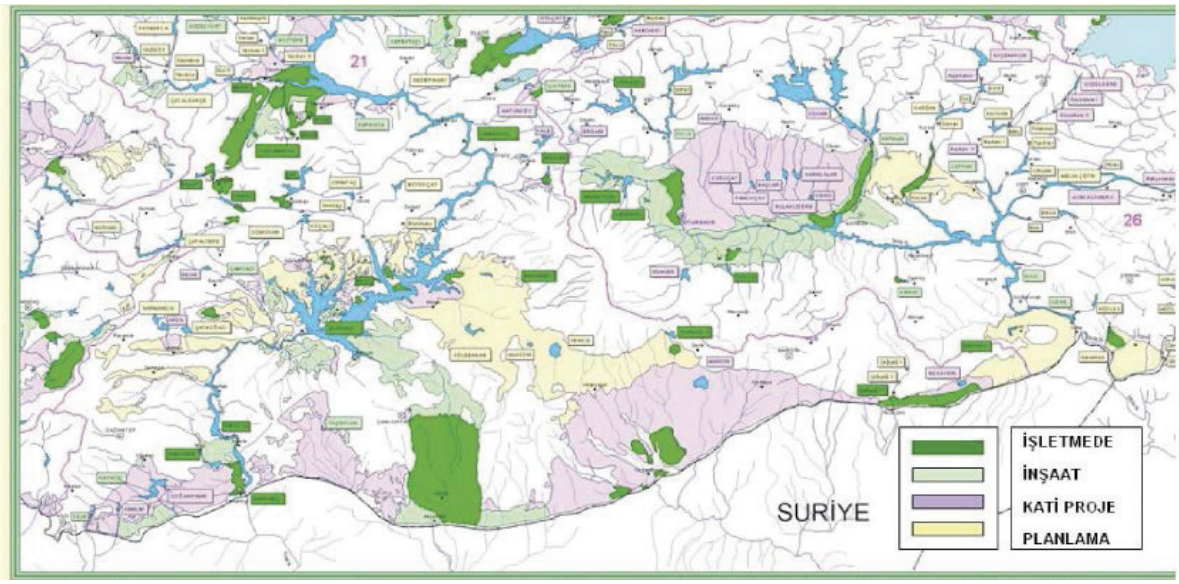

Figure 1. Map of GAP General Outlook - 22 Dam, 19 HES 1.822 million ha irrigation

Social Conditions of the Region

According to the 2007 address-based census, total population of Turkey is 70,586,256, and the region hosts 10 % of this population. The per capita income of the region is lower than the average rate of Turkey.

Unemployment rate in the region is well over the average Turkey rate. Educational, medical and social services are not sufficiently provided to people in the region. To sum up, the region severely needs an economic and social development project like GAP.

State of the Land and Production Patterns

Agricultural classification of the lands to be irrigated in Southeastern Anatolia Project area is as follows:

1. class land rate 2 %
2. class land rate 65 %
3. class land rate 18 %_____ 85 %
4. class land rate 2 %
5. class land rate 5 %
6. class land rate 8 %

With this project, 85 percent of the land to be irrigated consists of high quality agricultural land. Main products to be produced are beet, oilseed, corn, fresh vegetables, animal feed, cotton, rice, pistachio and fruit. Thanks to Southeastern Anatolia Project, the following increases are expected in the production of beet: 29%, oilseed: 3%, corn: 8%, fresh vegetables: 28%, animal feed: 23%, cotton: 118%, rice: 10%, pistachio: 286%, and fruit: 54%.

Irrigation Principles in Southeastern Anatolia Project

Two indispensable principles in Southeastern Anatolia Project are:

• Irrigation water should be used in the most appropriate way. Water shouldn't be wasted, and

• Soil should be protected. With an appropriate irrigation technique, necessary amount of water should be supplied for the soil while preventing salinization of the soil.

To be able to satisfy these principles,

• The most advanced irrigation technique should be applied.

• The most appropriate crop should be selected for the soil and the amount of water available.

• The farmer should be educated and made aware of the facts about the selected crops.

• From field to factory, agricultural activities should be executed by employing scientific methods.

Closed irrigation system (sprinkling, drip irrigation) is an advanced technology that provides water savings. Investment costs of these systems are 50-100 % more than the open systems. However, as they enable the controlled use of water in the facility and enable water savings, open systems were not preferred in the Southeastern Anatolia Project. Open irrigation systems provided up to now will be turned into closed irrigation systems and also from now on, irrigation systems will be constructed as closed irrigation systems.

Targets of Turkey in Southeastern Anatolia Project

Three targets of Turkey in Southeastern Anatolia are:

• Humanitarian target of Southeastern Anatolia Project: Everyone should benefit from this water equally.

• Social target of Southeastern Anatolia Project: Social welfare level of region's population should be augmented with economic opportunities gained via the project.

• Economic target of Southeastern Anatolia Project: Economic strength of Turkey must be augmented with this project.

For these targets to be realized, Turkey invested 20 billion US dollars up till now. For the project to be completed it will invest somewhat 20 billion US dollars again and by doing so, it will augment the life standard of the region's population. Turkey is determined in this subject.

TRANSBOUNDARY WATERS / THE EUPHRATES AND TIGRIS RIVERS

The future of Euphrates and Tigris is a concern for only Turkey, Syria and Iraq. The reason for this is that these rivers originate from the lands of these countries and at the same time they nourish the lands of these countries. There is no sense for others, apart from these three countries, to get involved in the discussions on this subject and furthermore they are not entitled to any legal rights. However, some circles feel they have the rights to govern the world and put forward some scenarios on this matter, claiming they are protecting the rights of some people and speaking on their behalf. These circles make systematical propagandas to the world public opinion against Turkey claiming that "Turkey cuts the water of downstream countries with the Southeastern Anatolia Project". Some Arabic countries, including Syria and Iraq, are directors and supporters of this propaganda which has influenced the third world countries. The European countries, USA and Israel also would like to openly intervene in the use of Euphrates and Tigris water and take side with the parties accusing Turkey.

Irrigable Lands

Irrigable lands with Euphrates and Tigris Rivers in Turkey have been determined by earlier studies conducted by Turkey. No such information has been made available from Syria and Iraq. Does this information exist? If it is, why it is not being made available? The situation is unknown. Areas that will be irrigated with Euphrates and Tigris Rivers are shown in Table 5 with estimated and approximate figures for Syria and Iraq:

Table5. Irrigable Lands with Euphrates and Tigris

Country	Euphrates (ha)	Tigris (ha)	Total (ha)
Turkey	1.800.000	650.000	2.450.000
Syria	800.000	150.000	950.000*
Iraq	2.500.000**	1.500.000	4.000.000
Total	5.100.000	2.300.000	7.400.000

(*) In the calculation of these areas, soils which have agricultural land classification values between 1 and 6 should be taken into consideration.
(**) Lands that Iraq will irrigate using the water of Euphrates are highly exaggerarated

Water Usage from the Euphrates and Tigris Rivers in the aftermath of GAP

Hydrological changes that will occur in Euphrates and Tigris after the Southeastern Anatolia Project is completed fully have been examined and various water budgets have been proposed by the experts of the subject or organizations related to this work. In Table 6, the water budgets of Euphrates and Tigris Rivers for open irrigation and for closed irrigation with 20% and 30% water are presented by using information from Kolars (1994) and Kliot (1994).

Table 6. Estimated Water Budgets for Euphrates and Tigris Rivers

Referans Irrigation Sytem	Kolars (1994)			Kilot (1994)			US Corps of Engineers		
	Open system %20 Closed system %30			Open system %20 Closed system %30			Open system %20 Closed system %30		
EUPHRATES									
Natural stream between Turkey and Syria border	30,67	30,67	30,67	28,20	28,20	28,20	28,20	28,20	28,20
Water drawn by Turkey	-21,60	-17,28	-15,12	-21,50	-17,20	-15,05	-21,50	-17,20	-15,05
Flowing through Syria	9,07	13,39	15,55	6,70	11,00	13,15	6,70	11,00	13,15
Water joining to Euphrates from Syria	9,484	9,484	9,484	10,70	10,70	10,70	6,70	11,00	13,15
Water drawn by Syria	-11,995	-9,596	-8, 397	-13,40	-10,72	-9,38	-4,30	-3,44	-3,01
Flowing through Iraq	6,559	13,278	16,637	4,00	10,98	14,47	6,90	12,06	14,64
Water drawn by Iraq	-13,00	-10,40	-9,100	-16,00	-12,80	-11,20	-17,60	-14,08	12,32
Flowing to Shatt Al- Arab	-6,441	+2,878	+7,537	-12,00	-1,82	+3,27	-10,70	-2,02	+2,32
TIGRIS									
Amount of water joining to Tigris from Turkey	18,50	18,50	18,50	18,50	18,50	18,50	18,50	18,50	18,50
Water drawn by Syria and Turkey	-6,70	-5,36	-4,60	-7,20	-5,76	-5,04	-6,70	-5,36	-4,60
Flowing through to Iraq	11,80	13,14	13,81	11,30	12,74	13,46	11,80	13,14	13,81
Water joining to Tigris in Iraq from river reaches	30,70	30,70	30,70	31,70	31,70	31,70	30,70	30,70	30,70
Water drawn by Iraq	-33,40	-26,72	-21,49	-40,00	-32,00	-28,00	-32,8	-26,24	-22,96
Flowing through Shatt Al-Arab	9,10	17,12	23,02	8,00	12,44	17,16	9,70	17,60	21,55
EUPHRATES+ TIGRIS	**2,659**	**19,998**	**30,557**	**-4,00**	**10,62**	**+20,43**	**-1,00**	**15,58**	**23,87**

Note 1: Water returned from irrigation hasn't been taken into account. The scientific studies carried on by Turkish Harran University, faculty members of Agriculture, showed that the quality of the water returned from Harran irrigation (irrigation tail) is acceptable for a second irrigation.
Note 2: Ground water potential of the region hasn't been taken into account

A close evaluation of the table indicates that;

• In comparison with Tigris River, Euphrates River is unsatisfactory in meeting the needs; as a result, transferring some water from Tigris to Euphrates within Iraq will be necessary,

• By means of expanding the application of closed system irrigation facilities, and under the condition that all three countries use water carefully, even according to the worst scenario, Euphrates and Tigris will be capable of meeting the needs of the people in the three countries, and furthermore, the needs of the wetlands will be met.

As such, it is impossible to understand the reasons of the negative opinions on Euphrates and Tigris water. The best way to avoid such opinions would be if Turkey, Syria and Iraq cooperate rapidly to develop a mutual management and execution plan to achieve water savings in the region, and urge for the realization of scientific and realistic studies on the use of Euphrates and Tigris waters.

TURKEY'S VIEWS ON THE USE OF EUPHRATES AND TIGRIS WATER: "A PLAN OF THREE STAGES"

Since Euphrates and Tigris rivers flow beyond the borders, their use concerns Turkey, Syria and Iraq. For these two rivers to be used in the augmentation of these countries' welfare, all three countries should agree on the common principles of the use of water.
Turkey has presented her opinions and attitudes on this subject with her "three-phase plan". To-date no clear agreement has been reached among Turkey, Syria and Iraq on the subject of peaceful use of these waters. Syria has softened its objections in the last few years and has started to take side with Turkey. However, Iraq hasn't yet shown a compromise on this subject, which might as well be due to the political instability in the last fifty years. In addition, the USA and the EU countries exhibit a deceitful approach by appearing to protect the interests of Arab countries and influencing the people of these countries against Turkey. Unfortunately, many third world countries have been taken by this deceitful act. The battles between Israel and Arabs in the Middle East for over fifty years have not been able to awaken the Iraqi people to the truth to recognize where their benefits lie. It is hoped that the last Crusade to Iraq carried on by the USA and its allies, and their looting and pillaging of Iraq have made Arab people recognize what is at stake so that they will look at the relations between Turkey and Iraq in a more positive way.

The "3 phase plan" offered by Turkey is a holistic approach for the region, and scope and the goal of the plan are presented as a collaborative work to be carried out by the three countries for rational and optimum use of Euphrates and Tigris water in a judicious way. The following is the outline of the 3-phase plan on Turkey's use of Euphrates and Tigris water basin - presented by Turkey to Syria and Iraq in 1984 via a joint technical committee of Turkey, Syria and Iraq:
• Euphrates and Tigris watersheds should be regarded as a single water basin.
• In order for all three countries to use this water judiciously, it is necessary to establish common scientific and technical committees that will employ scientific methods to provide the most appropriate solutions for the single basin by following a scientific approach as outlined below:
1. Gathering all kinds of hydrological information, e.g., the amount of water carried by the water basin, rain-flow relations, evaporation and water losses, sediment flows.
2. By using common data and criteria, determining the water demands for irrigation, drinking, and municipal and industrial use, and the demand needed for sustainability of the wetlands.
3. In the light of this information, developing joint projects under the condition that the most appropriate techniques are used, establishing the most economical operations models and putting them into practice, and providing the required coordination and organizations with collaboration of these three countries.
• This plan aims at benefiting each of the three countries objectively. The plan is humanistic, reasonable and fair. We hope that Turkey's plan will be received positively by Iraq, and

concrete steps will be taken by the three countries in order to use these waters for the benefit of their people.

In the use of Euphrates and Tigris waters, Turkey has good intentions for the region, and looks at the future with hope for collaboration of the three countries. The good will of Turkey has become obvious during the Atatürk Dam water retention works, as presented below:

• The construction work of Atatürk Dam was started with the construction of derivation tunnels in 1981 and afterwards Euphrates water was directed towards these tunnels in June 16, 1986.

No flow restrictions of Euphrates River were applied until the first and second tunnels of three derivation tunnels were closed in 1989, at which time water was channel downstream through the third derivation tunnel. The capacity of the third tunnel was 700 – 1000 m3/s.

• It is stated in item 6 of the Economic Cooperation Protocol between Turkey and Syria dated 07.17.1987, that during the process of water retention and filling of Atatürk Dam, "The Turkish side guarantees that on an average it will leave more than 500 m3/s water on a yearly basis at Syrian border until the Euphrates water is
allocated among the three countries. If the monthly flow drops below 500 m3/s, then the missing amount will be compensated the following month".

• In Atatürk Dam, before water retention took place, an average of 768 m3/s of water flow and a total of 3.453 billion m3 water was released to Euphrates riverbed for 52 days between November 23, 1989 and January 13, 1990.

• The third derivation tunnel was closed on January 13, 1990. During water retention period, the water level upstream was 392.20. Therefore, no water was released downstream until water reached number 1 and 2 derivation tunnels' inlet on February 13, 1990.

• As of February 14, 1990, the guaranteed amount of water was released downstream by opening valves of number 1 and 2 derivation tunnels. This operation has continued until July 26, 1992, at which time the energy production was realized in the dam.

• During this period, the water level was 508.07 m and water accumulated in reservoir was 25.871 billion m3. During this phase, the amount of water released to the downstream was over 40 billion m3, and the flow rate was over 500 m3/s. This information was summarized in Table 7.

• After July 26, 1992, energy production was started in the dam and the turbines were put into use every four months. On average 200 – 220 m3/s water could be released downstream from each turbine. When guaranteed amount of water was
met by the amount of water released downstream from turbines, the derivation tunnel valves were closed gradually.

• Currently, water passing through the turbines is released downstream; although the amount of this water released varies according to the number of turbines working, it is, in fact, far more than 500 m^3/s.

Above numbers show explicitly that Turkey was able to compensate the deficit realized during water collection for a period of 30 days by averaging at about 509 m^3/s over a period of 82 days, and hence was loyal to its promise.

Table 7. Amount of Water released to Syria During Water Retention in Atatürk Dam

1-Before Water Retention	
23-30 November 1989	625m3/s x 8 days = 0.432 x 109 m3
01-31 December 1989	818 m3/s x 31 days = 2.190 x 109 m3
01-13 January 1990	740 m3/s x 13 days = 0.831 x 109 m3
SubTotal	**52 days 3.453 x 109 m3**
2-During Water Retention	
14-31 January 1990	65 m3/s x 18 days = 0.102 x 109 m3
01-12 February 1990	50 m3/s x 12 days = 0.052 x 109 m3
SubTotal	**30 days 0.154 x 109 m3**
3-Final Total	82 days 3.607 x 109 m3
$Q_{Average}$	**3.607.000.000/82*86400=509.120m3/s**

CONCLUSIONS

The discussion of water rights has started with the construction of Atatürk Dam and the hydroelectric plants in the region of Southeastern Anatolia Project to tame the Euphrates River. Syria and Iraq, backed by the Arab countries and supported by major world propaganda centers, still continue to bring charges against Turkey andNtry to mold the world public opinion in their favor. The western press believes that tension between Turkey and other countries will augment because of water issues leading to possibly close combat. The western world provokes this subject since it sees itself as the spokesman of water rights and tries to set the agenda. It is necessary for Turkey to approach this subject decisively and prevent it from being an international problem. Waters in question should be waters making countries closer and their people close friends. They will all benefit if these waters stay away from being controversial.

Therefore, this subject is very important and deserves close attention. For these waters to remain as "peaceful" waters, the following are suggested:

• The role of engineers is to produce and then submit to the leaders of the three countries the most favorable projects.

• The role of country leaders is to provide the cooperation between the countries in the light of these projects and put these projects into service.

• The role of people is to come to the realization that only they will protect their interests in the best manner. In the light of the last 16 years the following evaluations can be made. If the subjects mentioned above are realized by each of the three country, then:

• Looting and pillaging going on in the region for nearly a century will be terminated.

• People of the region will use their resources for their own interests, and these regions will regain the peace, trust and welfare they long for.

Turkey's push in the field of civilization with Southeastern Anatolia Project has undergone important delays due to the activities of the foreign-supported terrorist organization, Kongra-Gel. Turkish public knows the identity and the intentions of these foreign supporters. Yet, this situation hasn't reduced the national will of

Turkey in the realization of Southeastern Anatolia Project; on the contrary, it only enforced it.

In spite of these obstacles, Turkey is determined to provide its population the desired life standards and is so determined to realize this project, while protecting the interests of the

region's population as a principle. Turkey is ready for close cooperation with the countries of the region on the use of Euphrates and Tigris rivers, and it is determined not to take side in the case of conflicts arising on these rivers. This will is guaranteed by the Turkish people who see the entire humanity as one.

REFERENCES

Altınbilek, D., 1972. "Fırat-Dicle Havzasının Gelişimi ve Yönetimi". Su Vakfı Yayınları. DSİ in Brief 1954-2007.

Kapan, İ., 1972. "Suyun Stratejik Dalgaları". Bahçeli Kültür Yayıncılığı.

Kliot, N., 1994. " Water resources and conflict in the Middle East" London; New York: Routledge Press, pp. 100-173, 1994.

Kolars, J.,1994. "Problems of International River Management: The Case of the Euphrates", International Waters of the Middle East From Euphrates-Tigrıs to Nile, Ed. Asit K. Biswas, Water Resources Management Series 2, Oxford University Press, p. 44-95.

Oğuz , S., 1992. "Güneydoğu Anadolu Projesi ve Kalkınmamızdaki Yeri" Su Dünyası, Su Dünyası, 2005

Şen, Z., "Ortadoğuda Su Sorunlu Bereketli Hilal ve Türkiye", Su Vakfı Yayınları.

5th International Symposium on Dam Safety

October 27-31, 2018

THE STRATEGIC BUT HAMPERED ENGINEERING PROJECT UNDER GAP: ILISU DAM AND HEPP CONSTRUCTION

Selami OĞUZ

ABSTRACT

The multi-dimensional South-East Anatolia Project (GAP) aims to utilize the Euphrates and the Tigris in for irrigation and energy purposes. Under the project, for which the planning process started in 60's, the first step was the construction of Karakaya Dam and HEPP on the Euphrates, followed by the other constructions over the Euphrates and the Tigris rivers. Ilısu Dam and HEPP come into prominence as its construction allows keeping the Tigris River under full control. GAP is an integrated development project with its promising economic and social aspects for the region's flourishment. The project cost is around 30-40 bio US$ providing opportunity to multiply the agricultural capacity of the country. There is a need for international support; however, on the contrary, the project has been hindered by foreign entities, mainly via the terrorism for the last 30 years in the region. Turkey is determined to realize the project with its own means.

Keywords: GAP, integrated development, Tigris River, International support, Terrorism.

HAMPERED ENGINEERING ARTIFACT ILISU DAM AN HPP CONSTRUCTION

It can be seen from the map below that Ilısu Dam and HPP construction is the most important dam planned over the Tigris under the GAP project. What Ataturk Dam over the Euphrates means, Ilısu over the Tigris is the same? It will be the 4th largest capacity hydroelectric power plant of Turkey.

Ilısu Dam and HPP project, with 1200 MW installed capacity, will be generating 4120 GW.h electricity annually. At its downstream, Cizre Dam and HPP with 240 MW installed capacity will be generating 1208 GW.h electricity.
Ilısu Dam will not only be valuable because of its energy production, but it will also help to control the Tigris water and ease construction of the Cizre Dam.
Besides electricity generation, Cizre Dam will be utilized for irrigation of 121.000 ha area of Nusaybin-Cizre-Idil savanna. These two dams will allow full control of the Tigris river.

Figure 1. General view of the projects over the Tigris River and Ilısu Dam sight (2018)

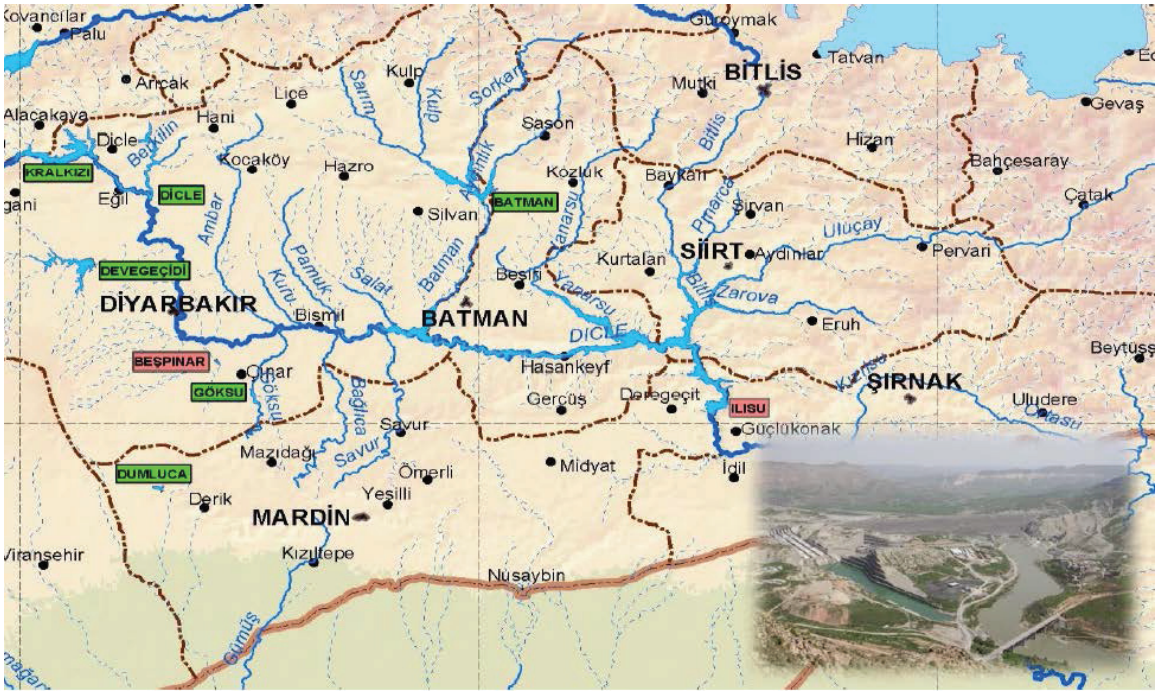

Units in Charge of the Project

-Owner of the project: DG Hydraulic Works

-Construction Works building group: Nurol İnşaat A.Ş , Cengiz İnşaat A.Ş, Çelikler İnşaat A.Ş. (Turkey) and Ed.Züblin AG (Germany)

-Construction Works project and coordination services group: Stucky Ltd. (Switzerland), Temel Su A.Ş. (Turkey)

-Electromechanical works group: Vatech GmbH & Co. (Austria). Alstom Ltd. (Switzerland)

-Engineering and Consultancy Services: Colenco Power Engineering Ltd. (Switzerland), Maggia Engineering Ltd. (Switzerland), Dolsar Mühendislik Ltd. Şti. (Turkey), Rast Mühendislik Ltd. Şti. (Turkey)

-Financing firm: Vatech Finance (Austria)

Use one blank line from the previous paragraph to create a 2nd Level Heading. The text of the following paragraph should immediately follow the 2nd Level Heading without any blank lines.

Operationalisation of the Credit

External Loan providers for the Ilısu Dam and HPP project

Austria ("OeKB"), Germany ("Euler-Hermes"), Switzerland ("ERG")

The key institution in the Ilısu project is DG Hydraulic Works (DSI). Facing many challenges, DSI should have adopted a unique approach for this project as it necessitates a strong intent. A decisive approach supported by a political support could have generated appropriate environment and financial means to implement the project. It is hard to give a positive answer to the question of whether DSI did thoroughly what must be done up to now.

According to the 04/06/1998 dated and 98/1123 numbered decree, South East Anatolia project was planned to be completed latest by 2010. However, construction of Ilısu Dam, as one of the most important milestones of GAP could only start in 2006. Again according to plans, the

construction period would be 8 years; however, it also took longer than the plan. The phase of water retain could only be initiated by the end of 2018, so energy production will not be possible any earlier than 2019.
What is the reason for so long lag behind the plans in Ilısu Dam construction?

Funding issues
Funding needed for the construction of dams and HPPs under GAP is approximately 30 mea US$. If the investment had been done using only domestic resources, it would have taken too long to complete the project. Therefore, from the very beginning, it is preferred to seek foreign credit opportunities, which is rather easy for the energy projects.
On the other side, we have the experience of Atatürk Dam. The institutions who provided finance to the Karakaya Dam, which is built only for providing energy, did not show interest in financing Atatürk Dam, as it was planned for irrigation purposes besides energy generation. These were mostly institutions from the EU Member States.
This decision was related to the policies of USA, EU and Israel. They considered against their interests the regional and national development project Turkey initiated with GAP, and sought ways to hinder. Funding organizations from these countries were accordingly biased.
Therefore except for the procurement of the energy equipment for Atatürk Dam and HPP, it was not possible to get international finance and the construction part was totally funded by domestic resources.

The funding need for Ilısu Dam and HPP was calculated to be 1.2 Mio €. The government decided this amount as "not affordable" by domestic resources, so they started seeking international finance, but overlooking the experiences of Ataturk Dam. It was possible to find international finance for Ilısu just as an energy provider. Unfortunately this process took a couple of years and financing agreement could only be signed on August 14, 2007, a year after the start of the construction date, August 05, 2006.

The breakdown of the 1 200 000 000 €, total amount of credit for Ilısu Dam and HPP was 925.6 Mio € + 134.6 Mio Swiss Frank for construction and electromechanical works, 17.7 Mio € + 26.09 Mio Swiss Frank for engineering and consultancy services. The amount needed for the reconstruction of roads, bridges and railways was 170.7 Mio TL, which would be funded by domestic resources in addition to confiscation and relocation expenses.

The financing institutions had a hidden agenda. There were some requirements to operationalize the credit. These requirements were:

Organisational requirements
On 6 October 2000, at the end of the meeting between the DG Hydraulic Works and representatives of the above-mentioned firms, a memorandum of understanding was signed. The parties agreed on the implementation principles and reporting requirements with this MoU. Accordingly, DSI, as the loan receiver, would pursue actions specified under relocation (68 related sub-articles), environmental issues (66 related sub-articles) and cultural entities (14 related sub-articles). Following units would be formed to undertake the tasks under these actions:

PIU-Project Implementation Unit

A Project Implementation Unit (PIU) would be set up to monitor the implementation process. The members of the committees would be bureaucrats and specialists. Under the PIU, there would be three regional committees formed, one for each action: relocation, cultural entities and environment. Related institution representatives and specialists would be the members of the committees.

CoS-Committee of specialists
To ensure the best practice according to international standards, CoS would provide guidance, technical support and inspection services for PIU. Main responsibilities of CoS were: "In accordance with the terms of reference agreed on 6 October 2006, monitioring and evaluation of the plans made and researches conducted by the PUB on the topics listed under Appendix 3 of the MoU, evaluation of the relocation plans and providing comments and suggestions on it, reporting the outcomes to the credit agencies". CoS would be formed by the relocation, environment, cultural heritage committees and the Board independent from the DSI and the consortium.

Operationalisation of the credit
External Loan providers for the Ilısu Dam and HPP project:
Austria ("OeKB"), Germany ("Euler-Hermes"), Switzerland ("ERG")
The key institution in the Ilısu project is DG Hydraulic Works (DSI). Facing many challenges, DSI should have adopted a unique approach for this project as it necessitates a strong intent. A decisive approach supported by a political support could have generated appropriate environment and financial means to implement the project. It is hard to give a positive answer to the question of whether DSI did thoroughly what must be done up to now.
According to the 04/06/1998 dated and 98/1123 numbered decree, South East Anatolia project was planned to be completed latest by 2010. However, construction of Ilısu Dam, as one of the most important milestones of GAP could only start in 2006. Again according to plans, the construction period would be 8 years; however, it also took longer than the plan. The phase of water retain could only be initiated by the end of 2018, so energy production will not be possible any earlier than 2019.
What is the reason for so long lag behind the plans in Ilısu Dam construction?

Funding issues
Funding needed for the construction of dams and HPPs under GAP is approximately 30 mea US$. If the investment had been done using only domestic resources, it would have taken too long to complete the project. Therefore, from the very beginning, it is preferred to seek foreign credit opportunities, which is rather easy for the energy projects.
On the other side, we have the experience of Atatürk Dam. The institutions who provided finance to the Karakaya Dam, which is built only for providing energy, did not show interest in financing Atatürk Dam, as it was planned for irrigation purposes besides energy generation. These were mostly institutions from the EU Member States.
This decision was related to the policies of USA, EU and Israel. They considered against their interests the regional and national development project Turkey initiated with GAP, and sought ways to hinder. Funding organizations from these countries were accordingly biased.
Therefore except for the procurement of the energy equipment for Atatürk Dam and HPP, it was not possible to get international finance and the construction part was totally funded by domestic resources.
The funding need for Ilısu Dam and HPP was calculated to be 1.2 Mio €. The government decided this amount as "not affordable" by domestic resources, so they started seeking

international finance, but overlooking the experiences of Ataturk Dam. It was possible to find international finance for Ilısu just as an energy provider. Unfortunately this process took a couple of years and financing agreement could only be signed on August 14, 2007, a year after the start of the construction date, August 05, 2006.

The breakdown of the 1 200 000 000 €, total amount of credit for Ilısu Dam and HPP was 925.6 Mio € + 134.6 Mio Swiss Frank for construction and electromechanical works, 17.7 Mio € + 26.09 Mio Swiss Frank for engineering and consultancy services. The amount needed for the reconstruction of roads, bridges and railways was 170.7 Mio TL, which would be funded by domestic resources in addition to confiscation and relocation expenses.

The financing institutions had a hidden agenda. There were some requirements to operationalize the credit. These requirements were:

Organisational requirement

On 6 October 2000, at the end of the meeting between the DG Hydraulic Works and representatives of the above-mentioned firms, a memorandum of understanding was signed. The parties agreed on the implementation principles and reporting requirements with this MoU. Accordingly, DSI, as the loan receiver, would pursue actions specified under relocation (68 related sub-articles), environmental issues (66 related sub-articles) and cultural entities (14 related sub-articles). Following units would be formed to undertake the tasks under these actions:

PIU-Project Implementation Unit

A Project Implementation Unit (PIU) would be set up to monitor the implementation process. The members of the committees would be bureaucrats and specialists. Under the PIU, there would be three regional committees formed, one for each action: relocation, cultural entities and environment. Related institution representatives and specialists would be the members of the committees.

CoS-Committee of specialists

To ensure the best practice according to international standards, CoS would provide guidance, technical support and inspection services for PIU.

Main responsibilities of CoS were: “In accordance with the terms of reference agreed on 6 October 2006, monitioring and evaluation of the plans made and researches conducted by the PUB on the topics listed under Appendix 3 of the MoU, evaluation of the relocation plans and providing comments and suggestions on it, reporting the outcomes to the credit agencies”.

CoS would be formed by the relocation, environment, cultural heritage committees and the Board independent from the DSI and the consortium.

Operationalization of the credit

Release of the credit for funding of the construction and electromechanical works of Ilısu Dam and HPP project was based on the progress reports submitted to the credit agencies on the action areas. If the progress reports are not satisfactory, namely if the tasks defined under each action were incomplete, fund would not be released.

External credit procurement process

In the letter sent to the Ministry of Environment and Forest, the credit agencies provided a summary of the current situation regarding relocation, cultural heritage and environment

issues and listed the precautions that should be taken by DSI to start the construction in dam area in October 2008. In this letter, it was mentioned that according to the specialists' reports the tasks that should have been completed before the start of the construction under relocation, environment and cultural heritage actions according to the MoU were not even started and if these were not completed, there would be a delay. DSI was responsible for the tasks mentioned under the MoU. Otherwise, the credit would not be released. On the other side, the committees formed by representatives of different organizations were not very effective and loss of time was indispensable. The articles of the agreement turned out to be a big challenge for DSI. Such a challenge in combination with the terrorist actions of PKK in the region, in a way supported by the governments of the countries of the financing agencies trapped DSI as this fact, was blinked during the signature stage of the financing agreement. Financing agreement of Ilısu Dam and HPP was suspended on December 23, 2008. The justification provided by the financing agencies for the suspension was not satisfactory. However, it came out that the project could not be implemented with this structure. DSI terminated the greater part of the financing agreement and took a decision to implement the project domestic funding, even though it would take a longer time. If we evaluate the approach of DSI to Ilısu Dam and HPP construction till then, we can say in short that:

- It was a serious mistake to consider external finance for such an investment project. Because the financing agents and related countries were against this project and they would create barriers. A similar case was faced for Atatürk dam and construction was completely funded by domestic resources. Having this experience, it was not realistic to try finding external finance. It was not possible to convince the Director of DSI at that time.
- The terms of the MoU signed by DSI at the end of the final evaluation meeting were not of any kind acceptable for and independent country. Sanctions were severe.

Project challenges

Modifications made in the dam projects

According to the article 17.1, paragraph 2 and 3 under the final project and revised final project heading it was stated that "the contracting authority will submit the revised final projects to the construction group before they start the work. In case the contracting authority sees necessary, there may be revisions to the project". In accordance with these articles, the contracting authority plans to revise the embankment project as "rockfilled with concrete encasement"

Ilısu dam body was designed similar to the Aatürk dam as clay core, zoned and rockfilled.

Body dimensions and characteristics were as follows:

Type: Clay core rockfilled

Thalweg level: 400.00 m crest level : 530.00 m Foundation level: 395.00 m

Elevation from the foundation: 135.00 m Elevation from the thalweg: 130.00 m

Crest Length: 1820.00 m

Crest Width: 15.00 m

Embankment volume : 43.79 x 106 m3

During this stage, there were views against the zoned earth dam or rockfilled dams. Some people considered these as old school and proposed new types of dam body types. They got the support of the top management, who do not know what a dam really is and tossed out DSI's 50 years of experience in dam building. The worst part of it was the DSI employees did not take a stand against these. In summary, the age of new dam body types was started in the country.

Based on this view, changing the body design of Ilısu dam was on the agenda. Such a design change decision was taken on January 19, 2007, 6 months after the groundbreaking. The

contract holder did not object to this revision as it was easier and more profitable. With this decision, the type was determined, but the axis took a long time as there were hesitations within DSI. They studied similar buildings, brought specialists from Columbia.
* Decision on the body axis of the dam could be taken in almost 20 months, in September 2008. What did DSI do in the meanwhile and what did the organization wait for? Is it acceptable for an organization to remain indecisive for such a long time in such a project and for this type of a decision?
* The characteristics of the new body project were as follows:
Dam body type: Rockfilled with concrete encasement in the face
Dam volume: 23.7 million m3
Dam Elevation: from foundation 136.00 m, from thalweg: 130.00 m
Crest length: RCEF length: 1775.00 m , concrete dam length:552.00 m Total 2327.00 m
Crest width: on RCEF 8.00 m, on concrete dam 10.00 m
Max dam reservoir volume: 10.4 billion m3
*The delay in the decision on design details of the axis affected diversion tunnels' entry and exit points. The revised final design of the diversion tunnels could only be approved by DSI on November 12, 2008, with 22 months delay. Diversion tunnels are on the critical path of dam construction. It would be a wise decision to issue a separate contract for the diversion tunnels in the beginning and to fund this contract b domestic resources, as it was done in Atatürk Dam. DSI decided to build these under credit content. Both the delay due to the revisions in the project and problems with the credit conditions caused latency in starting the building of the diversion tunnels.
*Revisions made on the dam body also affected the spillway and energy structures. Consequent changes in the projects of these structures increased the delay to 30 months.
* As the conclusion, the revisions made in the project accounted for 70-80% after the agreement.
Now, let's seek an answer to the question: Was it correct to make such a big revision in Ilısu Dam and HPP project after the contract was made?

Engineering review of the project revisions
Let's review the revisions from the two key engineering perspectives. 1. Is the technical safety of the building ensured with the revisions? 2. Is the project more economic after the project revisions?

Do the revisions make the dam body technically safer?
*Dam body is dimensioned in the light of the stabilization analysis considering the earthquake accelerations. The dam body should definitely be safe in this regard.
The Earthquake Regions of Turkey map published by the Ministry of Urban Planning in 1996, has been updated by Disaster and Emergency Management Authority (AFAD). On this map, it can be seen that Ilısu Dam and HPP region is in the 2nd-degree earthquake zone. Its distance to 1st-degree zone is 100-150 km and 10-15 km to the 3rd-degree zone. In the body stabilization analysis, earthquake accelerations should be well determined and body dimensions should be decided accordingly. According to the same earthquake map, under the reservoir of Ilısu dam fault lines that may cause 1st-degree earthquake can be seen. Effects of an earthquake on the reservoir and respectively on the body should be evaluated. I believe such analysis was made and design precautions were taken.
* There may be many examples of this type of dam ad DSI may be willing to have experience in this technology. However, it must be noted that type of a dam should be decided according

to the earthquake risk of the region, ground conditions and the topographic structure on which the dam will be built.
This type is viable on narrow and deep valleys, for dams with short crest and with vigorous side slop. In a similar type of dam built in Turkey, Kürtün dam, the ratio of height to crest length is between 1/3-1/4. However, in Ilısu Dam, we cannot talk about any of these conditions. Height to crest length ratio is 1/14. Since it diminishes the effect of the side slopes, I believe this ratio may multiply the risks on the body structure.
In addition, the linear axis of the dam worries me. I would prefer a slightly arched axis towards the head.
*The weakest aspect of this type of dams is possible leakage over the body. The concrete coating over the water retaining head side surface has been reinforced by special precautions. In this way, both the risk of cracks and fracture has been diminished and leakage risk has been eliminated by the membrane coating under the concrete.

90% of the dams DSI built up to now were clay core sand or rockfilled. In these dams, there is no risk of water leakage, earthquake safety is ensured and no problem has been faced due to the earthquakes lived except the case of Sürgü Dam.

DSI has a great experienced in building this type of dams. The agreement was built around this experience initially. DSI should have insisted on this type and should utilize its previous experiences in building Ilısu Dam. Whatever the reason is, I clearly express that I do not deem the revisions made in the body design as a sound decision.

Did the revisions make the project more economical?
Construction cost and time were the key issues in revisions made in the project. It was justified as the changes would decrease the construction period from 7 to 5 years. It is a key success criteria to complete such strategic investment projects as quickly as possible. It should be kept in mind that delay means loss of production and must be avoided.
In case of Ilısu Dam, did the revisions generated time-saving? Considering water retain could only be started by the end of 2018 earliest, the project period became 11.5 years since August 2006, the time of groundbreaking. In other words, there is no time-saving, but a time-loss, 3.5 years due to conditions of the agreement and 5.5 years due to revisions in the project.
*Longer construction period caused 5.5x4.120=22.660 billion KWh energy loss. Taking unit value as 0.06 US$/Kh, its economic value is 1,360 Billion US$. This figure equals almost the total cost of construction, for which you can find a breakdown below:
-The body initially referred in the Agreement was consisting of 20% clay and filter core and 80% rock filled. In 2016 unit cost rates, cost of a cubic meter was 15 TL and dam body cost was 43 790 000 x 15= 656.850 million TL.
-The revised body design cost was at the same year's rates (filling + concrete coating) nearly (474.000+220.000=) 694.000 million TL. I other words, there is no saving in dam body construction.

In summary; the revisions made on the Ilısu Dam body and its consequent effects on the other parts did not do any good but harm the dam economy. The sorry state of affairs nobody gets uncomfortable due to this loss. Who made these revisions are Turkish engineers. In such a significant investment project inconsiderate decisions both cost and time-wise are really disappointing. It is an evidence that engineering discipline DSI organization is fading out.
Economic aspects of Ilısu dam will be discussed below.

* Revisions on the project elevated the energy amount that can be generated in Ilısu Dam and HPP from 3.833 GWh to 4.120 GWh. We will see how correct these figures are only after the dam starts its operations.

Security issues

In the region, Ilısu Dam and HPP is built, starting with the GAP project PKK's terrorist actions have been intensive with the support of the EU, USA and Israel. Terrorists have taken to hamper the project as duty and intensified their actions in the region. The government of the Republic of Turkey secured road and work-sites by establishing military stations and did not allow the terrorist actions. With the security measures taken the project could come to the stage of water-retain.

Relocation problems

Like every dam project, for this one confiscation was done. In accordance with the existing code of confiscation, the government pays the expropriated price to the property owners and does not deal with the rest. It is not defendable to pay and expect the people, who spent all of their lives in this region, to leave without any support in their new life. Relocation principle entered into our agenda with the EU accession process. Under this project, the relocation actions offered a new life support to the people who had to leave their properties after confiscation. The Ilısu village built close to the work-site is a good example to this. The modern village has been the symbol of Turkish government's care and prudence. Confiscation and relocation actions together cost 2.2 billion TL.

Cultural heritage problems

As in most of the dam construction projects, cultural heritage items need to be preserved from remaining underwater. The common practice was taking all possible measures to preserve these assets. Assuan I and II Dams built in Egypt and the Three Passages Dam constructed in China can be given as examples.

In Ilısu dam Hasankeyf has been the focus. All efforts were channeled to preserve the remains. On the other hand, there were groups lobbying to stop the construction project while we have the option of preserving these items and continue the investment for the dam.

The main purpose was to hinder the dam. For this purpose, the terrorist incidents in the region were continuously supported by foreign powers, cultural heritage issues were used, especially Hasankeyf was used as political pressure area.

As Ilısu Dam and HPP will increase the economic and social welfare of the people in the region, so terrorism will lose its base gradually like the case in Şanlıurfa, which has become wealthier with irrigation systems.

During the construction of the Ilısu Dam, historical items, including those in those parts of Hasankeyf that would remain underwater, El Rızk mosque, Sultan Süleyman mosque, Kızlar mosque and Küçük mosque, Zeynel Bey mausoleum, Imam Abdullah Zaviyesi, Artuklu bridge were moved to the new Hasankeyf New Cultural Park above the max water level and rebuilt there.

The historical artifacts that are underwater are removed by excavation work and moved to the museums. To this end, 200 million TL was spent to preserve the cultural heritage items.

Similarly, in Atatürk Dam, Samsat Winter Palace being in the first place, the historical items was moved to new places. However, this work did not cause any delay in the water retention for Ataturk Dam.

In Ilısu dam case, financing, project revisions and preservation of cultural heritage resulted in 5.5 years of delay. Considering only the energy sales revenue, the loss corresponds to ((5.5 years x 4.120 billion KWh x 0.06 US$= 1.359 billion US$) the investment value of Ilısu Dam construction.
DSI, as the authority making both investments, has been more successful in time management in Atatürk Dam, but couldn't show the same performance in Ilısu Dam case. This is an indication of decline in engineering performance of DSI.

Current situation of Ilısu Dam and HPP construction
-Construction work could start on May 16, 2008, with 2 years delay.
- Diversion could be completed by August 29, 2012.
-Dam body construction could be started with cofferdam building on March 9, 2012. Body construction was completed in October 2017.
The dam body construction started on 09 March 2012 with the construction of the cofferdam. Construction of the body was completed in October 2017. For the first time, additional measures were taken to prevent leaks at the dam body. In the front face concrete coating joints, copper gasket was used.
-All construction works were completed in March 2018.
-Electromechanical equipment installation will be completed in August 2018.
- If there is no problem related to cultural heritage issues, water retaining will start on October 29, 2018. Since the lake has a volume of 10.4 km3, the water level can reach the level that makes energy production possible in 1 year.
- Energy production can start at the end of December 2019.
- If the critical dates mentioned above are met, the dam will have been taken into service with a delay of 5.5 years, in 13 years and 5 months from the date of groundbreaking, 5 August 2006.

*** Investment value of Ilısu Dam**: Estimated investment value was given above. Let's see the breakdown:
- Based on 2007 price index, Dam and HPP cost: 1 012 500 000 Euro = 1 383 286 000 US$
- Cost of Confiscation : 2 200 000 000 TL
- Cost of preservation of cultural heritage items: 300 000 000 TL
- Cost of relocation: 200 000 000 TL
- Total Cost: 2 700 000 000 TL = 2 064 220 000 US$
- Total cost of Ilısu Dam and HPP construction = 3 447 506 000 US$.
- Confiscation cost increased the tota investment value in this dam.
- The exchange rate referred in the Agreement is used for calculations 1 US$= 1.308 TL.

* As water retaining phase starts in Ilısu Dam and HPP construction, Tigris river will be under full control. Such a strategic investment project was unfortunately impeded and took too long time to complete. The plan was to complete in 2002; however, it will be in service after 18 years. It is anyway elating to have it completed.
.
Cost-Engineering prformance of Ilısu dam and HPP construction
Ilısu dam construction has been very late, unfortunately. Just following the completion of Atatürk Dam, Ilısu Dam should have started. It is a pity that DSI organization could not perceive what time loss means in energy projects.
The loss generated due to to18 years delay of Ilıs Dam and HPP is (18 years x 4.120 billion KWh x 1US$ =) 74.160 billion US$.

River dams were taken into agenda with the Renewable Energy Law No. 5346 issued on May 18, 2005, in our country. Due to the environmental destruction, there has been a great deal of public reaction to the construction of such facilities. How economical were these facilities? This issue has not been discussed much until this day. The number of HPPs carried out in this context is over 600.
The amount invested in 268 premises with less than 10 MW installed power, is about 2 billion USD. For such a size, expenses happen to be almost equal to the revenues. Hence, there is no real benefit from these power plants and the invested amount is for nothing. The amount of energy that these plants can produce is only 16.7% higher than the amount that can be obtained from the Ilisu Dam. If funds allocated to these facilities had been for Ilisu Dam and the subsequent Cizre Dam and HEPP, we can talk about a more sound decision from the engineering perspective.
There are two important reasons why the country cannot develop sufficiently. The first is that the investments have not been selected correctly, that is, the efficient investments have not been done in the first place. The second is poor time and cost management performance in critical investments. The same criticism is valid for almost all industries in the country, which is linked to weakened engineering performance and lack of people's commitment.

CONCLUSION

- It was a serious mistake to fund such a critical and strategic project with foreign credit.
- The memorandum of understanding signed by the DSİ for the credit was not a one that can be accepted by an independent country. The MoU with articles generating this much burden should not have been signed.
-The revisions made in the dam body caused consequent revisions in other parts. Redundantly 3 years were lost. The total delay has reached 5.5 years.

It was obvious that this situation was very favorable for those who do not want this dam to be built. In our country, we have people and civil society organizations who ask " What use does a dam have? " and answer this question as " So far dam is the worst invention of human beings".

I explain all in detail to help new generations understand and do not repeat similar mistakes in the future. I believe we should learn from our mistakes in order to progress. I'd like to mention that this country has reached the current level with the efforts and sacrifices of unknown heroes.

The experiences gained during the Ilısu Project is typical to GAP.
I wish Ilısu Dam and HPP construction become auspicious for my country and people and for their efforts in realizing such a significant investment for my country, I put aside the mistakes made and congratulate those who contributed.

REFERENCES

GAP Development Plan. DSİ 1972
DSİ Ilısu Dam 16. Region 2017 presentation Program
Concrete faced Dams. DSİ TAKK Directorate 2017
Ilısu Dam and HPP Construction Memorandum of Understanding 2000
Water Report 2009.Selami OĞUZ

5th International Symposium on Dam Safety

October 27-31, 2018

REAL TIME DAM STABILITY FORECASTING

Ton PETERS [1], Frans VAN DEN BERG [1], Ahmed ELKADI [1]

ABSTRACT

In cooperation with the Karnataka Water Resources Department (KaWRD) a pilot project, called DAMSAFE, is currently being completed at the Bhadra dam and reservoir, located in Karnataka (India). In DAMSAFE an operational monitoring and forecasting system is implemented and the results are demonstrated to the dam operator. The overarching goal of the pilot project is to contribute to enhancing dam safety and water management in India. The innovative technologies that will be integrated in DAMSAFE are: PS-InSAR satellite measurements, in-situ measurements and the Delft-FEWS software platform. Delft-FEWS is used to integrate global weather forecasting and (measurement) data from different sources with automatic computations using different hydrology, hydraulic and geotechnical numerical models. The system supplies information on forecasting of inflow and water levels in the reservoir that can be used for Real Time Control (RTC) of reservoir operation. Based on water pressure measurements in the dam body and dam foundation the stability of the dam is calculated real time. In future, the forecasting of water reservoir levels allows for forecasting of dam stability. This information can be used to control flood risk and for emergency response actions.

Keywords: In-situ Measurements, Satellite Measurements, Dam Stability Forecasting,

INTRODUCTION

Demand for water is steadily increasing throughout the world and conflicting interests generate a complex and delicate field of work. Multi-purpose water reservoirs and dams play a major role for water supply, irrigation, hydropower and flood protection in India. The dams are aging, but are also facing different circumstances than when designed, often decades or more ago. This is due to changes in land use, socio-economic developments and climate change. In order to ensure long-term operation and safety of the dams, continuing investments have to be made in adaptation planning and actions including monitoring, maintenance, repair and retrofitting. The on-going Dam Rehabilitation and Improvement Project (DRIP) in India is one of the major endeavors targeting at improving the existing situation of the large dams in India (Pillai & Giraud, 2014).

In cooperation with the Karnataka Water Resources Department (KaWRD), a pilot project, called DAMSAFE, is currently being completed in which a number of innovative technologies on dam safety and water reservoir performance will be demonstrated on a site in this state by a consortium led by Deltares (https://www.deltares.nl/en/). The Central Water Commission (CWC) is involved in the project as a major stakeholder at national level. One of the project challenges will be to focus information from these technologies to the needs in the Indian dam safety and water management sector. That is why close interaction with the end-user KaWRD was established. (Peters & Giri, 2017).

[1] Deltares, Geo-Engineering Department, Delft, the Netherlands, https://www.deltares.nl/en/
E-mail: ton.peters@deltares.nl

The Deltares led DAMSAFE consortium further consists of the Dutch companies SkyGeo and Royal Eijkelkamp and the Spanish company iPresas. These companies provide high tech, specialist technologies on PS-InSAR satellite measurements, online monitoring systems and risk-informed dam safety assessment. The ambition of the consortium partners is to use this pilot project for building a long-term cooperation with end-users in this sector and to offer integral solutions. The role of Deltares as a research organization is to provide the needed integrating, enabling software technologies (Delft-FEWS, RTC-Tool, SOBEK and DAM).

BHADRA DAM-RESERVOIR SYSTEM

The pilot case of the DAMSAFE project is the Bhadra dam-reservoir system. Bhadra Dam is located across Bhadra River near Lakkavalli village, Tarikere Taluk, Chikkamagalore District of Karnataka State at an elevation of 601.00 m above Mean Sea Level (MSL). This is a multi-purpose dam, including irrigation, water supply and hydropower generation. (Peters et al., 2018)

Figure 1. Bhadra dam-reservoir system. Left: masonry dam (back). Right: saddle dam (front)

The dam was finished in 1962. It includes a main masonry dam and two saddle (earthen) dams. The main dam includes a spillway with four gates and has a total length of 76.8 m. The reservoir capacity is 2026 hm^3 (1 hm^3=1000000 m^3). The maximum height is 76.8 m for the masonry dam (main dam). The maximum height is 49.4 m for saddle dam 1 and 32.3 m for saddle dam 2. The base level is located at 583.39 m in the masonry dam (main dam), and at 612.95 m and 630.02 m for saddle dams 1 and 2, respectively. The maximum water level in normal operation is established at 657.76 m, being 657.15 m during the monsoon season. The spillway has a maximum discharge of 3012 m^3/s. The spillway crest level is located at elevation 650.60 m. The maximum spillway opening height is 7.16 m.

ONLINE MONITORING SYSTEM

A system, available online, has been implemented for monitoring of the water reservoir, main dam and saddle dams. The online monitoring system consists of two components:

- High frequency in-situ measurements providing data on water reservoir and dams at a number of specific locations.
- Low frequency satellite based measurements providing data on dam deformation at a wide range of locations on the dams.

The data of the online monitoring system is stored and presented in the Delft-FEWS software platform. The measurement data in combination with weather forecasting and numerical calculations

is used to provide information on current and expected behavior of the dam-reservoir system. This is further explained in in the next sections.

In-situ measurement system

The focus of the in-situ measurement system is on weather, water flow, water levels and dam behavior. Therefore, the system includes:

- weather stations in the catchment area to measure rainfall, temperature, wind and sun radiation,
- devices for measuring surface water levels at the dam and at the rivers flowing into the reservoir, (pore) water pressures in the dam body and in the dam foundation, and
- outflow of water from the dam drainage systems.

Figure 2. Measurement station at the river inlet into the Bhadra reservoir

The measurement stations were installed by Royal Eijkelkamp with local assistance from the district in which the Bhadra dam and reservoir are located. Figure 2 shows an installed measurement station at the river inlet into the reservoir to determine the water inflow from the main river. It is equipped with a battery and solar panel for energy supply and a wireless connection for data transmission.

The acquired data in combination with other historical data from the pilot dam are the input for the numerical computations of dam stability. The measurements are fully automated and available real-time on a secured internet platform, which is accessible worldwide for stakeholders and project partners. Monitoring activities will also include a dashboard within the Bhadra dam control room to present the results to the dam operator and maintenance staff.

Satellite based measurement system

Persistent Scatterer Interferometric Synthetic Aperture Radar (PS-InSAR) is a radar technique used to generate maps of surface deformation, using differences in the phase of the waves returning to the satellite, as shown in Figure 3. The technique can potentially measure millimeter-precision changes in deformation over spans of days to years.

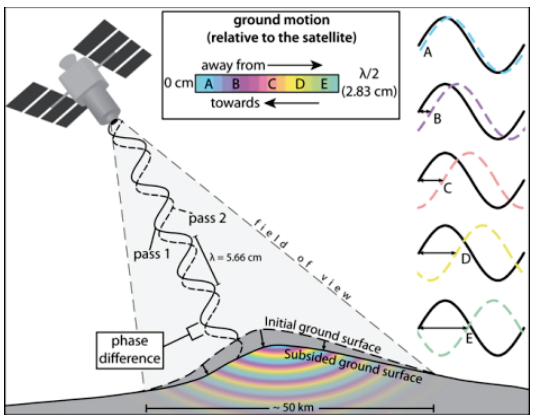

Figure 3. PS-InSAR Sattelite measurements

In general, there are two methods of applying PS-InSAR; using artificial reflection points and using natural reflection points. The method of natural reflection points has many advantages such as no access needed to the site, but it requires specialized data-processing (by partner SkyGeo) in order to optimize the measurements in terms of signal-to-noise ratio and allocation of the persistent scatterers.

The main limitation of the technology (McCormack et al. 2011) lies in the fact that not always sufficient energy is reflected back from the surface to the radar. This depends on the properties, direction and inclination of the reflecting surface.

An important advantage of the technology is that satellite images are 30x50 km or larger, meaning that, if sufficient reflectors are available, the whole dam can be monitored from the same source data. This includes many dam infrastructure assets (e.g. reservoir slopes, pumping stations, structural elements, supporting constructions, etc.), which cannot be achieved cost-effectively otherwise. The monitoring of dam deformation can be used to detect anomalies in dam behavior, of which the cause can subsequently be studied. New information can be added from future satellite images at a weekly, bi-weekly or monthly basis, depending on cost and availability of data.

Delft-FEWS FORECASTING

Delft-FEWS is a software platform developed by Deltares that is used to integrate **data** from different sources and to perform computations automatically using different numerical **models**, e.g. SOBEK

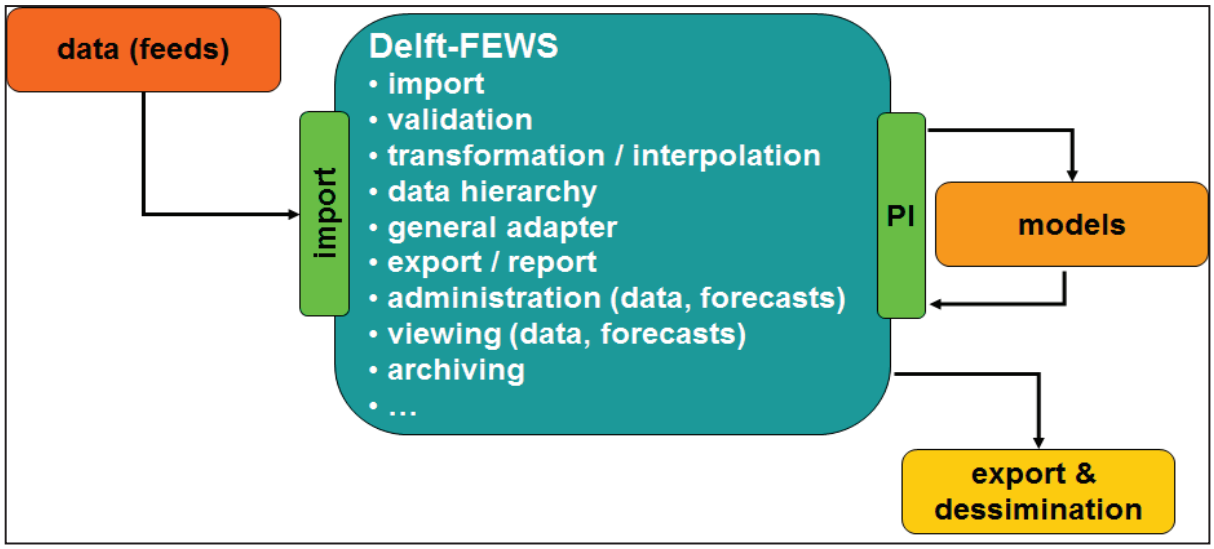

Figure 4. Overview Delft-FEWS software platform.

and DAM. SOBEK is a powerful modelling suite for hydraulic and morphological simulations including inundation, dam-break, dam/weir operation integrated with a Real-Time-Control (RTC) tool. DAM is software that assesses the strength of a dam or dike based on certain failure mechanisms (Peters and Van den Berg 2016). The DAM software is designed to routinely integrate data from different sources in a GIS environment, to perform automated, high density calculations of dam safety and to present the results in Delft-FEWS and in a GIS environment.

DISCUSSION OF RESULTS

In this section, the results are discussed of the measurements and the integration of measurements with numerical geotechnical modelling. The focus in this paper is on the aspect of dam safety, however the system also provides forecasting of inflow of water into the reservoir and expected water levels.

Dam deformation measurements

After processing of the PS-InSAR measurement data, the reflecting locations are presented on a map. Figure 5 shows the main (masonry dam), in which each dot represents a reflector on the surface. The colors indicate deformation in mm/year: downwards (yellow-orange-red) or upwards (blue). In green the deformation is small (only a few mm/year).

Figure 5. Main dam deformation (period 29 September 2016 to 11 March 2018)

During interpretation of the results it has to be noted that the direction of deformation is not necessarily exactly vertical but is depending on the position of the satellite compared to the reflecting surface. The results also have to be evaluated using information from the ground that can be supplied by the dam owner. The main conclusion from Figure 5 is that, though there a few reflectors showing some deformation, the overall situation of the masonry dam is stable.

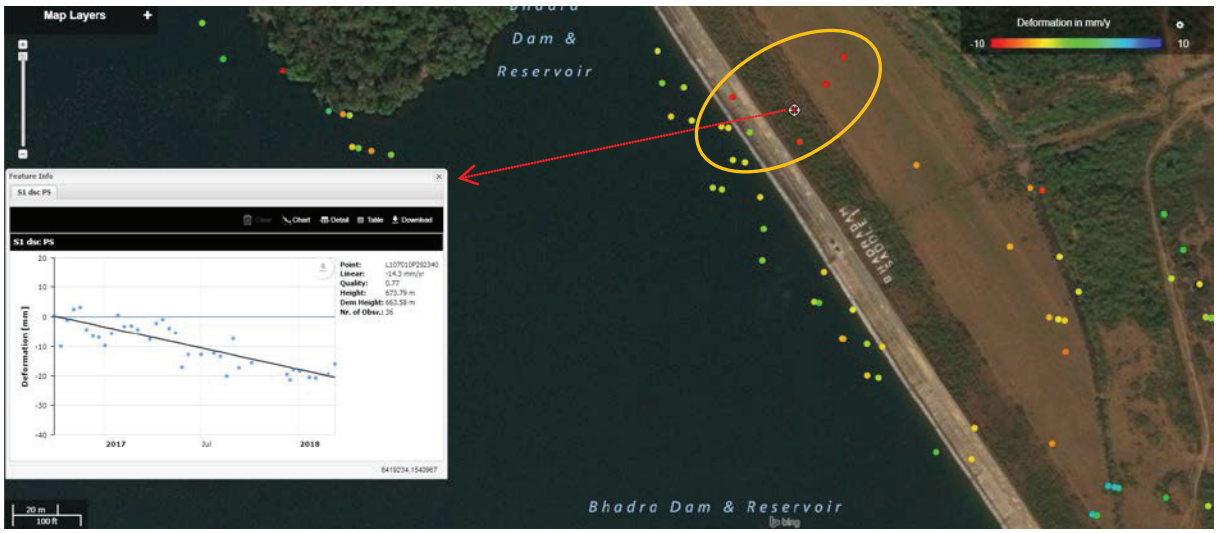

Figure 6. Saddle dam 1 deformation (period 29 September 2016 to 11 March 2018)

In Figure 6 the deformation of one of the embankment dams, including the deformation graph of a selected reflector, is presented. In the orange marked section of the dam there are locations on the crest of the dam, slope and hinterland that show deformation up to 14 mm/year. This is an indication of possible instability that needs further inspection to verify the observation and, if necessary, investigate the root cause and implement actions to prevent possible damage. These two examples show the added value of the used approach for verifying dam stability and to focus addition inspection to areas that show anomalies.

Integration of in-situ measurements with numerical calculations

Main dam

In Figure 7, the cross section of the spillway of the main dam is depicted including the installed monitoring instrumentation. The aim of the instrumentation is to feed the two stability models in real time. So the stability of the main dam is continuously known in detail. These two models are:

- Overturning of the main dam
- Horizontal sliding of the main dam

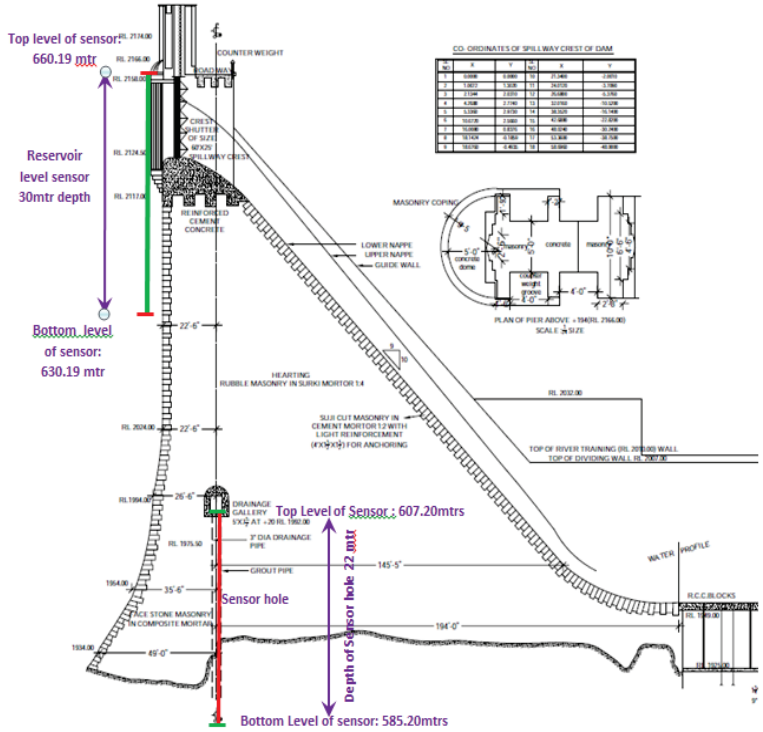

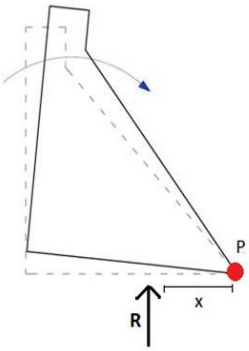

Overturning failure mechanism

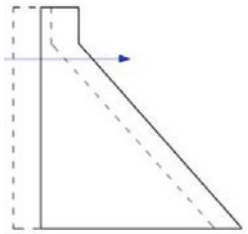

Sliding failure mechanism

Figure 7. Instrumentation of the main dam with a water level sensor and a pore-water pressure sensor in the dam foundation, including considered dam failure mechanisms

Figure 8 shows the real-time stability of the main dam as a graph in the operational Delft-FEWS system. The stability calculation is based on the measurements of the pore-water pressures sensors, which are installed under the gallery of the main dam, and the reservoir water level. The measurements of the pore-water pressures and the reservoir level are presented in this graph in meters to Reference Level (m RL) for the period from 17 March 2018 till 27 April 2018. Next to that the safety factor for real time dam stability for the overturning and sliding mechanisms are presented in this graph.

During the depicted time period, the Bhadra dam reservoir level was decreasing from 645.71 [m RL] till 638.74 [m RL], that is a diminution of approximately 7 m. This diminution is the result of the water use for irrigation and drinking water and because of evaporation.

The piezo-metric head sensors WA1 and WA2 showed in that period also a decrease of the piezo-metric head values as a result of the lowering of the Bhadra dam reservoir level. Probably due to grouting activities, as part of the rehabilitation program, some of the sensors show fluctuating pressures. This is shown as some irregular activities in the graph line of the sensors. However, the trend lines for the sensors are showing a decrease.

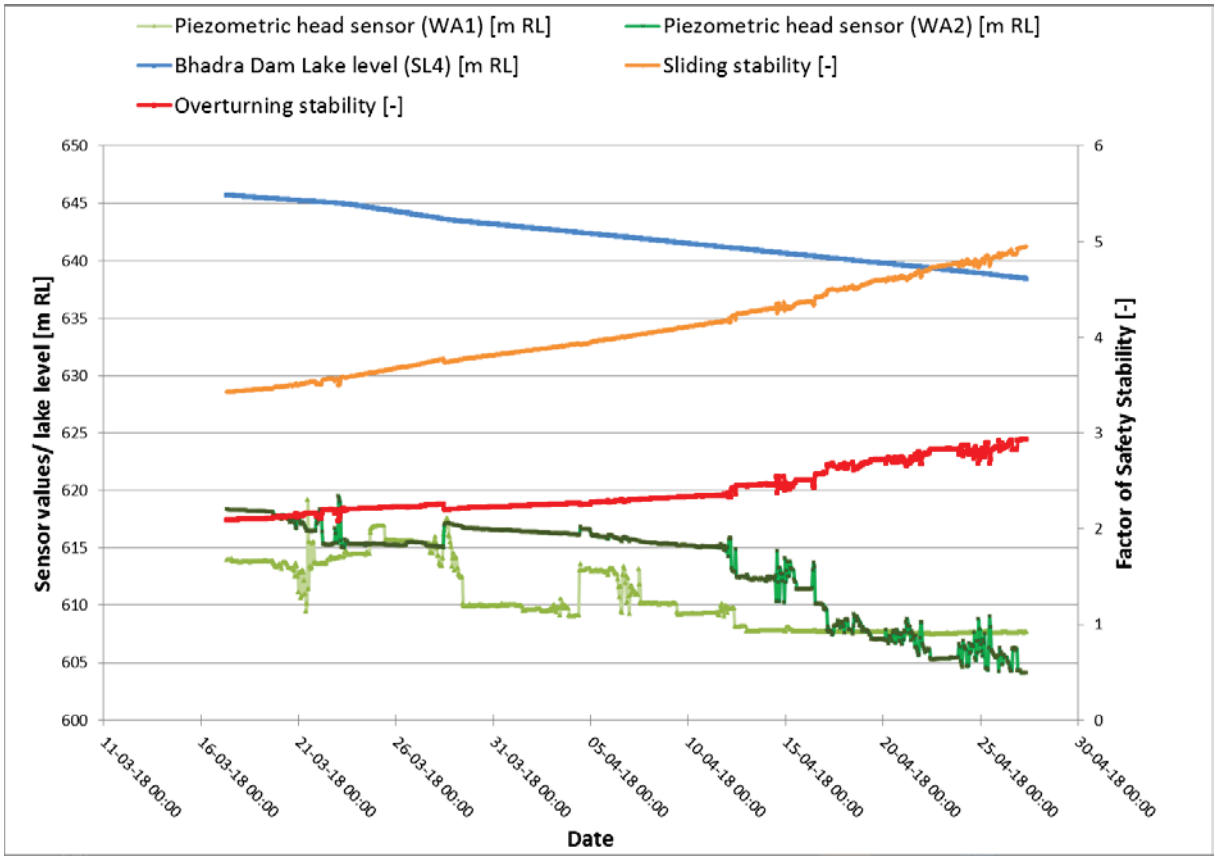

Figure 8. Stability Spillway (sliding and overturning)

Immediately after collecting the data from the sensors the system calculates the real time stability for overturning and horizontal sliding. As a result of the lowering of the reservoir level the stability for overturning and horizontal sliding will increase, this is as expected. The factor of safety for the overturning stability has increased from 2.09 to 2.93 in this period and for the horizontal stability there is an increase from 3.42 to 4.94. Based upon these result it can be concluded that lowering the reservoir level will result in an increase of stability of the main dam.

Saddle dam

In order to calculate the macro stability of the saddle dam, pore-water pressure sensors have been installed in the downstream slope, see Figure 9. The macro stability will be calculated in real time with the input of the installed pore-water pressure sensors and the reservoir level. In Figure 10, the results of the calculations for the period from March 17 till April 27, 2018 are shown.

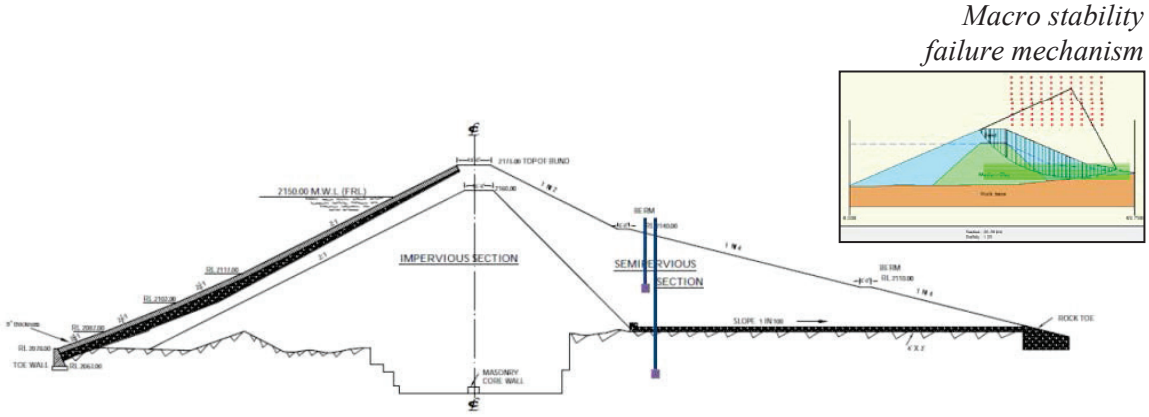

Figure 9. Instrumentation of Saddle dam 1 with a pore-water pressure sensor in the dam body and in the dam foundation, including considered failure mechanism

During the period from March 17 till April 27, 2018 the Bhadra dam reservoir level was decreasing from 645.71 [m RL] till 638.74 [m RL], that is a diminution of approximately 7 m. This diminution is result of the water use for irrigation and drinking water and because of evaporation.

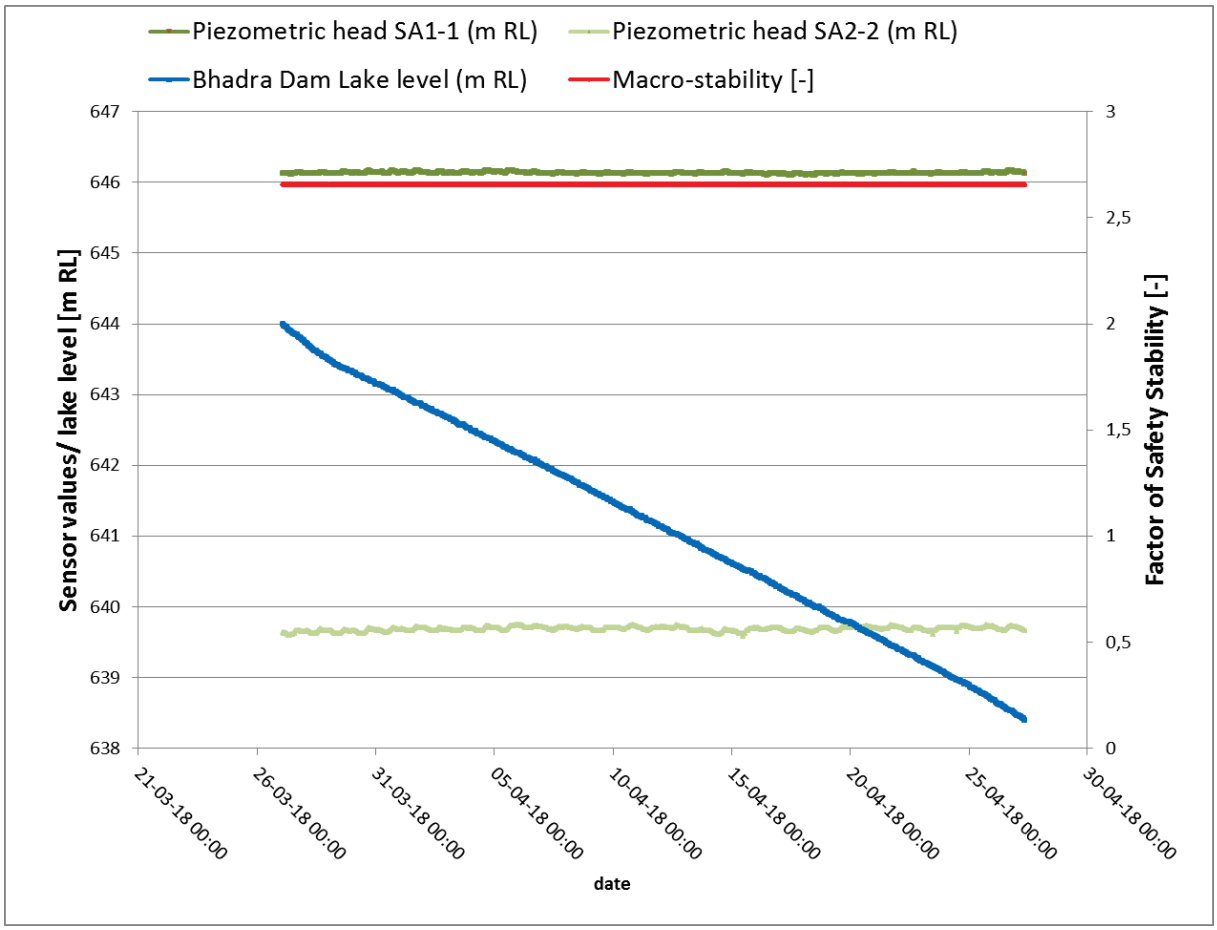

Figure 10. Macro stability down stream Sadde dam 1

The piezo-metric head of sensors SA1-1 and SA2-2 showed in that period no response to the decreasing of the Bhadra dam reservoir level. The sensors gave a relative flat line for that period. The reason for that is the impermeable core of the saddle dam. Because there is no direct response of the piezo-metric head to the lowering of the Bhadra dam reservoir (as shown in the graph of Figure 10), it can be concluded that on this location the dam core is functioning well. As a result also no change is observed in the safety factor of the real time calculated macro stability.

CONCLUSION

In this paper an innovative approach was presented on the monitoring of stability of dams. The use of PS-InSAR (radar) measurements from a satellite platform offers the possibility to detect anomalies in the dam deformation pattern indicating a possible deterioration process. Further inspection of detected anomalies is needed to verify the observation and, if necessary, investigate the root cause and implement actions to prevent possible damage. The systematic monitoring of dams with PS-InSAR will in the long-term contribute to optimization of Operation and Maintenance (O&M).

In the pilot of the Bhadra dam-reservoir system, the integration of in-situ measurements with numerical calculations is demonstrated using the Delft-FEWS software platform. Based on observed water levels in the reservoir and pore-water pressure measurements in the dam body and dam

foundation, the stability of the dam for certain failure mechanism is calculated in real time. This information can be used by the dam owner to control flood risk.

Based on weather forecasting, the Delft-FEWS system also supplies information on forecasting of water inflow and expected water levels in the reservoir. In combination with Real Time Control (RTC) of reservoir operation, this information can be used to improve water management and that will increase performance of the reservoir.

A next step will be the correlation between observed water levels in the reservoir and the pore-water pressure measurements. This will be possible when sufficient data becomes available of the reservoir at low water level and maximum water level during the monsoon. The forecasting of inflow of water in the reservoir and expected water levels at the dam will then allow us to go beyond real time stability monitoring. This means that the safety factor of the dam for the considered failure mechanisms can be forecasted days ahead. In critical situations this information will be important for dam owners, first responders and responsible government agencies and allow for a timely deployment of emergency response actions (e.g. evacuation).

AKNOWLEGDEMENTS

The DAMSAFE project (http://www.damsafe.eu/) in Karnataka is sponsored by the Dutch Partners for Water Program. The authors wish to thank the Central Water Commission, the Karnataka Water Resources Department and the Netherlands Enterprise Agency for their support to this project.

REFERENCES

Berg, van den, F. et al., 2012. “Real time Monitoring of Levees through Sensor Technology along the Yellow River”. Fifth International Yellow River Forum, Zhenghzou, China.

McCormack, H., Thomas, A. and Solomon, I., (2011). “The capabilities and limitations of satellite InSAR and terrestrial radar interferometry”. http://www.smartlevee.nl/en/

Peters, T., and Berg, van den , F (2016). “Rapid Assessment Tools for Dam Safety”. Second National Dam Safety Conference, Bengaluru, India.

Peters, T. and Giri, S., 2017. “the DAMSAFE project in Karnataka”. Third National Dam Safety Conference, Roorkee, India.

Peters, T. et al., 2018 “Enhancing dam safety and water resources management in India: the case of Bhadra dam (Karnataka)”. International Commission on Large Dams (ICOLD), Vienna, Austria.

Pillai, B.R.K. and Giraud, S., 2014 Dam Rehabilitation and Improvement Project (DRIP): 270 Dams to be rehabilitated”. First National Dam Safety Conference, Chennai, India.

5 DAM SAFETY İstanbul Turkey 2018

International
5th National Symposium on
Dam Safety

October 27-31, 2018

DAM SAFETY LEGISLATION – THE GOOD AND THE BAD

Dr Andy HUGHES [1]

ABSTRACT

This paper describes the development of legislation in the UK. It will demonstrate how the country has developed a system which places the responsibility of the assessment of safety squarely on an individual engineer assessed and appointed by Government to be capable of assessing safety. The paper will describe the benefits of such a system, but it also shows that the development has been largely reactive rather than proactive.

The paper will go on to describe how after a number of incidents in 2007 that the legislation was modified in an attempt to move towards a risk-based approach. This process and the outcomes will be discussed in detail and show that things could have been handled in a better way because the UK now has what are effectively four different legislative regimes – one for England, one for Wales, one for Scotland and one for Northern Ireland. The author thinks this is not a sensible outcome and will give suggestions on how best to manage a review of legislation or the formulation of new legislation.

Keywords: history, safety, legislation, accidents, risk.

INTRODUCTION

Reservoir safety legislation in the UK has, like most countries, developed with time. This has largely been by reactions to incidents, accidents and failures that have occurred. However, in contrast to may reservoir safety models around the world, the legislation still places the assessment of safety on an individual engineer, the Panel Engineer, assessed and appointed by Government.

THE HISTORY OF LEGISLATION IN THE UK

The first piece of legislation that can be traced is the Waterworks Clauses Act of 1863. This seems to be a reaction to a failure at Holmforth in 1852 where 64 people lost their lives. This legislation gave the powers to two justices of peace, if they were alerted to a problem, to investigate the problem and then to arrange, presumably with engineers, to resolve the problem.

The flooding of a mine by water from a reservoir basin near Manchester led to the farmers ruling of Rylands v Fletcher in 1868, which states that if anyone released anything onto another party they are liable – the reservoir contents were released into the mine causing the working of the mine to stop.

In 1864 the failure of Dale Dyke, a dam filling for the first time, led to more than 264 lives to be lost on the night of the 11th March. It is likely that more than 400 lives were lost due to disease and pestilence.

[1] Director, Dams & Reservoirs Ltd, Newark, United Kingdom
e-posta: andy.hughes@damsandreservoirs.co.uk

The coroner's jury of the time said dams should be subject to regular, frequent and adequate inspection.

Figure 1. Dale Dyke

This thread has been woven through all legislation since that date.

In 1925 the UK suffered two major accidents, one at Skelmorlie in Scotland where 5 people were killed when a reservoir with a capacity of 5 million gallons (22,700 cubic metres) failed, and then a further 16 people were killed in November 1925 when a cascade of 2 dams failed and destroyed part of the village of Dolgarrog in North Wales.

Figure 1. Dolgarrog

These events led the engineering profession to put pressure on the Government to bring in further legislation. The Reservoirs (Safety Provisions) Act, 1930 came into force early in 1931 and this introduced the Panel Engineer system, where an independent engineer carried out a statutory inspection and made recommendations in the interests of safety.

Unfortunately, although the Act was in place for more than 40 years, it was ineffective as there was no register of reservoirs and a large number of reservoirs were never inspected and when works were required there was no enforcement – no one made the owner carry out the work.

Failures at Malpasset and Vajont in the 1900's and discussions at the ICOLD meeting in Edinburgh led the UK Government to review the 1930 legislation via a committee in 1966. This committee made 12 recommends for change.

The most noteworthy changes were the formulation of an Enforcement Authority who had a duty to form a register of reservoirs and generally enforce the Act, including carrying out works if required. The other main recommendation, which is probably the most important feature of the current legislation, was the formation of the Supervising Engineer. The Supervising Engineer is a 'Panel Engineer' trained to examine the dam and to look for changes which could be an indication of a failure mode forming. That engineer would then seek advice from a more senior Panel Engineer – an Inspecting Engineer.

The Reservoirs Act, 1975 passed through Parliament in 1975 but political pressures meant, an Act, which stated it was there to protect persons and property against an escape of water, was not commenced until 1987.

In the 1990's various reviews were undertaken as to how the Act was performing and in 2003 the Water Act led to two significant changes; a change from more than 160 different Enforcement Authorities in England and Wales to one – the Environment Agency – a part of the Government department, DEFRA - the Department of the Environment, Fisheries and Rural Affairs. There was also a provision for the Secretary of State to order a flood plan to be written for the higher consequence dams. A flood plan consists of an onsite plan - what the owner can do to try to avoid a failure – containing such things as where to procure pumps, how many pumps are required and the hoses that go with them, what mobile phones work, where valves and located, how water can be turned away, where different accesses can be achieved – an inundation map – showing areas of inundation, water depths and velocities and time of travel defining areas where there is total destruction as opposed to partial destruction – this information feeds into the offsite plan, which is formulated and used by the emergency services to formulate their plans to evacuate people and ensure essential services are maintained, and as said many years earlier 'to protect persons and property against an escape of water'.

In 2007, the UK suffered a significant number of storms over a short period of time. This caused significant flooding and a number of small dams and reservoirs, not subject to the legislation – i.e. capacity of less than 25,000 m^3 were damaged and failed.

Sir Michael Pitt was commissioned by Government to review the situation and make recommendations for change to try to prevent reoccurrence of the problems in a time where people are talking about climate change and more severe hydrological events.

Sir Michael Pitt's report – Pitt Review – Learning Lessons from the 2007 Flood (2008) had written into its recommendations which included a move towards a risk-based approach for reservoir safety, a change to a lower threshold volume (10,000 cubic metres); and a desire to consider 'cascades' of reservoirs.

The Flood and Water Management Act of 2010 introduced these issues. Devolution of legislation to the counties of the UK have now meant that the Reservoirs Act 1975 as modified by the Flood and Water Management Act 2010 applies to England and Wales, the Reservoirs (Scotland) Act, 2011 applies to Scotland and Northern Ireland is developing and implementing its legislation called the Reservoirs Act (Northern Ireland) 2015.

The principles outlined by Sir Michael Pitt have been embodied into the legislation but now we have three different pieces of legislation with one piece of legislation applied differently by the legislators in England and Wales.

In England and Wales reservoirs are now constituted as either 'High Risk' or 'Not High Risk'. If designated as High Risk, then the reservoir has to be inspected and supervised as shown. If 'Not High Risk' then the reservoir is not subject to any legislation. If development took place downstream of a reservoir which had been designated as 'not high risk' then it would be reclassified as 'high risk'. A reservoir is considered high risk – a reservoir where one person's life is put at risk.

In Scotland they have three designations; high, medium and low risk – the medium risk ensures a Supervising Engineer (SE) is employed and a statutory inspection only is called for if the SE is concerned about something.

It remains to be seen what Ireland adopts but it is likely to be in line with Scottish arrangements.

Ireland, Scotland and Wales have adopted the new criteria for volume of the reservoir – 10,000 cubic metres – but England has not, even though the legislation in Wales and England is the same.

Cascades have not been adopted by any of the legislation to date and Scotland has accepted a true 'risk based' approach and owners are required to calculate the probability of failure, whereas the legislation in England and Wales is really a consequence-based system.

CONCLUSIONS

The UK in general reacted to situations which have occurred. Changes in legislation have been made after events which have occurred.

The UK has now three different elements of legislation applied in four different ways for a stock of reservoirs which are essentially similar across the geographic boundaries.

In my opinion, I believe that any Government considering changes to legislations should consult with the engineers having to operate within the legislative framework – get their views and collect knowledge on what the legislation should help them achieve in terms of tool to try to advise reservoir safety. Parliamentary draughtsmen would then be used to change the desires into the clauses required to be put into the Bill and subsequently the Act. This opportunity, when it is based on a reactionary response to incidents/accidents, only occurs every 30 years or so, and in my opinion, we have missed a fantastic opportunity to simplifying our legislation and achieve improvements.

It is unfortunate that we have three different pieces of legislation applied in four different ways. The opportunity to address difficulties and change clauses to address areas of uncertainty/confusion is difficult.

Parliamentary time is always limited and so opportunities for change arise unless it is a reaction to a problem.

However, the UK legislation is still based on the Panel Engineer system which I consider is a very powerful way in trying to ensure reservoir safety. It is considered that any proposed changes should be first discussed with Panel Engineers before discussing with Parliament Draughtsmen to achieve the 'correct' outcome for the amendments to the legislation.

Consistency across the four administrations with the same legislation is considered to be a desirable outcome from any future review.

The views expressed in this paper are those of the author only.

REFERENCES

HMSO, The Waterworks Clauses Act 1963
HMSO, The Reservoirs (Safety Provisions) Act, 1930
HMSO, The Reservoirs Act 1975
HMSO, The Water Act 2003
The Cabinet Office, 2007, The Pitt Review – Learning Lessons from the 2007 Floods.

5 DAM SAFETY
İstanbul Turkey 2018

5th International Symposium on Dam Safety

October 27-31, 2018

NUMERICAL SIMULATIONS OF THE WETTING EFFECT ON THE LONG-TERM BEHAVIOUR OF CONCRETE FACE ROCKFILL DAMS

Mohammadkeya KHOSRAVI [1], Linke LI [2] , Saeed SAFIKHANI [3] , Erich BAUER [4]

ABSTRACT

Wetting deformations of the rockfill material in a concrete face rockfill dam (CFRD) can lead to an increase of the bending of the concrete slabs and consequently to cracks and leakage points in concrete slabs. Heavy rainfall or defects of the concrete sealing causes a local increase of the moisture content in the dam body, which can lead, for moisture sensitive rockfill materials, to time dependent deformations.
In the present paper, numerical simulations are carried out to investigate the influence of the size and location of the wetted zone on the time dependent deformation of the CFRD. To this end an extended hypoplastic constitutive model by Bauer is used. The model takes into account the current void ratio, the effective stress, the strain rate, the moisture-sensitive solid hardness and its rate. Herein the moisture-sensitive solid hardness is a key parameter to model the inherent properties of moisture-sensitive and weathered coarse-grained rockfill materials. It is shown that the size and location of the wetted zone has a strong influence on the evolution of concrete slab deformation.

Keywords: Rockfill dam, solid hardness, wetting deformation, hypoplasticity

INTRODUCTION

The effect of wetting on the mechanical properties of weathered and moisture sensitive rockfill materials is an experienced fact and of great importance for the long term behaviour of rockfill dams, e.g. (Sowers et al., 1965; Clements, 1981; Oldecop and Agreda, 2004; Oldecop and Alonso, 2007; Chen et al., 2007; Bauer et al., 2010). Wetting deformations of rockfill material are caused by a degradation of the solid hardness leading to particle breakage and a reorientation of the grain skeleton into a denser state. The amount of particle crushing is mainly controlled by the state of weathering of the rock particle, the grain size distribution, the pre-compaction, the stress level and the change of the moisture content (Nobari and Duncan, 1972; Brauns et al., 1980; Alonso and Cardoso, 2010). The deformation and strength characteristic of the rockfill material differs in dry and wet conditions. The change of the moisture content of the granular material has a significant effect on the micro crack propagation in the rock particles and the degradation of the solid hardness subsequently leads to

[1] PhD student and Assistant Lecturer, Institute of Applied Mechanics, Graz University of Technology, Austria, e-posta: khosravi@student.tugraz.at
[2] PhD student and Assistant Lecturer, Institute of Applied Mechanics, Graz University of Technology, Austria, e-posta: linke.li@student.tugraz.at
[3] PhD student and Assistant Lecturer, Institute of Applied Mechanics, Graz University of Technology, Austria, e-posta: s.safikhani@student.tugraz.at
[4] Professor, Institute of Applied Mechanics, Graz University of Technology, Austria
e-posta: erich.bauer@tugraz.at

deformations in the rockfill body even if the stress is kept constant (Hang, 1990; Tedd et al., 1994; Oldecop and de Agreda, 2007; Fu et al., 2011; Bauer, 2018).

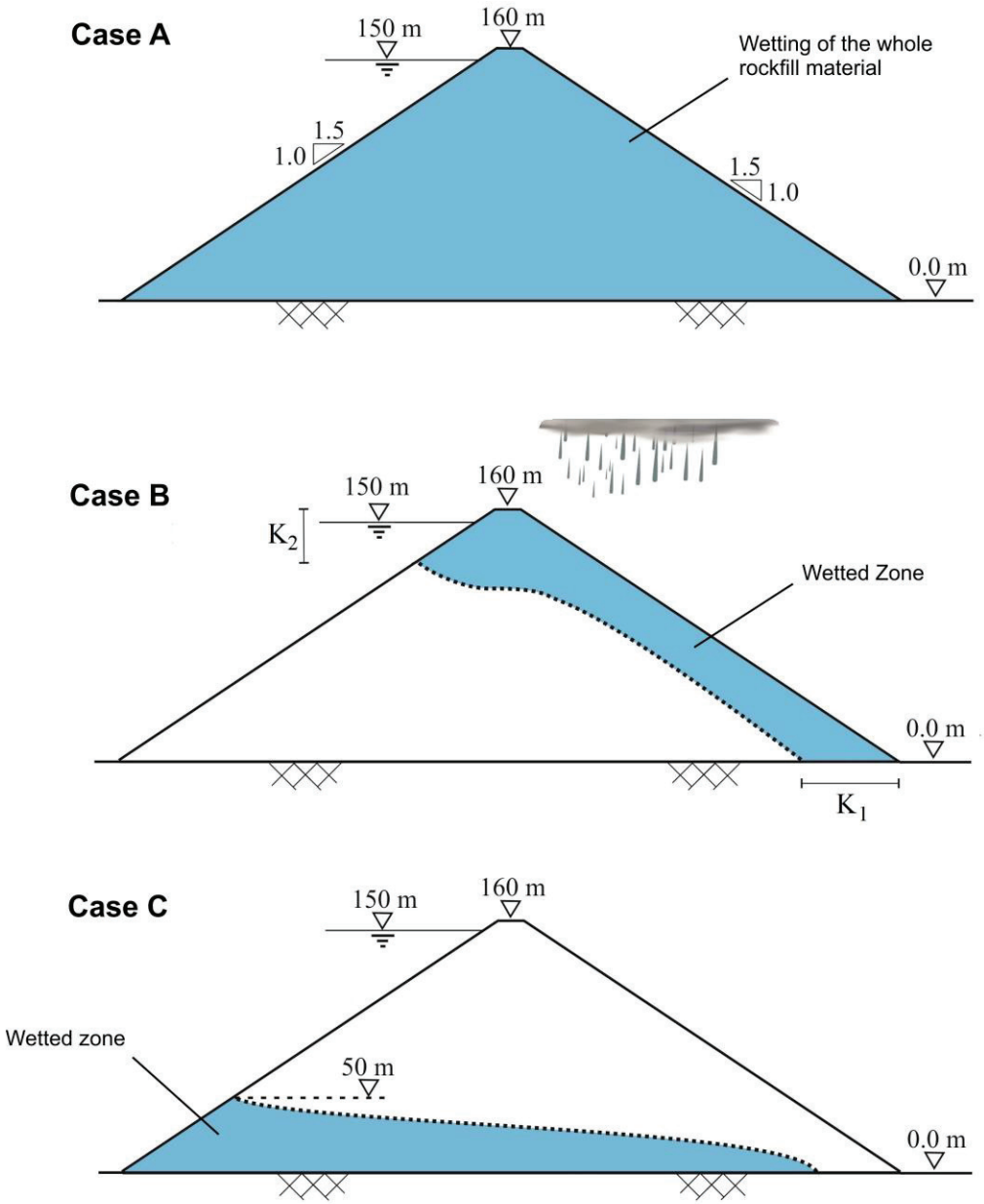

Figure 1. Section of an artificial CFRD with three different wetting scenarios:
Case A: wetting of the whole rockfill material;
Case B: wetting of a downstream part of the dam body caused by rainwater infiltration;
Case C: leakage into the lower part of the rockfill dam.

Long-term deformations of the rockfill material may have a strong influence on the amount of bending moments and crack propagation in the concrete slab of a concrete face rockfill dam (CFRD). The analysis of the wetting-induced deformation in CFRDs is thus of great importance already during the design phase. Wetting induced deformations are a function of the initial conditions in terms of the state of weathering of the solid hardness, void ratio, stress state and moisture content and the change of these quantities (Bauer, 2009; Lu et al., 2010). Depending on the reason for a change of the moisture content the corresponding time dependent degradation of the solid hardness can be limited to a specific area within the dam body.

In the present paper, numerical simulations are carried out to investigate the influence of the size and location of the wetted zone on the time dependent deformation of the rockfill material and the concrete slab of an artificial CFRD. Three different scenarios of wetting zones are investigated as illustrated in (Figure 1). In particular, in Case A it is assumed that the entire rockfill material is wetted, in Case B only a part of the downstream area is affected by rainwater infiltration and in Case C wetting of the bottom part of the rockfill material caused by leakage through the foundation is considered. For modeling wetting effects an extended hypoplastic constitutive model by (Bauer, 2009) is used. The model takes into account the current void ratio, the effective stress, the strain rate, the moisture-sensitive solid hardness and its rate. The moisture-sensitive solid hardness is described in the sense of a continuum description and it is a key parameter to model the inherent properties of moisture-sensitive and weathered coarse-grained rockfill materials.

CONSTITUTIVE MODEL

In order to model weathered and moisture sensitive rockfill materials the so-called solid hardness plays an important role in the constitutive model used in the present paper. In particular, the solid hardness, h_{st}, is a parameter in the compression law proposed by (Bauer, 1996, 2009) which is defined for an assembly of particles under monotonic isotropic loading. Thus, h_{st} should be distinguished from the hardness of individual grains. It is known that under the same pressure rockfill materials can show different packing density of the grain assembly, i.e. the void ratio can range between a maximum void ratio, e_i, and a minimum void ratio, e_d. For consistency, the solid hardness h_{st} is related to the compression curve obtained from an isotropic compression starting from the maximum void ratio. The decrease of the maximum void ratio, e_i, with an increase of the mean pressure, p, is described by the following compression law (Bauer, 2009):

$$e_i = e_{io} \exp\left[-\left(\frac{3p}{h_{st}}\right)^n\right] \tag{1}$$

Herein e_{i0} denotes the maximum void ratio at the stress-free state, h_{st} is the current value of the solid hardness and n is a constitutive parameter. The compressibility of weathered rockfill materials is higher for the wet material than for the dry material. When a reaction with water takes place the degradation of solid hardness is a time dependent, irreversible process and modelled by the following evolution equation (Bauer, 2009):

$$\dot{h}_{st} = -\frac{1}{c}(h_{st} - h_{sw}) \tag{2}$$

Herein the current state of the solid hardness, h_{st}, ranges within the upper limit h_{so}, i.e. the solid hardness before wetting and the lower limit h_{sw}, i.e. the final degraded state of the solid hardness.
Parameter c has the dimension of time and scales the velocity of degradation. It can be calibrated from a creep test. For general stress paths, the moisture and rate-dependent solid hardness and limit void ratio has been embedded into the hypoplastic model by (Bauer, 1996) and (Gudehus, 1996). In particular, for $\dot{h}_{st} \le 0$ the extended constitutive equation reads (Bauer, 2009):

$$\sigma_{ij}^{\nabla} = f_s [\hat{a}^2 \dot{\varepsilon}_{ij} + (\hat{\sigma}_{kl}\, \dot{\varepsilon}_{kl})\hat{\sigma}_{ij} + f_d\, \hat{a}\,(\hat{\sigma}_{ij} + \hat{\sigma}^*_{ij})\sqrt{\dot{\varepsilon}_{kl}\, \dot{\varepsilon}_{kl}}] + (\dot{h}_{st} / h_{st})\sigma_{ij} \tag{3}$$

In (Equation 3), σ_{ij}^{∇} denotes the effective objective stress rate, $\dot{\varepsilon}_{ij}$ is the rate of deformation, σ_{ij} is the effective Cauchy stress, $\sigma^*_{ij} = \sigma_{ij} - \sigma_{kk}\delta_{ij}/3$ is the deviatoric part, $\hat{\sigma}_{ij} = \sigma_{ij}/\sigma_{kk}$ and $\hat{\sigma}^*{}_{ij} = \hat{\sigma}_{ij} - \delta_{ij}/3$ are normalized quantities. Factor $\hat{a}$ is related to critical friction angle, φ_c, and can be adapted to the limit condition by (Matsuoka and Nakai, 1977) as shown in detail by (Bauer, 2000).
The effect of pressure level and current void ratio on the incremental stiffness is taken into account with factors f_s and f_d. In particular, the density factor f_d represent a relation between the current void ratio e, the critical void ratio, e_c and the minimum one e_d, i.e.

$$f_d = \left(\frac{e - e_d}{e_c - e_d} \right)^{\alpha} \tag{4}$$

where the pressure dependent quantities e_c and e_d are related to the compression law (Equation 1) via the postulate by (Gudehus, 1996), i.e.

$$\frac{e_i}{e_{io}} = \frac{e_c}{e_{co}} = \frac{e_d}{e_{do}} = \exp\left[-\left(\frac{3p}{h_{st}} \right)^n \right] \tag{5}$$

The stiffness factor f_s has the dimension of stress and reads:

$$f_s = \left(\frac{e_i}{e} \right)^{\beta} \frac{1}{\hat{\sigma}_{kl}\,\hat{\sigma}_{kl}} \frac{1 + e_i}{n\, h_i e_i} \left(\frac{h_{st}}{3} \right)^n p^{(1-n)} \tag{6}$$

Herein , α and β are constitutive constants (Bauer, 1996) and h_i can be obtained from a consistency condition by (Gudehus, 1996).

NUMERICAL SIMULATIONS

The effect wetting of the rockfill material on the long-term behavior of an artificial CFRD is numerically investigated using the extended hypoplastic constitutive model outlined in the previous section and the finite element program ABAQUS. The CFRD considered has a height of 160 m, a width of the crest of 16 m and a slope ratio of 1:1.5 on both upstream and downstream side of the dam as illustrated in (Figure 1). For the sake of simplicity, in all simulations a rigid foundation is assumed. For the rockfill material a weathered broken granite with a density of 2200 kg/m^3 and a corresponding void ratio of e_0 = 0.33 of the compacted state of the dam body after construction is considered. The hypoplastic constitutive parameters of the rockfill material are calibrated based on the data obtained from large scale triaxial experiments carried out by (Kast, 1992). The parameters are summarized in (Table 1). Herein the solid hardness of h_{s0} = 75.0 MPa is obtained from experiments under dry conditions. It can be noted that for a water saturated condition a value of h_{sw} = 25 MPa was obtained for a lower pre-compaction (Bauer, 2009), while in the current investigation a higher value is considered (Khosravi et al., 2017). In particular, for the effect of limited rainfall events (Case A and Case B) a value of h_{sw} = 68.8 MPa and for the long-term effect of leachate (Case C) a value of h_{sw} = 60.0 MPa is assumed.

Table 1. Constitutive parameters for the rockfill material

Case	h_{s0} [MPa]	n	h_{sw} [MPa]	c [Year]	φ_c [°]	e_{d0}	e_{c0}	e_{i0}	α	β
A	75	0.6	68.8	2.0	42.0	0.2	0.39	0.85	0.125	1.05
B	75	0.6	68.8	2.0	42.0	0.2	0.39	0.85	0.125	1.05
C	75	0.6	60.0	2.0	42.0	0.2	0.39	0.85	0.125	1.05

The corresponding reduction of the solid hardness with time is shown in (Figure 2). The concrete slab has a thickness of 0.3 m at the top and a thickness of 0.62 m at the bottom plinth. The latter is calculated according to the concept for design of CFRDs suggested by (ICOLD, 2004), i.e. for the 160 m high CFRD one obtains 0.3+0.002x160 = 0.62 m. At the bottom the concrete slab has a certain freedom to move along the concrete abutment. A linear elastic material behaviour is assumed. for the concrete, i.e. E_s = 20 GPa, υ = 0.17 and ρ = 2400 kg/m^3. Between the concrete slab and the cushion layer a friction coefficient of 0.5 is taken into account. The interface behaviour between the concrete slab and the cushion layer is modelled using the concept of Master and Slave surfaces provided by the finite element software of ABAQUS.

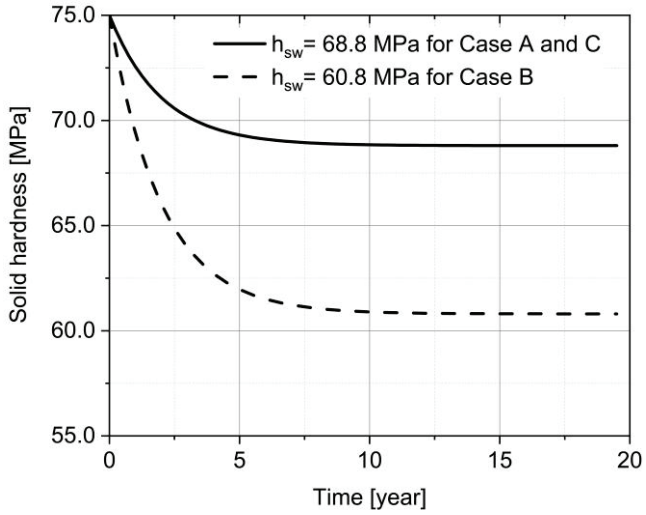

Figure 2. Degradation of the solid hardness with the time for two different wetting effects.

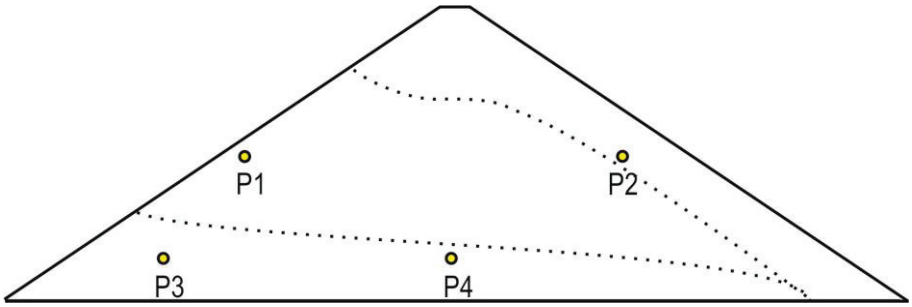

Figure 3. Selected points for comparing the void ratio caused by water impounding and wetting induced deformations (the dashed curves are related to the wetted zones in Case B and Case C.

Points	*e*
P1	0.3262
P2	0.3299
P3	0.3285
P4	0.3295

(a)

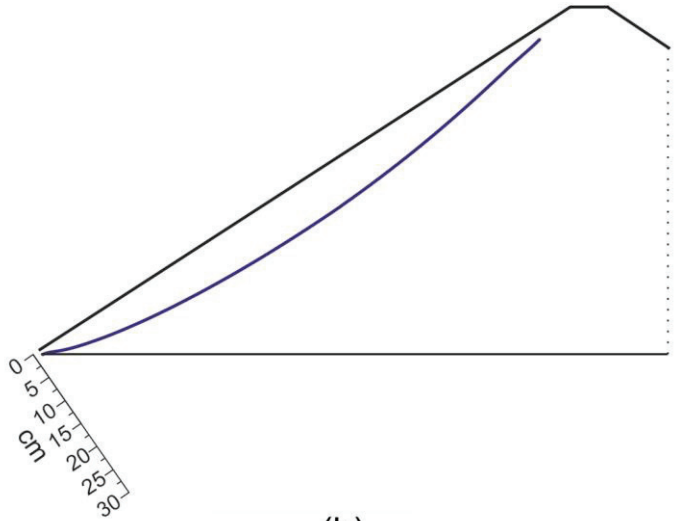

(b)

Figure 4. Deformation caused by water impoundment: (a) value of the void ratio at selected points defined in (Figure 3); (b) normal deflection of the concrete slab.

In the numerical simulation the following steps are considered: (i) construction of the dam body in 16 layers; (ii) construction of the concrete slab and the cushion layer; (iii) computation of the deformations caused by water impounding; (iv) additional deformations caused by degradation of the solid hardness for the wetting scenarios shown in (Figure 1).

Instantaneous deformation and additional compaction caused by water impounding

For computing the deformation caused by water impounding no degradation of the solid hardness is considered, i.e. for the instantaneous deformation the value of h_{s0} = 75 MPa is kept constant. Because of the high pre-compaction of the rockfill material assumed during construction the additional compaction is small. The evolution of void ratio at four points of the dam body is shown in (Figure 4a). The maximum reduction of the void ratio is located close to the concrete slab, (point P1), and the maximum void ratio is located in the downstream part of the dam body (point P2). The maximum normal deflection of the concrete slab is 7.5 cm and located nearly at the middle height of the dam (Figure 4b). Because of the rigid dam foundation, the concrete slab has only little freedom to move along the abutment joint and to penetrate into the thin cushion layer. This situation influences the shape of the slab deformation in the lower part.

Case A: Wetting of the whole rockfill material

After water impounding a degradation of the solid hardness, caused by wetting of the whole dam body, is considered over a period of 14 years. To this end, the reduction of the solid hardness from h_{st} = 75 MPa to h_{sw} = 68.8 MPa according to the evolution (Equation 2) is computed and taken into account in the hypoplastic constitutive (Equation 3). Although the degradation of the solid hardness is the same in the whole dam body, the evolution of the additional compaction is strongly related to the local stress state and density after water impounding. This is clearly visible by comparing the time dependent evolution of the relative void ratio, i.e. $e_{rel}(t) = (e_0 - e(t))/e_0$, in points P1, P2, P3 and P4 shown in (Figure 5a). The amount of reduction of the relative void ratio is greater at the lower level, i.e. for points P3 and P4, which can be explained by the combined effect of the higher vertical effective stress and the influence of wetting.

It can also be observed that the final value of the additional densification after degradation of the solid hardness is greater in point P4 than in point P3 although these two points are located at the same level. This is because of the influence of the higher vertical stress in point P4. It is clearly apparent that the change of the relative void ratio declines with increasing time and after 8 years the rate of the void ratio is almost the same in all points of the dam body. The normal deflection of the concrete slab after 14 years is shown in (Figure 5b). With respect to normal deflection caused by water impounding and degradation of the solid hardness the maximum value is 28 cm and located at the crest of the dam.

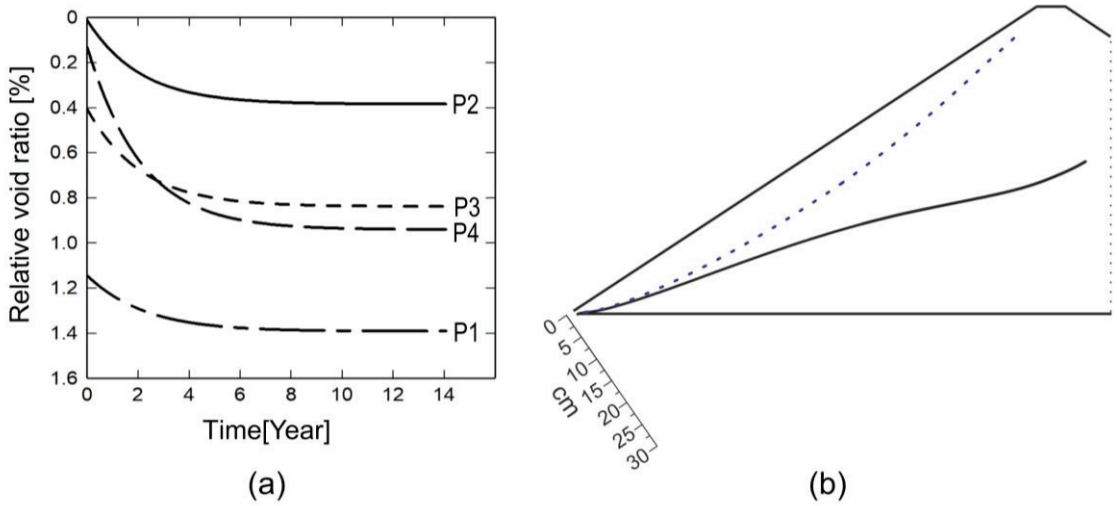

Figure 5. Wetting effect Case A: (a) changes of the relative void ratio at selected points defined in (Figure 3); (b) normal deflection of the concrete slab.

Case B: Wetting of a downstream part of the dam body caused by rainwater infiltration

In this case the deformations caused by wetting of a part of the rockfill material in the downstream part of the CFRD are investigated. In order to show the effect of rainwater infiltration, the creep deformation caused by gravity load and water impounding are not taken into account. The spatial area affected by the change of the moisture content of the rockfill material depends on the intensity and

duration of the rainfall events. Thus, the degradation of the solid hardness can be more pronounced within this area. To demonstrate this effect, four different areas are analyzed. The assumed extensions of these zones according (Figure 1b) are summarized in (Table 2).

Table 2. Size of the wetting zones for different rainfall event.

Subcase	K_1 [m]	K_2 [m]
B-1	30	20
B-2	40	30
B-3	50	40
B-4	60	50

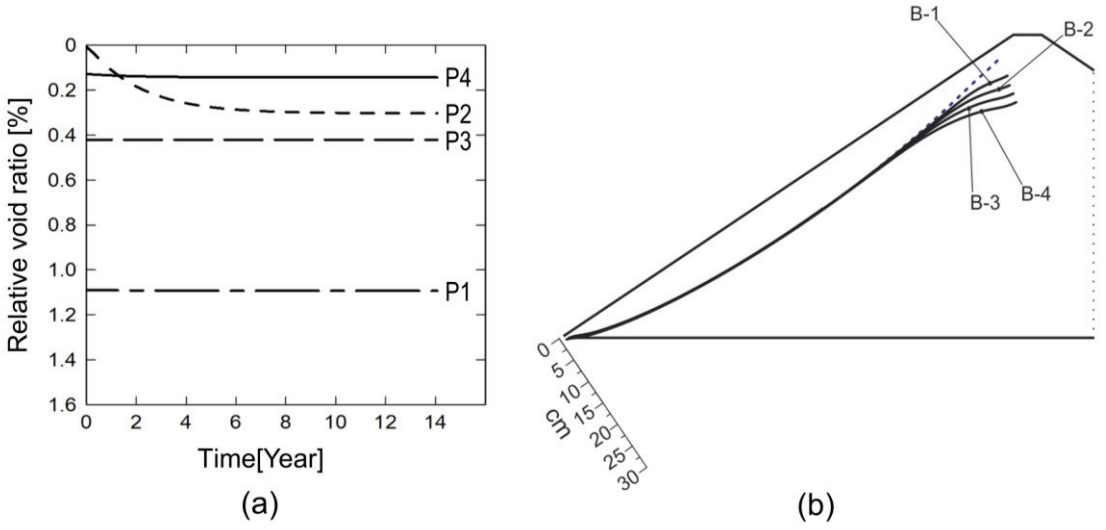

Figure 6. Wetting effect Case B: (a) changes of the relative void ratio at selected points defined in (Figure 3); (b) normal deflection of the concrete slab.

As can be seen in (Figure 6a) additional compaction occurs only in point P2, which is located in the wetted zone. The value of wetting-induced normal deflection of the concrete slab is only significant in the upper part and it is greater for a larger extension of the wetted zone (Figure 6b). The maximum normal deflection of the concrete slab and for the different subcases, their locations are summarized in (Table 3).

Table 3. Maximum normal deflection of the concrete slab for different subcases.

Case	Maximum of normal deflection [m]	Level of the Maximum of normal deflection [m]
B-1	0.08	90.0
B-2	0.085	96.0
B-3	0.097	160.0
B-4	0.112	160.0

Case C: Leakage into the lower part of the rockfill dam

This case investigates the effect of leakage through the foundations of the dam or a defect of the sealing of the concrete joints in the lower part of the dam. A wetted zone illustrated in (Figure 1c) is assumed for the analysis. In contrast to the limited duration of rainfall events, seepage caused by leakage can be considered as being stationary over long periods. Thus, a larger degradation of the

solid hardness is assumed, i.e. h_{sw} = 60 MPa. This also leads to larger compaction of the wetted zone as indicated by points P3 and P4 (Figure 7a). The vertical stress is higher in the middle of the dam, therefore, the additional densification is also more pronounced at point P4 than at point P3. Although a degradation of the solid hardness only takes place in the wetted zone the deformation of the concrete slab is pronounced in the upper part (Figure 7b).

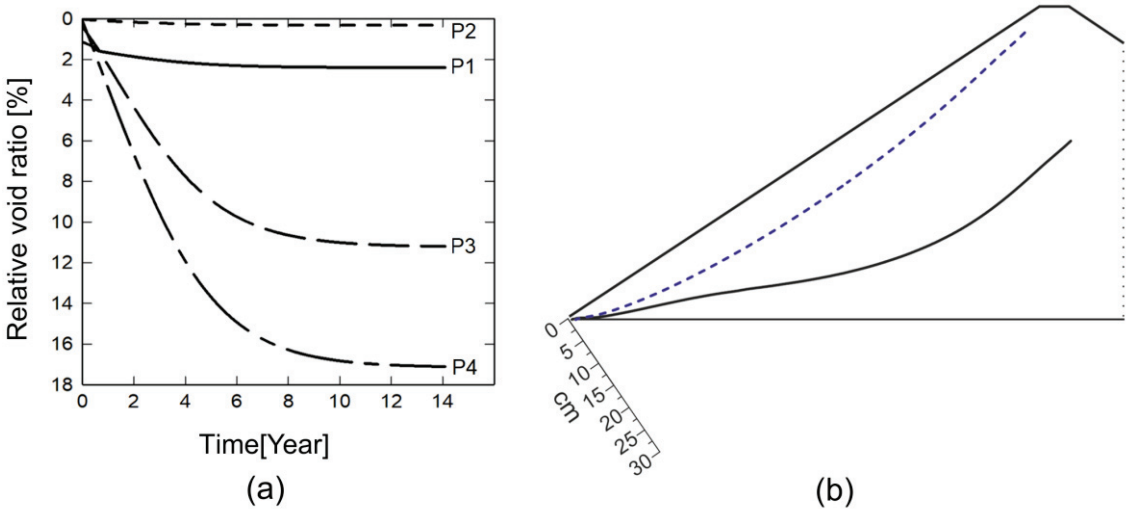

Figure 7. Wetting effect Case C: (a) changes of the relative void ratio at selected points defined in (Figure 3); (b) normal deflection of the concrete slab.

CONCLUSION

An extended hypoplastic constitutive model is used to investigate wetting induced long-term deformations of a concrete face rockfill dam (CFRD). For modelling the behavior of the weathered and moisture sensitive rockfill material a so-called solid hardness is a key parameter in the hypoplastic model. The solid hardness represents the current state of weathering and serves as a scaling factor of the stiffness. State changes of the solid hardness caused by repeated wetting are described by a corresponding evolution equation. In this paper three different scenarios of wetting deformations in a CFRD are investigated: wetting of the entire rockfill material, wetting of the downstream part of the rockfill material caused by heavy rainfall, and wetting of the bottom part of the rockfill material caused by leakage through the foundations. The results of the numerical simulations show that the extension and location of the wetted zone has a strong influence on both the shape and the amount of deformation of the concrete slab. The normal concrete slab deflection can be much higher than the instantaneous part that caused by water impounding and depends on the quality of the pre-compaction and the rockfill material used. As the concrete slab serves as a sealing, the focus of evaluation of the deformed concrete slab should also be on the value of curvatures, which are related to bending moments, and are thus indicators for the appearance of cracks in the concrete slab. The present investigations are based on a simplified 2-D CFRD model on a rigid foundation, and thus potential exists for more precise and qualitatively improved results. More detailed modeling is needed in order to take into account the influences of the dam foundation stiffness, the 3-D geometry of the dam in space, the properties of lateral abutments and the coupling of the computation of the deformation with the relevant seepage behavior.

REFERENCES

Abaqus 6.13, Dassault Systèmes Simulia Corp, Johnston, Rhode Island, United States.

Alonso, E. E., Cardoso, R., 2010. “Behavior of Materials for Earth and Rockfill Dams: Perspective from Unsaturated Soil Mechanics”. Frontiers of Architecture and Civil Engineering in China, vol. 4, N.1, pp. 1-39.

Bauer, E., 1996. “Calibration of a Comprehensive Hypoplastic Model for Granular Materials”. Soils and Foundations, vol. 36, N.1, pp. 13-26.
Bauer, E., 2009. “Hypoplastic Modelling of Moisture-Sensitive Weathered Rockfill Materials”. Acta Geotechnica, vol. 4, N.4, pp. 261-272.
Bauer, E., Fu, Z., Liu, S., 2010. “Hypoplastic Constitutive Modeling of Wetting Deformation of Weathered Rockfill Materials”. Frontiers of Architecture and Civil Engineering in China, vol.4, N.1, pp. 78-91.
Bauer, E., 2018. “Constitutive Modelling of Wetting Deformation of Rockfill Materials”. International Journal of Civil Engineering, pp. 1-6, doi: 10.1007/s40999-018-0327-7.
Brauns, J., Kast, K., Blinde, A., 1980. “Compaction Effects on the Mechanical and Saturation Behaviour of Disintegrated Rockfill”. Proc Int Conf Compact, vol. 1, pp. 107-112.
Chen, L. H., Zhou, X. G., Wei, Y. Q., 2007. “Wetting Effects of Rockfill on the Deformation of the Yellow River Xiaolangdi Dam”. Key Engineering Materials, vol. 353, pp. 2736-2739.
Clements, R. P., 1981. “The Deformation of Rockfill, Inter-Particle Behaviour, Bulk Properties and Behaviour in Dams”. University of London.
Fu, Z. Z., Liu, S. H., Gu, W. X., 2011. “Evaluating the Wetting Induced Deformation of Rockfill Dams Using a Hypoplastic Constitutive Model”. Advanced Materials Research, vol. 243, pp. 4564-4568.
Gudehus, G., 1996. “A Comprehensive Constitutive Equation for Granular Materials”. Soils and Foundations, vol. 36, N.1, pp. 1-12.
Hang, Y. Z. Z., 1990. “Deformation Analysis of Earth Dam during Reservoir Filling”. Chinese Journal of Geotechnical Engineering, vol. 12, N.2, pp. 1-8.
Khosravi, M., Li, L., Bauer, E., 2017. “Numerical simulation of post-construction deformation of a concrete face rockfill dam”. Proceedings of the 4th International Conference on Long-Term Behaviour and Environmentally Friendly Rehabilitation Technologies of Dams, LTBD 2017, (eds.) Noorzad, A., Bauer, E., Ghaemian, M., Ebrahimian, B., Published by Verlag der Technischen Universität Graz, ISBN 978-3-85125- 564-5, pp. 307-314.
Lu, N., Godt, J. W., Wu, D. T., 2010. “A Closed-Form Equation for Effective Stress in Unsaturated Soil”. Water Resources Research, vol. 46, N.5, doi:10.1029/2009WR008646.
Materon, B., 2009. “Concrete Face Rockfill Dams”. International Water Power and Dam Construction, Yearbook. (November), pp. 304-310.
Matsuoka, H, Nakai, T., 1977. “Stress-Strain Relationship of Soil Based on the SMP”. Proceedings of 9th ICSMFE, Constitutive Equations of Soils, pp.153-162.
Nobari, E. S., Duncan, J. M., 1972. “Movements in Dams Due to Reservoir Filling”. Performance of earth and earth-supported structures.
Oldecop, L. A., Alonso, E. E., 2004. “Theoretical Investigation of the Time-Dependent Behaviour of Rockfill”. Géotechnique, vol. 57, N.3, pp. 289-301.
Oldecop, L. A., de Agreda, E., 2007. “Testing Rockfill under Relative Humidity Control”. Geotechnical Testing Journal, vol.27, N.3, pp. 269-278.
Sower, N., Wratten, G. P., 1965. “Intussusception Due to Intestinal Tubes, Case Reports and Review of Literature”. The American Journal of Surgery, vol.110, N.3, pp. 441-444.
Tedd, P., Charles, J. A., Holton, R., Robertshaw, A. C., 1994. “Deformation of Embankment Dams Due to Changes in Reservoir Level”. Proceedings of the international conference on soil mechanics and foundation engineering, vol. 3, pp. 951-954.

5th International Symposium on Dam Safety

October 27-31, 2018

DAM-BREAK FLOW EXPERIMENTS OF WATER-GRANULAR MIXTURES

Yavuz OZEREN[1], Luc REBILLOUT[2], Mustafa ALTINAKAR[3]

ABSTRACT

A series of channelized and non-channelized dam-break flow experiments with dry granular materials and various concentrations of water-granular mixtures were carried out in a multipurpose experimental facility. The highly-transient nature of dam-break phenomena required the use of non-intrusive measurement techniques with high data acquisition rates. The flow characteristics were measured mainly by using imaging techniques using high-speed camera recordings. Velocity fields in both water and granular layers were measured by Particle Image Velocimetry (PIV). The evolution of the free surface and phreatic surface in the upstream reservoir was tracked using the high-speed and time-lapse camera images. Here, the measurement techniques used during this study and key findings will be presented.

Keywords: Dam break, granular flow, laboratory experiments, PIV, FTP, image measurements.

INTRODUCTION

Dam failures typically release sediment-laden water which usually contains high-concentrations of cohesive and non-cohesive granular particles. Due to the unpredictability of these events, in situ data is seldom available. The flow of water-granular mixtures is highly transient and three dimensional, and involves interaction of multiple phases; therefore, numerical models are often utilized to predict the essential flow characteristics. Laboratory experiments are therefore required to validate the numerical models and understand the complex flow dynamics.

In the past, dam-break and granular flow related problems have been studied both numerically and experimentally. Armanini et al. (2008) used cylindrical plastic particles as granular material to experimentally investigate the different collisional regimes in gravity induced flows in a tilted channel with continuous input of water and granular material. Spinewine and Zech (2007) used a downward sliding gate with similar particles on a channelized reservoir to perform dam-break experiments of water-granular material mix over a moveable bed. Similar experiments such as the one presented here were conducted by Rébillout et al. (2016) and Ozeren et al. (2014) using crushed walnut shells as granular material. Imaging techniques are often used to capture the highly transient features of the flow similarly as what was done in this study. Aleixo et al. (2014) used a combined PIV-PTV approach to capture more accurately the velocity field in dam-break experiments. Yet, none of these studies report the evolution of the phreatic surface and failure geometry.

[1] Research Scientist, National Center for Computational Hydroscience and Engineering, University of Mississippi, University, MS, US, e-mail: yozeren@ncche.olemiss.edu
[2] Research Assistant, National Center for Computational Hydroscience and Engineering, University of Mississippi, University, MS, US, e-mail: luc@ncche.olemiss.edu
[3] Research Professor, National Center for Computational Hydroscience and Engineering, University of Mississippi, University, MS, US, e-mail: altinakar@ncche.olemiss.edu

In this study, a series of dam-break flow experiments with dry granular materials were carried out in a multipurpose experimental facility. The highly-transient nature of dam-break phenomena combined with the added complexity of the granular phase required novel non-intrusive measurement techniques with high data acquisition rates. This paper focuses on the measurement techniques used in the experiments of dam-break flows with various types of dry granular materials and different concentrations of water-granular mixtures, into both channelized and non-channelized downstream floodplain. Some of the preliminary findings are also presented.

METHODS

Experimental Setup

The experiments were conducted in the dam-break facility of NCCHE at the USDA-ARS National Sedimentation Laboratory in Oxford, Mississippi, USA. The facility consists of a 3.66 m wide and 7.6 m long rectangular platform (Figure 1). The upstream reservoir was 3.24 m-long and the remaining 4.42 m-long portion of the platform served as the downstream floodplain. A sliding gate was located at the center of the wall separating the reservoir from the floodplain. The sliding gate was pulled upwards at high speeds to simulate dam failure. The gate was pulled by a cable and pulley system and actuated by dropping a weight onto a lever arm that was connected to the cable system. An air cylinder was used to slow the upward movement of the gate. The gate removal speed was controlled by setting the initial height of the weight. The reservoir bed was made of painted aluminum and the floodplain bed was painted smooth PVC.

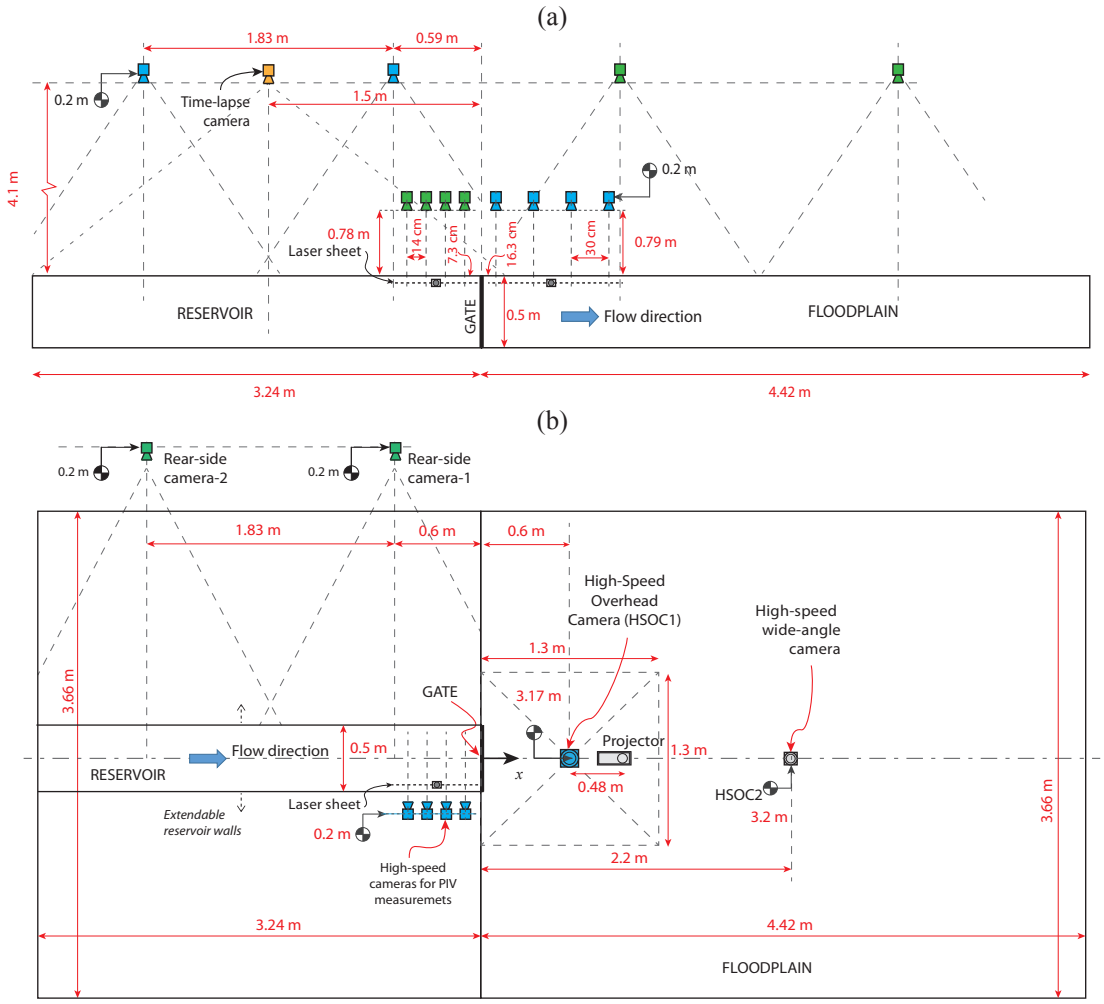

Figure 1. The dam-break test basin for (a) channelized and (b) non-channelized configurations with camera and projector layout.

The experiments described here were carried out in both channelized and non-channelized downstream conditions. The upstream reservoir was channelized in both cases by clear acrylic walls on both sides of the gate. The upstream channel was 0.50 m wide, 0.61 m high and 3.24 m. The downstream platform was left open for the non-channelized experiments; whereas, for the channelized downstream experiments, the channel cross-section was extended to the downstream of the gate by clear acrylic walls with free outflow at the downstream end. The two configurations are illustrated in Figure 1.

Materials

Three different types of artificial materials, Polyethylene terephthalate (PET) pellets, crushed walnut shells and Urea-formaldehyde (Urea), and natural sand were used during the experiments. Some of the physical properties of these materials are listed in Table l. PET pellets were white, cylindrical shaped particles of uniform size with a median diameter, d_{50} = 2.87 mm. Crushed walnut shells are commonly used as abrasive media for various industrial applications. The walnut shell particles used in this study were well-sorted with a dry median diameter d_{50} = 1.34 mm. The walnut shell particles swelled by almost 25% by volume when they were soaked in water. They had irregular but well-rounded shapes, and a uniform brown color. Urea particles were a mixture of crushed recycled material. These particles had irregular shapes with sharp edges and composed of a mixture of different colors (d_{50} = 2.23 mm).

The granular material was placed in the upstream reservoir and densely packed with a concrete vibrator using a standardized procedure to ensure repeatability. The packed material was then leveled by an adjustable sliding paddle. For saturated experiments, the reservoir was slowly filled with water at the upstream end of the reservoir.

Table 1. Properties of the materials used.

Material	d_{50} (mm)	Specific Gravity	Porosity	Friction angle, ϕ
PET	2.87	1.42	0.34	30.5
Walnut shells	1.34	1.48	0.42	31.5
Urea	2.23	1.28	0.46	34.9
Sand	0.20	2.65	0.30	34.5 (Shear box)

Dry granular flow experiments

Dry granular flow experiments were carried out in channelized and non-channelized downstream configurations (Table 2). The upstream reservoir was channelized in both cases (Figure 1). For the non-channelized floodplain case, packed and unpacked PET pellets and walnut shells were tested. For the unpacked case, the material was gradually poured in the channel and levelled, while for the packed case the material was packed with a concrete vibrator before levelling. PET, Urea, walnut shells, and 0.2 mm quartz sand were used for the channelized dry-granular dam-break flow experiments.

Wet granular flow experiments

Both PET and walnut shells were tested in the non-channelized configuration. Only PET was used for the channelized saturated and submerged cases. After packing the granular material, the water level was gradually increased feeding in the upstream channel. A diffuser was attached to the hose outlet to minimize bed deformation. The sediment particles that were set afloat due to surface tension were either removed or pushed down. In some experiments, blue dye was mixed in a separate barrel before introducing into the sediments.

Table 2. The experimental conditions

		Mixture		
		Dry	Wet	
			Saturated	Submerged
Floodplain	Channelized	PET, UREA Walnut shells, Sand	PET	PET
	Non-channelized	PET (packed/unpacked) WS (packed/unpacked)	PET WS	PET WS

Measurement Techniques

The highly-transient nature of dam-break flow requires the use of non-intrusive measurement techniques with high data acquisition rates. Imaging techniques have been successfully used in previous studies (Ozeren et al. 2014; Aleixo et al. 2014 and Rebillout et al. 2016). A variety of image-based measurement techniques were used during the study. Each technique was suited for the experimental configuration, materials used, and temporal and spatial resolution required. The images for these techniques were captured by using six high-speed cameras, a high-definition time-lapse camera and a wide-angle camera. Figure 1 shows the arrangement of these cameras.

During the channelized dam break flow experiments, an array of four high-speed cameras were used consecutively on the upstream and downstream sides of the gate for Particle Image Velocimetry (PIV), and the remaining two high-speed cameras were placed on the opposite side to monitor a wider view of the flow and the free surface. Flow depth was measured using Fourier Transform Profilometry on the non-channelized downstream floodplain in a small area around the gate. An overhead high-speed camera together with a pattern projector was used for this method. A wide-angle action camera was also used to track the wave front on the entire floodplain. Interface tracking was utilized to measure both the free surface and phreatic surface, using high-speed cameras and time-lapse cameras. Each of these methods are summarized below:

Particle Image Velocimetry (PIV)
The upstream PIV cameras had 1280 × 500 (vertical × horizontal) pixel resolution and 400 fps spatial resolution, and the downstream cameras had 640 × 1000 (vertical × horizontal) pixel resolution. The spatial resolution was around 3 mm in both cases. Lens distortion was corrected using a method similar to the one described by Proença (2009), which minimizes the error between at set of base points and control points on a reference grid using some common MATLAB functions. Vibration errors were corrected by tracking fixed markers placed on the walls and applying a sub-pixel registration method (Guizar-Sicairos et al.,2008). The PIVlab Matlab toolbox was used for PIV analysis (Rebillout et al. 2016, Rebillout et al. 2017). The toolbox used a Fast Fourier Transform (FFT) based cross-correlation method to calculate the displacement of two consecutive interrogation windows. Outliers of the vector fields were removed by applying local and global filters including a standard deviation test and local normalized median test. Parallax and refraction errors were geometrically corrected based on the actual particles location.

For the submerged granular flow experiment, Pliolite particles were added in the water for PIV analysis, while the granular material itself served as tracking particles to measure the flow velocity. A laser light sheet illuminated the Pliolite particles in a vertical plane parallel to the side wall. The illuminated plane was chosen to be as close as possible to the side wall (1 cm) onto which the camera was focused. LED lamps were used to illuminate the granular phase through the side wall. Figure

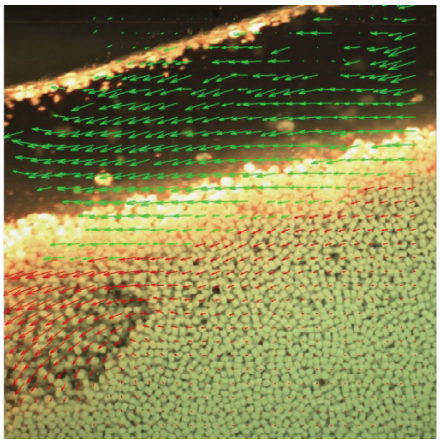

Figure 2. An example frame showing the velocity vectors in both granular (red) and water (green) phase.

For PIV analysis, Keane and Adrian (1990) recommends the interrogation window size to be greater than the displacement of a particle during a given frame rate, and the particle density to be around 0.005 ppp (particles per pixel) in order to have a reasonable correlation for each interrogation window. Yet, the flow time scales in the fluid and granular regions were significantly different during the submerged granular flow experiments. Also, the Pliolite® particle count in the water layer and the grain count in the sediment layer differed significantly which led to difficulties in meeting the above criteria everywhere in the flow. Therefore, two different sizes of interrogation windows used in the sediment and water phases of the flow. A HSV based interface tracking technique was used to separate the two regions. The interface tracking method is explained in more detail below.

Fourier Transform Profilometry (FTP)

For the non-channelized dam-break flow experiments, PIV cameras were installed only on the upstream reservoir sidewall. The time-varying flow depth on the downstream floodplain was measured by Fourier Transform Profilometry (FTP), a pattern projection technique (Takeda et al. 1982). To apply this method, a fringe pattern was projected on the water surface, and the deformed pattern reflected from the surface was captured by a high-speed camera. The fringe pattern was distorted from the camera's point of view, and displayed a phase shift with respect to a reference surface. The analysis of the distorted pattern using two-dimensional Fourier transform and phase unwrapping provided the time variation of the three-dimensional flow-depth field. The high-speed camera for FTP measurements was attached 3.17 m above the floodplain floor, looking vertically downward with its optical axis intersecting the floodplain centerline 0.6 m downstream from the gate (Figure 1). The camera covered an area of about 1.3 m × 1.3 m and recorded at a rate of 100 fps. The fringe pattern was projected onto the water surface by a slide projector that was also attached to the ceiling 0.48 m downstream of the high-speed camera along the centerline. To make the water opaque, so that the pattern is projected on the water surface, titanium dioxide was added to the water. Camera synchronization and the trigger mechanism were computer-controlled. Additional details of the methodology can be found in Ozeren, et al. (2012, 2013 and 2014).

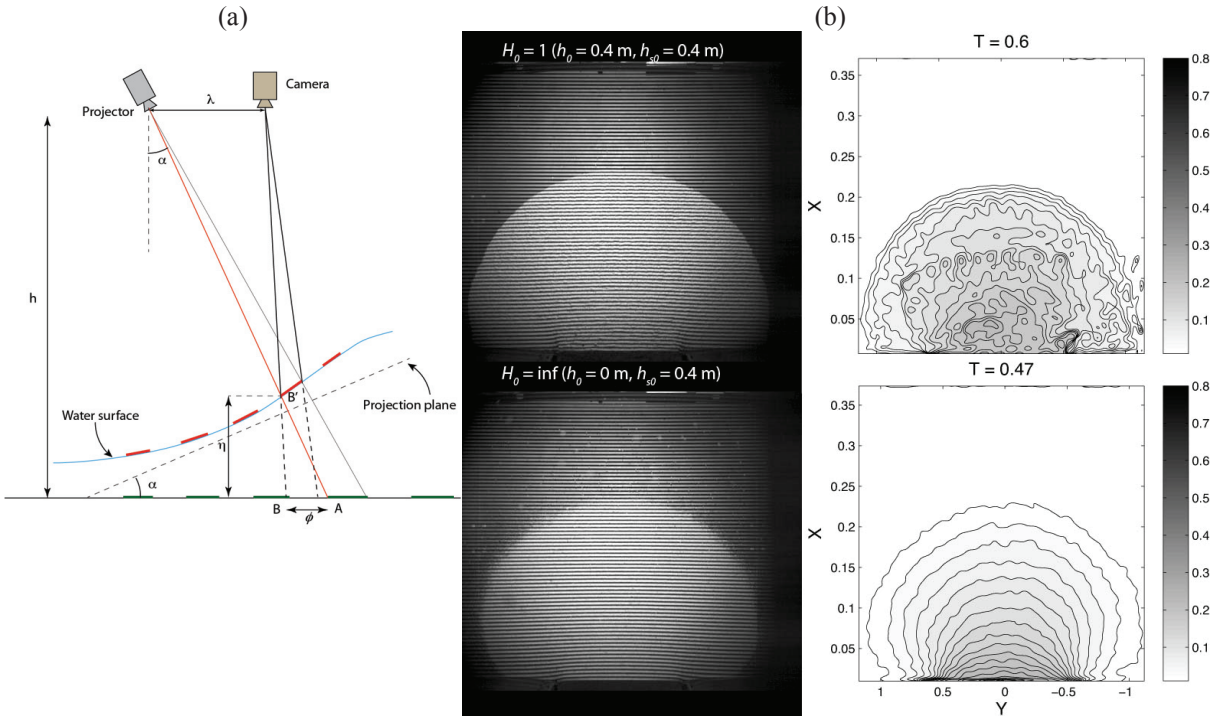

Figure 3. (a) Schematics of the optical geometry for a fringe projection and imaging system; (b) Top views of the dry (h_w = 0.0 m, h_s = 0.4 m) and saturated (h_w = 0.4 m, h_s = 0.4 m) configurations with PET and their respective elevation contours (X = x/L_r, Y = y/w_r, Z = z/h_0, T = $t(gh_0)^{0.5}/L_r$, where L_r is the reservoir length, w_r is reservoir width, h_0 is the initial water depth and g is gravity)

Interface tracking

The air-water and water-sediment interfaces were digitized using an empirical threshold, either in Grayscale or Hue-Saturation-Value (HSV) color space. Grayscale threshold relied on the contrast between bright and dark areas in the pictures. To extract the water-sediment interface, the color difference between the two phases was used to separate two regions during the analysis. The V-channel in the HSV domain produced the best contrast for interface detection. The threshold values were assigned by trial and error for each case.

High-speed cameras provided high-frequency image acquisition but only a few seconds of recording time due to memory limitations. When the concentration of the granular phase was high, a series of sudden failures were followed by drainage of porewater at a much slower timescale. Therefore, a time-lapse camera was used to capture long term evolution of the phreatic surface at higher spatial resolution. The time-lapse camera took high-definition pictures (6016 × 4016 pixels) at 5 second intervals producing 0.57 mm/pixel resolution on the reservoir sidewall. Blue dye was added in the water to make it visible in the PET pellets, and blue filter was used in the HSV domain to digitize the phreatic surface.

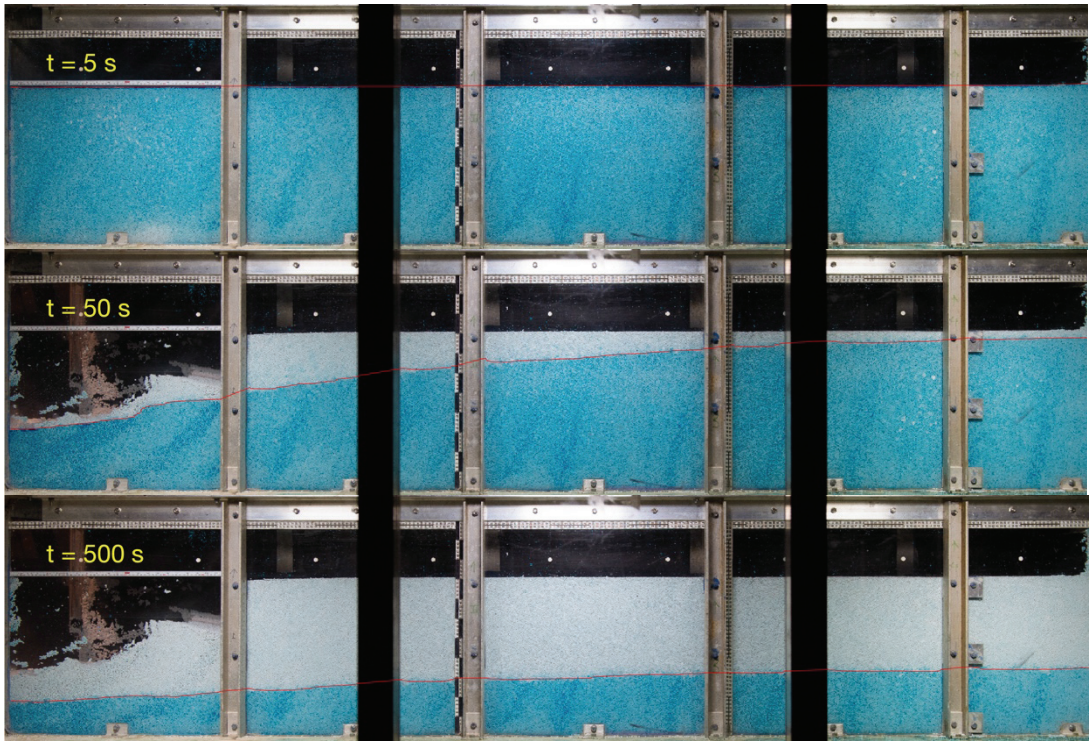

Figure 4. Time-lapse camera pictures, 5 s, 50 s, 500 s after the dam-break. Saturated conditions (h_w = 0.4 m, h_s = 0.4 m)

Interface tracking with the wide-angle camera

A wide-angle high-speed camera (GoPro Hero 3) was positioned 3.20 m above the floodplain pointing vertically downward with its optical axis 2.2 m away from the gate along the floodplain centerline, in order to track the wave front progression after gate removal (Figure 1). The images were captured with a resolution of 1920 × 1080 pixels at 60 frames per seconds. Camera distortion was corrected using reference markers with known coordinates. The recorded video was first filtered by a high-pass filter to increase the contrast between the water surface and the background, and then converted to a binary image. The interface was traced by a combined motion and interface-tracking algorithm. A motion detection procedure was used to eliminate the background and remove vibrations. The free surface was identified after enhancing the binary image through a series of morphological operations. Figure 5 shows the steps of this procedure.

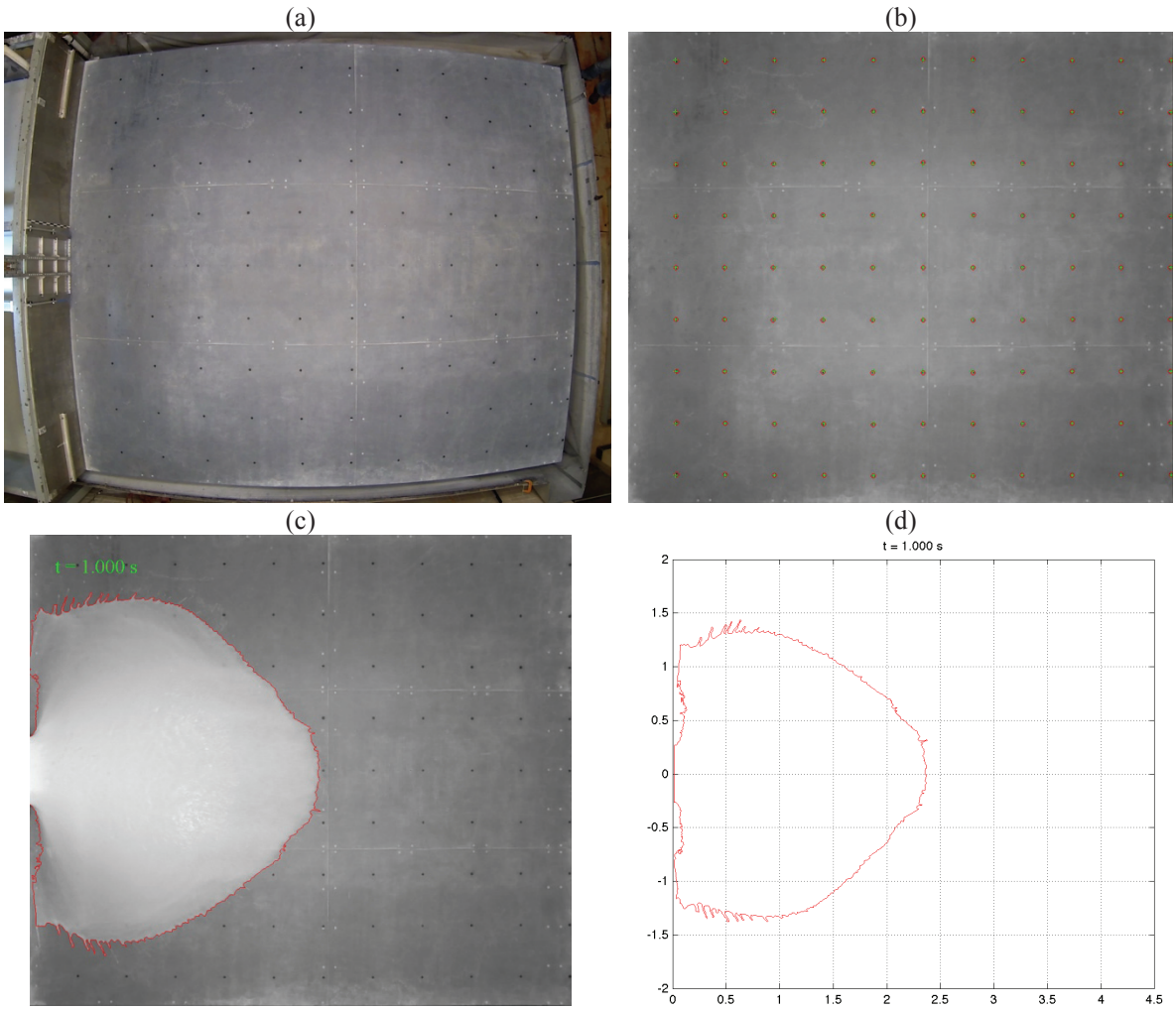

Figure 5. Figure 4. (a) Original undistorted image, (b) corrected image with the reference points marked (maximum error = 13.2 mm, mean error = 6.8 mm), (c) interface tracking and (d) scaled wave front.

DISCUSSIONS

Dry Granular Flow

Both PIV and interface tacking methods were successful in identifying the flow properties of the dry granular flow experiments. Lateral variations of the flow were minimum and side wall view represents the flow in the channel. The location of the wave front was the most problematic region to detect through the side wall. Also, distortion and parallax introduced additional challenges in the post processing.

Channelized dry granular dam-break flow experiments with PET, Walnut shells, Urea, and sand showed similarities in terms of the general behavior of the failure and the final failure profiles. Upon removal of the gate, the granular material collapsed to the floodplain and came to rest after some time. In the upstream reservoir, the slope of the failure surface at rest matched the internal angle of repose for all samples. The horizontal extent of the wave front downstream of the gate depended on the friction angle between the granular material and the channel floor. The time for finer grains and natural to sand come to rest was longer than that for the coarser materials. The depth of the granular material at the gate sections was approximately $4/9h_0$, where h_0 is the initial depth. Figure 6 shows a snapshot of a section of the upstream reservoir during the dry granular dam-break flow experiments with walnut shells. The velocity vectors are also shown in the pictures. The velocity contours at $t = 0.5$ s clearly show the plug flow region.

The upstream geometries of the non-channelized dry granular flow experiments were similar to that of the channelized experiments. Similar to the channelized counterparts, the slopes at rest were comparable to the internal angle of friction. The free surface elevation contours on the downstream floodplain were obtained by FTP using the projected fringe lines as shown in Figure 3 for 40 cm initial depth. The wave front assumed a mushroom-like shape with an approximately linear vertical profile.

In Figure 7 the dimensionless wave front position is plotted for various granular materials. Note that the horizontal location is normalized with the angle of repose for each material. One of the non-channelized open floodplain experiments with PET is also included in Figure 7. The centerline profiles of the non-channelized experiment were used for comparison. The results of the experiments with natural sand compared reasonably well with experiments of di Cristo et al. (2010). The large differences were observed during the earlier stages of the flow which depends on the initiation of the dam break flow. The experiments differed with their maximum horizontal extent at rest which depends on the friction angle between the grains and the channel bed.

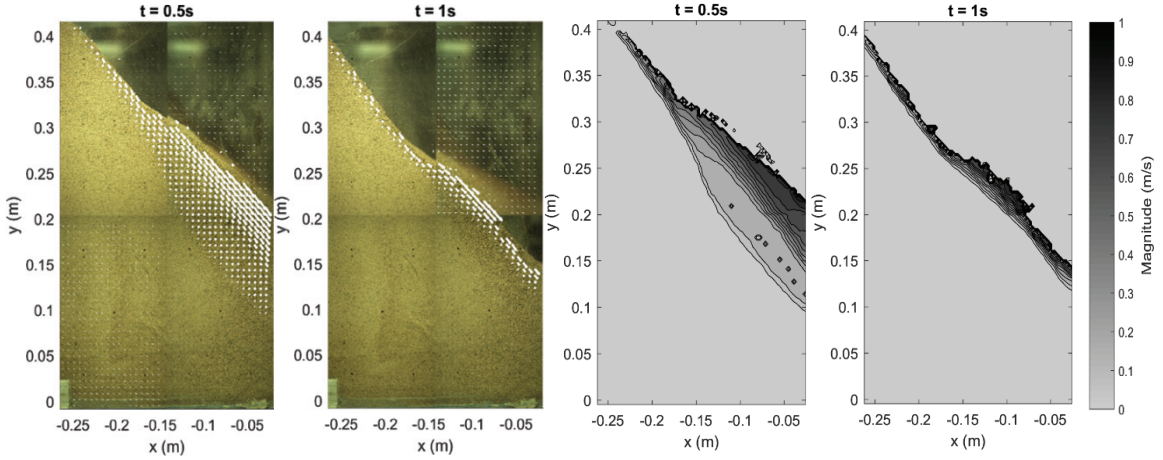

Figure 6. Dry granular flow experiments with densely packed walnut shells.

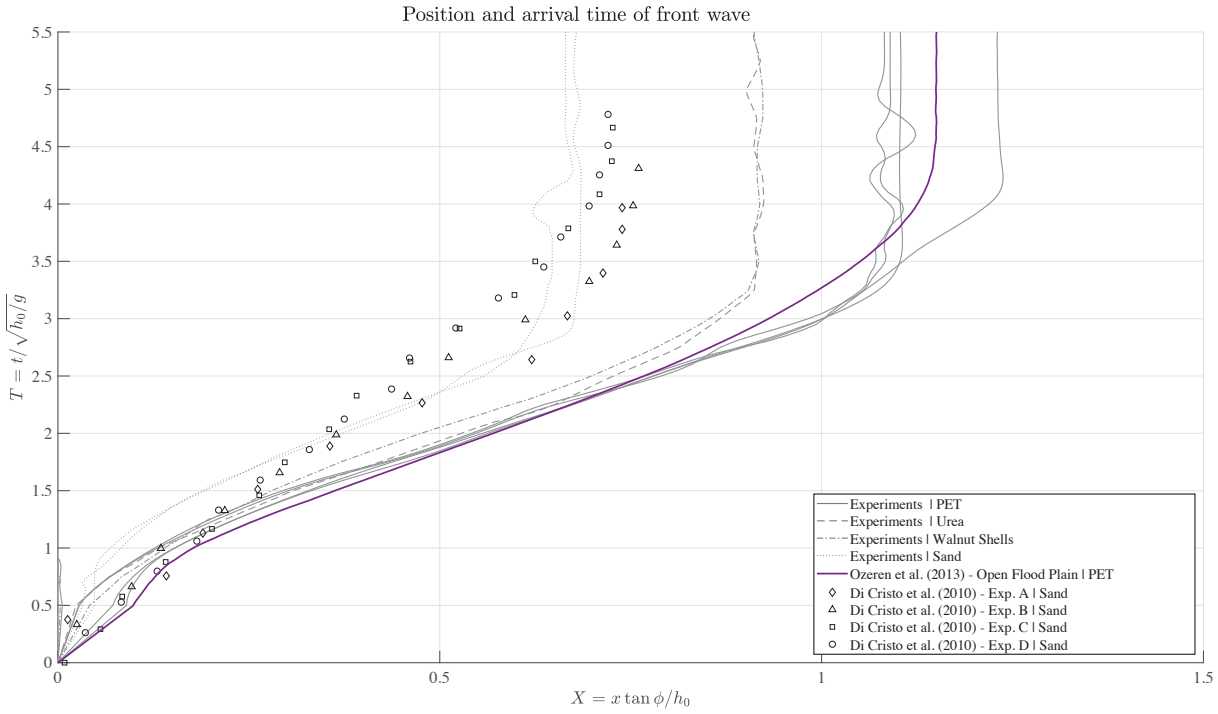

Figure 7. Comparison of the dimensionless wave front progression after for various dry-granular dam break flow experiments.

Wet Granular Flow

Saturated

Discrete block failures were observed during the saturated granular flow experiments in both channelized and non-channelized conditions. PIV method was successfully applied and was used to identify the velocity field and failure plane in the upstream reservoir. Figure 8 shows an example image of a section of the upstream reservoir during the experiments with PET, and the corresponding vorticity plot.

Following each failure, the collapsed material slowly creeped downstream. After the failures, the granular layer stayed virtually stationary in the upstream channel while the phreatic surface declined slowly. Using a blue color filter in the HSV domain, the free surface of the phreatic table was extracted (Figure 4). The phreatic surface profiles were smoothed with spline interpolation.

Failure planes, slump geometry and phreatic surface during the early stages were digitized using the high-speed camera images of the upstream and downstream channels and the beginning of each failure was identified by the formation of tension cracks in the upstream reservoir. Figure 9 shows the geometries just before each failure. The horizontal component of the velocity vectors in the downstream channel are also shown in these plots. The figure shows that saturated granular dam-break flows are strictly heterogenous and involved the unsteady flow of multiple phase at different time scales.

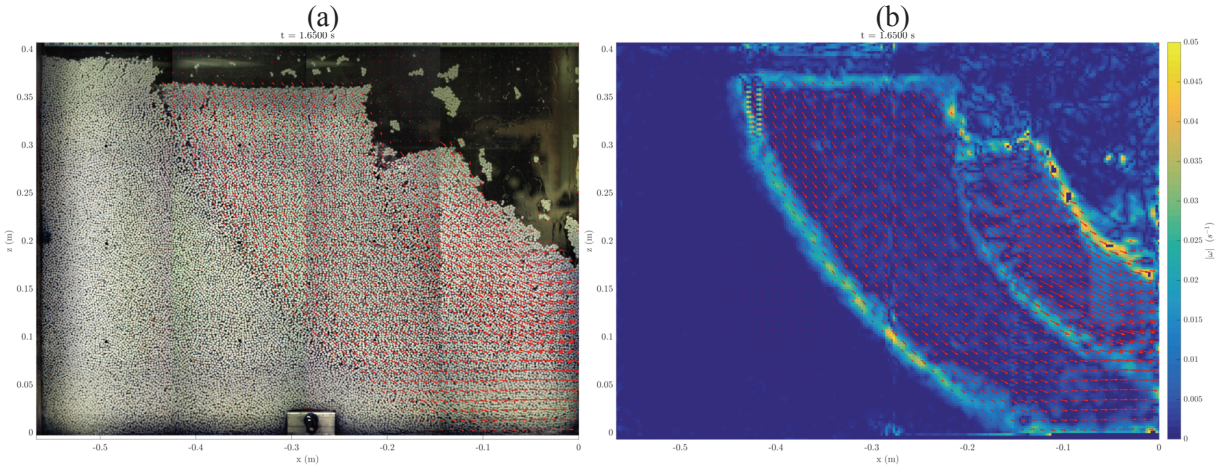

Figure 8. (a) The vector field calculated using PIV, overlaid on the picture of the granular collapse during a saturated channelized dam-break flow experiment with PET (h_w = 0.4, h_s = 0.4), and (b) vorticity field contours calculated using the same vector field.

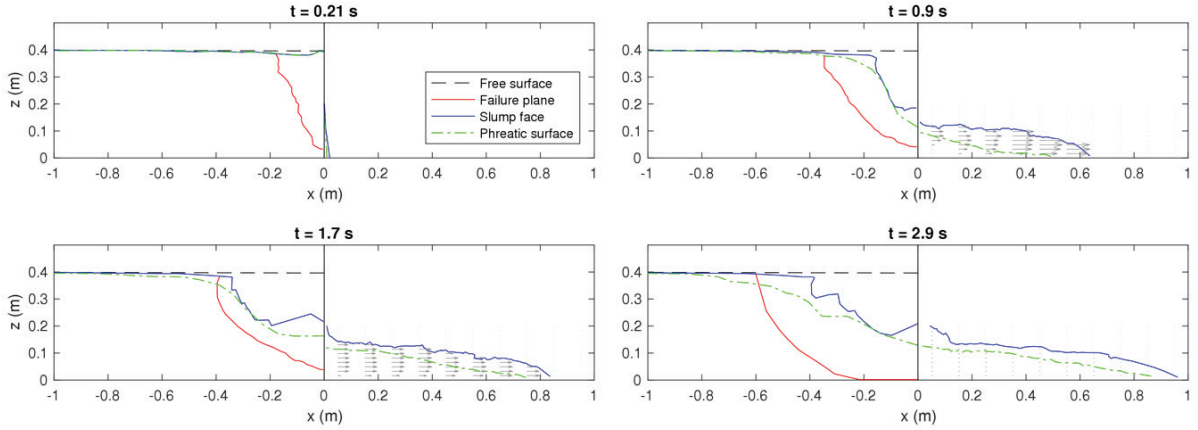

Figure 9. Failure geometry and phreatic surface at the beginning of each failure event with the downstream velocity profiles for the saturated case.

Submerged

Walnut shells and PET pellets were tested in the non-channelized configuration, while only the PET pellets were tested in the channelized case. The top water layer collapsed downstream in front of the granular after the removal of the gate, and entrapped air in the mixed flow. Figure 10 shows velocity and grain density fields of the submerged case at different times. Underwater mass failures were observed in the granular layer as the negative wave propagated inside the upstream reservoir. The failed material moved as plug flows with an average velocity much lower than that of the water layer above. The sediment-laden flow downstream of the slump was highly turbulent and well mixed. Three-dimensional rotational structures were observed in the flow (Figure 10). PIV measurement in the downstream channel was particularly challenging in because of the highly turbulent three-dimensional flow during later stages.

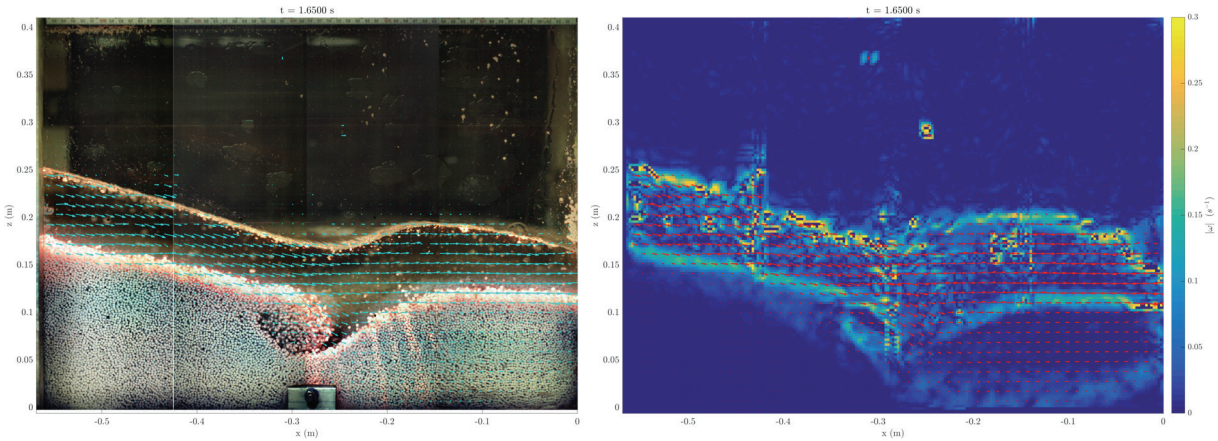

Figure 10. (a) The vector field calculated using PIV, overlaid on the picture of the granular collapse during a submerged channelized dam-break flow experiment with PET (h_w = 0.4, h_s = 0.2), and (b) vorticity field contours calculated using the same vector field.

On the non-channelized downstream, the progression of the wave front was measured using the wide-angle camera. Figure 11 shows the wave front contours at constant time intervals for the non-channelized experiments with PET (h_w = 0.4, h_s = 0.2). Each contour line indicates the wave front position at the indicated time on the contour line. Vectors denote the wave speed magnitude and direction derived from consecutive wave front contours assuming that the direction of wave propagation is perpendicular to the wave-front line. Color contours indicate the magnitudes of the wave front speed. The wave accelerates shortly after the gate removal and decelerates as it spreads on the floodplain.

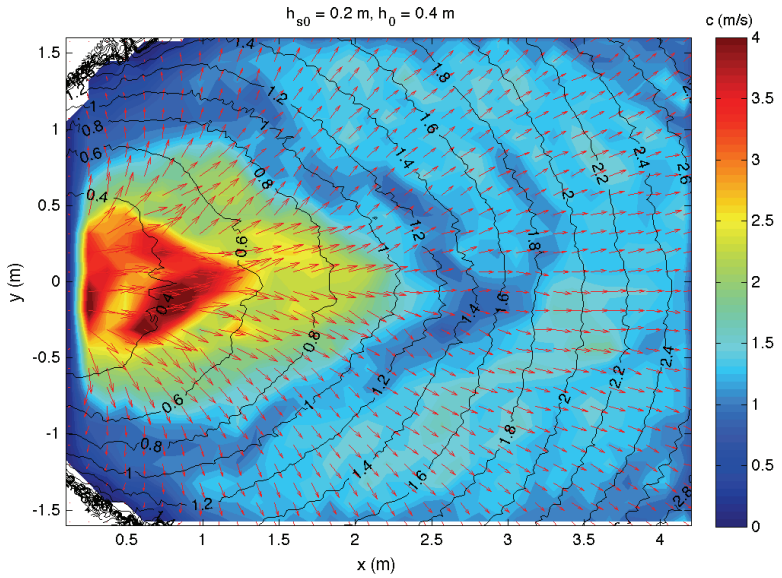

Figure 11. Wave front progression contours (PET, h_w = 0.4, h_s = 0.2).

In the upstream reservoir, slump failures of the saturated cases and underwater mass failures of the submerged cases progressed upstream as the reservoir emptied. This was similar for both channelized and non-channelized experiments with different materials, but there were significant differences between the saturated and submerged experiments in terms of the rate of the backward progression. This is compared in Figure 12. The failure progression for submerged experiments were at a nearly constant rate, but in the saturated case the failure progression rate slowed down. Both rates were much slower than the negative wave speed.

These failures also affected the flow hydrographs as shown in Figure 13. The discharge hydrographs were calculated using the instantaneous free surface profiles acquired by interface tracking. The hydrographs of the experiments with sediments showed an oscillatory pattern due to the discrete failures in the sediment layer, such that a local peak was observed following each failure.

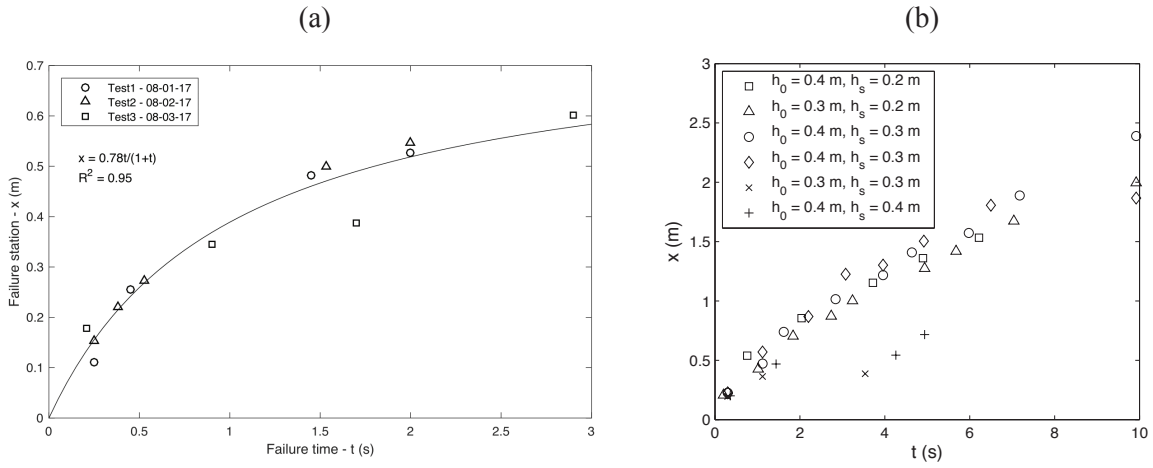

Figure 12. (a) Backward progression of the slump failures of the channelized saturated granular dam-break flow experiments, and (b) the underwater failures of the non-channelized granular dam-break flow experiments.

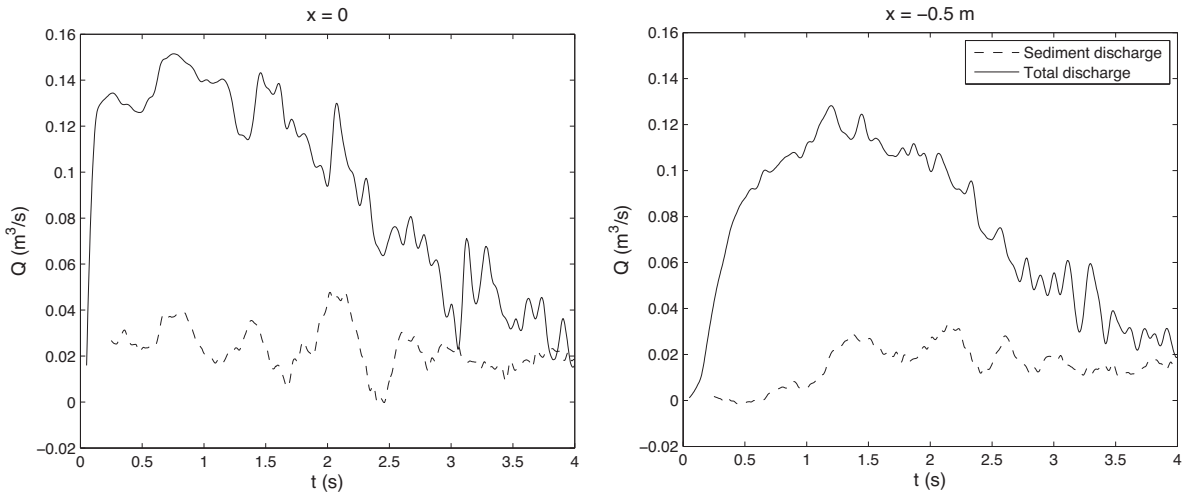

Figure 13. Discharge hydrographs for the water-granular mixture, and the granular phase at two different section in the upstream reservoir for non-channelized dam-break experiments with PET (h_w = 0.4, h_s = 0.2).

CONCLUSIONS

A variety of image-based flow measurement techniques were used during dry, saturated, and submerged granular dam-break flow experiments for both channelized and non-channelized open floodplain conditions using various granular materials. The techniques described here provided good temporal resolution and reasonable spatial resolution. The flow velocities in both water and granular layers were measured in channelized upstream reservoir. Free surface, the phreatic surface in the reservoir, water-granular interface wave front progression, mass failure geometries the wave front progressions were also detected using image-based methods. The example applications presented in this paper showed that saturated and submerged granular dam-break flows are three dimensional, highly turbulent and involved the interaction of multiple phases at different time scales.

ACKNOWLEDGEMENTS

This work is supported in part by USDA ARS under the Specific Research Agreement No. 6060-13000-025-00D, monitored by the USDA-ARS National Sedimentation Laboratory, and The University of Mississippi. The authors would like to thank Daniel Wren at NSL. Jacob Ferguson, Glen Gray, Alan Barger and Will Andrews provided technical support during the experiments.

REFERENCES

Aleixo, R., Ozeren, Y., Altinakar, M., & Wren, D. 2014. “Velocity field measurements in tailings dam failure experiments using a combined PIV-PTV approach”. Proceedings of the 3rd IAHR Europe conference. Porto, Portugal.

Armanini, A., Fraccarollo, L., & Larcher, M. 2008. “Liquid–granular channel flow dynamics”. Powder Technology, 182(2), 218-227.

Di Cristo, C., Vacca, A., & de Marinis, G. 2010. “Analytical solution of dam break wave in dry granular flows”. In Proc. of the 1st European IAHR Congress, Edimburgh (UK).

Guizar-Sicairos, M., S. T. Thurman, and J. R. Fienup (2008). “Efficient subpixel image registration algorithms”. In: Optics letters 33.2, pp. 156–158.

Keane, R. D. and Adrian, R. J. 1990 “Optimization of particle image velocimeters. I. Double pulsed systems”. Measure-ment science and technology, 1.11: 1202

Kocaman, S., & Ozmen-Cagatay, H. 2012. “The effect of lateral channel contraction on dam break flows: Laboratory experiment”. Journal of hydrology, 432, 145-153.

Ozeren, Y., Aleixo, R., Altinakar, A., & Wren, D. 2014. “Laboratory experiments on dam-break flow of water-sediment mixtures”. In Meeting Proceedings.

Ozeren, Y., Altinakar, M., and Wren, D. G., 2013. “Experimental Measurements of Dam-Break Flow”, 6th International Perspective on Water Resources & the Environment conference (IPWE 2013), January 7-9, 2013, Izmir, Turkey.

Proença, M. (2009). “Using Matlab for Expeditious Image Geometric Correction”. In: XXIIe colloque GRETSI (traitement du signal et des images), Dijon (France), 8-11 septembre 2009. GRETSI, Groupe d’Etudes du Traitement du Signal et des Images.

Rébillout, L., Ozeren, Y. & Altinakar, M., 2017. “Dam-break flow measurements of granular-liquid mixtures in a channelized reservoir”. In HMEM Conference Durham, New Hampshire, USA.

Rébillout, L., Ozeren, Y., & Altinakar, M. 2016. “Application of imaging techniques in dam-break flow experiments with crushed walnut shells”. In River Flow 2016 (pp. 212-213). CRC Press.

Spinewine, B., & Zech, Y. 2007. “Small-scale laboratory dam-break waves on movable beds”. Journal of Hydraulic Research, 45(sup1), 73-86.

Takeda, M., Ina, H., and Kobayashi, S. 1982. "Fourier-Transform Method of Fringe-Pattern Analysis for Computer-Based Topography and Inteferometry." Journal of the Optical Society of America 72 (1): 156-160.

Thielicke, W., & Stamhuis, E. 2014. “PIVlab–towards user-friendly, affordable and accurate digital particle image velocimetry in MATLAB”. Journal of Open Research Software, 2(1).

5 DAM SAFETY
İstanbul Turkey 2018

5th International Symposium on Dam Safety

October 27-31, 2018

STRUCTURAL HEALTH MONITORING OF LABORATORY ARCH DAM MODEL

Ahmet Can ALTUNIŞIK [1], Barış SEVİM [2], Murat GÜNAYDIN [3], Süleyman ADANUR [4], Ebru KALKAN [5]

ABSTRACT

Arch dams are important structures used in many fields such as energy, drinking water, irrigation and industrial needs. Failure or damages in the dams may result in pecuniary loss and intangible damages. In this study, it is aim to monitor the structural health of the arch dam by examining the changes over the years in the modal parameters of the Type-1 Arch Dam, which has a laboratory model. For this purpose, in order to examine the changes in the modal parameters of the laboratory model, experimental measurements were made at different times and under different between 2009-2017 years. Experimental measurements were performed under conditions damaged, repaired with high-strength structural mortar and strengthened with composite carbon fiber reinforced polymer. Ambient vibration tests are performed to extract the dynamic characteristics using Enhanced Frequency Domain Decomposition (EFDD) method. Measured natural frequencies and mode shapes for different cases are compared with each other. The compared values provide information about structural changes in the dam model over time.

Keywords: Arch dam, modal parameters, retrofitting, structural behavior, Type-1 arch dam.

INTRODUCTION

The actual performance of an arch dam under the earthquake loadings should be determined considering quantity of water in the reservoir. Because it is well known that the water considerably affects the dynamic behavior of arch dam during the earthquakes. When a dam-reservoir system is exposed to a dynamic loading like earthquakes, hydrodynamic pressures in excess of hydrostatic pressures occur on the dam due to the vibration of the dam and water in the reservoir. These hydrodynamic pressures and the deformation of the dam interact with each other (Perumalswami and Kar 1973). Hence, the water level effects on the dynamic behavior of arch dams must be considered.

In the literature, three approaches are used to consider the reservoir effects in the dynamic analyses: Westergaard, Euler, and Lagrangian approach. In Westergaard approach (Westergaard 1933), it is considered that a vibrated mass dispersion with the dam, which is similar to being hydrodynamic

[1] Professor, Department of Civil Engineering, Karadeniz Technical University, Trabzon, Turkey, e-posta: ahmetcan8284@hotmail.com
[2] Professor, Department of Civil Engineering, Yildiz Technical University, Trabzon, Turkey, e-posta: basevim@yildiz.edu.tr
[3] Asst. Prof., Department of Civil Engineering, Karadeniz Technical University, Istanbul, Turkey, e-posta: muratgunaydin@ktu.edu.tr
[4] Professor, Department of Civil Engineering, Karadeniz Technical University, Trabzon, Turkey, e-posta: sadanur@ktu.edu.tr
[5] Dr., Department of Civil Engineering, Karadeniz Technical University, Trabzon, Turkey, e-posta: ebrukalkan@ktu.edu.tr

effect dispersion towards the dam upstream face. In Eulerian approach (Dungar 1978), the displacements are the variables in the structure; the pressures are the variables in the fluid. However, in Lagrangian approach (Wilson and Khalvati 1983), the displacements are the variables in both the fluid and the structure. So, there is no need of any extra interface equations in Lagrangian approaches. Thus, compatibility and equilibrium are automatically satisfied at the nodes along the interfaces between fluid and structure (Bayraktar et al. 2011).

Beside these approaches, it is emphasized that dynamic behavior of arch dams must also be investigated and monitored experimentally. Dynamic characteristics (natural frequencies, mode shapes and damping ratios) are the key parameters to monitor the structural safety and performance of structures during their service period. Many structural monitoring methods, based on the dynamic characteristics have been developed recently. The main aim of methods is to fallow the changes of dynamic characteristics. It is well known that the changes in the physical properties of the structures such as boundary conditions, stiffness will cause changes in dynamic characteristics. Therefore, the dynamic behavior of structures can be monitored by following the changing of dynamic characteristics, especially after earthquakes.

The ambient vibration testing technique has been often used to determine the structural performance and/or structural safety of large dams. Deinum et al. (1982) performed the ambient and forced vibration tests on the Emmoson arch dam to estimate the dynamic properties of the dam. Loh and Wu (1996) determined the dynamic characteristics of Fei-Tsui arch dam using finite element analysis and experimental measurement tests. Ziyad (1998) carried out the finite element analysis and experimental measurements on Morrow Point arch dam to determine the dam-water interaction effect and water compressibility. Ambient vibration tests on a 56 meter high concrete gravity dam were conducted by Daniell and Taylor (1999) to measure its modal properties for validating a finite element model of the dam. Proulx et al. (2001) investigated the water level effects on the dynamic behavior of arch dams. Darbre and Proulx (2002) preferred the continuous ambient vibration monitoring studies and their results related to Mauvoisin arch dam. Validation of numerical model of Pacoima Arch Dam using ambient vibration testing data was studied by Alves and Hall (2006). The Berke Arch Dam, located in South Anatolia on Ceyhan River, was studied by Sevim et al. (2011). Calcina et al. (2014) worked on the ambient vibration tests of the Punta Gennarta Arch Dam in two different studying conditions to evaluate the effect produced by two different reservoir water levels on the structural vibration properties. Cheng et al. (2015) studied about the health monitoring method of a concrete dam based on the ambient vibration testing and kernel principal analysis. It has been seen from the literature that although the physical conditions are quite difficult for excitation of large dams, and tests become too expensive and require much time; results achieved by ambient vibration test are very useful. But, such kinds of difficulties motivate researchers to build scaled prototype dam models under laboratory conditions to determine the structural performance experimentally (Oliveira and Faria 2006, Mendes and Oliveira 2007, Sevim 2010, Wang and He 2007, Weng and Loh 2010, Pan et al. 2011, Sevim et al. 2011, Tarinejad et al. 2014, Türker et al. 2014, Altunışık et al. 2015, Hariri-Ardebili and Sayed-Kolbadi 2015, Altunışık et al. 2016, Liu et al. 2016, Altunışık et al. 2017). Apparently, from the literature, studies into water level effects with the different conditions (damaged, repaired, strengthened) on the dynamic characteristics are sufficient. This study seeks to contribute to relieve the deficit.

In this paper, the ambient vibration tests have been carried out with the purpose of determining the water level effects on the dynamics characteristics of damaged, repaired and strengthened arch dam models. The ambient vibration test has been conducted on each arch dam models for varying water levels to present the natural frequencies, mode shapes and damping ratios. Enhanced Frequency Domain Decomposition (EFDD) technique has been used to extract the dynamic characteristics from the ambient vibration measurements. As a result of study, experimentally identified dynamic characteristics have been compared with each other for each condition to determine the effects of water levels.

AMBIENT VIBRATION TESTING OF THE PROTOTYPE ARCH DAM MODEL

Description of laboratory arch dam model

There are five types of arch dams with different geometries proposed in the symposium "Arch Dams (1968)" held in England in 1968. From this dam types, in order to study in the laboratory were selected model small-scaled Type-1 arch dam. The Type-1 arch dam has geometry that a constant radius, angle and a single curvature. The geometrical characteristics of the Type-1 arch dam are shown in Figures 1 and 2.

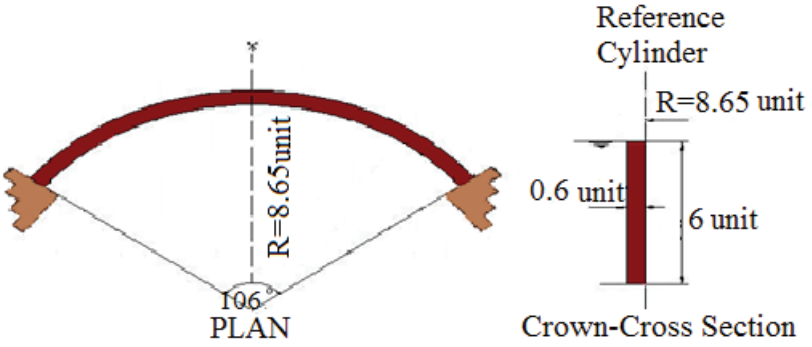

Figure 1. Geometry properties of Type-1 Arch Dam (Arch Dams, 1968)

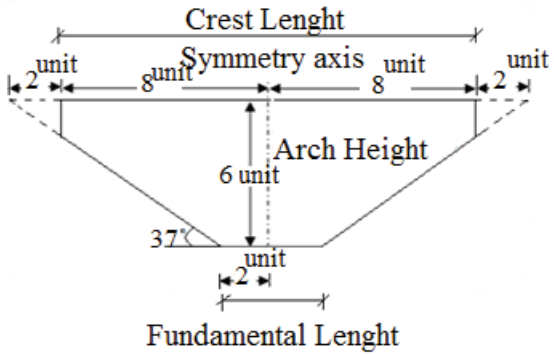

Figure 2. The cross-section of the valley where the Type-1 arch dam is located

Constitution of Laboratory Model

In the Type-1 arch dam whose dimensions are given in units, 1 unit=10cm is selected and the laboratory model is created. According to the obtained data, the dam height (H) is 60cm, the crest and the base width are 6cm and the crest length of the dam is calculated as 171.13cm in the upstream face and 160.03cm in the downstream face. In the studies conducted within the scope of the thesis, the dam model has been developed to include base and reservoir in order to realistically determine the dynamic behavior of the Type-1 arch dam (Sevim 2010). The three-dimensional soil-structure interaction model and laboratory model of the Type-1 arch dam prepared according to these properties and the dimensions of this model are given in Figure 3.

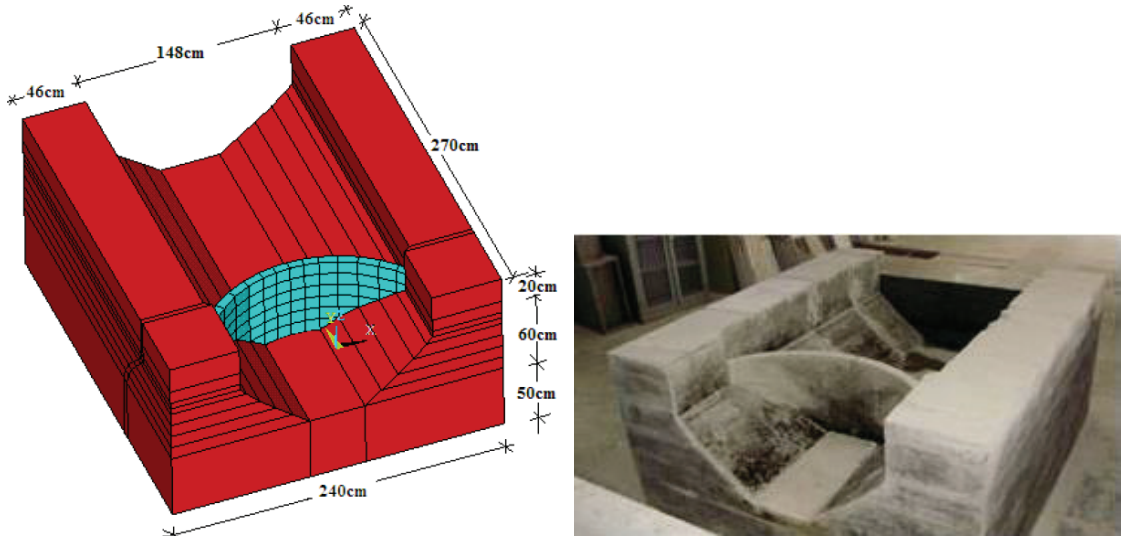

Figure 3. 3D and laboratory model of Type-1 arch dam

Ambient vibration tests

Ambient vibration tests are conducted on the dam model to determine its dynamic characteristics such as natural frequencies, mode shapes and damping ratios. The test measurements are carried out for three different conditions: damaged (Condition-1), repaired (Condition-2) and strengthened dam (Condition-3) models. Measurements are conducted with different water levels for empty reservoir (0 cm), 10 cm, 20 cm, 30 cm, 40 cm, 50 cm and full reservoir (60 cm) water levels. During the ambient vibration tests, a B&K 3560 data acquisition system with 17 channels and a B&K 4507-B005-type uni-axial accelerometers, uni-axial signal cables, a laptop, PULSE (PULSE 2006) and Operational Modal Analysis software (OMA 2006) are used. The frequency range is selected as 0-1000 Hz and eleven accelerometers are located on the crest surface, as shown in Fig. 4. The tests are carried out for 5 minutes.

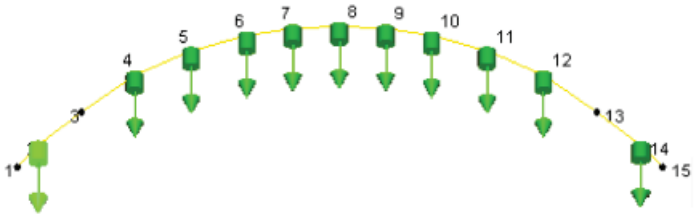

Figure 4. Locations of accelerometers used in the ambient vibration tests

- Ambient vibration tests for damaged dam model (Condition-1)

For the crack formation, the dam body is damaged by loading a random impact effect. The minor cracks were occurred in the middle of the upper part of the dam and distributed through the abutments. In addition to the minor cracks, some severe cracks and fractures were generated in the body of dam. These cracks distributed below to the sides of the first cracks. The formation of these new cracks is expected and similar conditions can be seen in the literature (USACE 2003, Karaton 2004, Oliveria and Faria 2006, Pan et al. 2011). Some views of the created cracks and fractures are shown in Fig. 5. Six natural frequencies and damping ratios were obtained from damaged model and are given in Table 1.

Figure 5. Views of the generated cracks and fractures

Table 1. Natural frequencies and damping ratios obtained from the condition-1

Mode	Water levels													
	Empty		10 cm		20 cm		30 cm		40 cm		50 cm		Full	
	Freq. (Hz)	Dr. (%)	Freq. (Hz)	Dr. (%)	Freq. (Hz)	Dr. (%)	Freq. (Hz)	Dr. (%)	Freq. (Hz)	Dr. (%)	Freq. (Hz)	Dr. (%)	Freq. (Hz)	Dr. (%)
1	151.5	4.35	149.2	4.73	146.1	2.99	146.5	4.00	146	4.73	145.9	3.79	145.6	3.49
2	178.0	3.15	178	3.15	181.5	3.93	179.7	3.77	200.2	3.06	192.8	2.57	176.3	3.55
3	247.9	2.15	243	2.68	239.5	2.26	239	1.22	243	0.46	238.9	2.16	229.1	0.65
4	305.9	0.98	302	1.02	293.8	2.24	287.3	1.65	302.1	1.00	293.8	2.24	281.1	2.93
5	406.5	2.30	387.6	1.19	372.4	3.60	367.2	2.68	372.4	3.61	357.9	1.85	358.5	3.47
6	441.2	1.33	439.8	1.21	431	0.26	429	0.84	439.8	1.20	420.8	0.84	381.7	1.46
*Freq: Frequency; Dr: Damping Ratio														

- Ambient vibration tests for repaired dam model (Condition-2)

In this test condition, the pre-damaged dam body was repaired using high-strength structural repair mortar. The commercially available epoxy-based repair mortar marked as CONCRESIVE®1406 including two components was implemented. The material properties of CONCRESIVE® 1406 type repair mortar are given in Table 2. The repair phases are given step by step in Fig. 6. Six natural frequencies and damping ratios were obtained from repaired model and are given in Table 3.

Table 2. Material properties of structural repair mortar

Material Property	Amount
Density of the mixture	1.70 ± 0.05 kg/liter
Compressive strength (7 days)	75 MPa
Flexural strength (7 days)	25 MPa
Bonding strength to concrete (7 days)	>3.0 MPa
Fully Cured at 20°C	7 Days

a) Removal of the damaged concrete pieces

b)Application of structural repair mortar using hand trowelling proces

c) Putting in the removed concrete pieces

d) Application of structural repair mortar on the surface of dam arc

Figure 6. Repair process of arch dam with epoxy mortar

Table 3. Natural frequencies and damping ratios obtained from the condition-2

Mode	Water levels													
	Empty		10 cm		20 cm		30 cm		40 cm		50 cm		Full	
	Freq. (Hz)	Dr. (%)	Freq. (Hz)	Dr. (%)	Freq. (Hz)	Dr. (%)	Freq. (Hz)	Dr. (%)	Freq. (Hz)	Dr. (%)	Freq. (Hz)	Dr. (%)	Freq. (Hz)	Dr. (%)
1	244.9	0.59	231.1	1.85	240.4	1.83	239.6	1.14	232.8	1.38	213.6	0.78	193.5	1.54
2	257.1	2.07	243.3	1.49	254.5	1.94	247.6	1.72	266.8	1.58	240.2	2.13	232	0.62
3	335	1.69	323.9	2.65	329.9	1.78	326.7	2.57	327.8	1.51	303.8	1.78	268.9	1.26
4	417.7	1.10	400.8	1.78	361.9	0.82	355.9	0.84	372.1	1.16	369.7	1.27	361.6	2.23
5	503.3	2.56	485.8	2.01	493.3	2.06	444.3	2.42	429	0.26	414	1.34	394.7	0.90
6	581.4	0.72	576	1.58	570.9	0.61	483.1	0.23	475.4	0.48	480.3	2.59	436.4	2.68
*Freq: Frequency; Dr: Damping Ratio														

- Ambient vibration tests for strengthened dam model (Condition-3)

CFRP sheet implementation is very effective method to the strengthen concrete members along with increasing stiffness. This paper also aimed to investigate how CFRP sheet implementation effects to dynamic characteristics with varying water levels. After repairing, the dam body was strengthened using unidirectional CFRP sheet. Unidirectional CFRP sheet and its components were provided by the BASF Corporation. MBT-MBrace®Fibre, its Saturant and Primer were used for strengthening. The properties of the dry carbon fiber sheet are; 4900 MPa tensile strength; 230 GPa elasticity modulus; 2.10% ultimate rupture strain and 0.111 mm nominal thickness per ply. Strengthening phases were practiced in some steps: a thin layer undercoat of MBT-MBrace®Primer was applied (Fig. 7(a)) to the dam body (only upstream direction), approximately 48 hour were waited to prepare the arch surface for epoxy implementation (Fig. 7(b)), MBT-MBrace Adesivo was used as an epoxy to achieve full bond between the concrete surface and CFRP sheet, and the CFRP sheets were wrapped to the dam body after curing (Fig. 7(c)). In the upstream direction, three plies of the CFRP sheet were wrapped to the surface of the arch dam body. After seven days of curing process, ambient vibration tests were carried out to obtain the experimental dynamic characteristics for same reservoir water levels. After the strengthening application, it is seen that water leakage is completely banned with the CFRP implementation (Fig. 8). As shown in Table 4, six natural frequencies are obtained between 0-1000 Hz for empty and full reservoir water levels as in similar above conditions.

a) Application of MBT-MBrace®Primer to the body surface

b) Application of MBT-MBrace®Adesivo to the body surface

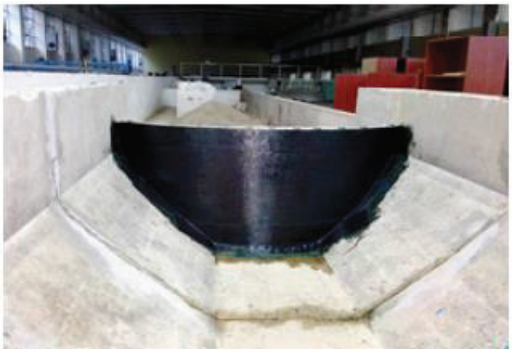

b) Wrapping of MBT-MBrace®Fibre Sheet to the body surface

Figure 7. Some phases of strengthening with CFRP sheet

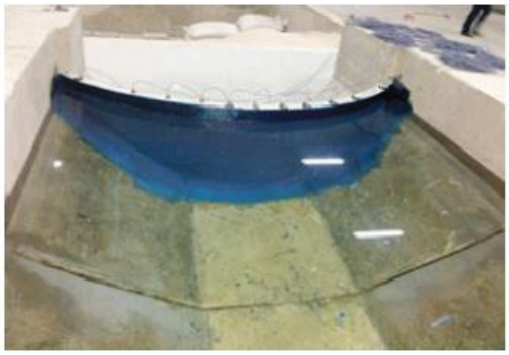

Figure 8. Some photos from condition-3

Table 4. Natural frequencies and damping ratios obtained from the condition-3

	Water levels													
Mode	Empty		10 cm		20 cm		30 cm		40 cm		50 cm		Full	
	Freq. (Hz)	Dr. (%)	Freq. (Hz)	Dr. (%)	Freq. (Hz)	Dr. (%)	Freq. (Hz)	Dr. (%)	Freq. (Hz)	Dr. (%)	Freq. (Hz)	Dr. (%)	Freq. (Hz)	Dr. (%)
1	290.4	1.49	272	1.41	266.2	1.41	264.3	1.03	256.4	2.03	236.2	2.13	235	1.10
2	312.9	1.39	301.3	1.37	292.8	1.89	288.9	2.19	277.7	1.13	258	1.32	252.7	3.09
3	409.9	1.93	373	2.97	363.3	4.42	373.3	2.57	364.7	2.97	331.9	2.47	328.1	2.21
4	495.1	0.98	475.3	0.97	461.6	1.92	456	1.66	454.9	2.51	427	1.95	425	0.81
5	593.5	1.52	570.6	1.75	547.7	2.79	523.3	4.11	513	0	483.5	4.09	478	1.13
6	689.6	0.97	627.1	0.41	650.4	0.10	647.6	1.89	619.9	1.60	595.9	0	587.4	1.18
*Freq: Frequency; Dr: Damping Ratio														

CONCLUSION

This study investigates the water level effects on the dynamic characteristics of damaged, repaired and strengthened arch dam models. To this end, ambient vibration tests are carried out on each model for different water levels to extract the natural frequencies, mode shapes and damping ratios. Ambient vibration testing is also used in this study as a method capable of assessing the stiffness variations due to both repairing and strengthening. Based on the results of this study the following conclusions are drawn:

- The first six natural frequencies before and after repairing range between 151.5 and 441.22 Hz, and 244.9 and 581.4 Hz for empty reservoir, respectively. The first six natural frequencies before and after repairing for the full reservoir range between 145.6 and 381.7 Hz, and 193.5 and 436.4 Hz. From the strengthened dam model, the obtained six natural frequencies for the empty and full reservoir are ranging between 290.4 and 689.6 Hz, and 235 and 587.4 Hz, respectively.
- The natural frequencies obtained from damaged, repaired and strengthened dam model have generally a decrease trend with increasing reservoir water levels. A decrease in frequencies associated with an augmentation of the dam mass due to added mass of water. The maximum difference between the frequencies for the empty and full reservoir are obtained as 16%, 33%, and 25% for damaged, repaired and strengthened model, respectively
- Mode shapes are obtained as symmetrical and antisymmetrical for each water level, and they are identical to each other. That is, mode shapes are not changed with increasing water levels. Apparently, mode shapes obtained from strengthened dam model are quite realistic and close to the possible modes of undamaged dam model.
- The increasing water levels affect damping ratios. But, there is no any harmony (regular increase or decrease) in damping ratios obtained from each water level for the all conditions. The damping ratios are calculated between 0.26-4.35%, 0.23-2.68% and 0.81-3.09% for the damaged, repaired and strengthened dam models, respectively.
- The repairing and strengthening implementations have a remarkable effect in restoring the initial dynamic characteristics of the dam model. After strengthening, the frequencies recoveries are obtained as between 46-92% and 43-62% for the empty and full reservoir respectively.

ACKNOWLEDGEMENTS

TUBITAK and Karadeniz Technical University supported this research under Research Grant No. 106M038 and 2005.112.001.1, respectively; that support is greatly appreciated. The authors also thank BASF Company, Türker SİNİCİ and Ali KÖSE for their collaboration.

REFERENCES

Altunışık, A.C., Günaydın, M., Sevim, B., Bayraktar, A., Adanur, S., 2015. "CFRP composite retrofitting effect on the dynamic characteristics of arch dams". Soil Dynamics and Earthquake Engineering, vol. 74, pp. 1-9.

Altunışık, A.C., Günaydın, M., Sevim, B., Bayraktar, A., Adanur, S., 2016. "Retrofitting effect on the dynamic properties of model-arch dam with and without reservoir water using ambient-vibration test methods". Journal of Structural Engineering, ASCE, vol. 142, N. 10, pp. 1-20.

Altunışık, A.C., Günaydın, M., Sevim, B., Adanur, S., 2017. "System identification of arch dam model strengthened with CFRP composite materials". Steel and Composite Structures, vol. 25, N. 2, pp. 231-244.

Alves, S.W., Hall, J.F., 2006. "System identification of a concrete arch dam and calibration of its finite element model". Earthq. Eng. Struct. Dyn., vol. 35, N. 11, pp. 1321-1337.

Arch Dams., 1968. "A review of British research and development". Proceedings of the Symposium Held at the Institution of Civil Engineers, London, England, March.

Bayraktar, A., Sevim, B., Altunışık, A.C., 2011. “Finite element model updating effects on nonlinear seismic response of arch dam-reservoir-foundation systems”. Finite Elem. Anal. Des., vol. 47, N. 2, pp. 85-97.

Calcina, S.V., Eltrudis, L., Piroddi, L., Ranieri, G., 2014. “Ambient vibration tests of an arch dam with different reservoir water levels: Experimental results and comparison with finite element modeling”. World J. DOI: 10.1155/2014/692709.

Cheng, L., Yang, J., Zheng, D., Li, B., Ren, J., 2015. “The health monitoring method of concrete dams based on ambient vibration testing and kernel principle analysis”. Shock Vib. DOI: http://dx.doi.org/10.1155/2015/342358

Daniell, W.E., Taylor, C.A., 1999. “Effective ambient vibration testing for validating numerical models of concrete dams”. Earthq. Eng. Struct. Dyn., vol. 28, N. 11, pp. 1327-1344.

Darbre, G.R., Proulx, J., 2002. “Continuous ambient vibration monitoring of the arch dam of Mauvoisin”. Earthq. Eng. Struct. Dyn., vol. 31, N. 2, pp. 475-480.

Deinum, P.J., Dungar, R., Ellis, B.R., Jeary, A.P., Reed, G.A.L., Severn, R.T., 1982. “Vibration tests on Emosson arch dam in Switzerland”. Earthq. Eng. Struct. Dyn., vol. 10, N. 3, pp. 447-470.

Dungar, R., 1978. “An efficient method of fluid-structure coupling in the dynamic analysis of structures”. Int. J. Numer. Meth. Eng., vol. 13, N. 1, pp. 93-107.

Hariri-Ardebili, M.A., Sayed-Kolbadi, S.M., 2015. “Seismic cracking and instability of concrete dams: Smeared crack approach”. Eng. Fail. Anal., vol. 52, pp. 45-60.

Karaton, M., 2004. “Dynamic damage analysis of arch dams including fluid-structure interaction”. Ph.D. Thesis; Fırat University, Elazığ, Turkey. [In Turkish].

Liu, J., Liu, F., Kong, X., Long, Y., 2016. “Large-scale shaking table model tests on seismically induced failure of concrete-faced rockfill dams”. Soil Dyn. Earthq. Eng., vol. 82, pp. 11-23.

Loh, C.H., Wu, T.S., 1996. “Identification of Fei-Tsui arch dam from both ambient and seismic response data”. Soil Dyn. Earthq. Eng., vol. 15, N. 7, pp. 465-483.

MBrace Composite Strengthening System., 2007. BASF Construction Chemicals UK, Version 10.

Mendes, P., Oliveira, S., 2007. “Study of dam-reservoir dynamic interaction using vibration tests on a physical model”. Proceedings of the 2nd International Operational Modal Analysis Conference, Copenhagen, Denmark, April, vol. 2, N. 18, pp. 477- 484.

Oliveira, S., Faria, R., 2006. “Numerical simulation of collapse scenarios in reduced scale tests of arch dams”. Eng. Struct., vol. 28, N. 10, 1430-1439.

OMA,. 2006. Operational Modal Analysis, Release 4.0; Structural Vibration Solutions A/S, Denmark.

Pan, J., Zhang, C., Xu, Y., Jin, F., 2011. “A comparative study of the different procedures for seismic cracking analysis of concrete dams”. Soil Dyn. Earthq. Eng., vol. 31, N. 11, pp. 1594-1606.

Perumalswami, P.R., Kar, L., 1973. “Earthquake behavior of arch dams-reservoir systems”. Proceedings of the 5th World Conference on Earthquake Engineering, Rome, Italy, July.

Proulx, J., Paultre, P., Rheault, J., Robert, Y., 2001. “An experimental investigation of water level effects on the dynamic behavior of a large arch dam”. Earthq. Eng. Struct. Dyn., vol. 30, N. 8, pp. 1147-1166.

PULSE., 2006, Analyzers and Solutions, Release 11.2; Bruel and Kjaer, Sound and Vibration Measurement A/S, Denmark.

Sevim, B., 2010. “Determination of Dynamic Behavior of Arch Dams using Finite Element and Experimental Modal Analysis Methods”, PhD Thesis, Karadeniz Technical University, Trabzon, Turkey.

Sevim, B., Bayraktar, A., Altunışık, A.C., Adanur, S., Akköse, M., 2010. “Modal parameter identification of a prototype arch dam using enhanced frequency domain decomposition and stochastic subspace identification techniques”. Journal of Testing and Evaluation, vol. 38, N. 5, pp. 588-597.

Sevim, B., Bayraktar, A., Altunışık, A.C., 2011. “Finite element model calibration of Berke arch dam using operational modal testing”. J. Vib. Control, vol. 17, N. 7, pp. 1065-1079.

Sevim, B., Bayraktar, A., Altunışık, A.C., Adanur, S., Akköse, M., 2011. “Dynamic characteristics of a prototype arch dam”. Experimantal Mechanics, vol. 51, pp. 787-791.

Tarinejad, R., Ahmadi Mohammad, T., Harichandran Ronald, S., 2014. “Full-scale experimental modal analysis of an arch dam: The first experience in Iran”. Soil Dyn. Earthq. Eng., vol. 61, pp. 188-196.

Türker, T., Bayraktar, A., Sevim, B., 2014. “Vibration based damage identification of concrete arch dams by finite element model updating”. Comput. Concrete, Int. J., vol. 13, N. 3, pp. 209-220.
USACE., 2003. Time-History Dynamic Analysis of Concrete Hydraulic Structures; Engineering and Design, USA.
Wang, H., Li, D., 2007. “Experimental study of dynamic damage of an arch dam”. Earthq. Eng. Struct. D., vol. 36, N. 3, pp. 347- 366.
Weng, J.H., Loh, C.H., 2010. “Structural health monitoring of arch dam from dynamic measurements”. Earth and Space 2010: Engineering, Science, Construction and Operations in Challenging Environments, ASCE, pp. 2518-2534.
Westergaard, H.M., 1933. “Water pressures on dams during earthquakes”. Transactions, ASCE, vol. 98, pp. 418-433.
Wilson, E.L., Khalvati, M., 1983. “Finite elements for the dynamic analysis of fluid-solid systems”. Int. J. Numer. Meth. Eng., vol. 19, N. 11, pp. 1657-1668.
Ziyad, D., 1988. “Experimental and finite element studies of a large arch dams”. Ph.D. Thesis; California Institute of Technology, USA.

5 DAM SAFETY
İstanbul Turkey 2018

5th International Symposium on Dam Safety

October 27-31, 2018

EXPERIMENTAL COMPARISON BETWEEN THICK-WALLED SPILLWAYS AND SPILLWAYS WITH DUG

Abderrahmane NOUI [1], Bachir SAKAA [2]

ABSTRACT

The major technological risks related to water, in particular dam failure, are generally due to insufficient drainage capacity of the spillway. To improve the safety of dams, several types of spillways are invented, such as rectilinear spillway and non-rectilinear spillway.
When the threshold of a spillway is in rectilinear alignment, this type of spillway is called rectilinear spillway, while the non-rectilinear spillway is characterized by its non-rectilinear alignment.
Non-rectilinear spillway dug are at the origin of non-rectilinear spillways in developed labyrinth, but they are characterized by the vertical digging of its cells. In this sense, three non-rectilinear spillway dug design models were selected. The first is characterized by a symmetrical digging of its cells; the second model is characterized by a unique digging downstream of its alveoli. While the third configuration is characterized by a unique digging of upstream cells.
In this sense, the present work is considered as a contribution to the comparative study between the rectilinear spillways with thick wall and the non-rectilinear spillways dug experimentally. The experimental study has shown that non-rectilinear spillway dug can be an effective solution for evacuating large flows under light loads compared to rectilinear spillway with thick wall.

Keywords: major technological risk, dam, rectilinear spillway with thick wall, non-rectilinear spillway dug, discharge capacity.

INTRODUCTION

The non-rectilinear spillways dug are the origin of the spillways of modified labyrinth (invented by LEMPRIERE and al 2003), but they are characterized by a vertical hollowing of its alveoli (Machiels and al, 2011).
Experimentally research on the yield of non-rectilinear spillways dug excavated has shown that the best performance of digging of the alveoli is that corresponding to a symmetrical digging of the alveoli.

[1] Research master (B), Scientific and Technical Research Center for Arid Areas (CRSTRA), Algeria.
e-posta: a.noui@univ-biskra.dz
[2] Research master (A),, Scientific and Technical Research Center for Arid Areas (CRSTRA), Algeria.
e-posta: sakaabachir@yahoo.fr

In this subject, it is recommended to compare the performance of non-rectilinear spillways dug symmetrically (with successive increase in digging depths) with the performance of rectilinear spillways of thick wall. We explain in this work the experimental results obtained on four reduced models.

DEFINITION OF THE NON-RECTILINEAR SPILLWAYS DUG

The non-rectilinear spillways dug are characterized by a non-rectilinear alignment; they take the name of "dug" by the digging of its alveoli (Machiels et al, 2011).
Its geometric configuration is based on:
- A rectangular disposition in plan.
- Existence of the upstream and downstream alveoli.
- A symmetrical or unique digging of the alveoli.

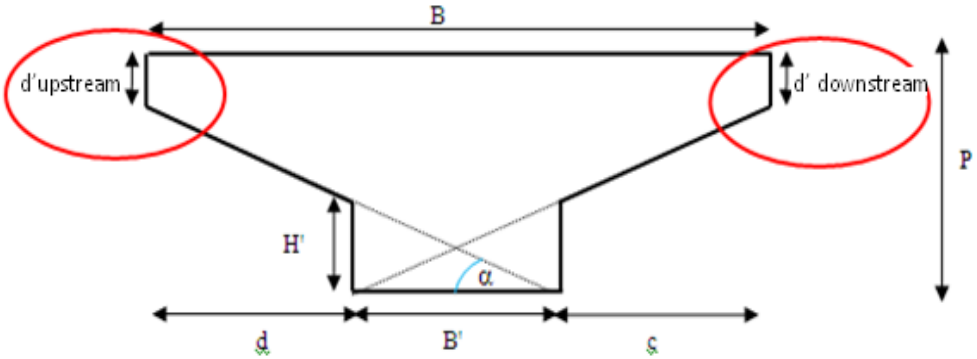

Figure 1. View of a non rectilinear spillway dug

With:
B: length of side wall (m)
B ': Width of spillway base (m)
P: Maximum upstream height of spillway (m)
c: length of the upstream overhang (m)
d: length of the downstream overhang (m)
d'a: depth of digging of the upstream alveoli (m)
d'v: depth of digging of the downstream alveoli (m)
H ': Maximum height of the side walls (m)
α : Wall angle (degree)

MATERIAL AND METHODS

For each experiment, the model of the spillway dug is installed at the exit of the basin of simulation. After verification of the correct installation of the model, a check of the parameters of the flowmeter and the pressure gauges is necessary.
Once the entire experimental system is verified, the pump is primed to fill the retention simulation basin to the spill along the crest of the spillway to be tested. After deactivation of the pump and stopping the flow on the crest of the weir, the threshold level is determined.
After this first step, the first pump is operated at a flow rate of about 30 l / s by manipulation of the first flow control valve. Once the flow is completely stabilized, measurements of the depth of water upstream of the weir tested are carried out by means of the readings on the manometric table, the flow being recorded directly on the computer (PC) by the flow Via the COMMUWIN II software.
This operation is repeated each time the flow rate is varied up to the maximum flow rate of the order of 170 l / s. A series of values (Q and h) is thus obtained (NOUI and al, 2018).
Experimentation of the reduced models of the spillways is carried out in this experimental device.

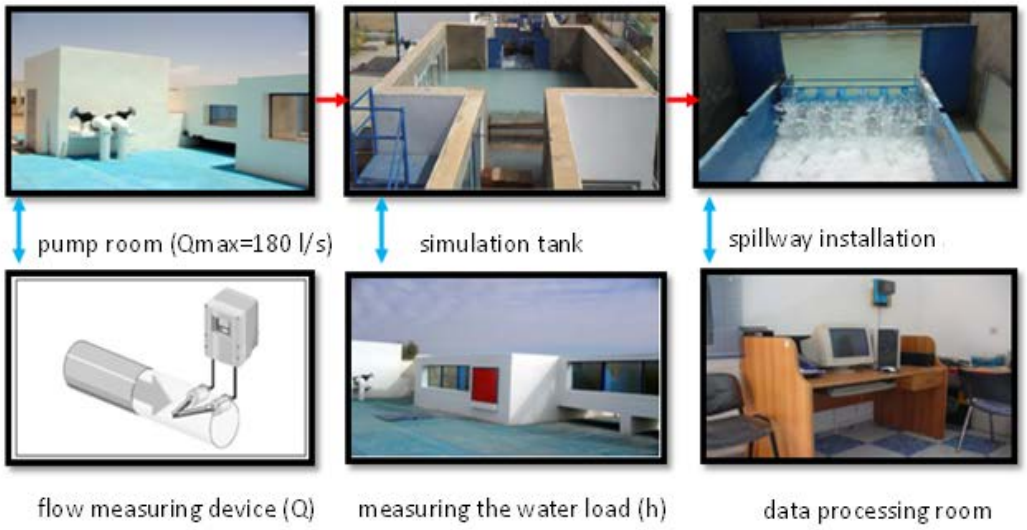

Figure 2.. Experimental protocol

RESULTS AND DISCUSSION

The graphic representation will be based on the torque of the measured values, the flow (Q) and the total relative hydraulic load on the spillway (H*/P).

Iin order to compare the yield of the non-rectilinear spillways dug and the yield of the thick-walled rectilinear spillways of the same width, four (4) models were tested (Table 1).

Table 1. Geometric characteristics of experienced models

Model	L (cm)	W_t (cm)	a (cm)	b (cm)	c=d (cm)	d'a (cm)	d'v (cm)	P (cm)	d'/P
D1	100	100	0	0	20	0	0	15	0
D2	600	100	9	7.5	10.25	2	2	15	0.13
D3	600	100	9	7.5	10.25	4	4	15	0.27
D4	600	100	9	7.5	10.25	6	6	15	0.4

a: width of the upstream alveoli (m)
b: width of the downstream alveoli (m)
d'/ P: ratio of the digging depth of the alveoli to the height
L: developed length of spillway (m)
W : spillway width (m)

Figure 3. Spillway of thick wall tested (Model D1)

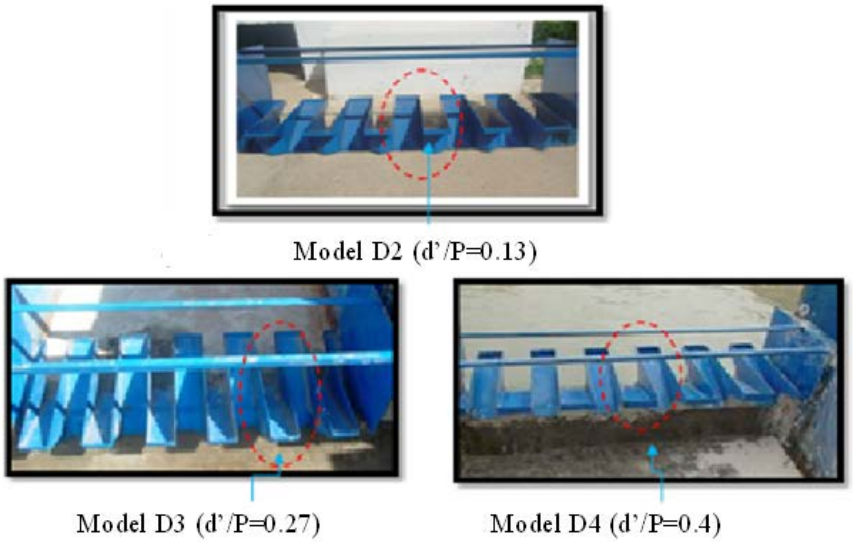

Figure.4. The tested models of spillways dug symmetrically

EXPERIMENTAL

Comparison between the yield of the spillway dug (d'/P=0.13) and the yield of rectilinear spillway with thick wall

The figure which represents a comparison between a non-rectilinear spillway dug symmetrically (d'/P = 0.13) with respect to a spillway in thick wall of the same width indicates that:

- The difference between the two flow curves is of the order of 40% for the relative hydraulic load (H*/P<0.5).
- Variation of the discharge range from 50% to 66% for medium and heavy relative hydraulic load (H*/P>0.5).

-The mean performance of the non-rectilinear weir with symmetrical digging (d'/P= 0.13) with respect to the rectilinear weir in thick wall of the same width is of the order of 2.3 times.

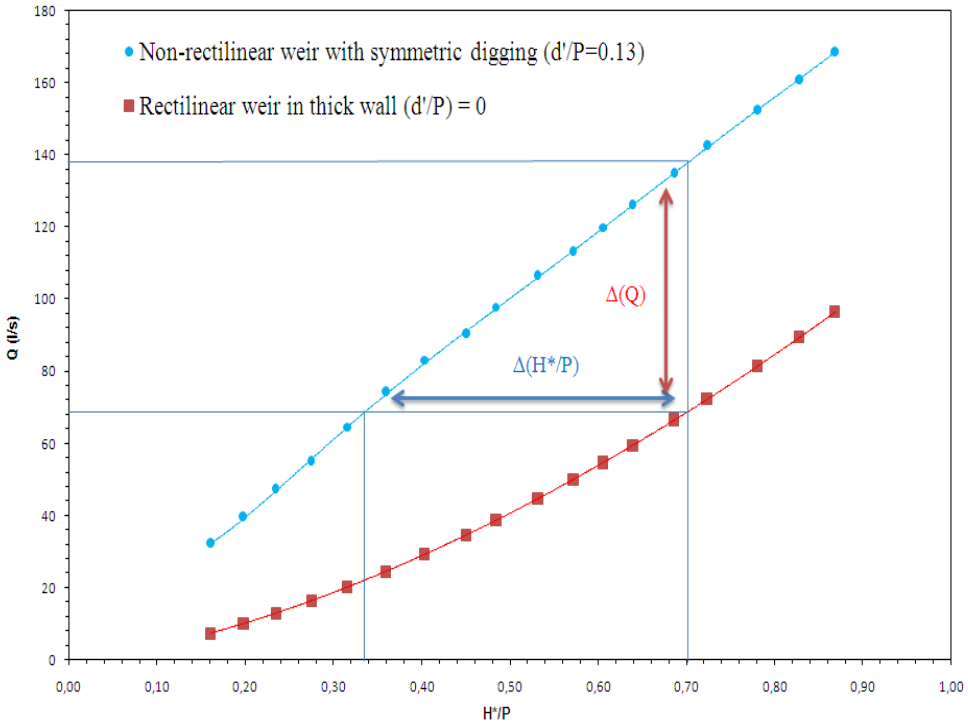

Figure 5. Flow curve of the spillway with symmetrical digging (d/P = 0.13) compared to that of the rectilinear spillway in thick wall

Comparison between the yield of the spillway dug (d'/P=0.27) and the yield of rectilinear spillway with thick wall

This figure indicates that:

- The difference between the two flow curves is of the order of 40 % for the relative hydraulic load (H*/P<0.5).
- Variation of the discharge range from 46% to 58% for medium and heavy relative hydraulic load (H*/P>0.5).
- The mean performance of the non-rectilinear spillway with symmetric digging (d'/P= 0.27) with respect to the rectilinear spillway in thick wall is of the order of 2.15 times.

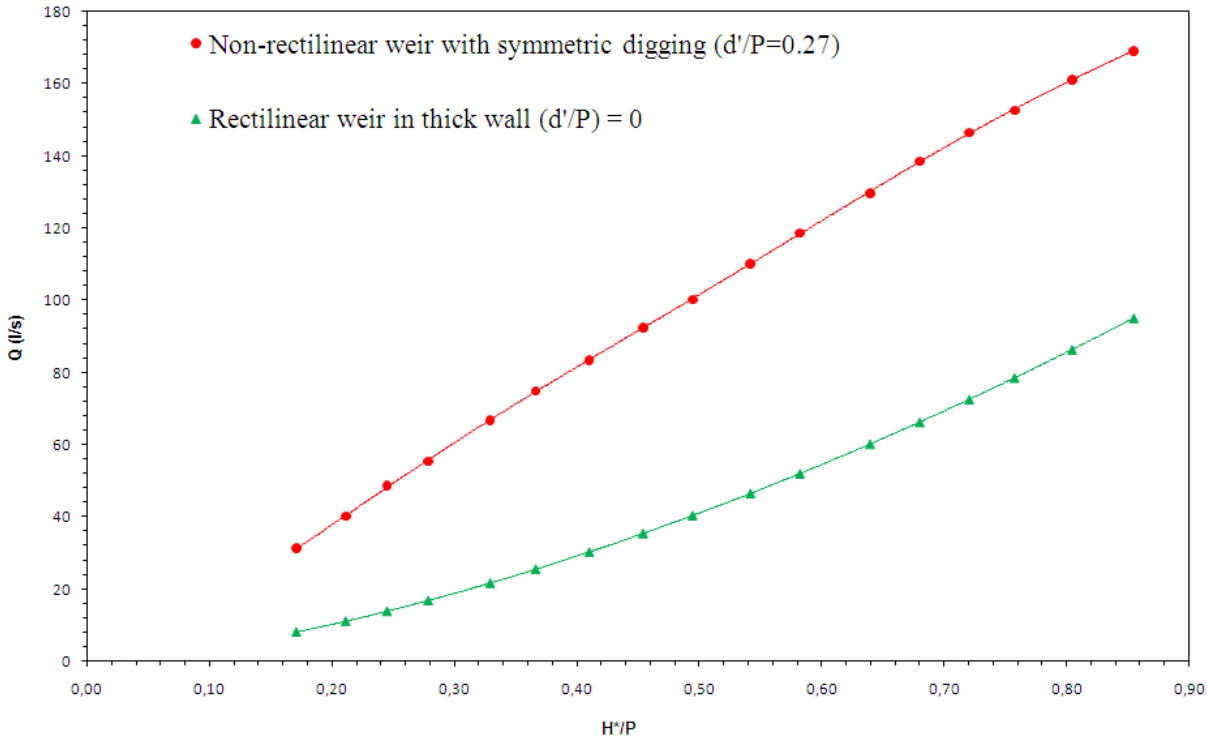

Figure 6. Flow curve of the spillway with symmetrical digging (d'/ P = 0.27) compared to that of the rectilinear spillway in thick wall

Comparison between the yield of the spillway dug (d'/P=0.4) and the yield of rectilinear spillway with thick wall

The figure which represents a comparison between a non-rectilinear spillway dug symmetrically (d'/P = 0.4) with respect to a spillway in thick wall of the same width indicates that:

- The difference between the two flow curves is of the order of 40% the relative hydraulic load (H*/P<0.5).
- Variation of the discharge range from 50% to 62% for medium and heavy relative hydraulic load (H*/P>0.5).

-The mean performance of the non-rectilinear weir with symmetrical digging (d'/ P = 0.4) with respect to the rectilinear weir in thick wall of the same width is of the order of 2 times.

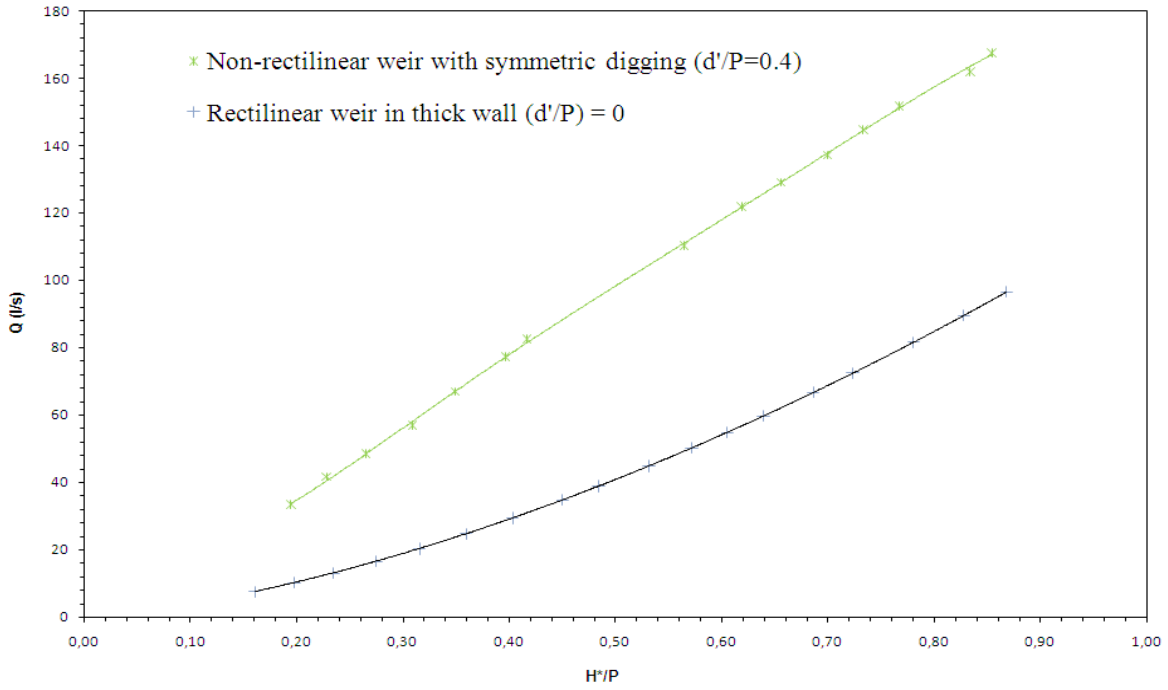

Figure 7. Flow curve of the spillway with symmetrical digging (d'/P = 0.4) compared to that of the rectilinear spillway in thick wall

Results interpretation

The very remarkable deviation of the evacuation capacity between the four models of the symmetrically dug spillways and the thick-walled spillway of the same width is reflected by the influence of;

- The slope generated by the symmetrical dug of non-rectilinear spillway.
- The developed length "L" of the not rectilinear spillway dug which favors the evacuation of the high flows in the same hydraulic load on the rectilinear spillways in thick wall.
- Increasing the digging slope increases the performance of the non - rectilinear spillway to a ratio doesn't exceed (1/3).

CONCLUSION

The results of the experimental tests on four models of symmetrically excavated non-rectilinear spillways and another model of the rectilinear spillway in thick wall of the same width showed that:

- Non rectilinear spillways dug are characterized by their geometrical configurations which favor superior performance compared to thick rectilinear spillways.
- The performance of the non-rectilinear spillways dug symmetrically is of the order 2 times the performance of the spillway in thick wall of the same width, and that in all the ranges of the hydraulic load.
- For better performance of symmetrically excavated non-rectilinear spillways, the slope of hollowing of the alveoli must not exceed (1/3).

REFERENCES

Lempérière F., Ouamane A., 2003. The Piano Keys Weir: a new cost-effective solution for spillways, The International Journal on Hydropower & Dams, Issue Four.

Machiels O., Erpicum S., Dewals B., Archambeau P. and Pirotton M. (2011), Experimental observation of flow characteristics over a Piano Key Weir, Journal of hydraulic research 49 (3), 359-366.

Noui A, Sakaa B. 2018. Comparative study between straight and non-rectilinear weirs. PhD Thesis in Hydraulic Sciences

Noui A, Sakaa B. The spillway in symmetrical digging of the alveoli and the rectilinear spillway (experimental study). J. Fundam. Appl. Sci., 2018, 10(2), 58-66.

5th International Symposium on Dam Safety

October 27-31, 2018

TIME VARIED WATER DEPTHS AND LOCAL VELOCITIES RESULTING FROM FLOOD WAVE PROPAGATION IN THE DISTORTED PHYSICAL MODEL OF ÜRKMEZ DAM IN THE CASE OF PARTIAL VEGETATION

Emrah SEVINC [1], Mehmet Sukru GUNEY[2]

ABSTRACT

The influence of the partial plant configuration on the flood wave propagation resulting from the sudden dam break was investigated experimentally. Experimental studies were carried out on a distorted physical model of Urkmez Dam and its downstream region, built in the scope of the TUBITAK 110M240 project. The model was built in the open area of Hydraulics Laboratory of Dokuz Eylul University Civil Engineering Department, with a horizontal scale of 1/150 and vertical scale of 1/30. The distorted physical model contains the reservoir, the residential area in the downstream of the dam until the sea and partially the plant configuration. The geometrical dimensions of the physical model were determined by using the Froude similitude law, topographic maps and the dam projects. The model crest length is 2.84 m and its height from the foundation is 1.07 m.

In the experiments; the water depths, the local velocities and the flood wave propagation times were measured. Water depths were determined by using e+ WATER L ultrasonic sensors placed in various locations. The velocities were measured from UVP (Ultrasonic Velocity Profiler) transducers. The wave propagation was recorded by means of the high definition cameras located at the downstream part. The time varied water depths and local velocities obtained in the case of partial plant configuration are presented and they are compared to those obtained from experiments carried out without any plant configuration.

Keywords: Dam break, Distorted physical model, Wave propagation, Partial plant configuration, Froude similitude law.

THE DISTORTED PHYSICAL MODEL

The distorted physical model of Urkmez dam with its reservoir and downstream part was designed to investigate flood wave propagation resulting from partial and sudden dam failure (Guney at al., 2013, 2014, 2015). The Urkmez dam was chosen due to its reasonable dimensions and it has a residential area on the downstream. The Figure 1 shows general view of the studied area.

[1] PhD Student, Department of Civil Engineering, Dokuz Eylul University, Izmir, Turkey, e-posta: emrahsvnc@yahoo.com

[2] Professor, Department of Civil Engineering, Izmir Economics University, Izmir, Turkey, e-posta: sukru.guney@ieu.edu.tr

Figure 1. General view of the studied area (http://maps.google.com)

The distorted physical model of Urkmez dam was designed according to the Froude similitude law because the gravitational force is dominant. The horizontal and vertical scales of the model were selected so that it can be built and operated conveniently and still be big enough to measure flow depths and velocities with sufficient accuracy. According to the available space in the open area of Hydraulics Laboratory of Dokuz Eylul University Civil Engineering Department, the horizontal and vertical scales were selected as ℓ_{xr} : 1/150 and ℓ_{zr} : 1/30, respectively.

The distortion coefficient is;

$$n = \ell_{zr} / \ell_{xr} = 5 \tag{1}$$

The slope scale is;

$$S_r = \ell_{zr} / \ell_{xr} = 5 \tag{2}$$

The cross-sectional area scale is;

$$A_r = \ell_{xr}\ \ell_{zr} = 1/4500 \tag{3}$$

The volume scale is;

$$V_r = \ell_{xr}^{\ 2}\ \ell_{zr} = 1/675000 \tag{4}$$

The geometric characteristics of Urkmez Dam (prototype) and its distorted physical model are given in Table 1.

Table 1. The Geometric characteristics of the prototype and the physical model

Characteristics	Prototype	Physical model
Crest length (m)	426	2.84
Crest width (m)	12	0.08
Dam height from its base (m)	32	1.07
Lake volume at minimum water level (m^3)	375 000	0.556
Lake volume at maximum water level (m^3)	8 625 000	12.778
Lake volume at normal water level (m^3)	7 950 000	11.778
Lake active volume (m^3)	7 575 000	11.222

The Froude number is formed by a typical velocity in the x direction of the flow (Yalin, 1971). Therefore, the Froude velocity scale is interpreted as;

$$\nu_r = \nu_{xr} = \sqrt{\ell_{zr}} = 1/5.48 \quad (5)$$

which gives for the time scale of the distorted model;

$$t_r = \frac{\ell_{xr}}{\sqrt{\ell_{zr}}} = \frac{1}{n}\sqrt{\ell_{zr}} = 1/27.4 \quad (6)$$

The distorted physical model of the Urkmez dam involving its reservoir and downstream part without any plant configuration is given in Figure 2.

Figure 2. Distorted physical model of the Urkmez dam involving its reservoir and downstream part without any plant configuration

Plastic brushes were installed at the upper upstream part of the downstream area to simulate partial plant configuration (Figure 3) (Sevinc and Guney, 2016).

Figure 3. Distorted physical model of the Urkmez dam involving its reservoir and downstream part with partial plant configuration

MEASUREMENT DEVICES AND METHODS

The sudden dam failure was simulated by toppling the gate suddenly, hence the flood hydrograph was generated as a result of this sudden failure (Figure 4).

Figure 4. Simulation of the sudden failure of the dam

The flood wave propagation was recorded by HD cameras located at the downstream part.

The time varied water depths were measured by e+ WATER L level sensors (Figure 5). These level sensors were distributed over the lake and downstream part of the Urkmez dam. The level measurement values are automatically compensated for variations in air pressure and water density variations due to temperature fluctuations. The local velocities were measured from UVP (ultrasonic velocity profiler) transducers (Figure 6).

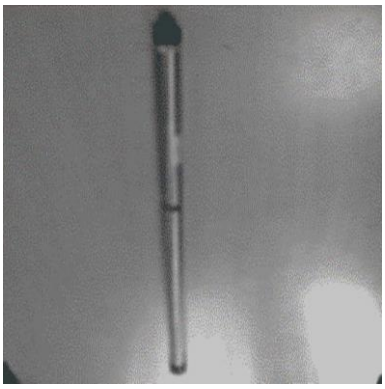

Figure 5. e+ WATER L level sensors

Figure 6. UVP transducers

Locations of the level sensors (S1, S2, S3, S4, S5, S6, S7, S10, S11) and the UVP transducers (T01, T03, T04, T05, T06, T07, T08) are shown in Figure 7.

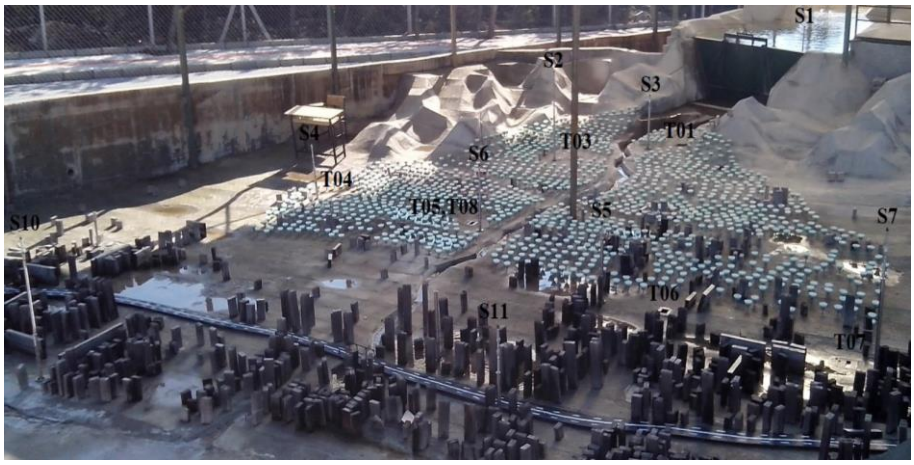

Figure 7. Locations of the level sensors and the UVP transducers

EXPERIMENTAL FINDINGS

Flood Hydrograph

The model reservoir volume-water depth curve obtained by means of the calibration performed initially is given in Figure 8. The measurements of the level meter S1, located in the lake, is given in Figure 9. The measured depth values were converted to the volume values by using the previously obtained volume-water depth curve. The discharge values of the hydrograph were determined by means of the records of the level meter S1 (Figure 10).

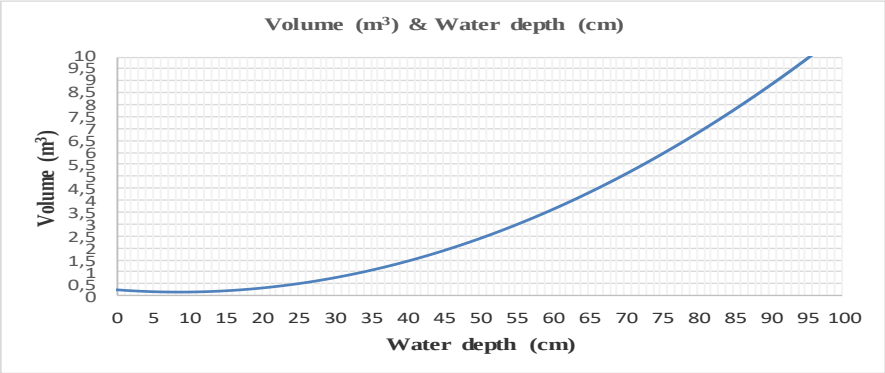

Figure 8. The model reservoir volume-water depth curve

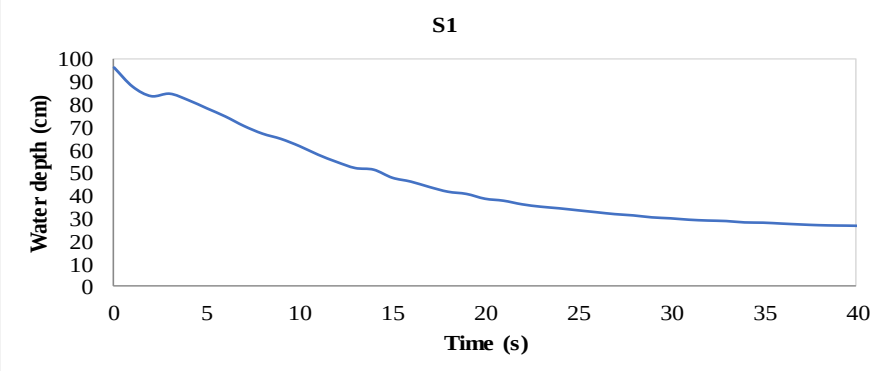

Figure 9. The measurements of level meter S1

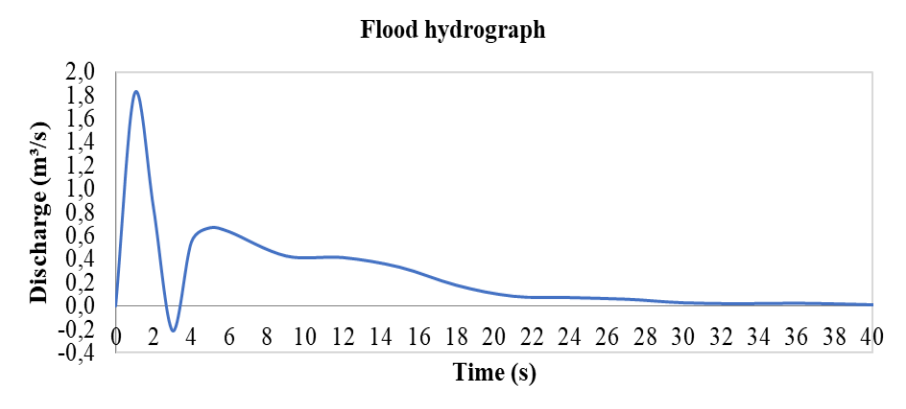

Figure 10. The flood hydrograph

Time Varied Water Depths

Time varied water depths at different locations corresponding to the experiments without vegetation and with vegetation are given in Figure 11.

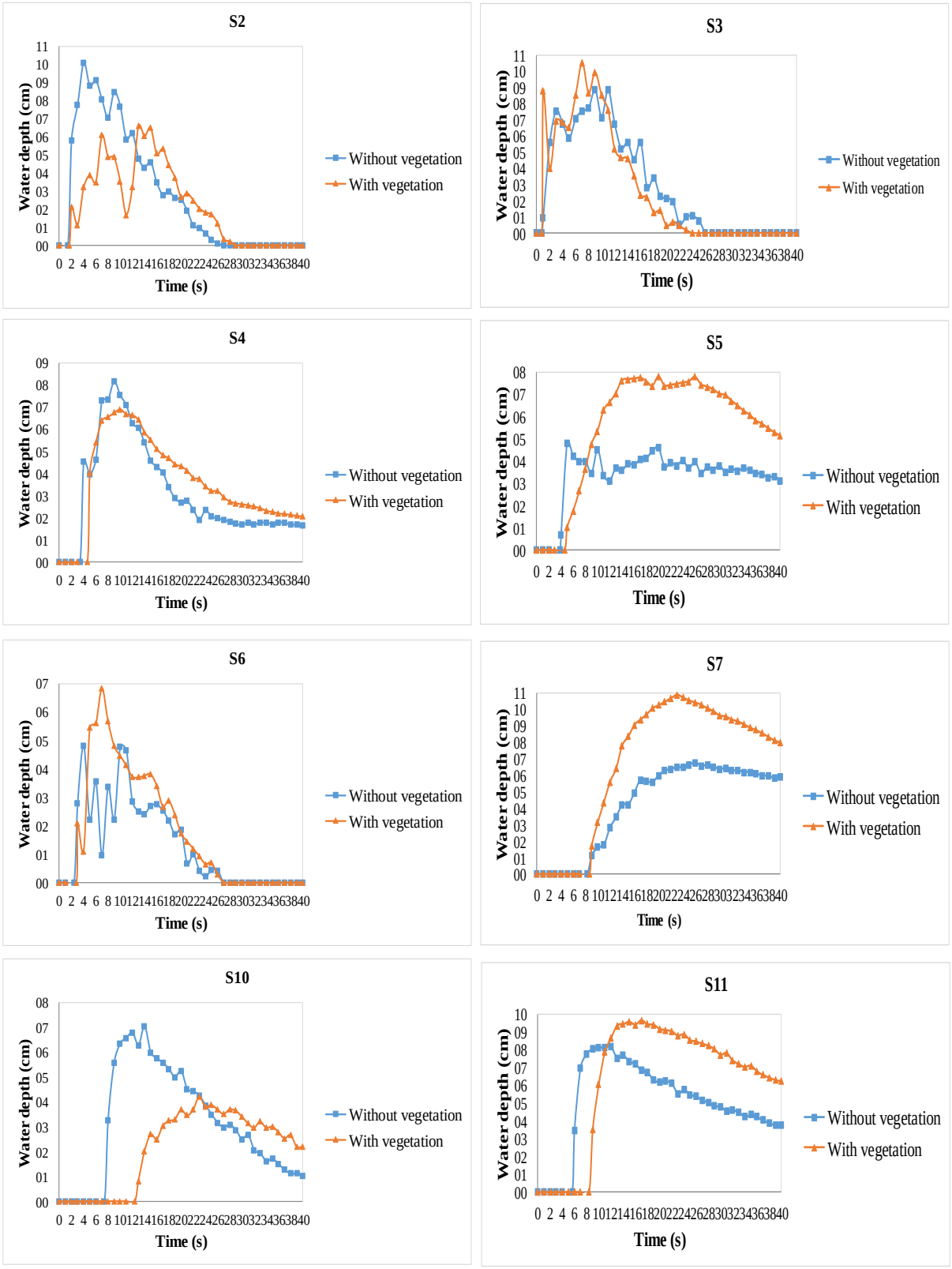

Figure 11. Time varied water depths at different locations

Local Velocities

Local velocities at different locations corresponding to the experiments without vegetation and with vegetation are given in Figure 12.

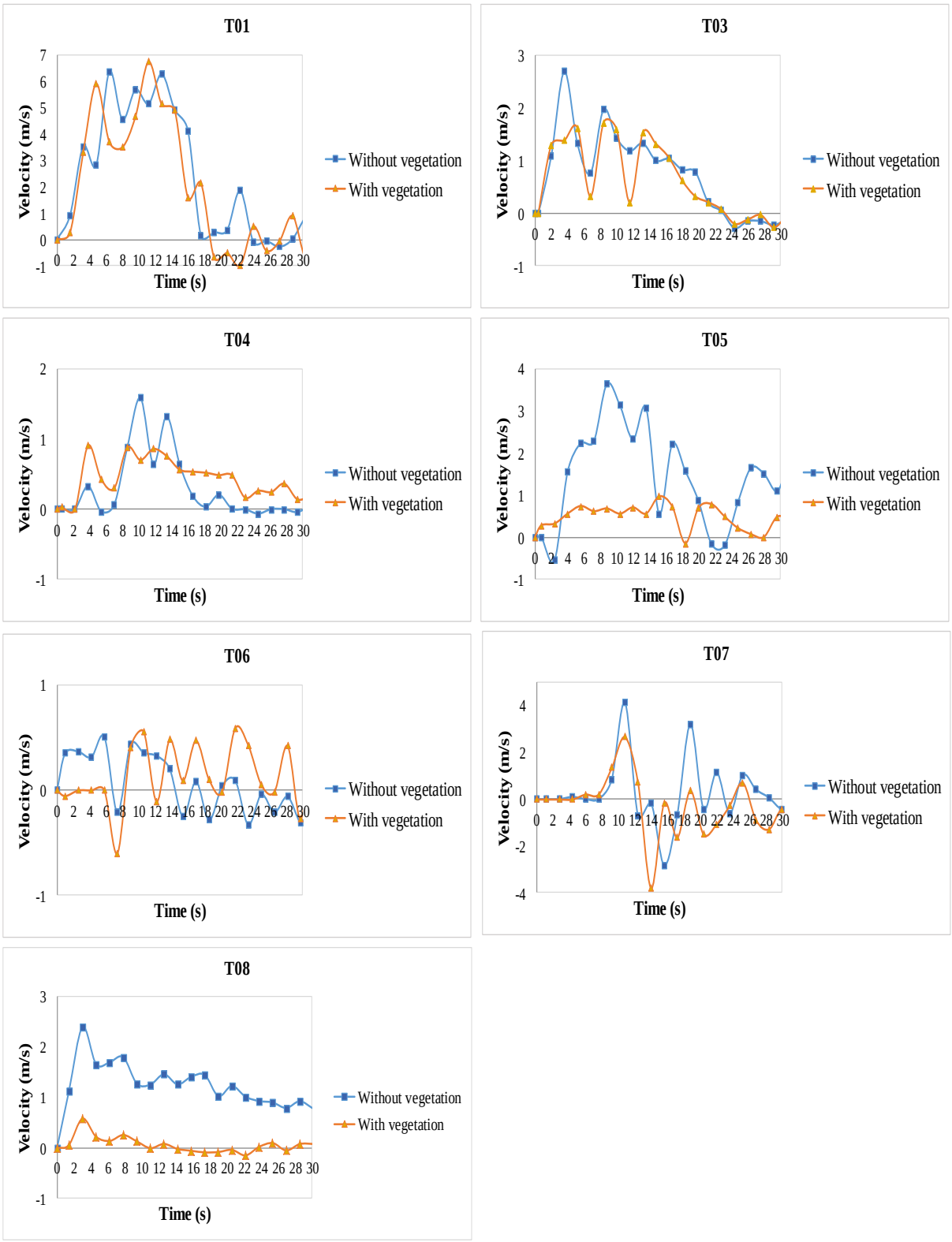

Figure 12. Local velocities at different locations

Flood Wave Propagation

Flood wave propagations in the experiments without vegetation and with vegetation were recorded by high definition cameras. The regions that flood wave reached at time 2 s, 3 s, and 6 s are given in Figure 13, Figure 14 and Figure 15, respectively.

Figure 13. The regions that flood wave reached at time 2 s

Figure 14. The regions that flood wave reached at time 3 s

Figure 15. The regions that flood wave reached at time 6 s

Maximum depths (cm) and times at which maximum depths were reached (s) during the experiments with and without vegetation at different locations are given in Table 2.

Table 2. Maximum depths (cm) and times at which maximum depths reached (s) during the experiments with and without vegetation at different locations

Measurement point	Without vegetation max. depth (cm)	Without vegetation Time at which max. depth reached (s)	With vegetation max. depth (cm)	With vegetation Time at which max. depth reached (s)
S2	10.1	4	6.63	13
S3	8.91	11	10.59	7
S4	8.19	9	6.93	10
S5	4.82	5	7.82	20
S6	4.84	4	6.87	7
S7	6.76	26	10.93	23
S10	7.05	14	4.25	23
S11	8.2	12	9.69	17

Maximum velocities (m/s) and minimum velocities (m/s) measured during the experiments with and without vegetation at different locations are given in Table 3.

Table 3. Maximum velocities (m/s) and minimum velocities (m/s) measured during the experiments with and without vegetation at different locations

Measurement point	Without vegetation max. velocity (m/s)	Without vegetation min. velocity (m/s)	With vegetation max. velocity (m/s)	With vegetation min. velocity (m/s)
T01	6.4	-0.3	6.8	-1
T03	2.7	-0.3	1.7	-0.3
T04	1.6	-0.1	0.9	0
T05	3.7	-0.5	1	-0.2
T06	0.5	-0.3	0.6	-0.6
T07	4.1	-2.8	2.7	-3.8
T08	2.4	0.8	0.6	-0.1

Times elapsed (s) to reach different locations in the experiments with and without vegetation are given in Table 4.

Table 4. Times elapsed (s) to reach different locations in the experiments with and without vegetation

Location reached	Without vegetation time elapsed (s)	With vegetation time elapsed (s)
S3	1	1
S6	3	3
Highway	4	6
Seaside	6	10

CONCLUSIONS

Maximum Water Depths

S2 is located near the dam and on the right side of the creek. The measured maximum water depths of 10.1 cm and 6.63 cm correspond to 3.03 m and 1.99 m, respectively, in the prototype. The water depths decreased significantly and there was an important time lag. These water depths were attained earlier in the case of non-vegetation; at 4 s (110 s in nature) instead of 13 s (356 s in nature)

S4 is located in sparse residential region and on the right side of the creek. The measured maximum water depths of 8.19 cm and 6.93 cm correspond to 2.46 m and 2.08 m, respectively, in the prototype. The water depths were not affected significantly and there was a small time lag, thereby 9 s (247 s in prototype) and 10 s (274 s in prototype).

S10 is located in residential region and on the right side of the creek. The measured maximum water depths of 7.05 cm and 4.25 cm correspond to 2.12 m and 1.28 m, respectively, in the prototype. The water depths were affected significantly and there was a significant time lag, thereby 23 s (630 s in prototype) instead of 14 s (384 s in prototype).

S5 is located in sparse residential region and on the left side of the creek. The measured maximum water depths of 4.82 cm and 7.82 cm correspond to 1.45 m and 2.35 m, respectively, in the prototype. The water depths increased significantly and a significant time lag was observed; 20 s (548 s in prototype) instead of 5 s (137 s in prototype).

S7 is located in sparse residential region and on the left side of the creek. The measured maximum water depths of 6.76 cm and 10.93 cm correspond to 2.03 m and 3.28 m, respectively, in the prototype. The water depths increased significantly but the time elapsed was nearly the same; 23 s (630 s in prototype)

and 26 s (712 s in prototype), the maximum water depth being reached 3 s earlier in the case of vegetation presence.

S11 is located in residential region and on the left side of the creek. The measured maximum water depths of 8.20 cm and 9.69 cm correspond to 2.46 m and 2.91 m, respectively, in the prototype. The vegetation induced an increase in water depth and an important time lag was observed; 17 s (466 s in prototype) instead of 12 s (329 s in prototype).

S3 is located near the dam and near the creek. The measured maximum water depths of 8.91 cm and 10,59 cm correspond to 2.67 m and 3.18 m, respectively, in the prototype. The vegetation induced an increase in water depth and a decrease in time elapsed; 7 s (192 s in prototype) instead of 11 s (301 s in prototype).

S6 is located in sparse residential region and near the creek. The measured maximum water depths of 4.84 cm and 6.87 cm correspond to 1.45 m and 2.06 m, respectively, in the prototype. The vegetation induced an increase in water depth and an important time lag was observed; 7 s (192 s in prototype) instead of 4 s (110 s in prototype).

Experimental findings revealed that the presence of the vegetation increased the maximum water depths in regions near the creek (S3 and S6) and in regions on the left side of the creek (S5, S7 and S11). By contrast, the maximum water depths decreased in regions on the right side of the creek (S2, S4 and S10).

Maximum and Minimum Velocities

T01 is located near the dam body and velocities measured as 6,4 m/s and 6,8 m/s correspond to 35,1 m/s and 37,3 m/s, respectively in prototype. These velocities can cause serious damages.

When there is no vegetation, the velocity of 2,7 m/s measured from T03 corresponds to 14,8 m/s in nature. When the vegetation exists this velocity decreased to 1,7 m/s (9,3 m/s in prototype).

When there is no vegetation, the velocity of 1,6 m/s measured from T04 corresponds to 8,8 m/s in nature. When the vegetation exists this velocity decreased to 0,9 m/s (4,9 m/s in prototype).

When there is no vegetation, the velocity of 3,7 m/s measured from T05 corresponds to 20,3 m/s in nature. When the vegetation exists this velocity decreased to 1,0 m/s (5,5 m/s in prototype).

When there is no vegetation, the velocity of 4,1 m/s measured from T07 corresponds to 22,5 m/s in nature. When the vegetation exists this velocity decreased to 2,7 m/s (14,8 m/s in prototype).

When there is no vegetation, the velocity of 2,4 m/s measured from T08 corresponds to 13,2 m/s in nature. When the vegetation exists this velocity decreased to 0,6 m/s (3,3 m/s in prototype).

Experimental findings revealed that maximum velocities decreased significantly when the vegetation exists.

Wave Propagation Times

Regions near the dam were totally affected by the wave in about 2 s (55 s in prototype) in the both cases of with and without vegetation. Water reached the highway in about 4 s (110 s in prototype) and reached the seaside in about 6 s (164 s in prototype) when there is no vegetation, while there was a significant time lag when the vegetation exists; the time elapsed to reach the highway was about 6 s (164 s in prototype) and for the seaside was about 10 s (274 s in prototype). Experimental findings revealed that the vegetation induced a mitigation of the flood wave.

The experimental findings are continued to be analyzed and interpreted in the light of existing literature knowledge. The numerical study and thus the comparison between the experimental and numerical findings are also being carried out by using the software FLOW3D. The elaborated results will be presented in the scope of the Ph. D. thesis of the first author.

ACKNOWLEDGEMENTS

This study was supported by the Scientific and Technological Research Council of Turkey (TUBITAK) with the project number 110M240.

REFERENCES

Güney, M. Ş., Tayfur, G., Bombar G., and Bayram D., 2013. "Experimental investigation of flood propagation due to trapezoidal breach in the distorted physical model of Ürkmez dam". IWPE 2013, 6 th International Perspective of Water Resources & the Environment, İzmir, Turkey.

Güney, M.Ş., Tayfur, G., Bombar, G., and Elçi, Ş., 2014. "A distorted physical model to study sudden partial dam break flows in an urban area". Journal of Hydraulic Engineering, DOI:10.1061//(ASCE)HY.19437 900.0000926.

Güney, M.Ş., Tayfur G., Arkış T., Bombar G., 2015. "Experimental and numerical investigation of flood propagation due to trapezoidal breach in the distorted physical model of Ürkmez dam". Dam Engineering, Vol XXV,issue 4, p 171-187.

http://maps.google.com

http://en.eijkelkamp.com/products/water/hydrological-research/water-level-measurements

http://www.met-flow.com

Sevinc, E., Güney, M. Ş., 2016. "Experimental study of the influence of plant configuration on the wave propagation resulting from dam break". 6th Annual International Conference on Civil Engineering, Athens, Greece.

Yalın, M. S., 1971. "Theory of hydraulic models". The Macmillan Press Ltd, London.

5 DAM SAFETY
İstanbul Turkey 2018

5th International Symposium on Dam Safety

October 27-31, 2018

NUMERICAL SIMULATIONS OF THE WETTING EFFECT ON THE LONG-TERM BEHAVIOUR OF CONCRETE FACE ROCKFILL DAMS

Mohammadkeya Khosravi [1], Linke Li [2], Saeed Safikhani [3], Erich Bauer [4]

ABSTRACT

Wetting deformations of the rockfill material in a concrete face rockfill dam (CFRD) can lead to an increase of the bending of the concrete slabs and consequently to cracks and leakage points in concrete slabs. Heavy rainfall or defects of the concrete sealing causes a local increase of the moisture content in the dam body, which can lead, for moisture sensitive rockfill materials, to time dependent deformations.
In the present paper, numerical simulations are carried out to investigate the influence of the size and location of the wetted zone on the time dependent deformation of the CFRD. To this end an extended hypoplastic constitutive model by Bauer is used. The model takes into account the current void ratio, the effective stress, the strain rate, the moisture-sensitive solid hardness and its rate. Herein the moisture-sensitive solid hardness is a key parameter to model the inherent properties of moisture-sensitive and weathered coarse-grained rockfill materials. It is shown that the size and location of the wetted zone has a strong influence on the evolution of concrete slab deformation.

Keywords: Rockfill dam, solid hardness, wetting deformation, hypoplasticity

INTRODUCTION

The effect of wetting on the mechanical properties of weathered and moisture sensitive rockfill materials is an experienced fact and of great importance for the long term behaviour of rockfill dams, e.g. (Sowers et al., 1965; Clements, 1981; Oldecop and Agreda, 2004; Oldecop and Alonso, 2007; Chen et al., 2007; Bauer et al., 2010). Wetting deformations of rockfill material are caused by a degradation of the solid hardness leading to particle breakage and a reorientation of the grain skeleton into a denser state. The amount of particle crushing is mainly controlled by the state of weathering of the rock particle, the grain size distribution, the pre-compaction, the stress level and the change of the moisture content (Nobari and Duncan, 1972; Brauns et al., 1980; Alonso and Cardoso, 2010). The deformation and strength characteristic of the rockfill material differs in dry and wet conditions. The change of the moisture content of the granular material has a significant effect on the micro crack propagation in the rock particles and the degradation of the solid hardness subsequently leads to

[1] PhD student and Assistant Lecturer, Institute of Applied Mechanics, Graz University of Technology, Austria, e-posta: khosravi@student.tugraz.at
[2] PhD student and Assistant Lecturer, Institute of Applied Mechanics, Graz University of Technology, Austria, e-posta: linke.li@student.tugraz.at
[3] PhD student and Assistant Lecturer, Institute of Applied Mechanics, Graz University of Technology, Austria, e-posta: s.safikhani@student.tugraz.at
[4] Professor, Institute of Applied Mechanics, Graz University of Technology, Austria
e-posta: erich.bauer@tugraz.at

deformations in the rockfill body even if the stress is kept constant (Hang, 1990; Tedd et al., 1994; Oldecop and de Agreda, 2007; Fu et al., 2011; Bauer, 2018).

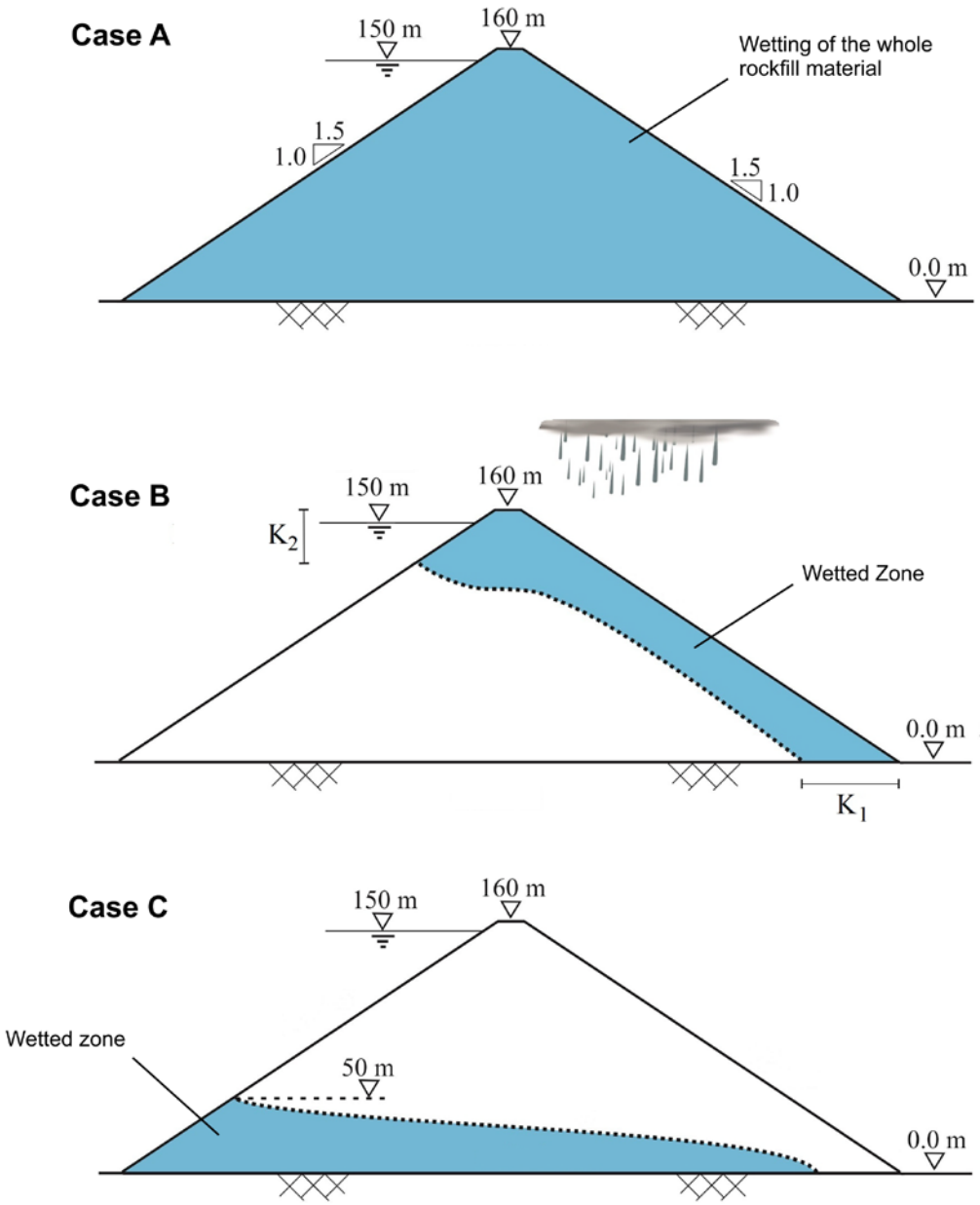

Figure 1. Section of an artificial CFRD with three different wetting scenarios:
Case A: wetting of the whole rockfill material;
Case B: wetting of a downstream part of the dam body caused by rainwater infiltration;
Case C: leakage into the lower part of the rockfill dam.

Long-term deformations of the rockfill material may have a strong influence on the amount of bending moments and crack propagation in the concrete slab of a concrete face rockfill dam (CFRD). The analysis of the wetting-induced deformation in CFRDs is thus of great importance already during the design phase. Wetting induced deformations are a function of the initial conditions in terms of the state of weathering of the solid hardness, void ratio, stress state and moisture content and the change of these quantities (Bauer, 2009; Lu et al., 2010). Depending on the reason for a change of the moisture content the corresponding time dependent degradation of the solid hardness can be limited to a specific area within the dam body.

In the present paper, numerical simulations are carried out to investigate the influence of the size and location of the wetted zone on the time dependent deformation of the rockfill material and the concrete slab of an artificial CFRD. Three different scenarios of wetting zones are investigated as illustrated in (Figure 1). In particular, in Case A it is assumed that the entire rockfill material is wetted, in Case B only a part of the downstream area is affected by rainwater infiltration and in Case C wetting of the bottom part of the rockfill material caused by leakage through the foundation is considered. For modeling wetting effects an extended hypoplastic constitutive model by (Bauer, 2009) is used. The model takes into account the current void ratio, the effective stress, the strain rate, the moisture-sensitive solid hardness and its rate. The moisture-sensitive solid hardness is described in the sense of a continuum description and it is a key parameter to model the inherent properties of moisture-sensitive and weathered coarse-grained rockfill materials.

CONSTITUTIVE MODEL

In order to model weathered and moisture sensitive rockfill materials the so-called solid hardness plays an important role in the constitutive model used in the present paper. In particular, the solid hardness, h_{st}, is a parameter in the compression law proposed by (Bauer, 1996, 2009) which is defined for an assembly of particles under monotonic isotropic loading. Thus, h_{st} should be distinguished from the hardness of individual grains. It is known that under the same pressure rockfill materials can show different packing density of the grain assembly, i.e. the void ratio can range between a maximum void ratio, e_i, and a minimum void ratio, e_d. For consistency, the solid hardness h_{st} is related to the compression curve obtained from an isotropic compression starting from the maximum void ratio. The decrease of the maximum void ratio, e_i, with an increase of the mean pressure, p, is described by the following compression law (Bauer, 2009):

$$e_i = e_{io} \exp\left[-\left(\frac{3p}{h_{st}}\right)^n\right] \tag{1}$$

Herein e_{i0} denotes the maximum void ratio at the stress-free state, h_{st} is the current value of the solid hardness and n is a constitutive parameter. The compressibility of weathered rockfill materials is higher for the wet material than for the dry material. When a reaction with water takes place the degradation of solid hardness is a time dependent, irreversible process and modelled by the following evolution equation (Bauer, 2009):

$$\dot{h}_{st} = -\frac{1}{c}(h_{st} - h_{sw}) \tag{2}$$

Herein the current state of the solid hardness, h_{st}, ranges within the upper limit h_{so}, i.e. the solid hardness before wetting and the lower limit h_{sw}, i.e. the final degraded state of the solid hardness.
Parameter c has the dimension of time and scales the velocity of degradation. It can be calibrated from a creep test. For general stress paths, the moisture and rate-dependent solid hardness and limit void ratio has been embedded into the hypoplastic model by (Bauer, 1996) and (Gudehus, 1996). In particular, for $\dot{h}_{st} \le 0$ the extended constitutive equation reads (Bauer, 2009):

$$\overset{\nabla}{\sigma}_{ij} = f_s[\hat{a}^2\dot{\varepsilon}_{ij} + (\hat{\sigma}_{kl}\,\dot{\varepsilon}_{kl})\hat{\sigma}_{ij} + f_d\,\hat{a}(\hat{\sigma}_{ij} + \hat{\sigma}^*_{ij})\sqrt{\dot{\varepsilon}_{kl}\,\dot{\varepsilon}_{kl}}] + (\dot{h}_{st}/h_{st})\sigma_{ij} \tag{3}$$

In (Equation 3), $\overset{\nabla}{\sigma}_{ij}$ denotes the effective objective stress rate, $\dot{\varepsilon}_{ij}$ is the rate of deformation, σ_{ij} is the effective Cauchy stress, $\sigma^*_{ij} = \sigma_{ij} - \sigma_{kk}\delta_{ij}/3$ is the deviatoric part, $\hat{\sigma}_{ij} = \sigma_{ij}/\sigma_{kk}$ and $\hat{\sigma}^*{}_{ij} = \hat{\sigma}_{ij} - \delta_{ij}/3$ are normalized quantities. Factor $\hat{a}$ is related to critical friction angle, φ_c, and can be adapted to the limit condition by (Matsuoka and Nakai, 1977) as shown in detail by (Bauer, 2000).
The effect of pressure level and current void ratio on the incremental stiffness is taken into account with factors f_s and f_d. In particular, the density factor f_d represent a relation between the current void ratio e, the critical void ratio, e_c and the minimum one e_d, i.e.

$$f_d = \left(\frac{e - e_d}{e_c - e_d} \right)^{\alpha} \tag{4}$$

where the pressure dependent quantities e_c and e_d are related to the compression law (Equation 1) via the postulate by (Gudehus, 1996), i.e.

$$\frac{e_i}{e_{io}} = \frac{e_c}{e_{co}} = \frac{e_d}{e_{do}} = \exp\left[-\left(\frac{3p}{h_{st}} \right)^n \right] \tag{5}$$

The stiffness factor f_s has the dimension of stress and reads:

$$f_s = \left(\frac{e_i}{e} \right)^{\beta} \frac{1}{\hat{\sigma}_{kl}\,\hat{\sigma}_{kl}} \frac{1 + e_i}{n\, h_i e_i} \left(\frac{h_{st}}{3} \right)^n p^{(1-n)} \tag{6}$$

Herein , α and β are constitutive constants (Bauer, 1996) and h_i can be obtained from a consistency condition by (Gudehus, 1996).

NUMERICAL SIMULATIONS

The effect wetting of the rockfill material on the long-term behavior of an artificial CFRD is numerically investigated using the extended hypoplastic constitutive model outlined in the previous section and the finite element program ABAQUS. The CFRD considered has a height of 160 m, a width of the crest of 16 m and a slope ratio of 1:1.5 on both upstream and downstream side of the dam as illustrated in (Figure 1). For the sake of simplicity, in all simulations a rigid foundation is assumed. For the rockfill material a weathered broken granite with a density of 2200 kg/m^3 and a corresponding void ratio of e_0 = 0.33 of the compacted state of the dam body after construction is considered. The hypoplastic constitutive parameters of the rockfill material are calibrated based on the data obtained from large scale triaxial experiments carried out by (Kast, 1992). The parameters are summarized in (Table 1). Herein the solid hardness of h_{s0} = 75.0 MPa is obtained from experiments under dry conditions. It can be noted that for a water saturated condition a value of h_{sw} = 25 MPa was obtained for a lower pre-compaction (Bauer, 2009), while in the current investigation a higher value is considered (Khosravi et al., 2017). In particular, for the effect of limited rainfall events (Case A and Case B) a value of h_{sw} = 68.8 MPa and for the long-term effect of leachate (Case C) a value of h_{sw} = 60.0 MPa is assumed.

Table 1. Constitutive parameters for the rockfill material

Case	h_{s0} [MPa]	n	h_{sw} [MPa]	c [Year]	φ_c [°]	e_{d0}	e_{c0}	e_{i0}	α	β
A	75	0.6	68.8	2.0	42.0	0.2	0.39	0.85	0.125	1.05
B	75	0.6	68.8	2.0	42.0	0.2	0.39	0.85	0.125	1.05
C	75	0.6	60.0	2.0	42.0	0.2	0.39	0.85	0.125	1.05

The corresponding reduction of the solid hardness with time is shown in (Figure 2). The concrete slab has a thickness of 0.3 m at the top and a thickness of 0.62 m at the bottom plinth. The latter is calculated according to the concept for design of CFRDs suggested by (ICOLD, 2004), i.e. for the 160 m high CFRD one obtains 0.3+0.002x160 = 0.62 m. At the bottom the concrete slab has a certain freedom to move along the concrete abutment. A linear elastic material behaviour is assumed. for the concrete, i.e. E_s = 20 GPa, υ = 0.17 and ρ = 2400 kg/m^3. Between the concrete slab and the cushion layer a friction coefficient of 0.5 is taken into account. The interface behaviour between the concrete slab and the cushion layer is modelled using the concept of Master and Slave surfaces provided by the finite element software of ABAQUS.

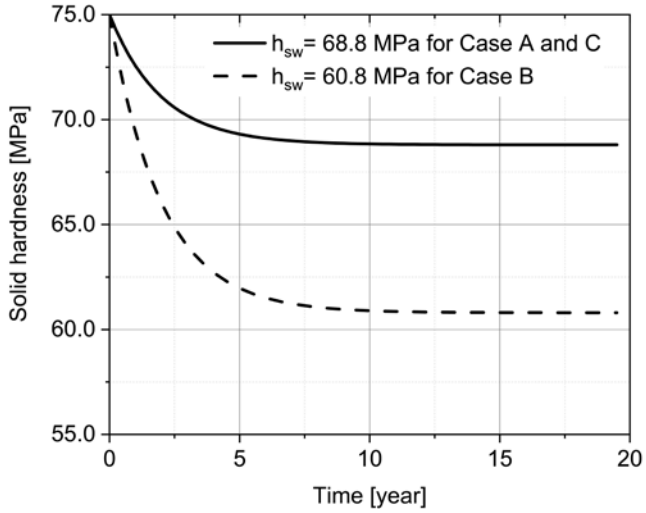

Figure 2. Degradation of the solid hardness with the time for two different wetting effects.

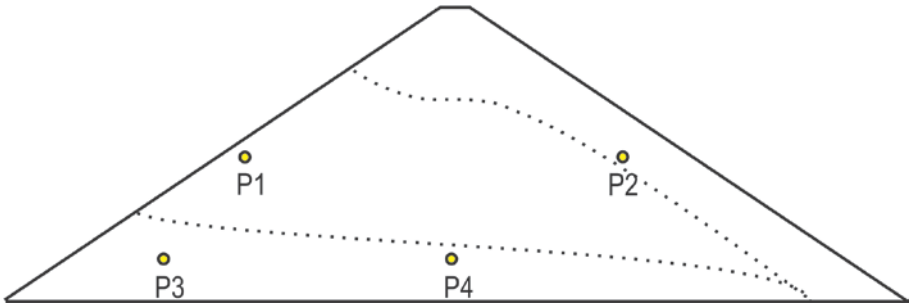

Figure 3. Selected points for comparing the void ratio caused by water impounding and wetting induced deformations (the dashed curves are related to the wetted zones in Case B and Case C.

Points	e
P1	0.3262
P2	0.3299
P3	0.3285
P4	0.3295

(a)

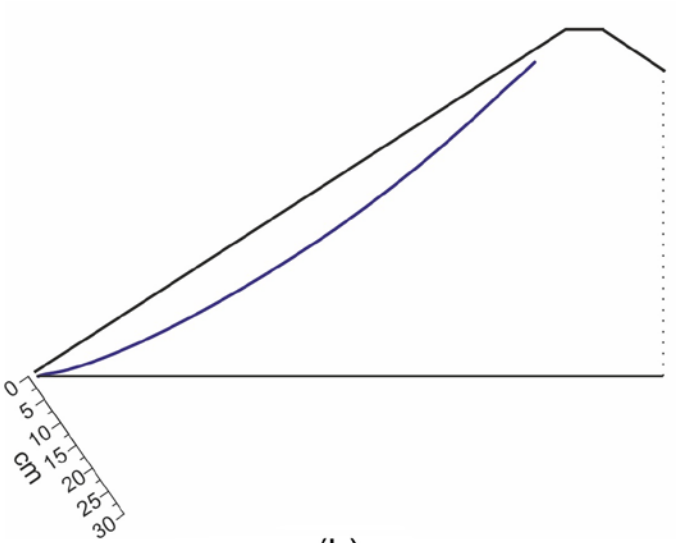

(b)

Figure 4. Deformation caused by water impoundment: (a) value of the void ratio at selected points defined in (Figure 3); (b) normal deflection of the concrete slab.

In the numerical simulation the following steps are considered: (i) construction of the dam body in 16 layers; (ii) construction of the concrete slab and the cushion layer; (iii) computation of the deformations caused by water impounding; (iv) additional deformations caused by degradation of the solid hardness for the wetting scenarios shown in (Figure 1).

Instantaneous deformation and additional compaction caused by water impounding

For computing the deformation caused by water impounding no degradation of the solid hardness is considered, i.e. for the instantaneous deformation the value of h_{s0} = 75 MPa is kept constant. Because of the high pre-compaction of the rockfill material assumed during construction the additional compaction is small. The evolution of void ratio at four points of the dam body is shown in (Figure 4a). The maximum reduction of the void ratio is located close to the concrete slab, (point P1), and the maximum void ratio is located in the downstream part of the dam body (point P2). The maximum normal deflection of the concrete slab is 7.5 cm and located nearly at the middle height of the dam (Figure 4b). Because of the rigid dam foundation, the concrete slab has only little freedom to move along the abutment joint and to penetrate into the thin cushion layer. This situation influences the shape of the slab deformation in the lower part.

Case A: Wetting of the whole rockfill material

After water impounding a degradation of the solid hardness, caused by wetting of the whole dam body, is considered over a period of 14 years. To this end, the reduction of the solid hardness from h_{st} = 75 MPa to h_{sw} = 68.8 MPa according to the evolution (Equation 2) is computed and taken into account in the hypoplastic constitutive (Equation 3). Although the degradation of the solid hardness is the same in the whole dam body, the evolution of the additional compaction is strongly related to the local stress state and density after water impounding. This is clearly visible by comparing the time dependent evolution of the relative void ratio, i.e. $e_{rel}(t) = (e_0 - e(t))/e_0$, in points P1, P2, P3 and P4 shown in (Figure 5a). The amount of reduction of the relative void ratio is greater at the lower level, i.e. for points P3 and P4, which can be explained by the combined effect of the higher vertical effective stress and the influence of wetting.

It can also be observed that the final value of the additional densification after degradation of the solid hardness is greater in point P4 than in point P3 although these two points are located at the same level. This is because of the influence of the higher vertical stress in point P4. It is clearly apparent that the change of the relative void ratio declines with increasing time and after 8 years the rate of the void ratio is almost the same in all points of the dam body. The normal deflection of the concrete slab after 14 years is shown in (Figure 5b). With respect to normal deflection caused by water impounding and degradation of the solid hardness the maximum value is 28 cm and located at the crest of the dam.

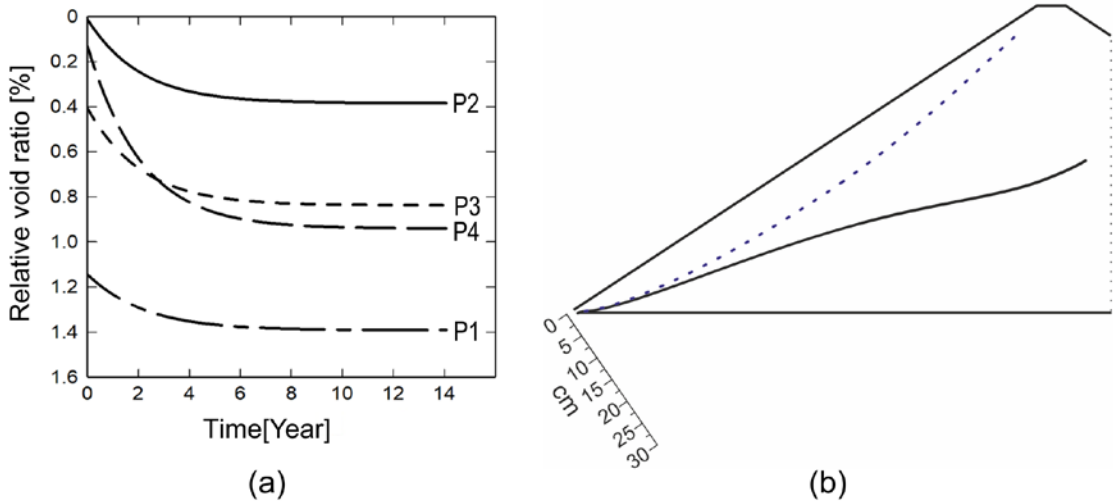

Figure 5. Wetting effect Case A: (a) changes of the relative void ratio at selected points defined in (Figure 3); (b) normal deflection of the concrete slab.

Case B: Wetting of a downstream part of the dam body caused by rainwater infiltration

In this case the deformations caused by wetting of a part of the rockfill material in the downstream part of the CFRD are investigated. In order to show the effect of rainwater infiltration, the creep deformation caused by gravity load and water impounding are not taken into account. The spatial area affected by the change of the moisture content of the rockfill material depends on the intensity and

duration of the rainfall events. Thus, the degradation of the solid hardness can be more pronounced within this area. To demonstrate this effect, four different areas are analyzed. The assumed extensions of these zones according (Figure 1b) are summarized in (Table 2).

Table 2. Size of the wetting zones for different rainfall event.

Subcase	K_1 [m]	K_2 [m]
B-1	30	20
B-2	40	30
B-3	50	40
B-4	60	50

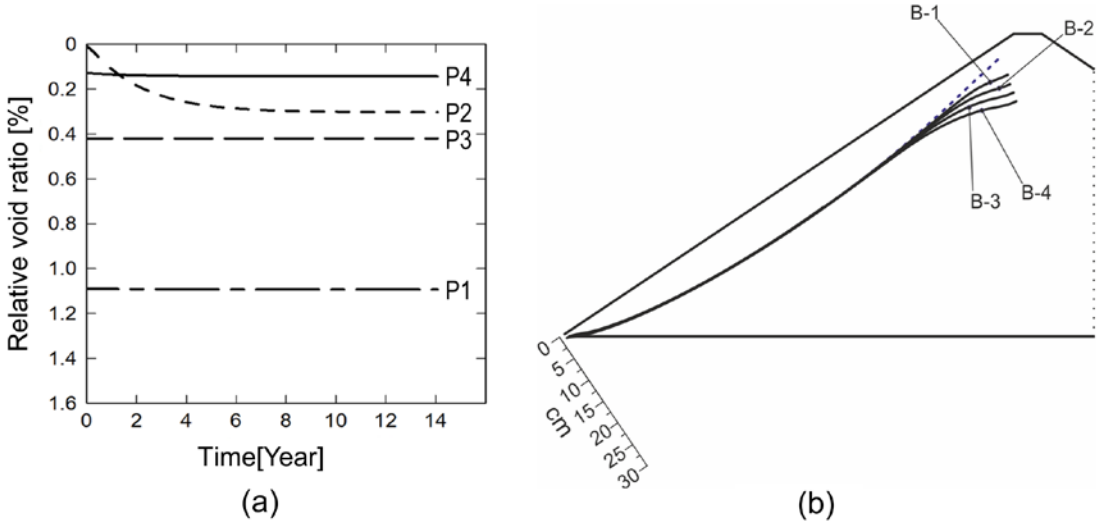

Figure 6. Wetting effect Case B: (a) changes of the relative void ratio at selected points defined in (Figure 3); (b) normal deflection of the concrete slab.

As can be seen in (Figure 6a) additional compaction occurs only in point P2, which is located in the wetted zone. The value of wetting-induced normal deflection of the concrete slab is only significant in the upper part and it is greater for a larger extension of the wetted zone (Figure 6b). The maximum normal deflection of the concrete slab and for the different subcases, their locations are summarized in (Table 3).

Table 3. Maximum normal deflection of the concrete slab for different subcases.

Case	Maximum of normal deflection [m]	Level of the Maximum of normal deflection [m]
B-1	0.08	90.0
B-2	0.085	96.0
B-3	0.097	160.0
B-4	0.112	160.0

Case C: Leakage into the lower part of the rockfill dam

This case investigates the effect of leakage through the foundations of the dam or a defect of the sealing of the concrete joints in the lower part of the dam. A wetted zone illustrated in (Figure 1c) is assumed for the analysis. In contrast to the limited duration of rainfall events, seepage caused by leakage can be considered as being stationary over long periods. Thus, a larger degradation of the

solid hardness is assumed, i.e. h_{sw} = 60 MPa. This also leads to larger compaction of the wetted zone as indicated by points P3 and P4 (Figure 7a). The vertical stress is higher in the middle of the dam, therefore, the additional densification is also more pronounced at point P4 than at point P3. Although a degradation of the solid hardness only takes place in the wetted zone the deformation of the concrete slab is pronounced in the upper part (Figure 7b).

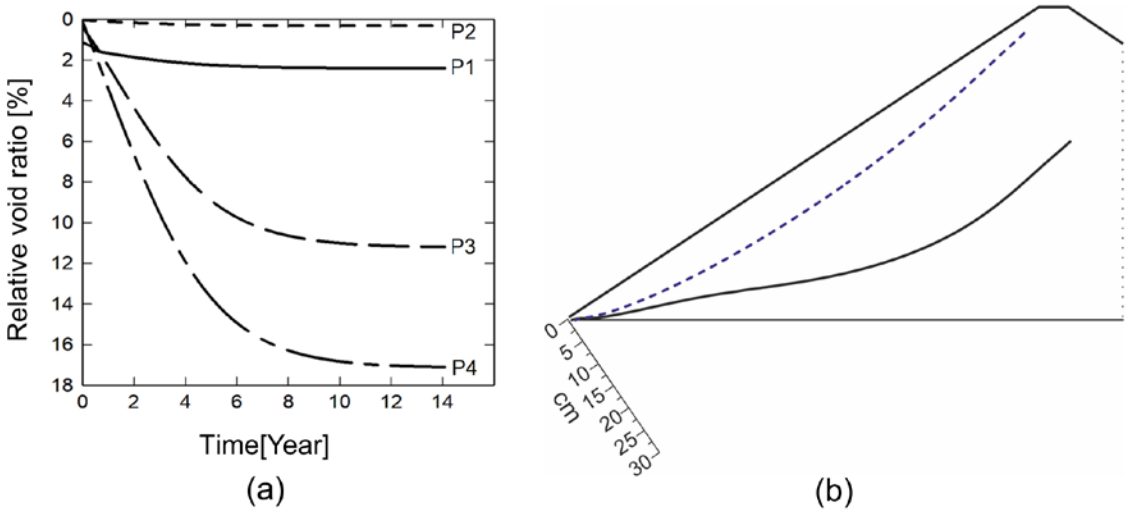

Figure 7. Wetting effect Case C: (a) changes of the relative void ratio at selected points defined in (Figure 3); (b) normal deflection of the concrete slab.

CONCLUSION

An extended hypoplastic constitutive model is used to investigate wetting induced long-term deformations of a concrete face rockfill dam (CFRD). For modelling the behavior of the weathered and moisture sensitive rockfill material a so-called solid hardness is a key parameter in the hypoplastic model. The solid hardness represents the current state of weathering and serves as a scaling factor of the stiffness. State changes of the solid hardness caused by repeated wetting are described by a corresponding evolution equation. In this paper three different scenarios of wetting deformations in a CFRD are investigated: wetting of the entire rockfill material, wetting of the downstream part of the rockfill material caused by heavy rainfall, and wetting of the bottom part of the rockfill material caused by leakage through the foundations. The results of the numerical simulations show that the extension and location of the wetted zone has a strong influence on both the shape and the amount of deformation of the concrete slab. The normal concrete slab deflection can be much higher than the instantaneous part that caused by water impounding and depends on the quality of the pre-compaction and the rockfill material used. As the concrete slab serves as a sealing, the focus of evaluation of the deformed concrete slab should also be on the value of curvatures, which are related to bending moments, and are thus indicators for the appearance of cracks in the concrete slab. The present investigations are based on a simplified 2-D CFRD model on a rigid foundation, and thus potential exists for more precise and qualitatively improved results. More detailed modeling is needed in order to take into account the influences of the dam foundation stiffness, the 3-D geometry of the dam in space, the properties of lateral abutments and the coupling of the computation of the deformation with the relevant seepage behavior.

REFERENCES

Abaqus 6.13, Dassault Systèmes Simulia Corp, Johnston, Rhode Island, United States.

Alonso, E. E., Cardoso, R., 2010. “Behavior of Materials for Earth and Rockfill Dams: Perspective from Unsaturated Soil Mechanics”. Frontiers of Architecture and Civil Engineering in China, vol. 4, N.1, pp. 1-39.

Bauer, E., 1996. “Calibration of a Comprehensive Hypoplastic Model for Granular Materials”. Soils and Foundations, vol. 36, N.1, pp. 13-26.
Bauer, E., 2009. “Hypoplastic Modelling of Moisture-Sensitive Weathered Rockfill Materials”. Acta Geotechnica, vol. 4, N.4, pp. 261-272.
Bauer, E., Fu, Z., Liu, S., 2010. “Hypoplastic Constitutive Modeling of Wetting Deformation of Weathered Rockfill Materials”. Frontiers of Architecture and Civil Engineering in China, vol.4, N.1, pp. 78-91.
Bauer, E., 2018. “Constitutive Modelling of Wetting Deformation of Rockfill Materials”. International Journal of Civil Engineering, pp. 1-6, doi: 10.1007/s40999-018-0327-7.
Brauns, J., Kast, K., Blinde, A., 1980. “Compaction Effects on the Mechanical and Saturation Behaviour of Disintegrated Rockfill”. Proc Int Conf Compact, vol. 1, pp. 107-112.
Chen, L. H., Zhou, X. G., Wei, Y. Q., 2007. “Wetting Effects of Rockfill on the Deformation of the Yellow River Xiaolangdi Dam”. Key Engineering Materials, vol. 353, pp. 2736-2739.
Clements, R. P., 1981. “The Deformation of Rockfill, Inter-Particle Behaviour, Bulk Properties and Behaviour in Dams”. University of London.
Fu, Z. Z., Liu, S. H., Gu, W. X., 2011. “Evaluating the Wetting Induced Deformation of Rockfill Dams Using a Hypoplastic Constitutive Model”. Advanced Materials Research, vol. 243, pp. 4564-4568.
Gudehus, G., 1996. “A Comprehensive Constitutive Equation for Granular Materials”. Soils and Foundations, vol. 36, N.1, pp. 1-12.
Hang, Y. Z. Z., 1990. “Deformation Analysis of Earth Dam during Reservoir Filling”. Chinese Journal of Geotechnical Engineering, vol. 12, N.2, pp. 1-8.
Khosravi, M., Li, L., Bauer, E., 2017. “Numerical simulation of post-construction deformation of a concrete face rockfill dam”. Proceedings of the 4th International Conference on Long-Term Behaviour and Environmentally Friendly Rehabilitation Technologies of Dams, LTBD 2017, (eds.) Noorzad, A., Bauer, E., Ghaemian, M., Ebrahimian, B., Published by Verlag der Technischen Universität Graz, ISBN 978-3-85125- 564-5, pp. 307-314.
Lu, N., Godt, J. W., Wu, D. T., 2010. “A Closed-Form Equation for Effective Stress in Unsaturated Soil”. Water Resources Research, vol. 46, N.5, doi:10.1029/2009WR008646.
Materon, B., 2009. “Concrete Face Rockfill Dams”. International Water Power and Dam Construction, Yearbook. (November), pp. 304-310.
Matsuoka, H, Nakai, T., 1977. “Stress-Strain Relationship of Soil Based on the SMP”. Proceedings of 9th ICSMFE, Constitutive Equations of Soils, pp.153-162.
Nobari, E. S., Duncan, J. M., 1972. “Movements in Dams Due to Reservoir Filling”. Performance of earth and earth-supported structures.
Oldecop, L. A., Alonso, E. E., 2004. “Theoretical Investigation of the Time-Dependent Behaviour of Rockfill”. Géotechnique, vol. 57, N.3, pp. 289-301.
Oldecop, L. A., de Agreda, E., 2007. “Testing Rockfill under Relative Humidity Control”. Geotechnical Testing Journal, vol.27, N.3, pp. 269-278.
Sower, N., Wratten, G. P., 1965. “Intussusception Due to Intestinal Tubes, Case Reports and Review of Literature”. The American Journal of Surgery, vol.110, N.3, pp. 441-444.
Tedd, P., Charles, J. A., Holton, R., Robertshaw, A. C., 1994. “Deformation of Embankment Dams Due to Changes in Reservoir Level”. Proceedings of the international conference on soil mechanics and foundation engineering, vol. 3, pp. 951-954.

5 DAM SAFETY
İstanbul Turkey 2018

5th International Symposium on Dam Safety

October 27-31, 2018

THE PROJECTION OF RESERVOIR VOLUME OF MARMARA LAKE UNDER RCP SCENARIOS

Umut KIRDEMIR [1], Umut OKKAN[2]

ABSTRACT

In the study prepared, the reservoir volume of Marmara Lake, operated for irrigation purposes in Gediz Basin, was tried to be projected between 2016-2050 water years in the context of climate change. In the study, RCP4.5 and RCP8.5 scenarios and twelve global circulation models (GCMs) specified in the IPCC's 5th Assessment Report were utilized and the meteorological and hydrological changes that may occur in Marmara Lake basin were aimed to foreseen for the future term. First, the atmospheric variables which capture the meteorological characteristics of basin were determined and coarse-resolution GCM data were downscaled to basin scale by means of statistical downscaling methods. Subsequently, the results of 12 GCMs were weighted through Bayesian Model Averaging (BMA) method and obtained combination of multi-model outputs. The bias of model results was corrected by quantile mapping (QM) method. Following this process, the irrigation water that can be demanded from the lake in the future was projected by Blaney-Criddle method. The inflow components feeding Marmara Lake were modeled mathematically by means of a conceptual hydrological model and total flows arriving to the lake were computed. The precipitation, temperature, crop water demand and streamflow projections were derived through the previous results and obtained that decreases in precipitation and inflows and increases in temperature and irrigation water demand may be experienced in the future. The performance of Marmara Lake was tried to be foreseen between 2016-2050 water years under the conditions of current operation policy and it was estimated that the lake may failure in the future in terms of supplement of irrigation water under RCP scenarios.

Keywords: Representative concentration pathways, downscaling, irrigation water, hydrological modeling, reservoir operation.

INTRODUCTION

Global warming is influencing the Earth unfavourably in terms of water availability, agricultural productivity, biodiversity, human health and etc. In regard to gradual changes in water, the planning studies of water resources have to be done by all countries for an efficient management of them. In order to do these studies, the possible effects of climate change should be precisely estimated so that the relevant authorities may take measures to avoid water shortage in the future. When the climate change studies are reviewed from past to present, it can be seen that global circulation models (GCMs) are very practical tools to simulate past and future climate. However, GCMs are required to

[1] PhD Student, Department of Civil Engineering, Dokuz Eylul University, Izmir, Turkey, e-posta: umut.kirdemir@gmail.com
[2] Asst. Prof., Department of Civil Engineering, Balikesir University, Balikesir, Turkey, e-posta: umutokkan@balikesir.edu.tr

be downscaled because they are relatively coarse-resolution so that sensitive simulations can be derived. In this regard, various downscaling strategies were applied by the researchers (Okkan and Inan, 2015; Schimidli et al, 2006) such that they were generally categorized into two groups such as statistical and dynamical.

GCMs were constituted by various research centers in accordance with the scenarios made up after the assessment reports of Intergovernmental Panel on Climate Change (IPCC). Following the First Assessment Report (FAR) of IPCC, same scenarios namely Special Report on Emissions Scenarios (SRES) were utilized until the Fourth Assessment Report (AR4) such that many downscaling studies were done in terms of climate models derived under SRES. In the last assessment report, AR5, IPCC in 2013 provides new scenarios termed "Representative Concentration Pathways" (RCPs) for users. RCPs represent groups of several scenarios that produce emission pathways related with the future emissions of greenhouse gases, aerosols, ozone, and land use/land cover changes, while preceding AR4 scenarios only included forcing by greenhouse gases and aerosols (Moss et al., 2010). These emission pathways in RCPs are classified by means of the radiative forcing generated by the end of the twenty-first century.

In this study, the possible effects of climate change on one of the most important water resources of Gediz Basin, Marmara Lake, were investigated under RCP4.5 and RCP8.5 scenarios. A statistical downscaling procedure was applied for meteorological variables such as precipitation and temperature so that inflow series of Marmara Lake can be derived to fulfill the reservoir operation in the future term 2015-2050. Subsequently, a conceptual rainfall-runoff model was utilized to simulate Marmara Lake inflows in which precipitation and temperature simulations were utilized as basic variables. Blaney-Criddle method was employed to estimate the past and future irrigation water demanded from Marmara Lake. At the end, reservoir operation by behavior analysis method was carried out so that future reservoir performance of Marmara Lake can be projected under different RCP scenarios. Basically, the study consists of 4 parts: a) generation of precipitation and temperature projections, b) crop water demand projections, c) streamflow projections and d) reservoir operation. In the study, the detailed information about Marmara Lake basin and utilized data are given in next section.

STUDY AREA AND DATA

Marmara Lake is one of the most important water resources existing in Gediz Basin. Marmara Lake has a natural dam lake which is operated for irrigation purposes such that it serves major parts of the irrigated fields with Demirkopru Dam in Gediz Basin. It has a embankment dam body with the volume of 7.2 hm^3 and active storage volume of 306 hm^3 such that it has the second largest storage volume in Gediz Basin behind Demirkopru Dam which has active storage volume of 1022 hm^3. The drainage area of the lake basin is 389 km^2. The annual mean areal precipitation in the lake basin is about 479 mm and the annual mean temperature is about 16 °C. The meteorological stations existing in the basin are operated by Turkish Meteorological Service (MGM) and General Directorate of State Hydraulic Works (DSI) In the study, the utilized meteorological and flow gauging stations were defined with respect to analyzing strategy of lake basin system in which Marmara Lake reservoir were fed by different parts of Gediz Basin such that they constitute the inflows of the lake. The inflows of Marmara Lake consist of accumulation of five components elucidated as follows:

1- Surface flow drained in the lake basin naturally. At the stage of calculation of this component, the data of Salihli meteorological station nearby Marmara Lake were utilized. The RCP scenario-based projection data were utilized from Okkan vd. (2016) for Salihli meteorological station.

2- The water released through spillway of Demirkopru Dam ($V_{spilled,dkopru}$) is conveyed to Marmara Lake reservoir by Adala regulator and 20.245 m-long Adala channel with maximum discharge

capacity of 30 m^3/s. Accordingly, the relationship for the water volume conveyed through Adala channel (V_{Adala}) can be constituted as follows:

$$V_{Adala} = \frac{n_{day} \text{ x } 86400 \text{ x } 30}{10^6} \quad if \quad V_{spilled,dkopru} \geq \frac{n_{day} \text{ x } 86400 \text{ x } 30}{10^6}$$
$$V_{Adala} = V_{spilled,dkopru} \quad if \quad V_{spilled,dkopru} < \frac{n_{day} \text{ x } 86400 \text{ x } 30}{10^6} \tag{1}$$

where n_{day} denotes the number of days in the related month. Units are in hm^3. In order to calculate the data of $V_{spilled,dkopru}$, the results of Okkan and Kirdemir (2018) were utilized. In their work, they used the data of 15 meteorological stations for precipitation and 9 meteorological stations for temperature series and the data of 4 flow-gauging stations.

3- The water spilled from Gordes Dam reservoir ($V_{spilled,gordes}$). In order to utilize the related data, the authors used the results of Okkan and Kirdemir (2016a) in which the data of 5 meteorological stations measuring both precipitation and temperature and the data of 1 flow-gauging station were utilized.

4- The streamflow discharge above the value of 5 m^3/s ($V_{floodwater}$) is conveyed to Marmara Lake reservoir by Comlekci regulator over Kum Creek. At this stage, it was decided to utilize the data of Kayalıoglu flow-gauging station over Medar Creek with the station number E05A009 which is operated by General Directorate of State Hydraulic Works (DSI). Contribution of flood water to Marmara Lake reservoir was calculated by the relationship defined as

$$V_{floodwater} = 0 \quad if \quad V_{\text{E05A009}} - \frac{n_{day} \text{ x } 86400 \text{ x } 5}{10^6} \leq 0$$
$$V_{floodwater} = V_{\text{E05A009}} - \frac{n_{day} \text{ x } 86400 \text{ x } 5}{10^6} \quad if \quad V_{\text{E05A009}} - \frac{n_{day} \text{ x } 86400 \text{ x } 5}{10^6} > 0 \tag{2}$$

In order to prepare the streamflow projection of Medar Creek, precipitation and temperature time series of past period were obtained by 2 meteorological stations for precipitation and 1 meteorological station for temperature.

5- The water which is in excess of the Adala channel capacity and ($V_{spilled,dkopru} - V_{Adala}$) and flows of Alasehir Creek are pumped through Ahmetli pumping station, existing at upstream side of Ahmetli Regulator, to the 15.52 km-long Marmara Lake drainage channel with the maximum capacity of 15 m^3/s and subsequently conveyed to the lake reservoir. This operation is carried out between the months May and November. Hence, monthly streamflow time series of Ahmetli Regulator ($V_{Ahm,reg}$) can be calculated by the data of flow-gauging station with the station number D05A031 which is scaled with respect to Alasehir Creek and Ahmetli Regulator drainage areas and the relationship can be obtained as

$$V_{Ahm,reg} = V_{spilled,dkopru} - V_{Adala} + 1.39438 V_{\text{D05A031}} \tag{3}$$

The volume of water pumped by Ahmetli pumping station and conveyed through Marmara Lake drainage channel ($V_{Ahm,pump}$) is calculated by Equation 4 as follows:

$$V_{Ahm,pump} = \frac{n_{day} \text{ x } 86400 \text{ x } 15}{10^6} \quad if \quad V_{Ahm,reg} \geq \frac{n_{day} \text{ x } 86400 \text{ x } 15}{10^6}$$
$$V_{Ahm,pump} = V_{Ahm,reg} \quad if \quad V_{Ahm,reg} < \frac{n_{day} \text{ x } 86400 \text{ x } 15}{10^6} \tag{4}$$

The data representing 1980-2005 and 1976-2010 time periods were extracted from each meteorological station and flow-gauging stations, respectively. The meteorological and flow gauging stations which were utilized in the study are presented in the Table 1 together with the operator institutions of them.

Marmara Lake supplies irrigation water demanded from 7 irrigation water associations (Table 2). According to the data obtained from irrigation associations between the years 1995-2007, water-melon, cotton, maize, vineyard, olive, orchard, vegetables, clover, cereals, animal feeds were cultivated and it was considered that the production trend of the related crops would continue in the future term 2015-2050. According to this scenario, the irrigated areas were estimated with a function of time and irrigation water that can be demanded from the associations was tried to be foreseen for each RCP scenarios. In this respect, the quantity of area irrigated by each associations was assumed not to exceed the net irrigation area in the future.

ERA-Interim monthly reanalysis data set (Dee *et al.*, 2011) of the European Centre for Medium-Range Weather Forecasts (ECMWF) were selected for the study region as large-scale predictors to calibrate statistical downscaling models. The location of the meteorological stations and ERA-Interim reanalysis grids used in the study are shown in the Figure 1. The large-scale output databases from twelve GCMs (BCC-CSM1, CCSM4, CESM1(CAM5), CSIRO-Mk3.6, GFDL-CM3, GFDL-ESM2M, GISS-E2-H, GISS-E2-R, HadGEM2-ES, IPSL-CM5A-LR, MIROC-ESM, MRI-CGCM3) which include both historical scenario outputs representing 20th century climate (1980-2005) and 21st century climate simulations under the RCP4.5, and RCP8.5 scenarios (2015-2050), were selected for the downscaling exercise under RCP scenarios (Okkan and Kirdemir, 2016b). The information of selected GCMs are given by Okkan and Kirdemir (2016b).

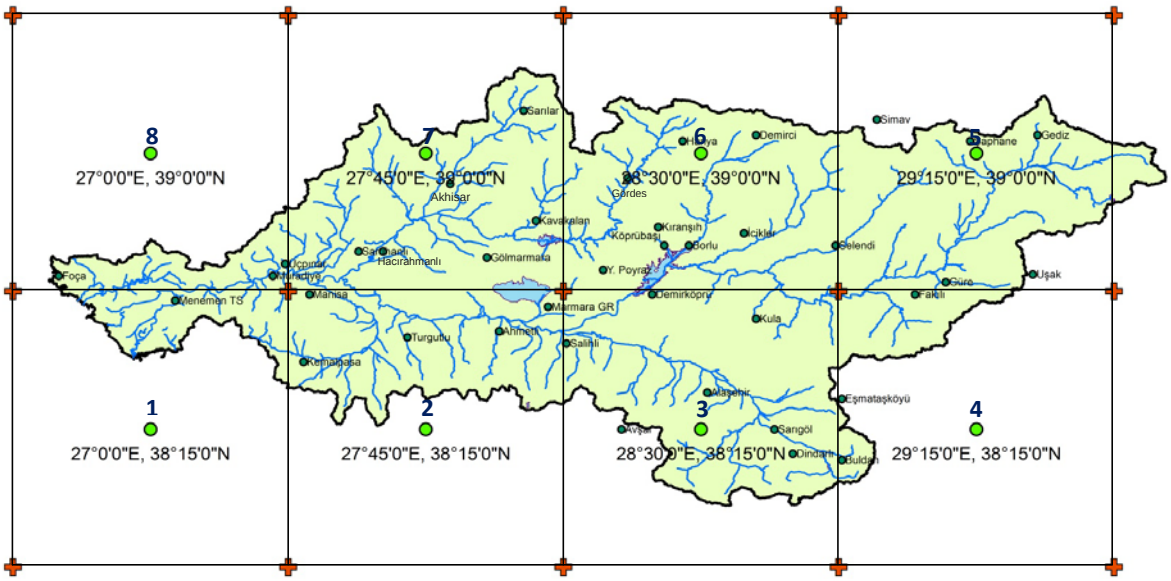

Figure 1. Location of Marmara Lake and ERA-Interim reanalysis grids over Gediz Basin.

In this study, twelve ERA-Interim variables, which were common to data involved in twelve GCMs having two RCP scenarios, were extracted with an intention to establish statistical downscaling models in order to transform GCM outputs to the monthly total precipitation and monthly mean temperature. The content of data set consists of several variables including mean air temperature (air), geo-potential height (hgt), and relative humidity (rhum) at different atmospheric levels (200, 500, and 850 hPa), large scale precipitation (pr) and sea level pressure (slp) at surface, which are the potential predictor variables. Referencing various correlation-regression experiments carried out by Okkan and Kirdemir (2016b), the combination including only large-scale pr variable is determined as the optimum for the downscaling of monthly precipitation over basin. Similarly, only mean air temperature (air) variable is adequate for the temperature downscaling study.

DOWNSCALING STRATEGY

GCMs are coarse-resolution mathematical models which may not represent the local climate characteristics precisely. Hence, it was decided to apply a downscaling procedure to derive future term projections that are more explanatory than coarse-resolution GCMs. Large scale atmospheric patterns to downscale were the predictors which were determined as above-mentioned experiments. In the study, statistical downscaling methods were utilized due to the fact that dynamical downscaling methods have obstacles such as its complicated design, and high computational cost. Accordingly, large scale pr variable for precipitation and air variable for temperature were downscaled to the local scale by means of the two machine learning techniques namely, artificial neural networks (ANN) and least square support vector machines (LSSVM). These predictors were used as inputs for the statistical downscaling method and this procedure was applied for all meteorological stations. The performances of statistical downscaling were measured by utilizing statistical performances criteria such as determination coefficient (R^2), root mean square error (RMSE), Nash-Sutcliffe coefficient (NS), percent bias (PBIAS) and proportion of RMSE to standard deviation of measured data (RSR) (Moriasi et al., 2007). For each meteorological station, the optimal downscaling model structure was chosen in terms of statistical performances in testing period. Generally, both models showed 'very good' and 'good' skills in simulating precipitation for the related meteorological stations. The models performed as 'very good' in temperature downscaling with R^2 and NS values above %98. In order to summarize to study, readers are referred to Okkan and Kirdemir (2018) and Okkan Kirdemir (2016b) where downscaling results corresponding to the downscaling strategy are available for several meteorological stations.

Following the validating downscaling models and choosing the best one, raw GCM data were integrated into the calibrated downscaling models and downscaled precipitation and temperature time series data were obtained for historical, RCP4.5 and RCP8.5 climate scenarios. In the study, it is emphasized on a hybrid model (ENSEMBLE) which includes all GCM forecasts, since these time series were obtained for 12 different GCMs. For this purpose, the ENSEMBLE procedure was performed by Bayesian Model Averaging (BMA) method and all the GCMs were weighted to avoid controversy in individual model selection. The aforementioned process was applied for dry and wet periods of the time period. The details of BMA method were presented by Okkan and Kirdemir (2016c). The biases of weighted ensemble outputs were also corrected by the quantile mapping based-bias correction (QM) approach. QM approach employed in this study, which utilizes cumulative distribution functions (Gamma function for precipitation and Normal function for temperature), was also preferred by Kirdemir (2017) to reduce biases originated from GCMs.

To have confidence on the climate change scenarios statistically downscaled from GCMs, it must be at least assured that the downscaled values can represent the historical climate conditions in terms of a significance level. (Dibike *et al.*, 2007). After bias correction, Mann-Whitney U test was employed in the study to analyze the confidence levels of both downscaled results of twelve GCMs and ensemble simulations derived from BMA scheme. Hypothesis testing on historical scenario results was also suggested by Dibike *et al.* (2007) in uncertainty analysis of downscaled precipitation and temperature regimes. Monthly areal total precipitation and monthly areal mean temperature changes for Salihli meteorological station are shown by box-plots in Figure 2. According to these changes monthly areal total precipitation was predicted for 2015-2050 future term that 8.5% and 18.2% decreases are foreseen for RCP4.5 and RCP8.5, respectively and for monthly areal mean temperature is expected to increase 3.8 and 5.2 °C for RCP4.5 and RCP8.5, respectively.

Table 1. Information about the meteorological stations (A) and flow-gauging stations (B) used in the study

Station Name	Station No.	MGM/DSI	Altitude (m)	Latitude (°) N	Longitude (°) E	Intended use
Akhisar*	17184	MGM	93	38.917	27.817	C4
Alaşehir*	5974	MGM	189	38.350	28.517	C5
Borlu	2425	MGM	250	38.750	28.467	C2
Demirci*	17746	MGM	851	39.050	28.650	C2
Gediz*	17750	MGM	825	39.050	29.417	C2
Gördes*	4930	MGM	550	38.933	28.300	C2, C3
Güre*	5458	MGM	650	38.650	29.167	C2
Köprübaşı*	5278	MGM	250	38.750	28.400	C2
Kula*	5624	MGM	675	38.550	28.650	C2, C5
Salihli*	17792	MGM	111	38.483	28.133	C1, C5
Şaphane	4765	MGM	925	39.033	29.233	C2
Sarıgöl*	6143	MGM	225	38.250	28.700	C5
Selendi*	5282	MGM	575	38.750	28.867	C2
Avşar	05-026	DSI	275	38.250	28.283	C5
Buldan	05-027	DSI	470	38.167	28.883	C5
Demirköprü	05-003	DSI	290	38.617	28.367	C5
Dindarlı	05-006	DSI	685	38.183	28.750	C5
Eşmataşköyü	05-001	DSI	930	38.333	28.883	C5
Fakılı	05-012	DSI	715	38.617	29.083	C2
Hanya	05-010	DSI	640	39.033	28.450	C2, C3
İcikler	05-018	DSI	710	38.783	28.617	C2
Kavakalan	05-011	DSI	460	38.817	28.050	C3
Kıranşıh	05-016	DSI	670	38.800	28.383	C2, C3
Sarılar	05-008	DSI	340	39.117	28.017	C4
Y. Poyraz	05-013	DSI	630	38.683	28.233	C3
Uşak*	17188	MGM	919	38.671	29.404	C2
Simav*	17748	MGM	809	39.093	28.979	C2

**: Meteorological stations measuring both precipitation and temperature.*

Station Number	River/Creek	Station Name	Altitude (m)	Latitude (°) N	Longitude (°) E	Intended use
E05A023	Gediz	Acısu	348	38.64	28.72	C2
E05A014	Selendi	Derekoy	345	38.70	28.70	C2
E05A022	Demirci	Borlu	245	38.76	28.48	C2
E05A015	Deliinis	Topuzdamları	381	38.72	28.56	C2
D05A031	Alasehir	Taytan Koprusu	91	38.50	28.18	C5
E05A009	Medar	Kayalıoglu	77	38.89	27.77	C4
D05A028	Gordes	Hacıhıdır	305	38.77	28.18	C3

The intended use of each meteorological station in terms of inflow calculation of Marmara Lake is denoted by 'C' (e.g., C1 denotes that the related meteorological station is used for calculation of first inflow component expressed in Section 2).

Table 2. Information about elements of irrigation system in the study area.

Irrigation Channels	Irrigation Associations	Net Irrigation Area (ha)	Water Resources
Ahmetli Left	Ahmetli & Turgutlu	9347	Demirkopru Dam and Marmara Lake
	Mesir	13679	
Ahmetli Right	Ahmetli & Turgutlu	2568	
	Sarikiz	13702	
	Gediz	10962	
Menemen Left	Menemen Left Beach	16500	
Menemen Right	Menemen Right Beach	6365	

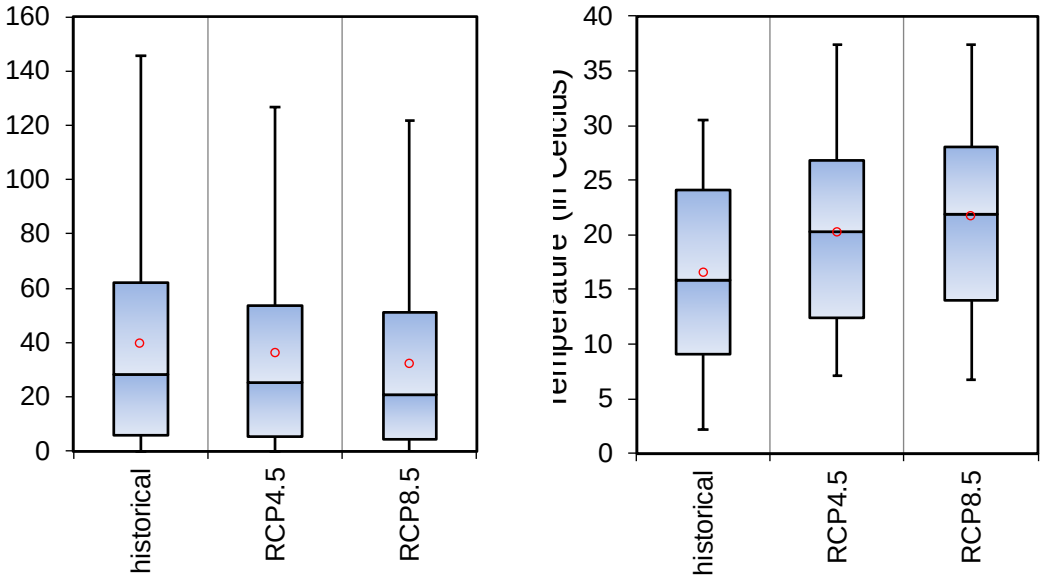

Figure 2. The box-plots of historical and projection results for precipitation and temperature.

CROP WATER DEMANDS

Marmara Lake is operated to supply irrigation water demands in study area and serves 7 irrigation associations such that 4 irrigation channels convey irrigation water to the related associations namely Ahmetli Left/Right Beach and Menemen Left/Right Beach irrigation channels. As seen in Table 2, the irrigation water is supplied to the demandant associations by not only Marmara Lake but also Demirkopru Dam. Upon evaluating the operating policies of Marmara Lake and Demirkopru Dam, it was distinguished that the irrigation water released to the irrigation channels by Demirkopru Dam is 3 times more than Marmara Lake. Hence, in the lights of above-mentioned evidences, it is possible to calculate the total irrigation water demanded from Marmara Lake for both and future periods. As stated before, the calculations are based on the assumption that the trends for the period 1995-2007 may continue in the future. Blaney Criddle method was utilized in order to calculate crop water demands such that precipitation and temperature data underlie the calculation of demands by the definition of the related method. In the phase of calculation of irrigation water requirements, the water conveyance and farm efficiencies were regarded in order to take into consideration the possible losses in conveyance through the channels and irrigation over the agricultural fields. In the study, it is assumed that the irrigation water will be conveyed to the fields by canalet and concrete channels (efficiency of %95) and the surface irrigation methods will be completely abandoned to reduce irrigation water loss, sprinkler and drip irrigation methods (efficiency of 90%) will be performed in the fields. Hence, the total efficiency was taken as 0.855 in the study. According to the calculations, mean annual irrigation water of 114 hm^3 was demanded from Marmara Lake by the irrigation associations in the 1996-2007 water year periods. Since the negative effects such as decrease in precipitation and increase in temperature are expected to be experienced in the study area, increases of 78% and 89% in irrigation water demand from Marmara Lake are foreseen for RCP4.5 and RCP8.5 scenarios. Generally, the total irrigation water released from the lake and conveyed through the irrigation channels are expected to be averagely 203 and 216 hm^3/year for RCP4.5 and RCP8.5 scenarios, respectively (Figure 3).

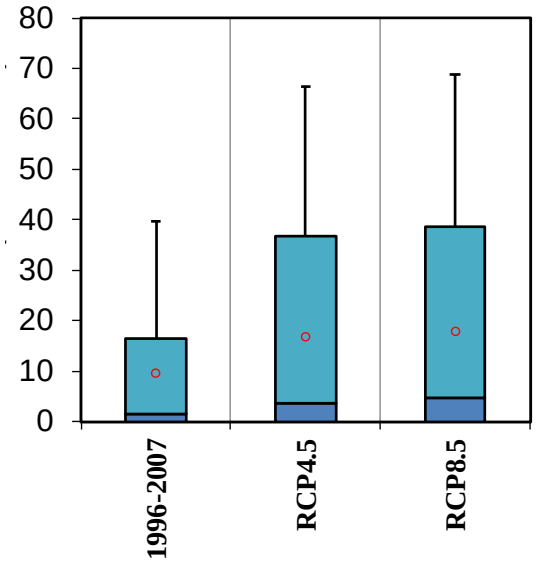

Figure 3. The box-plots of irrigation water demanded from Marmara Lake

DYNAMICAL WATER BUDGET MODEL AND STREAMFLOW PROJECTIONS

In this section, the inflow computation of Marmara Lake was carried out for each of five components expressed in Section 2. First component, the water accumulated naturally in the lake basin was calculated by rational method in which the parameter values of surface flow constant, precipitation height and drainage area were used as inputs. In the rest of components a deterministic, lumped and conceptual rainfall-runoff model, Dynamic Water Budget Model (DYN-WBM) developed by Zhang et al. (2008) were utilized. Zhang et al. (2008) developed the model as a 4-parameter model to simulate streamflow time-series. In this study a modified version of DYN-WBM was used to obtain the streamflow projections for the related components. The detailed expression of modified DYN-WBM can be accessed in Okkan and Kirdemir (2018). The streamflow projections of the second and third component was obtained from the works of Okkan and Kirdemir (2018) and Okkan and Kirdemir (2016b). For the sake of brevity, the readers are referred to these related researchs in which detailed expression of streamflow projections are available. In model construction for fourth and fifth components, the calibration of model was carried out to simulate Medar Creek and Alasehir Creek flows with the observed monthly runoff series of 1976-1993 for water year period and the verification is carried out for water year period 1994-2010. The calibration of the model is based on minimization of RMSE statistics and observed and calibrated runoff series with the model performances for Medar and Alasehir Creeks were shown in Figure 4a,b. Generally, DYN-WBM showed ‘very good’ results in both calibration and verification processes of runoff modeling of Medar Creek and Alasehir Creek, separately. However, the model performed at the verification stage as ‘adequate’ with respect to PBIAS criterion in the modeling of Alasehir Creek.

The streamflow projections for each component were derived through related precipitation and temperature projections constituted for RCP4.5 and RCP8.5 scenarios, respectively. In view of the fact that the data of historical irrigation water demands encapsulate 1996-2007 water years, the comparisons were made with repsect to this related time period. Overall, this time period was selected as the reference time period to be analogous with the demands in reservoir operations studies. The mean annual values of contribution of each component to the Marmara Lake reservoir is presented in Figure 5a for the reference period and RCP scenarios. According to calculations made for each component, the water conveyed from Ahmetli pumping station and Adala Regulator channel have the major proportions in terms of feeding the Marmara Lake reservoir in the reference time period. On the contrary, the water spilled from Gordes Dam and Kum Creek flood water have the minor contribution

to the Marmara Lake reservoir. The inflow accumulated in the lake basin captures the 17% of the total inflow. The summation of these components, that is, the total inflow of Marmara Lake has the highest values in the months April, March and February, respectively. The contributions to the lake are low in between the months June and October.

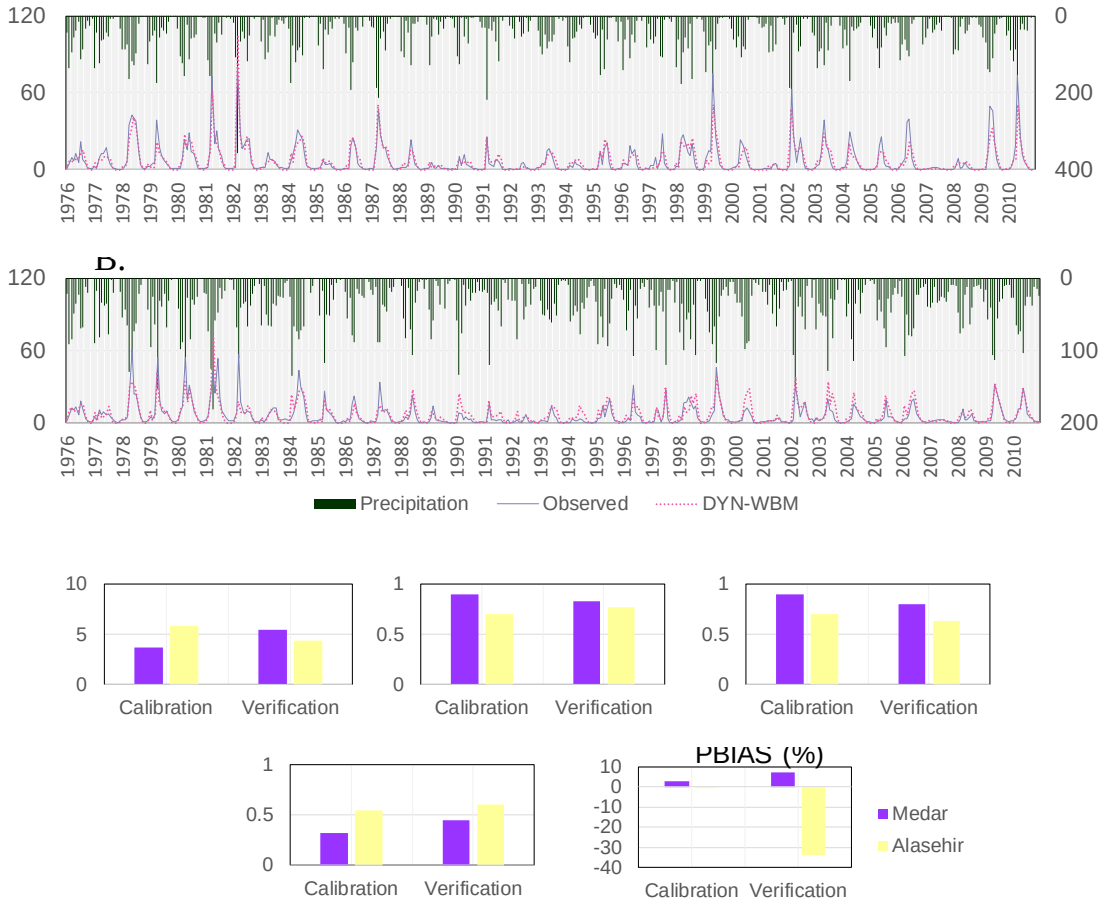

Figure 4. Modeling of runoff time series of Medar (A) and Alasehir (B) Creeks by DYN-WBM.

According to the Figure 5a, decreases of %11 and %20 for RCP4.5 and RCP8.5 scenarios are foreseen in the water accumulated in the lake basin in consequence of possible decreases of precipitation in the related area. The inflow component of Adala Regulator and conveyance channel, which has the major contribution to the lake reservoir in the reference period, is foreseen to have 20% decrease in annual efficiency among the other components in the future and significant decreases in the amount of mean annual flows are predicted as well. The related decrease is mainly due to the fact that significant reductions in the amount of water spilled from Demirkopru Dam are expected for the period 2015-2050. With regard to the amount of water spilled from Demirkopru Dam, while the mean annual flow conveyed through Adala Regulator is about 105 hm^3 in the reference period, it is estimated as in the order of 23 hm^3 and 16 hm^3 for RCP4.5 and RCP8.5 scenarios, respectively. Correspondingly, decreases of 78% and 85% in the contribution of the flow conveyed through Adala Regulator are expected in the future term 2015-2050 for RCP4.5 and RCP8.5 scenarios, respectively. The contributions of spillway flows of Gordes Dam and flood water of Kum Creek are expected to be insignificant in the future as is in the reference period. However, it may be claimed that it is possible to experience decreases of 35% and 65% in Kum Creek flood water contribution for RCP4.5 and RCP8.5 scenarios, respectively. Marmara Lake reservoir is expected to majorly satisfy the water from the component of Ahmetli pumping station in the future due to the fact that the efficiency of Adala Regulator component in feeding Marmara Lake is foreseen to reduce significantly. This ratio is expected to be about 63% in the future term while it is about %43 in the reference period. The mean

annual flow conveyed through Ahmetli pumping station is 128 hm^3 in the future period for both RCP scenarios while this value is about 150 hm^3 for reference period, that is, it corresponds to an expected decrease of 14% in the contribution of Ahmetli pumping station in the future. Overall, in accordance with the possible changes in contribution of each component, the total inflow of Marmara Lake is expected to decrease by 26% and 41% for RCP4.5 and RCP6.0 scenarios, respectively (Figure 5b).

RESERVOIR OPERATION

Following the calculation of irrigation water demands and inflows, the reservoir operation studies were performed by means of behavior analysis in which monthly water budget relationships were constituted for consecutive months. In addition to the data of demands and inflows, net evaporation from the lake surface are required to be calculated to take into account the losses. In order to calculate the evaporative losses, an exponential relationship was constituted between the temperature data of Salihli meteorological station and pan evaporation data of Marmara Lake Regulator meteorological station of General Directorate of State Hydraulic Works with the station number 05-023. The pan coefficient was taken as 0.7 at the stage of reservoir operation. The reservoir operation studies were performed such that it was accepted the reservoir is at full state in the beginning of the time periods. Figure 6a shows the time-varying water volume at the beginning of the month for reference period and RCP scenarios. According to the Figure 6a, the reservoir volume shows a resilient behavior in most of the reference period in spite of the demands and evaporations. In RCP4.5 scenario, it is expected that the reservoir volume is not be able to get back to the maximum operating after the beginning of the 2030s. This situation is foreseen in the beginnings of 2020s for the pessimistic scenario, RCP8.5. In the study, the results were also interpreted by designating the amount of water deficits which can emerge on the months when the demands were not satisfied as well as calculation of failure ratios of the dam. The changes in water deficit over time that may emerge under both reference period and RCP scenarios are given in Figure 6b. As seen in Figure 6b, the reservoir completely satisfies the water demands in reference period, that is, it is not experienced any water deficit in terms of supplying irrigation water. In RCP4.5 scenario, it is estimated that there may be increases in water deficits in the last 25 years of the future time period and it is expected water deficits in the 17.9% of the time period. Under RCP8.5 scenario, it is predicted that critical increases may emerge at the last 30 years of the future time period and the reservoir is expected to satisfy the irrigation water with a limited extent in the %26.9 of the related time period. In addition, it is not expected to experience any years in which the demand will be completely satisfied by Marmara Lake between the years 2031 and 2050 except 2044 in RCP8.5 scenario.

CONCLUSIONS

In the study prepared, the effects of the climate change on Marmara Lake, which has an important role on agricultural sector in Gediz Basin, were investigated. In preparing the climatological projections, 12 GCMs which were prepared in the scope of IPCC's AR5 and two different concentration pathways data were utilized. ANN and LSSVM based statistical downscaling models were used for precipitation and temperature projections. The ERA-Interim predictors representing each precipitation and temperature station on the basin scale were used in the calibration and verification processes of the statistical downscaling models. Even though only one meteorological station data was utilized to capture the precipitation and temperature of lake basin, 26 more meteorological data were used for calculating the all inflow components such that 12 of them observes air temperature as well. In the study, it was obtained that ANN and LSSVM perform as ‘good’ and ‘very good’ in most of the meteorological stations and they show very consistent results in downscaling of temperature with high values of statistical performance criteria. A multi-model ensemble and bias correction strategy was applied for ultimate projections of precipitation and temperature for all meteorological stations. Hence, it was obtained the time series with highher significance levels and less uncertainty for both precipitation and temperature simulations.

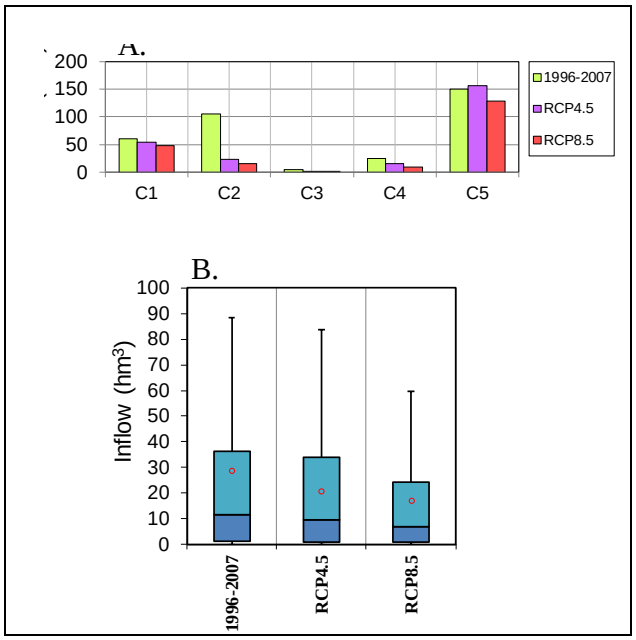

Figure 5. The amount of inflow components (A) and box-plot illustrations of total inflow (B) of Marmara Lake with respect to the reference period and RCP scenarios.

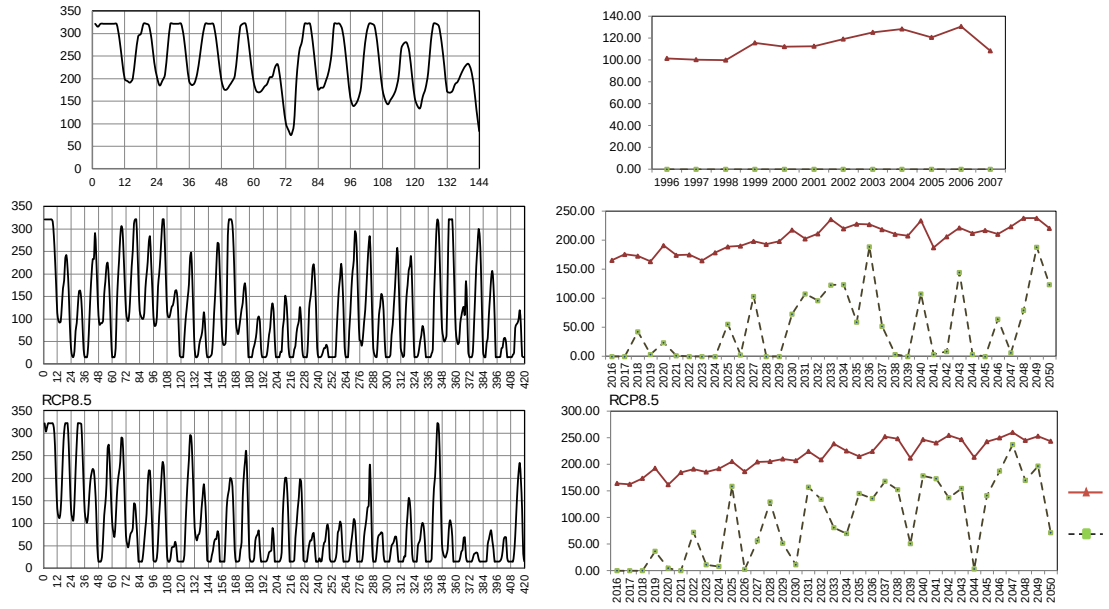

Figure 6. Time-varying reservoir volume changes with respect to the related months (A) and the water demanded from Marmara Lake and the response of reservoir against the demand (B). The vertical axis of graphs denotes the water volume in hm^3 as volume at the beginning of the months for those on A column and demanded and water deficit volume for those on column B.

The irrigation water demand projections were derived by Blaney-Criddle method in which the projected precipitation and temperature time series were used as inputs. Following, the five components which constitute total inflow of Marmara Lake were calculated by means of rational method (for component 1) and modified DYN-WBM model (for component 4 and 5). At the end, the reservoir operation studies which captures the reference and scenario-based performance of Marmara Lake reservoir was performed for the related time periods. Overall, it is expected decreases between %8.5 and %18.2 in precipitation and increases between 3.8 and 5.2 °C in temperatu
RCP8.5 scenarios. Hence, total inflow of Marmara Lake is expected to decrease in the future term up

to 26% and 41% for RCP4.5 and RCP8.5 scenarios, respectively. With the above-mentioned expectations which may force the Marmara Lake reservoir in the future, it is expected the lake to failure in certain months of the future period which corresponds to approximately 18% and 27% of the time period for RCP4.5 and RCP8.5 scenarios, respectively.

ACKNOWLEDGEMENTS

The research leading to this study is funded by the Scientific and Technological Research Council of Turkey (TUBITAK) under Grant No. 114Y716.

REFERENCES

Dibike, Y.B., Gachon, P., St-Hilaire, A., Ouarda, T.B.M.J., Nguyen, V.T.V., 2007. Uncertainty analysis of statistically downscaled temperature and precipitation regimes in Northern Canada. Theor. Appl. Climatol. 91, 149–170. https://doi.org/10.1007/s00704-007-0299-z

Kirdemir, U., 2017. İklim değişikliğinin baraj havzası hidrolojisi üzerindeki olası etkilerinin modellenmesi: AR5-RCP senaryoları ve Demirköprü Barajı örneği. Balıkesir Üniversitesi Fen Bilimleri Enstitüsü, Yüksek Lisans Tezi, 105 sayfa.

Moriasi, D.N., Arnold, J.G., Van Liew, M.W., Binger, R.L., Harmel, R.D., Veith, T.L., 2007. Model evaluation guidelines for systematic quantification of accuracy in watershed simulations. Trans. ASABE 50, 885–900. https://doi.org/10.13031/2013.23153

Moss, R.H., Edmonds, J.A., Hibbard, K.A., Manning, M.R., Rose, S.K., Van Vuuren, D.P., Carter, T.R., Emori, S., Kainuma, M., Kram, T., Meehl, G.A., Mitchell, J.F.B., Nakicenovic, N., Riahi, K., Smith, S.J., Stouffer, R.J., Thomson, A.M., Weyant, J.P., Wilbanks, T.J., 2010. The next generation of scenarios for climate change research and assessment. Nature 463, 747–756. https://doi.org/10.1038/nature08823

Okkan, U., Fistikoglu, O., 2014. Evaluating climate change effects on runoff by statistical downscaling and hydrological model GR2M. Theor. Appl. Climatol. 117, 343–361. https://doi.org/10.1007/s00704-013-1005-y

Okkan, U., Inan, G., 2015. Bayesian Learning and Relevance Vector Machines Approach for Downscaling of Monthly Precipitation. J. Hydrol. Eng. 20, 04014051-1-04014051-13. https://doi.org/10.1061/(ASCE)HE.1943-5584.0001024.

Okkan, U., Kirdemir, U., 2018. Investigation of the Behavior of an Agricultural-Operated Dam Reservoir Under RCP Scenarios of AR5-IPCC. Water Resour. Manag. https://doi.org/10.1007/s11269-018-1962-0

Okkan, U., Kirdemir, U., 2016a. Investigation of A Dam Reservoir Behaviour Under Climate Change Scenarios of IPCC-AR5, in: 3rd International Scientific Meeting in the Field of Civil and Environmental Engineering. Tuzla, Bosnia and Herzegovina.

Okkan, U., Kirdemir, U., 2016b. Downscaling of monthly precipitation using CMIP5 climate models operated under RCPs. Meteorol. Appl. 23. https://doi.org/10.1002/met.1575

Okkan, U., Kirdemir, U., 2016c. Bayes Model Ortalaması Yöntemiyle Kavramsal Yağış-Akış Modeli Çıktılarının Değerlendirilmesi. DSİ Tek. Bülteni 121.

Okkan, U., Kirdemir, U., Serbes, Z.A., 2016. Rcp İklim Değişikliği Senaryoları İle Salihli Sol Sahil Sulaması'nda Sulama Suyu İhtiyacının 2015-2050 Gelecek Dönemi İçin İrdelenmesi. 13. Kültür Teknik Kongresi, Kundu, Antalya.

Schmidli, J., Frei, C., Vidale, P.L., 2006. Downscaling from GCM precipitation: A benchmark for dynamical and statistical downscaling methods. Int. J. Climatol. 26, 679–689. https://doi.org/10.1002/joc.1287

Zhang, L., Potter, N., Hickel, K., Zhang, Y., Shao, Q., 2008. Water balance modeling over variable time scales based on the Budyko framework - Model development and testing. J. Hydrol. 360, 117–131. https://doi.org/10.1016/j.jhydrol.2008.07.021

So many large dams were constructed
for irrigation of lands
and also production of electricity.
DSA desires to be a non-profit organization
for providing
"dam safety concept" in Turkey.

ATA

We are thankful to executive committee
of ATA Companies Group
for their contribution